Scottish Government
Riaghaltas na h-Alba
gov.scot

The Scottish Coastal Observatory 1997-2013

Part 2 - Description of Scotland's Coastal Waters

Scottish Marine and Freshwater Science Vol 7 No 26

E Bresnan, K Cook, J Hindson, S Hughes, J-P Lacaze, P Walsham, L Webster and W R Turrell

marinescotland

The Scottish Coastal Observatory 1997-2013
Part 2 – Description of Scotland's coastal waters

Scottish Marine and Freshwater Science Vol 7 No 26

E Bresnan, K Cook, J Hindson, S Hughes, J-P Lacaze, P Walsham,
L Webster and W R Turrell

Published by Marine Scotland Science
ISSN: 2043-772
DOI: 10.7489/1881-1

Marine Scotland is the directorate of the Scottish Government responsible for the integrated management of Scotland's seas. Marine Scotland Science (formerly Fisheries Research Services) provides expert scientific and technical advice on marine and fisheries issues. Scottish Marine and Freshwater Science is a series of reports that publishes results of research and monitoring carried out by Marine Scotland Science. It also publishes the results of marine and freshwater scientific work carried out by Marine Scotland under external commission. These reports are not subject to formal external peer-review.

This report presents the results of marine and freshwater scientific work carried out by Marine Scotland Science.

Contents

1. Introduction 1
   1.1 Supporting Policy 1
   1.2 Impact 2
   1.3 Underpinning Science 2
   1.4 The 2016 Baseline Review 3
   1.5 Accompanying Data Set 3
   1.6 The Scottish Coastal Observatory 3
   1.7 Summary - Introduction 4
   1.8 References - Introduction 4
2. Report Methodology 6
   2.1 Sampling Temporal Resolution 6
   2.2 SCObs Data Set 6
   2.3 Data transformation 6
   2.4 Plot 1 - Seasonal Variability 7
   2.5 Plot 2 – Annual Variability 7
   2.6 Plot 3 and 4 Inter and Intraannual variability 8
   2.7 Quality Control and Quality Flagging 10
   2.8 References – Report Methodology 11
3. Site Descriptions 12
   3.1 Millport 16
   3.2 Mallaig 17
   3.3 Loch Maddy 17
   3.4 Loch Ewe 18
   3.5 Scapa Bay 20
   3.6 Fair Isle 20
   3.7 Scalloway 21
   3.8 Cromarty 22
   3.9 East Coast (Findon, Cove Bay, Stonehaven) 23
   3.10 Stonehaven 23
   3.11 Summary - Site Descriptions 25
   3.12 References – Site Descriptions 25
4. Context Setting - Physical Conditions 27
   4.1 Meteorology 27
   4.2 Summary – Meteorology 31

4.3 Plots - Meteorology 32
4.4 River Flow 34
4.5 Summary – River Flow 40
4.6 Plots - River Flow 41
4.7 Offshore Temperature 44
4.8 Summary – Offshore Temperature 46
4.9 References - Physical Conditions 47
4.10 Plots – Offshore Temperature 48
5. Temperature and Salinity 49
5.1 Introduction 49
5.2 Methods 50
5.3 Results 54
5.4 Summary – Temperature and Salinity 59
5.5 References - Temperature and Salinity 59
5.6 Plots – Temperature and Salinity – Context Setting 60
5.7 Plots - Temperature and Salinity at the Coastal Monitoring Sites 63
6. Secchi Depth 77
6.1 Introduction 77
6.2 Methods 77
6.3 Results 77
6.4 Summary – Secchi Depth 78
6.5 References – Secchi Depth 78
6.6 Plots – Secchi Depth 79
7. Inorganic Nutrients 81
7.1 Introduction 81
7.2 Methods 82
7.3 Results 84
7.4 Summary– Inorganic Nutrients 88
7.5 References – Inorganic Nutrients 90
7.6 Plots – Inorganic Nutrients 91
8. Ocean Acidification – Carbonate Chemistry Parameters 117
8.1 Introduction 117
8.2 Methods 118
8.3 Results 121
8.4 Summary – Ocean Acidification 122
8.5 References – Ocean Acidification 123
8.6 Plots – Carbonate Chemistry Parameters 125

9. Phytoplankton 133
9.1 Introduction 133
9.2 Methods 135
9.3 Results - Diatoms 136
9.4 Plots – Diatoms 139
9.5 Results - Dinoflagellates 145
9.6 Plots – Dinoflagellates 147
9.7 Results – *Alexandrium* 153
9.8 Plots – *Alexandrium* 155
9.9 Results - *Dinophysis* 162
9.10 Plots – *Dinophysis* 164
9.11 Results - *Pseudo-nitzschia* 170
9.12 Plots - *Pseudo-nitzschia* 172
9.13 Summary - Phytoplankton 178
9.14 References - Phytoplankton 179
10. Chlorophyll ‘a’ 183
10.1 Introduction 183
10.2 Methods 183
10.3 Results 184
10.4 Summary- Chlorophyll ‘a’ 184
10.5 References – Chlorophyll ‘a’ 186
10.6 Plots – Chlorophyll ‘a’ 187
11. Algal toxins 189
11.1 Introduction 189
11.2 Methods 191
11.3 Results 195
11.4 Discussion 198
11.5 Summary - Biotoxins 200
11.6 References – Algal toxins 202
11.7 Plots – Algal toxins 204
12. Zooplankton 216
12.1 Introduction 216
12.2 Methods 220
12.3 Results - Total Copepod Biomass 221
12.4 Plots – Total Copepod Biomass 223
12.5 Results - *Calanus finmarchicus* Stages C5-6 Biomass 225
12.6 Plots - *Calanus finmarchicus* Stages C5-6 Biomass 226

12.7 Results - *Calanus helgolandicus* Stages C5-6 Biomass 228
12.8 Plots - *Calanus helgolandicus* Stages C5-6 Biomass 229
12.9 Results - *Centropages hamatus* Stages C1-6 Biomass 231
12.10 Plots - *Centropages hamatus* Stages C1-6 Biomass 232
12.11 Results - *Centropages typicus* Stages C1-6 Biomass 234
12.12 Plots - *Centropages typicus* Stages C1-6 Biomass 235
12.13 Results - *Acartia clausi* Stages C1-6 Biomass 237
12.14 Plots - *Acartia clausi* Stages C1-6 Biomass 238
12.15 Results - *Paracalanus parvus* Stages C1-6 Biomass 240
12.16 Plots - *Paracalanus parvus* Stages C1-6 Biomass 241
12.17 Results - *Pseudocalanus* spp. Stages C1-6 Biomass 243
12.18 Plots - *Pseudocalanus* spp. Stages C1-6 Biomass 244
12.19 Results - *Temora longicornis* stages C1-6 biomass 246
12.20 Plots - *Temora longicornis* stages C1-6 biomass 247
12.21 Results - Oithonidae stages C1-6 biomass 249
12.22 Plots - Oithonidae stages C1-6 biomass 250
12.23 Results - Benthic Larvae Biomass 252
12.24 Plots - Benthic Larvae Biomass 253
12.25 Results - Decapod Larvae Biomass 255
12.26 Plots - Decapod Larvae Biomass 256
12.27 Results - Bivalve Larvae Biomass 258
12.28 Plots - Bivalve Larvae Biomass 259
12.29 Results - Barnacle Larvae Biomass 261
12.30 Plots - Barnacle Larvae Biomass 262
12.31 Results - Cnidarian Biomass 264
12.32 Plots - Cnidarian Biomass 265
12.33 Results - Calcifying Plankton Biomass 267
12.34 Plots - Calcifying Plankton Biomass 268
12.35 Summary – Zooplankton 270
12.36 References - Zooplankton 271
13. Acknowledgments 275

Chapter Authors

1	Introduction	Eileen Bresnan
2	Report Methodology	Bill Turrell Sarah Hughes Eileen Bresnan
3	Site Descriptions	Sarah Hughes Jenny Hindson Eileen Bresnan Bill Turrell
4	Physical Conditions	Sarah Hughes Jenny Hindson
5	Temperature and Salinity	Sarah Hughes Jenny Hindson
6	Secchi Depth	Eileen Bresnan
7	Inorganic Nutrients	Lynda Webster Pam Walsham
8	Ocean Acidification – Carbonate Chemistry Parameters	Pam Walsham Lynda Webster
9	Phytoplankton	Eileen Bresnan
10	Chlorophyll	Eileen Bresnan Pam Walsham
11	Algal toxins	Jean-Pierre Lacaze
12	Zooplankton	Kathryn Cook

Text editors

Bill Turrell, Eileen Bresnan

1. Introduction

Scotland's seas are an intrinsic part of its cultural history, identity and economic success. Scottish fishing, aquaculture, tourism, renewable energies, and oil and gas industries are all supported by the oceans around Scotland. Part of the vision of Marine Scotland is to protect Scotland's marine ecosystem while maintaining its economic prosperity. Underpinning this is a need for a comprehensive understanding of how the marine ecosystem functions and how it responds to local environmental pressures such as anthropogenic nutrient input or global drivers such as climate change.

Scotland's coastal waters play an important role in the Scottish rural economy. They provide fertile fishing grounds for stocks such as *Nephrops*, lobsters and crabs and are also the main areas where the aquaculture and maritime tourism industries are located. This coastal environment is subject to pressures from natural and anthropogenic drivers which may impact these industries.

Changes in the ocean circulation offshore, or multi decadal large scale climatic cycles can influence ambient temperature and salinity in coastal areas (Edwards et al., 2002). Weather patterns can result in harmful algal blooms being advected into areas where shellfish farms are located (Whyte et al., 2014). Larger scale drivers such as climate change and ocean acidification (Hoegh-Guldberg and Bruno 2010) can impact the coastal marine ecosystem. The impacts of these longer term changes are unknown and scientists are developing models to try and predict these.

Realising the importance of this situation, Marine Scotland identified 'understanding how the marine ecosystem functions' and 'responding to climate change and its interaction with the marine environment' as two of its high priorities in the 2010-2015 Scottish Marine Science Strategy.

1.1 Supporting Policy

The state of the oceans is recognised as an important concern at an international scale. The vision of 'Clean & Safe', 'Healthy & Biodiverse', and 'Productive' seas is a key driver of marine policy at a national, European and North Atlantic level. The Oslo Paris Commission (OSPAR) has a number of assessment criteria which oblige European states to ensure their waters are not negatively impacted by anthropogenic pressures (OSPAR 2013). The EU has implemented directives such as the Water Framework Directive (WFD) and Marine Strategy Framework Directive (MSFD) which require member states to ensure their waters achieve '*Good Ecological Status'* and *'Good Environmental Status*' respectively. Thus governments are obliged to provide the data to ensure that these assessments can be made.

Coastal ecosystems are very variable with dramatic changes in some parameters e.g. plankton biomass, taking place over a time scale of hours or days. Some aspects of the coastal ecosystem have been poorly studied. For example, studies of the coastal plankton community in Scotland are limited to a number of short term discrete investigations with little description of baseline community structure and how this changes from year to year. Multi-decadal time series of data are required if long term changes in Scotland's coastal ecosystem are to be identified above the pattern

of short term variability. A minimum of three decades of data is required to identify these changes with statistical robustness. Time series data sets are scarce in UK and European waters and this has been flagged in the scientific (Hensen et al., 2014, Boero et al., 2015) and policy based (Edwards et al., 2010, Owens 2014, McQuattors-Gollop et al., 2015) literature over the last number of years.

Marine Scotland Science (MSS) established its first ecosystem monitoring site in 1997, 5 km offshore from the fishing village of Stonehaven in northeast Scotland. Initially established to understand the ecology of the zooplankter *Calanus finmarchicus,* this monitoring site has evolved and is now considered an important monitoring site by the national and international scientific community. It is a key site for the implementation of the WFD and MSFD (Devlin et al., 2013, Scherer et al., 2015) and has been used to describe the status of the zooplankton and phytoplankton communities on a North Atlantic scale (O'Brien et al., 2012, O'Brien et al., 2013). It is providing baseline data about carbonate chemistry (Ostle et al., 2016), climate change (Edwards et al., 2013) and how algal blooms can be transported around the Scottish coast (Davidson et al., 2009).

Stonehaven represents the start of the efforts by Marine Scotland to monitor Scotland's coastal waters. Additional sites were introduced into the programme from 1999 and different combinations of temperature, salinity, nutrients, pigments, algal toxins and plankton were monitored at a further five sites although two are now discontinued. Temperature miniloggers were also installed in an additional five sites. The location of these monitoring sites can be seen in Figure 3.1.

1.2 Impact

Since 2000 data from these time series have addressed a number of policy driven issues:

(i) Supported a challenge to WFD phytoplankton assessment tools and ensured that tools were appropriate for Scottish waters,

(ii) Provided the data for the assessment of GES for the pelagic water column for the MSFD (Scherer et al., 2015),

(iii) Formed part of Scottish Climate Status Report (Hughes 2007),

(iv) Contributed towards the UK assessment of state in Charting Progress 2 (UKMMAS 2010), Scotland's Marine Atlas (Baxter et al., 2011), UK Marine Climate Change Impacts Partnership report cards (Edwards et al., 2013).

1.3 Underpinning Science

Data from this programme have expanded the state of knowledge about the Scottish marine ecosystem with 37 peer review publications, 15 internal and 13 external reports produced by MSS using data from this monitoring programme. Data or samples requested from this programme have also contributed to ten further peer reviewed manuscripts, reports and theses. Since its inception this time series has supported five Ph.D. students with a further six Ph.D. projects underway, five M.Sc.

and three B.Sc. students. This programme is also providing opportunities for future scientists with eight secondary school Nuffield students having worked on the time series since 2005. A full list of the outputs of this programme can be found in Appendix A in Part 3 of this report.

1.4 The 2016 Baseline Review

As the importance of time series is increasing at an international level (Koslow and Couture 2013) this Scottish programme is receiving more attention. Requests to Marine Scotland to contribute data from this programme to assessments, provide material for diversity investigations and to validate modelling studies are becoming more frequent. This dataset is becoming a national resource for policy makers and academics in Scotland, the UK and worldwide.

To aid this and to further flag the variety of data available, Marine Scotland presents a basic description of the seasonality and variability of the main parameters (temperature, salinity, nutrients, carbonate chemistry, phytoplankton, chlorophyll 'a', algal toxins and zooplankton) measured at these coastal monitoring sites. This description takes the form of a MSS report in three parts (Part 1- Executive Summary, Part 2 – Description of Scotland's Coastal Waters, Part 3 – Appendices), along with an accompanying data set.

This report provides baseline descriptions of 135 parameters monitored in this programme. To place these data in a broader context, 68 supporting parameters from external sources, are also presented describing meteorology, riverine inputs and offshore temperatures. More detailed analysis of the data will appear in the peer reviewed scientific literature.

1.5 Accompanying Data Set

The data set that has been published alongside this report contains all the monthly mean values for 135 parameters and 68 supporting parameters. This data set has been given a doi number 10.7489/1761-1 and can be accessed remotely using the Marine Scotland web site or by emailing Scobs@gov.scot. A summary of all parameters in the data set is given in 'Appendix B in Part 3' of this report where this data is described.

1.6 The Scottish Coastal Observatory

Prior to this baseline review a number of names have been used for this monitoring programme. From this date the programme will be renamed "the Scottish Coastal Observatory".

1.7 Summary – Introduction

- This report provides baseline descriptions of 135 parameters derived from sampling performed at ten coastal ecosystem monitoring sites which make up the Scottish Coastal Observatory.
- The report covers the period from 1997 when monitoring first started to the end of 2013.
- To place the monitoring into context, 68 supporting parameters are also presented describing background meteorology, riverine inputs and offshore temperatures.
- Data from the Scottish Coastal Observatory has already had documented policy deliverables and impact, and provided the basis for an extensive portfolio of published research and supporting studies.
- The aim of the report is to provide a single accessible citation describing the Scottish Coastal Observatory which will support future analyses, peer reviewed publications, and further promote the use of the data amongst the scientific community.
- To accompany the report, a quality controlled summary data set consisting of monthly means of all 203 parameters has also been published (doi 10.7489/1761-1)

1.8 References - Introduction

Baxter, J.M., Boyd, I.L., Cox, M., Donald, A.E., Malcolm, S.J., Miles, H., Miller, B., Moffat, C.F., (Editors) (2011) Scotland's Marine Atlas: Information for the national marine plan. Marine Scotland, Edinburgh. 191pp. http://www.scotland.gov.uk/Publications/2011/03/16182005/0.

Boero, F., Kraberg, A.C., Krause, G., Wiltshire, K. (2015) Time is an affliction: Why ecology cannot be as predictive as physics and why it needs time series. Journal of Sea Research, 101, 12 – 18.

Davidson, K., Miller, P., Wilding, T., Shutler, J., Bresnan, E., Kennington, K., Swan, S.(2009) A large and prolonged bloom of Karenia mikimotoi in Scottish waters in 2006. Harmful Algae, 45, 692 – 703.

Devlin, M.J., Best M., Bresnan E., Baptie, M. (2013) Water Framework Directive: The development and status of phytoplankton tools for ecological assessment of coastal and transitional waters. United Kingdom. Update Report to UK Technical Advisory Group for the Environment Agency (May 2013).

Edwards, M., Beaugrand, G., Reid, P.C., Rowden, A.A., Jones, M.B. (2002) Ocean climate anomalies and the ecology of the North Sea. Marine Ecology-Progress Series, 239, 1-10.

Edwards, M., Beaugrand, G., Hays, G.C., Koslow, J.A., Richardson, A.J. (2010) Multidecadal oceanic ecological datasets and their application in marine policy and management. Trends in Ecology and Evolution, 25, 602 – 610.

Edwards, M., Bresnan, E., Cook, K., Heath, M., Helaouet, P., Lynam, C., Raine, R., Widdicombe, C. (2013) Plankton Report Card. MCCIP Science Review 2013,98-112, doi:10.14465/2013.arc12.098-112.

Henson, SA. (2014) Slow science: the value of long ocean biogeochemistry records. Philosophical Transactions of the Royal Society A, 372, 20130334. http://dx.doi.org/10.1098/rsta.2013.0334.

Hoegh-Guldberg, O. and Bruno, J.F. (2010) The Impact of Climate Change on the World's Marine Ecosystems. Science, 328(5985), 1523-1528.

Hughes, S. (2007) Scottish Ocean Climate Status Report 2004 - 2005. Aberdeen. Fisheries Research Services.

Koslow, J.A. and Couture, J. (2013) Follow the Fish, Nature 502, 163 – 165.

McQuatters-Gollop, A., Edwards, M., Helaouet, P. Johns, D.G., Owens, N., Raitos, D.E., Schroeder, D., Skinner, J., Stern, R. (2015) The Continuous Plankton Recorder survey: How can long-term phytoplankton datasets contribute to the assessment of Good Environmental Status? Estuarine and Coastal Shelf Science, 162, 88 -97.

O'Brien, T.D., Wiebe, P.H., Falkenhaug, T. (2013) ICES Zooplankton Status Report 2010/2011. ICES Cooperative Research Report No. 318, 208pp.

O'Brien, T., Li WKW, Moran X. (2012) ICES Phytoplankton and Microbial Ecology Status Report 2009/2010. ICES Cooperative Research Report No. 313, 197pp.

OSPAR (2013) Common Procedure for the Identification of the Eutrophication Status of the OSPAR Maritime Area. OSPAR decision 2013-8, 66pp.

Ostle, C., Williamson, P., Artioli, Y., Bakker, D.C.E., Birchenough, S., Davis, C.E., Dye, S., Edwards, M., Findlay, H.S., Greenwood, N., Hartman, S., Humphreys, M.P., Jickells, T., Johnson, M., Landschützer, P., Parker, R., Pearce, D., Pinnegar, J., Robinson, C., Schuster, U., Silburn, B., Thomas, R., Wakelin, S., Walsham, P., Watson, A.J. (2016) Carbon dioxide and ocean acidification observations in UK waters: Synthesis report with a focus from 2010 - 2015. doi:10.13140/RG.2.1.4819.4164.

Owens, N.J.P. (2014) Sustained UK marine observations. Where have we been? Where are we now? Where are we going? Philosophical Transactions of the Royal Society A, 372, 20130332. http://dx.doi.org/10.1098/rsta.2013.0332.

Scherer, C., Gowen, R.J., Tett, P., Atkinson, A., Baptie, M., Best, M., Bresnan, E., Cook, K., Forster, R., Keeble, S., McQuatters-Gollop, A. (2015) Development of a UK integrated plankton monitoring programme. Report to DEFRA. http://randd.defra.gov.uk/Document.aspx?Document=13580_ME5312LifeformFinalReport.pdf.

UK Marine Monitoring and Assessment Strategy (2010) Charting Progress 2 Healthy and Biological Diverse Seas Feeder report. (Eds. Frost, M., Hawkridge, J.). Published by Department for Environment Food and Rural Affairs on behalf of UK MARINE MONITORING AND ASSESSMENT STRATEGY. 682pp. http://chartingprogress.defra.gov.uk/healthy-and-biologically-diverse-seas-feeder-report.

Whyte, C., Swann, S., Davidson, K. (2014) Changing wind patterns linked to unusually high *Dinophysis* blooms around the Shetland Islands, Scotland. Harmful Algae, 39, 365 – 373.

2. Report Methodology

This report presents basic descriptive summaries of the seasonal, inter-annual and intra-annual variability of the parameters measured in the Scottish Coastal Observatory alongside a selection of climatic variables which place the MSS data in a broader context. The report does not attempt to perform robust statistical analyses of the different parameters but rather attempts to provide a basic description of the monitoring programme and its data, from when it began in 1997 to the end of 2013. More indepth analysis of the data will appear in the peer reviewed scientific literature.

Details of all sampling and sample analysis methodologies and quality assurance are presented in each specialised parameter chapter. A standard layout of data analysis and plots has been used in this report, which is described here. Plots 1-4 have been produced by different software programmes. In Chapters 4 and 5 plots were produced using MATLAB (MATLAB 2014) and in Chapters 6-12 using R (R core team, 2013) and the TTA package within R (Devreker and Lefebve 2015).

2.1 Sampling Temporal Resolution

Parameters derived from physical samples, including salinity, nutrients and plankton, have been collected on a weekly basis (weather/equipment permitting). Temperatures recorded using manual thermometers have also been collected on a weekly basis, while automatically logged temperatures have been recorded at intervals down to 30 minutes. Supporting data from external sources such as meteorology and river flow data was collected on varying time scales, typically hours.

Appendix C, in Part 3 of this report, presents further details about sample numbers for each parameter.

2.2 SCObs Data Set

In order to present a coherent data set, monthly means have been calculated for all parameters, and are recorded in the accompanying data set (doi number 10.7489/1761-1).

Point to Note: *Please be aware that that there can be missing values owing to operational reasons. Please contact Scobs@gov.scot or staff at the Marine Laboratory Aberdeen if you require access to raw data.*

2.3 Data transformation

Owing to the numeric spread of some parameters (e.g. plankton) these data have been transformed prior to the calculation of monthly and annual statistics. This is described in the relevant chapters. Data in the accompanying data set have not been transformed.

2.4 Plot 1 - Seasonal Variability

The seasonal cycle describes the short-term changes in each parameter over the time scale of one calendar year. For most parameters, changes caused by the seasonal cycle, can be much greater than the interannual variability. Box whisker plots are used to present the seasonal cycle (Figure 2.1).

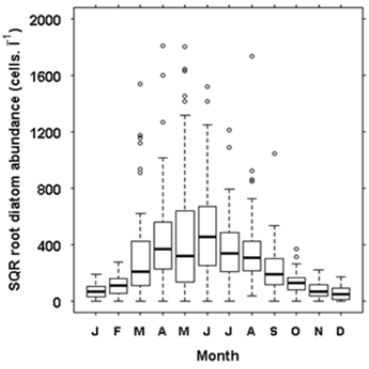

Figure 2.1 Example of standardised plot 1 – seasonal variability and the seasonal cycle.

In these plots the box, or rectangle, represents the boundary values where 25% to 75% of the data, collected in that calendar month through the entire observing period lie. The bold horizontal line within the box represents the median value of all the weekly data recorded in that calendar month from all years observed. The dashed whiskers represent the maximum and minimum values recorded that calendar month, if within 1.5 times the interquartile range (the length of the box). Data points (weekly) exceeding these values are considered outliers and are represented with a circular symbol.

2.5 Plot 2 – Annual Variability

A box whisker plot presents the variability encountered across the whole observation period, and within individual years (Figure 2.2).

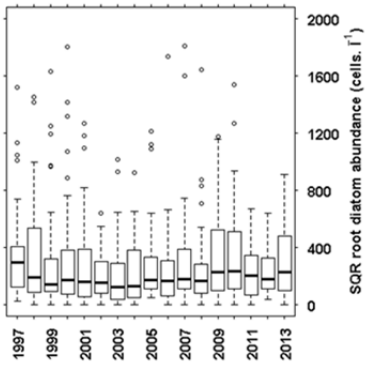

Figure 2.2 Example of plot 2 – annual values.

In these plots, the box or rectangle represents the boundary values where 25% to 75% of the data of the weekly data, collected that year lie. The bold horizontal line within the box represents the median value of all the weekly data recorded in that year. The dashed whiskers represent the maximum and minimum values recorded that year, if within 1.5 times the interquartile range (the length of the box). Data points (weekly) exceeding these values are considered outliers and are represented with a circle symbol.

2.6 Plot 3 and 4 Inter and Intraannual Variability

Plot 3 presents annual anomaly values (interannual variability) and Plot 4 presents monthly anomaly values (intraannual variability) for each parameter. Different calculation methods were used to suit the individual parameters as described below. We describe them here in reverse order.

Anomalies are the differences between an individual measurement and the average values (monthly or yearly) of a parameter at each location. Positive anomalies mean higher than normal conditions; negative anomalies mean lower than normal conditions. In both Plots 3 and 4 positive anomalies are coloured red, and negative anomalies coloured blue.

The anomalies have been normalised by dividing the anomaly values by the standard deviation (sd) of the data calculated over the base period ($sd_{base\ period}$). An anomaly value of +2 represents data which is two standard deviations higher than the base period mean.

Plot 4

In Plot 4, monthly anomalies are presented, i.e. the differences between the means calculated over individual calendar months and the averaged monthly means calculated over the base period i.e.;

$$A_{M,Y} = P_{M,Y} - P_{M,base\ period}$$

where $A_{M,Y}$ is the monthly anomaly for month $_M$ in year $_Y$, $P_{M,Y}$ is the average of parameter P over month $_M$ in year $_Y$, and $P_{M,base\ period}$ is the average of parameter P calculated for all data in month $_M$ throughout the base period.

The normalised monthly anomaly $Anorm_{M,Y}$ is;

$$Anorm_{M,Y} = A_{M,Y} / sd_{M,base\ period}$$

where $sd_{M,base\ period}$ is the standard deviation of all data collected in month $_M$ throughout the base period and $A_{M,Y}$ is the monthly anomaly for month $_M$ in year $_Y$.

Hence in Plot 4, the average seasonal cycle over the base period has been removed from the monthly averages, leaving the monthly anomalies (Figure 2.3).

For Chapters 4-5 the base period is 2001–2010 or the duration of the data record if it is less than this. For Chapters 6-12, the base period is taken as the entire data record.

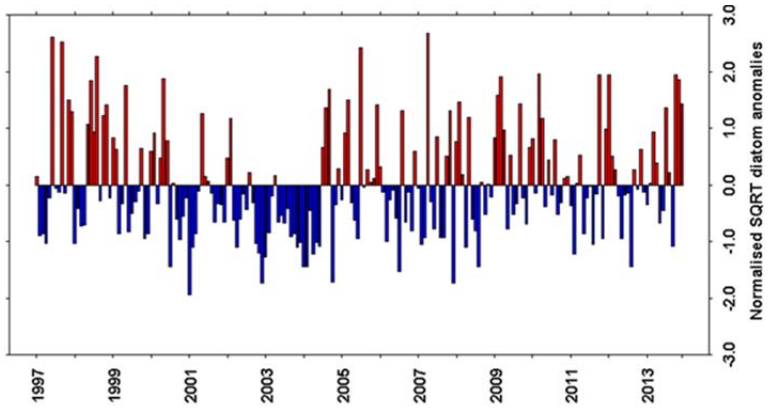

Figure 2.3 Example of plot 4 – normalised monthly mean anomalies.

Plot 3

In Plot 3, annual anomalies are presented, i.e. the differences between the means calculated over individual calendar years and the mean calculated over a base period. For Chapters 4-5 the annual mean anomalies (A_{normY}) presented in Plot 3 are calculated as the average of the monthly anomalies used in Plot 4 i.e.;

$$A_{normY} = (\text{sum}(A_{normM,Y})_M) / _M$$

For Chapters 6-12 the annual mean anomalies are calculates using the formula below;

$$A_Y = P_Y - P_{base\ period}$$

$$A_{normY} = A_Y / sd_{base\ period}$$

where A_Y is the annual anomaly for year $_Y$, P_Y is the average of parameter P over year $_Y$, and $P_{base\ period}$ is the average of parameter P over the base period (Figure 2.4).

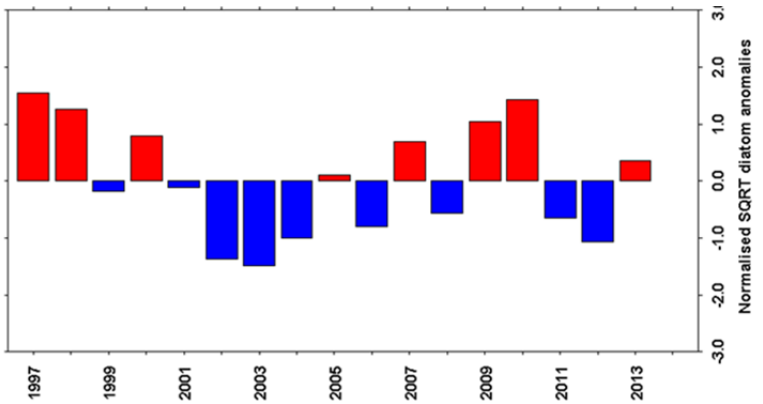

Figure 2.4 Example of plot 3 – normalised annual mean anomalies.

Time Offset

In Plot 3, vertical bars representing annual means of year Y are centred on the year value (Y), with an approximate width of one year. Thus they appear to sit between Y-0.5 and Y+0.5, in terms of decimal year. In Plot 4, vertical bars representing the monthly means of year Y fit between the year marks Y and Y+1.

Missing Values

Missing values are discussed individually in each chapter.

2.7 Quality Control and Quality Flagging

In order to prepare this report, the datasets were all quality controlled. A summary of the detailed QC procedure for each parameter can be found in Chapters 4-12.

For historic temperature, salinity and nutrient data, Quality Flags (QF) have been used in order to record the outcome of various QC procedures applied to the data. Quality flags were assigned according to the Seadatanet system (SEADATANET 2010 – see Appendix D, in Part 3 of this report, for list). Data with a QF value of 3 and 4 (representing probably bad/bad data) were excluded from the analysis.

In order to assign quality flags to temperature, salinity and nutrient data, a MATLAB script was produced to examine their seasonal trends. Data points, prior to any transformation, falling outside +/- 2 standard deviations of the seasonal mean were flagged and each individual point was manually checked to see if this was a natural event or an analytical error. The final QF is assigned at the end of each calendar year when a seasonal cycle could be examined. Further details are presented in the methods section of the relevant chapters.

Figure 2.5 shows the different data streams contributing to this report and their internal location in MSS.

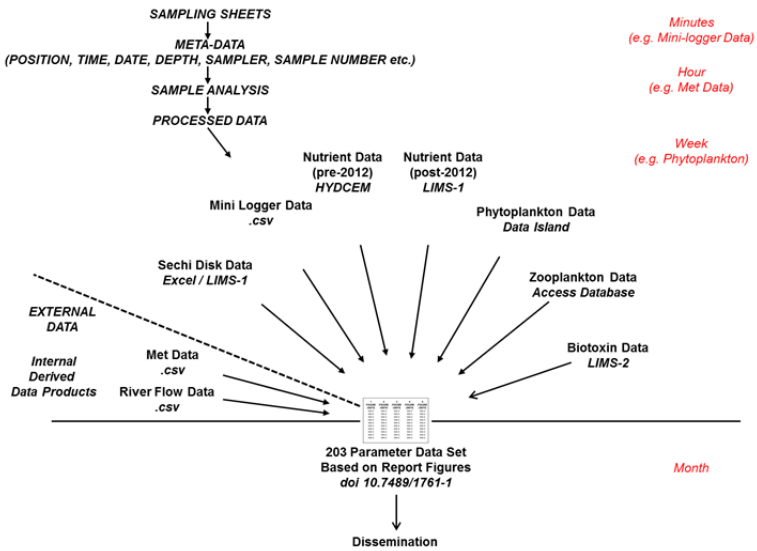

Figure 2.5 Summary of the different data streams and internal MSS storage location described in this report and presented in the accompanying data set (doi number 10.7489/1761-1).

2.8 References – Report Methodology

Devreker, D. and Lefebve, A. (2015) TTAinterfaceTrendAnalysis: A R GUI for Routine Temporal Trend Analysis and Diagnostics. 14pp. https://cran.r-project.org/web/packages/TTAinterfaceTrendAnalysis/vignettes/TTAVignette.pdf

MATLAB (2014) The MathWorks, Inc., Natick, Massachusetts, United States

R Core Team (2013). R: A language and environment for statistical computing. R Foundation for Statistical Computing, Vienna, Austria. URL http://www.R-project.org/

SEADATANET (2010) DATA QUALITY CONTROL PROCEDURES. 78pp. http://www.seadatanet.org/content/download/18414/119624/file/SeaDataNet_QC_procedures_V2_(May_2010).pdf.

3. Site Descriptions

The first mulitparameter monitoring site in this Scottish Coastal Observatory was started at Stonehaven in 1997 where a number of physical, chemical and biological parameters were measured to examine the ecology of the copepod *Calanus finmarchicus*. This programme was expanded from 1999 to include a number of locations around the Scottish coast. The aim is to generate a long term time series of data to allow variability and change within the Scottish coastal environment to be identified and investigated.

Since 1997 the number of sites has changed, with some new sites started and others discontinued. The parameters measured at each site can differ. For this report, data from the ten coastal stations are presented. Out of these, four measured sea surface temperature only, while a further six measured additional parameters (a combination of physics, chemistry and biology). Samples are collected weekly, however, weather or operational issues may mean a sampling event is missed. A summary list of location and exposure of each monitoring site is given in Table 3.1 and the parameters measured in Table 3.2. Fundamental to the success of this programme has been the contribution of the voluntary collectors who gave up their time to collect samples and maintain sampling equipment. Without their input this observatory could not happen.

The monitoring sites are often in harbours, which by their very design, tend to be the most sheltered spots along a particular coastline. However, each harbour has a different aspect and can be exposed to wind driven waves and storms from a particular direction. Prevailing winds in the UK are from the south and south-west, therefore we would expect unsheltered coasts with this aspect to be the most exposed.

Site Exposure

In order to try and characterise each site in a similar way, the relative exposure of the site has been determined from an exposure index dataset prepared during a wave exposure study (Burrows et al., 2008). We have used these data to determine the average exposure of the sampling site and also the exposure of the surrounding area. The average exposure takes account of the exposure from each of the 16 wind directions, however, for this analysis we haven't differentiated between these. Where sites have an average wave exposure index below (above) the median for the UK coastlines, they are described as sheltered (exposed). If the site has an exposure index lower than the 10^{th} percentile compared to the UK wide dataset, they are described as 'very sheltered' and conversely above the 90^{th} percentile it is described as 'very exposed'.

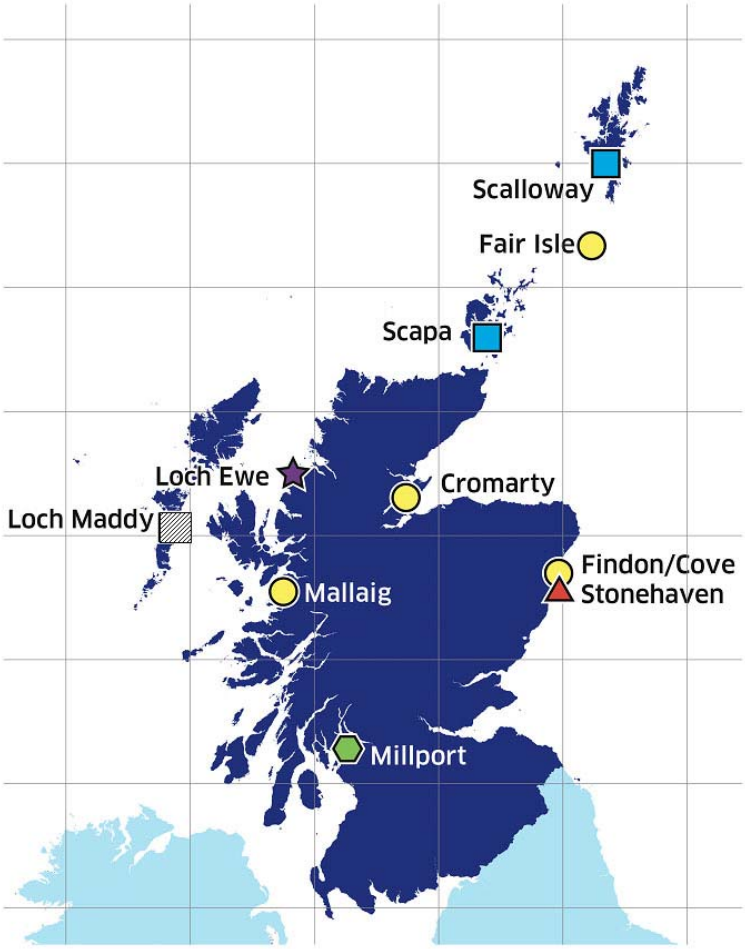

Figure 3.1 Map of monitoring stations in the Scottish Coastal Observatory. The different symbols represent the different combination of parameters measured; ● temperature only, ⬢ temperature and phytoplankton, ▨ temperature, salinity, phytoplankton, ■ temperature, salinity, nutrients, algal toxins, phytoplankton, ★ temperature, salinity, secchi, nutrients, pigments, algal toxins, phytoplankton, zooplankton, ▲ temperature, salinity, secchi, nutrients, carbonate chemistry, pigments, phytoplankton, zooplankton.

	Site	Location Name	Position changes	Latitude		Longitude		Site Exposure	Coastline Exposure
1	Millport	Keppel Pier	55	44.97	004	54.33		sheltered	sheltered
	Millport	Fairlie Channel	55	44.61	004	54.32		sheltered	sheltered
2	Mallaig	Fishery Pier	57	00.40	005	49.50		sheltered	exposed
3	Loch Maddy	Ferry Pier	57	35.77	007	09.34		very sheltered	very sheltered
		nr Hamarsay	57	03.09	007	08.48		sheltered	very sheltered
4	Loch Ewe	Mooring	57	50.14	005	36.61		sheltered	sheltered
		Mouth Loch Ewe	57	50.99	005	38.97		exposed	sheltered
5	Scapa	Scapa Pier	58	57.42	002	58.37		very sheltered	sheltered
6	Fair Isle	North Haven Pier	59	32.28	001	36.23		very sheltered	very exposed
7	Scalloway	Clift Sound	60	07.04	001	16.87		sheltered	sheltered
		Boat Club Pontoon	60	08.07	001	16.95		very sheltered	sheltered
8	Cromarty	Cromarty Pier	57	40.98	004	02.39		sheltered	sheltered
9	East Coast	Findon	57	03.81	002	06.25		exposed	very exposed
		Cove	57	05.74	002	04.59		exposed	very exposed
		Stonehaven Harbour	56	57.61	002	12.01		exposed	very exposed
10	Stonehaven	Offshore	56	57.81	002	06.78		very exposed	very exposed

Table 3.1 Position of Scottish Coastal Observatory monitoring sites.

Site	Physics			Chemistry						Biology				
	Temp	Sal	Sec	DIP	DSi	TOxN	Amm	TA	DIC	$Phyto_{tox}$	Phyto	Al_{tox}	Chl	Zoo
1 Millport	1997									2005-2013	2005-2013			
2 Mallaig	1999													
3 Loch Maddy	2003	2003-2011		2003-2011	2003-2011	2003-2011	2003-2011			2003-2011	2003-2011			
4 Loch Ewe	1999	2003	2008	2003	2003	2003	2003			1999	2001	2005-2016	2002	2002
5 Scapa	1999	1999		1999	1999	1999				1997	2000	2011-2016		
6 Fair Isle	1997 (2000-2003 missing)													
7 Scalloway	2000	2000		2000	2000	2000	2000			2000	2001	2011-2016		
8 Cromarty	2004													
9 East Coast	1997													
10 Stonehaven	1997	1997	2002	1997	1997	1997	1997	2008	2008	1997	1997		1997	1999

Table 3.2 Details of parameters measured at the 10 coastal monitoring sites. First data indicate start date of monitoring. Finish date entered where appropriate. Parameters are: Temp – temperature; Sal – salinity; Sec – secchi disk; DIP - dissolved inorganic phosphorus; DSi – dissolved inorganic silicate; TOx - total oxidised nitrogen; Amm – ammonia; TA- total alkalinity; DIC - dissolved inorganic carbon; Al_{tox} – dissolved algal toxins; Phyto –total diatoms and dinoflagellates; $Phyto_{tox}$ – toxic phytoplankton; Chl - chlorophyll 'a'; Zoo – Zooplankton.

3.1 Millport

The monitoring station at Millport is situated on the Isle of Cumbrae in the Firth of Clyde. Most of the coastline of Millport is sheltered but its position within the Firth of Clyde makes it exposed at the south and south-west only. The minilogger is deployed at Keppel Pier which extends into the north-south oriented Fairlie channel between Millport Island and the mainland. The Keppel Pier site is a sheltered location in a sheltered coastline.

Data collection at the Millport station was started by the Scottish Marine Biological Association in 1953,although records exist from as early as 1909, and sea surface temperature measurements were collected at weekly intervals using a bucket thermometer. The contribution of Dr Peter Barnett, originally based at the Millport Marine Biological Station, for the initial collections and his continued assistance with the minilogger deployments is gratefully acknowledged.

MSS adopted the station and started collecting temperature data in 2003. From this point data collection was automated using temperature loggers. The minilogger is deployed on a surface-following buoy, so data are recorded at a fixed depth (approximately 15 cm) below sea surface.

Phytoplankton samples were collected between October 2005 and October 2013 from Fairlie Channel and the sampling site is approximately 35 m in depth. When weather was rough these samples were collected from Keppel Pier. An integrated tube sampler is used to collect samples for phytoplankton community analysis. Samples were collected by staff at the University Marine Biological Station Millport between 2005 and 2013 and their input into the success of this programme is gratefully acknowledged.

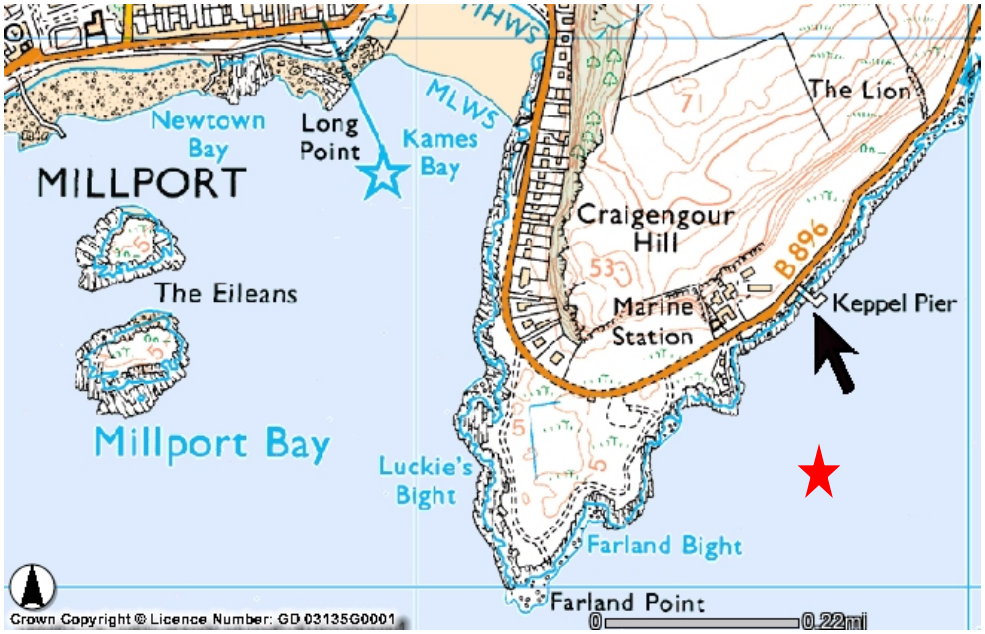

Figure 3.2 Position of Minilogger at Keppel Pier (55° 44.97' N, 004° 54.33' W), black arrow indicates minilogger position, red star indicates sampling position further offshore in Fairlie channel.

3.2 Mallaig

Mallaig harbour lies on the mainland of Scotland. Although this is a site on the west coast of Scotland and thus relatively exposed to the North Atlantic, the harbour of Mallaig lies in the lee of the Island of Skye which is north-west of Mallaig. The smaller offshore islands of Eig and Rhum also afford some protection to this coastline.

Mallaig was set up as a temperature monitoring site in 1999. In 2003 after some data losses, the minilogger was removed from its original position and a more secure site was established close to the fishery pier. Whilst the minilogger is in a sheltered site within the harbour, the coastline outside the harbour is exposed. The minilogger recorder is deployed at a fixed datum point (approximately 0.5 m below chart datum) within a metal pipe attached to the pier.

Figure 3.3 Position of Minilogger at Mallaig harbour (57° 00.40' N, 005° 49.50' W), West Coast Scotland.

3.3 Loch Maddy

Loch Maddy is located on the Island of North Uist, part of the Western Isles. Although the Western Isles are exposed to the North Atlantic, the site of Loch Maddy, on the eastern coast is generally very sheltered. Although named Loch Maddy, this site is not defined as a 'loch' in the sense of having limited exchange with the ocean (Edwards and Sharples, 1986). It is, however, a unique site with a diverse saline lagoon system opening into the main bay area, which contains a mix of rocky reefs and soft sediment habitats.

This system supports a rich diversity of marine life and as a result it has been designated a marine special area of conservation (SAC). The water sampling site is at one of the most exposed positions within the sheltered bay.

Loch Maddy was established as a monitoring site in 2003 however salinity, nutrient and phytoplankton sampling ceased in 2011. Samples have been collected by Comann na Mara and Loch Duart Salmon and their input into the success of this programme is gratefully acknowledged.

Water sampling at this site was done from a small boat at a site close to the island of Hamarsay (Figure 3.4). The minilogger recorder was suspended on the sheltered side of the concrete, at the end of the pier at a depth of around 5 metres (0.5 m from the sea bed). This pier is a very sheltered site and is used by the passenger ferry that runs from North Uist to the mainland. In 2004 the minilogger was moved to beneath a buoy closer to the water sampling site, but was lost from this location so the position at the end of the pier was resumed.

Conditions in Loch Maddy can be expected to reflect those in the bays and channels of the inshore side of the Hebrides archipelago.

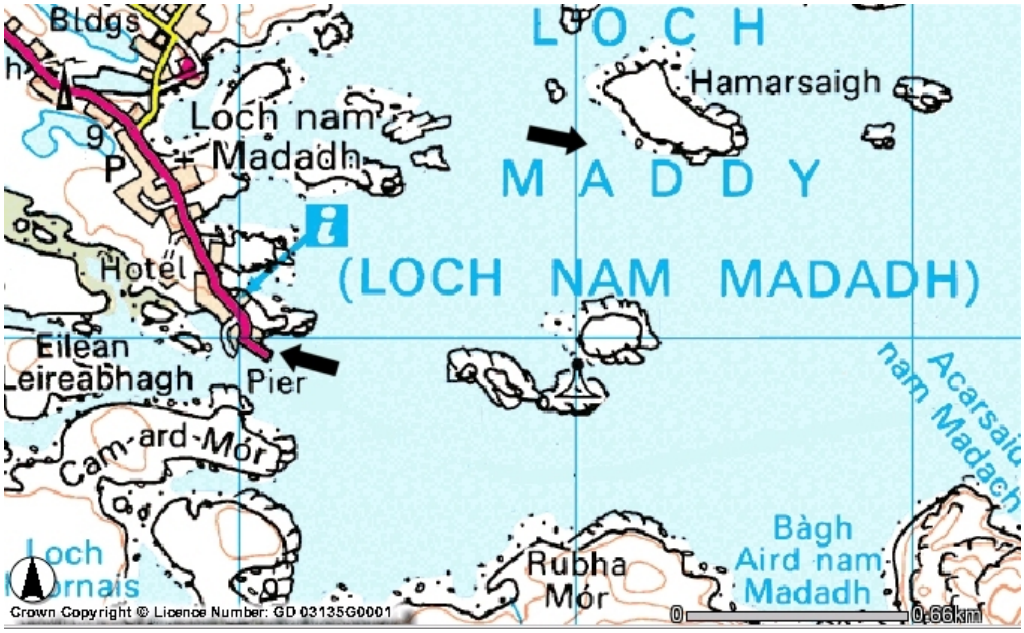

Figure 3.4 Position of Minilogger at Loch Maddy, West Coast Scotland. The lowermost arrow indicates the minilogger position (57° 35.77' N, 007° 09.34' W) at the Pier and the uppermost arrow indicates the water/phytoplankton sampling site (57° 36.09' N, 007° 08.48' W).

3.4 Loch Ewe

Multiple parameters have been measured at Loch Ewe since 2000, however, temperature measurements have been recorded since 1999. This site acts as a reference site to fulfil the requirements of the EU Water Framework Directive and the EU Marine Strategy Framework Directive. The input of Jane and Willie Grant into the success of the monitoring programme is gratefully acknowledged.

Loch Ewe is a sea loch on the west coast of Scotland. The loch has a narrow entrance and is sheltered from the worst of Atlantic storms by the Hebrides Island chain, however, the coastline outside of Loch Ewe is exposed in a northward direction to the North Atlantic. Loch Ewe has a volume of 945 $x10^6$ m^3 making it one

of the larger sea lochs in Scotland by volume. It is relatively shallow for a Scottish sea loch and has a round shape, only 11 km long, giving it a low aspect ratio (length to width). The loch faces north and has variable exchange with the North Minch, which is influenced by influxes of Atlantic water. There is some riverine influence with 9% of the flow in the loch coming from freshwater (Edwards and Sharples, 1986).

The Loch Ewe monitoring site is 40 m in depth and located in the outer basin of the loch, which has a maximum depth of 62 m and a sill depth of 33 m. As the water sampling site is close to the northerly opening of the sea loch, this is an exposed site. Since April 2002 temperature, salinity, nutrients, phytoplankton and zooplankton have been sampled weekly from a small boat near the mouth of the loch, initially operated by MSS staff and latterly by Isle of Ewe Shellfish.

The minilogger is positioned further into the loch at a sheltered site, attached to a mooring. Due to its position in the loch, the minilogger site is likely to be influenced more by fresh water flowing into the loch. During the winter this water is colder than the surrounding loch water and during the summer this water is warmer than the surrounding loch water. The SPATT bag for algal toxin analysis is located at this site and phytoplankton samples before 2002 were also collected here.

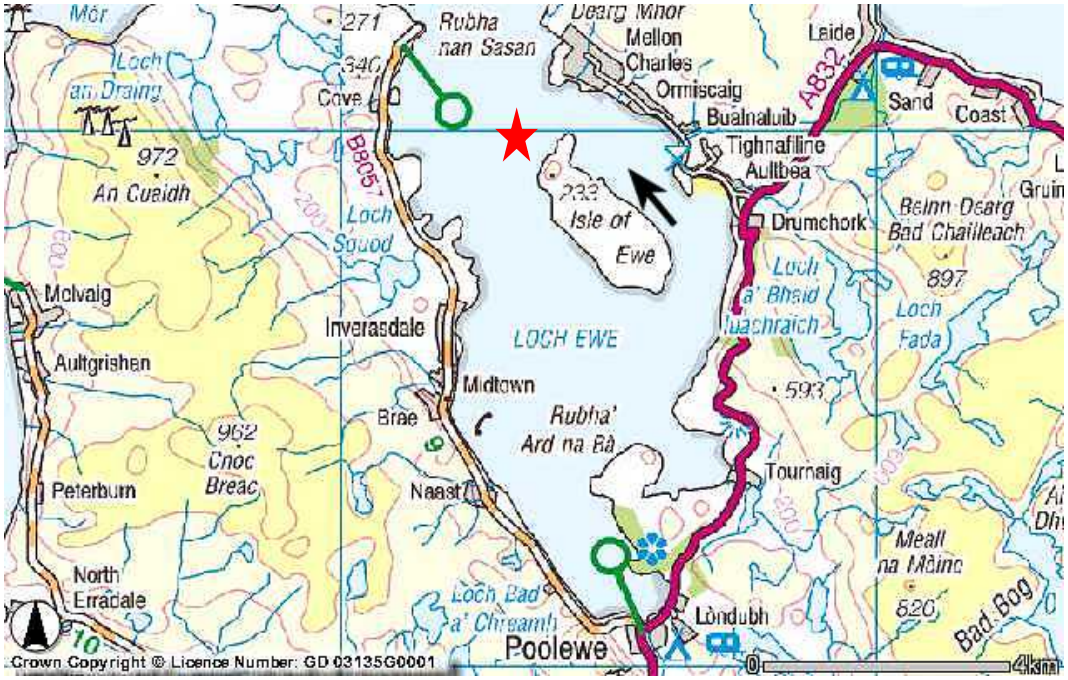

Figure 3.5 Position of Sampling Station at Loch Ewe, West Coast Scotland. The black arrow indicates minilogger position (57° 50.14'N, 005° 36.61'W), the red star indicates the water/plankton sampling position (57° 50.99'N, 005° 38.97'W). .

3.5 Scapa Bay

The Orkney Isles are an archipelago of up to 70 islands which lie just over 50 miles north of the Scottish mainland. They are separated from the UK mainland by the Pentland Firth, a tidally dynamic area where the waters of the Atlantic meet the waters of the North Sea. Compared to the outer coastline of Orkney Islands, Scapa Flow is a very sheltered region in a central position, surrounded by the islands and protected from exchange with the open seas by the Churchill barriers. Scapa Bay, in the north east of Scapa Flow is a very sheltered site in a sheltered coastline.

Multiple parameters have been measured at the Scapa Bay site, in Orkney since 2001, whilst toxin producing phytoplankton have been sampled since 1997, temperature measurements have been recorded at Scapa Pier since 1999. The minilogger recorder is suspended from the pier at a fixed datum, a depth of 1 m below the level of the lowest tide. Samples are collected by Orkney Islands Council Marine Services and their input into the success of this programme is gratefully acknowledged.

Prior to 2003 phytoplankton samples were taken from the centre of Scapa Bay. Since 2003 these samples have been taken from Scapa pier.

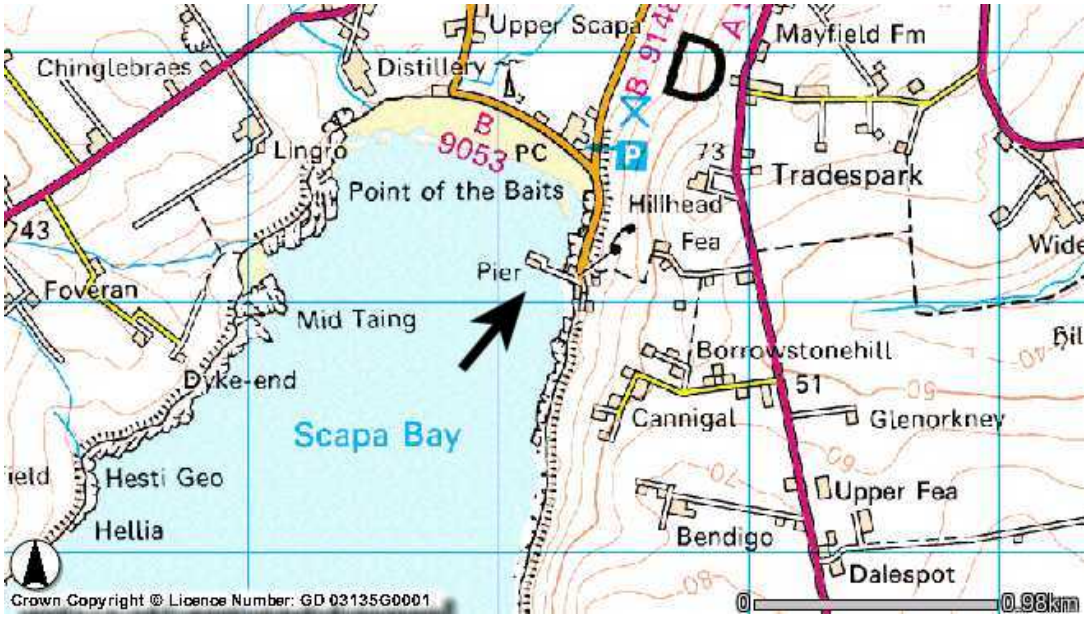

Figure 3.6 Position of Sampling Station at Scapa Bay (58° 57.42' N, 2° 58.37' W), Orkney, Scotland. The black arrow indicates the pier from which all samples are taken.

3.6 Fair Isle

Temperature data from the Fair Isle site dates back to 1979, when Dave Wheeler, a local resident and meteorologist, collected daily data using a bucket thermometer until 2000. The Fair Isle site was adopted by MSS in 2003 and after this time data collection was automated using a minilogger recorder.

Fair Isle is an island lying half-way between the Orkney Islands and Shetland, exposed to the influences of the surrounding seas. Atlantic water enters the northern

North Sea through the Fair Isle gap and this site is therefore very exposed to the influence of saline Atlantic Water. The minilogger at Fair Isle is deployed from a harbour pier. This pier is in a very sheltered position on the island, but this offers only localised protection as the rest of the island is very exposed.

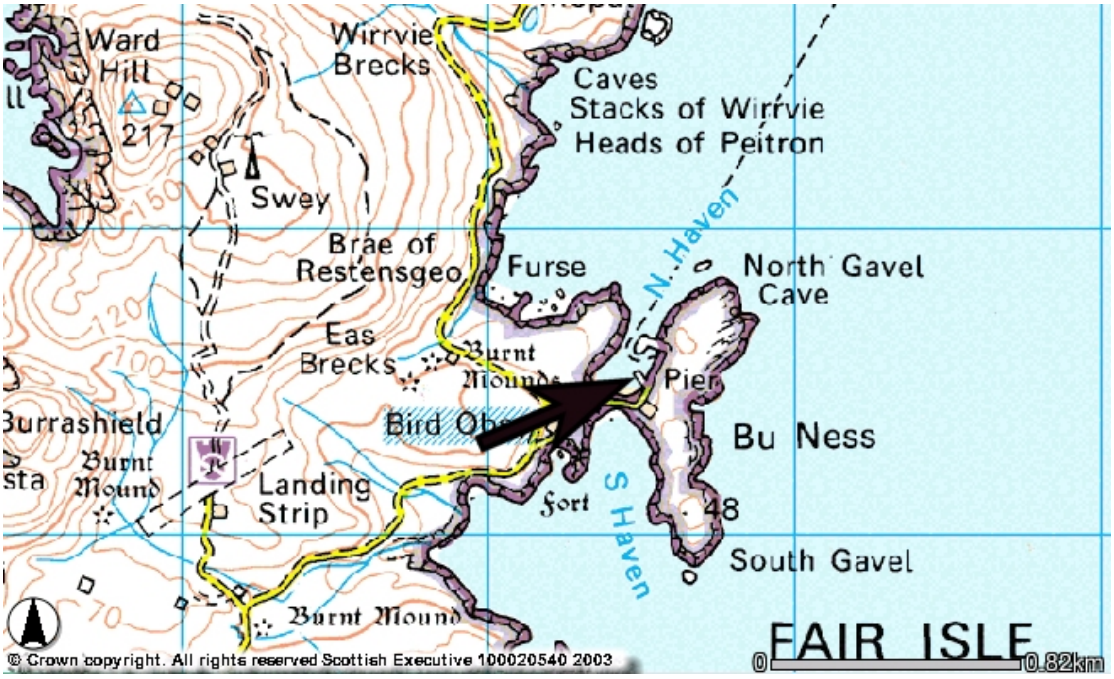

Figure 3.7 Position of minilogger at North Haven pier, Fair Isle, Scotland. Scapa Bay (59° 32.25'N, 001° 36.25'W). The black arrow indicates the pier from which the minilogger is suspended.

3.7 Scalloway

Scalloway in the Shetland Isles has been part of this monitoring programme since 2002, although temperature monitoring began prior to this in 1999 and toxic phytoplankton monitoring in 2000. Samples are collected by the North Atlantic Fisheries College (http://www.nafc.ac.uk) and their input into the success of this programme is gratefully acknowledged.

The Shetland Isles lie over 100 miles north of the UK mainland. Atlantic water from west of the UK enters the North Sea between the Orkney and Shetland Islands and around north east of Shetland through the Norwegian trench. Scalloway is a harbour on the south west coast of the Shetland mainland, sheltered from the North Atlantic by a number of small islands.

At the start of the measurement period, a minilogger was first deployed in Clift Sound at position, 60° 07.04' N, 001° 16.87' W, near Scalloway in December 1999. In December 2001 the recorder was moved to a different site in Scalloway which was easier to service. The minilogger recorder is suspended at 2 m below the sea surface under a floating pontoon at Scalloway boat club so this is never at risk of exposure to the air. The exact position of the site has changed slightly over the years due to a collapse of the original boat club pontoon, which also resulted in a gap in the data. The water samples are taken from the same boat club pontoon,

which is at a location with less than 10 m water depth and is a very sheltered location on a sheltered part of the coastline.

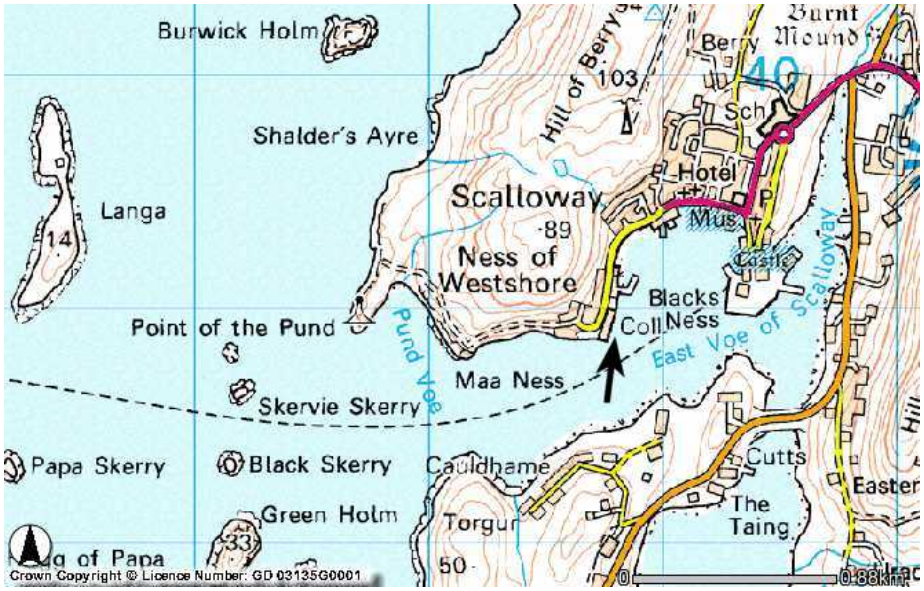

Figure 3.8 Position of Minilogger and sampling site in Scalloway Bay (60° 08.07'N, 01° 17.08'W), Shetland, Scotland.

3.8 Cromarty

Cromarty harbour is located on the north east coast of Scotland, it is situated within the narrow entrance that separates the Cromarty Firth with the North Sea. As it sits within the entrance this site is a sheltered spot in a sheltered coastline.

Although the recorder is within the shelter of Cromarty Firth, it is deployed on the outside wall of the harbour and subject to strong tidal flows of water. The minilogger recorder is deployed below Cromarty pier fixed at a depth of approximately 1 m above the seabed. Temperature measurements have been recorded at Cromarty since 2003.

Figure 3.9 Position of Minilogger in the mouth of Cromarty Firth (57° 40.98'N, 004° 02.39'W), East Coast Scotland.

3.9 East Coast (Findon, Cove Bay, Stonehaven)

On the east coast of Scotland temperature measurements have been made at a number of sites relatively close to one another. Temperature measurements were made at a coastal site at Findon (57°03'48.6"N, 2°06'14.8"W) from 1996 to 2009. The Findon site was in an exposed location in a small inlet on the east coast of Scotland, approximately seven miles south of Aberdeen, subjected to the North Sea conditions.

Due to logistical reasons the Findon site was re-located to Cove Bay (57°05'44.5"N, 002°04'35.2"W), three miles north of Findon, where temperature measurements were collected between 2008 and 2015. However, data suggested that the instrument became dry at certain times, so in 2015 the Minilogger recorder was relocated to a site at Stonehaven harbour (56°57'36.5"N, 002°12'00.8"W).

Like Stonehaven (see section 3.10), all of these sites are very exposed, particularly to the east, with the only shelter occurring from the lee of the coastline.

3.10 Stonehaven

The Stonehaven monitoring site is on the east coast of Scotland (Figure 3.10), approximately eight miles to the south of Aberdeen, and has been an active monitoring site since 1997. This site fulfils the monitoring requirements of EU Water Framework Directive and EU Marine Strategy Framework Directive.

The Stonehaven monitoring site is 50 m in depth and located 5 km offshore. The coastline in this region is relatively straight and the whole area is very exposed to the North Sea. At the site tidal stirring mixes the water column, but stratification due to freshwater run-off and the seasonal heating/cooling cycle can also occur at times.

Since 2000, water column profiles using CTDs were made, in addition to the water samples collected from the site, using the RV Temora (Figure 3.11). In addition, in 2015 the minilogger from Findon/Cove bay was deployed to a site in Stonehaven harbour (See section 3.9 above).

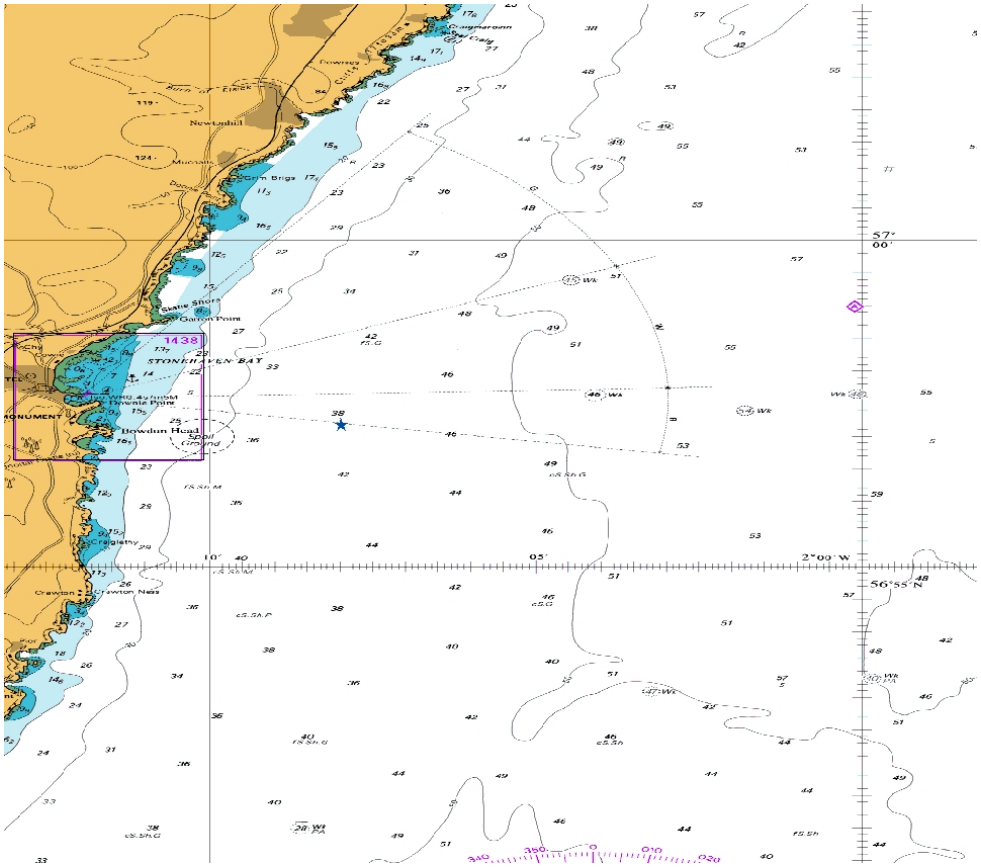

Figure 3.10 The Stonehaven ecosystem monitoring site (56°57.8' N 002°06.2' W), east coast Scotland (red star). The black arrow indicates the position of the new minilogger site at Stonehaven harbour.

3.11 Summary - Site Descriptions

- Full descriptions of each of the ten monitoring sites which make up the Scottish Coastal Observatory are presented.
- These document the location, physical conditions, exposure and sampling history of each site.
- A full range of physical, chemical and biological parameters are monitored at two of the sites; Stonehaven on the east coast and Loch Ewe on the west coast.
- At the other sites, different combinations of physical, chemical and biological parameters are monitored.
- The station with the longest, continuous and most complete data set is Stonehaven, where data collection started in 1997.
- Other start dates vary between 1999 and 2005.
- Some parameters and sites have ceased operation for operational and resource reasons. These data continue to offer useful insights into seasonality and variability.

3.12 References – Site Descriptions

Burrows, M.T., Harvey, R., Robb, L. (2008) Wave exposure indices from digital coastlines and the prediction of rocky shore community structure. Marine Ecology Progress Series, 353, 1–12, doi: 10.3354/meps07284.

Edwards, F., Sharples, F. (1986) Scottish sea lochs: a catalogue. Scottish Marine Biological Association; 1986.

Hill, A. (1998) Buoyancy effects in coastal and shelf seas. In K.R. Brink, The Sea, Volume 10: The Global Coastal Ocean: Processes and Methods (pp. 21-62). Harvard University Press.

Figure 3.11 Upper: The Stella, a small boat used for sampling at Stonehaven between 1997 and 2003 Lower: The catamaran Temora tied up in Stonehaven harbour. This vessel has been used for sampling at the Stonehaven monitoring site since 2003.

4. Context Setting - Physical Conditions

Data from external sources was summarised to support the environmental data collected as part of the Scottish Coastal Observatory.

4.1 Meteorology

Data Sources

Meteorological data were obtained from the historic climate datasets from eight different sites (Figure 4.1, Table 4.1) prepared by the UK Meteorological Office and downloaded via their website[1]. The data have been collected from long running synoptic stations around Scotland and the data have been quality controlled and processed by the UK Meteorological Office.

The data provided by UK Meteorological Office were as follows: monthly averages of daily maximum and minimum air temperature, and mean air temperature recorded over the period 0900-0900 UTC. Days of air frost, total daily rainfall and total sunshine duration (sun). Values for mean temperature were calculated from the average of the mean daily maximum and mean daily minimum temperature i.e. (tmax+tmin)/2.

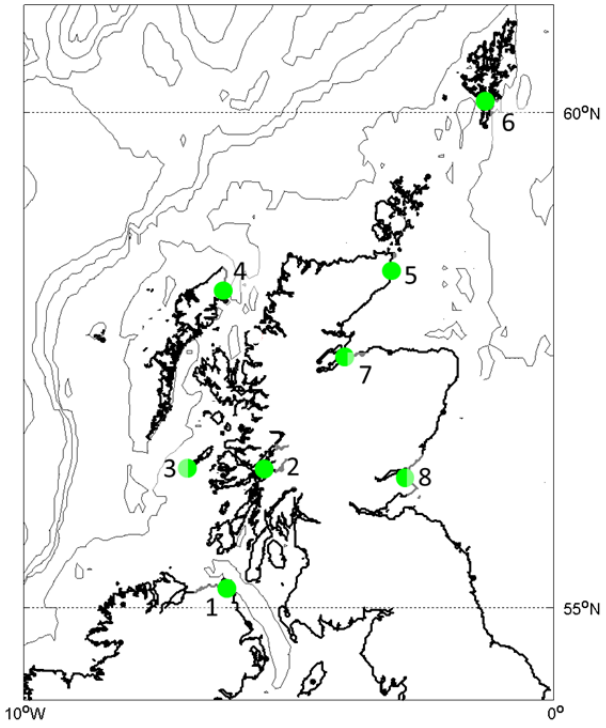

Figure 4.1 Position of eight meteorological data sites from which air temperature, (max and min), days of frost, rainfall and sunshine have been recorded. Key: 1) Ballypatrick, 2) Dunstaffnage, 3) Tiree, 4) Stornoway, 5) Wick Airport, 6) Lerwick Airport, 7) Nairn, 8) Leuchars.

[1] http://www.metoffice.gov.uk/public/weather/climate-historic

Table 4.1 Details of Meteorological Stations

Station Name	Start Date	Latitude	Longitude	Height (amsl)	Kipp and Zonen[2]
Ballypatrick	1961	55.181	-6.153	156 m	Jun 2009 only
Dunstaffnage	1971	56.451	-5.439	3 m	Jun 2009 only
Tiree	1928	56.500	-6.880	12 m	Sep 2001 onwards
Stornoway	1873	58.214	-6.318	15 m	Sep 2002 onwards
Lerwick	1930	60.139	-1.183	82 m	Jun 2008 onwards
Wick Airport	1914	58.454	-3.088	36 m	-
Nairn	1931[3]	57.593	-3.821	8m[4]/23 m	-
Leuchars	1957	56.377	-2.861	10 m	Sep 2005 onwards

Data Quality Control and Processing

Data from all stations were processed and formatted into a standard data format.. The standard quality flags applied to all internal data (See Appendix D, Part 3 of this report) were incorporated into these files. As the data have already been quality controlled by the UK Meteorological Office, all data were given the Quality Flag '1'. Missing data (when there were more than two days missing in a month) were marked as 'QF 9'. Where estimated data have been provided, these have been marked as 'QF 8' in the raw data file, these data have been incorporated into the analysis without further consideration.

Sunshine data were mainly recorded by a Campbell-Stokes recorder. In more recent years the automated Kipp and Zonen photosensitive detectors have been used at some sites. Comparison of the two types of sensor has shown the newer automated sensors to be an improvement on the Campbell-Stokes recorder (Kerr and Tabony, 2004; Legg, 2014) which is read manually, often requires subjective analysis to remove artefacts in the data and tends to overestimate sunshine hours in summer. In this analysis, data from either sensor have been treated in exactly the same way, with no distinction or correction in the data analysis. No allowances have been made for small site changes or other changes in instrumentation, although these have been noted in Table 4.1 and in the figure legends where appropriate.

Data Analysis

Data have been analysed to examine the typical variability and the long and short term trends. All data have been treated in the same manner using methodology from the time series analysis toolbox (TTA) (R core team (2013), Devreker and Lefebve (2015)). Figures from every parameter and site included in Table 4.1 are presented as supplementary figures in Appendix E, in Part 3 of this report.

[2] Periods in which an automated Kipp and Zonen sunshine recorder was used, all other records are from a Campbell-Stokes sunshine recorder.

[3] Site changed in 1998 and station height increased

[4] Prior to 1998

Long Term Trend

When considering the conditions observed in the measurement period (1997-2013), it is important to examine the data in the context of the long term trend. Time series of both global and more local air temperatures demonstrate that the measurement period was exceptionally warm. Examining the global average air temperature record up until the end of 2013, for example CRUTEM[5] (Jones et al., 2012), the ten warmest years in the record (which started in 1850) all occurred during the period covered by this dataset. In descending order these years are 2007, 2010, 2005, 1998, 1999, 2013, 2003, 2012, 2002, 2009, with the warmest year being 2007[6].

In the UK the Central England Temperature (CET) (Parker et al., 1992) is the longest air temperature time series representing a region of the southern UK between Bristol, Lancashire and London. For this dataset, records began in 1659. Examining the Central England Temperature[7] annual mean air temperature time series up to and including the year 2013, shows that the warmest year on record was 2006, and the years 2011,1999, 1997 and 2003 all feature in the top ten warmest years on record. As the CET time series extends back as far as 1659, this observation adds to the evidence that the observations presented in this report were made at a time of unusually warm temperatures.

Trends and Variability 1997-2013

Examining the data from eight meteorological stations (Figure 4.1) around Scotland, at all stations there appears to be a similar pattern in the annual mean. Compared to a decadal average (2001-2010) temperatures were cooler than normal in the years 1998 to 2001, warmer than normal between 2002 and 2007, and then in the period 2008 to 2013 temperatures once again cooled to below average. Annual mean air temperatures in 2003 were particularly high in the north and east of Scotland, specifically Nairn, Wick and Lerwick (Figure 4.2), and this was the warmest year, on average, during the measurement period (1997-2013). Annual mean air temperatures were particularly low at all stations in 2010.

Although 2003 was the warmest year overall, the maximum monthly temperature anomaly was measured in February 1998 at Ballypatrick, Dunstaffnage, Nairn and Leuchars. Minimum monthly temperature anomalies were observed in December 2010 at all stations; on the west coast in Dunstaffnage the minimum monthly average temperature of 1.05°C was measured, 3.86°C lower than average, and on the East coast, Leuchars had a minimum monthly average temperature of -0.9°C, 4.28°C lower than average.

The conditions observed at these Scottish stations are typical of the pattern observed across the UK. The year 2003 was a very warm year across the UK, however northern Scotland was the most extreme of all UK regions, annual mean air

[5] http://www.metoffice.gov.uk/hadobs/crutem4/

[6] Note that at the time of publication, warmer global air temperatures were observed in 2014 and 2015

[7] http://www.metoffice.gov.uk/hadobs/hadcet/index.html

temperatures for 2003 were 7.99°C, being 0.69°C higher than the long term average (1981-2010)[8].

The year 2010 was the twelfth-coldest year in the 100-year series and the coldest since 1986. This was a consequence of a sequence of cold winters. There was cold weather in January, February of 2010 and then again at the end of the year in late November and December - which was one of the coldest calendar months in the last 100 years[9].

Rainfall is very variable and does not show any strong trend throughout this period and there is a high degree of variability between sites as well as between years. The west coast tended to have higher rainfall than the east coast, which is the pattern that is expected for Scotland. There are large areas of western Scotland that can experience annual average rainfall of greater that 2000 mm/yr, whereas on the east coast of Scotland annual rainfall values are typically less than 1000 mm/yr (Jenkins et al, 2008).

During the measurement period (1997-2013), average annual rainfall was at its highest during 1999, although in both 1998 and in 2009 every station had higher than normal annual average anomalies. The year 2003, as well as being the warmest year, was also the driest year with lowest rainfall anomalies at all stations. The maximum monthly average rainfall of 418 mm, was measured at Dunstaffnage in December 2011, this value was 276 mm greater than normal. The most unusual rainfall event occurred in April 2000 at Nairn, when the monthly rainfall was 138 mm, more than four standard deviations higher than the average for April (35 mm).

Although sunshine and rainfall are not exactly correlated, the driest places can often be the sunniest. The patterns of sunshine across Scotland are, therefore, broadly opposite to those of rainfall. Sites along the east coast of Scotland, can typically expect twice as many sunshine hours as those on the west coast[10]. Sunshine hours also tend to be highest in May at all stations across Scotland[11]. Not all of the meteorological stations had sunshine recorders in operation during the measurement period, so there are more limited data than the other parameters. Like rainfall, sunshine hours are very variable throughout the time period, with no obvious trend and with marked differences between stations.

The sunniest year overall though, was 2003, with the station at Stornoway and Nairn the sunniest stations. Higher than average sunshine anomalies were particularly apparent between 1997 and 2001. During the measurement period the station with highest monthly sunshine hours was Tiree, with 313 hours recorded in May 2000. In January 2001, Stornoway was unusually sunny, with the monthly sunshine hours of 78, being almost four standard deviations above normal.

Frost days only occur at the start and the end of the year, there are usually no days of frost expected from June to September. The frostiest year was 2010 across most

[8] http://www.metoffice.gov.uk/climate/uk/summaries/2003/annual/regional-values [anomalies have been recalculated relative to 1981-2010 values]
[9] http://www.metoffice.gov.uk/climate/uk/summaries/2010/annual
[10] http://www.metoffice.gov.uk/public/weather/climate
[11] http://www.metoffice.gov.uk/climate/uk/regional-climates

stations, with the least frost occurring in 2007 and 2011. The general trend seen in air temperatures is also reflected in the frost readings with the period 2002-2007 having fewer frosty days than the period either before or after. The maximum monthly frost measured was 26 days in December 2010 at Leuchars, 12 days longer than the average.

4.2 Summary – Meteorology

- Monthly mean values of air temperature, days of frost, sunshine hours and rainfall are presented for eight stations around Scotland.
- The meteorological data sets cover the full observation period (1997-2013) with few gaps, and allow robust seasonal cycles to be described.
- The period 2003-2006 was a consistently warm period, with cooler air temperatures before 2003 and more variable air temperatures after 2006.
- The year 2003 had the lowest average rainfall across all sites. This year was also particularly sunny in the north and east of Scotland and was, on average, the warmest year of the measurement period.
- The year 2010 was very cold, with highest frost and lowest temperatures of the record at all sites. Both the early part of 2010 (January, February) and the latter part of the year (November, December) were very cold.
- The year 2013 also had very low rainfall in north and east of Scotland.

4.3 Plots - Meteorology

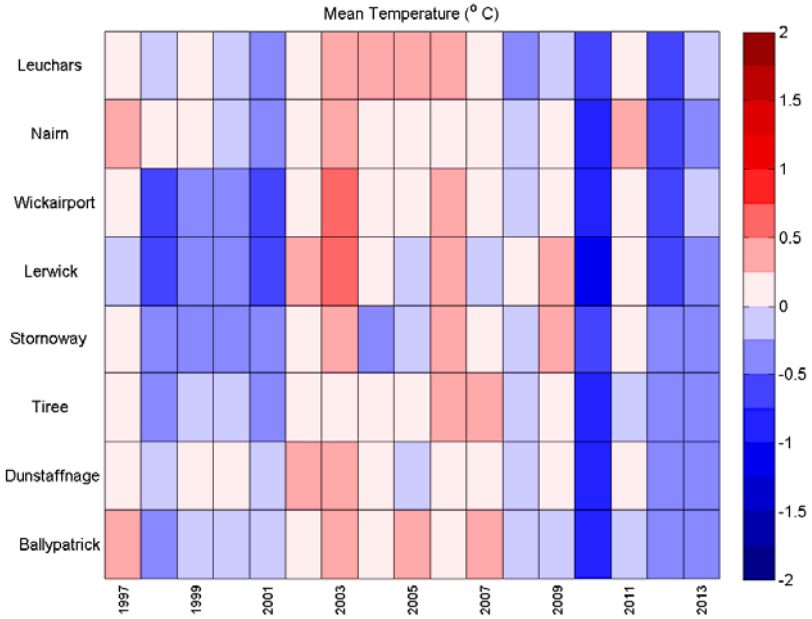

Figure 4.2 Annual mean anomalies of mean air temperature at eight sites around Scotland. The anomalies are normalized with respect to the standard deviation (sd) (e.g. a value of +2 indicates 2 sd above normal). Anomalies are with respect to base period 2001-2010. Base period Colour intervals 0.25 sd; reds = positive/warm, blues = negative/cool. See Figure 4.1 for a map showing the locations of the meteorological stations in this figure.

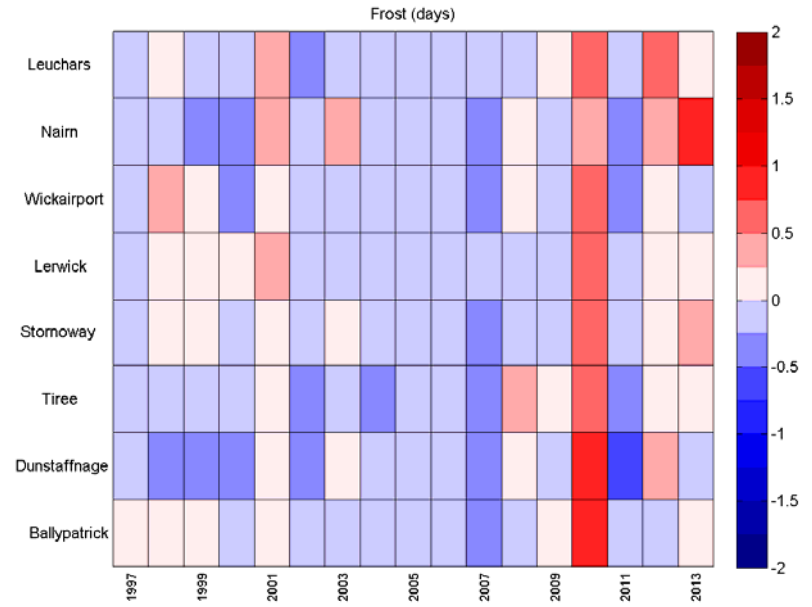

Figure 4.3 Annual mean anomalies of mean number of days of frost at eight sites around Scotland. The anomalies are normalized with respect to the standard deviation (sd) (e.g. a value of +2 indicates 2 sd above normal). Anomalies are with respect to base period 2001-2010.Colour intervals 0.25 sd; reds = positive/more days, blues = negative/less days. See Figure 4.1 for a map showing the locations of the meteorological stations in this figure.

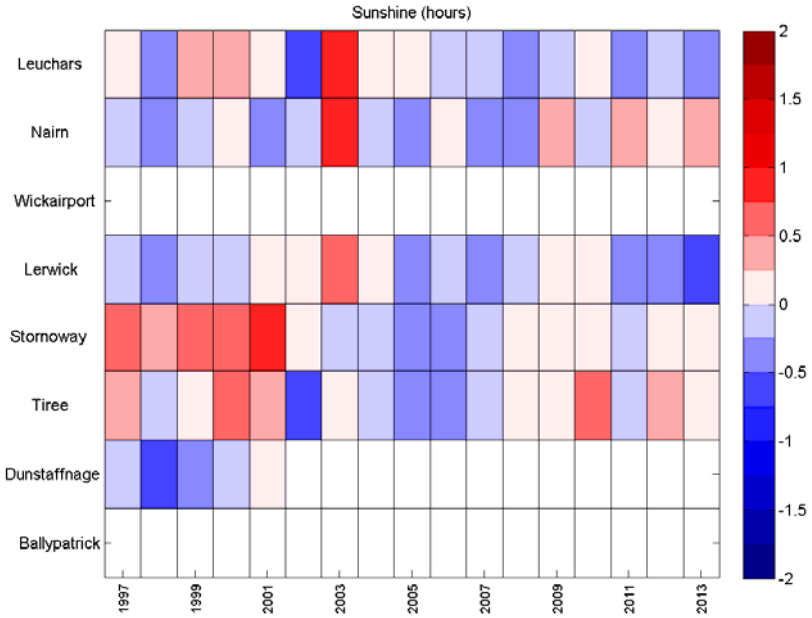

Figure 4.4 Annual mean anomalies of mean number of sunshine hours at eight sites around Scotland. The anomalies are normalized with respect to the standard deviation (sd) (e.g. a value of +2 indicates 2 sd above normal). Anomalies are with respect to base period 2001-2010.Colour intervals 0.25 sd; reds = positive/sunnier, blues = negative/less sunny. White boxes indicate no data available for analysis. See Figure 4.1 for a map showing the locations of the meteorological stations in this figure. Note Ballypatrick and Wick Airport did not report sunshine hours.

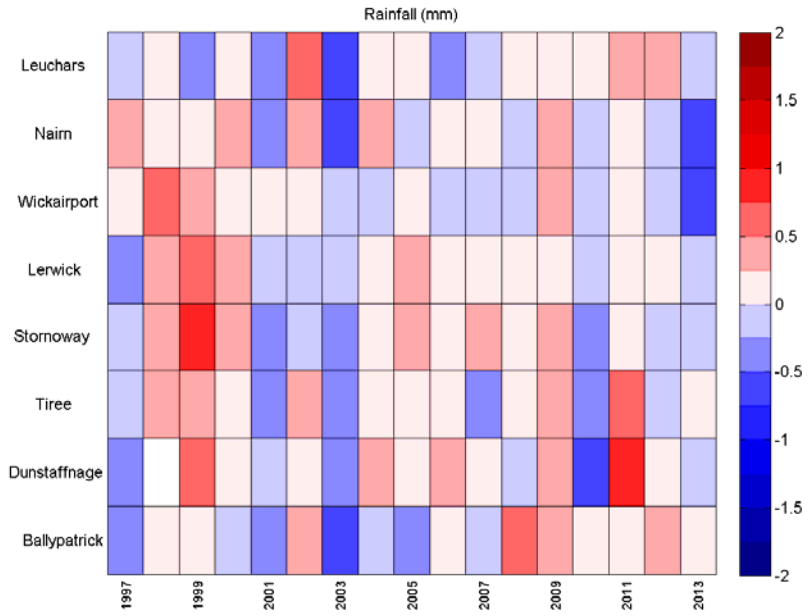

Figure 4.5 Annual mean anomalies of average rainfall at eight sites around Scotland. The anomalies are normalized with respect to the standard deviation (sd) (e.g. a value of +2 indicates 2 sd above normal). Anomalies are with respect to base period 2001-2010.Colour intervals 0.25 sd; reds = positive/sunnier, blues = negative/less sunny. White boxes indicate no data available for analysis. See Figure 4.1 for a map showing the locations of the meteorological stations in this figure.

4.4 River Flow

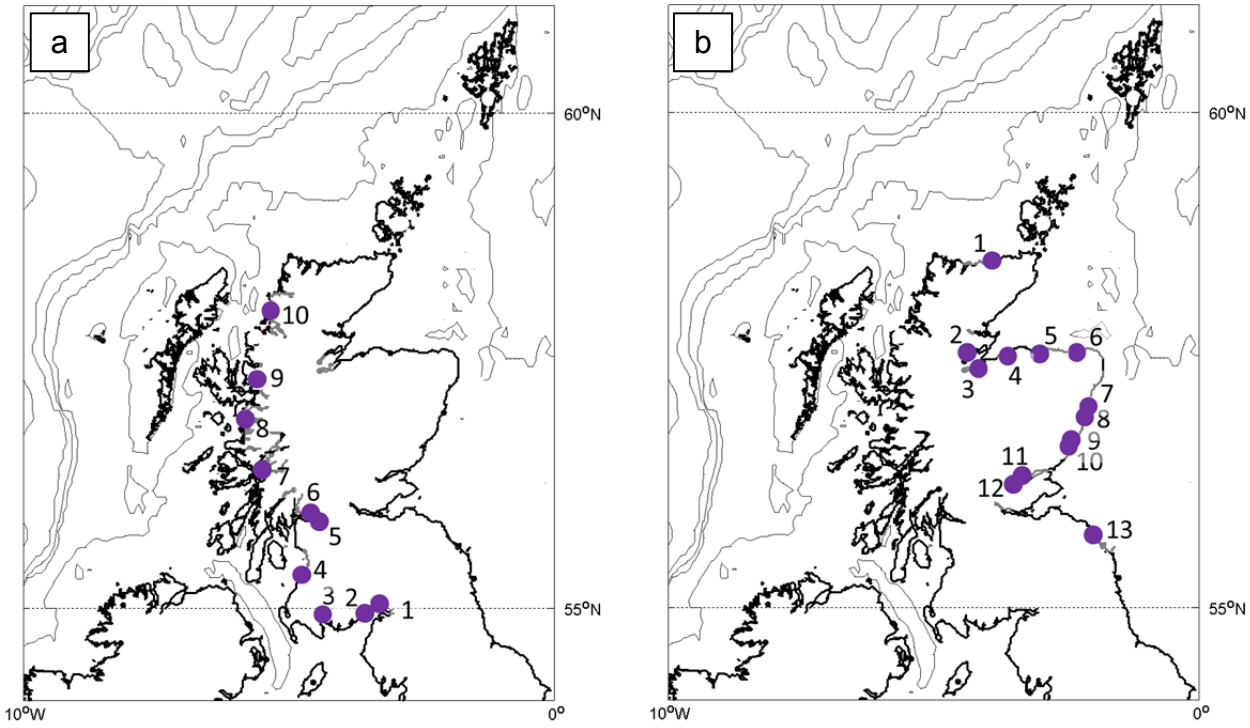

Figure 4.6 River Data monitoring sites for a) West Coast Flow (10 rivers): 1) Annan, 2) Nith) 3) Cree, 4) Ayr 5) Clyde, 6) Leven (Loch Lomond), 7) Orchy (Loch Etive), 8) Shiel, 9) Carron, 10) Ewe; and b) East Coast Flow (13 rivers): 1) Naver, 2) Conon, 3) Ness, 4) Findhorn, 5) Spey, 6) Deveron, 7) Don, 8) Dee, 9) North Esk, 10) South Esk 11) Earn, 12) Tay and 13) Tweed.

Data Source

Variability in river flow was derived by combining data from a number of gauged (measured) rivers across Scotland. The rivers were selected to give reasonable spatial coverage and to capture the largest and therefore most representative river flows. The location of these rivers can be seen in Figure 4.6. The river gauging network is maintained by the Scottish Environment Protection Agency (SEPA) and the original data files were downloaded from the National River Flow Archive (NRFA) via their website[12]. Some gauged data on the NRFA is not freely available for public download. Due to the restrictions in obtaining these data, these data have not been used and the data from the station is treated as if it had not been gauged. Gauged stations with flows of less than $10 m^3 s^{-1}$ were ignored in the analysis.

Climatological averages of total river flow across the whole of Scotland for the period 2007-2010 and 1961-2012 were obtained from a Grid 2 Grid (G2G) modelled dataset (Cole et al., 2014). This model uses data from rainfall across Scotland combined with information about shape of river catchments and knowledge of land runoff. The model was developed by Centre for Ecology and Hydrology, and has been tuned and tested against the gauged river flows.

[12] http://www.ceh.ac.uk/data/nrfa/data/search.html

The modelled data is used in this report to give estimates of what percentage of the total freshwater inflow to Scottish coastal waters is covered by the gauged rivers whose data is presented here.

Data Quality Control and Processing

Daily gauged river flow values ($m^3 s^{-1}$) were averaged to calculate monthly mean river flow at each river gauging station. Monthly average data values were only calculated if there was gauged flow available for every day in that particular month. The total monthly gauged river flow on the east and west coasts of Scotland was calculated using the sum of monthly values from each river. A dividing point on the North Coast of Scotland (4°6'W) was used to divide these two regions.

Gauged river flow provides one estimate of freshwater input into the coastal zone. However, a large proportion of total freshwater flow into Scottish waters is not gauged. This proportion is more significant on the west coast of Scotland than on the east coast and is partly due to the remote nature of the region and the distribution of the freshwater discharge across a greater number of smaller rivers.

Tables 4.2 and 4.3 summarise the key statistics for river flow on the east and west coast. Each table lists the largest points of freshwater discharge on each coast – determined using climatological averages from the G2G model for the period 1961-2012. Each of these rivers has an average monthly mean flow of greater than 13 $m^3 s^{-1}$ and these are referred to as the 'major' rivers in the following text.

River Network

Although rainfall over Scotland is one of the highest in Europe (Cole et al., 2014) the freshwater inputs to the coastal zone tend to be distributed across many small discharge points rather than in large single rivers. Scotland has a network of more than 125,000 km of rivers. The River Tay is Scotland's largest river and has an annual average discharge of ~170$m^3 s^{-1}$. In comparison, the Rhine has a discharge of 2,900 $m^3 s^{-1}$.

Around 32 (of ~508) rivers on mainland Scotland have a mean flow >15 $m^3 s^{-1}$ (calculated from G2G, period 1961-2012). Modelled averages of freshwater flow from mainland Scotland show that input on the east and west coasts (divided by a line at 4°6'W) are very similar. Total annual flow on west coast (1191 $m^3 s^{-1}$) is similar to the east coast (1115 $m^3 s^{-1}$ – Cole et al., 2014).

Three of the major rivers on the west coast are entirely ungauged. A further three have gauging stations that cover less than 60% of the catchment, two of the gauged stations had mean flow less than 10$m^3 s^{-1}$ and three of the gauged stations have restricted access data. In total 36% of the runoff from the major rivers are gauged and included in the accompanying data set. This represents approximately 20% of the total estimated runoff in the west coast region (Table 4.2).

On the east coast the gauging of river flow is much more complete. Of the 17 rivers with annual mean flow greater than 13 $m^3 s^{-1}$, data from 12 of these rivers is freely available. These rivers also represent a much higher percentage of the total

estimated freshwater inflow, with more than 75% of the largest rivers being represented in the gauged data. The gauged flow, however, still represents only 60% of the total runoff to the coastal waters on the east coast (Table 4.3).

It is the gauged river flow (rather than the modelled flow) that is plotted in Figures 4.7 to 4.10, and included in the accompanying data set. However, we expect a high correlation between total flows and gauged flows. In a similar analysis, Marsh et al., (2015) showed that, taken over the whole of Scotland, there was a correlation of 0.993 between gauged and modelled river flow. All of the index rivers selected in their analysis are included here with the exception of the Firth of Forth as it was not freely available for download.

Table 4.2 Major rivers discharging into coastal waters on the West Coast of Scotland.

River/Discharge Point	Position						G2G Mean Flow (m^3s^{-1})	Catchment Area (m^3)	% Area Gauged	Gauging Station	Gauged Flow (m^3s^{-1})	NOTES
BROOM	57	54.51	N	5	12.00	W	16.84	331	43	95002 - Broom at Inverbroom	7.25	Data not included
EWE	57	45.76	N	5	36.46	W	27.52	444	100	94001 - Ewe at Poolewe	29.64	
LOCH TORRIDON	57	32.68	N	5	41.18	W	15.11	224	0		0.00	Catchment ungauged
LOCH CARRON	57	21.53	N	5	35.07	W	16.67	247	55	93001 - Carron at New Kelso	10.70	
LOCH LONG	57	17.34	N	5	30.68	W	18.20	251	0		0.00	Catchment ungauged
LOCH SHEIL	56	46.58	N	5	49.41	W	20.22	258	100	92001 - Shiel at Shielfoot	21.07	
LOCH EIL	56	47.71	N	5	9.22	W	105.21	1,628	82	91002 - Lochy at Camisky	59.48	Data not available
LOCH LEVEN	56	41.20	N	5	10.64	W	23.48	329	0		0.00	Catchment ungauged
ORCHY	56	27.38	N	5	23.12	W	94.80	1,327	3	89003 - Orchy at Glen Orchy	22.41	
LEVEN	55	56.74	N	4	34.30	W	42.68	802	37	85001 - Leven at Linnbrane	45.17	
CLYDE	55	55.24	N	4	28.44	W	68.17	2,996	89	84005 - Clyde at Blairston	43.54	
IRVNE	55	36.13	N	4	39.62	W	15.24	477	98	83005 - Irvine at Shewalton	7.64	Data not included
AYR	55	28.07	N	4	38.12	W	12.55	583	83	83006 - Ayr at Mainholm	15.94	
CREE	54	54.91	N	4	24.71	W	18.58	468	79	81002 - Cree at Newton Stewart	15.77	
DEE (BORDERS)	54	50.46	N	4	2.95	W	41.98	969	83	80002 - Dee at Glenlochar	41.20	Data not available
NITH	55	0.05	N	3	34.36	W	43.48	1,219	85	79002 - Nith at Friars Carse	27.99	
ESK (BORDERS)	54	58.77	N	3	3.37	W	34.43	1,174	70	77001 - Esk at Netherby	26.23	Data not available
ANNAN	54	58.64	N	3	16.49	W	32.60	957	97	78003 - Annan at Brydekirk	30.60	
	Total Significant River Mean Flow						**647.78**	**Total Gauged River Mean Flow**			**233.19**	
								% of Significant flow that is gauged			**36%**	
								% of Total west coast flow that is gauged			**20%**	

Table 4.3 Major rivers discharging into coastal waters on the East Coast of Scotland.

River/Discharge Point	Position						G2G Mean Flow (m3s-1)	Catchment Area (m^3)	% Area Gauged	Gauging Station	Gauged Flow (m^3s^{-1})	NOTES
NAVER	58	31.34	N	4	13.51	W	16.26	509	92	96002 - Naver at Apigill	15.86	
HELMSDALE	58	7.06	N	3	39.40	W	13.46	571	96	2001 - Helmsdale at Kilphedir	13.26	Data not available
CARRON/SHIN	57	51.90	N	4	18.15	W	68.77	1,634	82	3005 - Shin at Inveran	4.97	Data not available
CONON	57	35.06	N	4	25.11	W	52.69	1,207	80	4001 - Conon at Moy Bridge	50.07	
BEAULY	57	29.66	N	4	25.76	W	53.48	1,008	79	5001 - Beauly at Erchless	45.63	Data not available
NESS	57	29.34	N	4	13.72	W	87.16	1,864	99	6007 - Ness at Ness-side	89.90	
FINDHORN	57	37.97	N	3	38.07	W	17.77	786	99	7002 - Findhorn at Forres	19.64	
SPEY	57	39.94	N	3	5.97	W	74.07	2,950	97	8006 - Spey at Boat o Brig	65.63	
DEVERON	57	39.62	N	2	30.77	W	19.09	1,240	78	9002 - Deveron at Muiresk	17.00	
DON	57	10.58	N	2	5.56	W	20.73	1,323	96	11001 - Don at Parkhill	21.15	
DEE	57	8.42	N	2	4.56	W	46.62	2,090	88	12002 - Dee at Park	47.29	
N ESK	56	45.20	N	2	26.10	W	17.55	772	96	13007 - North Esk at Logie Mill	19.94	
S ESK	56	41.96	N	2	27.04	W	12.63	603	81	13008 - South Esk at Brechin	12.72	Data not available
EARN	56	21.12	N	3	18.25	W	29.93	956	81	16004 - Earn at Forteviot Bridge	29.21	
TAY	56	21.66	N	3	18.27	W	175.88	5,091	94	15006 - Tay at Ballathie	170.88	
FORTH	56	5.13	N	3	46.64	W	63.25	1,632	89	18011 - Forth at Craigforth	46.86	Data not available
TWEED	55	46.49	N	2	0.57	W	101.49	5,007	98	21009 - Tweed at Norham	81.27	
Total Significant River Mean Flow (m^3s^{-1})							**870.84**	**Total Gauged River Mean Flow (m^3s^{-1})**			**657.59**	
								% of significant flow that is gauged			**59%**	
								% of Total east coast flow that is gauged			**76%**	

Seasonal and Spatial Patterns

In Scotland, only a small portion of the precipitation that falls in winter lies as snow. As a result the highest freshwater flows occur in the winter months as rain falls and runs into the rivers and then into the sea (Figures 4.7 and 4.8). This is not the case for rivers in continental Europe that tend to have maximum freshwater flow after spring (May-June) as a result of snow melting in the high mountains.

The largest amount of rainfall falls on the western regions of Scotland, and there is a strong seasonal pattern with rainfall higher in winter months. On the west coast, the coastline is complex and indented and much of freshwater flow comes via sea lochs. Compared to the east coast of Scotland there are many more points were freshwater discharges into the coastal waters (more than 290 rivers) and these tend to be smaller rivers. The annual average freshwater flow on the west coast of Scotland based on modelled data is 1191 $m^3 s^{-1}$, much higher than the averaged gauged flow which is ~233 $m^3 s^{-1}$ (Table 4.2).

The eastern region of Scotland has much lower rainfall and overall there are fewer rivers and, therefore, fewer points where freshwater discharges into the coastal waters. However, these rivers tend to be much larger and longer than those on the west coast and many of these rivers actually have their catchment in the west of Scotland. The annual average freshwater flow on the east coast of Scotland, based on modelled data, is actually very similar to that of the west coast, being 1115 $m^3 s^{-1}$. This is much higher than the averaged gauged flow which is ~658 $m^3 s^{-1}$ (Table 4.3). Compared to the west coast, the coastline is generally much straighter and rivers flow into estuarine basins rather than sea lochs. The largest river, Tay has a discharge twice as large as any other river.

Long Term Trends

Overall river flow has increased over the period 1971-2013 (Cole et al., 2014). Increased freshwater input is likely to lead to a decrease in the salinity of coastal waters of the long term. Over the same period offshore waters have become increasingly more saline driven by changes in North Atlantic circulation (see Chapter 5). The pattern of salinity in coastal waters actually reflects the trends in oceanic salinity.

Trends and Variability 1997-2013

The total river flow on the east and the west coasts are very similar and shows the same pattern of falling and rising anomalies throughout the time period. The year 2006 is the only year where the flow is lower than normal on the east coast but higher than normal on the west.

The highest annual average anomaly in total river flow on the west coast was recorded in 2011, with the total river flow 1.0 sd higher than normal. On the east coast, river flow was high in 2011, but the highest annual flow was observed in 2002, when the flow was around 0.8 sd higher than normal. The year 2003 is a particularly noticeable year for lower than average river flow at all locations around the Scottish coast. Both the west and east coast had lower flow than normal. The west coast had

an annual average total river flow 0.5 sd lower than normal, and on the west coast flow was 0.8 sd lower than normal.

In 1997 there was generally lower than average flow at all locations and this was followed by a year of higher than normal flow in 1998. The years 1999 and 2000 continued to have higher than normal river flows at most locations, although a couple of sites had lower than normal flow. There was variability in flow in 2001 and 2002 before the lower than normal flow in 2003.

Figures 4.9 and 4.10 allow a comparison of the spatial differences in interannual variability between rivers on the east and west coasts. The gauging station on the river Ewe, on the west coast is close to the monitoring site at Loch Ewe. At Stonehaven monitoring site, river flow at the Dee and Don are likely to be indicative of the local freshwater flow.

There were also differences between the west and east coast rivers. Between 2003 and 2005 and in 2007, the rivers on the east coast generally had higher than average river flow, whilst in this same time period on the west coast river flows remained closer to the average. The years 2008 and 2009 had generally higher than normal flow in rivers on both the east and west coasts, but the difference from normal values are more pronounced in the west coast rivers. The two exceptions to this are the rivers Naver and Spey on the east coast which had lower than normal flow in 2009. In 2010 all rivers on the west coast had lower than normal flow levels, whilst on the east coast more than half of the rivers had higher than normal flow. Despite this variation within the east coast, total flow remained lower than normal for this year on both coasts.

4.5 Summary – River Flow

- Monthly mean river flows at ten gauged rivers on the west coast of Scotland and 13 gauged rivers on the east coast are presented.
- Comparison with modelled data suggest that the gauged rivers capture 20% of the total runoff on the west coast and 76% of the total runoff on the east coast.
- The variability in the gauged river flows most likely match those of the total flows
- Published model results suggest that total runoff is about the same on the west and east coasts, with annual totals of approximate 1,100 $m^3 s^{-1}$.
- The data is consistent over the observation period (1997-2013) with few gaps, allowing clear seasonal cycles in runoff to be described (minimum in June/July, maximum in winter on both coasts).
- Lowest freshwater flows were observed in 2003.
- Highest freshwater flows occurred in 2002 on the west coast but in 2011 on the east coast.

4.6 Plots - River Flow

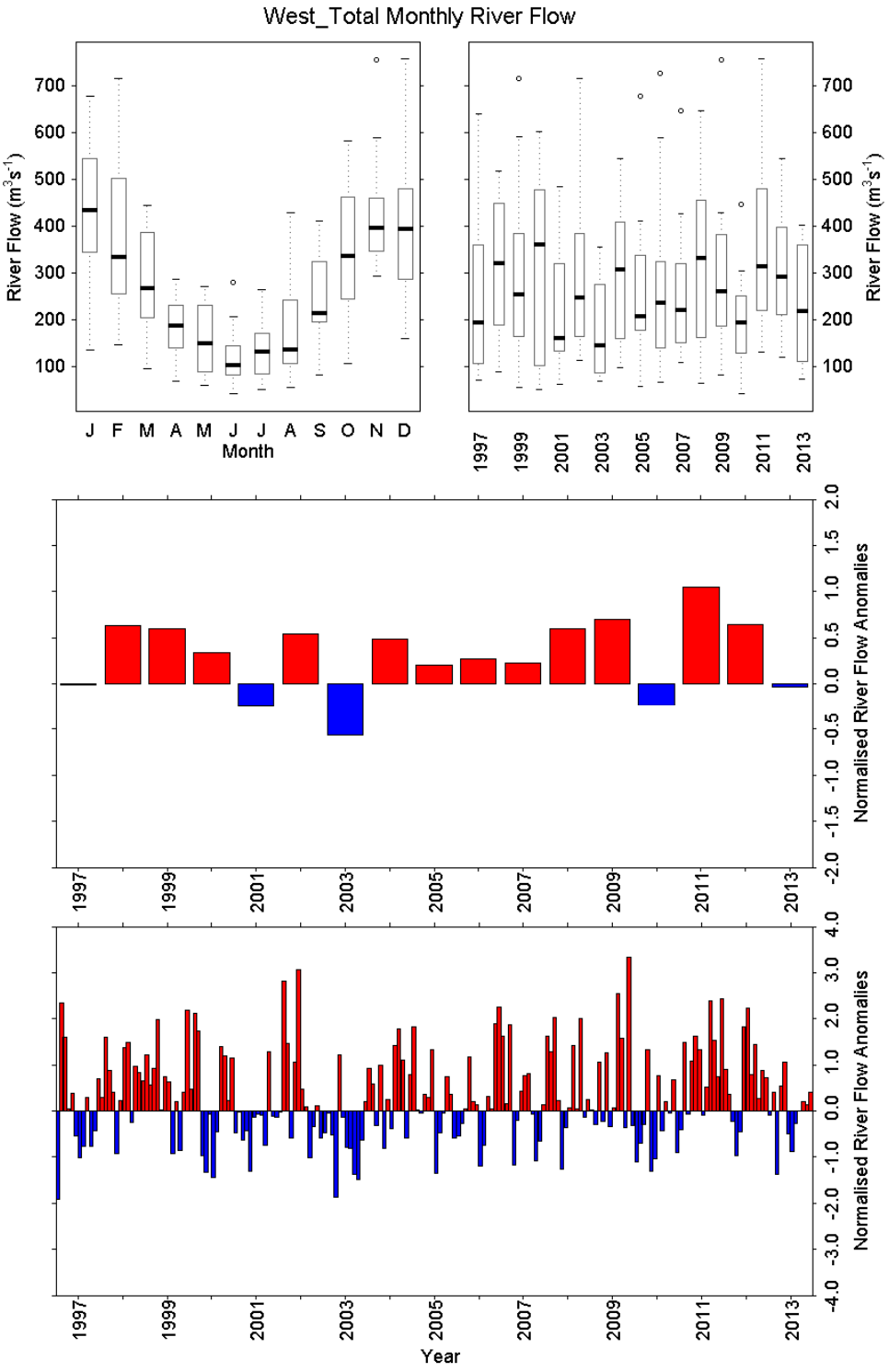

Figure 4.7 Sum of river flow on west coast of Scotland calculated from 10 from selected gauged rivers (see Table 4.2). a) Monthly boxplot of river flow. b) Annual boxplot of river flow. c) Annual mean anomaly time series d) Monthly mean anomaly time series. Anomalies are with respect to base period 2001-2010.

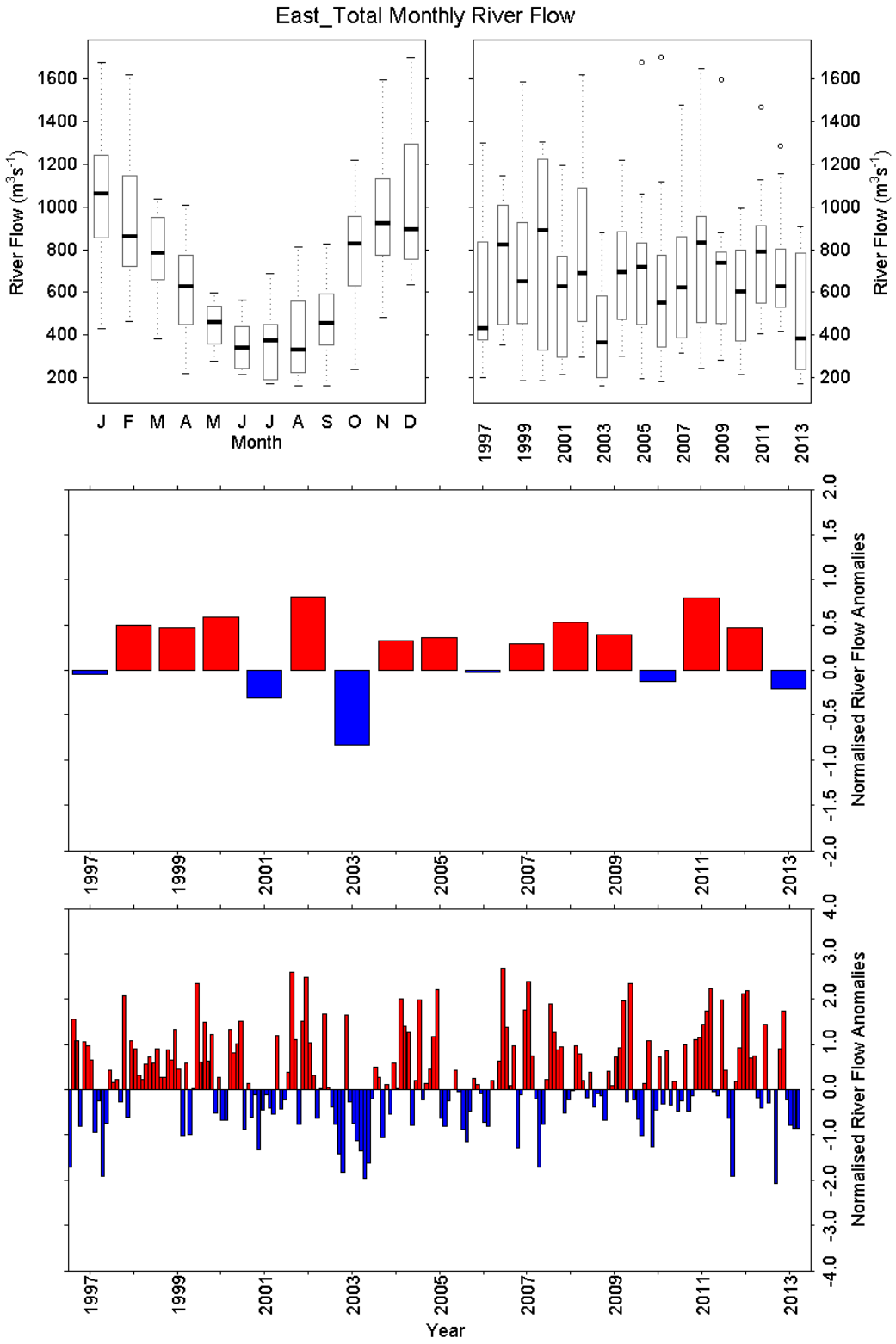

Figure 4.8 Sum of river flow on east coast of Scotland, calculated from 13 selected gauged rivers (see Table 4.3). a) Monthly boxplot of river flow. b) Annual boxplot of river flow. c) Annual mean anomaly time series d) Monthly mean anomaly time series. Anomalies are with respect to base period 2001-2010.

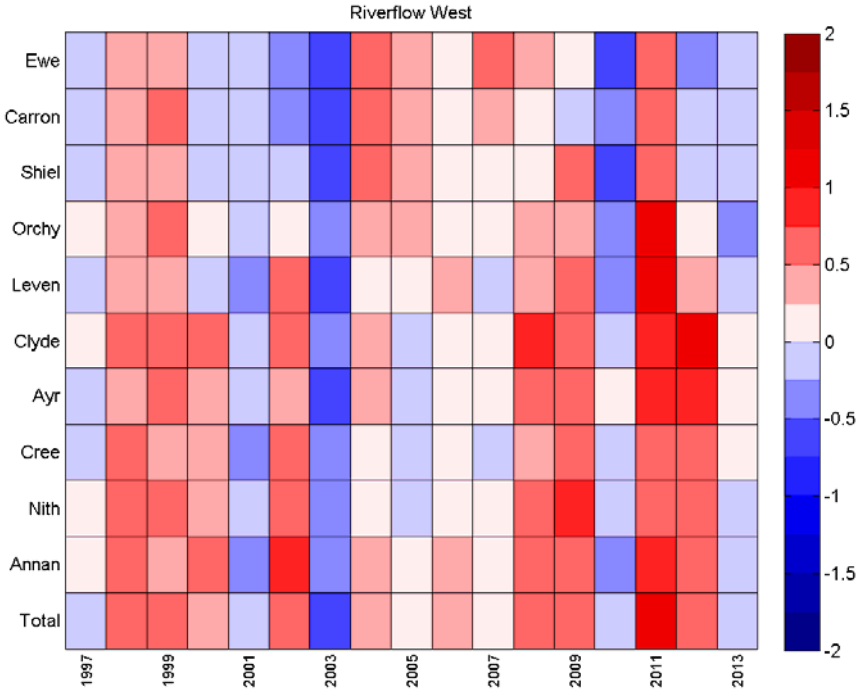

Figure 4.9 Yearly anomalies of river flow on the west coast of Scotland, including the total over all ten selected gauged rivers. The anomalies are normalized with respect to the standard deviation (sd) (e.g. a value of +2 indicates 2 sd above normal). Anomalies are with respect to base period 2001-2010. Colour intervals 0.25 sd; reds = positive/high flow, blues = negative/low flow. See Figure 4.6 for a map showing the locations of rivers in this figure.

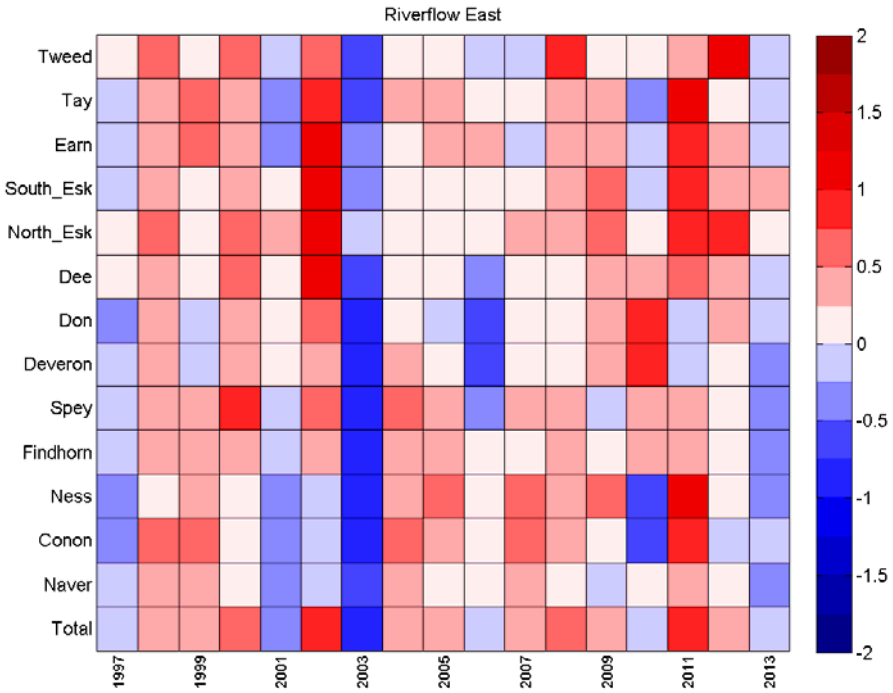

Figure 4.10 Yearly anomalies of river flow on the east coast of Scotland, including the total over all 13 selected gauged rivers. The anomalies are normalized with respect to the standard deviation (sd) (e.g. a value of +2 indicates 2 sd above normal). Anomalies are with respect to base period 2001-2010. Colour intervals 0.25 sd; reds = positive/high flow, blues = negative/low flow. See Figure 4.6 for a map showing the locations of rivers in this figure.

4.7 Offshore Temperature

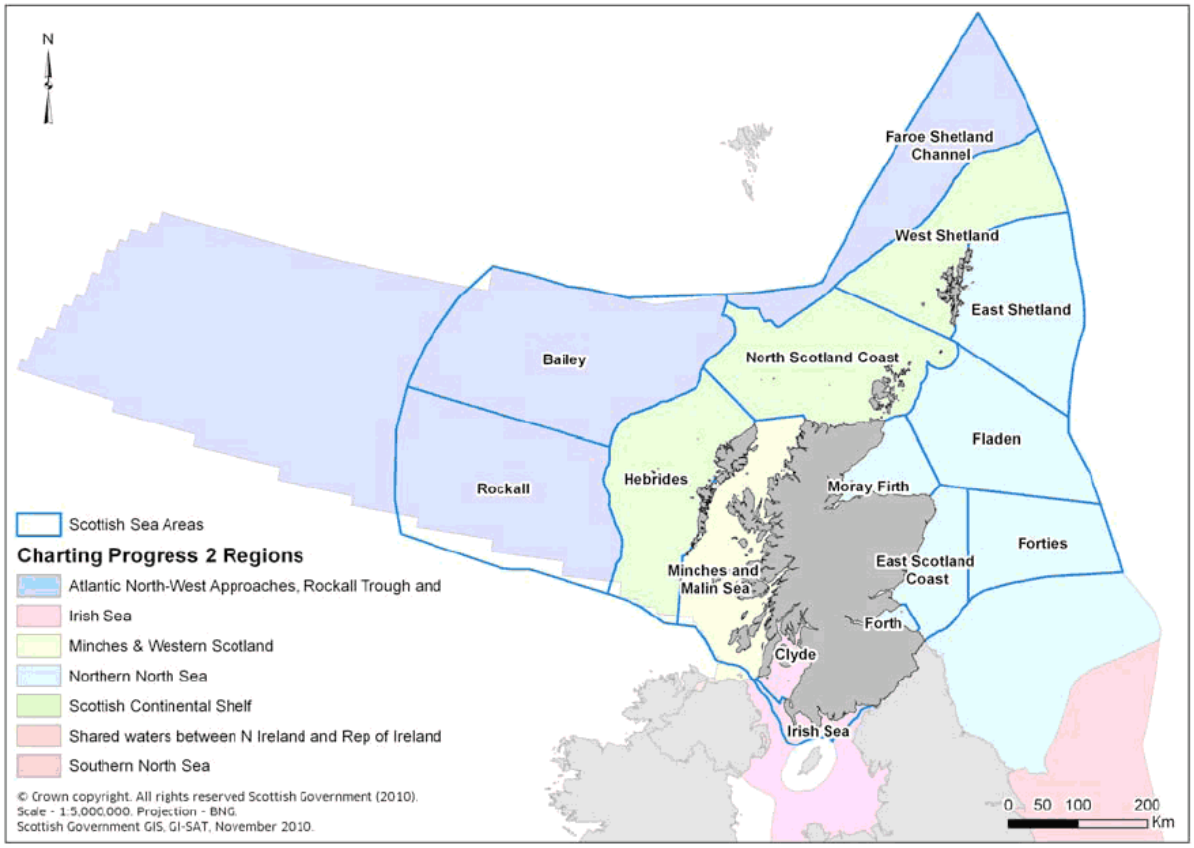

Figure 4.11 Scottish Sea Regions described in Charting Progress 2 (UKMMAS 2010).

Data Source

Figure 4.11 shows the area of each designated Scottish Sea Region. Sea surface temperatures in Scottish waters have been obtained from a combined satellite and *in situ* gridded dataset. The data are a subset of the Optimum Interpolation SST dataset (OISST) produced on a 1° grid and provided by the NOAA–CIRES Climate Diagnostics Centre in the USA. The 1981-2010 climatology was prepared from a combination two data sets[13]. This climatology was recently constructed to meet the World Meteorological Organization's standard for climatology to reflect the most recent 30-year period[14]. The 1981–2000 climatology, which was utilized in past State of the Climate reports, is about 0.2°C higher than the 1971–2000 climatology (Xue et al., 2003) over much of the tropical oceans and North Atlantic[15].

Data Quality Control and Data Processing

Monthly averaged sea surface temperature from the OISST, 1° (latitude and longitude) gridded dataset have been combined to make a single spatially averaged time series of monthly data for each of 13 Scottish Sea Areas. Note that because of

[13] http://www.cpc.ncep.noaa.gov/products/people/yxue/sstclim/Note_SST_Climatology_1981-2010.doc
[14] http://www.wmo.int/pages/prog/wcp/wcdmp/documents/WCDMPNo61.pdf
[15] see details in http://www.cpc.ncep.noaa.gov/products/people/yxue/sstclim/Note_SST_Climatology_1981-2010.doc

the small size and coastal nature of the Irish Sea and Forth Sea Areas, no data were available from this dataset in these areas. The Scottish Sea Areas have previously been used to assess data in reports such as the Scottish Marine Atlas (Baxter et al., 2011) and are subsets of larger sea areas presented in the Charting Progress 2 report (UKMMAS 2010).

Data Analysis

Sea surface temperature anomalies have been calculated with reference to climatology for the period 2001-2010. For each sea area, a single index has been prepared which is calculated as the average temperature across all of the grid cells that lie within the region.

Seasonal and Spatial Patterns

Seasonal patterns of sea surface temperature across Scottish Waters reflect the latitudinal variability in surface heat flux as well as the effect of heat being stored in deeper oceanic waters. As a result, the lowest temperatures overall are found in the northernmost areas (Faroe Shetland Channel) whereas the highest average temperatures are found in the southernmost of the offshore regions to the west of Scotland. Here the influence of Atlantic Water keeps average temperatures much higher than in coastal regions.

Annual temperatures vary by just over 8°C in the Forties region, in the North Sea, whereas the difference between the maximum and minimum temperatures is only 4.3°C in the Bailey and Rockall areas. Winter temperatures are lowest on the East Scotland coast, with the lowest winter temperatures (averaged over the 2001-2010 period) being only 6.8°C. In the Rockall area, the lowest monthly mean temperature was 10°C.

The pattern of annual temperature anomalies shows a relatively strong spatial coherence. The more inshore regions around Scotland's coast also have a similar pattern. The main differences are observed in the year-to-year pattern in the offshore regions to the west of Scotland (Rockall and Bailey) and also the Clyde Sea region.

Trends and Variability 1997-2013

The period 2002-2006 was relatively warm compared to the rest of the measurement period, and the warmest year across all regions was 2003. The year 2009 was also a warm year, particularly in the offshore regions of Bailey and Rockall (Figure 4.12) and the more northern areas which are also influenced by Atlantic waters (West Shetland, North Coast, Faroe Shetland Channel).

From 1999 to 2001 and 2010 to 2013 there were Scottish-wide cold periods. The year 2000 was the coldest year overall for these sea areas and temperatures were particularly low in the Rockall and Bailey areas. Although 2010 was a very cold year for air temperature, particularly in the winter, there is not such a strong signal observed in sea surface temperatures. The year 2010 was the second coldest year

in the Clyde and Minches regions as well as the Moray Firth, Forties and East Shetland.

Between 1997 and 2001 the eastern region sea surface temperatures were cooler than normal, 2002 was close to normal but following this, 2003 and 2004 were two very warm years.

May 2013 was a very cool month in the Clyde area, with temperature of 8.55°C more than 3 sd below normal (10.12°C) for that time of year. In the East Scotland coast area, the lowest monthly average temperatures were observed in December 2010, with average temperatures of 8.09°C, 1.34° lower than average for December.

The most unusually warm period occurred at Rockall in May 2008, when temperatures of 11.92°, almost 1° higher than normal, were observed. In many areas, October 2006 was the warmest month, with average temperatures 2.5 sd higher than average in the West and East Shetland regions. Higher than average October temperatures also occurred in the Clyde, Fladen and the East Scotland Coast areas.

4.8 Summary – Offshore Temperature

- Sea surface temperature for 13 Scottish Sea Areas have been calculated from a combined satellite and in situ gridded dataset.
- The data has no gaps over the observation period (1997-2013), and hence robust seasonal cycles can be determined.
- Highest sea surface temperatures were observed in 2003.
- The year 2009 was also warm but mainly in offshore regions where the Atlantic influence is the greatest.
- Lowest temperatures were observed in 2000 across all sea areas.
- The very cold winter of 2010 did not have as strong an impact on sea surface temperatures as it did on air temperatures, although North Sea and Clyde temperatures were relatively low in December 2010.

4.9 References - Physical Conditions

Baxter, J.M., Boyd, I.L., Cox, M., Donald, A.E., Malcolm, S.J., Miles, H., Miller, B., Moffat, C.F., (Editors) (2011) Scotland's Marine Atlas: Information for the national marine plan. Marine Scotland, Edinburgh. 191pp. http://www.scotland.gov.uk/Publications/2011/03/16182005/0.

Cole, S.J., Moore, R.J., and Davies, H.N. (2014) River discharge datasets for the coastlines of Scotland and Northern Ireland. Natural Environment Research Council, Centre for Ecology and Hydrology.

Devreker, D. and Lefebve, A. (2015) TTAinterfaceTrendAnalysis: A R GUI for Routine Temporal Trend Analysis and Diagnostics. 14pp. https://cran.r-project.org/web/packages/TTAinterfaceTrendAnalysis/vignettes/TTAVignette.pdf

Jenkins, G.J., Perry, M.C., Prior, M.J. (2008) The climate of the United Kingdom and recent trends. Met Office Hadley Centre, Exeter, UK.

Jones, P.D., Lister, D.H., Osborn, T.J., Harpham, C., Salmon, M., Morice, C.P. (2012) Hemispheric and large-scale land surface air temperature variations: An extensive revision and an update to 2010, Journal of Geophysical Research, 117, D05127, doi:10.1029/2011JD017139.

Kerr, A. and Tabony, R. (2004) Comparison of sunshine recorded by Campbell–Stokes and automatic sensors. Weather, 59(4), 90-95, doi: 10.1256/wea.99.03.

Legg, T. (2014) Comparison of daily sunshine duration recorded by Campbell–Stokes and Kipp and Zonen sensors. Weather, 69(10), 264-267, doi: 10.1002/wea.2288.

Marsh, T., Sanderson, F., Swain, O. (2015) The National Hydrological Monitoring programme: Derivation of the UK national and regional runoff series: Centre for Ecology and Hydrology.

Parker, D.E., Legg, T.P., Folland, C.K. (1992) A new daily Central England Temperature Series, 1772-1991. International Journal of Climatology, 12, 317-342.

R Core Team (2013). R: A language and environment for statistical computing. R Foundation for Statistical Computing, Vienna, Austria. URL http://www.R-project.org/

UK Marine Monitoring and Assessment Strategy Community (UKMMAS) (2010). Charting Progress 2 Feeder report: Clean and Safe Seas. (Eds. Law, R. and Maes, T.). Published by Department for Environment Food and Rural Affairs on behalf of UKMMAS. 366pp.

Xue, Y., Smith, T.M., Reynolds, R.W. (2003) Interdecadal Changes of 30-Yr SST Normals during 1871–2000. American Meteorological Society, http://dx.doi.org/10.1175/1520-0442-16.10.1601
.

4.10 Plots – Offshore Temperature

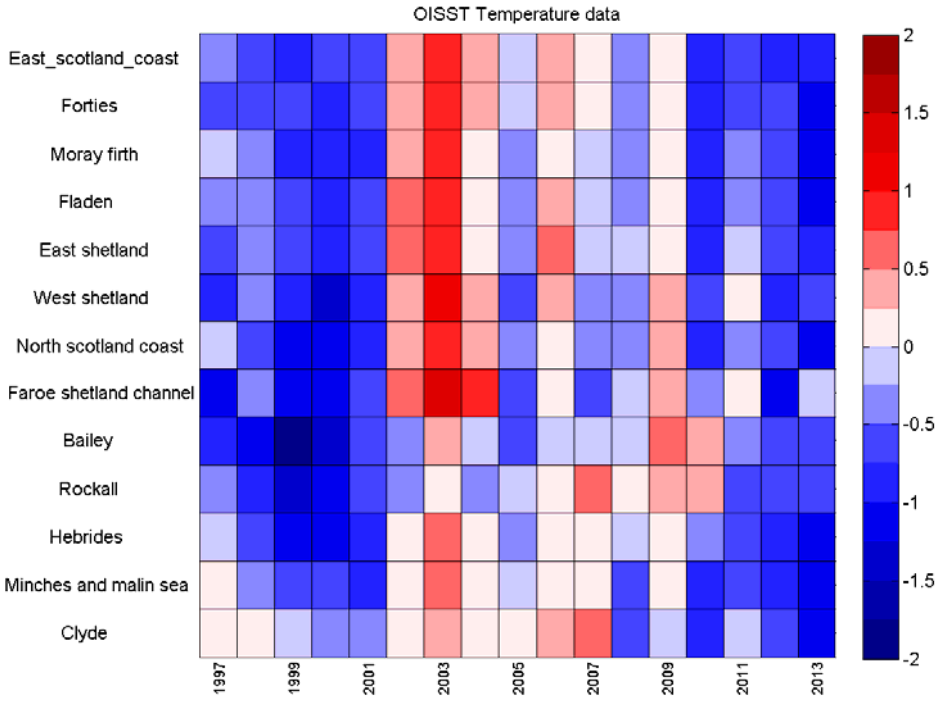

Figure 4.12 Yearly anomalies of sea surface temperature relative to a 2001-2010 base period, averaged over 13 Scottish Sea Areas. The anomalies are normalized with respect to the standard deviation (sd) (e.g. a value of +2 indicates 2 sd above normal). Colour intervals 0.25 sd; reds = positive/warm; blues = negative/cool. See Figure 4.11 for a map supplying more details about the locations in this figure. No gridded SST data are available in the Irish Sea or Firth of Forth Areas.

5. Temperature and Salinity

5.1 Introduction

In Chapter 4 observed changes in temperature around the coast of Scotland were described along with additional meteorological drivers and river runoff. In this section, the temperature and salinity measured at each of the monitoring sites in the Scottish Coastal Observatory are described. Some of the sites have temperature data only. Salinity is measured at five sites; Loch Maddy, Loch Ewe, Scapa, Scalloway and Stonehaven (Figure 5.1).

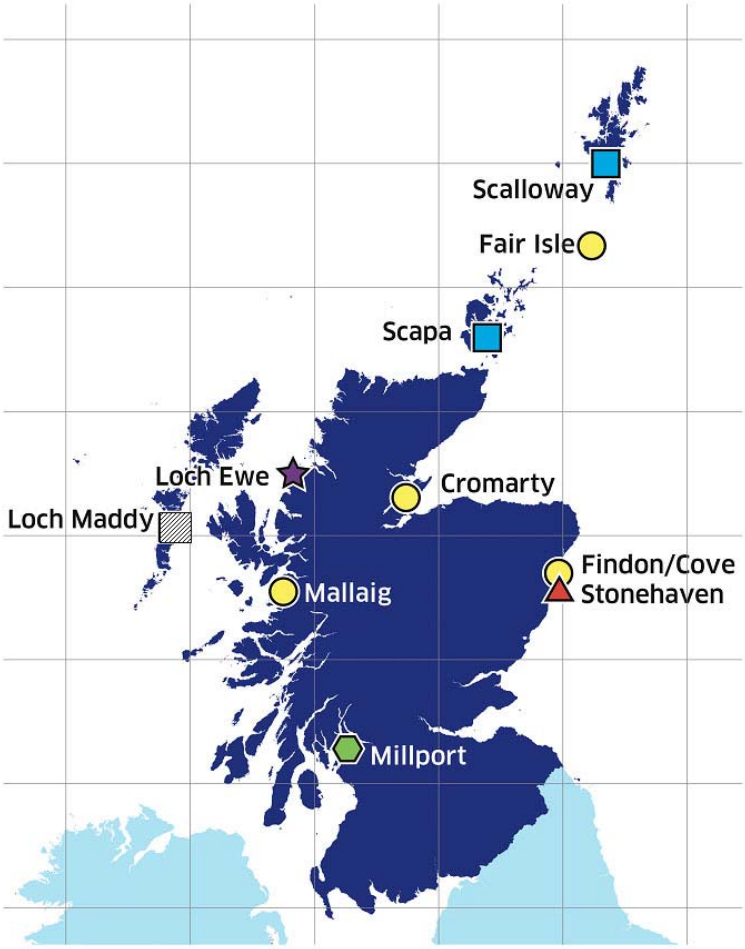

Figure 5.1 Location of the Scottish coastal temperature monitoring sites. The different symbols represent the different combination of parameters measured. Temperature is a core measurement at all sites; ● temperature only, ⬢ temperature and phytoplankton, ▩ temperature, salinity, phytoplankton, ■ temperature, salinity, nutrients, algal toxins, phytoplankton, ★ temperature, salinity, secchi, nutrients, pigments, algal toxins, phytoplankton, zooplankton, ▲ temperature, salinity, secchi, nutrients, carbonate chemistry, pigments, phytoplankton, zooplankton.

5.2 Methods

Sample/Data Collection and Storage

Sampling methodologies for temperature and salinity vary between sites. Table 5.1 summarises the key differences. Unless specifically mentioned, samples are taken at close to the surface of the water column.

Site Name	Fixed Depth	Fixed Datum	Minilogger Temperature	Bottle Temperature	Sampling in Lower layers	Salinity
Millport	X		X			
Mallaig		X	X			
Loch Maddy		X	X			X
Loch Ewe	X		X	X	X	X
Scapa		X	X			X
Fair Isle		X	X			
Scalloway	X		X			X
Cromarty		X	X			
East Coast		X	X			
Stonehaven		X		X	X	X

Table 5.1 Sampling methods for measuring temperature and salinity at the coastal ecosystem monitoring sites.

Temperature Sampling

There are two methods used to record temperature data here. At most sites, sea temperature is measured automatically and continuously using an electronic temperature recording device (Vemco Minilogger) installed at the monitoring site. These data are generally referred to as minilogger data. Miniloggers are used at Loch Maddy, Scapa and Scalloway and is the only method of measuring temperature at these sites. Measurements are only made in the surface layers at these sites. At both Loch Ewe and Stonehaven, where the monitoring programme is more intensive, temperature is recorded at the time, position and depth of each water sample using an electronic reversing thermometer attached to a reversing water bottle, these temperature data are referred to as 'Bottle' temperature data.

Temperature Sampling (Bottle) - Reversing Thermometers

Where bottle temperature data were collected these measurements were made using reversing water bottles fitted with reversing thermometers, initially mercury and laterally digital model RTM 4002X, made by SIS (Sensoren, Instrumente, Systeme) in Germany. The SIS digital reversing thermometer is a precision instrument with an accuracy of 0.003ºC, resolution 0.001ºC over the measurement range -2 ºC to 40 ºC. The digital thermometers are regularly sent for factory calibration. The reversing water bottles were used to sample the water for salinity analysis. At Stonehaven and Loch Ewe this method was used to sample two different depths; the upper layer (<10m depth) and the bottom layers (approximately 5m above the sea bed).

Temperature Sampling (Logger Temperature) - Vemco Minilogger

Where continuous records of sea surface temperature were made, this was done using Vemco Minilogger temperature recorders. These small instruments were deployed in the near surface layer (approximately 5 m deep) and set to record usually at 30 minute intervals. Prior to 2010 most of the Miniloggers were 8-bit, model Minilog-T with a measurement range of -4 to 20ºC, a resolution of 0.1°C and a stated accuracy of 0.2°C. From 2011 onwards a programme of upgrade and replacement resulted in new instruments, model Minilog-II-T being used, these new instruments have a measurement range of -30 to 80ºC and an improved resolution of 0.01 ºC and an accuracy of +/-0.1ºC.

Vemco Minilogger Deployment Methods

At some sites, the minilogger was deployed at a fixed depth, usually by being suspended from a floating platform. In Millport temperature is measured using a Minilogger which is suspended below a floating buoy attached to a pier, maintaining records from a constant depth of 0.5 m below sea surface. Similarly in Loch Ewe, the Minilogger is deployed from a buoy in a sheltered location at a fish farm, at a depth of 3 m below the platform.

At the Scalloway site, the minilogger is suspended at 2 m below the sea surface under a floating pontoon at Scalloway boat club. The exact position of the site has changed slightly over the years due to a collapse of the original boat club pontoon, which also resulted in a gap in the data.

At other sites, the minilogger is deployed at a fixed position (termed fixed datum), and its depth therefore varies with the state of the tide. At Mallaig, the Minilogger is fixed inside a pipe and deployed from a pier. The Minilogger at Findon was also fixed inside a pipe that afforded it some shelter from storms, and was deployed at a depth of 1 m below the level of the lowest tide. In Loch Maddy the Minilogger was suspended on the sheltered side of the concrete at the end of the pier at a depth of around 5 metres (0.5 m from the sea bed). In 2004 it was moved to beneath a buoy, but was lost from this location so the position at the end of the pier was resumed.

In Scapa Bay the Minilogger is also suspended from a pier. It sits at a depth of 1 m below the level of the lowest tide. Similarly, in Fair Isle the Minilogger sits below North Haven pier recording temperature. The Minilogger in Cromarty is close to a pier but is deployed using a subsurface buoy and rope system fixing it at approximately 1 m above the seabed.

Because of the offshore nature of the Stonehaven site, there is no permanent mooring to deploy a minilogger. A minilogger site was established at Findon in 1997, with the minilogger deployed in a pipe at fixed datum. After the site became unsafe and a replacement site at Cove proved to be unsuitable, a new site was eventually found at the pier in Stonehaven Harbour in 2015.

Salinity Sampling

Salinity samples are collected weekly at the Loch Maddy, Loch Ewe, Scapa, Scalloway and Stonehaven sites (Figure 5.1 and Table 5.1). Throughout the project, water samples were collected for salinity at both surface and near bed at Stonehaven and Loch Ewe. However, during periods when additional mid-depth samples were taken for nutrients, for example at 5 m and 10 m, coincident samples were also taken for salinity.

A subsample of water for salinity analysis is taken from a larger water sampling bottle, with the salinity sample bottle being rinsed three times before filling. The sample is stored in a glass bottle, which is dried with a paper towel to prevent salt crystals forming around the neck and then sealed tightly using a plastic insert to protect against evaporation. Salinity bottles are stored in protective crates and boxes and kept at ambient temperature until they are moved to a temperature controlled environment prior to analysis.

Sample Processing, Analysis and Archiving

Salinity Analysis

Salinity analysis is undertaken using a Guildline Portasal Salinometer Model 8410A, to determine the salt content of a seawater sample using a measure of the conductivity ratio on the Practical Salinity Scale 1978 (UNESCO, 1981). The salinometer is designed to make precision conductivity comparisons between a water sample and a reference sample, results are recorded in Practical Salinity Units (PSU). The salinometer is standardised using a known reference material, International Association for Physical Sciences of the Ocean (IAPSO) Standard Seawater, which is the internationally recognized calibration standard for the measurement of Practical Salinity.

The current definition for Practical Salinity states: a seawater sample, at a temperature of 15ºC and at atmosphere pressure, of Practical Salinity 35 has a conductivity ratio of unity with a potassium chloride (KCl) solution containing a mass of 32.4356 grams of KCl per kilogram of solution. Marine Scotland operate two Portasal salinometers on rotation, with a calibration and service schedule that ensures that the operational Portasal that has been calibrated within the last twelve months.

Using this method, salinity can be determined in the range of 10 to 36 PSU (Guildline Instruments Ltd, 2002). The accuracy of the instrument is better than 0.003 equivalent Practical Salinity Units.

Data Quality, Handling and Archiving

All data presented here have been quality controlled as described in Chapter 2. Data assigned a quality flag of bad and probably bad (QF 3 and QF4) were excluded from the assessment, but all other values accepted.

Instrument errors are well controlled as the instruments used are very accurate and calibrated regularly. The main source of error in temperature or salinity data is likely to be human error in data recording and transcription. This is a result of either surface and bottom samples being mixed up (water depth incorrectly recorded) or values from the reversing thermometer and/or salinometer being incorrectly transcribed into the data record. When using temperature data from automated loggers another source of error is the inaccuracy of water sampling time and the variability in temperature between the depth/position of the water sample and the depth/position of the logger.

Gross errors made in this way can be captured, firstly by searching for physically impossible values (such as unstable water column) or by values that are outside of the expected seasonal range for each parameter. Minor transcription errors, for example those in the second decimal place cannot be identified.

At some sites (e.g. Scapa and Scallaway), temperate measurements were not made at the same point as the discrete water sample but were measured continuously using an automated temperature sensor located nearby. In this case, water temperatures associated with the water sample are interpolated to the time of the discrete sample from hourly averages of the logged water temperature. It should be noted that the sample times are not always recorded with high precision and may differ by up to +/- one hour of the actual sample. In such cases the temperature has been recorded with a data Quality Flag of 8, indicating an interpolated sample.

Overall, only a small number of temperature and salinity records were rejected and so there is high confidence in these data.

Sampling at these monitoring sites is usually undertaken weekly however there are gaps in the record resulting from adverse weather preventing the boat reaching the sampling site safely or kit failures. Each monthly average is thus calculated from between one and five samples in that month. Missed sampling is more likely in winter months, particularly at Stonehaven as its offshore location and boat based sampling is more vulnerable to weather disruption. Over the 17 years of measurement at Stonehaven there were an average of three samples per month in December, January and February and an average of four samples per month throughout the rest of the year. Owing to its position close to shore, interruption in sampling is not an issue at Loch Ewe.

For the annual and monthly analysis, months with less than two samples were not included and years with less than nine months of data were not included in the yearly anomaly calculations. For years with between 9 and 11 months of data, missing months were replaced with climatological average values when calculating annual mean values for each parameter. This ensures that annual mean temperatures are not unduly skewed by missing years, and makes it likely that estimates of anomalies in missing years will be underestimates of the actual value. The number of samples collected in each month is given in Appendix C in Part 3 of this report.

5.3 Results

Long Term Trends

When considering trends in the observed time series, it is important to bear in mind the long term trends that have been observed in the coastal data as well as in other long term datasets. Using evidence from the Millport coastal temperature time series, for example (Figure 5.2), we know that in the period 1997-2013, average coastal sea temperatures were above the long term mean as a result of a long term trend in rising temperatures. Figures 5.2 and 5.3 illustrate the difference in comparing conditions during the measurement period to a 30-year baseline (1981-2010) or a 10-year baseline (2001-2010).

The temperature trends observed over the 15 year period of this monitoring programme are important in as much as they are likely to be significant drivers of the observed ecosystem variability, but they are not indicators of the long term climate trends.

Temperature data from the Millport monitoring site represent one of the longest coastal temperature time-series in Scotland. Continuous and regular monitoring mean that the seasonal cycle is well described and the long term mean has been established. To allow comparison between the measurement period (1997-2013) discussed here and the long term record, data from 1997-2013 are presented but also data from 1971-2013.

It is clear from the long term record that conditions between 1997 and 2013 can mostly be characterised as warm with the exception of 2013, when the annual temperature was actually colder than the long term average (Figure 5.2). Therefore, in the context of long term climate change, the measurement period should be considered as unusually warm. The high temperatures observed at this site in 2002 were the highest observed in 30 years and actually represent the highest temperatures in the measured record, which extends back to the early 1900s. The long term trend in coastal temperature at Millport is also consistent with evidence from average UK coastal temperatures (MCCIP, 2013). The period 1997-2013 was warmer than any other period observed since 1875.

Seasonal and Spatial Patterns

The seasonal patterns of temperature in Scottish waters are well described in Hughes (2007) and Berx (2009) and the data presented here show the expected variability between east and west coast with the season. On the west coast of Scotland, winter temperatures tend to remain higher than in the North Sea, average winter (Jan-Mar) temperatures at Loch Maddy, at 8.2ºC were 1.8ºC higher than average winter temperatures at Stonehaven (6.5ºC).

The coastal waters of Scotland are fresher than those offshore as a consequence of freshwater runoff. The annual average salinity at the surface is higher in locations such as Scapa (34.70) and Scalloway (34.93), than in the sea lochs of the west coast (Loch Ewe 33.77 and Loch Maddy 34.43). The annual average salinity at Stonehaven is 34.52, higher than in the West Coast sea loch environment but lower

than the North Atlantic influenced island regions of Orkney and Shetland. At both Loch Ewe and Stonehaven, average salinity increases with water depth, which is to be expected as any local surface runoff will tend to remain in the upper layers.

The seasonal pattern of salinity at each site also conforms to the expected broad scale patterns. At all sites on the west and north coasts of Scotland, maximum salinity occurs in the summer months (June-July) and lower salinities are observed in autumn/winter months (November, December, Januaray, February). This correlates to the seasonal pattern of rainfall and river flow and suggests that on seasonal timescales, the coastal freshwater content is locally influenced. At Stonehaven, however, the seasonal pattern of salinity is quite different. Minimum salinity is observed in spring (March) and maximum salinity is observed in September. Salinities remain high during the autumn and early winter when there is high Atlantic inflow and then begin to decrease in January-February. Rather than simply reflecting the patterns of precipitation and runoff, the seasonal pattern of salinity at Stonehaven is similar to that across the whole of the northern North Sea and is a consequence of varying Atlantic Water influence (Hughes et al., 2011) balanced with the freshwater inputs to the North Sea.

At sites where there are both surface and near bed salinity records, it is clear that variability in salinity is greater in the surface layers responding probably to local freshwater events. Salinity at the near bed level is a more stable indicator of the coastal water freshwater content and is taken to be more representative of the broader scale changes in coastal waters.

Near surface temperature shows a typical seasonal pattern, similar to that of air temperature with maximum temperature occurring in late summer August/September and minimum temperatures at the end of winter February/March time. Near bottom temperature can show a different pattern, as during the stratified period, the near-bed water masses are isolated from the surface and tend to warm much more slowly than the waters of the upper layers. In well stratified waters, a sharp increase in temperature may be seen at the end of summer, when mixing of the water column breaks down the water column and distributes the heat of the upper layers rapidly down through the water column. This mixing can sometimes trigger an autumn bloom in phytoplankton growth as a result of nutrient resuspension into the surface waters. However, at these shallow coastal sites, stratification is not strong enough to isolate the lower layers, which demonstrate a marked seasonal cycle, but with a slightly reduced range compared to the upper layers.

A comparison of the annual variability in coastal sea surface temperatures demonstrates a similar patter to that observed across the Scottish Sea Areas (Figure 4.12). Maximum temperatures are observed in 2003 at most of the sites, with cooler periods prior to 2003 and a notably colder period from 2009-2013.

Variability and Trends

Millport

It should be noted that the warmest year observed at Millport is 2002, whereas it was 2003 at all of the other coastal measurement sites. It is possible that this reflects

true spatial variability in the maximum temperature but evidence from other temperature records (see Figure 4.15) suggests that because there were data missing from January-February at this site in 2003, the anomaly for that year is biased downwards.

Loch Maddy

Temperature and salinity were measured in surface waters at Loch Maddy between 2003 and 2013. The variability in salinity changed markedly in the latter part of the measurement period. Prior to this time surface salinity was in the range 30-35, whereas after 2010 surface salinities of less than 30 were regularly observed in winter and spring. This may have been due to the sampling site moving position. With a relatively short and sparse dataset it is difficult to determine any significant trends in temperature data at this site.

Loch Ewe

Temperature and salinity have been measured in Loch Ewe surface and bottom waters since 2003. In both surface and bottom waters the later years of the observation period were cooler than the earlier years. The year 2003 was the warmest year in the observations, with an annual mean temperature anomaly of 0.35 and 0.43 sd above average at upper and lower levels.

Following a pattern seen at most of the measurement sites, 2010 and 2013 were the coldest years of this record at Loch Ewe. In both of these years temperatures in all months and at all levels were below average. A similar trend can be seen in the salinity record at Loch Ewe, with salinity in the latter part of the time series being lower than at the start. It is notable that 2013 was both cool and fresh, whereas 2010 was cool but of average salinity for the time period.

Scapa

Temperature and salinity have been measured in surface waters at Scapa, Orkney since October 1999. There were some gaps in the temperature record due to lost Miniloggers in 2006 and 2008, but apart from this the record is almost complete. The lowest annual average salinity was observed in 2013, with values of 0.98 sd lower than average. The years 2001 and 2007 also had low salinity. The warmest year in the measurement period was 2003, with higher than average temperatures in all months throughout the year and an average temperature of 0.79 sd above average.

Scalloway

Temperature and salinity have been measured in surface waters in Shetland since October 2000. The temperature record at Scalloway was not particularly consistent with large gaps in 2005 and 2007, when there were only eight months of data in each year. Data from these years are not, therefore, included in the monthly analysis. The salinity record was slightly more complete. However, there were still data missing in 2002, 2004 and 2008.

Comparison with the closest nearby sites of Scapa and Scalloway suggests that there is a common pattern to the temperature and salinity. At both sites 2003 stands out as the warmest year of observation with cooler conditions from 2009 onwards. Also consistent with Scapa, 2001 and 2013 were years with fresher than average for the measurement period.

Stonehaven

At Stonehaven, the Minilogger was sited at a coastal site (East Coast), 5.4 km away from the sampling site. Correlation analysis between weekly surface (bottle) temperatures at the sampling site and the weekly subsampled data at the coast was ($p<0.01$), showing that the coastal site captures the same variability as the Stonehaven monitoring site further offshore (Figure 5.4). In this section bottle temperature data are presented.

Of all the long-term monitoring sites, Stonehaven is the longest and most complete, with data collection starting in 1997. These data clearly show that temperatures were higher in the period 2003-2009 than at the start or at the end of the measurements period. The warmest year of the record was 2003, with annual mean temperatures at 0.71 sd above the average value for the period in both upper and lower layers. The coldest year was 2013 at both upper and lower levels, with annual temperatures of 0.76 and 1.34 sd below the average for the measurement period respectively.

Overall there was no significant trend in the 17 year measurement period, although it must be remembered that evidence from longer datasets in coastal waters and the northern North Sea (MCCIP, 2013) show that in this period, sea temperatures were always above the long term mean (1971-2000).

The year 2001 stands out as significantly anomalous when the annual mean salinity at both upper and lower levels was much lower than average. There was a period of higher salinity between 2003 and 2006 and then 2007 was again a year of low salinity. In contrast to other sites on the west coast, at Stonehaven 2013 was not particularly fresh.

Discussion

When placed in the context of longer term trends the measurement period 1997-2013 should be considered warmer than normal, however, there was no overall warming trend. The warmest years occurred around 2003 and the latter part of the measurement period was characterised by more variable and often cooler conditions, with a series of very cold winters in 2010 and 2011. Patterns of atmospheric and ocean temperatures follow similar patterns but the cold winter air temperatures in 2010 had the most influence on conditions in the shallower coastal areas such as the Clyde and the North Sea while areas influenced by the North Atlantic remained warm.

The year 2003 was a very warm year at inshore and offshore sites. Air temperatures across Scotland were also higher than normal during this year and it was very sunny and dry. This year was also characterised by lower than normal river flow across all

regions. In offshore regions, the year was on average very warm across all areas. Data from offshore monitoring sites indicate that 2003 was a record year of warm and salty conditions in the North Atlantic (Hughes et al., 2011). The year 2010 stands out as a cold year, with higher than normal river flow on the east of Scotland (although not such a strong pattern on the west coast). It is important to note that the cold conditions in 2010 were skewed by a particularly cold winter and this is shown in the much lower than average air temperatures and higher than average days of frost. In contrast to 2003, these conditions were not reflected particularly strongly in offshore areas showing that the main driver of this cold year was atmospheric conditions rather than broader patterns in oceanic circulation.

The highest freshwater flows occurred in 2002 on the west coast but in 2011 on the east coast. There is little evidence in the data that local freshwater flows influence salinity in the coastal areas. The lowest salinities observed at Stonehaven occurred in 2001 and again in 2007. The interannual variability in salinity appears more closely related to the salinity of oceanic waters.

5.4 Summary – Temperature and Salinity

- Temperatures at nine sites around Scotland, measured using electronic automatic data recorders, are presented.
- Temperature recorded at Millport is presented from 1971 in order to examine base period selection and its effect on anomalies.
- Salinity and temperature recorded manually at five sites (Stonehaven, Loch Ewe, Scalloway, Scapa and Loch Maddy) is presented.
- Temperature, as expected, has a strong seasonal cycle at all stations, with maxima in August/September.
- Salinity has a much weaker seasonal cycle, although most pronounced at Stonehaven, with maxima in July to September.
- The measurement period 1997-2013 is likely to be the warmest 17 year period for coastal sea temperature on record.
- 2001 was a very fresh year at all sites.
- 2003 was the warmest year at all sites (where data existed for 2003).
- Highest salinities were observed in 2004.
- 2010 was cold, linked to cold atmospheric conditions.
- 2013 was very cold and also fresh at Loch Ewe, Scapa and Scalloway.

5.5 References - Temperature and Salinity

Berx, B.H. (2009) Climatology of Surface and Near-bed Temperature and Salinity on the North-West European Continental Shelf for 1971-2000. Continental Shelf Research, 29, 2286-2292.

Guildline Instruments Ltd. (2002) 8410A Portasal Portable Salinometer. Ontario.

Hill, A. (1998) Buoyancy effects in coastal and shelf seas. In K.R. Brink, The Sea, Volume 10: The Global Coastal Ocean: Processes and Methods (pp. 21-62). Harvard University Press.

Hughes, S.L., Holliday, N.P., Beszczynska-Moller, A. (2011) The ICES Report on ocean Climate 2010. ICES Co-operative Research Report No. 69.

Hughes, S. (2007) Scottish Ocean Climate Status Report 2004 - 2005. Aberdeen: Fisheries Research Services.

MCCIP (2013) Marine Climate Change Impacts Report Card. Summary Report. Lowestoft.

UNESCO (1981) Tenth report of the Joint Panel on Oceanographic Tables and Standards. Technical Paper in Marine Science, 25.

5.6 Plots – Temperature and Salinity – Context Setting

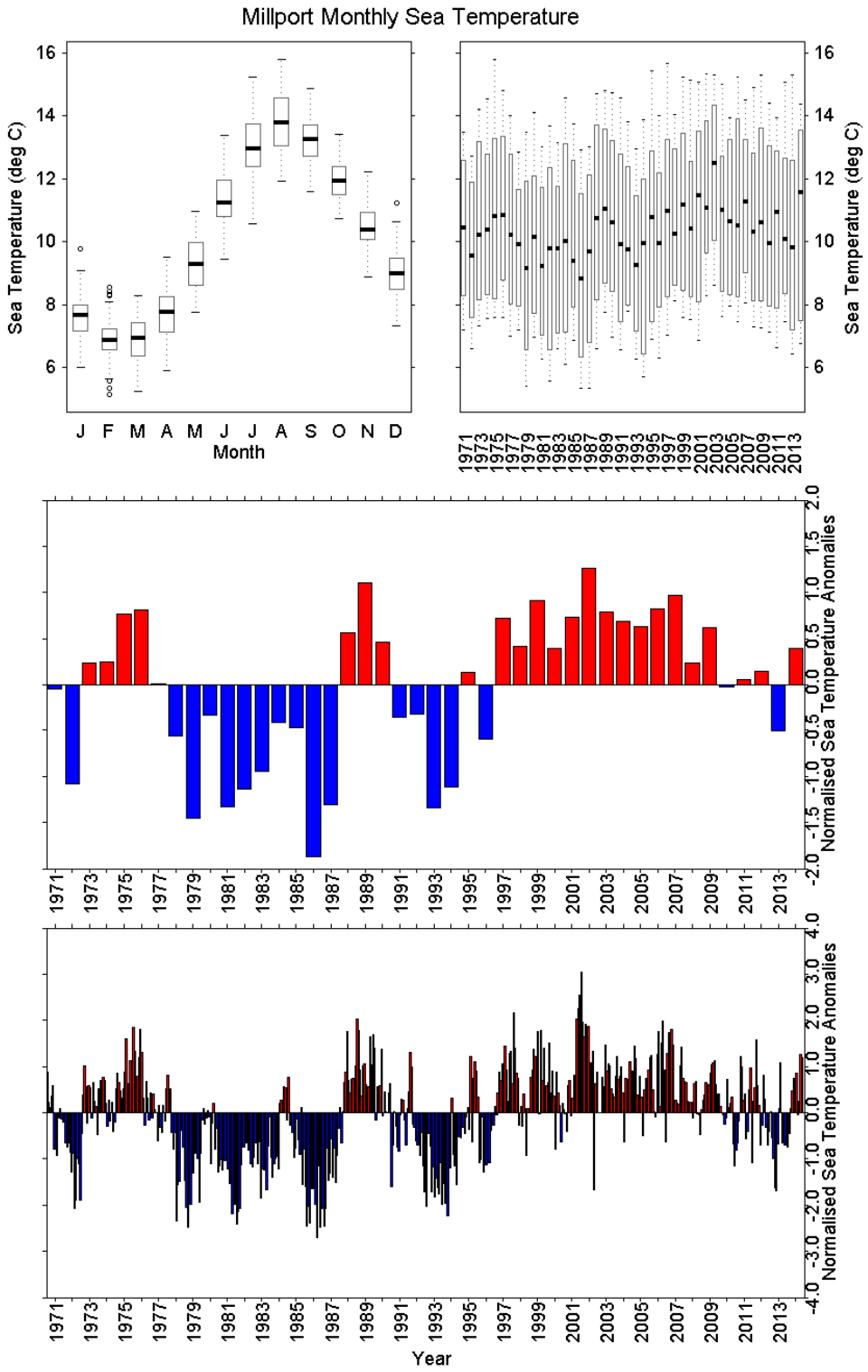

Figure 5.2 Long term variability in sea surface temperature data between 1971 and 2013 at Millport. a) Monthly boxplot of sea surface temperature data. b) Annual boxplot of sea surface temperature data. c) Annual mean anomaly time series d) Monthly mean anomaly time series. Anomalies calculated relative to 1981-2010 base period.

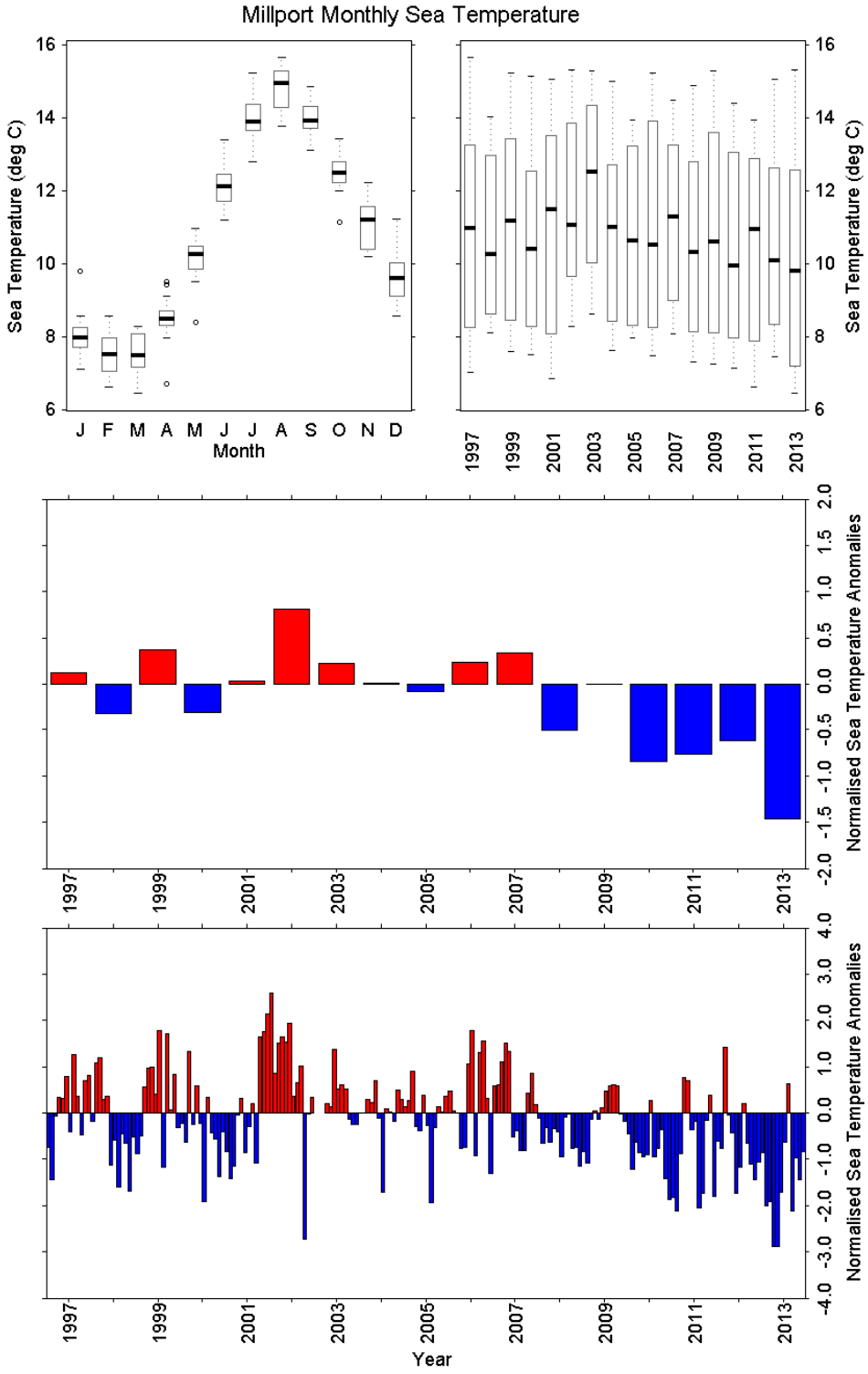

Figure 5.3 Sea surface temperature data from long term monitoring site at Millport (1997 – 2013). a) Monthly boxplot of sea surface temperature data. b) Annual boxplot of sea surface temperature data. c) Annual mean anomaly time series d) Monthly mean anomaly time series. Anomalies calculated relative to 2001-2010 base period.

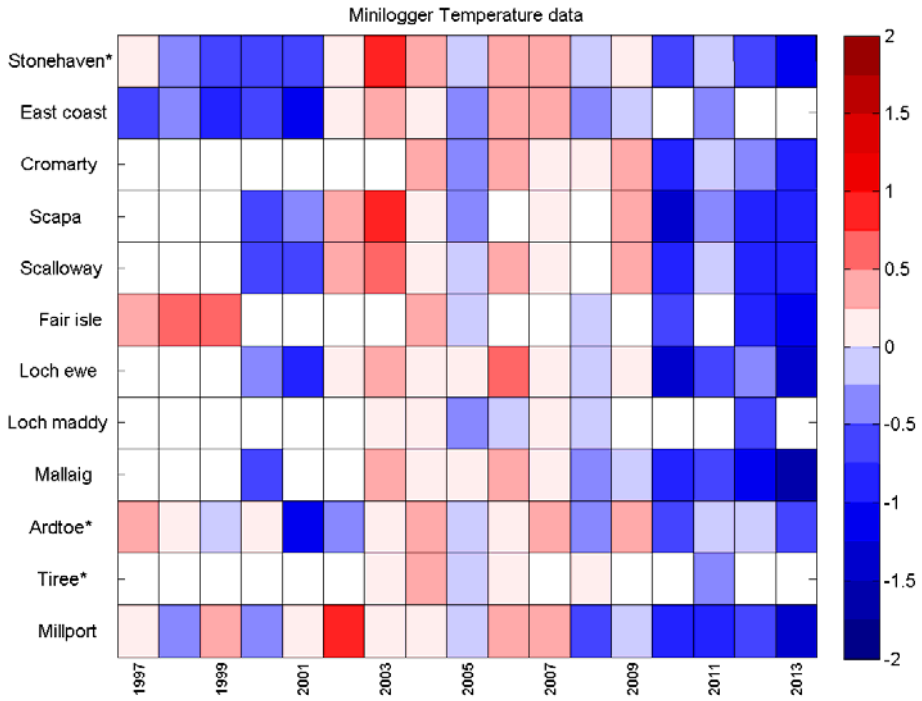

Figure 5.4 Yearly anomalies of sea surface temperature relative to 2001-2010 base period, from minilogger data at nine coastal monitoring sites around the Scottish coast and additional monitoring stations at Ardtoe, Tiree and Stonehaven. Data from the additional stations (marked with *) are included for comparison although these are not minilogger records. The anomalies are normalized with respect to the standard deviation (sd) (e.g. a value of +2 indicates 2 sd above normal). Colour intervals 0.25 sd; reds = positive/warm; blues = negative/cool. See Figure 4.13 for a map supplying more details about the locations in this figure.

5.7 Plots - Temperature and Salinity at the Coastal Monitoring Sites

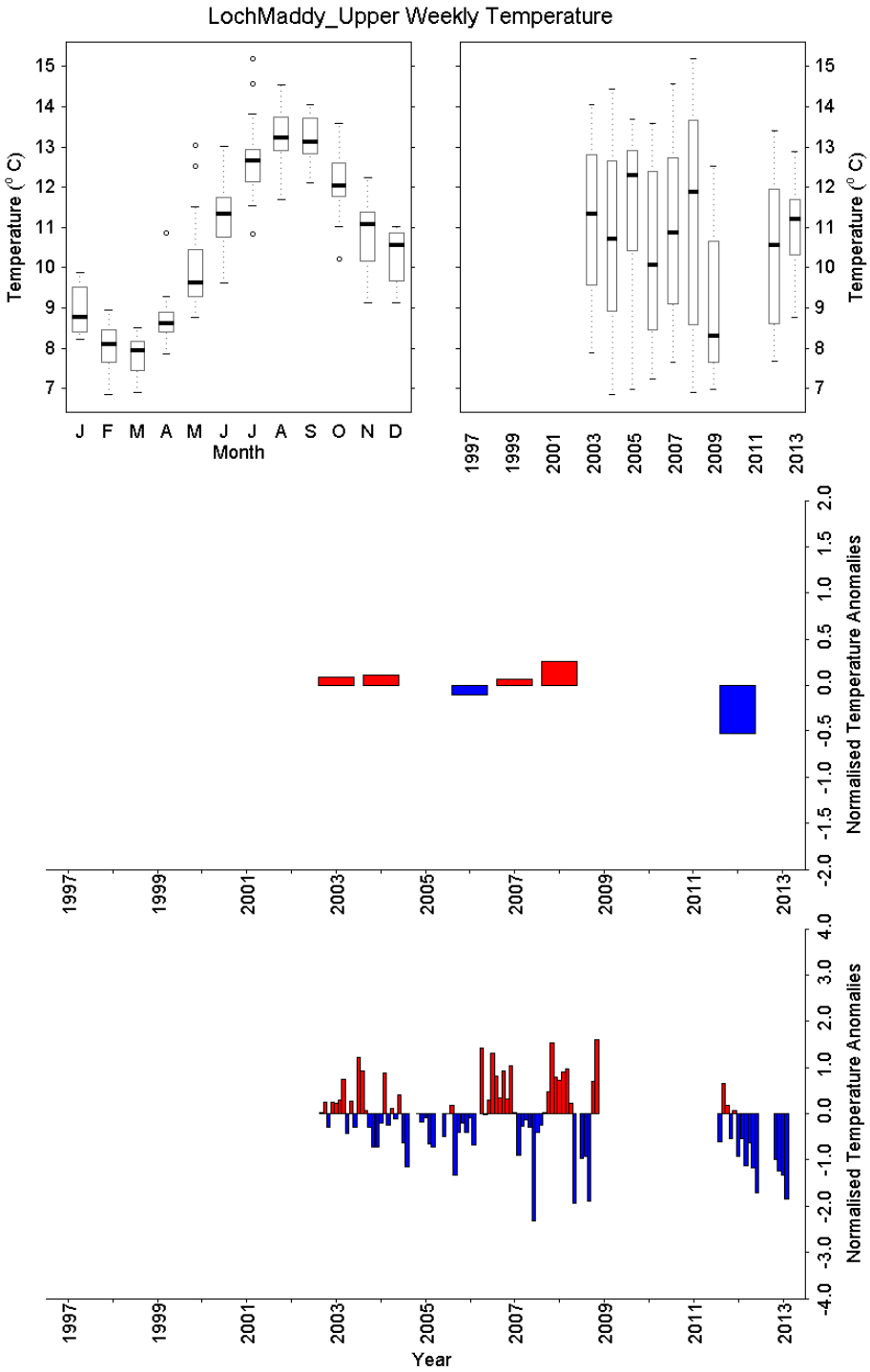

Figure 5.5 Sea surface temperature data from long term monitoring site at Loch Maddy. Data are interpolated to the sample time from hourly temperature records a) Monthly boxplot of sea surface temperature data. b) Annual boxplot of sea surface temperature data. c) Annual mean anomaly time series d) Monthly mean anomaly time series. Data was only available from 2003 to 2013. Only 8 months of data were available in 2005, and 5 months in 2009. In 2010-2011 instrument losses resulted in a large gap in the temperature record. There are also missing data at the end of 2012 and the start of 2013. Anomalies calculated relative to average of all data.

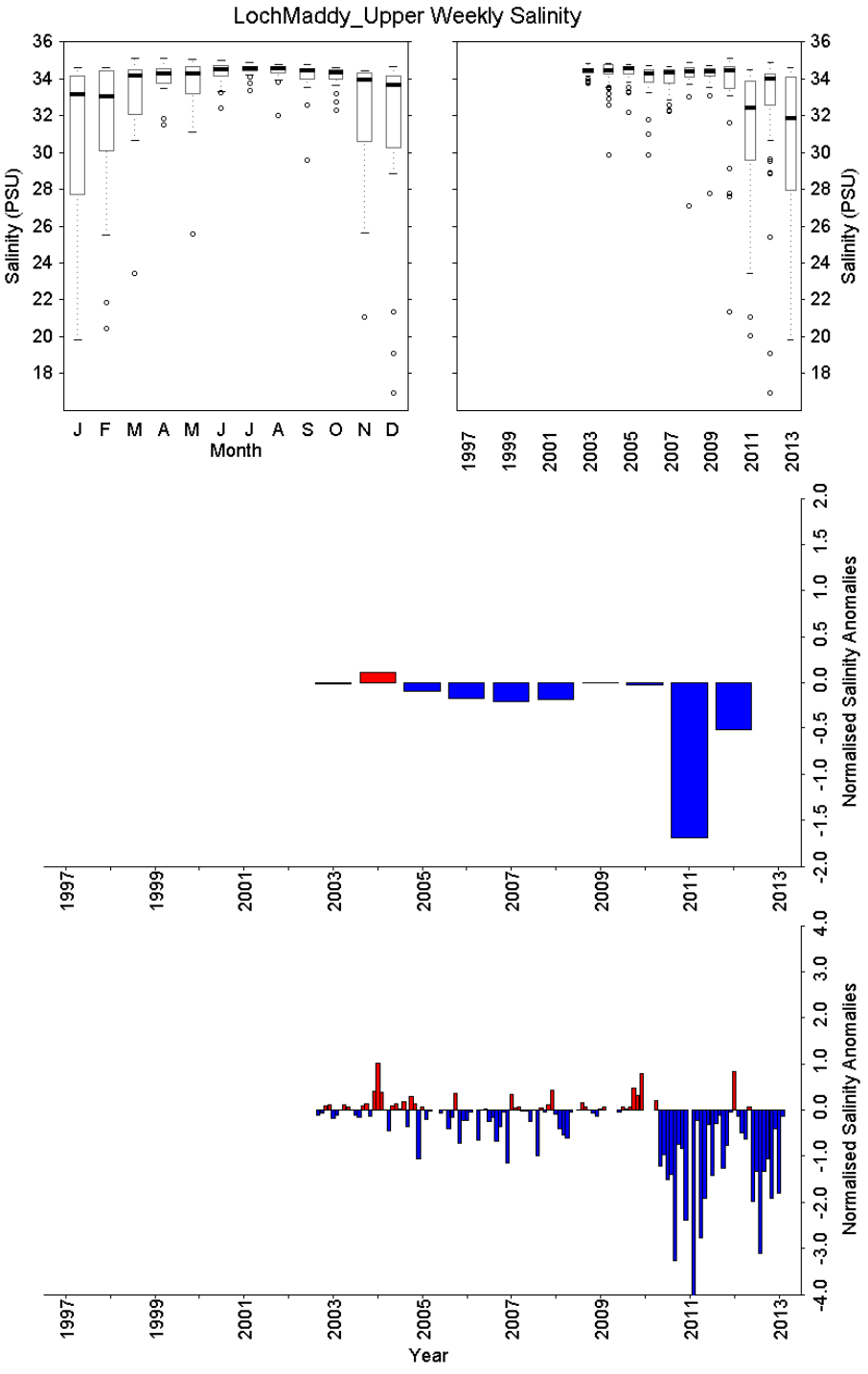

Figure 5.6 Sea surface salinity data from long term monitoring site at Loch Maddy. Data are calculated from discrete weekly samples a) Monthly boxplot of salinity data. b) Annual boxplot of salinity data. c) Annual mean anomaly time series d) Monthly mean anomaly time series. Data were only available from March 2003 to 2013. Sampling at this site was very irregular with missing months in all years except 2004, 2007 and 2012. Anomalies calculated relative to average of all data.

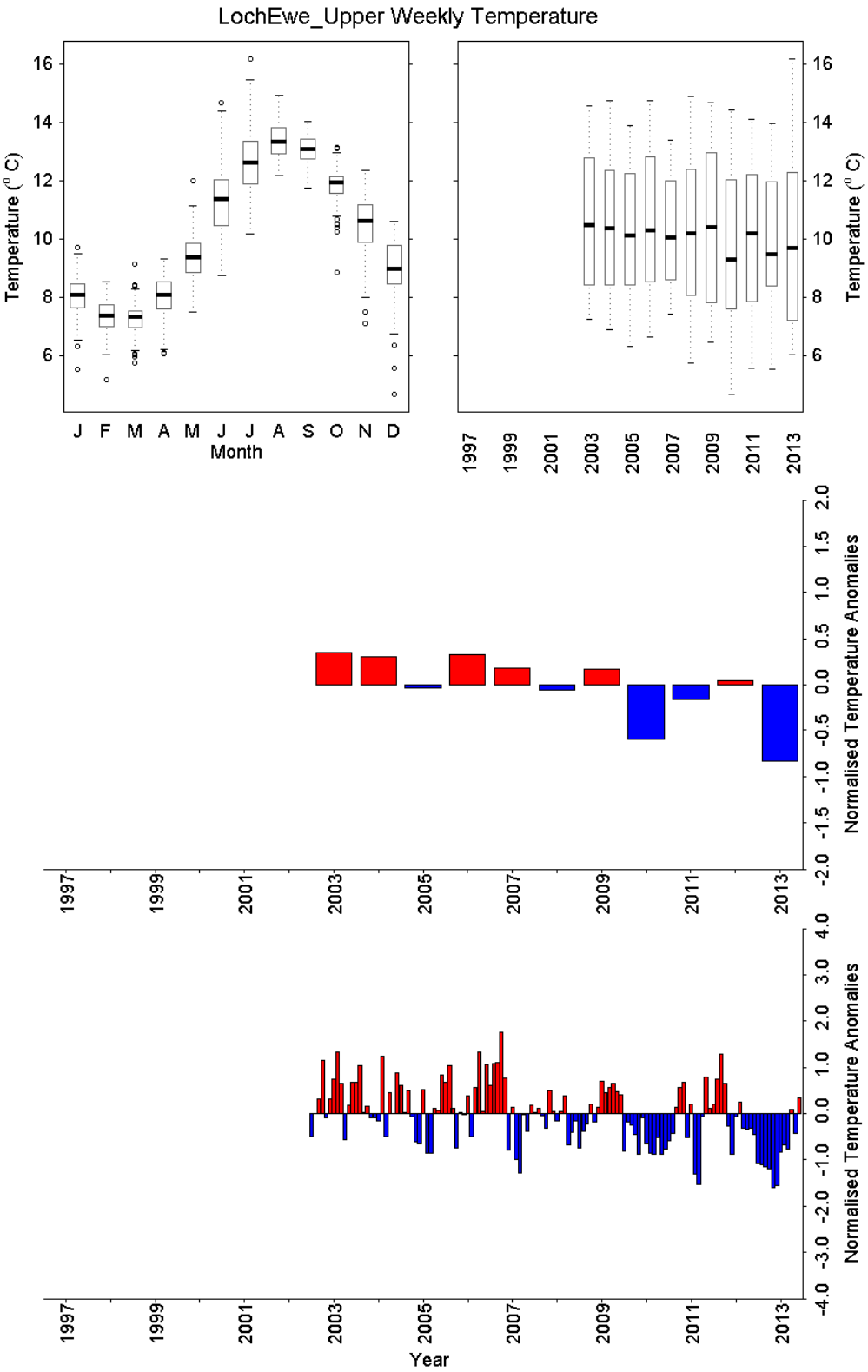

Figure 5.7 Upper layer temperature data (0-10m) from long term monitoring site at Loch Ewe collected using a digital thermometer a) Monthly boxplot of sea surface temperature data. b) Annual boxplot of sea surface temperature data. c) Annual mean anomaly time series d) Monthly mean anomaly time series. Data were only available from 2003 to 2013. Anomalies calculated relative to average of all data.

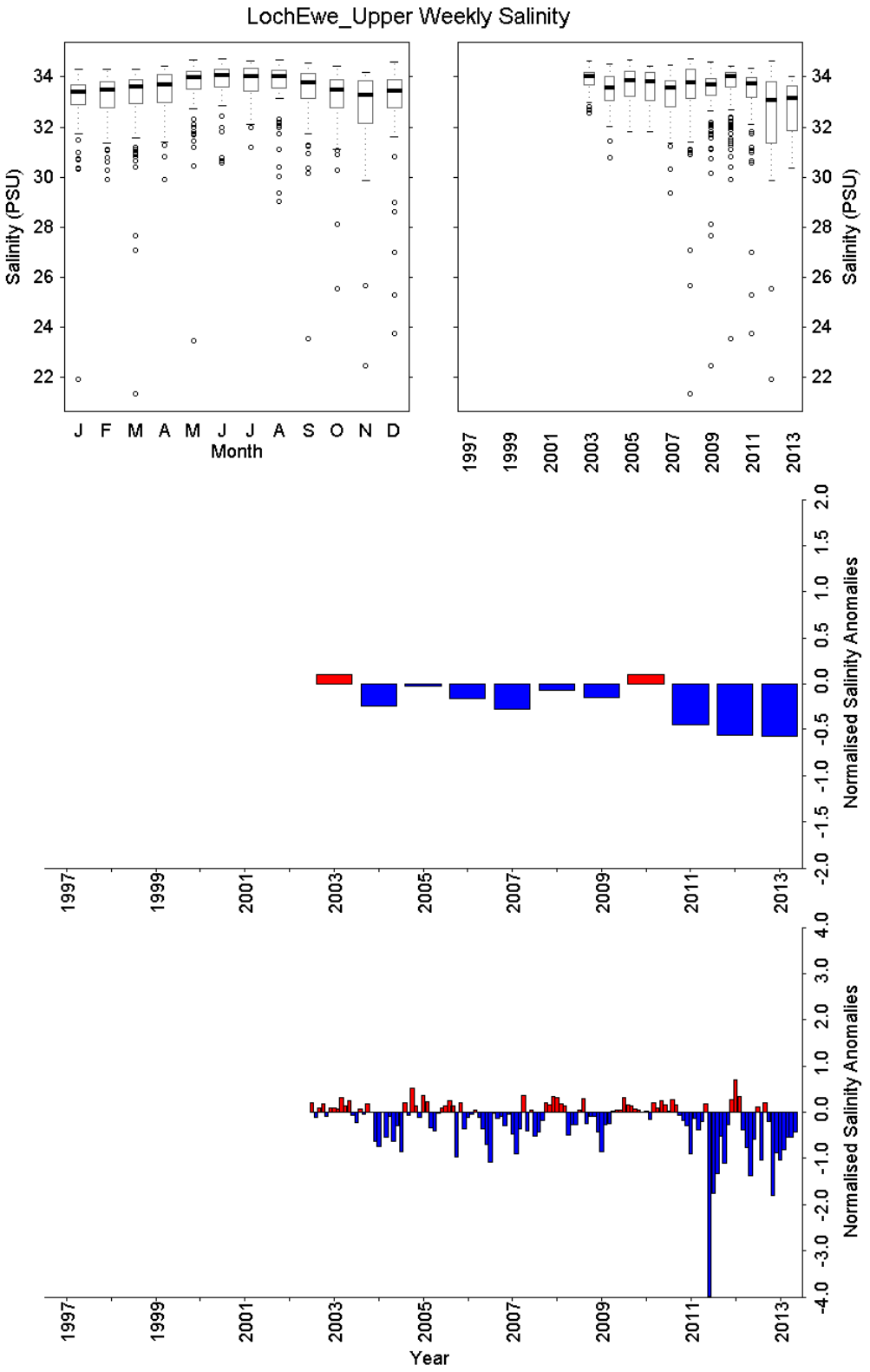

Figure 5.8 Upper layer salinity data (0-10m) from long term monitoring site at Loch Ewe. Data are calculated from discrete weekly samples a) Monthly boxplot of salinity data. b) Annual boxplot of salinity data. c) Annual mean anomaly time series d) Monthly mean anomaly time series. Data were only available from 2003 to 2013. Anomalies calculated relative to average of all data.

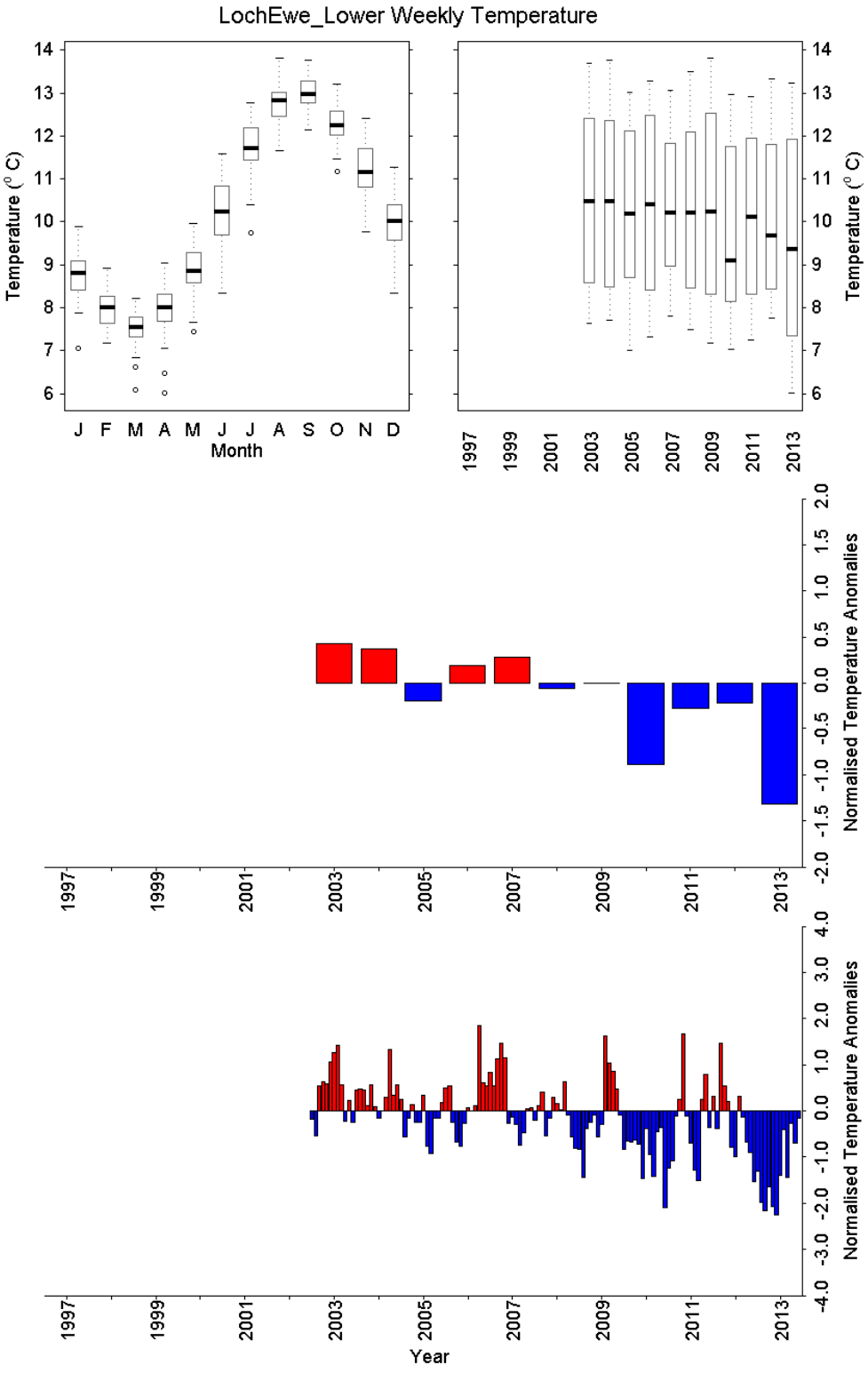

Figure 5.9 Lower layer temperature data (>30m) from long term monitoring site at Loch Ewe collected using a digital thermometer; a) Monthly boxplot of sea surface temperature data. b) Annual boxplot of sea surface temperature data. c) Annual mean anomaly time series d) Monthly mean anomaly time series. Data were only available from 2003 to 2013. Anomalies calculated relative to average of all data.

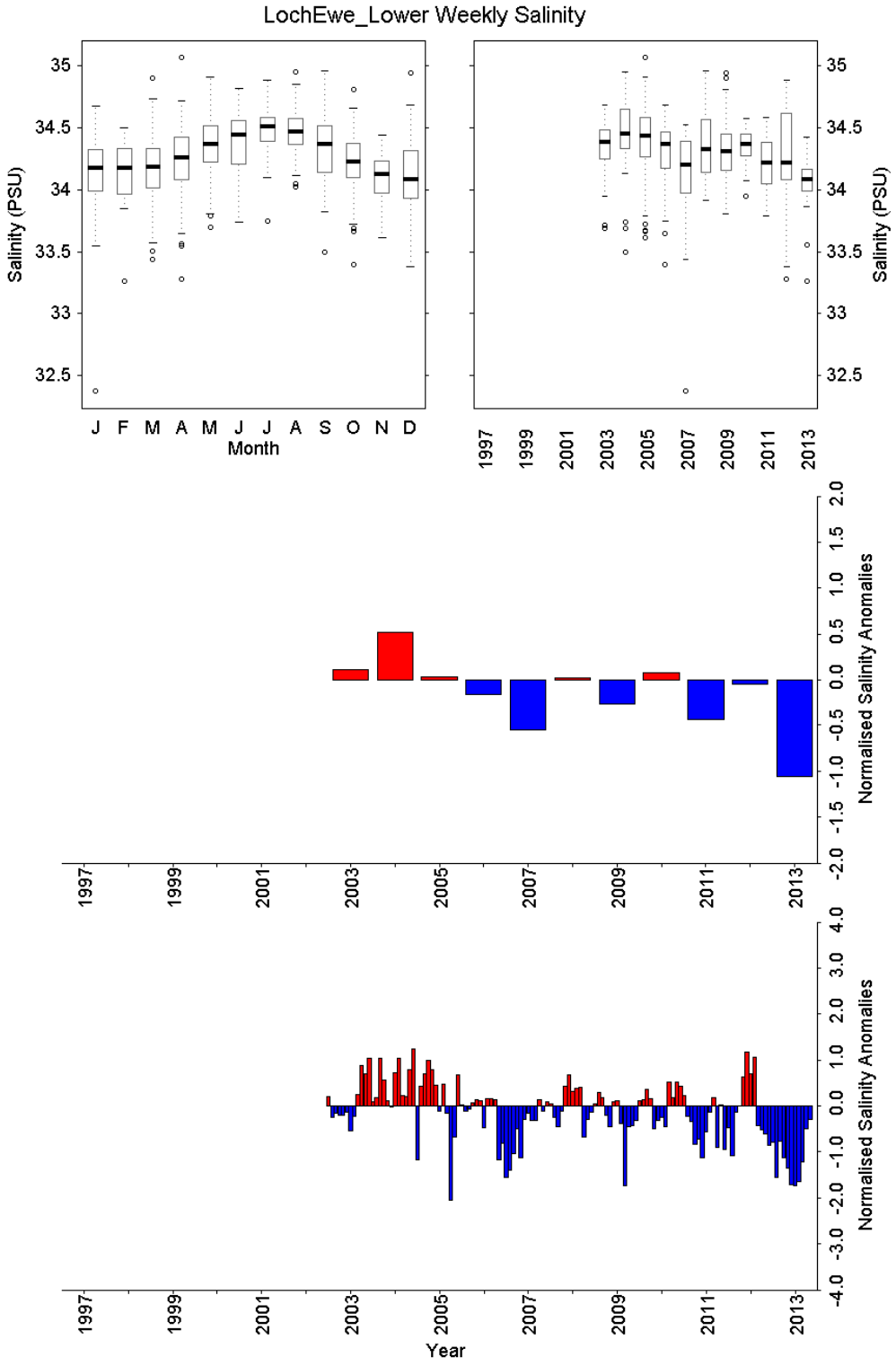

Figure 5.10 Lower layer salinity data (>30m) from long term monitoring site at Loch Ewe. Data are calculated from discrete weekly samples a) Monthly boxplot of salinity data. b) Annual boxplot of salinity data. c) Annual mean anomaly time series d) Monthly mean anomaly time series. Data were only available from 2003 to 2013. Anomalies calculated relative to average of all data.

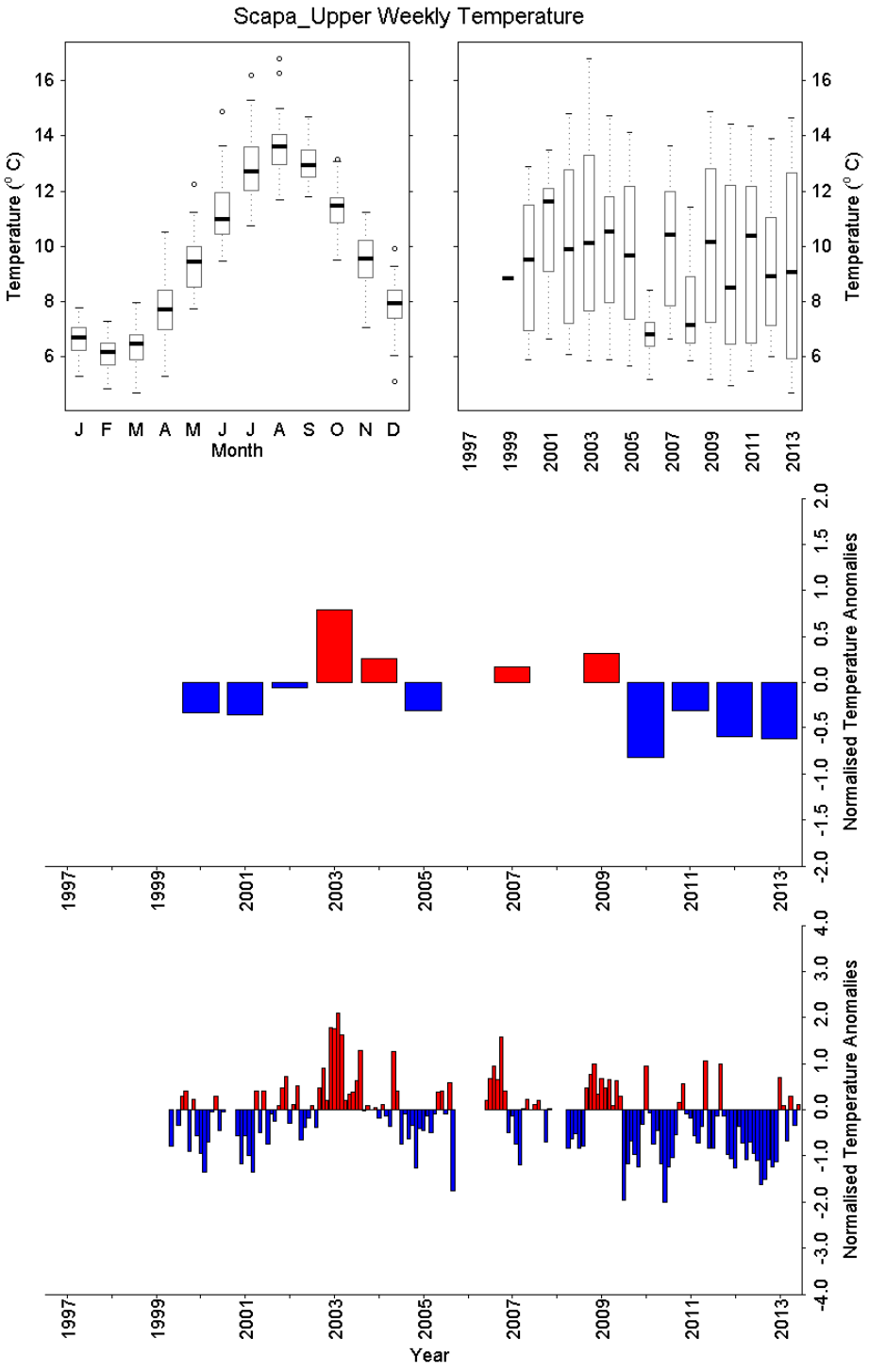

Figure 5.11 Sea surface temperature data from long term monitoring site at Scapa. Data are calculated from discrete weekly samples of temperature at the times that match the other in-situ sampling a) Monthly boxplot of sea surface temperature data. b) Annual boxplot of sea surface temperature data. c) Annual mean anomaly time series d) Monthly mean anomaly time series. The data collection started in November 1999 and only one month of temperature data are available in this year. Records for 2006 and 2008 are incomplete (only 4 months of data in 2006 and 8 months in 2008). Anomalies calculated relative to 2001-2010 base period.

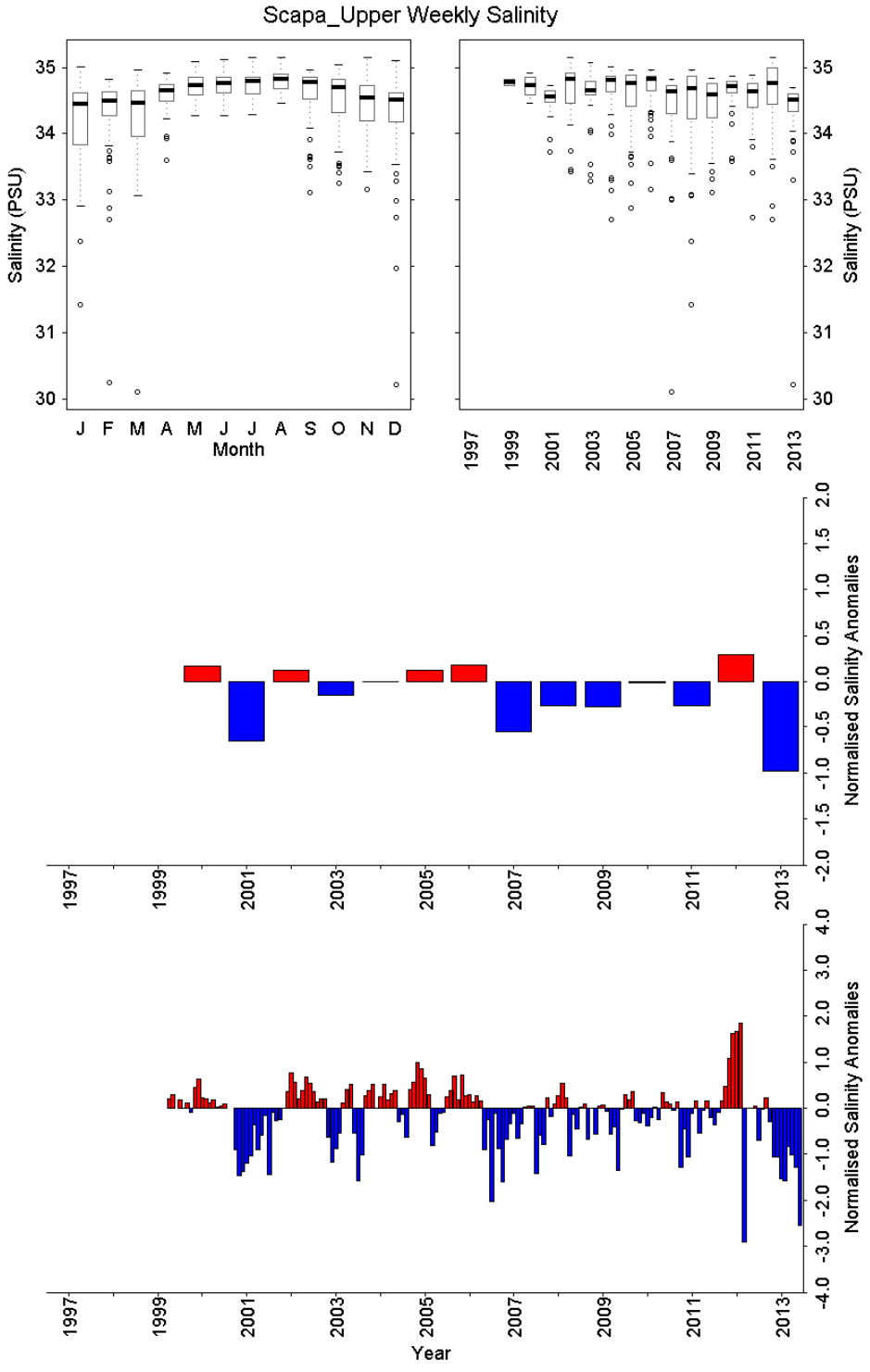

Figure 5.12 Sea surface salinity data from long term monitoring site at Scapa. Data are calculated from discrete weekly samples a) Monthly boxplot of salinity data. b) Annual boxplot of salinity data. c) Annual mean anomaly time series d) Monthly mean anomaly time series. The data collection started in October 1999 and only two months of salinity data are available in this year. Records for 2001 are incomplete with only 10 months of data. Anomalies calculated relative to 2001-2010 base period.

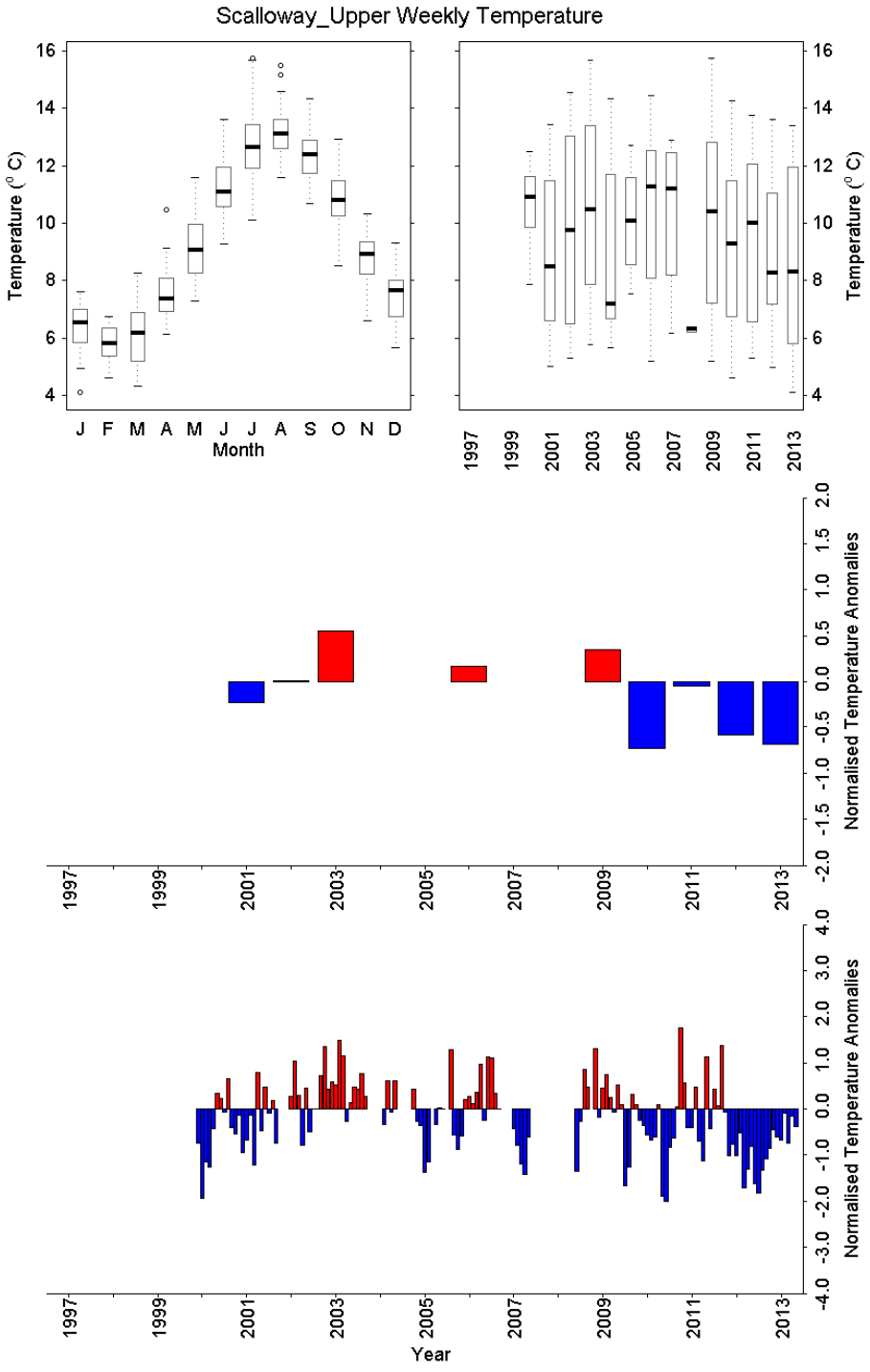

Figure 5.13 Sea surface temperature data from long term monitoring site at Scalloway. Data are calculated from discrete weekly samples of temperature at the times that match the other in-situ sampling a) Monthly boxplot of sea surface temperature data. b) Annual boxplot of sea surface temperature data. c) Annual mean anomaly time series d) Monthly mean anomaly time series. The data collection started in June 2000 and only seven months of salinity data. Anomalies calculated relative to 2001-2010 base period sarah. are available in this year. Records for 2004, 2005 and 2007, 2008 are incomplete (only 8 months of data in 2004 and 2005, 7 months of data in 2007 and 1 month in 2008). Anomalies calculated relative to 2001-2010 base period.

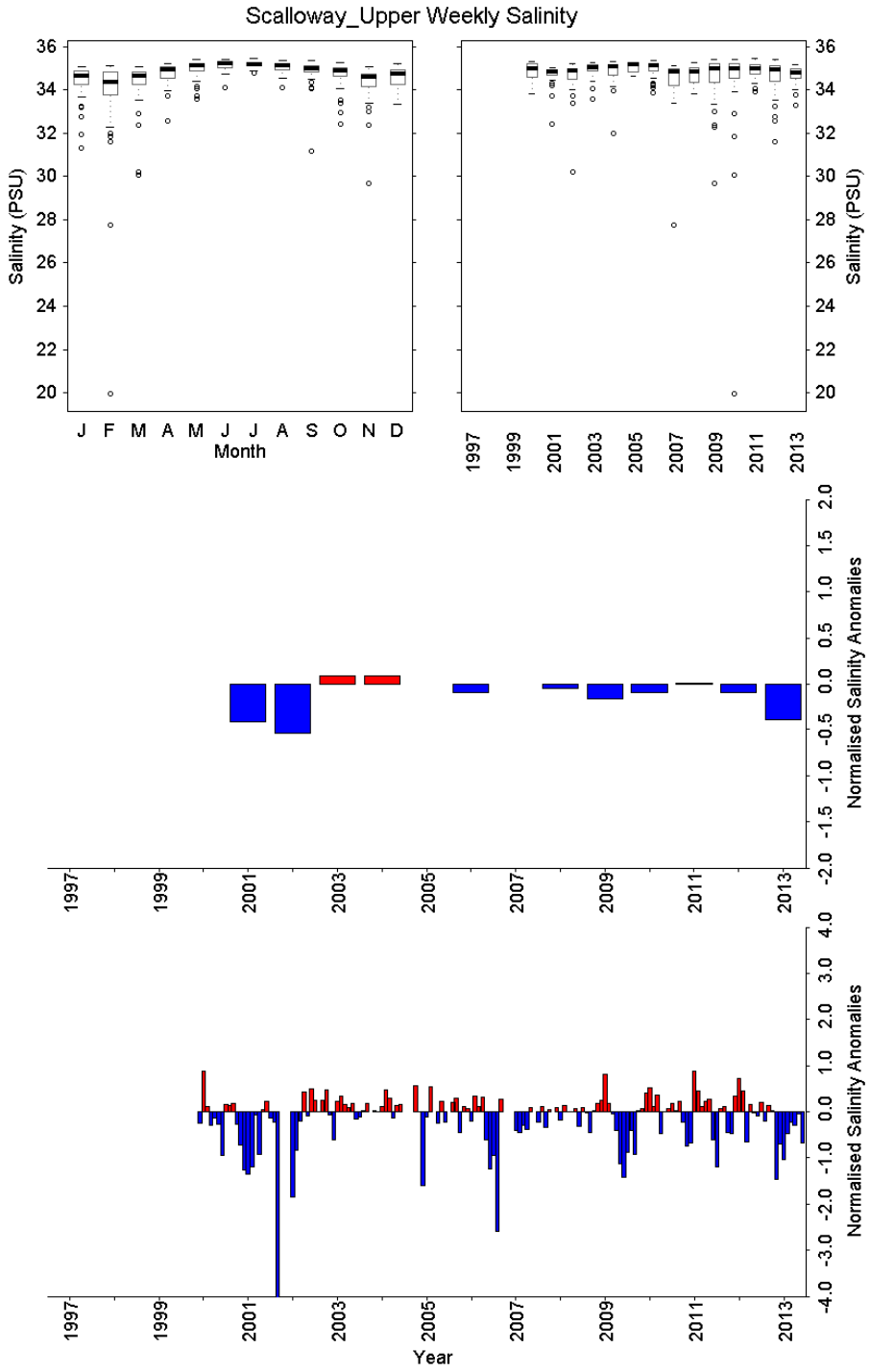

Figure 5.14 Sea surface salinity data from long term monitoring site at Scalloway. Data are calculated from discrete weekly samples a) Monthly boxplot of salinity data. b) Annual boxplot of salinity data. c) Annual mean anomaly time series d) Monthly mean anomaly time series. The data collection started in June 2000 and only seven months of salinity data are available in this year. Records for 2002, 2005, 2007 and 2008 are incomplete. (Anomalies calculated relative to 2001-2010 base period.

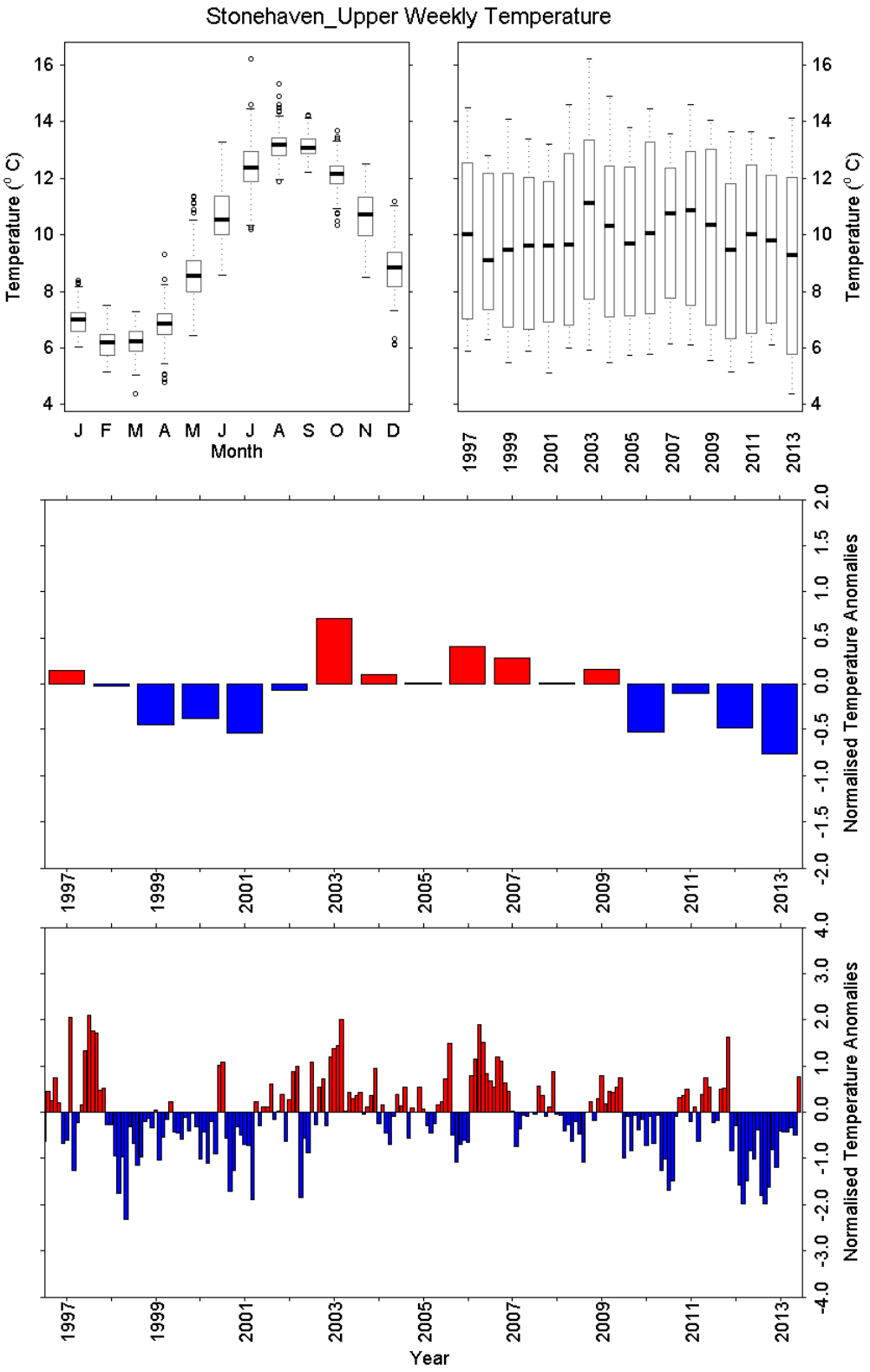

Figure 5.15 Upper layer temperature data (0-10m) from long term monitoring site at Stonehaven collected using a digital thermometer a) Monthly boxplot of sea surface temperature data. b) Annual boxplot of sea surface temperature data. c) Annual mean anomaly time series d) Monthly mean anomaly time series. Anomalies calculated relative to 2001-2010 base period.

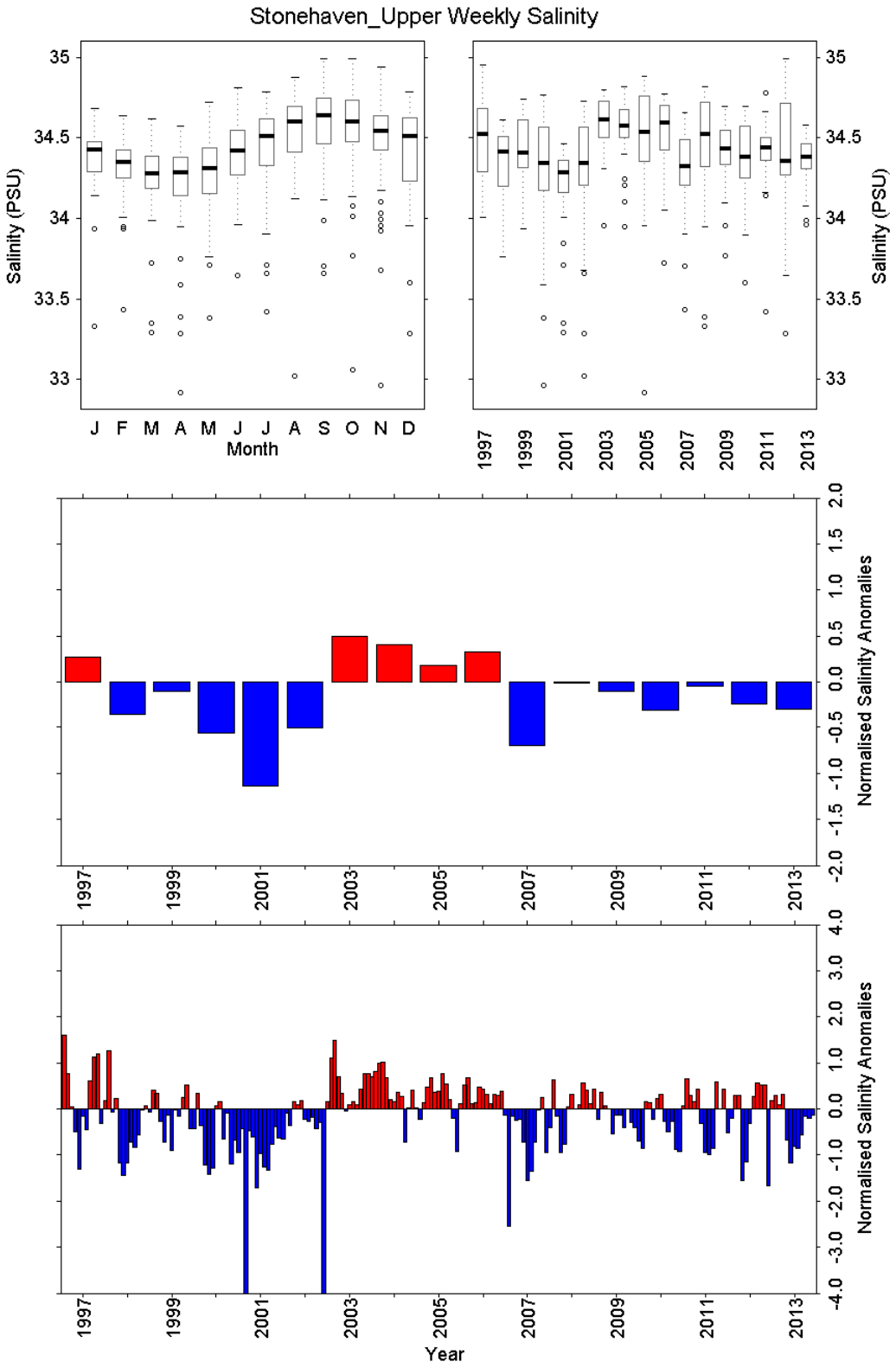

Figure 5.16 Upper layer salinity data (0-10m) from long term monitoring site at Stonehaven. Data are collected using a digital thermometer samples a) Monthly boxplot of salinity data. b) Annual boxplot of salinity data. c) Annual mean anomaly time series d) Monthly mean anomaly time series. Anomalies calculated relative to 2001-2010 base period.

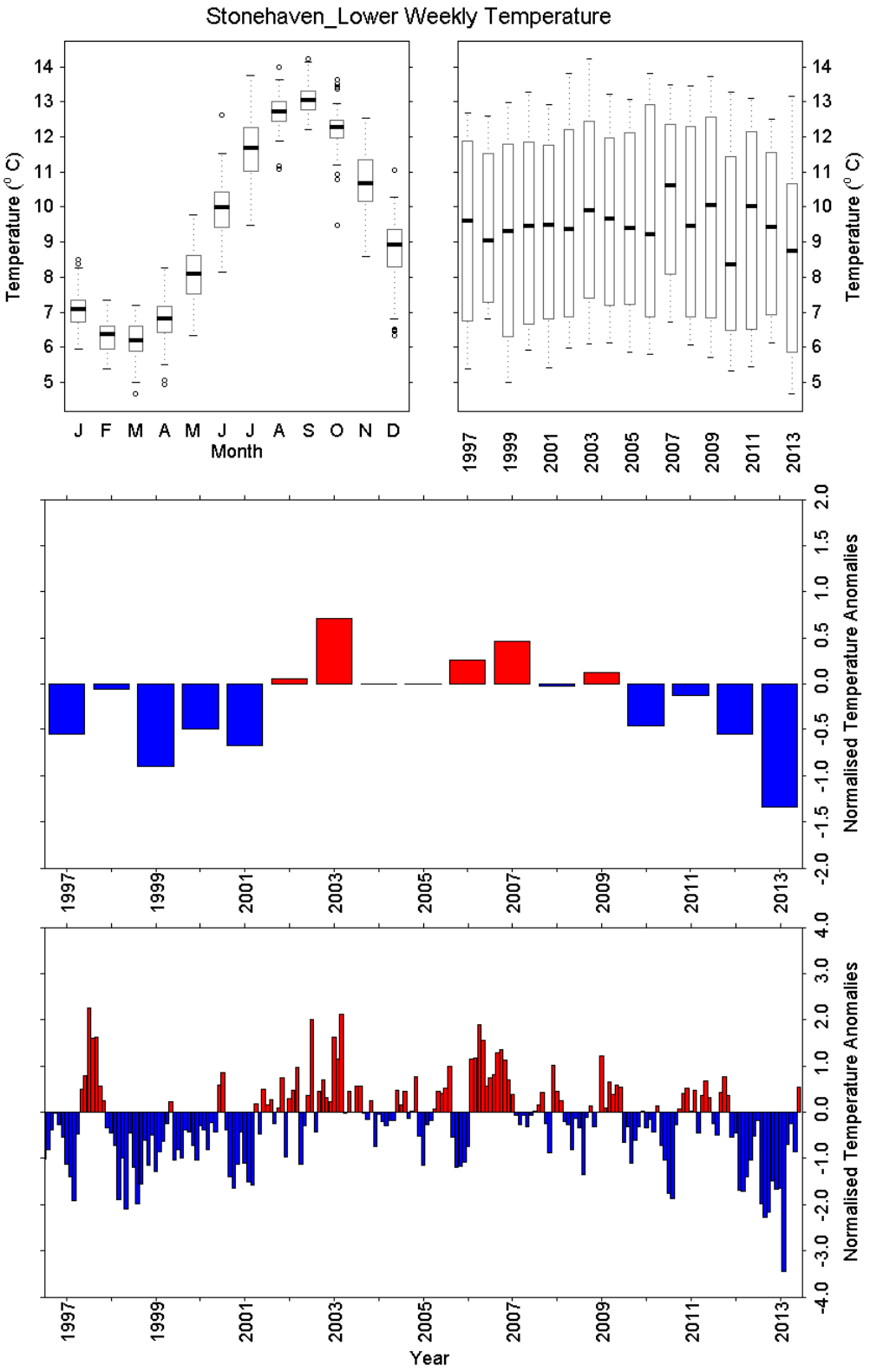

Figure 5.17 Lower layer temperature data (>30m) from long term monitoring site at Stonehaven. Data are collected using a digital thermometer a) Monthly boxplot of sea surface temperature data. b) Annual boxplot of sea surface temperature data. c) Annual mean anomaly time series d) Monthly mean anomaly time series. Anomalies calculated relative to 2001-2010 base period.

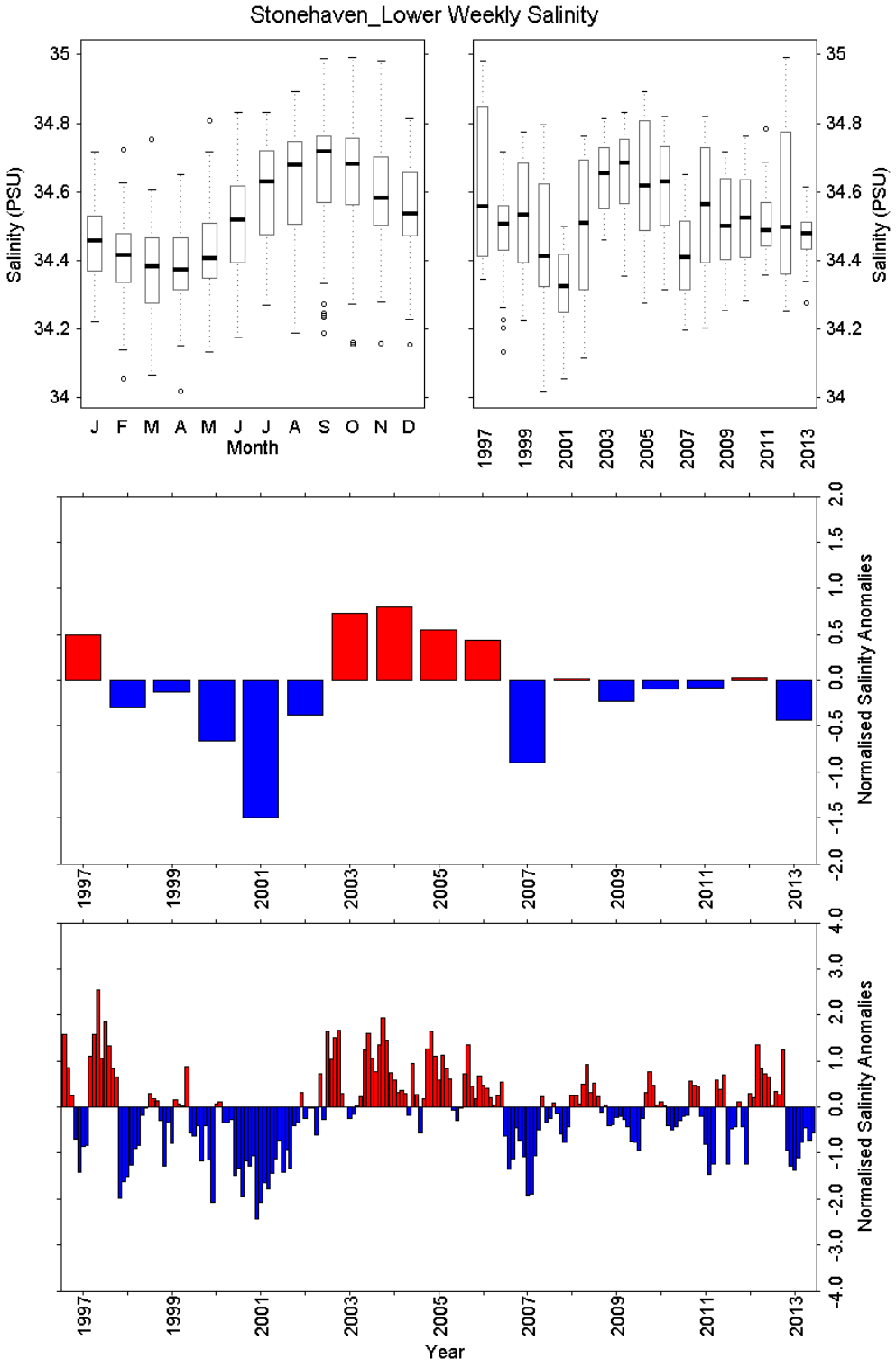

Figure 5.18 Lower layer salinity data (>30m) from long term monitoring site at Stonehaven. Data are calculated from discrete weekly samples a) Monthly boxplot of salinity data. b) Annual boxplot of salinity data. c) Annual mean anomaly time series d) Monthly mean anomaly time series. Anomalies calculated relative to 2001-2010 base period.

6. Secchi Depth

6.1 Introduction

Light availability is one of the primary drivers of primary production in the marine environment. Light availability can be impacted by turbidity in the water column, which can result from sediment resuspended from the sea floor or the biomass of plankton growing in the water column. A simple measure of turbidity in the water column is measured with a Secchi disk (Secchi 1866). A Secchi disk is a black and white disk that is lowered into the water. The depth at which the disk disappears from view is known as the Secchi depth and is indicative of the turbidity in the water column. Suspended sediment, coloured dissolved organic matter or bulk plankton biomass can increase turbidity and reduce Secchi depth measurements (Fleming-Lehtinen and Laamanen 2012). Secchi disk measurements are now being used in a worldwide citizen science project to estimate phytoplankton abundance in the world's oceans (http://www.secchidisk.org/).

6.2 Methods

The disk is lowered over the side of the boat facing away from direct sunlight. The depth at which the Secchi disk disappears from view is recorded. Secchi depth measurements began in 2002 at Stonehaven and 2008 at Loch Ewe.

Data Handling and Quality Control

Secchi data is stored in an access database and all values are checked against paper records to ensure there are no typographic errors.

6.3 Results

Loch Ewe

The Secchi disk depth at Loch Ewe ranges from 3.5 m – 12.5 m. It is at its shortest during the spring bloom period in April when chlorophyll 'a' concentration in the water column is at its maximum.

Stonehaven

Secchi disk depth at Stonehaven ranges from 2.0 m – 14.0 m. It is at its shortest during the winter months. As chlorophyll 'a' concentrations are low during this time this suggests that resuspended sediment is present in the water column. Secchi depth increases during the summer months.

Discussion

A comparison of the median spring time Secchi depth at both sites shows that it is approximately 1 m greater at Loch Ewe than at Stonehaven. This suggests that turbidity is less in Loch Ewe. This reduced turbidity increases the amount of light available for phytoplankton cells to utilize and is thought to influence the earlier development of the spring diatom bloom at the Loch Ewe site (Bresnan et al., 2015).

6.4 Summary – Secchi Depth

- Secchi disk data is presented from Stonehaven (12 years) and Loch Ewe (6 years).
- Monthly means vary between 3.5 m – 12.5 m and 2 m – 14 m at both sites, with a contrasting seasonal cycle observed.
- Minimum secchi depths are observed in April, May and June in Loch Ewe suggesting light transmission may be most influenced by phytoplankton biomass.
- At Stonehaven minimum secchi depths are recorded in December, January and February suggesting that suspended sediment influences light transmission in the watercolumn at this site.

6.5 References – Secchi Depth

Bresnan, E., Cook, K., Hughes, S., Hay, S., Smith, K., Walsham, P., Webster, L. (2015) Seasonality of the plankton community at an east and west coast monitoring site in Scottish waters. Journal of Sea Research, 105,16-29.

Fleming-Lehtinen, V. and Laamanen, M. (2012) Long-term changes in Secchi depth and the role of phytoplankton in explaining light attenuation in the Baltic Sea. Estuarine and Coastal Shelf Science, 102-103, 1 – 10.

Secchi, A. (1866) Relazione della Esperienze Fatta a Bordo della Pontificia Pirocorvetta L'Immacolata Conceziorze per Determinare La Transparenza de1 Mare (Reports on Experiments made on Board the Papal Steam Sloop L'Immacolata Concezione to Determine the Transparency of the Sea). From Cmdr. A. Cialdi, Sul moto ondoso de1 mare e su le correnti di esso specialment auquelle littorali (second ed.) Dep. of the Navy, Office of Chief of Naval Operations (1866) ON1 Transl. A-655, Op-923 M4B., pp. 258–288 (in Italian).

6.6 Plots – Secchi Depth

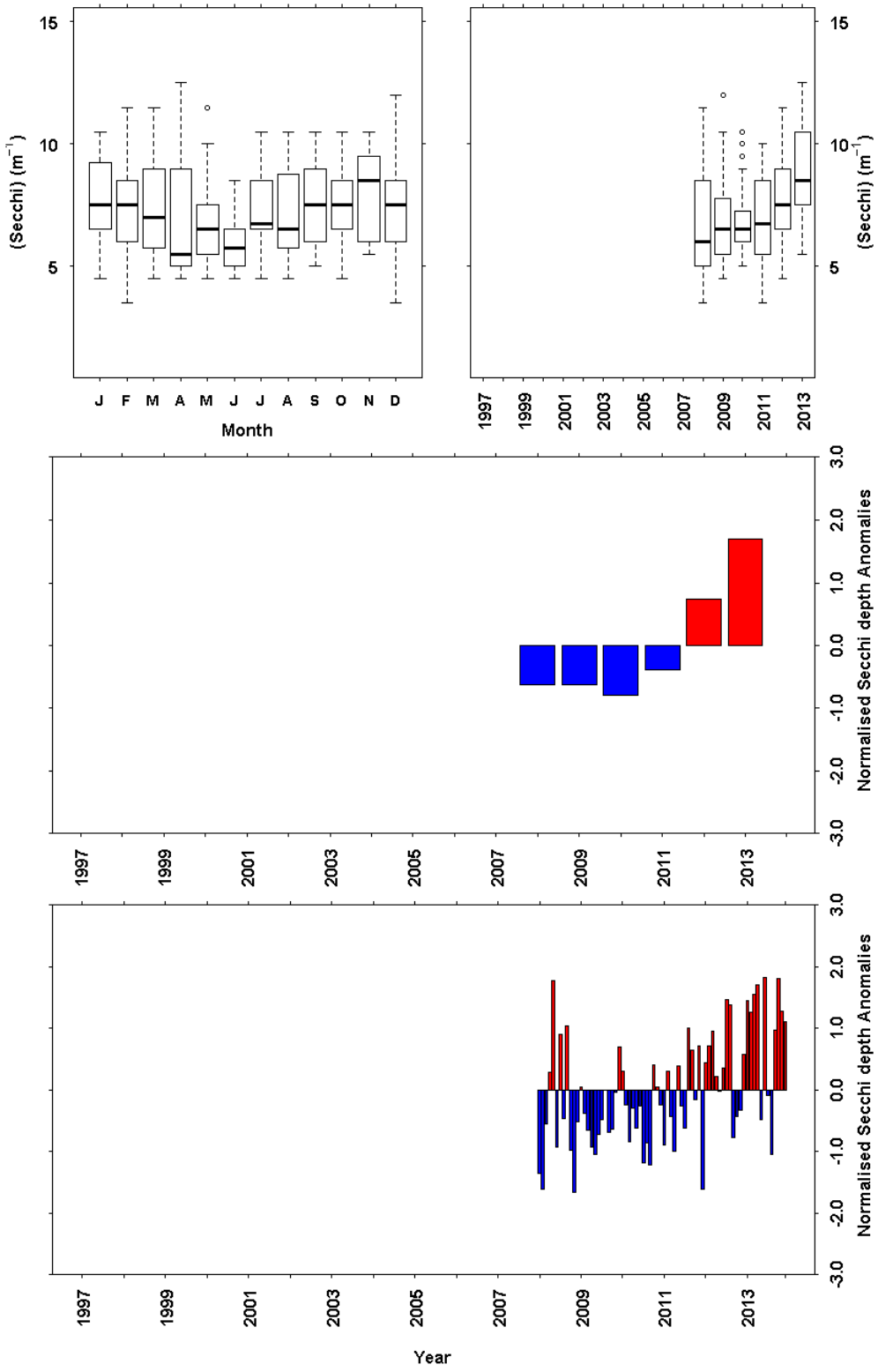

Figure 6.1 Secchi depth (m) from the long term monitoring site at Loch Ewe. a) Monthly boxplot of Secchi depth. b) Annual boxplot of Secchi depth. c) Annual mean anomaly time series d) Monthly mean anomaly time series. Sampling for Secchi depth began in 2007. Anomalies calculated relative to average of all data.

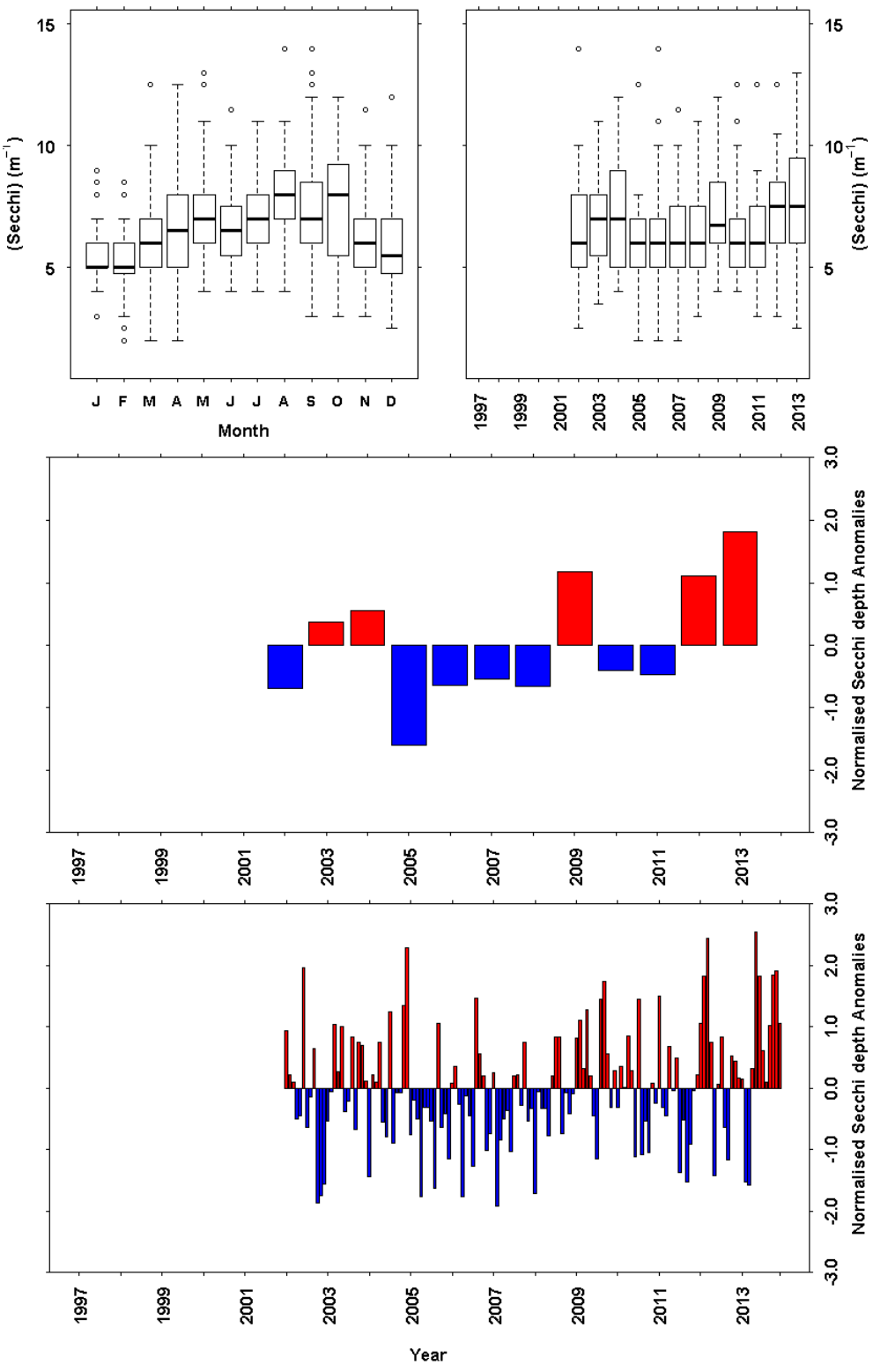

Figure 6.2. Secchi depth (m) from the long term monitoring site at Stonehaven. a) Monthly boxplot of Secchi depth. b) Annual boxplot of Secchi depth. c) Annual mean anomaly time series d) Monthly mean anomaly time series. Sampling for Secchi depth began in 2002. Sampling for Secchi depth began in 2007. Anomalies calculated relative to average of all data.

7. Inorganic Nutrients

7.1 Introduction

A limiting factor on the growth of primary producers in the marine environment is the availability of inorganic nutrients. Dissolved inorganic nitrogen (DIN), dissolved inorganic phosphorus (DIP) and dissolved silicate (DSi) are the three most commonly limiting nutrients. Anthropogenic sources of nitrogen and phosphorous, including agricultural run-off and domestic and industrial waste disposal can result in elevated nutrient concentrations, particularly in coastal waters. In Scotland, highest inputs of nitrate are on the east coast from agricultural run-off and inputs of phosphate and ammonia are highest from urban areas in the east and west (Baxter et al., 2011). The main source of silicate in the marine environment is from the weathering of rocks, therefore local geology will influence silicate concentrations. Nutrient enrichment may result in eutrophication where waters have low dissolved oxygen and can be of poor quality.

The Marine Strategy Framework Strategy (MSFD) sets out eleven qualitative descriptors against which Good Environmental status (GES) should be assessed. Descriptor 5 (Eutrophication) states that 'Human-induced eutrophication is minimised, especially adverse effects thereof, such as losses in biodiversity, ecosystem degradation, harmful algal blooms and oxygen deficiency in bottom waters'. One of the common indicators for the MSFD Descriptor 5 is 'Winter nutrient concentrations'. In the UK, a two-tiered approach will be used for Descriptor 5 targets and indicators. In areas designated non-problem areas under the OSPAR Common Procedure (OSPAR, 2013) there should be 'no increase in the assessed DIN or DIP concentration resulting from anthropogenic nutrient input'. In OSPAR problem areas the UK MSFD target is 'for a downward trend in DIN and DIP resulting from decreasing anthropogenic nutrient input over a ten year period'. Progress towards these targets is to be assessed using data from periodic surveys (at least once per MSFD reporting cycle of 6 years).

An assessment of the eutrophication status of the OSPAR area was undertaken in 2008, as required for the OSPAR Joint Assessment and Monitoring Programme (JAMP) (OSPAR, 2008). All Scottish open coastlines were classed as non-problem areas and, therefore, there should be no increasing trends for DIN and DIP if is GES is to be achieved for Descriptor 5.

OSPAR Ecological Quality Objectives (EcoQOs) for nutrient enrichment in the UK have been developed for dissolved inorganic nitrogen (DIN; the sum of the concentration of Total Oxidised Nitrogen (TOxN) and ammonia) in coastal waters (defined as having salinities between 30 and 34.5) and offshore waters (salinities greater than 34.5 - Table 7.1). The elevated concentrations are defined as 50% above the background concentration for DIN (OSPAR, 2013; Cefas, 2008). The coastal criteria requires DIN concentrations to be normalised to a salinity of 32 by assuming conservative mixing along a constant gradient with a 0 salinity endpoint of 42 µM (Devlin et al., 2007). This freshwater value was determined in the river Leven in Cumbria, UK, and was assumed to be representative of a relatively unpolluted rural river system. The offshore criteria are for non-normalised DIN concentrations. Smith et al., (2014) proposed new background concentrations for TOxN in Scottish

coastal and offshore waters, taking into account that Scottish shelf sea waters are depleted in TOxN relative to oceanic waters (Table 7.1). The ammonia contribution to the DIN concentration in offshore water was considered negligible (Smith et al., 2014) and therefore there should be little difference between DIN and TOxN concentrations.

Table 7.1 Proposed (Smith et al., 2014) and current background (OSPAR, 2013) and elevated TOxN/DIN concentrations derived using Minches and Malin Sea data.

Area	Proposed (TOxN) (µM)		Current (DIN) (µM)	
	Background	Elevated	Background	Elevated
Offshore	7.5	10.5	10	15
Coastal	9.5	14.25	12	18

7.2 Methods

Collection and Storage of Sea Water Samples

Water samples for nutrients at four depths (1 m, 5 m, 10 m & 45 m at Stonehaven and 1 m, 5 m, 10 m and 35 m at Loch Ewe) were collected using a Niskin Sampling bottle, which was also fitted with a digital reversing thermometer. At all other sites surface water samples only were collected.

Samples for nitrate and phosphate were stored in glass bottles at -20^{o}C and allowed to thaw for 24 hours before analysis. Samples for silicate analysis were stored in plastic bottles and either stored in a refrigerator maintained between 0 and 8^{o}C (1997 - 2010) or at -20^{o}C (2011 onwards). Refrigerated samples were allowed to come to room temperature before analysis while frozen samples were thawed in the dark for 48 hours to allow for depolymerisation.

Determination of TOxN, PO_4 and DSi

Water samples were analysed for DIP, TOxN and DSi by colorimetry using a continuous flow analysis (CFA) system based on the techniques of Armstrong et al., (1967) for oxidised nitrogen (nitrate plus nitrite), Murphy and Riley (1962) for PO_4 and Koroleff (1971) for DSi. Samples collected prior to 2002 were analysed using a Skalar system. From 2002-2006 a Bran and Luebbe Analyser (AA3) and from 2006 a Bran and Luebbe QuAAtro (SEAL Analytical, UK) was used. Aliquots of each sample (5 ml) were aspirated using an auto-sampler and transmitted through the complete system by a peristaltic pump. The sample stream was split with a pump continuously adding the reagents required to each sample stream using tubes of a specific internal diameter. Air bubbles are evenly pumped through each stream to reduce inter-sample dispersion and improve sample throughput. Once the chemical reaction to allow detection was complete each stream flowed through a specific detector. Concentrations were determined with the wavelengths set at 520 nm for TOxN and at 880 nm and 820 nm for PO_4 and DSi, respectively. Dual-beam operation with same-wavelength compensation gives low drift, even at very high sensitivities. Data was collected as an analogue voltage that was fed through a digitising interface to a computer and analysed using either the Bran & Luebbe data

processing package Versions 5.31 – 6.02 or with the Skalar data processing package Version 6. Further details of the methodology can be found in Webster et al., (2007), Rose et al., (2009) and Smith et al., (2014).

Determination of Ammonia

Samples were analysed for ammonia using a manual method. Buffer solution was added to the samples to prevent the precipitation of calcium and magnesium hydroxides, followed by the phenol catalyst and an oxidising agent (dichloro-s-2,4,6-trione). Samples were then incubated and exposed to UV light for at least 40 minutes. In the presence of the phenol catalyst and excess chlorine, ammonia reacts with phenol to form indophenol blue, which was determined calorimetrically at 630 nm using a spectrophotometer. Further details of the methodology can be found in Webster et al., (2007) and Rose et al., (2009).

Data Handling

Since 2012 all nutrient data and the sample information from the Oceanography Environmental Record sheets is held on LIMS. Prior to 2012 nutrient data was saved by analytical Batch number on a shared folder on the internal computer system and in-house developed data base (Chemdat). Nutrient data was sent to the MSS Oceanography Group who would add the nutrient data on to their own databases along with the sample information.

Quality Control

A system suitability standard (highest calibration standard) was analysed each day using the CFA. Calibration standards covering the range 0.2-19.3 µM for TOxN, 0.2-13.3 µM for DSi, 0.05 - 5 µM for PO_4 were analysed at the start and the highest concentration analysed at the end of each batch, to account for drift. In both cases correlation coefficients of at least 0.999 were achieved for all nutrients. The limits of detection were dependent on the instrument used and were based on 4.65 times the standard deviation of the mean value from repeat analysis of ten low standards and can be found in Webster et al., (2007), Rose et al., (2009) and Smith et al., (2014).

Calibration standards, covering the range 0.2 to 10.00 µM for ammonia, were prepared in low nutrient sea water (LNSW) and analysed with each batch. The absorbance readings were used to compute the calibration curve. Correlation figures of at least 0.995 were achieved. The limit of detection (LoD), based on 4.65 times the standard deviation of the mean value from repeat analysis of ten low standards was 0.19 µM.

Prior to 2010, QUASIMEME sea water samples were used as reference materials, whilst from 2010 onwards reference standards were prepared from standards procured from OSIL (Havant, Hampshire, UK). The data obtained from the reference samples were plotted on Shewhart charts with warning and action limits drawn at ± 2 x and ± 3 x the standard deviation of the mean. Further quality control was assured through successful participation in the nutrient programme of QUASIMEME (Quality Assurance of Information for Marine Environmental Monitoring in Europe). All methods are accredited by the United Kingdom Accreditation Service (UKAS).

Data assigned a Quality Flag of 3 or 4 ("probably bad" and "bad" – see Section 2.8) were excluded from the assessment. Phosphate data from water samples collected from Stonehaven and Loch Ewe in 2004, 2005 and 2006, from Scapa and Loch Maddy in 2006, and from Scalloway in 2003 and 2006 were not included in the data assessment as this data was assigned a Quality Flag of 4. In these years phosphate concentrations tended to be higher than expected for the seasonal cycle. However, there was no obvious explanation for this; the analytical quality control (internal QC and external proficiency testing QC) was acceptable during this time period. Ammonia data from samples collected between 2006 and 2009 inclusive were also assigned a Quality Flag of 4. The analysis during this period was undertaken on the Bran & Luebbe QuAAtro analyser with detection with a digital colorimeter, although the internal analytical quality control was acceptable external proficiency QC indicated a potential problem with the technique. The data from this period were therefore excluded from the data assessment.

7.3 Results

Loch Maddy

Total oxidised nitrogen (TOxN), dissolved inorganic phosphorus (DIP) and dissolved silicate (DSi) were measured in surface waters at Loch Maddy between 2003 and March 2010. TOxN, DIP and DSi concentrations are shown as monthly and yearly boxplots (Figures 7.1-7.3). The monthly boxplots for DIP, TOxN and DSi show seasonal trends in both the surface and bottom waters. Concentrations are lowest, often below detection limits for all three nutrients, in the summer months (May to August) and highest in winter (November to February). Low light intensities and high turbulence ensure that phytoplankton numbers are minimal during the winter so nutrients tend to accumulate, reaching a maximum prior to the start of the growing season. DIP concentrations rarely exceeded 0.6 µM and winter (November to February) annual averages ranged from 0.33 µM to 0.50 µM. TOxN winter annual means ranged from 4.95 µM to 6.41 µM and DSi from 3.70 µM to 5.31 µM. Winter DSi concentrations at Loch Maddy were similar to Loch Ewe, Stonehaven, Scapa and Scalloway. TOxN and DIP concentrations were similar to Loch Ewe, but significantly lower than Scalloway, Scapa and Stonehaven (ANOVA with Tukey's pair-wise comparisons, $p<0.005$). Nutrient concentrations have previously been shown to be low in the Minches and Malin Sea as it is shielded by the Outer Hebrides against the inflow of Atlantic water from the west and local inputs of freshwater do not appear to be an important source of nutrients (Smith et al., 2014).

The Loch Maddy site is in a non-problem area and therefore there should be no increasing trends in DIN or DIP concentrations. Yearly boxplots showed no significant temporal trend for any of the nutrients. Concentrations were highest in 2009 and 2010 as only winter nutrients were included in the boxplots, in 2009 only January and February data was used, all other months had a Quality Flag of 4, and in 2010 only samples collected between January and March were analysed for nutrients.

Ammonia was not measured at Loch Maddy and therefore TOxN (normalised) concentrations were compared to the DIN assessment criteria. The highest TOxN (normalised) concentration at Loch Maddy was 10.99 µM, well below the current UK

coastal elevated and background concentrations. Only one sample exceeded the proposed Scottish coastal background concentration for TOxN of 9.5 µM.

Loch Ewe

Total oxidised nitrogen (TOxN), dissolved inorganic phosphorus (DIP), dissolved silicate (DSi) and ammonia have been measured in Loch Ewe surface waters since 2003 and in bottom waters since 2008. Concentrations are shown as monthly and yearly boxplots (Figures 7.4-7.11) for both upper and lower waters. The monthly boxplots for DIP, TOxN and DSi clearly show seasonal trends, with concentrations lowest in the summer months (May to August) and highest in winter. Concentrations for TOxN, DIP and DSi are most variable in March or April, around the start of the spring bloom. Low light intensities and high turbulence ensure that phytoplankton numbers are minimal during the winter so nutrients tend to accumulate, reaching a maximum prior to the spring bloom. Loch Ewe winter DSi concentrations (November to February) were similar to those observed at Stonehaven, Scapa and Scalloway, with average winter annual average concentrations ranging from 3.99 µM to 6.11 µM. Winter TOxN and DIP concentrations were similar to Loch Maddy but significantly lower compared to Stonehaven, Scapa and Scalloway (ANOVA with Tukey's pair-wise comparisons, $p<0.005$). As discussed above, nutrient concentrations are generally low in the Minches and Malin Sea (Smith et al., 2014). DIP concentrations rarely exceeded 0.7 µM and winter annual averages ranged from 0.38 µM to 0.53 µM, whilst winter mean TOxN concentrations ranged from 4.01 µM to 6.95 µM.

Similar to Stonehaven, Loch Ewe monthly boxplots for ammonia do not show a seasonal trend in either the surface or bottom water. Concentrations were often below detection limits (12% of samples) and only occasionally exceeded 2 µM.

The Loch Ewe site is in a non-problem area and, therefore, there should be no increasing trends in DIN or DIP concentrations. Yearly boxplots showed no significant temporal trend for any of the nutrients. Both the anomaly and annual boxplot showed that DIP, TOxN and DIP concentrations were lower in 2003. However, this is a result of there being no data for some of the winter months; samples were collected for nutrients from April 2003.

All winter Loch Ewe water samples (upper and lower) gave DIN (normalised) concentrations below the current UK coastal elevated concentration of 18 µM as well as the proposed Scottish elevated coastal TOxN concentration of 14.25 µM (Smith et al., 2014). In addition all concentrations were below both the current UK coastal DIN background concentration of 12 µM and the proposed Scottish coastal TOxN background of 9.5 µM.

Scapa

Total oxidised nitrogen (TOxN), dissolved inorganic phosphorus (DIP) and dissolved silicate (DSi) have been measured in the surface waters at Scapa since October 1999. Ammonia was been measured in 2013 only. TOxN, DIP and DSi concentrations are shown as monthly and yearly boxplots (Figures 7.12-7.14). The monthly boxplots for DIP, TOxN and DSi show seasonal trends. Concentrations are

lowest, often below detection limits for all 3 nutrients, in the summer months (May to August) and highest in winter (November to February). Low light intensities and high turbulence ensure that phytoplankton numbers are minimal during the winter so nutrients tend to accumulate, reaching a maximum prior to the growing season. DIP concentrations rarely exceeded 0.8 µM and winter (November to February) annual averages ranged from 0.47 µM to 0.59 µM. TOxN winter annual means ranged from 5.66 µM to 7.76 µM and DSi from 4.62 µM to 6.11 µM. Winter DSi concentrations at Scapa were similar to Loch Ewe, Stonehaven and Scalloway. TOxN and DIP concentrations were similar to Stonehaven but significantly lower than Scalloway and significantly higher than Loch Ewe and Loch Maddy (ANOVA with Tukey's pair-wise comparisons, $p<0.005$). Ammonia concentrations (not shown here) were only measured in 2013 did not show a seasonal pattern and rarely exceeded 3 µM.

The Scapa site is in a non-problem area and, therefore, there should be no increasing trends in DIN or DIP concentrations. Yearly boxplots showed no significant temporal trend for any of the nutrients Sampling began at Scapa in October 1999 and, therefore, the 1999 annual mean is higher than the subsequent years as there are only winter nutrient for this year. Ammonia was only measured in 2013 and, therefore, winter (November to February) TOxN (normalised) concentrations were compared to the proposed Scottish coastal assessment criteria (Smith et al., 2014). Only two out of 147 samples exceeded the proposed elevated TOxN concentration of 14.25 µM and 75% of samples were below the proposed Scottish coastal TOxN background concentration of 9.5 µM.

Scalloway

Total oxidised nitrogen (TOxN), dissolved inorganic phosphorus (DIP), dissolved silicate (DSi) and ammonia have been measured in surface waters at Scalloway since 2000. TOxN, DIP, DSi and ammonia concentrations are shown as monthly and yearly boxplots (Figures 7.15-7.18). The monthly boxplots for DIP, TOxN and DSi show seasonal trends in both the surface and bottom waters. Concentrations are lowest, often below detection limits for all three nutrients, in the summer months (May to August) and highest in winter (November to February). Low light intensities and high turbulence ensure that phytoplankton numbers are minimal during the winter so nutrients tend to accumulate, reaching a maximum prior to the growing season. DIP concentrations rarely exceeded 0.8 µM and winter (November to February) annual averages ranged from 0.50 µM to 0.72 µM. TOxN winter annual averages ranged from 5.81 µM to 9.52 µM and DSi from 3.91 µM to 6.33 µM. Winter DSi concentrations at Scalloway were similar to Loch Ewe and Stonehaven, however, winter TOxN and DIP concentrations were significantly higher than the other four sites (ANOVA with Tukey's pair-wise comparisons, $p<0.005$). The higher TOxN and DIP concentrations at Scalloway reflect the greater proportion of Atlantic water in this area. Scalloway had the highest annual average salinity (34.93) and in most cases when nutrient concentrations were high the salinity was also high, which suggests the high concentrations were not due to freshwater inputs.

The monthly boxplot for ammonia did not show the typical nutrient seasonal pattern. Ammonia concentrations exceeded the detection limit more frequently at Scalloway than at the other sites, and concentrations were significantly higher than all other sites. Highest ammonia concentrations were found in October, November and

December. The Scalloway sampling site is located close to a harbour and therefore anthropogenic inputs may have resulted in higher ammonia concentrations.

The Scalloway site is in a non-problem area and, therefore, there should be no increasing trends in DIN or DIP concentrations. Yearly boxplots showed no significant temporal trend for any of the nutrients. Both the anomaly and annual boxplot showed that DIP, TOxN and DIP concentrations were lower in 2005, this is a result of there being no data for the winter months in this year. For ammonia there were more positive anomalies between 2010 and 2013.

All winter Scalloway water samples gave DIN (normalised) concentrations below the current UK coastal elevated concentration of 18 µM and only five out of 126 winter samples exceeded the proposed elevated TOxN concentration of 14.25 µM (Smith et al., 2014). The majority (65%) of samples also gave concentrations below the current UK coastal DIN background concentration of 12 µM and 72% of samples were below the proposed Scottish TOxN background concentration of 9.5 µM.

Stonehaven

Total oxidised nitrogen (TOxN), dissolved inorganic phosphorus (DIP), dissolved silicate (DSi) and ammonia have been measured in upper and lower waters at the Stonehaven site since 1997. TOxN, DIP, DSi and ammonia concentrations are shown as monthly and yearly boxplots (Figures 7.19-7.26) for both surface and bottom waters. The monthly boxplots for DIP, TOxN and DSi show seasonal trends at both depths. Concentrations are lowest, often below detection limits for all three nutrients, in the summer months (May to August) and highest in winter (November to February). Concentrations for TOxN, DIP and DSi are most variable in March or April, around the start of the phytoplankton growing season. Low light intensities and high turbulence ensure that phytoplankton numbers are minimal during the winter so nutrients tend to accumulate, reaching a maximum prior to the growing season. DIP concentrations rarely exceeded 0.8 µM and winter (November to February) annual averages ranged from 0.45 µM to 0.61 µM. TOxN winter annual averages ranged from 6.40 µM to 8.43 µM and DSi from 3.53 µM to 6.08 µM. Winter TOxN and DIP concentrations were similar to Scapa but significantly higher compared to Loch Ewe and Loch Maddy (see below), possibly due to greater riverine inputs at this site, but significantly lower compared to Scalloway (ANOVA with Tukey's pair-wise comparisons, $p<0.005$).

Ammonia does not follow the same seasonal pattern as TOxN. Ammonia sampling and analysis is more prone to contamination, which may mask any seasonal changes. Possible sources of ammonia contamination include sampling equipment, the atmosphere and the analyst (Kirkwood, 1996). Ammonia concentrations were often below the detection limit in all months, including winter, and rarely exceeded 3 µM. The highest monthly mean ammonia concentration in both the surface and bottom waters was found in October, although concentrations were also the most variable in this month.

Yearly boxplots show no significant temporal trend for any of the nutrients. However, the monthly and yearly anomaly plots for DSi, TOxN and DIP showed more positive anomalies (coloured red in the plots) prior to 2003 (Figures 7.19-7.24). This change

does not correspond to the change in instrument as samples collected from 2002 to 2006 were analysed using the same instrument. Between 2001 and 2005 phytoplankton numbers at Stonehaven were lower, which may partly explain the higher nutrient anomalies prior to 2003.

The Stonehaven site is in a non-problem area and, therefore, there should be no increasing trends in DIN or DIP concentrations. There is no evidence of any increasing trends in either DIN or DIP concentrations at Stonehaven. All winter Stonehaven water samples (surface and bottom) gave DIN (normalised to salinity) concentrations below the current UK coastal elevated concentrations of 18 µM and the majority (98%) of samples also gave concentrations below the current UK coastal DIN background concentration of 12 µM. Only one out of 638 winter samples exceeded the proposed coastal elevated TOxN concentration of 14.25 µM (Smith et al., 2014) and 63% of samples were below the proposed Scottish coastal TOxN background concentration of 9.5 µM.

7.4 Summary– Inorganic Nutrients

- Inorganic nutrients (Total oxidised nitrogen (TOxN), dissolved inorganic phosphorus (DIP) and dissolved silicate (DSi)) are presented from five coastal stations (Stonehaven, Loch Ewe, Scapa, Scalloway and Loch Maddy). Ammonia is presented from 3 stations (Stonehaven, Loch Ewe and Scalloway).
- Concentrations of DIP, TOxN and DSi exhibit a seasonal cycle at all stations, driven by the uptake of nutrients by phytoplankton during the spring, an event known as the spring bloom. Nutrient concentrations are lowest, often below detection limits, during the summer months (May to August) and begin to increase during Sept.
- Nutrient concentrations are highest in winter (November to February), when phytoplankton growth is reduced. The timing of inorganic nutrient uptake by the spring bloom varied by station and year.
- Ammonia concentrations were often below detection limits and did not show a seasonal trend. Ammonia sampling and analysis is more prone to contamination, which may mask any seasonal changes.
- Nutrient enrichment can be assessed using OSPAR Ecological Quality Objectives (EcoQOs). However, the UK Dissolved Inorganic Nitrogen (DIN; the sum of the concentration of TOxN and ammonia) background and elevated concentrations (50% above background) have been shown to be too high for Scottish waters so new estimates of TOxN background values were proposed by Smith et al., (2014).
- DIN and TOxN (normalised) concentrations were below the current UK and proposed Scottish elevated concentrations, consistent with the relatively low

population densities and industrial activities in Scotland. The majority of samples were also below the UK background concentrations.

- Spatial differences were observed in winter nutrient concentrations. In the winter, the highest monthly average TOxN (5.81-9.52 µM) and DIP (0.50-0.72 µM) concentrations were found at Scalloway, suggesting a greater proportion of Atlantic water in this area, as evidenced by the highest average annual salinity.
- Lower TOxN (Loch Maddy 4.95-6.41 µM; Loch Ewe 4.01-6.95) and DIP (Loch Maddy 0.33-0.50 µM; Loch Ewe 0.38-0.53) concentrations were in the west coast sea lochs of Loch Maddy and Loch Ewe. Nutrient concentrations have previously been shown to be low in the Minches and Malin Sea as it is shielded by the Outer Hebrides against the inflow of Atlantic water from the west and local inputs of freshwater do not appear to be an important source of nutrients (Smith et al., 2014).
- All sites were within non-problem areas as defined by the Water Framework Directive (WFD), and, therefore, there should be no increasing trends in DIN or DIP concentration. Yearly boxplots showed high interannual variability and no obvious temporal trend for any of the nutrients at any station.

7.5 References – Inorganic Nutrients

Armstrong, F.A.J., Stearns, C.R., Strickland, J.D.H. 1967. The measurement of upwelling and subsequent biological processes by means of the Technicon AutoAnalyzer and associated equipment. Deep Sea Research, 14, 381-389.

Baxter, J.M., Boyd, I.L., Cox, M., Donald, A.E., Malcolm, S.J., Miles, H., Miller, B., Moffat, C.F., (Editors). 2011. Scotland's Marine Atlas: Information for the national marine plan. Marine Scotland, Edinburgh. 191pp. http://www.scotland.gov.uk/Publications/2011/03/16182005/0.

Cefas. 2008. Common procedure for the identification of the eutrophication status of the OSPAR maritime area - UK National Report. Technical Report.

Devlin, M., Painting, S., Best, M. 2007. Setting nutrient thresholds to support an ecological assessment based on nutrient enrichment, potential primary production and undesirable disturbance. Marine Pollution Bulletin, 55, 65-73.

Kirkwood, D. 1996. Nutrients: Practical notes on their determination in sea water, ICES Techniques in Marine Environmental sciences No. 17.

Koroleff, F. 1971. On the determination of reactive silicate in natural waters. ICES CM 1971/C:43.

Murphy, J., Riley, J.P. 1962. A modified single solution method for the determination of phosphate in natural waters. Analytica Chimica Acta, 27, 31-36.

OSPAR Commission. 2008. OSPAR Integrated Report on the Eutrophication Status of the OSPAR Maritime Area.

OSPAR. 2013. Common Procedure for the Identification of the Eutrophication Status of the OSPAR Maritime Area. OSPAR decision 2013-8, 66pp.

Rose, M., Webster, L., Walsham, P., Moffat, C. 2009. The nutrient status of Scottish coastal waters: 2001-2008. Technical Report FRS Internal Report No. 05/09. Fisheries Research Services. http://www.scotland.gov.uk/Uploads/Documents/Int0509.pdf.

Smith, A.F., Fryer, R.J., Webster, L., Berx, B., Taylor, A., Walsham, P., Turrell, W.R. 2014. Setting background nutrient levels for coastal waters with oceanic influences. Estuarine, Coastal and Shelf Science, 145, 69 -79.

Webster, L., Rose, M., Walsham, P., Shaw, C., Davies, I.D., Moffat, C. F. 2007. The nutrient status of Scottish coastal waters: 2001-2007, FRS Internal Report No 13/07.

7.6 Plots – Inorganic Nutrients

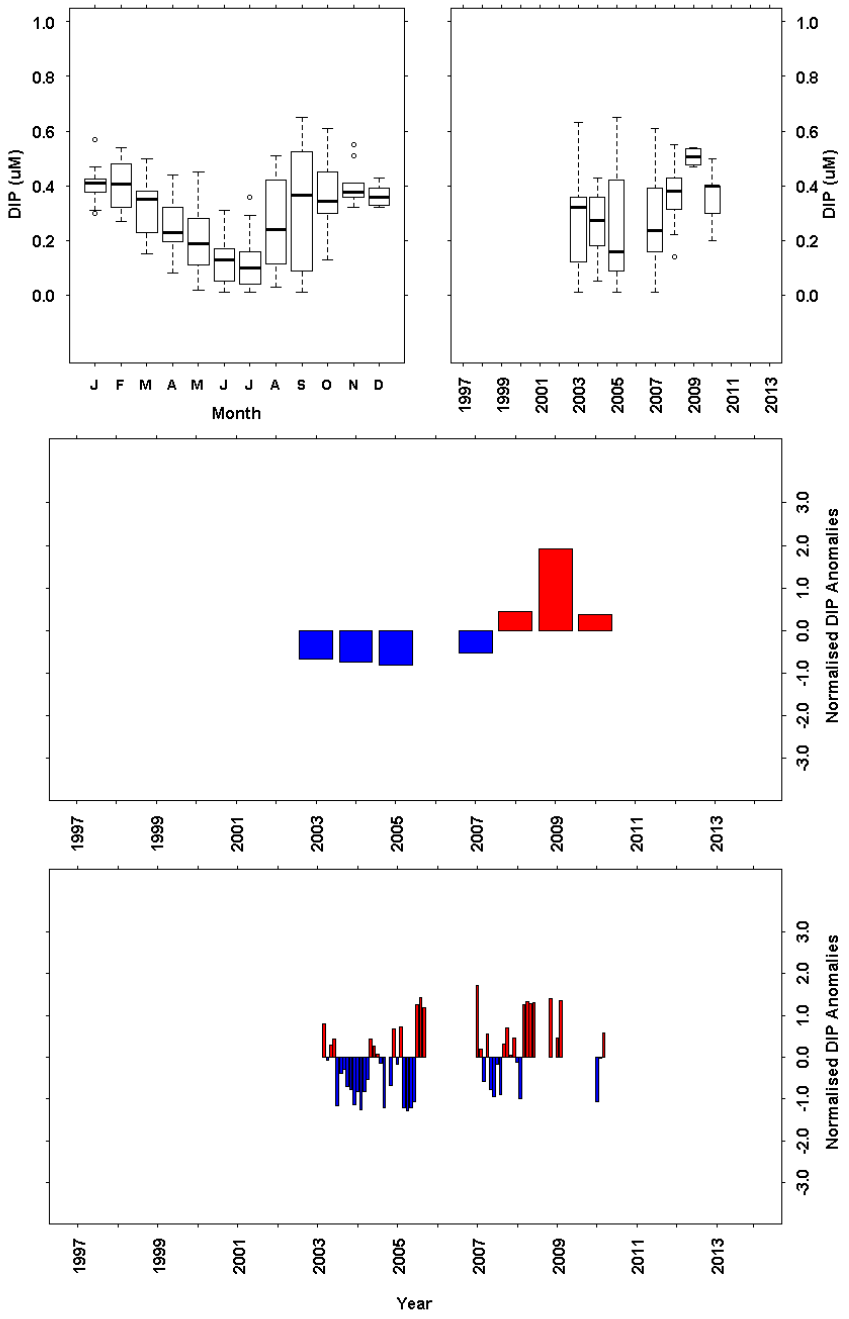

Figure 7.1 Dissolved inorganic phosphorus (DIP, µM) data from long term monitoring site at Loch Maddy. a) Monthly boxplot DIP data. b) Annual boxplot of DIP data. c) Annual mean anomaly time series d) Monthly mean anomaly time series. Data was only available from 2003 to March 2010, inclusive. in 2009 only January and February data was used, all other months had a Quality Flag of 4, and in 2010 only samples collected between January and March were analysed for nutrients. The full data set was used as the base period for the anomaly calculations.

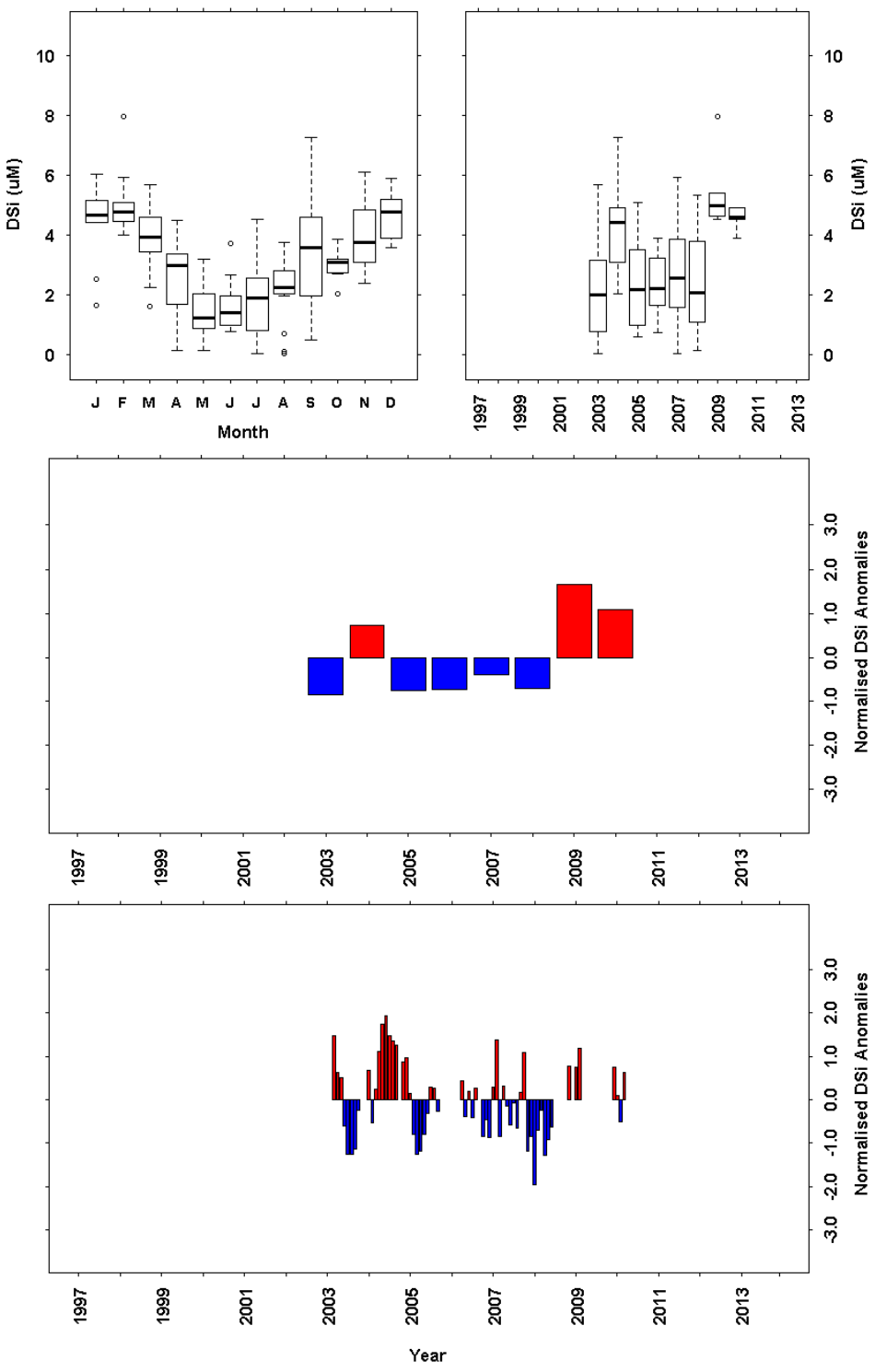

Figure 7.2 Dissolved silicate (DSi, µM) data from long term monitoring site at Loch Maddy. a) Monthly boxplot DSi data. b) Annual boxplot of DSi data. c) Annual mean anomaly time series d) Monthly mean anomaly time series. Data was only available from 2003 to March 2010, inclusive. in 2009 only January and February data was used, all other months had a Quality Flag of 4, and in 2010 only samples collected between January and March were analysed for nutrients. The full data set was used as the base period for the anomaly calculations.

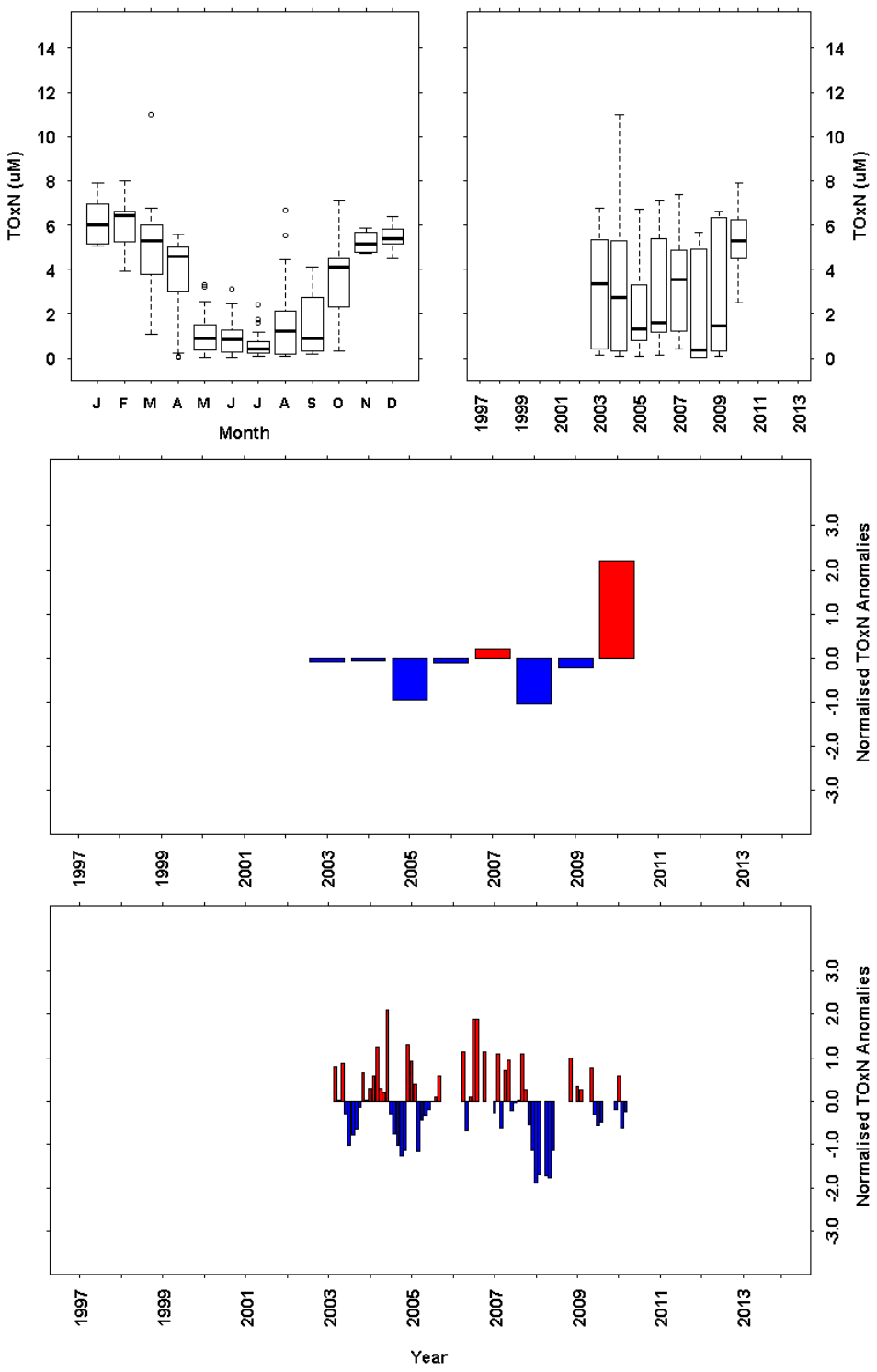

Figure 7.3 Total oxidised nitrogen (TOxN, µM) data from long term monitoring site at Loch Maddy. a) Monthly boxplot TOxN data. b) Annual boxplot of TOxN data. c) Annual mean anomaly time series d) Monthly mean anomaly time series. In 2009 only January and February data was used, all other months had a Quality Flag of 4, and in 2010 only samples collected between January and March were analysed for nutrients. The full data set was used as the base period for the anomaly calculations.

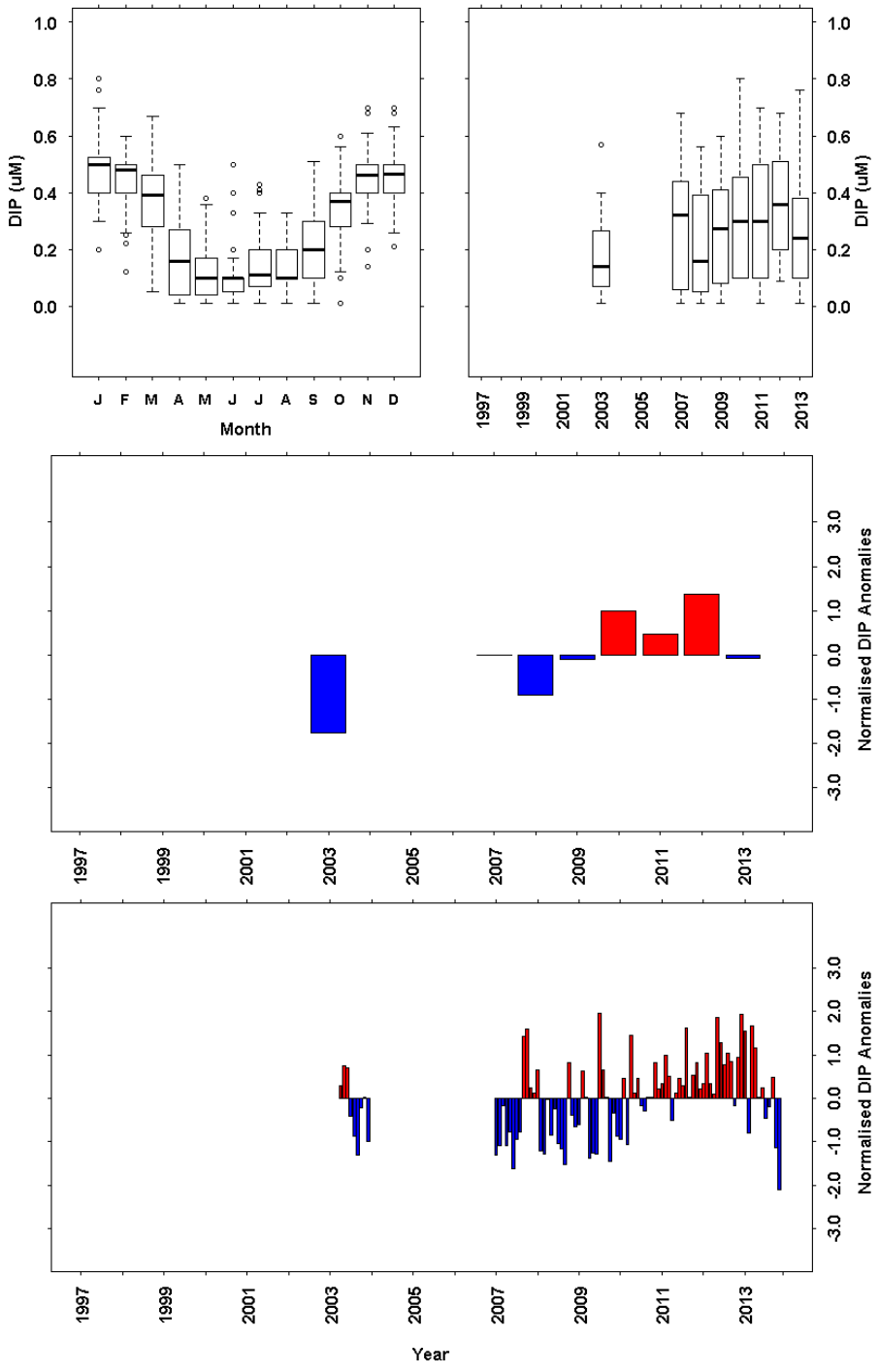

Figure 7.4 Upper layer (0 -10 m) dissolved inorganic phosphorus (DIP, µM) data from long term monitoring site at Loch Ewe. a) Monthly boxplot DIP data. b) Annual boxplot of DIP data. c) Annual mean anomaly time series d) Monthly mean anomaly time series. There were no data available prior to 2003. DIP data for samples collected in 2004, 2005 and 2006 were assigned a Quality Flag of 4 and therefore excluded from the data assessment. The full data set was used as the base period for the anomaly calculations.

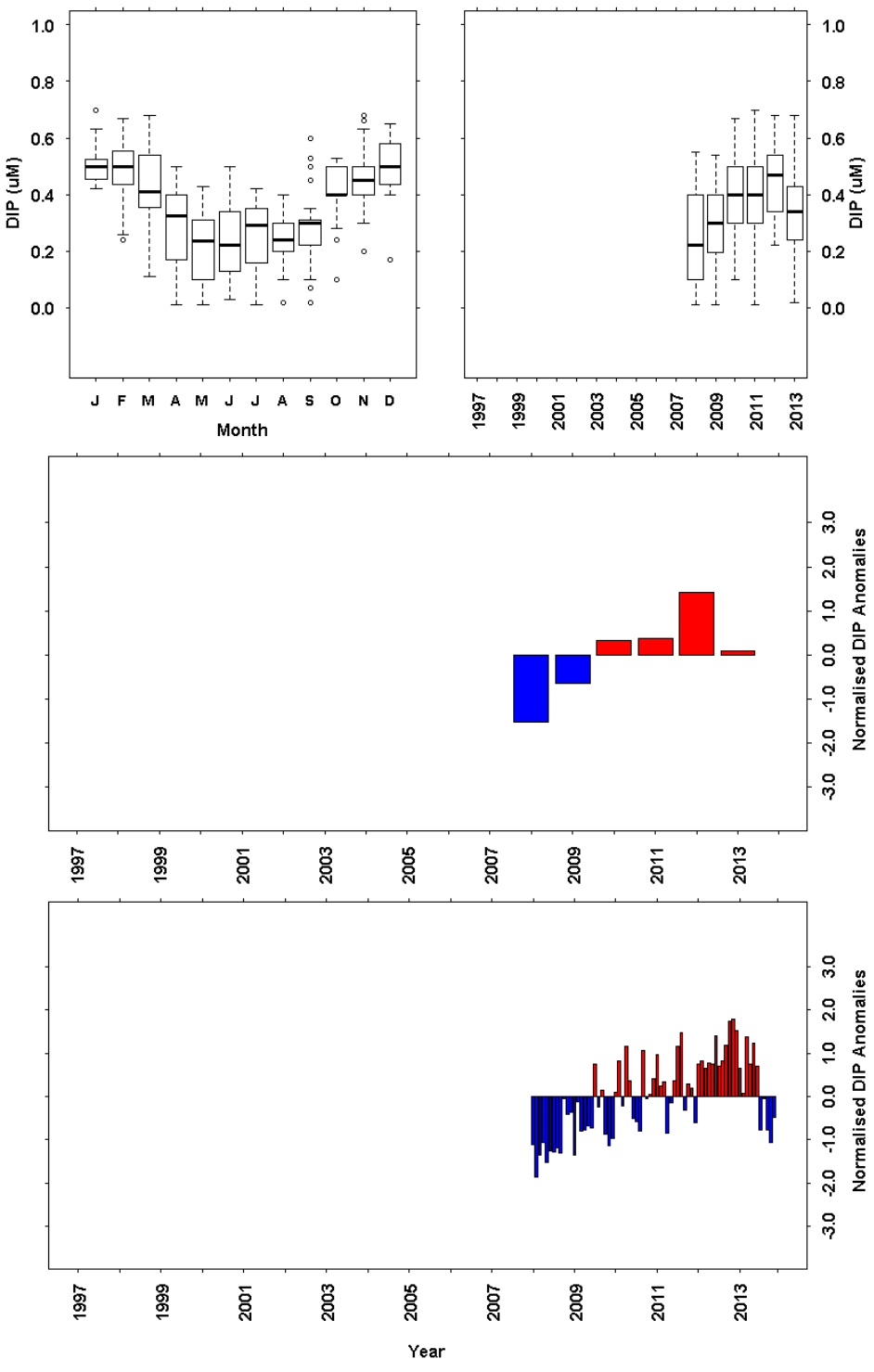

Figure 7.5 Lower layer (>30m) dissolved inorganic phosphorus (DIP, µM) data from long term monitoring site at Loch Ewe. a) Monthly boxplot DIP data. b) Annual boxplot of DIP data. c) Annual mean anomaly time series d) Monthly mean anomaly time series. There were no data available prior to 2008. The full data set was used as the base period for the anomaly calculations.

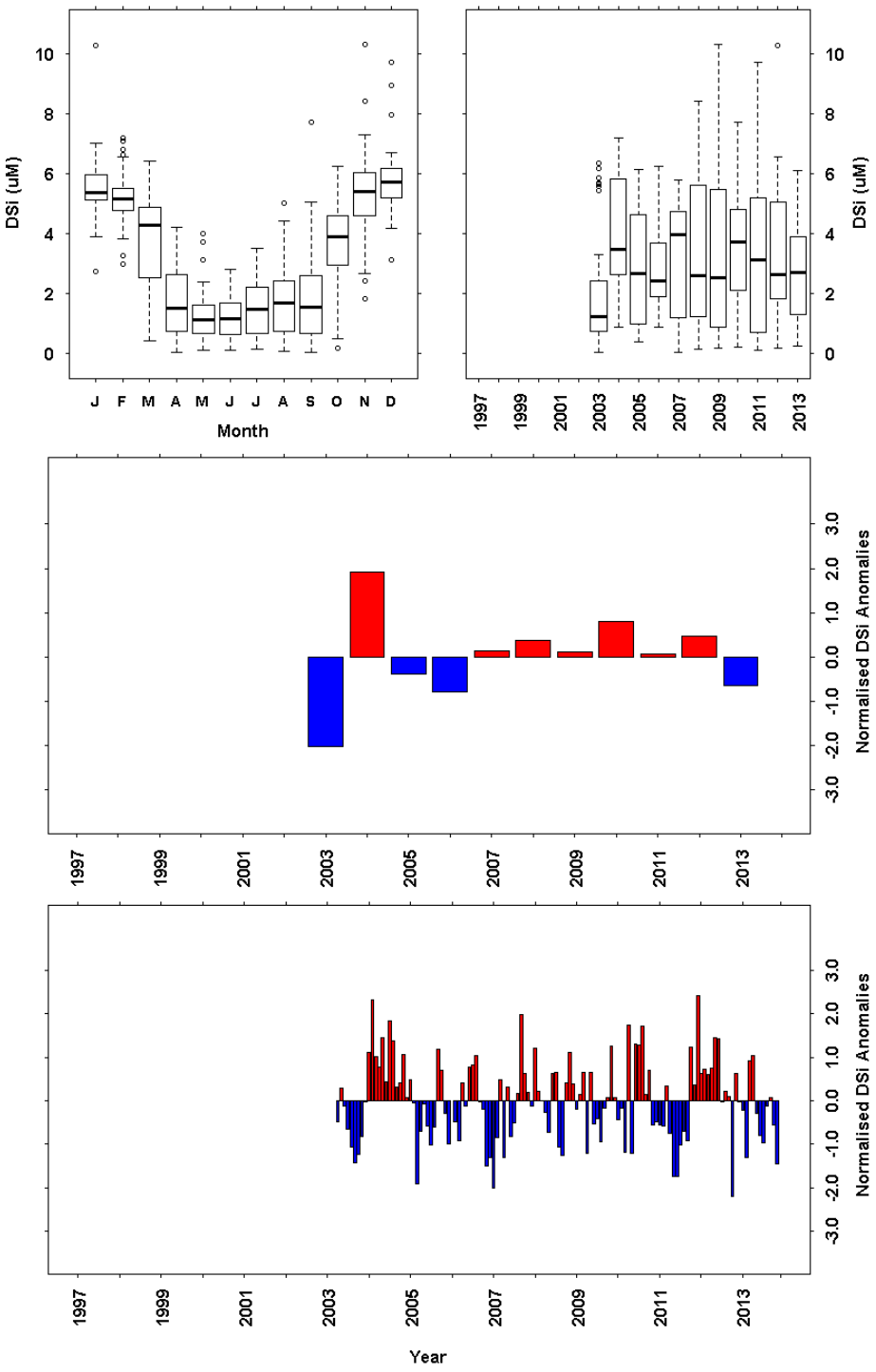

Figure 7.6 Upper layer (0 -10 m) dissolved silicate (DSi, µM) data from long term monitoring site at Loch Ewe. a) Monthly boxplot DSi data. b) Annual boxplot of DSi data. c) Annual mean anomaly time series d) Monthly mean anomaly time series. There were no data available prior to 2003. The full data set was used as the base period for the anomaly calculations.

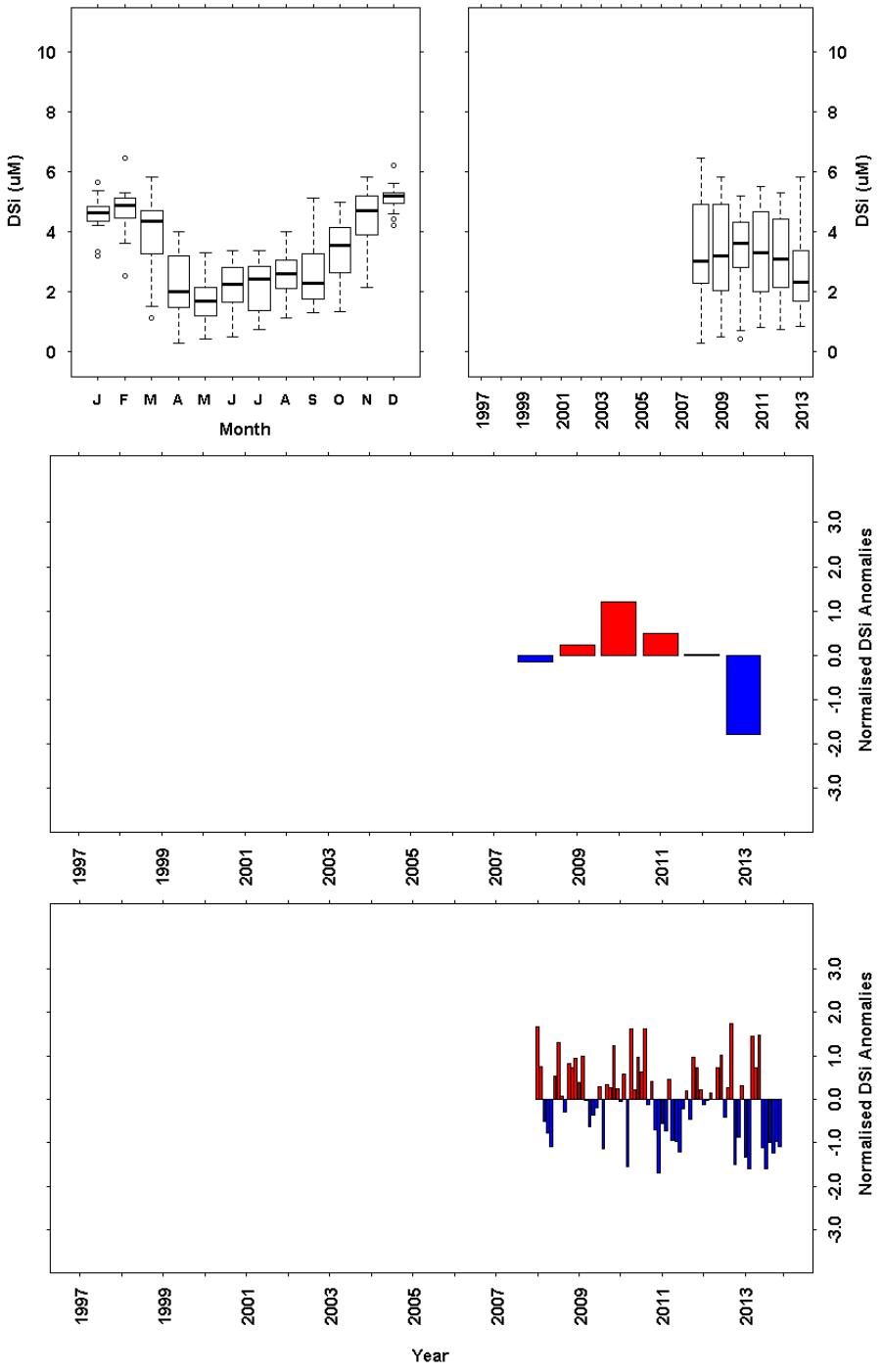

Figure 7.7 Lower layer (>30m) dissolved silicate (DSi, µM) data from long term monitoring site at Loch Ewe. a) Monthly boxplot DSi data. b) Annual boxplot of DSi data. c) Annual mean anomaly time series d) Monthly mean anomaly time series. There were no data available prior to 2008. The full data set was used as the base period for the anomaly calculations.

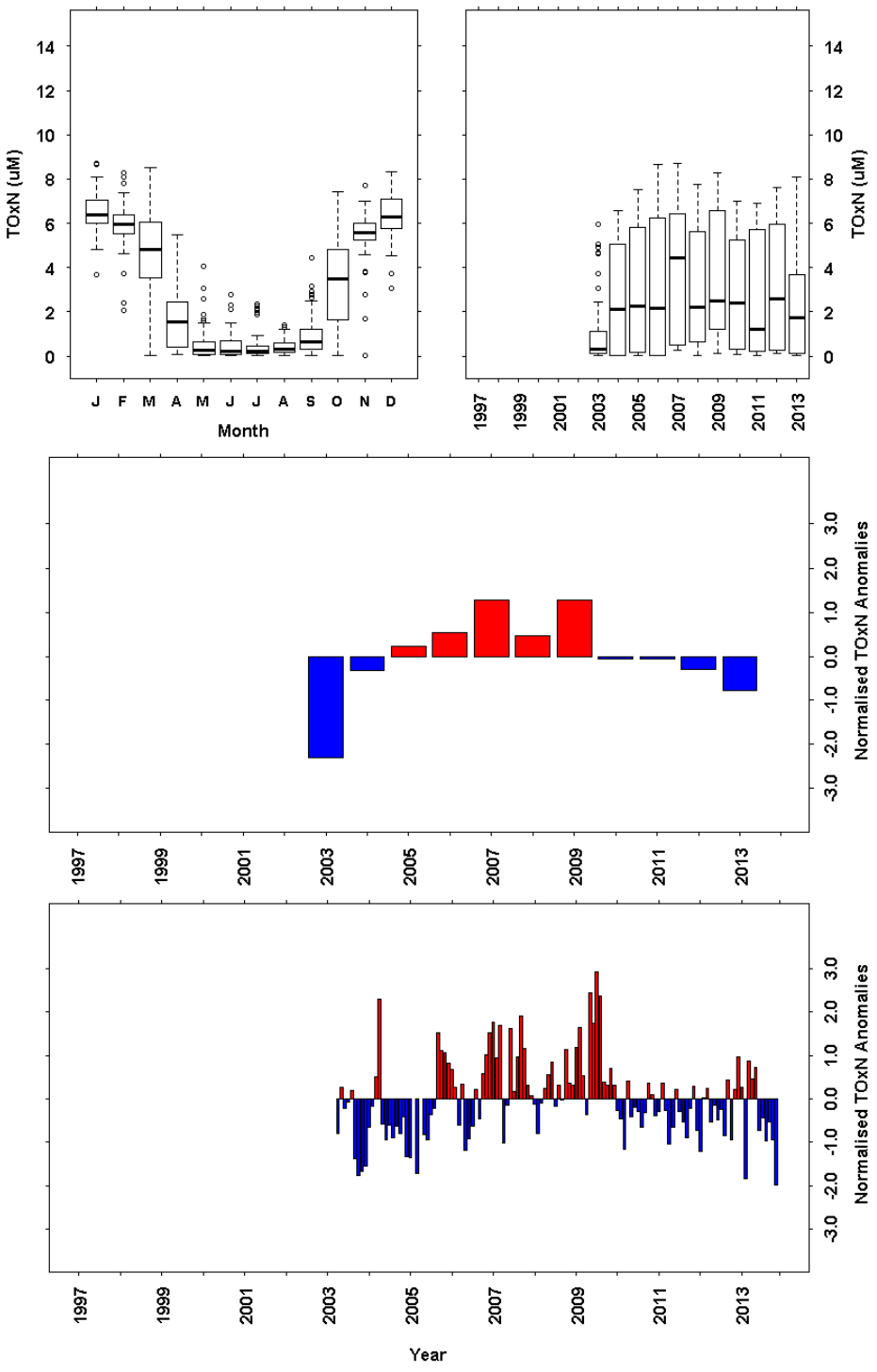

Figure 7.8 Upper layer (0 -10 m) total oxidised nitrogen (TOxN, µM) data from long term monitoring site at Loch Ewe. a) Monthly boxplot TOxN data. b) Annual boxplot of TOxN data. c) Annual mean anomaly time series d) Monthly mean anomaly time series. There were no data available prior to 2003. The full data set was used as the base period for the anomaly calculations.

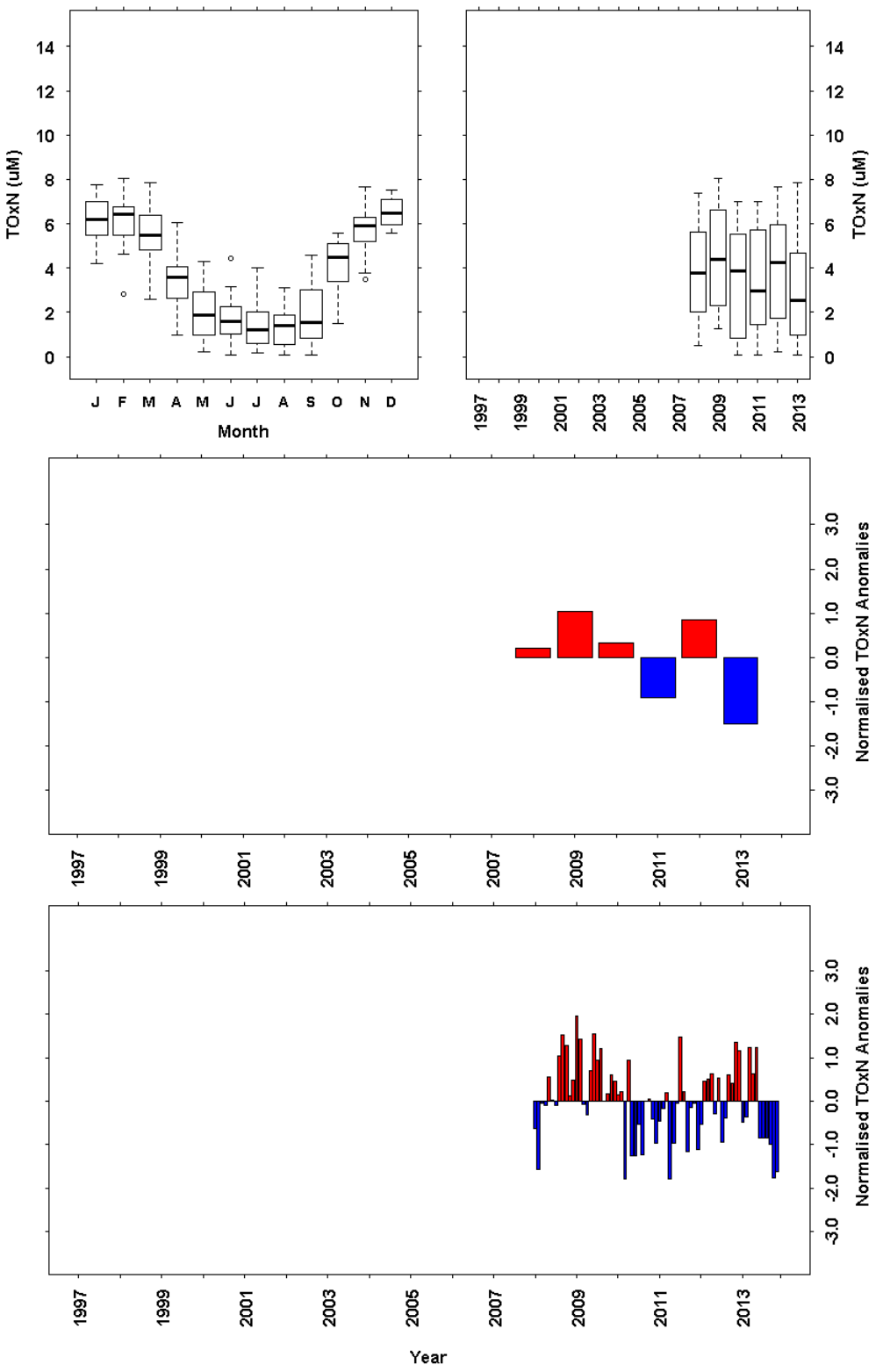

Figure 7.9 Lower layer (>30m) total oxidised nitrogen (TOxN, µM) data from long term monitoring site at Loch Ewe. a) Monthly boxplot TOxN data. b) Annual boxplot of TOxN data. c) Annual mean anomaly time series d) Monthly mean anomaly time series. There were no data available prior to 2008. The full data set was used as the base period for the anomaly calculations.

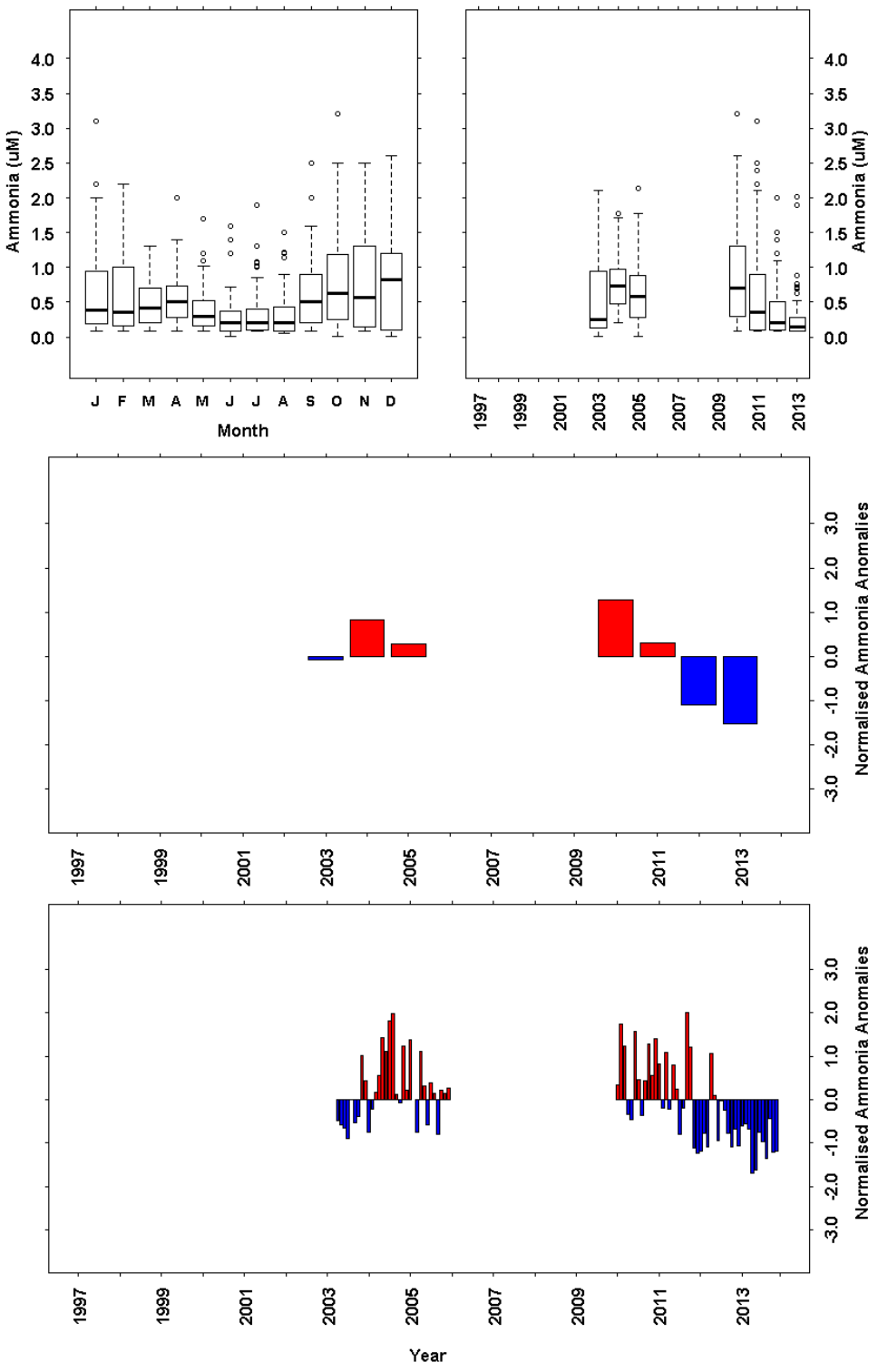

Figure 7.10 Upper layer (0 -10 m) ammonia (µM) data from long term monitoring site at Loch Ewe. a) Monthly boxplot ammonia data. b) Annual boxplot of ammonia data. c) Annual mean anomaly time series d) Monthly mean anomaly time series. Ammonia data from samples collected between 2006 and 2009 inclusive were also assigned a Quality Flag of 4 and were therefore excluded. There were no data available prior to 2003. The full data set was used as the base period for the anomaly calculations.

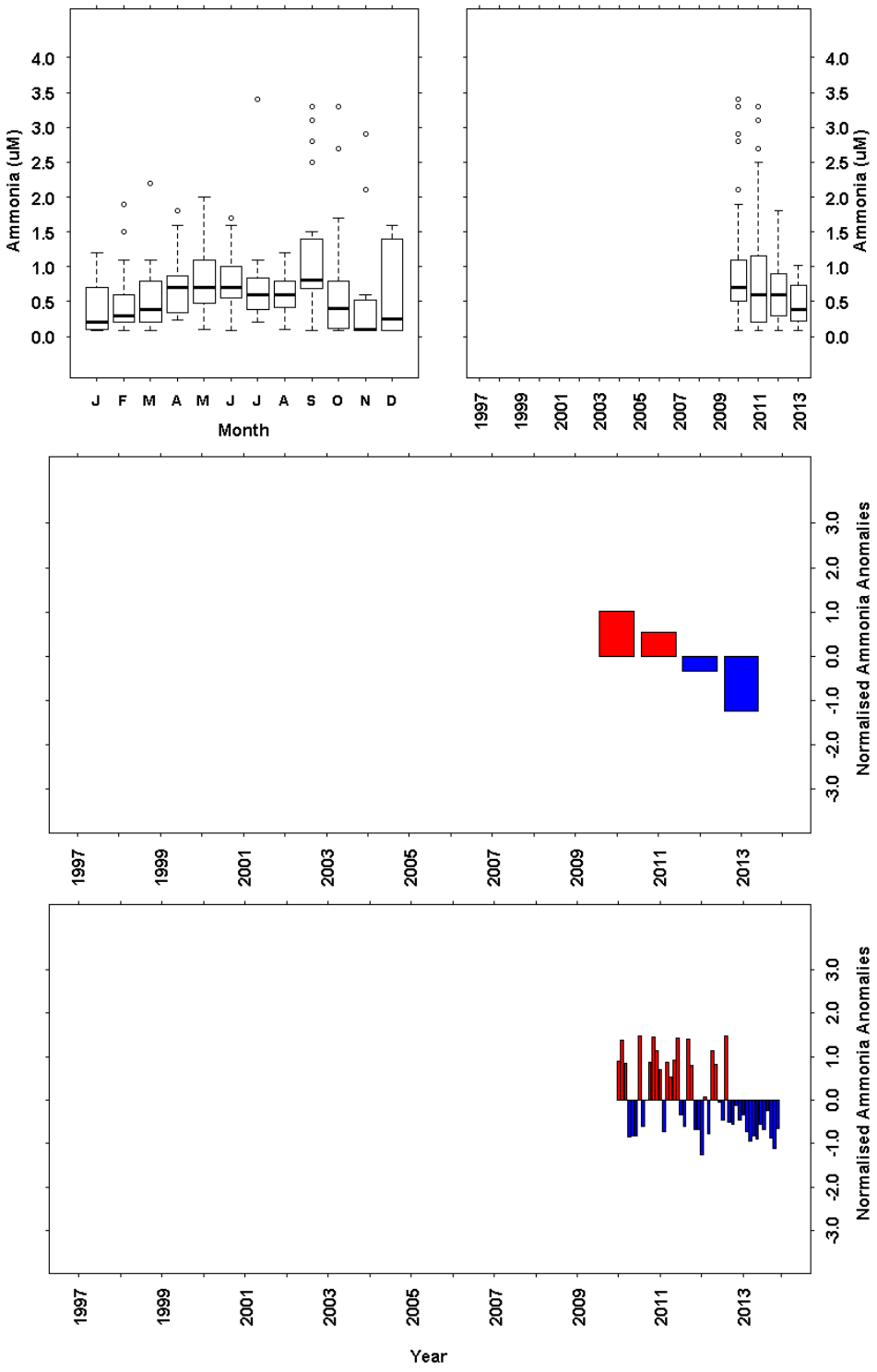

Figure 7.11 Lower layer (>30m) ammonia (µM) data from long term monitoring site at Loch Ewe. a) Monthly boxplot ammonia data. b) Annual boxplot of ammonia data. c) Annual mean anomaly time series d) Monthly mean anomaly time series. There were no data available prior to 2008, and data from 2008 and 2009 was assigned a Quality Flag of 4 and therefore excluded. The full data set was used as the base period for the anomaly calculations.

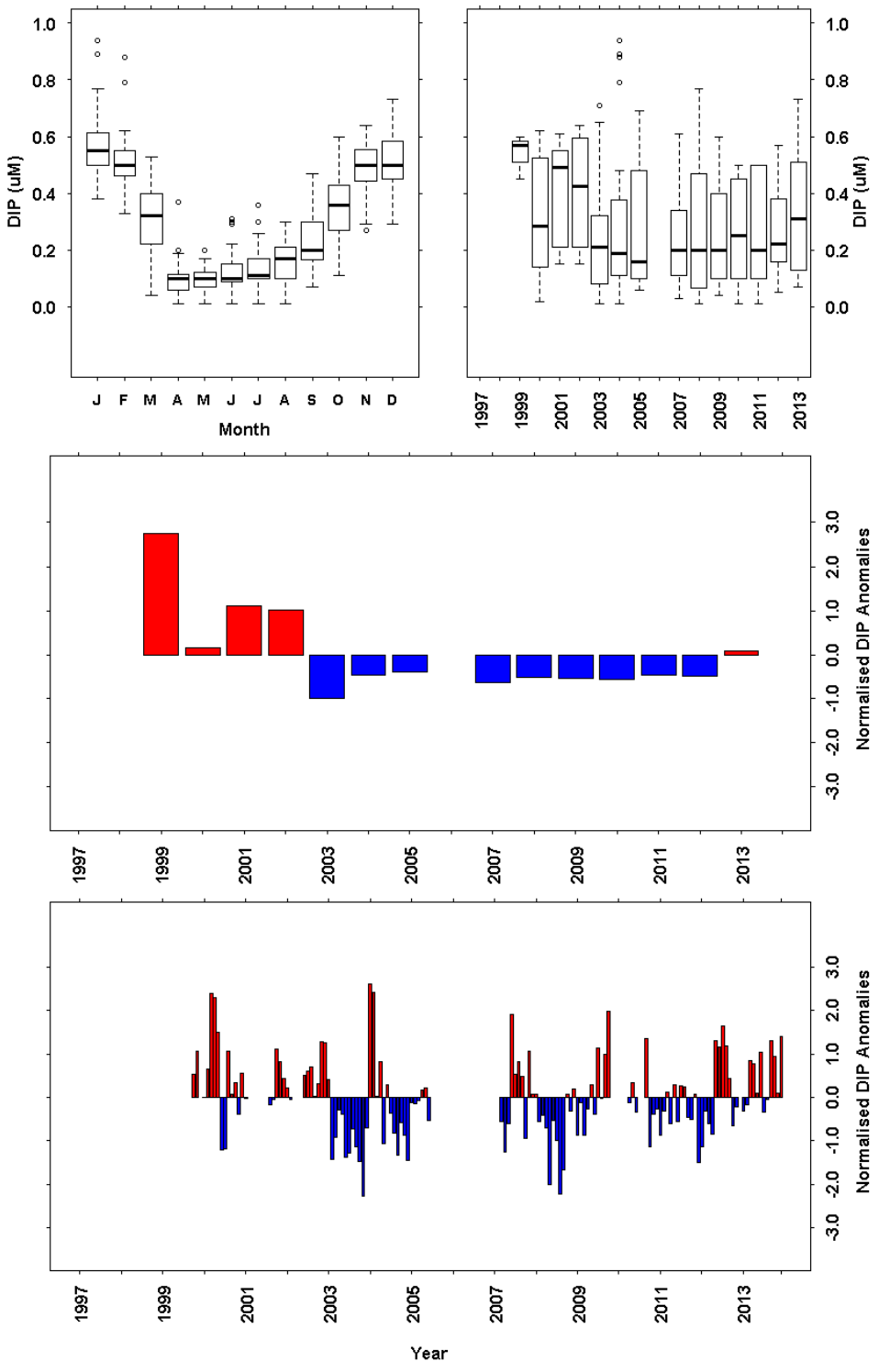

Figure 7.12 Dissolved inorganic phosphorus (DIP, µM) data from long term monitoring site at Scapa. a) Monthly boxplot DIP data. b) Annual boxplot of DIP data. c) Annual mean anomaly time series d) Monthly mean anomaly time series. There were no data available prior to October 1999. All DIP data was assigned a Quality Flag of 4 in 2006 and was therefore excluded from the data assessment. The full data set was used as the base period for the anomaly calculations.

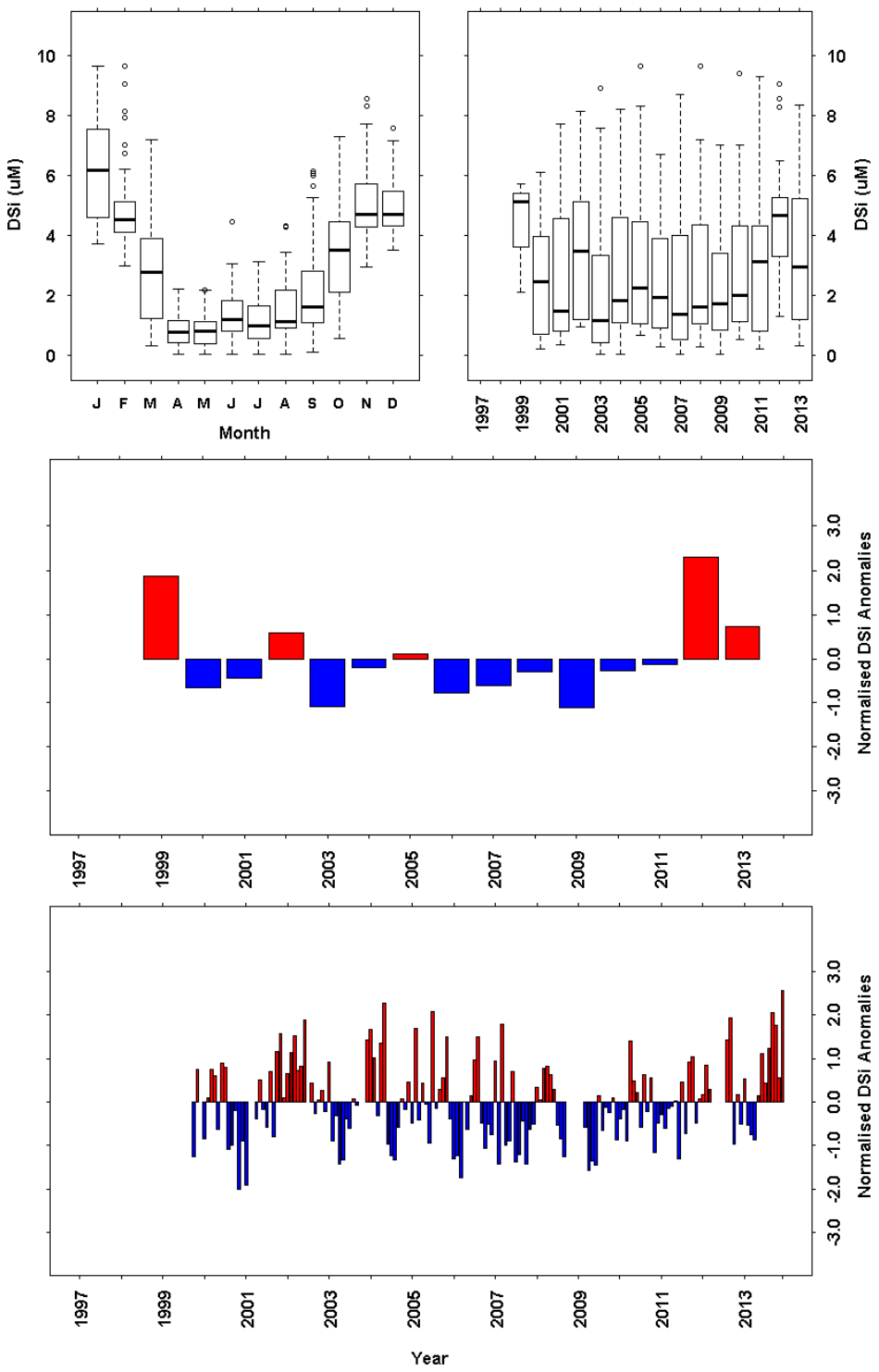

Figure 7.13 Dissolved silicate (DSi, µM) data from long term monitoring site at Scapa. a) Monthly boxplot DSi data. b) Annual boxplot of DSi data. c) Annual mean anomaly time series d) Monthly mean anomaly time series. There were no data available prior to October 1999. The full data set was used as the base period for the anomaly calculations.

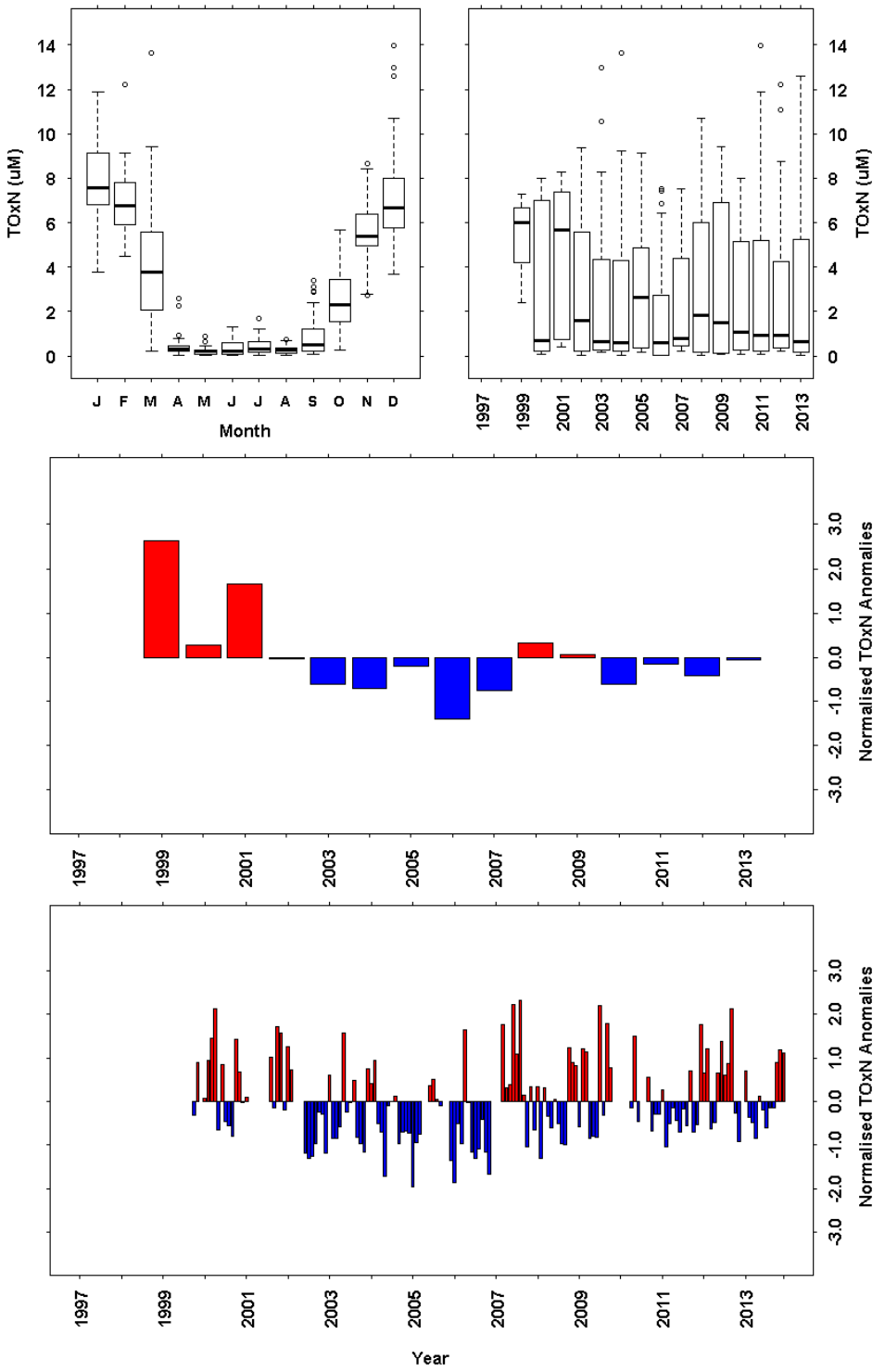

Figure 7.14 Total oxidised nitrogen (TOxN, µM) data from long term monitoring site at Scapa. a) Monthly boxplot DSi data. b) Annual boxplot of DIP data. c) Annual mean anomaly time series d) Monthly mean anomaly time series. There were no data available prior to October 1999. The full data set was used as the base period for the anomaly calculations.

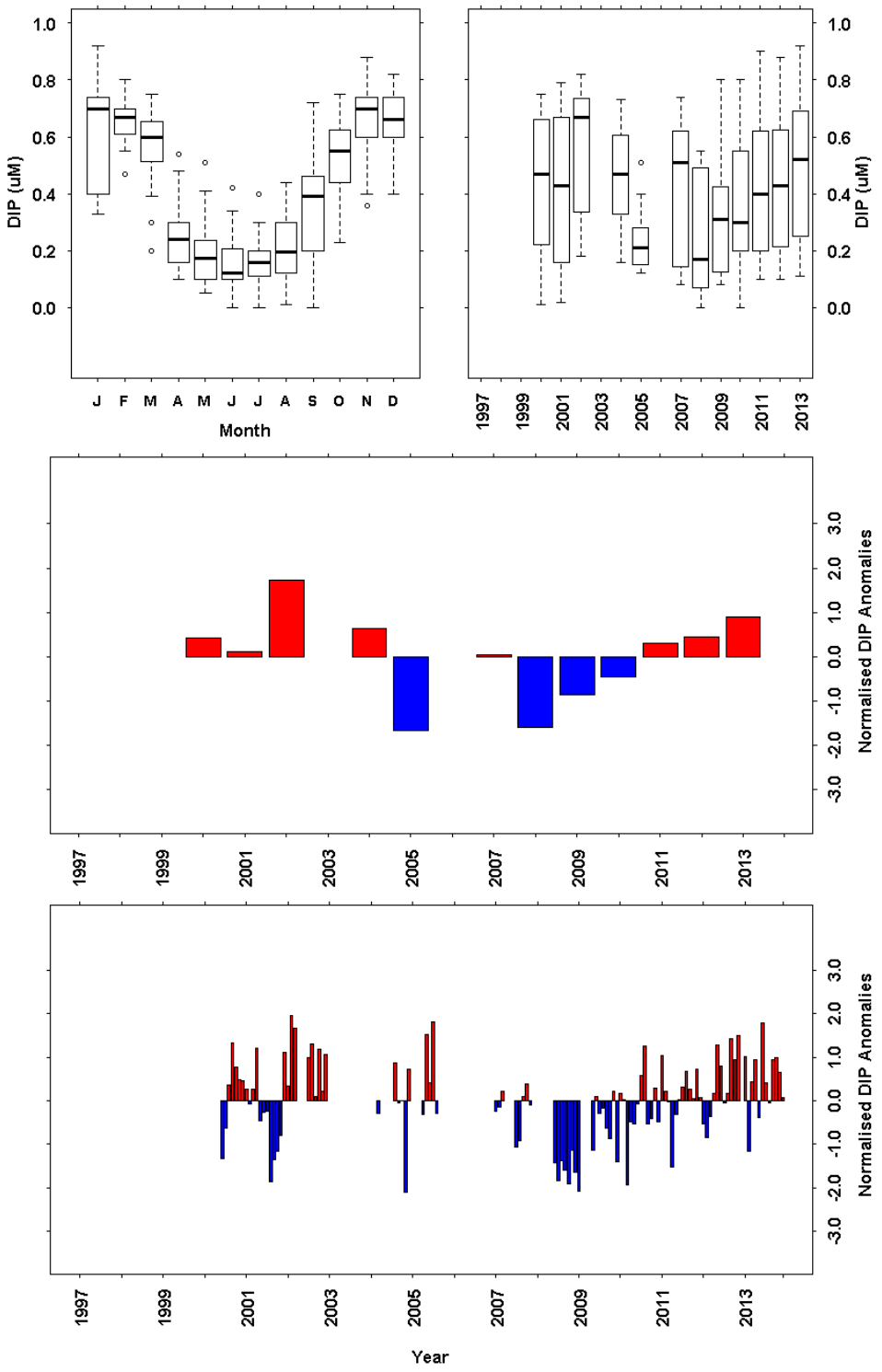

Figure 7.15 Dissolved inorganic phosphorus (DIP, µM) data from long term monitoring site at Scalloway. a) Monthly boxplot DIP data. b) Annual boxplot of DIP data. c) Annual mean anomaly time series d) Monthly mean anomaly time series. There were no data available prior to 2000. In 2005 data is only available from April – August. All DIP data was assigned a Quality Flag of 4 in 2003 and 2006 and therefore was excluded The full data set was used as the base period for the anomaly calculations.

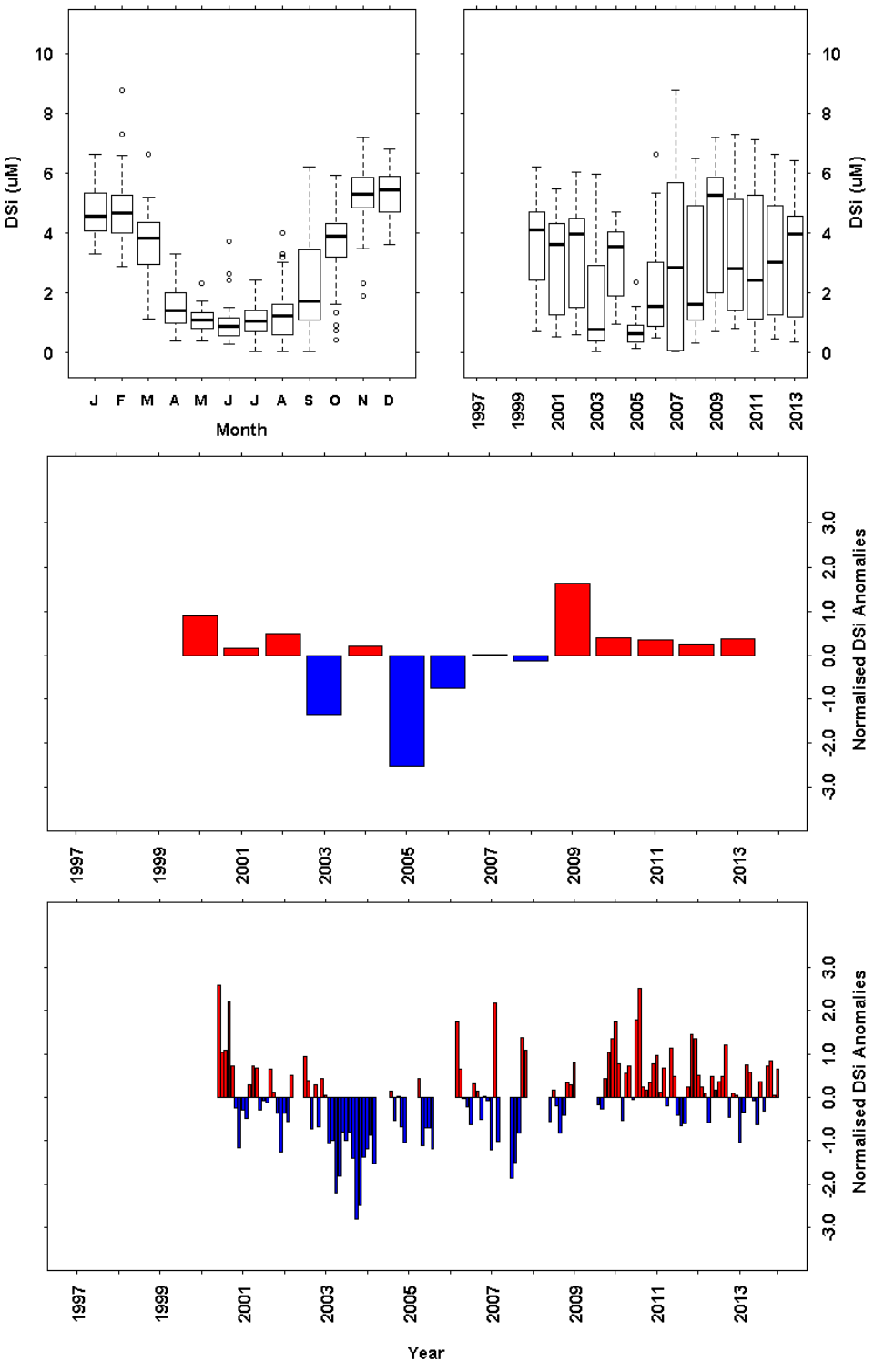

Figure 7.16 Dissolved silicate (DSi, µM) data from long term monitoring site at Scalloway. a) Monthly boxplot DSi data. b) Annual boxplot of DSi data. c) Annual mean anomaly time series d) Monthly mean anomaly time series. There were no data available prior to 2000. In 2005 data is only available from April – August. The full data set was used as the base period for the anomaly calculations.

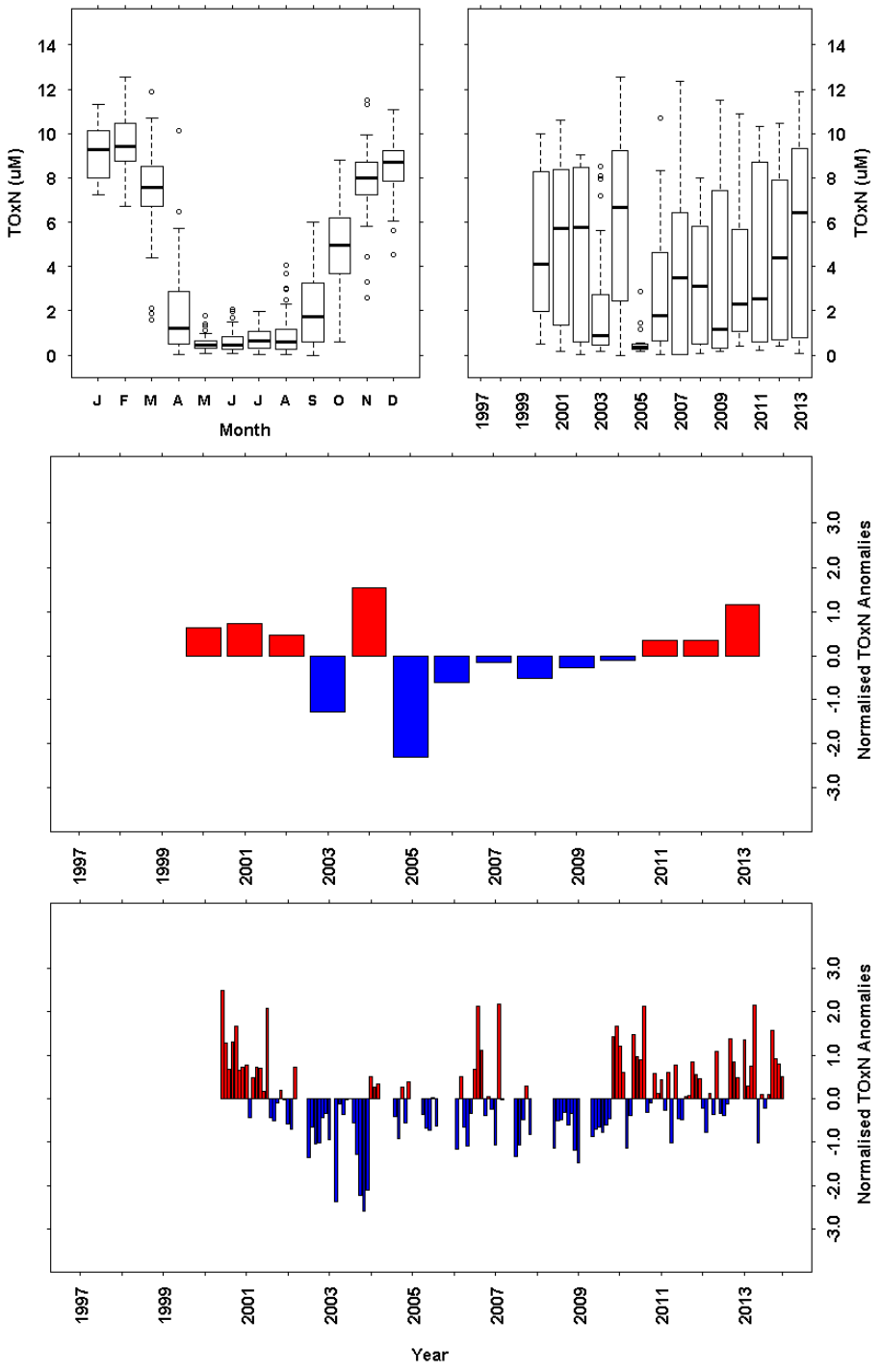

Figure 7.17 Total oxidised nitrogen (TOxN, µM) data from long term monitoring site at Scalloway. a) Monthly boxplot TOxN data. b) Annual boxplot of TOxN data. c) Annual mean anomaly time series d) Monthly mean anomaly time series. There were no data available prior to 2000. In 2005 data is only available from April – August. The full data set was used as the base period for the anomaly calculations.

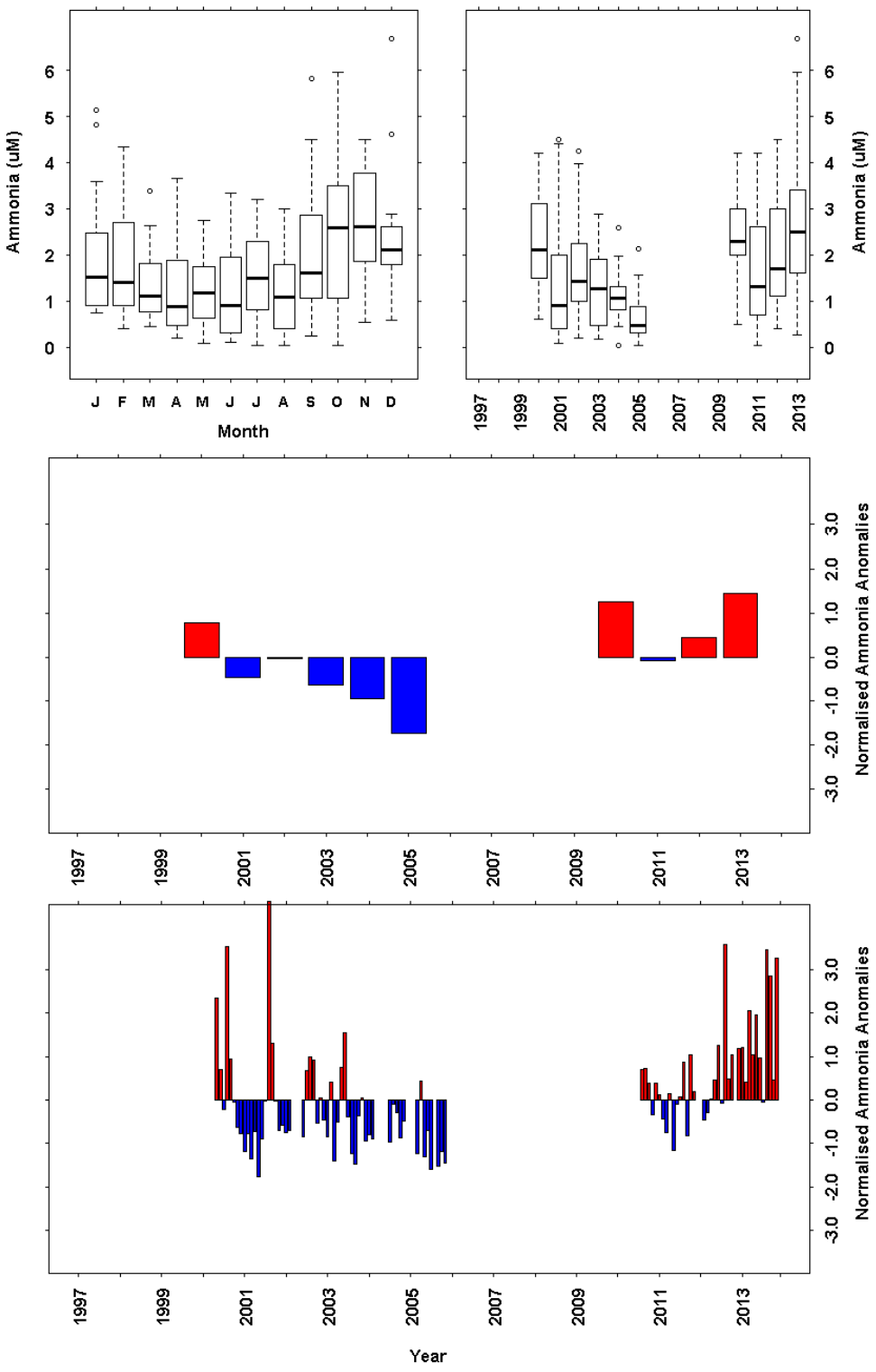

Figure 7.18 Ammonia (µM) data from long term monitoring site at Scalloway. a) Monthly boxplot ammonia data. b) Annual boxplot of ammonia data. c) Annual mean anomaly time series d) Monthly mean anomaly time series. There were no data available prior to 2000. In 2005 data is only available from April – August. The full data set was used as the base period for the anomaly calculations.

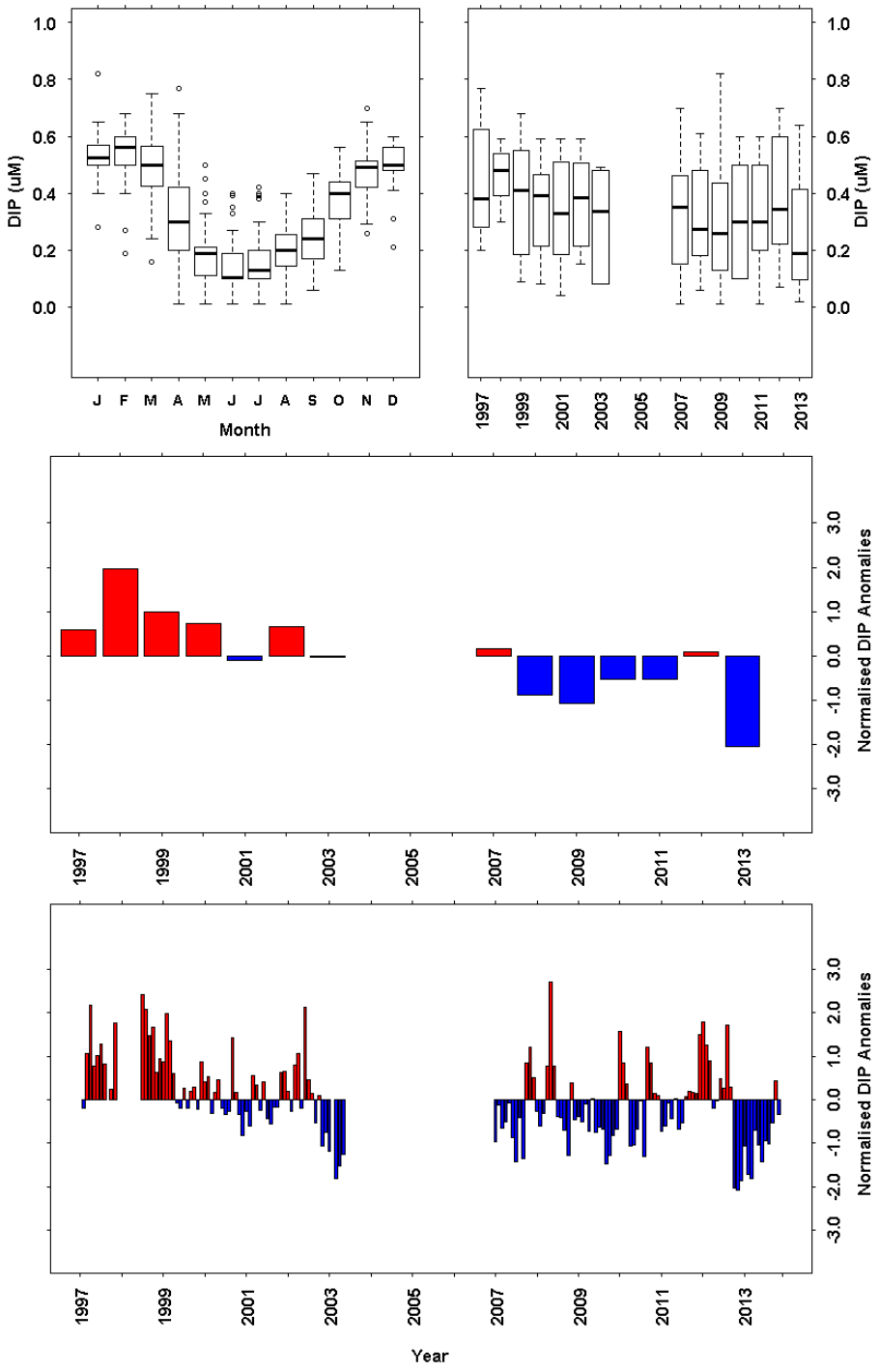

Figure 7.19 Upper layer (0 -10 m) dissolved inorganic phosphorus (DIP, µM) data from long term monitoring site at Stonehaven. a) Monthly boxplot DIP data. b) Annual boxplot of DIP data. c) Annual mean anomaly timeseries d) Monthly mean anomaly timeseries. DIP data for samples collected in 2004, 2005 and 2006 were assigned a Quality Flag of 4 and were therefore excluded from the data assessment. The full data set was used as the base period for the anomaly calculations.

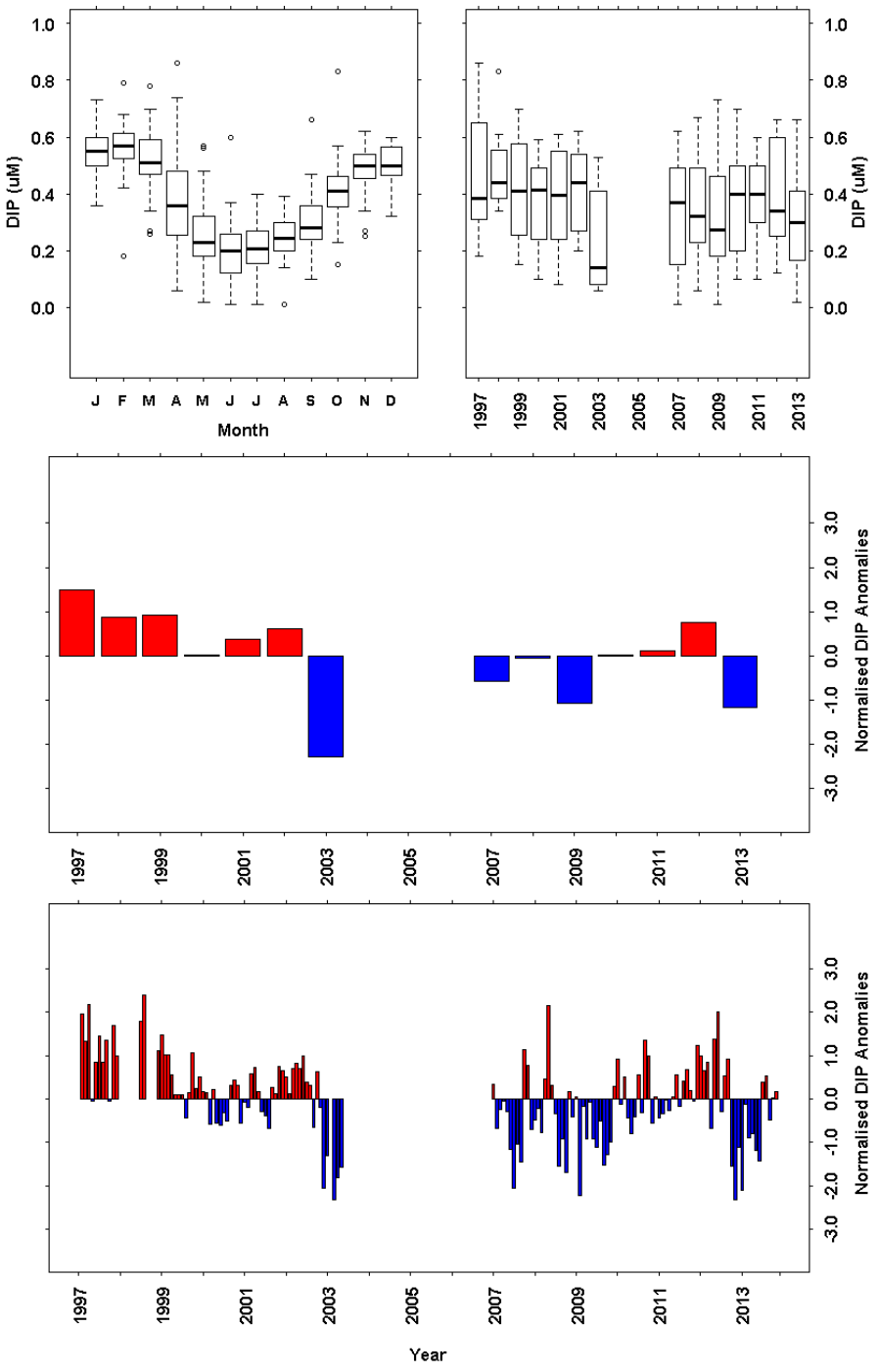

Figure 7.20 Lower layer (>30m) dissolved inorganic phosphorus (DIP, µM) data from long term monitoring site at Stonehaven. a) Monthly boxplot DIP data. b) Annual boxplot of DIP data. c) Annual mean anomaly timeseries d) Monthly mean anomaly timeseries. DIP data for samples collected in 2004, 2005 and 2006 were assigned a Quality Flag of 4 and were therefore excluded from the data assessment. The full data set was used as the base period for the anomaly calculations.

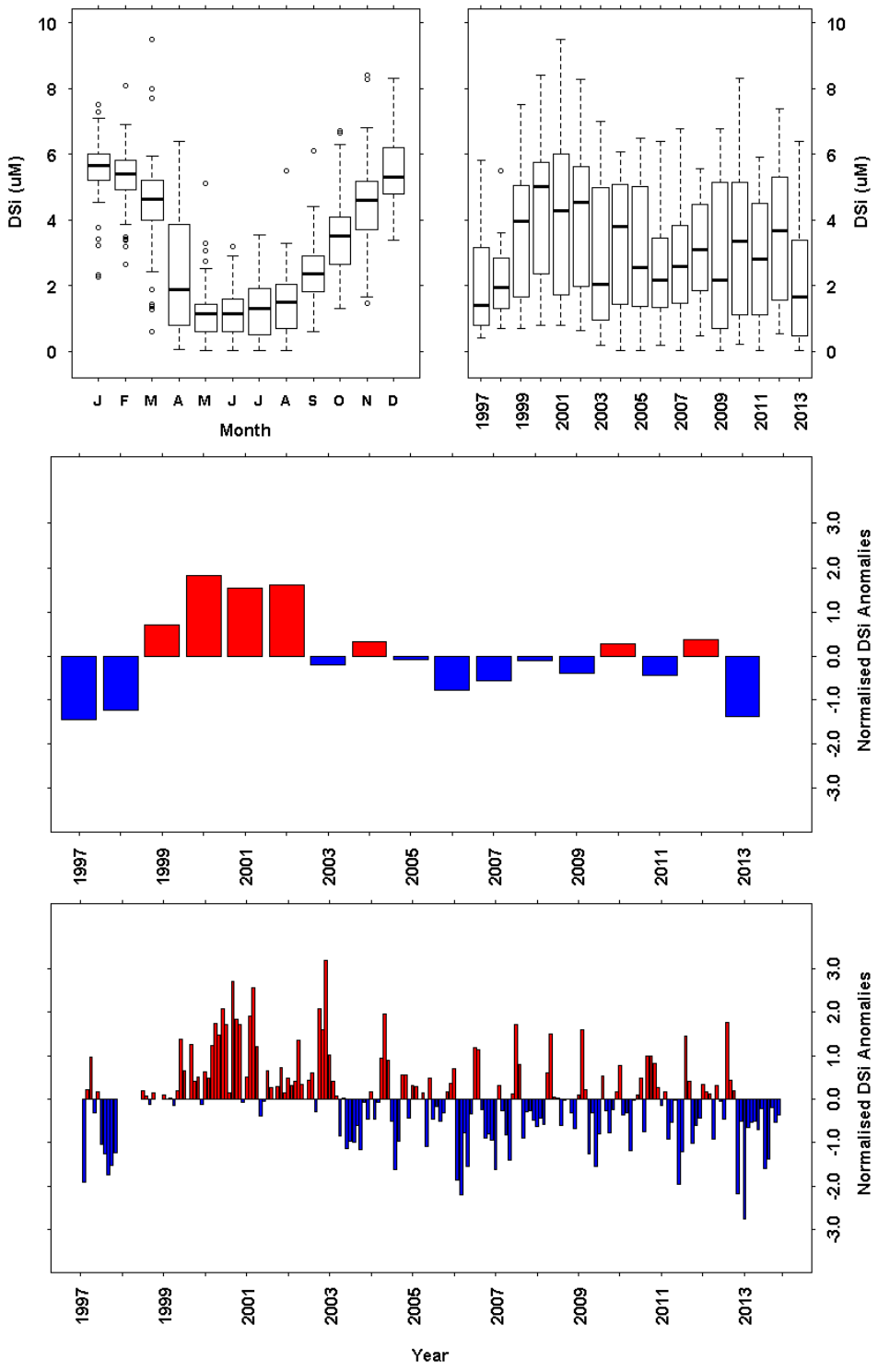

Figure 7.21 Upper layer (0 -10 m) dissolved silicate (DSi, µM) data from long term monitoring site at Stonehaven. a) Monthly boxplot DSi data. b) Annual boxplot of DSi data. c) Annual mean anomaly time series d) Monthly mean anomaly time series. The full data set was used as the base period for the anomaly calculations.

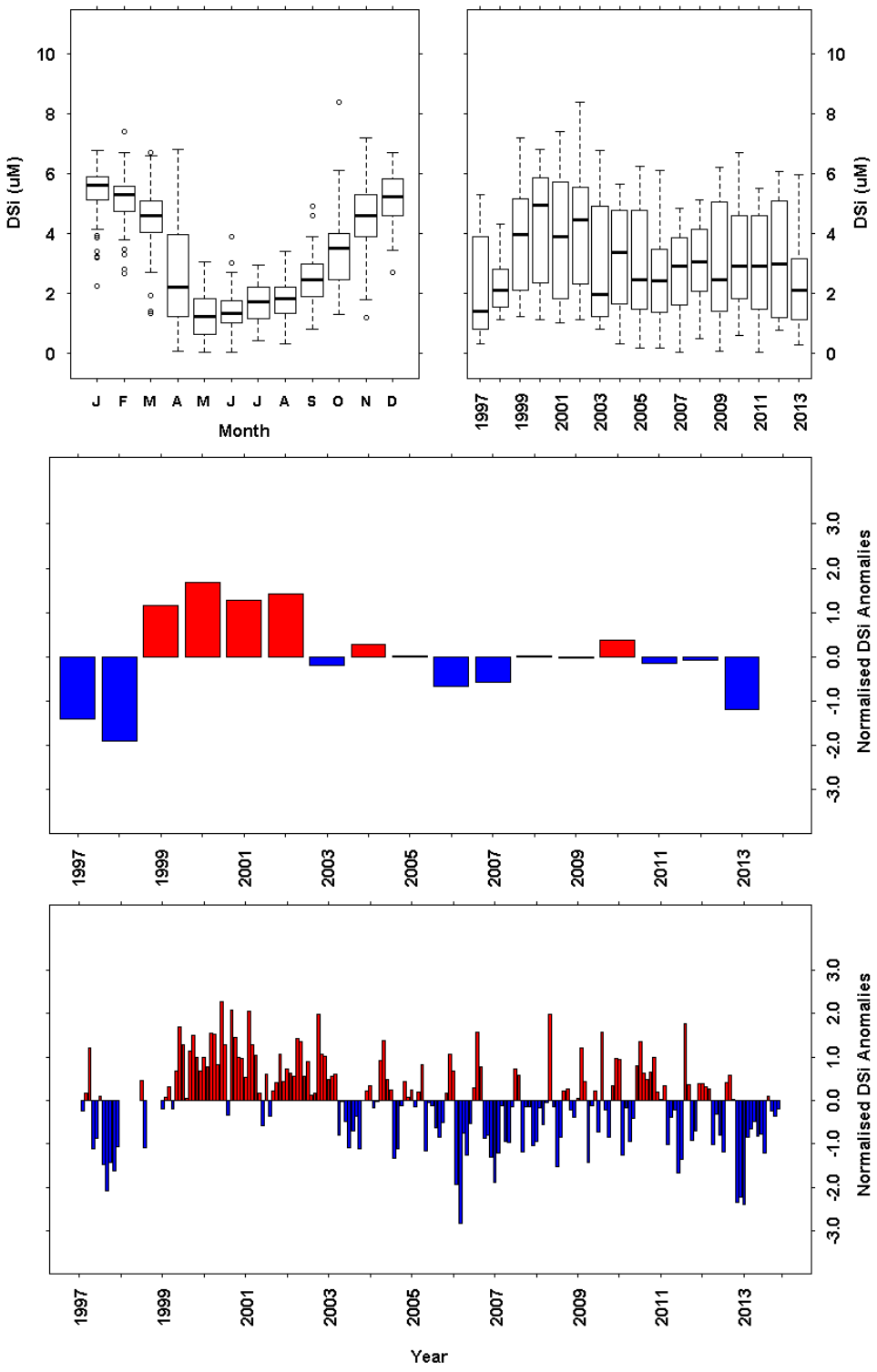

Figure 7.22 Lower layer (>30m) dissolved silicate (DSi, µM) data from long term monitoring site at Stonehaven. a) Monthly boxplot DSi data. b) Annual boxplot of DSi data. c) Annual mean anomaly time series d) Monthly mean anomaly time series. The full data set was used as the base period for the anomaly calculations.

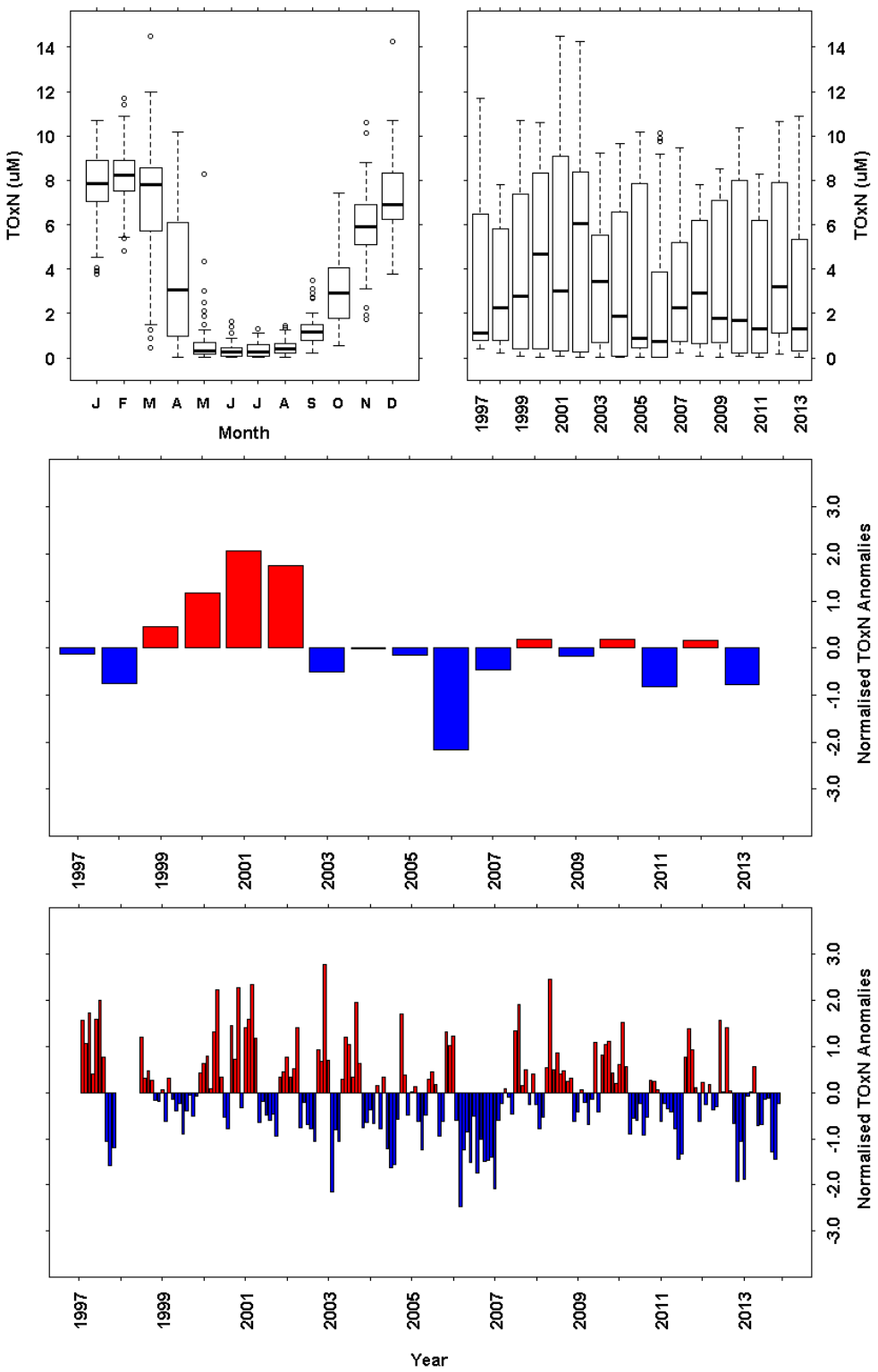

Figure 7.23 Upper layer (0 -10 m) total oxidised nitrogen (TOxN, µM) data from long term monitoring site at Stonehaven. a) Monthly boxplot TOxN data. b) Annual boxplot of TOxN data. c) Annual mean anomaly time series d) Monthly mean anomaly time series. The full data set was used as the base period for the anomaly calculations.

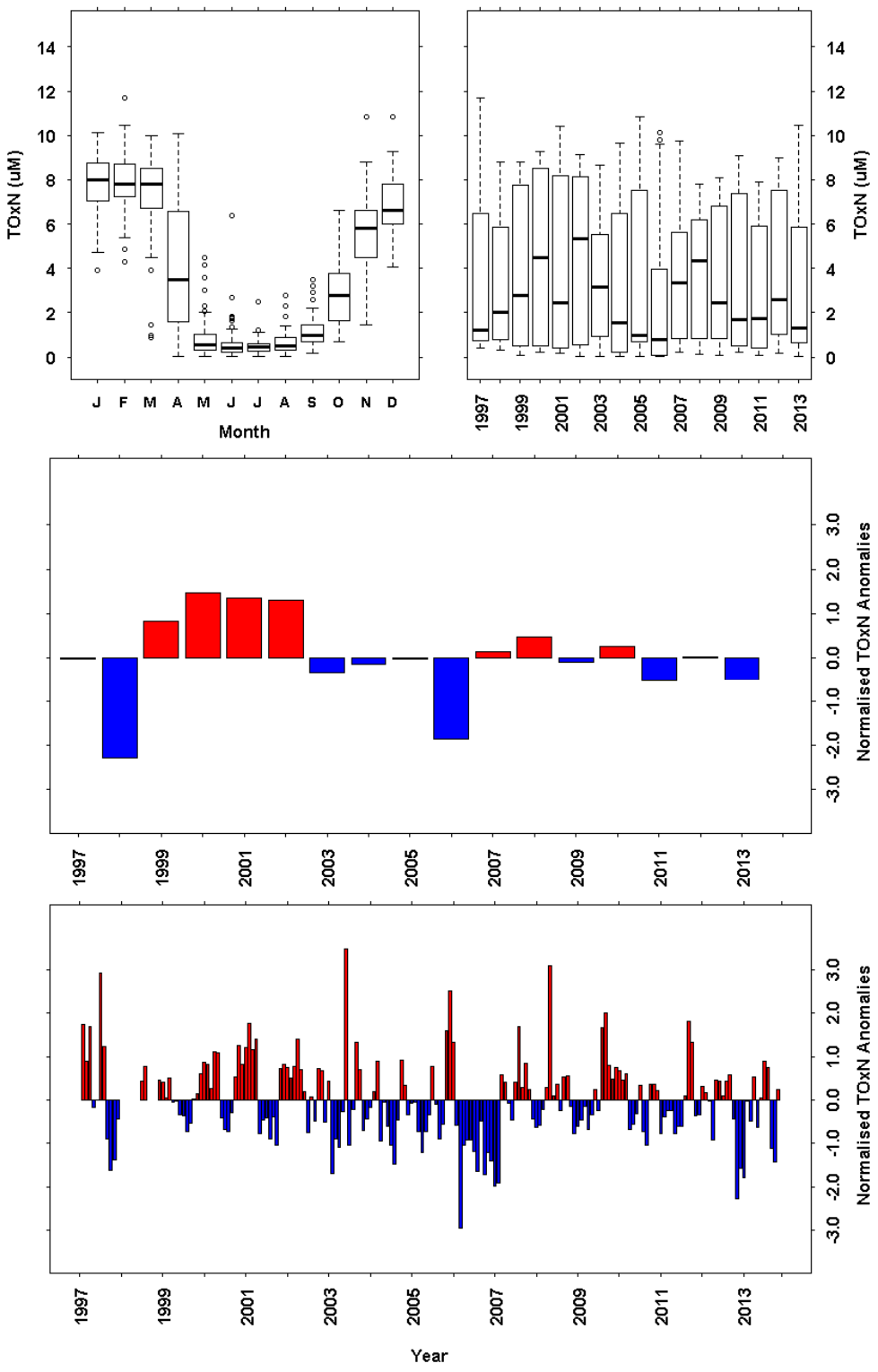

Figure 7.24 Lower layer (>30m) total oxidised nitrogen (TOxN, µM) data from long term monitoring site at Stonehaven. a) Monthly boxplot TOxN data. b) Annual boxplot of TOxN data. c) Annual mean anomaly time series d) Monthly mean anomaly time series. The full data set was used as the base period for the anomaly calculations.

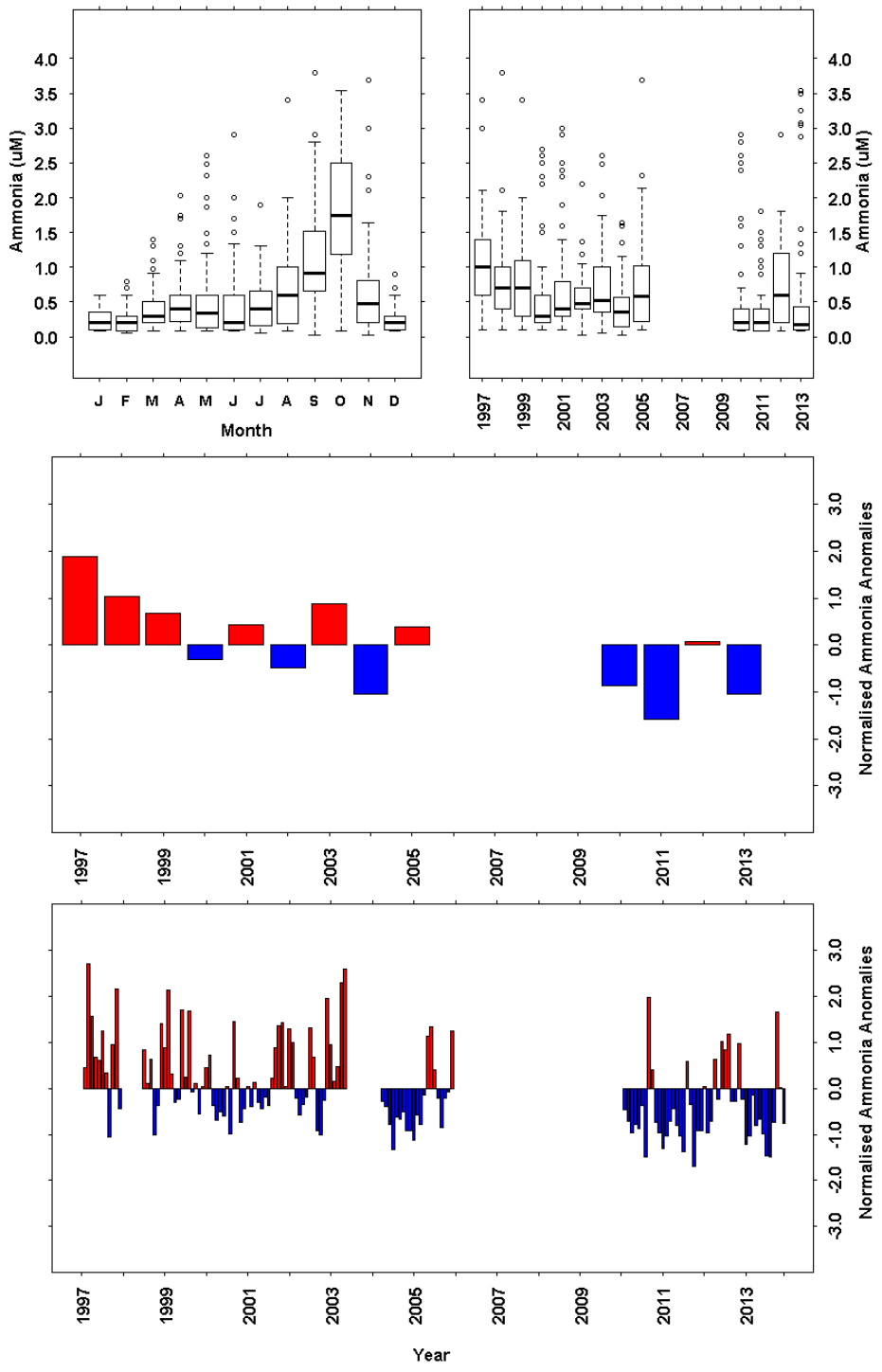

Figure 7.25 Upper layer (0 -10 m) ammonia (µM) data from long term monitoring site at Stonehaven. a) Monthly boxplot ammonia data. b) Annual boxplot of ammonia data. c) Annual mean anomaly time series d) Monthly mean anomaly time series. Ammonia data from samples collected between 2006 and 2009 inclusive were assigned a Quality Flag of 4 and were therefore excluded from the data assessment. The full data set was used as the base period for the anomaly calculations.

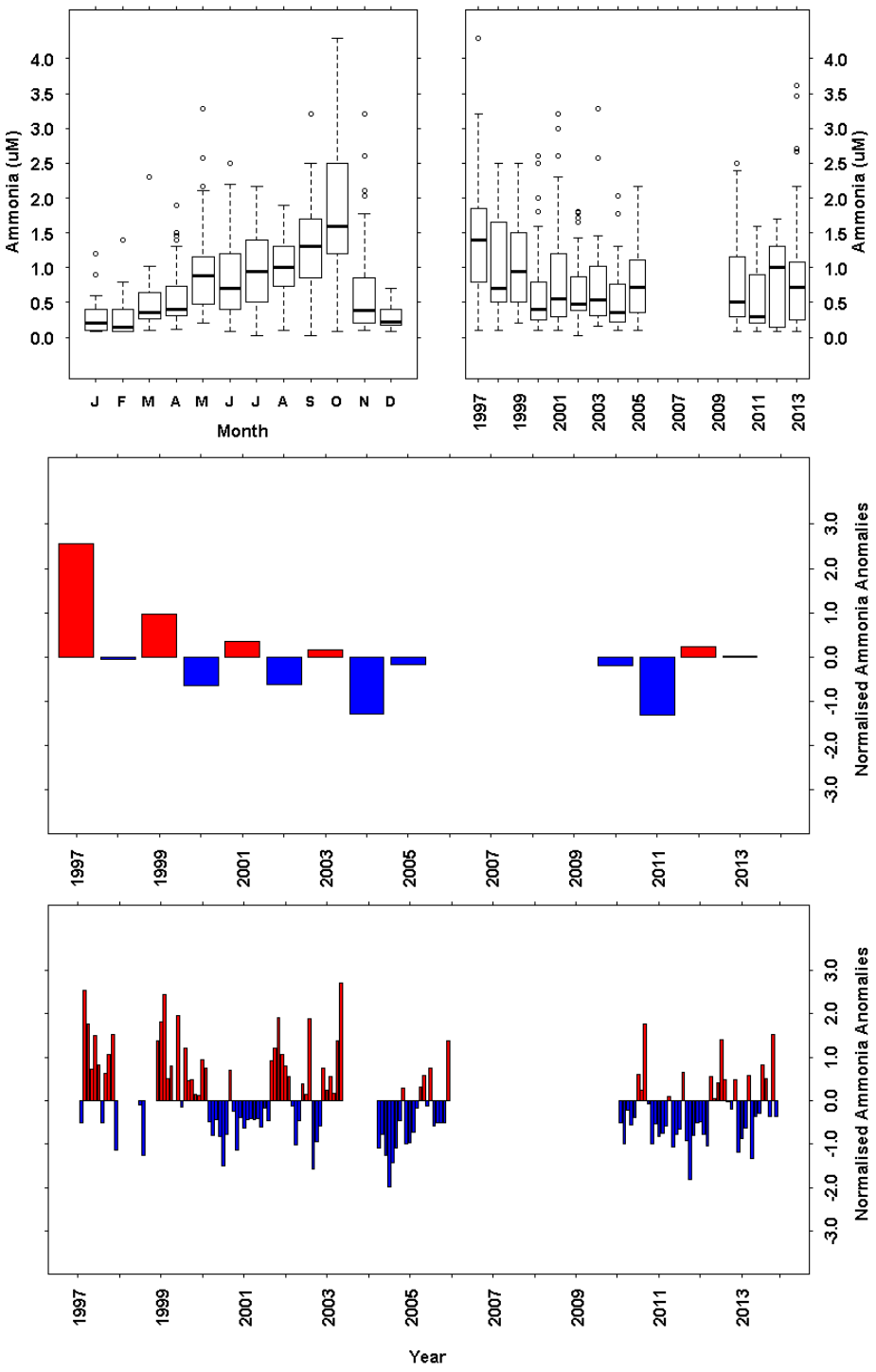

Figure 7.26 Lower layer (>30m) ammonia (µM) data from long term monitoring site at Stonehaven. a) Monthly boxplot ammonia data. b) Annual boxplot of ammonia data. c) Annual mean anomaly time series d) Monthly mean anomaly time series. Ammonia data from samples collected between 2006 and 2009 inclusive were also assigned a Quality Flag of 4 and were therefore excluded from the data assessment. The full data set was used as the base period for the anomaly calculations.

8. Ocean Acidification – Carbonate Chemistry Parameters

8.1 Introduction

Ocean acidification is the decrease in the pH of the earth's oceans as a result of uptake of anthropogenic carbon dioxide (CO_2) from the atmosphere (Calderia and Wickett, 2003). It has been reported that a third of the anthropogenic CO_2 (from activities such as fossil fuel burning) produced over the past 200 years has been absorbed by the oceans, resulting in a decrease in pH of 0.1 units (Sabine et al., 2004). By 2100 the pH is predicted to decrease by up to 0.4 units (Gattuso et al., 2014). Although the input of CO_2 from the atmosphere has only small spatial variation, some marine regions will be more rapidly affected; the susceptibility of water chemistry to change is dependent on the chemical composition and temperature of the water.

The limited data available worldwide shows that acidification does not occur uniformly. Spatial, seasonal and annual variations have been reported (Bates and Peters, 2007; Dore et al., 2009; OSPAR, 2010a), with variability naturally highest in coastal regions. It is, therefore, important to identify these natural variations by routine monitoring before changes due to anthropogenic inputs can be assessed. Ocean acidification and climate change share a common cause, increasing carbon dioxide (CO_2) in the atmosphere. However, ocean acidification must be distinguished from climate change as it is not a climate process but rather an alteration to the chemistry of seawater.

There has been a great deal of interest in ocean acidification in recent years because of its potential effects on marine biogeochemistry and ecosystems. Atmospheric CO_2 is in equilibrium with CO_2 in the aqueous phase. As concentrations of CO_2 increase in the atmosphere, dissolved inorganic carbon (DIC) will increase resulting in an alteration to the carbonate system such that HCO^{-3} and CO_2 will increase while CO_3^{-2} and pH will decrease. $CaCO_3$ saturation decreases with water depth, therefore, any reduction of CO_3^{-2} will potentially result in lowered saturation levels with increased dissolution and reduced saturation depths of marine carbonates such as aragonite, calcite and magnesian calcites (Rost et al., 2008; Feely et al., 2004).

The effects of the decrease in seawater pH and changes to the saturation states of carbonates may be corrosive to the shells and skeletons of marine organisms, while the decrease in carbonate ions may affect organisms' abilities to build skeletons and shells, particularly among calcifying organisms (Feely, 2004). In planktonic and benthic communities many may require more energy to obtain and produce the calcium carbonate required for skeletal or shell production. This may impact on other energy using functions such as fertilisation, development and growth. Studies have shown a decreased calcification when pH is decreased, with early life stages being particularly sensitive to acidification. CO_2 effects will impact the metabolism and physiology of organisms in many ways, since factors such as acid - base status and oxygen transport in cells and body fluids are affected by their pH.

Ocean acidification may also have socio-economic implications for the UK economy as a potential consequence of marine species loss or shift. Estimating the impact of

ocean acidification to the economy, however, is difficult because the ability of marine species to adapt is unknown. Any impact on fertilisation, development and growth of marine species, as a result of ocean acidification, may impact fisheries as a food resource. It is estimated that 20% of the world's protein intake is from marine sources (United Nations, 2007). In 2010, 606,295 tonnes fish and 245,856 tonnes shellfish were landed in the UK and Ireland. It is estimated that 30,000 people in the UK alone are dependent on fishing for their livelihoods (MCCIP, 2012).

The Marine Climate Change Impacts Partnership (MCCIP) 2013 science review (Williamson et al., 2013) predicted that ocean acidification (assuming a doubling of atmospheric CO_2 and a 10-25% reduction in growth calcification) would result in a 10-25% loss in shellfish landings, equating to a loss of £100-500 million per year by 2080 from the UK economy. Coastal areas are also an important part of the UK leisure and recreation industry supporting employment and small businesses for activities such as diving, kayaking, sea angling, and marine mammal observations. Any change in coastal marine biodiversity as a result of ocean acidification may impact potential revenue. The effects of ocean acidification may, therefore, impact those involved in the fisheries and aquaculture industry, retailers, consumers and coastal communities.

In September 2010 the UK signed up to the OSPAR Bergen Statement, to which effect ministers have agreed to respond to new challenges and priorities including ocean acidification. Following on from the Bergen statement the OSPAR Coordination Group (CoG) met and agreed that ocean acidification will be a requirement of the Joint Assessment and Monitoring Programme (JAMP) 2010- 2014 (OSPAR, 2010b). The UK also has a commitment to fulfill Marine Strategy Framework Directive (MSFD) requirements. Annex 3 of the Directive includes pH, pCO2 (partial pressure of CO_2) profiles or equivalent information used to measure marine acidification as a characteristic under physical and chemical features. The OSPAR Quality Status Report, published in September 2010 (OSPAR, 2010a), identified ocean acidification as an emerging concern for ecosystems and indicated that ecosystem wide effects would be observed in the next 50 years.

ICES highlighted the lack of data on seasonal and inter-annual variability, and advised that measurements should cover a range of waters (Hydes et al., 2013). Charting Progress 2 also highlighted the lack of baseline measurements of pH against which changes can be judged and indicated that there was an upward trend in ocean acidification which could pose a threat to marine species and ecosystems. Both the OSPAR/ICES Study Group on Ocean Acidification (SGOA; ICES, 2014) and the Global Ocean Acidification Observing Network (GOA-ON; Newton et al., 2015) have identified particular gaps in data for coastal and inshore waters. This time series begins to address this knowledge gap.

8.2 Methods

Collection and Storage of Sea Water Samples

Between 2009 and 2013 water samples were collected from two depths (1 m and 45 m) on a weekly basis (weather permitting) at the Stonehaven ecosystem monitoring site with the aim of providing a baseline for a coastal region in Scottish waters.

Water samples collected between January 2009 and February 2011 and analysed, by the National Oceanography Centre Southampton (NOC), as part of the Defra PH project and UK Ocean Acidification (UKOA) project. Since August 2011, water samples have been collected at the Stonehaven monitoring site. Samples were collected using a Niskin sampling bottle, which was also fitted with a digital reversing thermometer. Discrete water samples were collected for the determination of Dissolve Inorganic Carbon (DIC) and Total Alkalinity (TA) into 250 ml glass bottles (Schott Duran) and poisoned with 50 µl saturated $HgCl_2$ solution to prevent biological alteration during storage. A head-space of 2.5 mL was left to allow for water expansion and the bottles were sealed using a greased ground glass stoppers to ensure they remained gas-tight.

Samples were shipped to the National Oceanography Centre Southampton (NOC) for analysis at the Natural Environment Research Council (NERC) laboratory.

Determination of Total Alkalinity (TA) and Dissolved Inorganic Carbon (DIC)

Analysis was performed using colorimetric and potentiometric open titration cell techniques. Samples were analysed using the Versatile Instrument for Analysis of Titration Alkalinity (VINDTA 3C, Marianda, Germany) on the two NERC Ocean Biogeochemistry and Ecosystems group carbonate facility (VINDTA units 11 and 24). All the samples were heated to 25ºC using a water bath (F12, Julabo, Germany) immediately before analysis. Standard guidelines were followed for analysis (Mintrop, 2005 and Hartman et al., 2011). DIC and TA were analysed in batches of between 9 and 24 samples. Duplicate samples were, where possible, analysed on different NOC Vindta instruments.

Dissolved Inorganic Carbon (DIC)

DIC was measured by a coulometric titration (coulometer 5011, UIC, USA) following the extraction of CO_2 from a ~20 ml sub-sample. The DIC section of the VINDTA 3C consists of two main parts where reactions take place. In the first, the sample is acidified with phosphoric acid (H_3PO_4, 10%) and bubbled through with the inert carrier gas (nitrogen), thereby reducing the pH and converting the carbon species into CO_2 gas. The CO_2 gas is then transferred into the second part by the inert carrier gas being cooled to remove water vapour enroute into the coulometer cell, where it is titrated colorimetrically.

The coulometer cell consists of two chambers separated by a sintered glass frit, the cathode and the anode chamber, with a platinum and silver electrode, respectively, and connected to the coulometer to produce a current. The cathode cell is filled with a dimethylsulfoxide solution containing monoethanolamine ($HOCH_2CH_2 NH_2$,) and the pH indicator thymol blue. The produced CO_2 reacts with the monoethanolamine to form hydroxyethyl carbamic acid ($HOCH_2CH_2NHCOOH$) causing the indicator to turn colourless, increasing the transmittance. The current is activated and the electrons titrate the hydroxethyl carbamic acid returning the pH to the value before the CO_2 addition, returning the indicator to blue and the transmittance to 29.6%. At the beginning of each session, a blank measurement was undertaken adding only H_3PO_4, generating an amount of counts (ideally below 100), which then are

subtracted from the end count as well as used to determine the titration endpoint. Analysis concluded after four end-points had been achieved.

Total Alkalinity

Total alkalinity (TA) was determined by a potentiometric open-cell titration on a ~100 ml sub-sample using a pH half-cell electrode (Orion, Ross, USA) and Ag/AgCl reference electrode (Metrohm, Switzerland). The sample was titrated against hydrochloric acid (HCl, 0.1M) prepared in sodium chloride solution (NaCl, 0.7 M). HCl was added via a Metrohm titrator (0.15 ml additions) until the carbonic acid equivalence point was reached. The pH of the titration was monitored by the pair of electrodes which measured the difference in electromotive force (emf) caused by the change in pH. The emf and the amount of acid added allows the calculation of total alkalinity by a curve fitting method based on a Gran plot approach (Dickson et al., 2007) by the VINDTA software.

Quality Control

Precision

Repeat measurements on previously analysed samples were undertaken before sample analysis each day (n>3). Instrument precision was better than ± 1.5 µM/kg for DIC and TA. The standard deviation for DIC and TA was calculated for each day of analysis.

Instrument Calibration and Monitoring Analytical Performance

Reference Materials (RM) from Dr Andrew Dickson (Scripps Institution of Oceanography) were used for calibration to assure the accuracy of the measurements. RMs were analysed at the beginning, middle and end of the sessions. The result of the first RM analysis was used in the final calculation to avoid bias in DIC due to gas exchange providing a correction factor (k) for each analysis session.

K= RM measured/ RM certificate

RMs were monitored on control charts for each individual instrument.

Data Handling - Correction for Salinity

The VINDTA software assigns a default salinity of 35 PSU. However, if the sample salinity was known at the time of analysis the TA was corrected for this within the instrument software. The DIC was corrected for salinity post analysis (Friis et al., 2003).

Data Handling - CO2SYS Routine

The marine carbonate system can be characterised from any two of the four parameters: DIC, TA, pCO_2 and pH. The Excel program “CO2SYS” can be used to calculate the partial pressure of CO_2 (pCO_2), pH, calcite and aragonite saturation

states, Revelle factor, carbonate and bicarbonate ion concentrations (Periott et al., 2006). The combination of input parameters DIC, TA, DIP and DSi concentrations and laboratory pressure and temperature (0 dbar, 25 Cº) and output conditions (real temperature and pressure when the sample was taken) were used to calculate the two other carbonate chemistry parameters pCO_2 and pH.

The dissociation constants of carbonic acid (pK1 and pK2) determined in real seawater (Millero et al., 2006) were used as constants in the CO2SYS calculation. The pCO_2 calculation comes from the inaccuracies of the thermodynamic dissociation constants (mainly pK1 and pK2) and the experimental measurements of the variables used for calculation and can be in the order of ± 7 µatm (Millero et al., 2006).

8.3 Results

There are four parameters of the marine carbonate system which can be measured directly; TA, pH, ρCO_2 andDIC. Measurements of any two components allow the concentration of the other two to be calculated. TA and DIC have been measured in surface and bottom waters at the Stonehaven long term monitoring site since 2009. TA and DIC concentrations are shown as monthly and year box plots (Figures 8.1-8.4) for both surface and bottom waters.

The monthly box plot shows a seasonal trend for TA in bottom waters with maximum concentrations in the summer months coinciding with the phytoplankton growing season. This is a consequence of nitrate uptake by phytoplankton cells during the growing season which reduces nitrate concentrations in the water which impacts TA. There was a slight increase in TA concentrations in surface waters during the summer months but the trend was not as pronounced as bottom waters possibly as a consequence of surface mixing at the site. DIC concentrations increased over the winter months to a maximum in March before decreasing to a minimum around June in surface and bottom waters. This annual cycle was strongest in surface waters.

The winter DIC maximum could potentially be attributed to calcite dissolution in the area and lack of uptake by phytoplankton due to low growth. The pH and calcite saturation were derived using CO2SYS. Monthly box plots of both surface and bottom pH showed pH was highest during April and May and corresponded with the phytoplankton growing season. Derived calcite saturation, of surface and bottom waters, was lowest during the winter months increasing to a maximum around June and July (Figures 8.5-8.8).

Ocean acidification is a long term process requiring decadal scale monitoring and it is therefore difficult to determine trends over the short timescale of this work (2008 to 2013). It should be noted that sampling only began in November 2008 and the boxplot for this year is based on two months of data.

Yearly boxplots of TA concentrations in both surface and bottom waters appear to show a drop in the alkalinity at the site in 2013. This corresponds to a negative anomaly on the anomaly plots for both the surface and bottom waters in 2013. DIC concentrations of both surface and bottom waters appear to have increased during

the period of the analysis and this corresponds to a positive anomaly plot from 2011 onwards.

Yearly box plots of both the derived pH and calcite saturation appear to show a downward trend at the site. The pH anomaly plots at both depths are negative in 2012 and 2013 while the calcite saturation anomaly plots are negative at both depths in 2011 and 2013. If this data is reviewed in isolation it would appear there is a downward trend. However, this does not account for any changes in salinity during the period. In late 2012 the salinity at the site increased to almost 35 PSU possibly as a consequence of offshore waters entering the site followed by very cold spring water temperatures. The downward trend in pH is not unique to Stonehaven, a recent publication by Ostle (2016) observed decreasing pH during the same period at the Western Channel Obervataory (Western English Channel) and the CEFAS Smartbuoy sites located in the Southern North Sea and Liverpool Bay. The Ostle publication did not consider changes to salinity or temperature and its impact on carbonate chemistry.

It is not currently possible to assess the data collected against assessment criteria as there are none available for carbonate chemistry parameters in relation to OA. The joint OSPAR/ICES Ocean Acidification Study Group (SGOA) noted that the existing concept of OSPAR assessment criteria is not readily transferrable to OA due to the long-term and global nature of the issue. SGOA concluded that the primary focus should be on temporal trend assessments. However, the calcite saturation at the site remains >1 indicating the waters at Stonehaven are supersaturated and organisms should be able to calicify. The long-term monitoring at Stonehaven highlights the requirement for a robust data set to distinguish changes as a consequence of anthropogenic inputs from that of the natural seasonal and inter-annual variability.

8.4 Summary – Ocean Acidification

- Ocean acidification driven by anthropogenic inputs is a long term process requiring high frequency decadal scale monitoring to identify established changes in carbonate chemistry.
- The carbonate chemistry parameters TA and DIC, pH and calcite saturation are presented from the Stonehaven coastal station. TA and DIC were measured directly from duplicate samples in surface (1m) and bottom waters (45m) between 2009 and 2013. Calcite saturation and pH values were derived.
- This dataset represents the only high frequency coastal carbonate chemistry time series in Scottish waters and provide a unique insight into the seasonality, short-term and interannual variability.
- The data reveal considerable variability on a weekly time scale at the Stonehaven monitoring site. On a seasonal scale it shows a relationship with the phytoplankton growing season as DIC is lowest and pH and TA highest when phytoplankton numbers are elevated.

- Both the derived pH and calcite saturation state decreased at the Stonehaven site during 2012 - 2013. This is consistent with other observations around UK waters over the same period. At Stonehaven, this event coincided with unusually high salinity water in the autumn 2012, followed by very low temperatures in spring 2013, both of which can be indicative of factors that affect carbonate chemistry.
- There are currently no asssessment criteria available for carbonate chemistry parameters in relation to OA. Changes in the saturation states of the carbonates, however, can give an indication of an organisms ability to calcify. Waters must be supersaturated (saturation > 1) to maintain calcification. The derived calcite saturation at Stonehaven remains >1, indicating the waters at Stonehaven are supersaturated and organisms should be able to calcify.
- The monitoring at Stonehaven highlights the requirement for a robust data set to distinguish changes as a consequence of anthropogenic inputs from that of the natural seasonal and inter-annual variability. Therefore, it is important that time series are maintained and supported, particularly in the coastal and inshore waters which have been identified as data gaps internationally.

8.5 References – Ocean Acidification

Bates, N.R. and Peters, A.J. 2007. The contribution of atmospheric acid decomposition to ocean acidification in the subtropical North Atlantic Ocean. Marine Chemistry, 107, 547-558.

Caldeira, K. and Wickett, M.E. 2003. Anthropogenic carbon and ocean pH. Nature, 425, 365-366.

Dickson, A.G., Sabine, C.L., Christian, J.R. 2007. Guide to best practices for ocean CO_2 measurements, North Pacific Marine Science Organization (PICES), Sidney, British Columbia, 191 pp.

Dore, J.E., Lukas, R., Sadler, D.W., Church, M.J., Karl, D.M. 2009. Physical and biogeochemical modulation of ocean acidification in the central North Pacific. Proceedings of the National Academy of Sciences, 106, 12235-12240.

Feely, R.A, Sabine, C.L., Lee, K., Berelson, W., Kleypas, J., Fabry, V.J., Millero, F.J. 2004. Impact of Anthropogenic CO_2 on the $CaCO_3$ system in the oceans. Science, 305, 362-366.

Friis, K., Kortzinger, A., Wallace, D.W.R. 2003. The salinity normalization of marine inorganic carbon chemistry data. Geophysical Research Letters,30(2), 1085, doi: 10.1029/2002gl015898.

Gattuso, J.-P., Brewer, P.G., Hoegh-Guldberg, O., Kleypas, J.A., Portner, H.-O., Schmidt, D.N. 2014. Cross-chapter box on ocean acidification. In: Climate Change 2014: Impacts, Adaptation, and Vulnerability. Part A: Global and Sectoral Aspects. Contribution of Working Group II to the Fifth Assessment Report of the Intergovernmental Panel on Climate Change [Field, C.B., Barros, V.R., Dokken, D.J., Mach, K.J., Mastrandrea, M.D., Bilir, T.E., Chatterjee, M., Ebi, K.L., Estrada, Y.O., Genova, R.C., Girma, B., Kissel, E.S., Levy, A.N., MacCracken, S., Mastrandrea, P.R., White, L.L. (eds.)]. Cambridge University Press, Cambridge, United Kingdom and New York, NY, USA, pp. 129-131.

Hartman, S.E., Dumousseaud, C., Roberts, A. 2011. National Oceanography Centre Internal Document No. 01 Operating manual for the Marianda (Versatile INstrument for the Determination of Titration Alkalinity) VINDTA 3C for the laboratory based determination of Total Alkalinity and Total Dissolved Inorganic Carbon.

Hydes, D.J., McGovern, E., Walsham, P. (Eds.). 2013. Chemical aspects of ocean acidification monitoring in the ICES marine area. ICES Cooperative Research Report No. 319. 78 pp.

ICES 2014. Final Report to OSPAR of the Joint OSPAR/ICES Ocean Acidification Study Group (SGOA). ICES CM 2014/ACCOM:67.141pp.

MCCIP 2012. Marine Climate Change Impacts on Fish, Fisheries and Aquaculture. (Frost M., Baxter J.M., Buckley P.J., Cox M., Dye S.R., Withers Harvey N. eds.) Summary Report, MCCIP, Lowstoft, 12pp.

Millero, F.J., Graham T.B., Huang, F., Bustos-Serrano, H., Pierrot, D. 2006. Dissociation constants of carbonic acid in seawater as a function of salinity and temperature. Marine. Chemistry, 100(1-2), 80-94.

Mintrop, L. 2005. The Versatile INstrument for the Determination of Titration Alkalinity; manual for versions 3s and 3c. In: Marianda 2.

Newton J.A., Feely R.A., Jewett E.B., Williamson P., Mathis J. 2015. Global Ocean Acidification Observing Network: Requirements and Governance Plan Second Edition, GOA-ON, http://goa-on.org/

OSPAR QSR 2010 a – Climate Change. http://qsr2010.ospar.org/en/index.html

OSPAR CoG 10/6/1, 2010 b, 2010/11 Product 5 - Initial list of parameters associated with climate change and ocean acidification needed in OSPAR monitoring and assessment work under the JAMP.

Ostle C., Williamson, P., Artioli, Y., Bakker, D.C.E., Birchenough, S., Davis, C.E., Dye, S., Edwards, M., Findlay, H.S., Greenwood, N., Hartman, S., Humphreys, M.P., Jickells, T., Johnson, M., Landschützer, P., Parker, R., Pearce, D., Pinnegar, J., Robinson, C., Schuster, U., Silburn, B., Thomas, R., Wakelin, S., Walsham, P., Watson A.J. 2016. Carbon dioxide and ocean acidification observations in UK waters: Synthesis report with a focus on 2010- 2015. doi:10.13140/RG.2.1.4819.4164.

Pierrot, D., Lewis, E., Wallace, D.W.R. 2006. MS Excel program developed for CO2 system Calculations, ORNL/CDIAC-105a. Carbon Dioxide Information Analysis Center, Oak Ridge National Laboratory, US Department of Energy, Oak Ridge, TN.

Rost,B., Zondervan, I., Wolf-Gladrow, D. 2008. Sensitivity of phytoplankton to future changes in the ocean carbonate chemistry: current knowledge, contradictions and research directions. Marine Ecology Progress Series, 373, 227-237.

Sabine, C.L., Feely, R.A., Gruber, N., Key, R.M., Lee, K., Bullister, J.L., Wanninkof, R., Wong, C.S., Wallace, D.W.R., Tilbrook, B., Millero, F.J., Peng, T-H., Kozyr, A., Ono, T., Rios, C.S. 2004. The ocean sink for CO_2. Science, 305,367-371.

United Nations. Food and Agriculture Organisation of the United Nations 2007. The State of World Fisheries and Aquaculture, 2006. Food and Agricultural Organisation Fisheries and Aquaculture Department, Rome.

Williamson,P., Turley, C., Brownlee, C., Findlay, H.S., Ridgwell, A., Schmidt, D.N., Schroeder, D.C., Blackford, J., Tyrrell, T., Pinnegar, J.K. 2013. Impacts of ocean acidification. MCCIP Science Review 2013, 34-48, doi:10.14465/2013.arc05.034-048.

8.6 Plots – Carbonate Chemistry Parameters

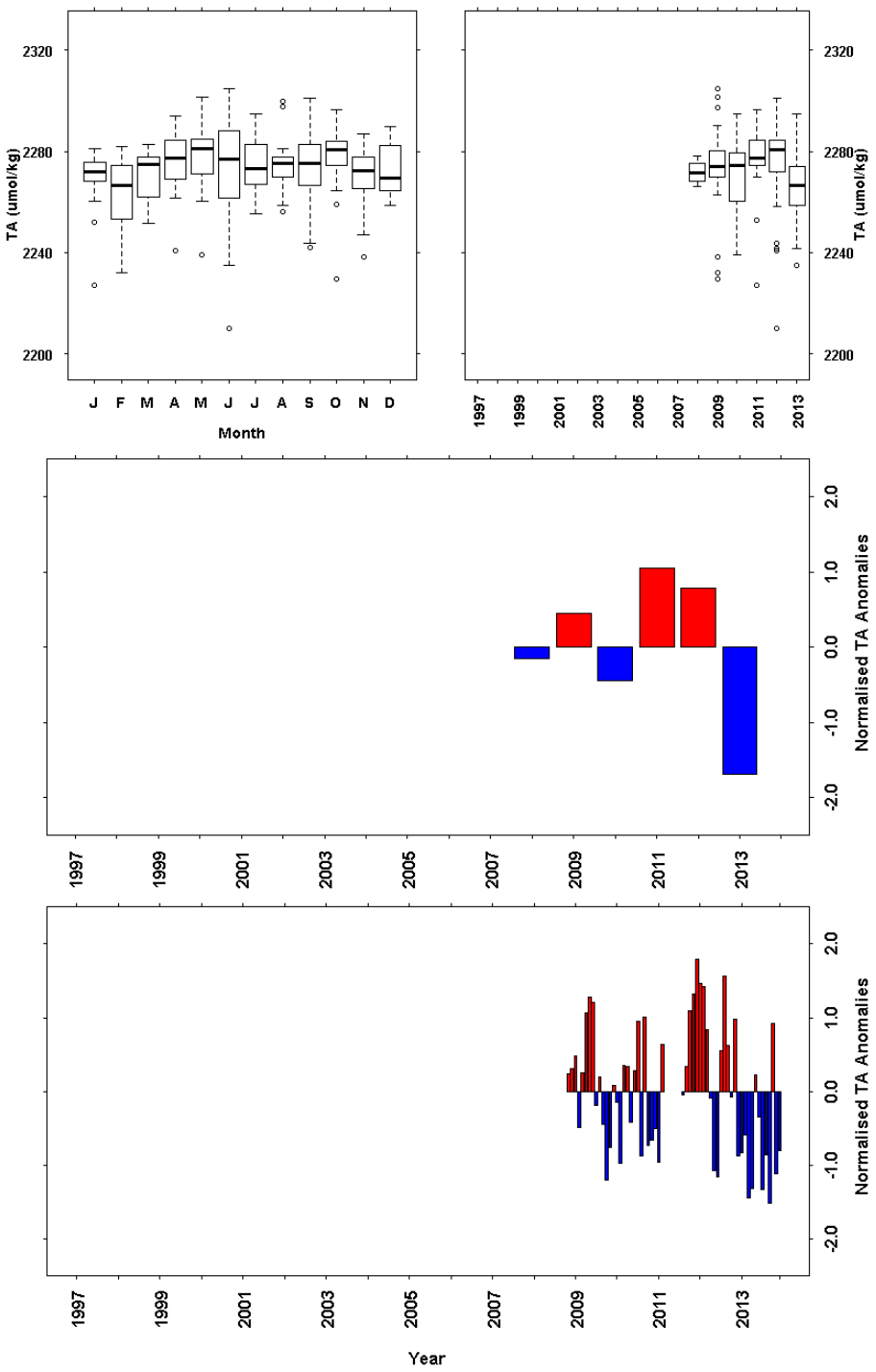

Figure 8.1 Upper layer (0-10 m) Total Alkalinity (TA) data from the long term monitoring site at Stonehaven. a) monthly boxplot of TA data, b) annual boxplot of TA data, c) annual TA anomaly time series data and d) monthly TA anomaly timeseries data. There were no data available prior to November 2008. The full data set was used as the base period for the anomaly calculations.

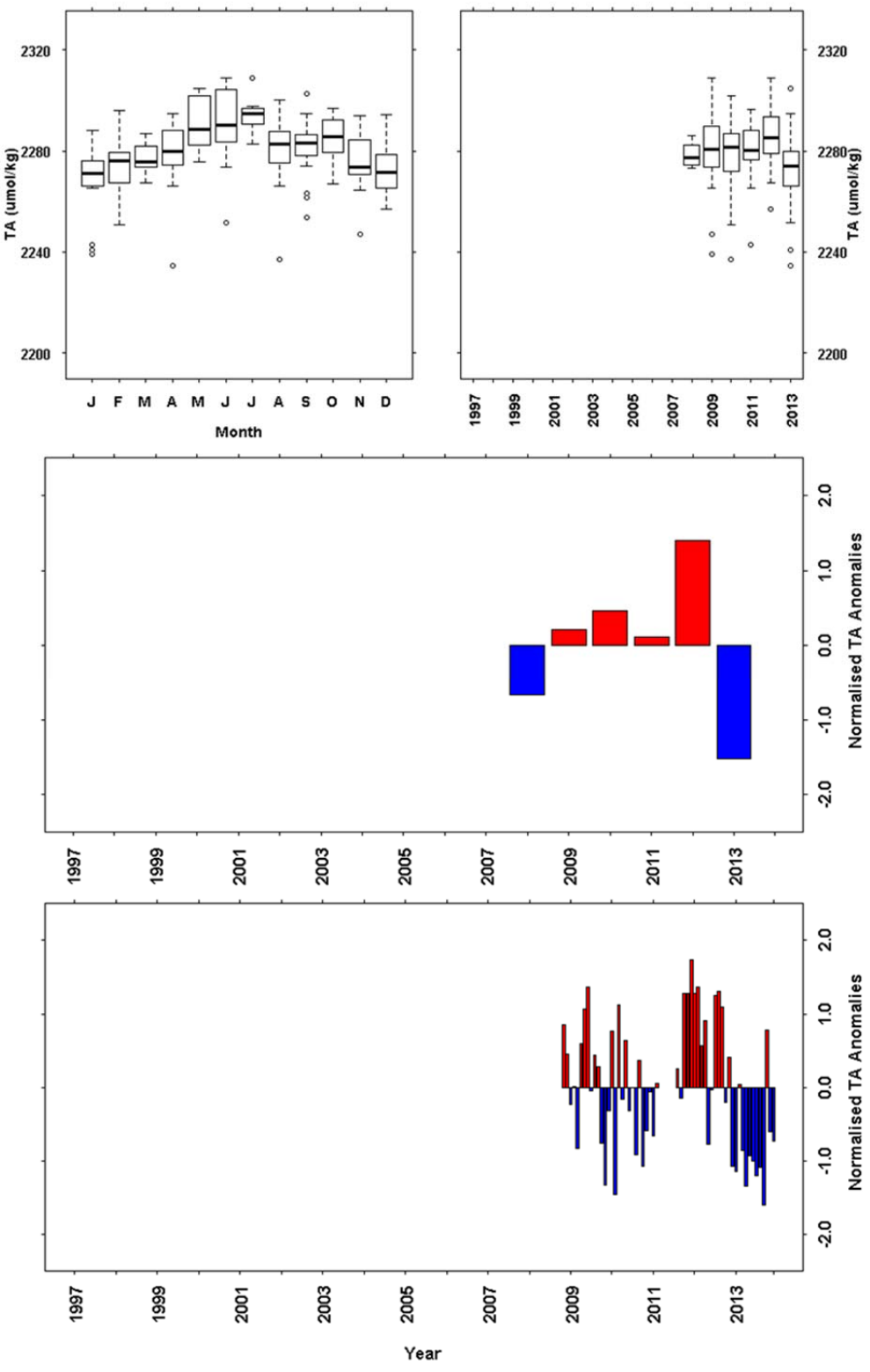

Figure 8.2 Lower layer (> 30 m) Total Alkalinity (TA) data from the long term monitoring site at Stonehaven. a) monthly boxplot of TA data, b) annual boxplot of TA data, c) annual mean TA anomaly timeseries data and d) monthly mean TA anomaly timeseries data. There were no data available prior to November 2008. The full data set was used as the base period for the anomaly calculations.

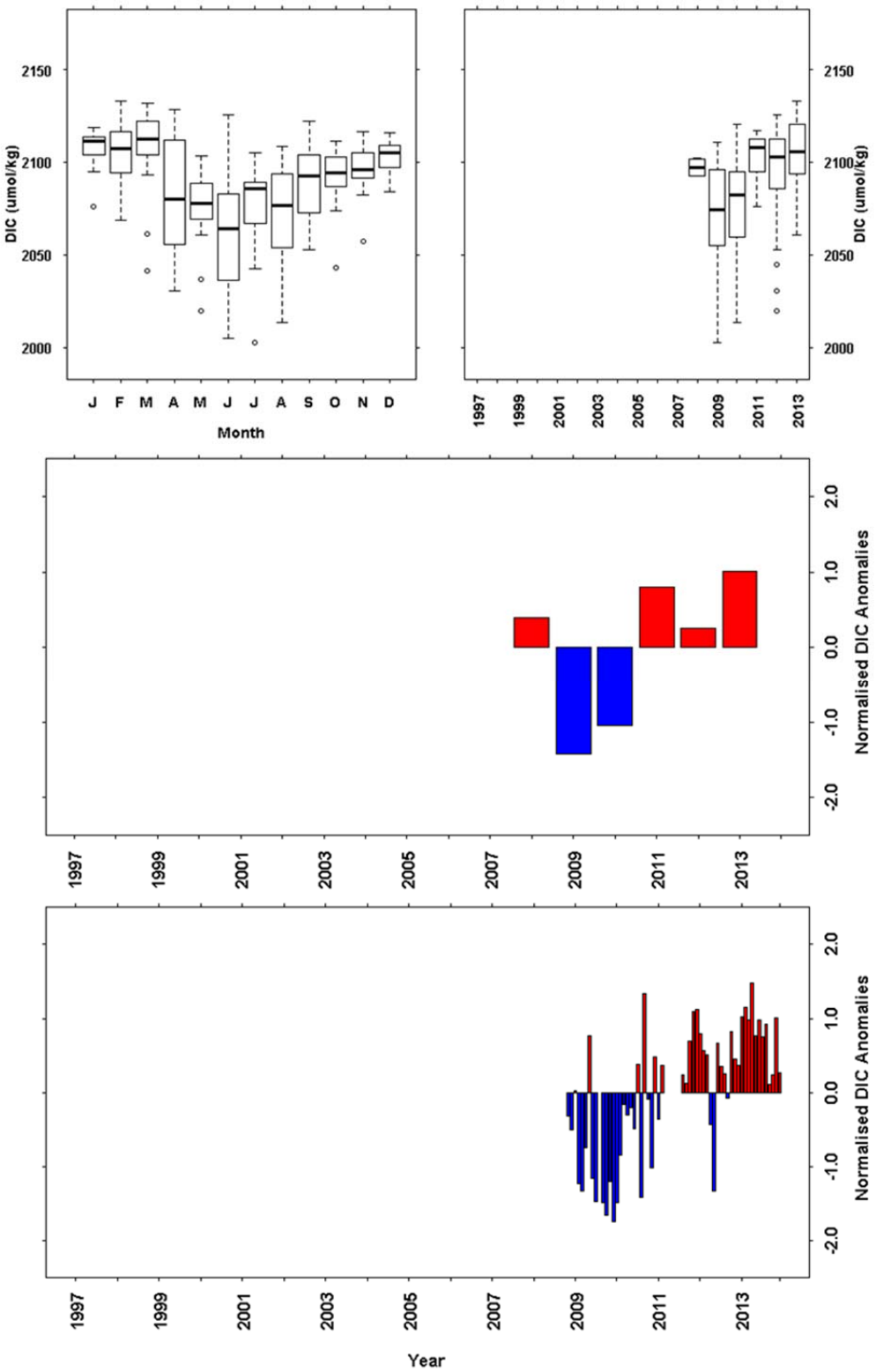

Figure 8.3 Upper layer (0-10 m) Dissolved Inorganic Carbon (DIC) data from the long term monitoring site at Stonehaven. a) monthly boxplot of DIC data, b) annual boxplot of DIC data, c) annual mean DIC anomaly timeseries data and d) monthly mean DIC anomaly timeseries data. There were no data available prior to November 2008. The full data set was used as the base period for the anomaly calculations.

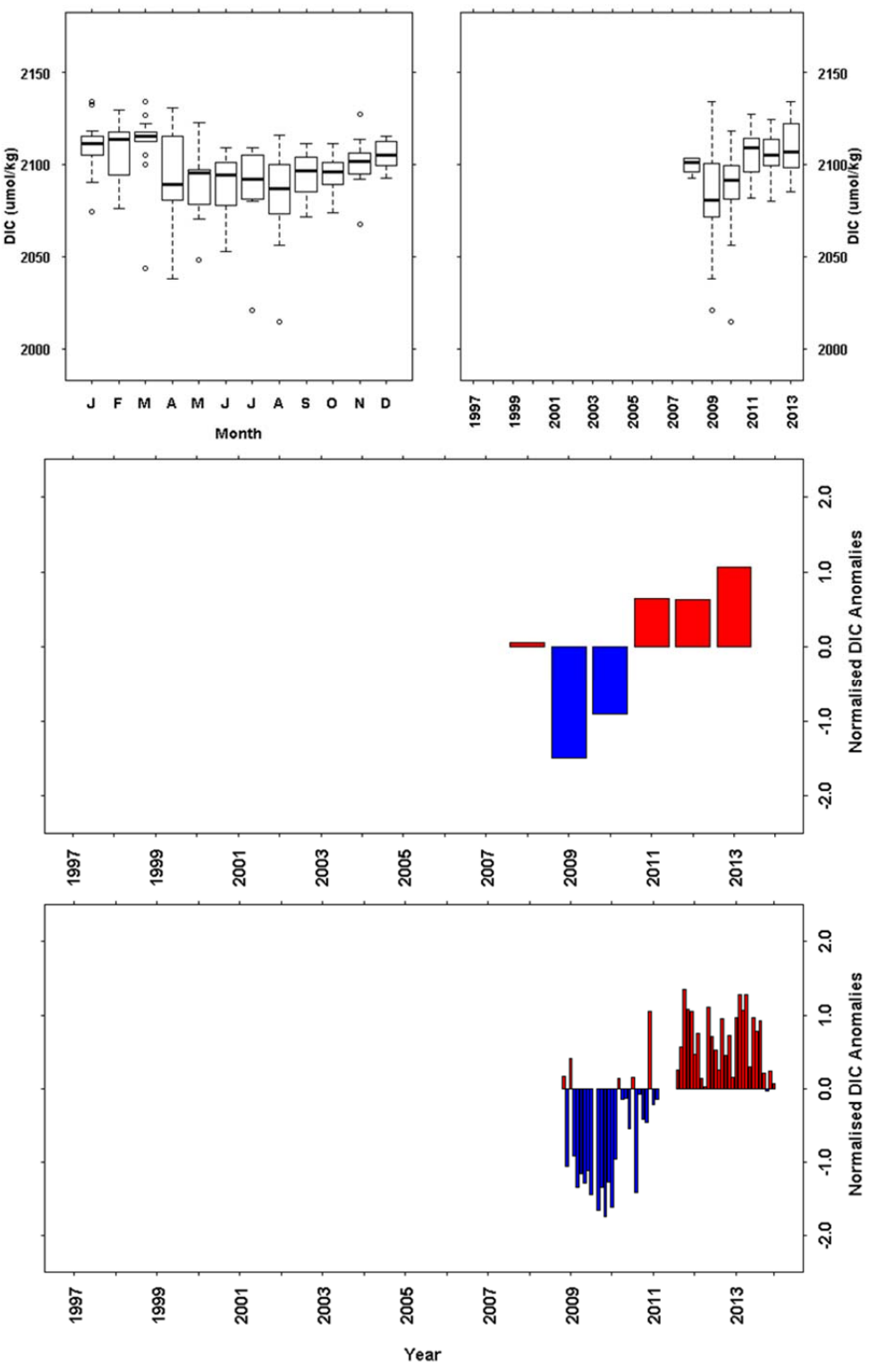

Figure 8.4 Lower layer (> 30 m) Dissolved Inorganic Carbon (DIC) data from the long term monitoring site at Stonehaven. a) monthly boxplot of DIC data, b) annual boxplot of DIC data, c) annual mean DIC anomaly timeseries data and d) monthly mean DIC anomaly timeseries data. There were no data available prior to November 2008. The full data set was used as the base period for the anomaly calculations.

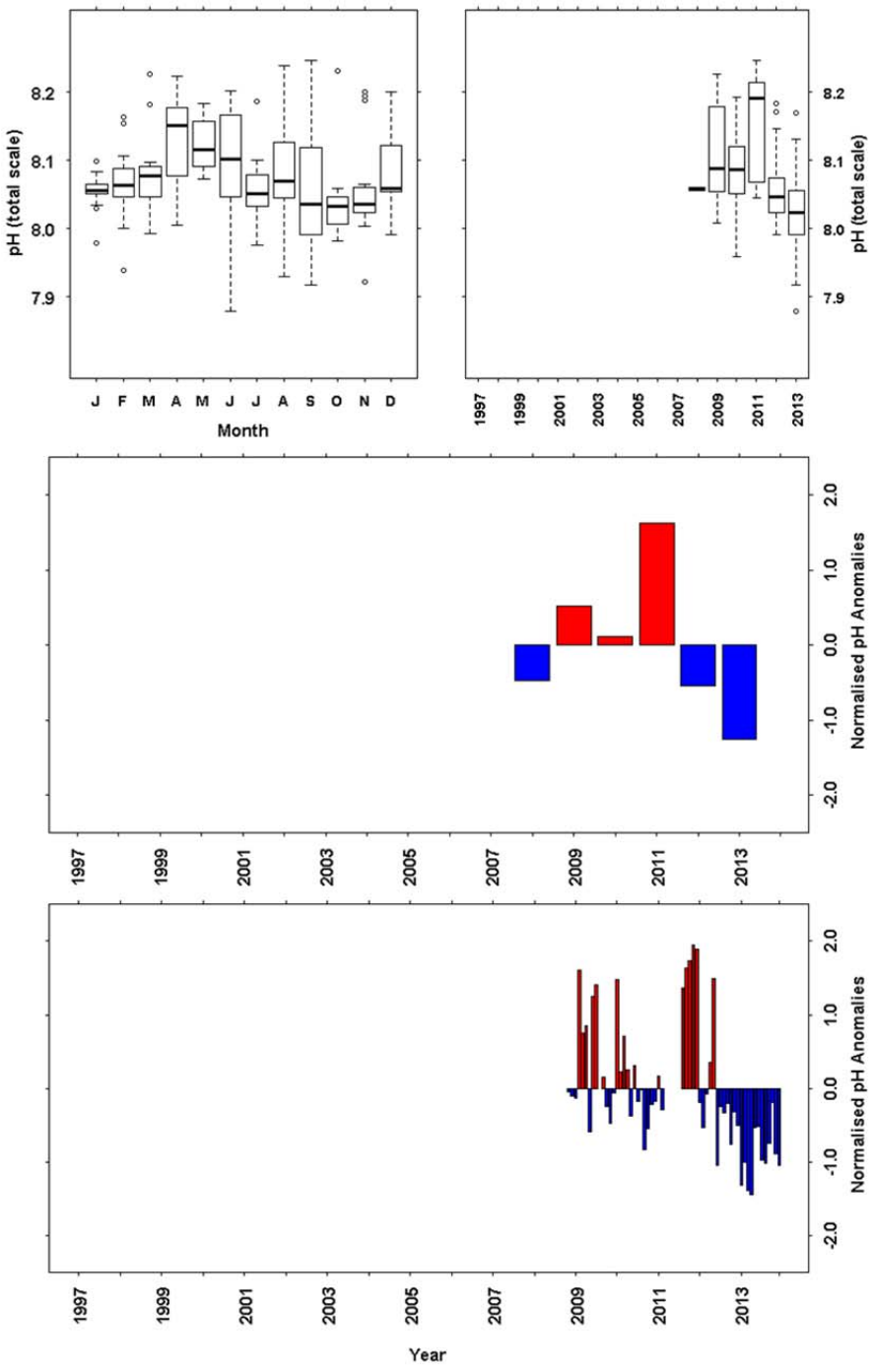

Figure 8.5 Upper layer (0-10 m) Derived pH (CO2SYS derived pH, Total Scale) data from the long term monitoring site at Stonehaven. a) monthly boxplot of pH data, b) annual boxplot of pH data, c) annual mean pH anomaly timeseries data and d) monthly mean pH anomaly timeseries data. There were no data available prior to November 2008. The full data set was used as the base period for the anomaly calculations.

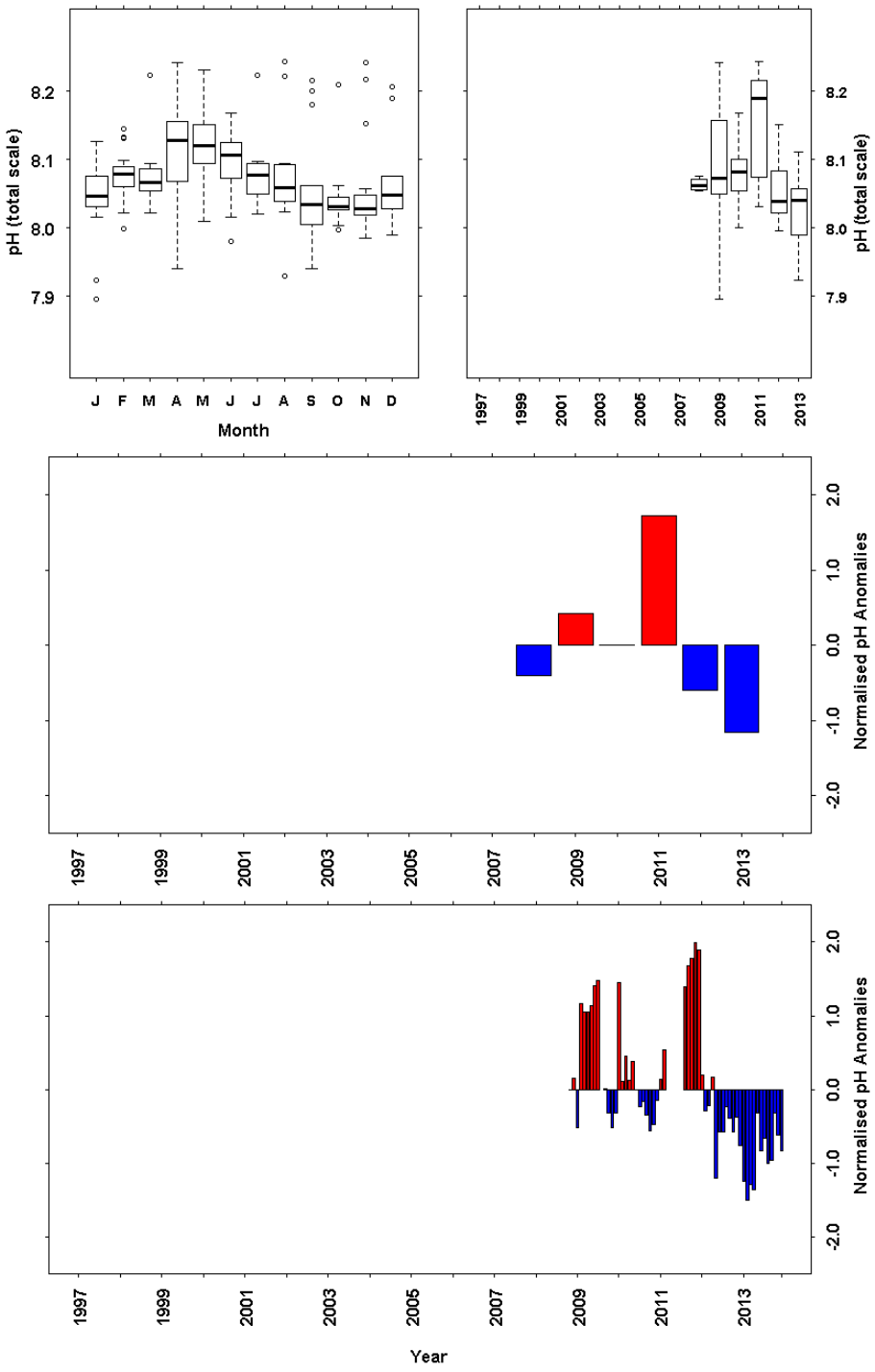

Figure 8.6 Lower layer (> 30 m) Derived pH (CO2SYS derived pH, Total Scale) data from the long term monitoring site at Stonehaven. a) monthly boxplot of pH data, b) annual boxplot of pH data, c) annual mean pH anomaly timeseries data and d) monthly mean pH anomaly timeseries data. There were no data available prior to November 2008. The full data set was used as the base period for the anomaly calculations.

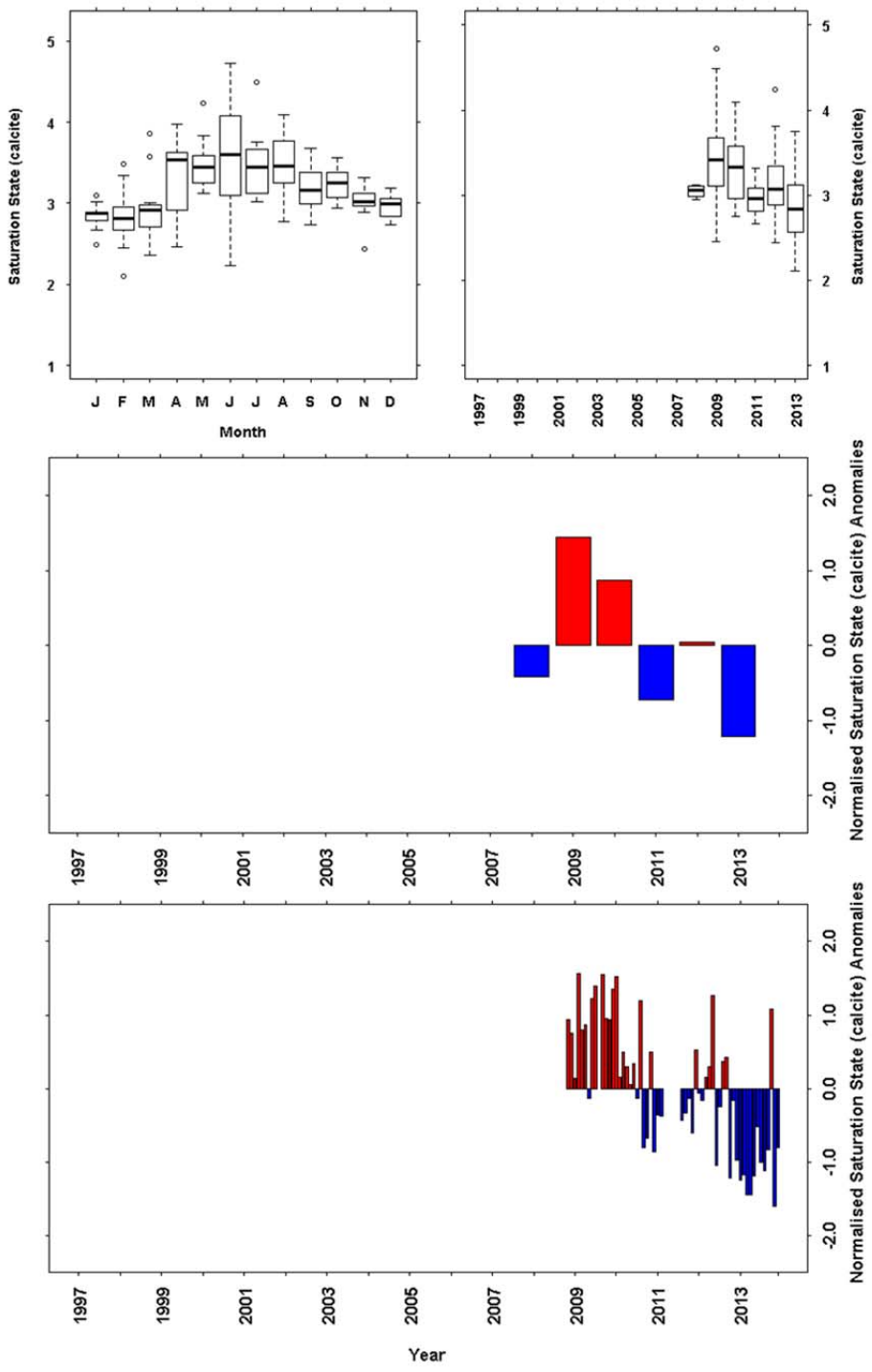

Figure 8.7 Upper layer (0-10 m) derived calcite saturation (CO2SYS derived) data from the long term monitoring site at Stonehaven. a) monthly boxplot of calcite saturation data, b) annual boxplot of calcite saturation data, c) annual mean calcite saturation anomaly timeseries data and d) monthly mean calcite anomaly timeseries data. There were no data available prior to November 2008. The full data set was used as the base period for the anomaly calculations.

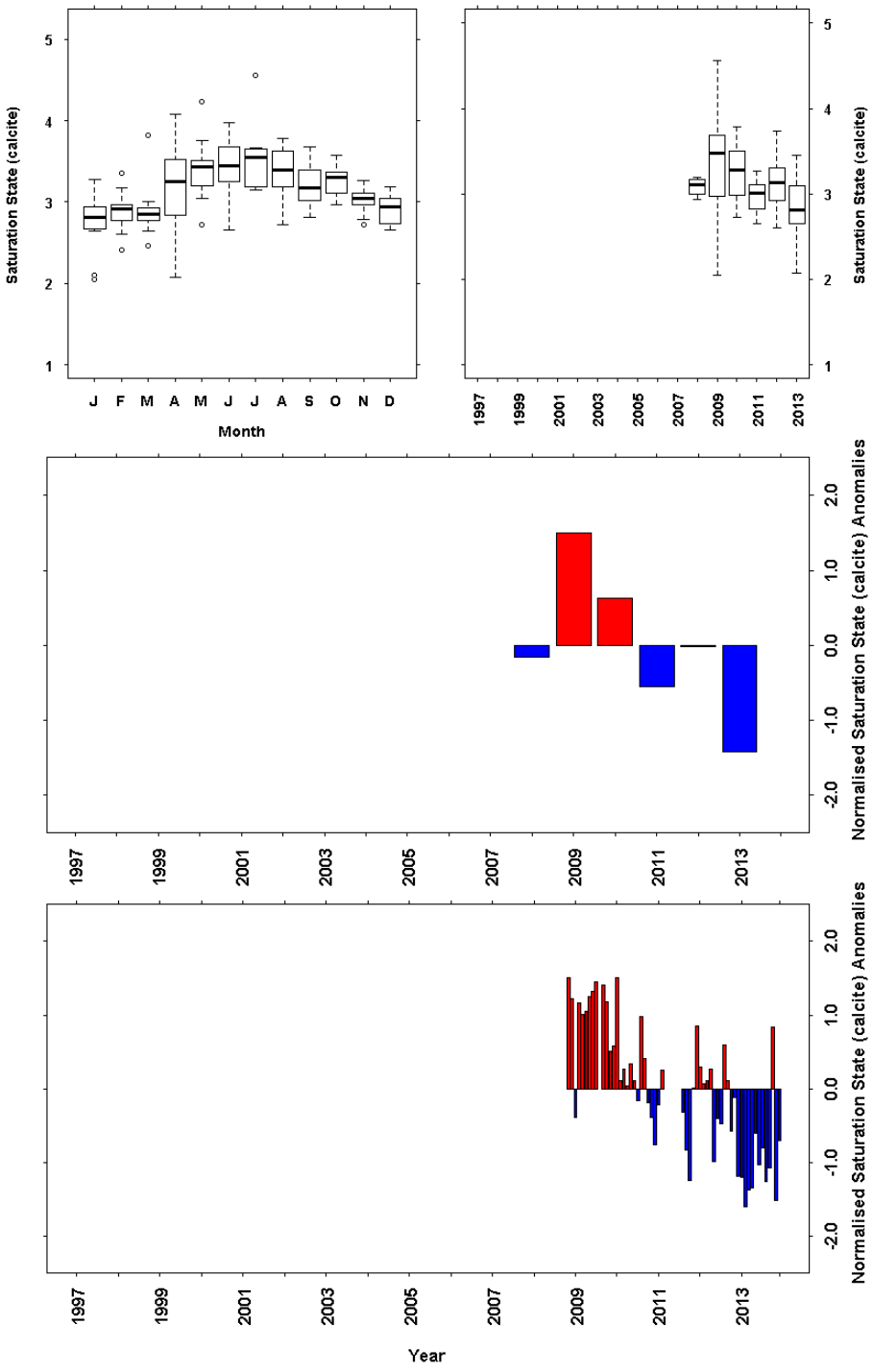

Figure 8.8 Lower layer (>30 m) derived calcite saturation (CO2SYS derived) data from the long term monitoring site at Stonehaven. a) monthly boxplot calcite of saturation data, b) annual boxplot of calcite saturation data, c) annual mean calcite saturation anomaly timeseries data and d) monthly mean calcite anomaly timeseries data. There were no data available prior to November 2008. The full data set was used as the base period for the anomaly calculations.

9. Phytoplankton

9.1 Introduction

Phytoplankton are microscopic unicellular organisms which inhabit the watercolumn. They occupy the base of the food chain and harvest light energy from the sun which they use to convert H_2O and CO_2 to carbohydrate and O_2 via the process called photosynthesis. This energy is passed up through the food web via grazing and predation and thus changes to the phytoplankton community have the potential to impact higher levels in the food web (Chavez et al., 2011). Under certain environmental conditions phytoplankton cell numbers can increase and form what is termed an 'algal bloom'. The formation of algal blooms is a natural part of the seasonal cycle in the oceans with a spring and autumn bloom commonly observed in marine ecosystems at temperate latitudes (Cushing 1989).

Some phytoplankton blooms can have a negative impact on the marine ecosystem and the goods and services it supports. Blooms of these species are referred to as 'harmful algal blooms' or HABs. It should be noted that this is a societal term and there are few biological similarities between the species that are included in this grouping (Gowen et al., 2012). HABs have a diverse range of negative impacts on the environment. Impacts recorded in Scottish waters include benthic mortalities from high biomass blooms, mortalities of farmed fish from high densities of the dinoflagellate *Karenia mikimotoi* (Davidson et al., 2009) and enforced closures of shellfish harvesting areas as a result of high concentrations of the toxins responsible for paralytic, lipophilic and amnesic shellfish poisoning (Davidson and Bresnan 2009).

There is a pressing requirement to understand the dynamics of the phytoplankton community in Scottish waters. Environmental drivers such as climate change, ocean acidification and eutrophication all have the potential to impact the phytoplankton community which can affect all levels of the marine food web. The Scottish Government is currently promoting a 50% increase in the production of farmed fish and 100% increase in the shellfish aquaculture industry between 2010 and 2020.

The EU Water Framework Directive (WFD) and EU Marine Strategy Framework Directive (MSFD) require member states to achieve 'Good Ecological Status' and 'Good Environmental Status' respectively in their marine waters. For the WFD, the phytoplankton community is included as a biological element used to assess water quality (Devlin et al., 2007). For the MSFD, 'Good Environmental Status' is assessed under eleven different descriptors with phytoplankton included as part of the Biodiversity, Food Webs and Eutrophication descriptors (DEFRA, 2010). The Stonehaven and Loch Ewe monitoring sites currently act as monitoring sites for both the WFD and MSFD with Scapa and Scalloway being included in the proposed UK MSFD monitoring plan. The phytoplankton data already collected as part of this MSS monitoring programme have contributed towards tool development to meet these directives (Devlin et al., 2013, Scherer et al., 2015).

Data from offshore phytoplankton populations collected by the Continuous Plankton Recorder (CPR) reveal a number of episodic events which have altered the phytoplankton community in the North East Atlantic over the last six decades. These

include a ‘cold boreal’ anomaly which was identified in the late 1970s, associated with low temperature and salinity and resulted in a reduction of the intensity of the spring diatom bloom (Edwards et al., 2002). A ‘warm temperate’ event identified at the end of the 1980s as a regime shift was associated with marked synchronous changes in plankton in the CPR and other time series from the North Sea and Baltic areas (Edwards et al., 2002, Edwards et al., 2006, Wiltshire et al., 2008). A shift in the spatial distribution of some HAB genera has been recorded in the North Sea over the last five decades. High cell densities of the lipophilic shellfish toxin producer *Dinophysis* along the north east coast of England in the 1970s are no longer observed and higher densities are now recorded in the northwest North Sea (Edwards et al., 2006). More recently, Alvarez-Fernandez et al., (2012) and Beaugrand et al., (2014) have reported another shift in the North Sea plankton community in 1998. This shift has been associated with a reduction in dinoflagellates and neritic copepods.

Data from coastal waters is much more sparse. Sporadic studies have been performed along the west coast in the 1970s and 80s (Gamble et al., 1977, Tett and Wallis 1978, Gowen et al., 1983, Jones et al., 1984, Morris 1984, Joint et al., 1987, Savidge and Lennon 1987) with more recent descriptions of the phytoplankton community on the east and west coast emerging in the last ten years (Bresnan et al., 2009, Whyte 2012, Tett 2013, Bresnan et al., 2015a, Siemering et al., 2016). There have been two published descriptions of the phytoplankton community from the ‘Ellet line’ which is monitored on an annual basis between Oban on the west coast of Scotland and Rockall (Savidge and Lennon 1987, Fehling et al., 2012). Since the 1990s most phytoplankton studies in Scotland have focused on harmful species owing to their negative impacts on the aquaculture industry (Fehling et al., 2004, 2005, 2006, Hart et al., 2007, Bresnan et al., 2008, Brown and Bresnan, 2008, Collins et al., 2009a, Davidson et al., 2009, Brown et al., 2011, Gowen et al., 2012, Whyte et al., 2014, Bresnan et al., 2015b).

Full Community Phytoplankton Analysis

Marine Scotland Science has commenced routine phytoplankton community monitoring in 1997 when this analysis began at the Stonehaven site. This analysis was included at Loch Ewe, Scapa and Scalloway from 2000, Loch Maddy from 2003-2011 and Millport from October 2005 to October 2013.

Diatoms and dinoflagellates were identified to species level when possible. The use of lugol’s iodine as a preservative, the limitations of using light microscopy and cryptic speciation mean that in many cases a species (or at times genus) level identification is not possible. Molecular, electron and fluorescent microscopy microscopy methods have been used to identify phytoplankton cells to species level for target groups and genera such as coccolithophores, *Phaeocystis, Alexandrium* and *Pseudo-nitzschia*. These data are not presented here. For this report the diatom and dinoflagellate cells identified and enumerated in each sample were summed to produce a total diatom and total dinoflagellate cell count and these values were used to generate the plots. Three shellfish toxin producing genera (*Alexandrium*, *Dinophysis* and *Pseudo-nitzschia*) are presented. Their seasonality and interannual variation in abundance is described and any regional differences flagged.

The Marine Plants Task Team for the WFD generated a phytoplankton species list to compile data from the UK for WFD assessment. This list is given in Appendix F in Part 3 of this report.

9.2 Methods

Sample Collection and Storage

Phytoplankton samples are collected using a 10 m integrated tube sampler. The tube is slowly lowered into the water from a boat or pier and the upper valve closed to ensure the water remains in the tube when it is extracted. The water from the tube is emptied into a bucket where it is mixed. A 1L subsample is poured into a 1L Nalgene bottle and 5 mL of acidic Lugol's iodine solution is added (Throndsen 1978). The bottle is labelled with site name, date, time, depth placed in a box and posted to the Phytoplankton Lab at the Marine Laboratory in Aberdeen. The mean time in transit is approximately 2-3 days. A full methodology can be found in Kelly and Fraser (1999).

Sample Processing, Analysis and Archiving

Phytoplankton samples are transferred to labelled amber glass jars immediately on receipt in the phytoplankton laboratory. Phytoplankton samples are analysed using a modified Utermöhl technique (Utermöhl 1958). Between 1997 and 1998, 10 mL of water sample was settled for four hours for analysis. In 1998 the volume settled was increased to 50 mL with a minimum settling time of 40 hours.

Phytoplankton samples were analysed using an inverted Zeiss axiovert microscope (model numbers 10, 20S, 100, 200). A number of target species were counted in the entire base plate and the presence/absence of all species in the sample were noted from 2001 from Stonehaven and 2005 for all other sites. Full community densities were estimated by counting the first 400 cells at X400 magnification from 1997 to 1999. From 2000, fields of view across a transect were also counted at X200 magnification.

Phytoplankton species data was held in a combination of Excel spreadsheets and a paradox database. In 2016 a web based data island was developed to hold this data.

Data Quality, Handling and Archiving

All analysts undergo approximately 12 months of internal training and participate on the Intergovernmental Oceanographic Commission's course in advanced harmful algal bloom taxonomy before they are signed off as competent to perform full community phytoplankton analysis. The length of time it takes for an analyst to be signed off depends on the individual and their prior taxonomic identification experience. Interanalyst ring trials are performed on an annual basis within MSS to examine interanalyst variability. Analysts participate on the BEQUALM international phytoplankton ring trial on an annual basis. They are also encouraged to participate on external training courses when funding is available.

Since 2005 the identification and enumeration of toxin producing phytoplankton cells has been accredited to the ISO 17025 standard. Sample log in, processing and data QC is also covered by this method (PHY01). This method also includes protocols for training and checking for procedural errors. Data from the phytoplankton database are checked for typographic errors after entry. At the end of the year the seasonal cycle is examined for extreme outliers. Should sample data look suspicious the sample is reanalysed from the 100 ml aliquot although this has happened infrequently during the time series. All data is assigned a QF0 (not QCed) until the data has been signed off at the end of the year. A final plot of the annual cycle is reviewed before the the relevant QF is assigned.

Data was square root transformed prior to plotting to reduce the impact of extreme values.

9.3 Results - Diatoms

Diatoms are small unicellular phytoplankton cells which have a silicon frustule. Morphological features of this silica frustule alongside size and shape are used to identify diatoms cells to genus and species level. In some instances the resolution of light microscopy and the preservation using Lugol's iodine is insufficient to allow a species identification and a genus level or broad grouping e.g. 'centric diatom' is used to record the cells. Cryptic speciation where two different species can not be distinguished using morphological criteria alone can occur in diatoms (e.g. *Pseudo-nitzschia delicatissima* and *Pseudo-nitzschia arayensis*). In this instance molecular methods are required to make a true assessment of the diversity present.

Diatoms play an important role in the marine food web. At northern latitudes light levels are low and the water column is turbulent over the winter months. At this time phytoplankton populations are sparse and as a result nutrients accumulate in the water column (see Chapter 7). As spring arrives, light levels begin to increase and the water column begins to stabilise. During most years there is a rapid burst of phytoplankton growth at this time, which is mostly dominated by smaller, rapidly growing diatoms. This group is favoured owing to their short generation times and ability to withstand agitation in the water column. This rapid increase in diatom numbers is referred to as the 'spring bloom'. This natural event plays an important role in the marine ecosystem as it represents the major food resource for zooplankton copepods and post winter egg production (Bresnan et al., 2015a).

Once the spring bloom has depleted the nutrients in the water column, diatom levels decline. Dinoflagellates begin to increase and at times the small colonial forming flagellate *Phaeocystis* can become more abundant. Dinoflagellates tend to be most abundant over the summer months (Cushing, 1989). This group prefer calm, stratified water and thus their abundance is strongly influenced by the prevailing weather conditions from year to year. In the autumn months dinoflagellates decline as the water column gets more agitated and nutrients in the water column increase. At this time there can be another bloom of diatoms known as the 'autumn bloom'. Once these diatom cell densities decline, diatoms are present in very low concentrations in the water column over the winter. Long term studies have shown that diatom cell densities are increasing during the summer months in the northeast

Atlantic area and have related the increase to increasing wind intensity during the summer months (Hinder et al., 2012).

One group of phytoplankton that are poorly studied are the microflagellates (< 20µm in diameter). These are flagellated cells whose small size and lack of distinguishing features in Lugol's iodine preserved samples make them difficult to identify and enumerate in a routine monitoring context. A 'relative' count of microflagellates is perfomed but not presented here. Since 2014 flow cytometric analysis of the nano (2-20 µm diameter) and pico (<2 µm) diameter has been performed at the Stonehaven monitoring site.

Diatoms: Millport

The diatom community in Millport follows a distinct seasonal cycle. Diatoms increase sharply during March, forming an intense spring bloom. This spring time community is dominated by the diatom *Skeletonema marinoi*. Diatom cell densities decrease over the summer months and the 'autumn diatom bloom' is largely absent at this site. The time series is too short to allow robust examination of trends over time but an increased abundance of diatoms was recorded from 2008 compared to the earlier years of the time series.

Diatoms: Loch Maddy

The spring bloom occurs during April/May in Loch Maddy. The population during this time is dominated by *Skeletonema marinoi* and *Thalassiosira* spp. There is a slight increase in cell numbers during the autumn. This population is dominated by *Pseudo-nitzschia* spp. and *Leptocylindrus* spp. cells. Infrequent sampling between 2008 and 2011 makes interpretation of the results from Loch Maddy during these years difficult.

Diatoms: Loch Ewe

Loch Ewe exhibits a seasonal cycle typical of temparate waters with a spring diatom bloom dominated by *Pseudo-nitzschia* '*delicatissima* type' cells, *Skeletonema marinoi, Thalassiosira* and *Chaetoceros* spp. Diatom numbers during the summer months are generally low with an autumn bloom comprising of *Pseudo-nitzschia 'seriata* type' cells and *Rhizosolenia* species observed between August and September. Interannual variation can be seen in the abundance of diatom cells observed throughout the year at this site with higher diatom abundances recorded during 2005-2009.

Diatoms: Scapa

A typical diatom cycle can be seen in Scapa with an increase in diatoms in spring and again in late summer/early autumn. The spring community is dominated by *P. 'delicatissima* type' cells, *Skeletonema marinoi*, *Guinardia delicatula, Chaetoceros* and *Thalassiosira* spp. The autumn community is dominated by *Pseudo-nitzschia 'seriata* type' cells and *Rhizosolenia* spp. Considerable interannual variability can be seen at this site during the time series with 2006-2009 showing positive anomalies in the abundance of diatoms observed.

Diatoms: Scalloway

Some differences can be observed between the seasonal diatom cycle at Scalloway and sites on the west coast of Scotland. Diatom cell densities begin to increase during the spring months but reach their maximum abundance during the summer in June and July. These summer populations are comprised of *Chaetoceros* spp., *Guinardia delicatula*, *Pseudo-nitzschia* spp. and *Thalassiosira* spp. An increase in diatom abundance can be observed from 2005.

Diatoms: Stonehaven

The diatom community at Stonehaven follows a seasonal cycle with cell numbers increasing in spring. This increase can generally be observed approximately a month later than at sites on the west coast. The spring bloom diatom community is dominated by *Pseudo-nitzschia* '*delicatissima* type' cells and *Chaetoceros* spp. From 2005 *Skeletonema marinoi* has become adominant member of this community during some years. In contrast to sites along the west coast and in Orkney, the autumn bloom is much less pronounced at this site and is not observed every year. If it occurs, it is comprised of *P. 'seriata* type' cells and *Rhizosolenia* spp.

Considerable interannual variation can be observed with a decrease in diatom abundance observed between 2001 and 2004. The spring bloom was particularly reduced during this period.

9.4 Plots – Diatoms

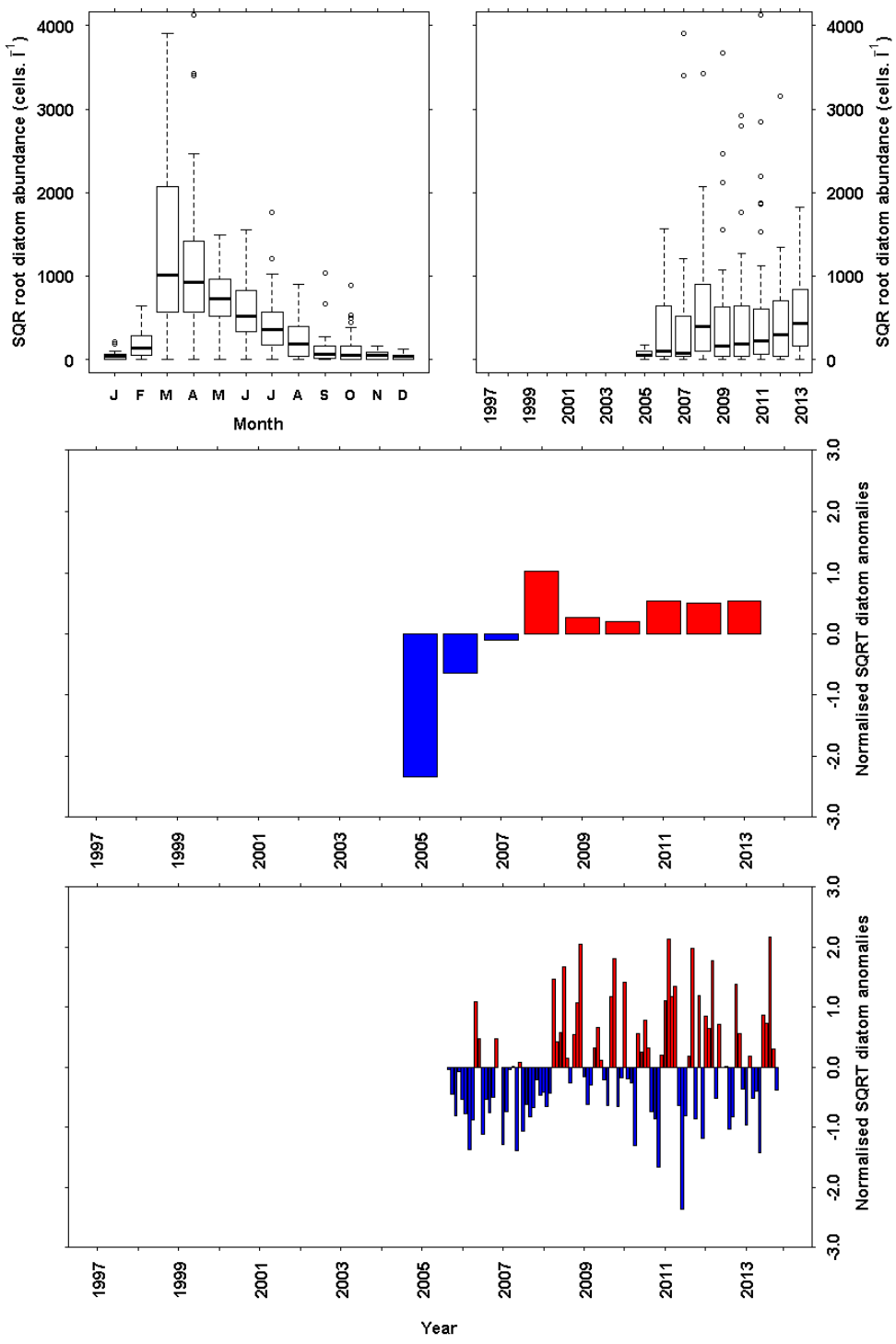

Figure 9.1 Diatom abundance (cells L^{-1}) from the long term monitoring site at Millport. SQRT transformed data has been plotted. a) Monthly boxplot of diatom abundance. b) Annual boxplot of diatom abundance. c) Annual mean anomaly time series d) Monthly mean anomaly time series. Sampling began in October 2005 and finished in October 2013. The full data set was used as the base period for the anomaly calculations.

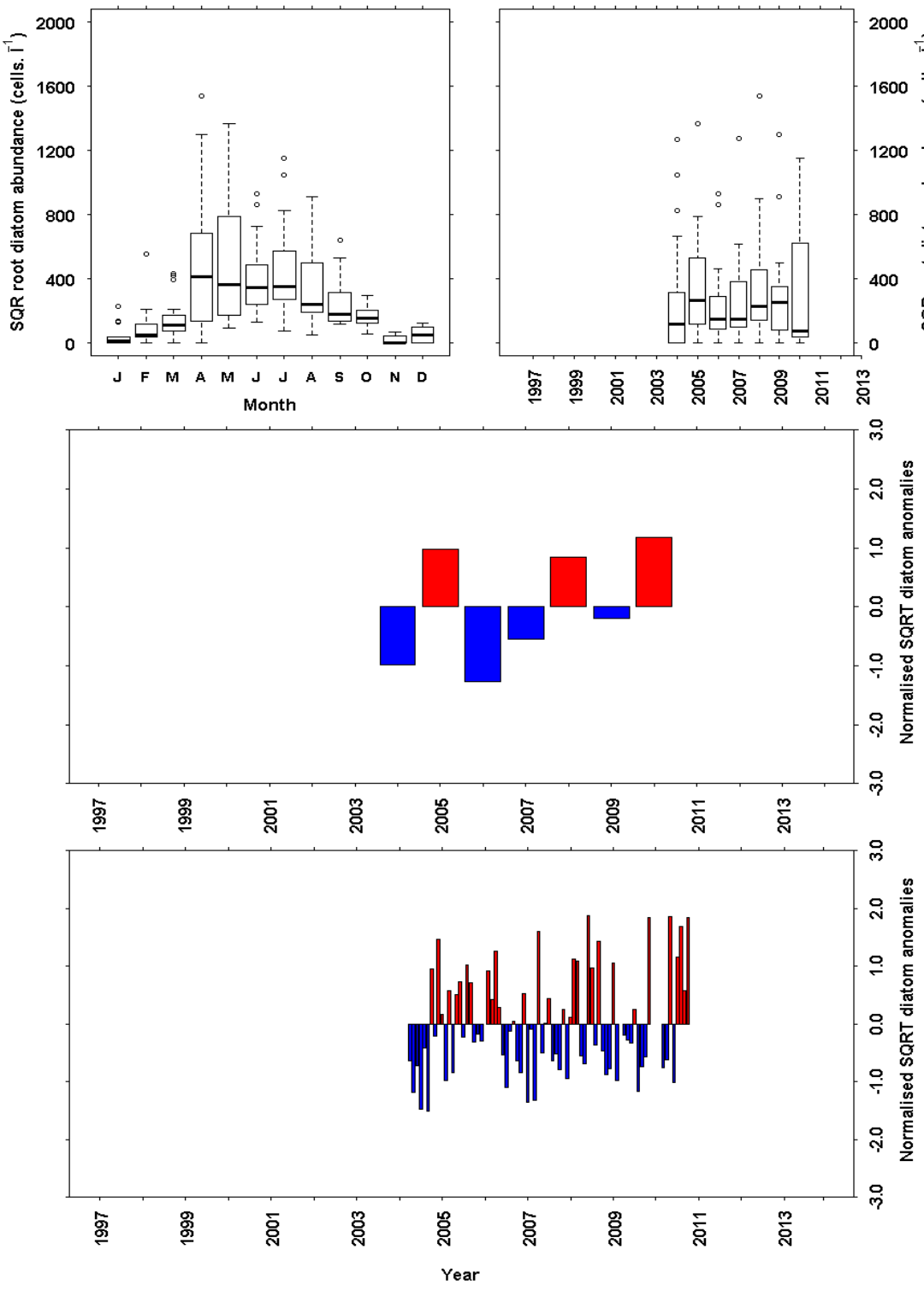

Figure 9.2 Diatom abundance (cells L^{-1}) from the long term monitoring site at Loch Maddy. SQRT transformed data has been plotted. a) Monthly boxplot of diatom abundance. b) Annual boxplot of diatom abundance. c) Annual mean anomaly time series d) Monthly mean anomaly time series. Sampling began in 2003 and sampling was infrequent during the latter part of the time series. The full data set was used as the base period for the anomaly calculations.

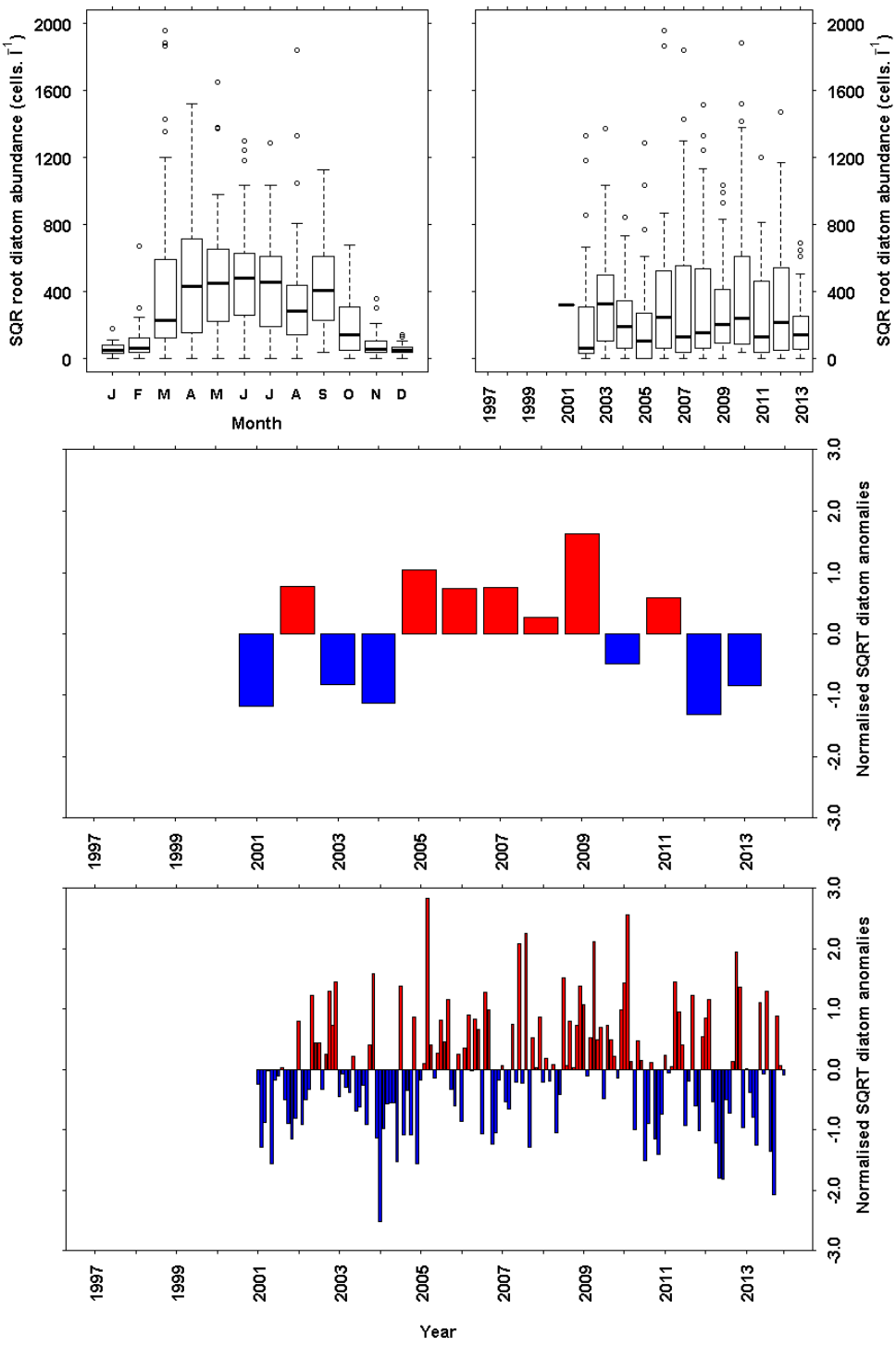

Figure 9.3 Diatom abundance (cells L^{-1}) from the long term monitoring site at Loch Ewe. SQRT transformed data has been plotted. a) Monthly boxplot of diatom abundance. b) Annual boxplot of diatom abundance. c) Annual mean anomaly time series d) Monthly mean anomaly time series. Sampling began in 2001 with the position of the site changing in 2002. The full data set was used as the base period for the anomaly calculations.

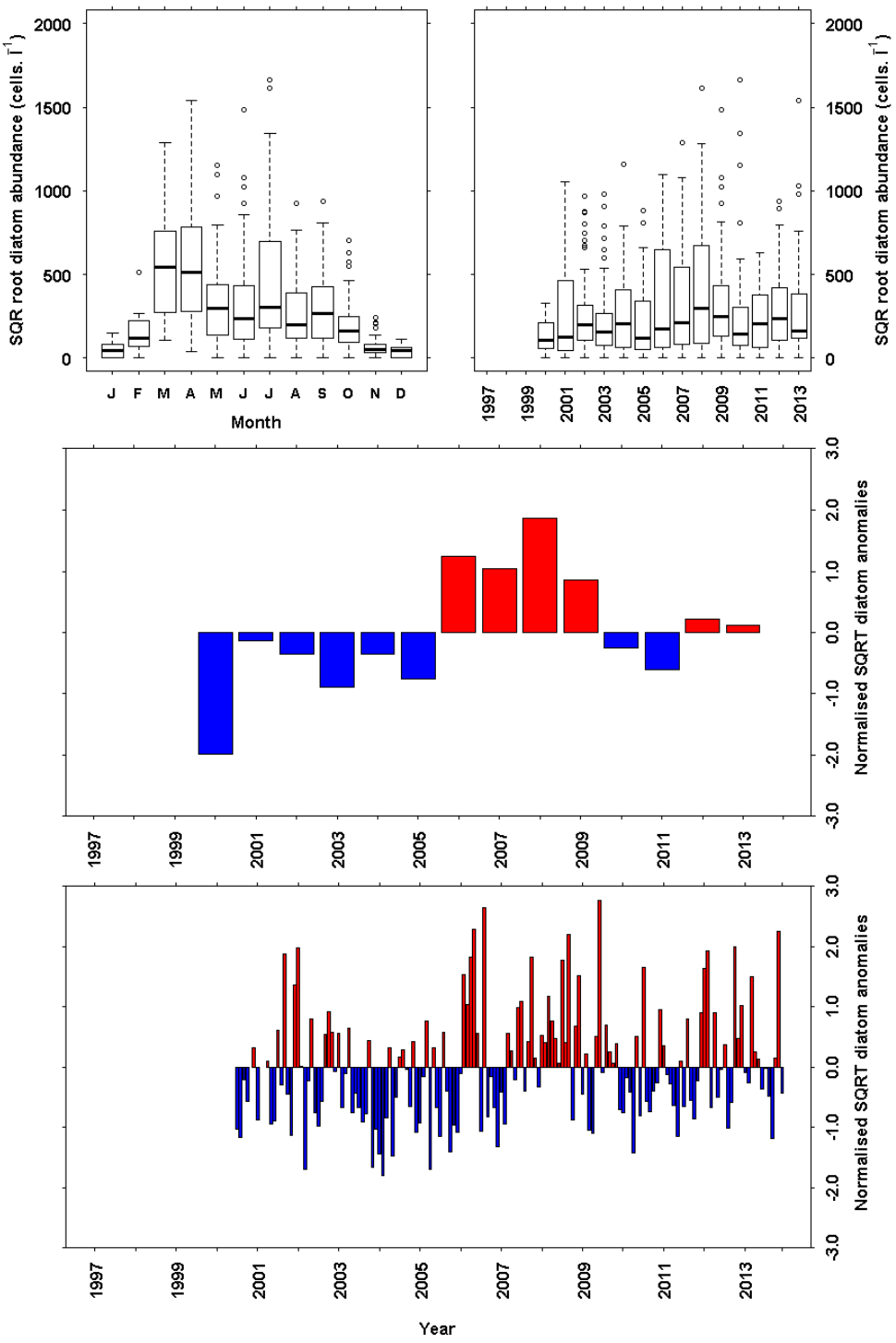

Figure 9.4 Diatom abundance (cells L^{-1}) from the long term monitoring site at Scapa. SQRT transformed data has been plotted. a) Monthly boxplot of diatom abundance. b) Annual boxplot of diatom abundance. c) Annual mean anomaly time series d) Monthly mean anomaly time series. Sampling began in 2001. The full data set was used as the base period for the anomaly calculations.

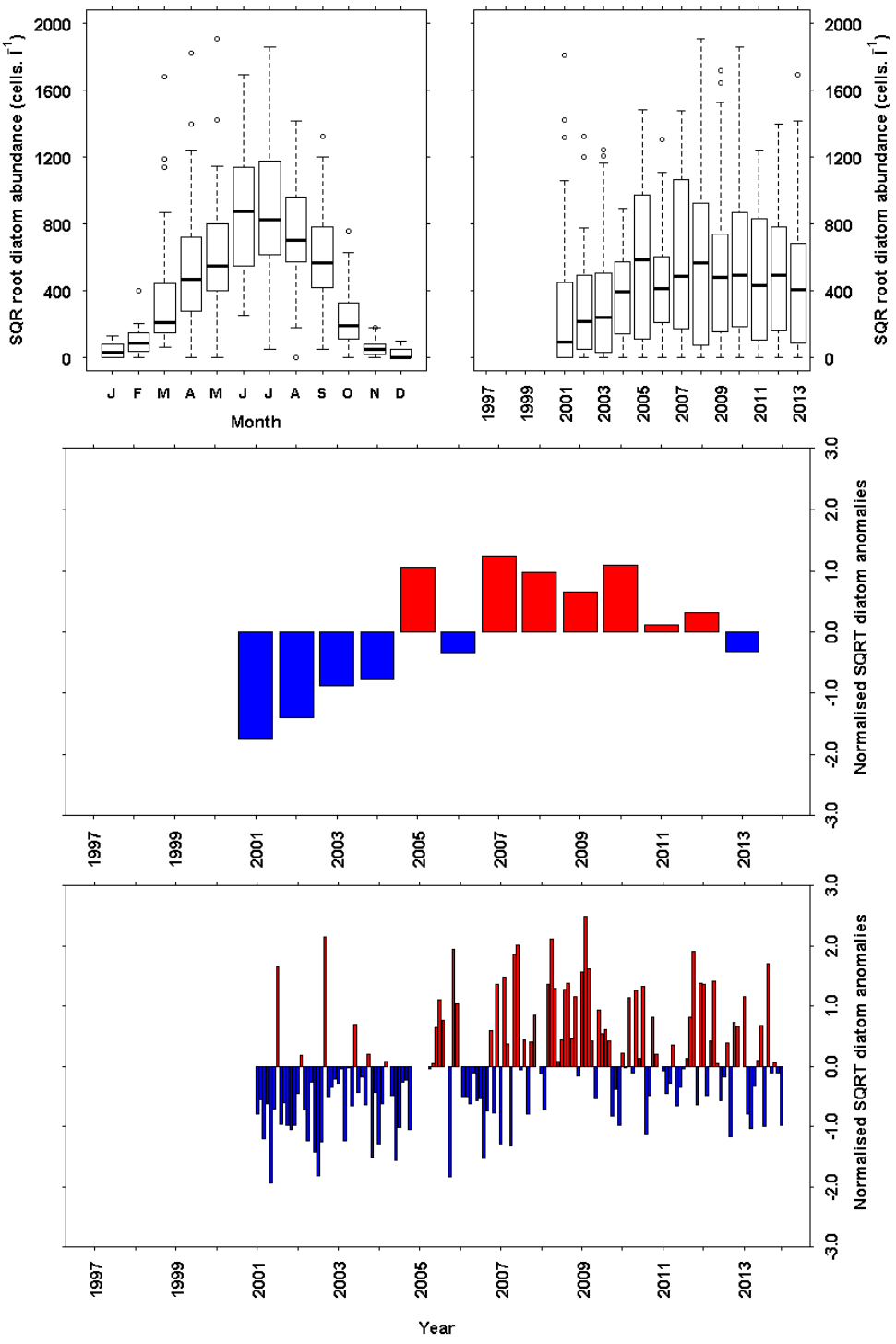

Figure 9.5 Diatom abundance (cells L^{-1}) from the long term monitoring site at Scalloway. SQRT transformed data has been plotted. a) Monthly boxplot of diatom abundance. b) Annual boxplot of diatom abundance. c) Annual mean anomaly time series d) Monthly mean anomaly time series. Sampling began in 2001. The full data set was used as the base period for the anomaly calculations.

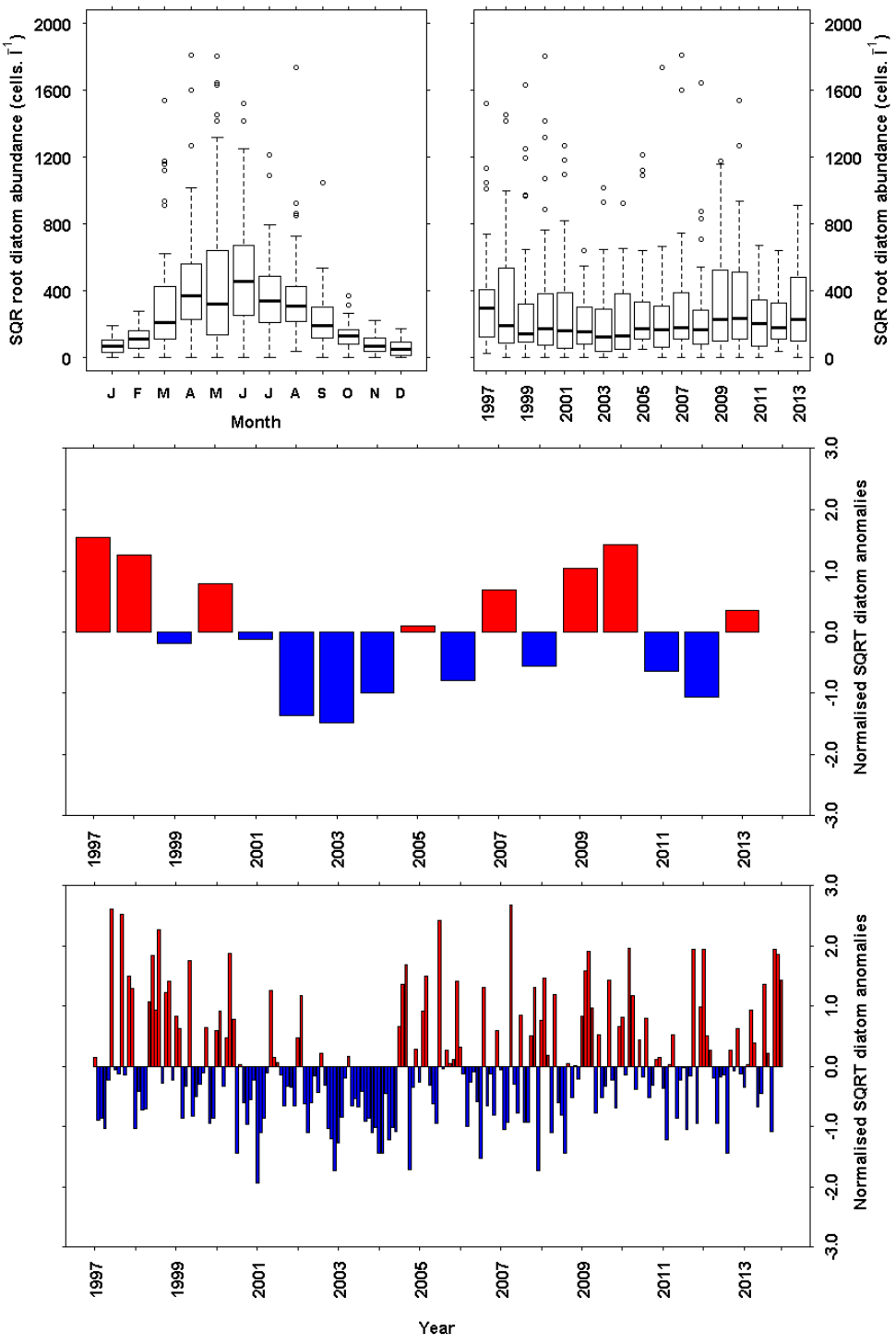

Figure 9.6 Diatom abundance (cells L^{-1}) from the long term monitoring site at Stonehaven. SQRT transformed data has been plotted. a) Monthly boxplot of diatom abundance. b) Annual boxplot of diatom abundance. c) Annual mean anomaly time series d) Monthly mean anomaly time series. Sampling began in 1997. The full data set was used as the base period for the anomaly calculations.

9.5 Results - Dinoflagellates

Dinoflagellates are important members of the summer phytoplankton community in Scottish waters. Dinoflagellates have two hair like flagella that they use to move about in the water column. They favour conditions when the water column is stable, usually during the summer when the water column is thermally stratified. During these periods dinoflagellates swim to the thermocline to utilise the nutrients there (Cushing 1989).

Dinoflagellates have many different modes of nutrition. As well as being autotrophs (using nutrients in the water column to produce sugars via the process of photosynthesis) some are heterotrophs and feed only on bacteria or other phytoplankton cells. Members of the *Protoperidinium* genus employ this feeding trait. Some dinoflagellates are mixotrophs and can alternate which mode they use. This range of feeding mechanisms increases the diversity of habitats they can inhabit (Gomez 2012).

A decrease in dinoflagellate abundances have been observed in the northeast Atlantic over the last number of decades (Edwards et al., 2002, 2006). The common summer dinoflagellates genus *Tripos* (reclassified from *Ceratium*) has shown a decrease in cell densities as a result of increasing and changing wind speeds (Hinder et al., 2012).

Some dinoflagellates can cause negative impacts through the production of shellfish toxins e.g. *Alexandrium* and *Dinophysis* resulting in enforced closures of shellfish harvesting areas (Bresnan et al., 2008, Davidson and Bresnan 2009) while *Karenia mikimotoi* can result in mortalities of the benthos and farmed fish (Davidson et al., 2009).

Dinoflagellates: Millport

The dinoflagellate community follows a typical seasonal cycle for temperate latitudes with cell densities dominating during the summer months. The dinoflagellate population is dominated by the genera *Tripos*, *Gymnodinium* and *Dinophysis*. Interannual variation can be observed at this site with maximum cells observed in 2009 and 2011.

Dinoflagellates: Loch Maddy

The dinoflagellate community at this site follows a typical seasonal cycle for temperate latitudes. The population is dominated by *Protoperidinium* and *Prorocentrum*. A bloom of *Karenia mikimotoi* was observed at this site in 2006.

Dinoflagellates: Loch Ewe

The dinoflagellates at this site follow a typical seasonality for temperate latitudes. The dinoflagellate population is dominated by *Tripos* and *Dinophysis*. Cell densities of *Tripos* observed a decline between 2003 and 2010. Blooms of *Karenia mikimotoi* have also impacted this site with mortalities of the benthos observed during 2006.

Dinoflagellates: Scapa

The seasonality of the dinoflagellate community at this site is similar to that of temperate latitudes with *Tripos* and *Dinophysis* dominant during the summer months. Cell densities of *Tripos* observed a decline between 2003 and 2010. This site has also experienced concentrated *Karenia mikimotoi* blooms during 2001, 2003, 2006 and 2009. Mortalities of benthic animals such as lug worms were observed at this site during the 2003 and 2006 blooms.

Dinoflagellates: Scalloway

Dinoflagellates dominate during the summer months at this site although peak numbers can be observed in May and June. In contrast to other sites *Tripos* is not routinely observed at this site and the summer community is dominated by gonyaulacoid dinoflagellates such as *Alexandrium* and *Gonyaulax*. This site has been impacted by blooms of *Karenia mikimotoi* which caused mass mortalities of farmed fish in Shetland in 2003. Interannual variation can be observed at this site with an increase in dinoflagellates observed since 2005.

Dinoflagellates: Stonehaven

Dinoflagellates dominate during the summer months at Stonehaven. The dinoflagellate community can be dominated by *Dinophysis* and *Tripos*. In addition a number of short lived blooms of *Prorocentrum* cf. *cordatum* have been observed during the early summer at this site. Interannual variation has been observed at this site since the monitoring began with an increase in the number of positive anomalies being observed in dinoflagellate abundance since 2005.

9.6 Plots – Dinoflagellates

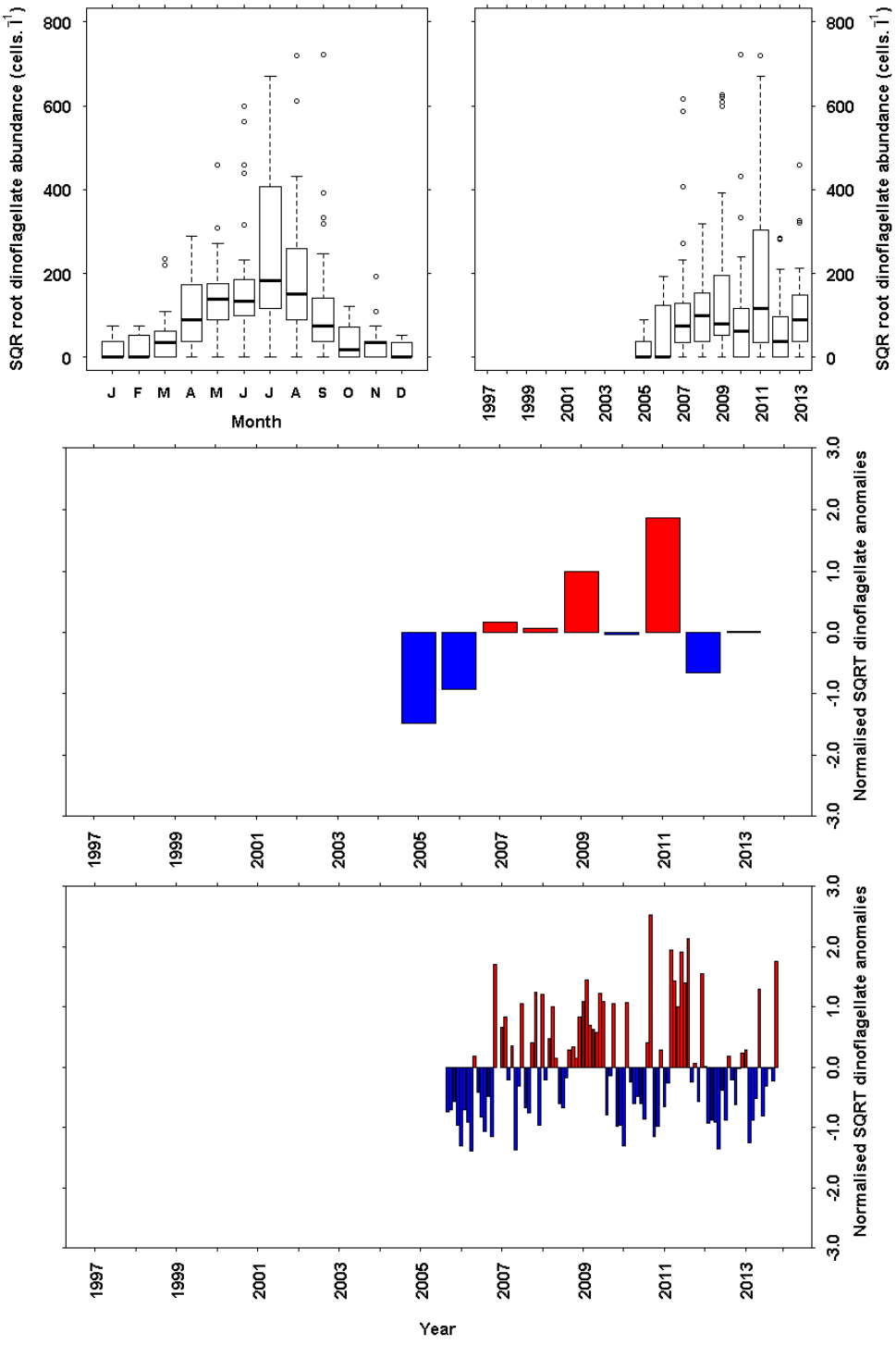

Figure 9.7 Dinoflagellate abundance (cells L^{-1}) from the long term monitoring site at Millport. SQRT transformed data has been plotted. a) Monthly boxplot of dinoflagellate abundance. b) Annual boxplot of dinoflagellate abundance. c) Annual mean anomaly time series d) Monthly mean anomaly time series. Sampling began in October 2005. The full data set was used as the base period for the anomaly calculations.

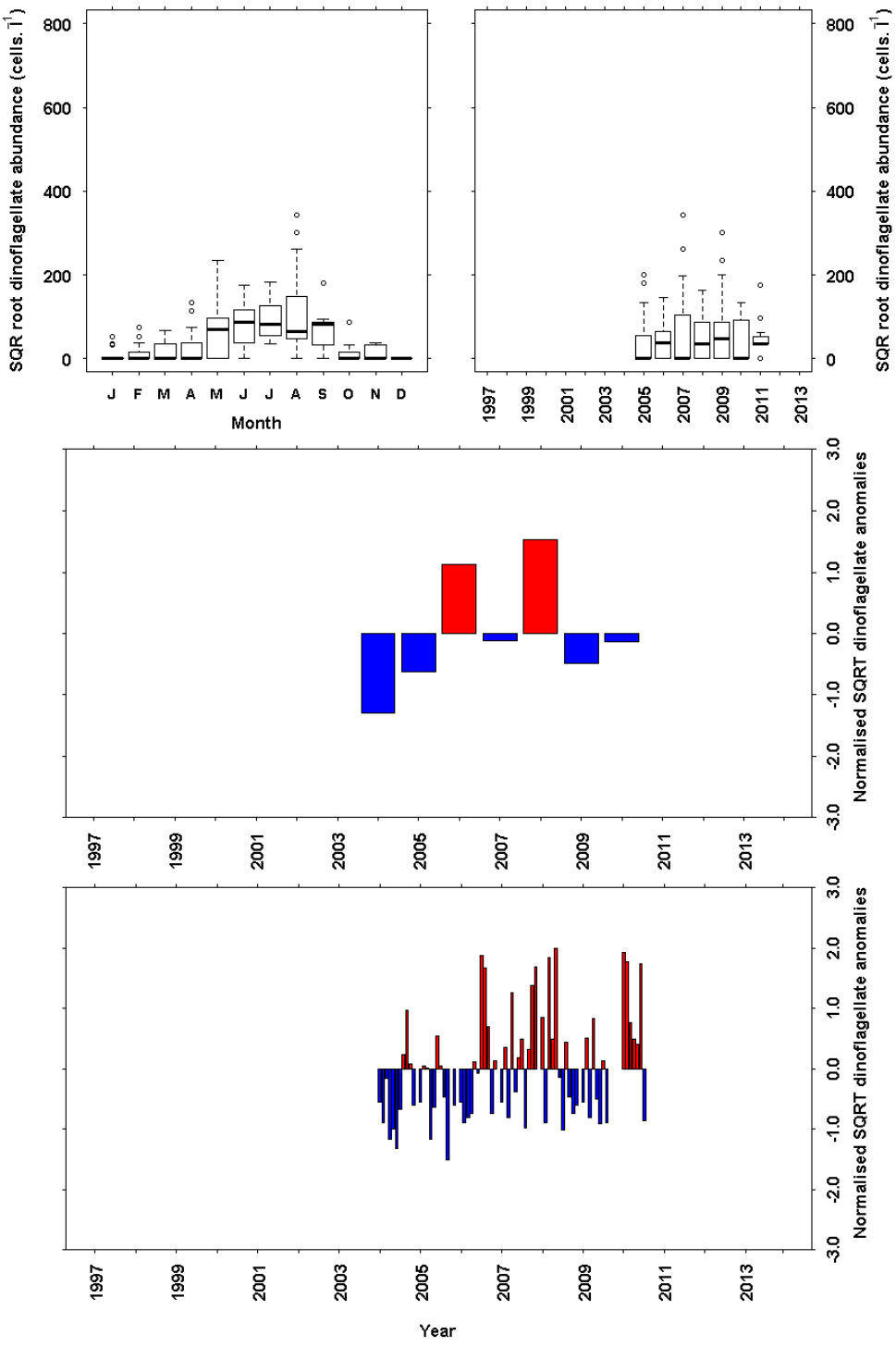

Figure 9.8 Dinoflagellate abundance (cells L^{-1}) from the long term monitoring site at Loch Maddy. SQRT transformed data has been plotted. a) Monthly boxplot of dinoflagellate abundance. b) Annual boxplot of dinoflagellate abundance. c) Annual mean anomaly time series d) Monthly mean anomaly time series. The full data set was used as the base period for the anomaly calculations.

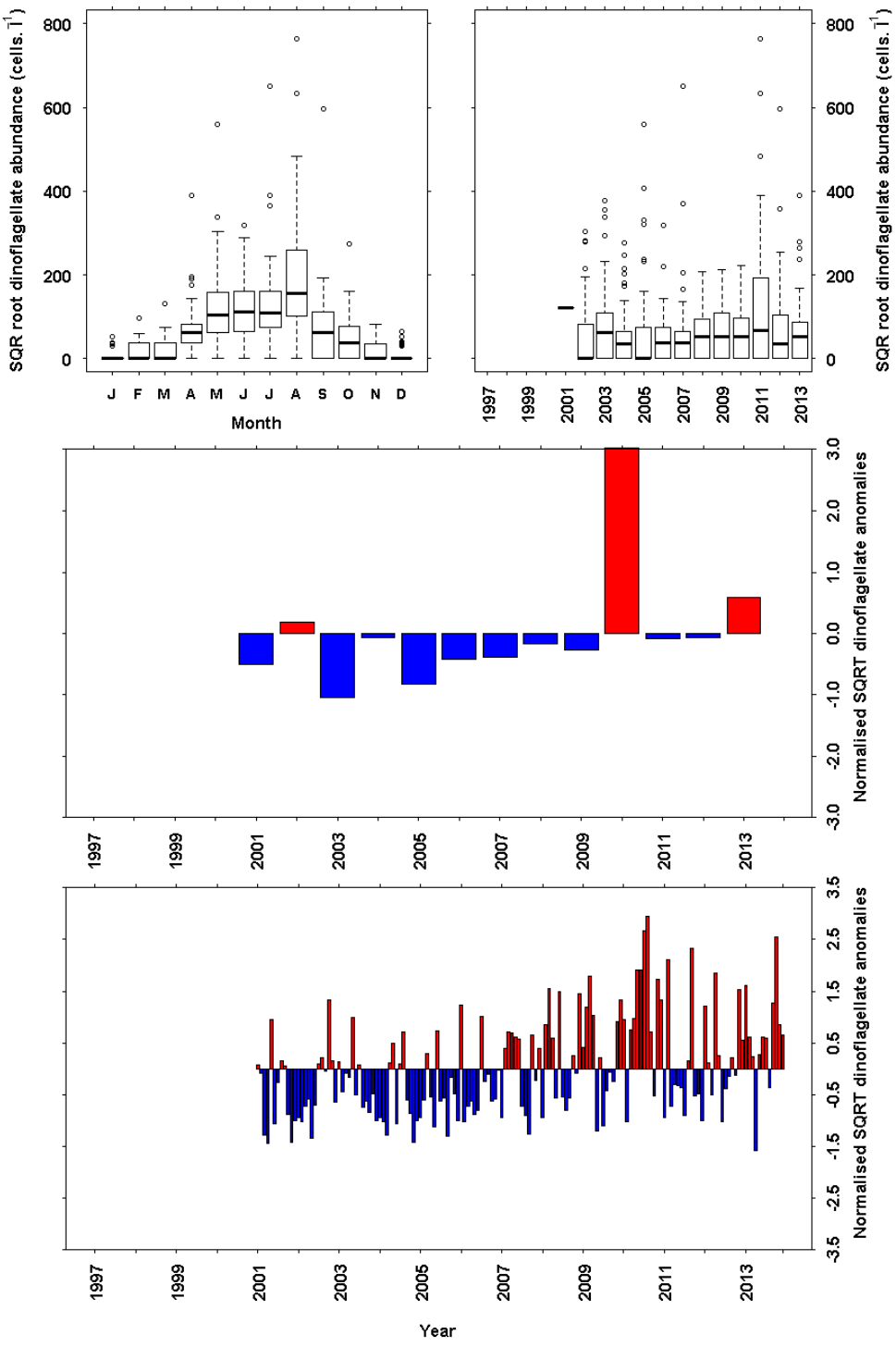

Figure 9.9 Dinoflagellate abundance (cells L^{-1}) from the long term monitoring site at Loch Ewe. SQRT transformed data has been plotted. a) Monthly boxplot of dinoflagellate abundance. b) Annual boxplot of dinoflagellate abundance. c) Annual mean anomaly time series d) Monthly mean anomaly time series. Sampling began in 2001. The full data set was used as the base period for the anomaly calculations.

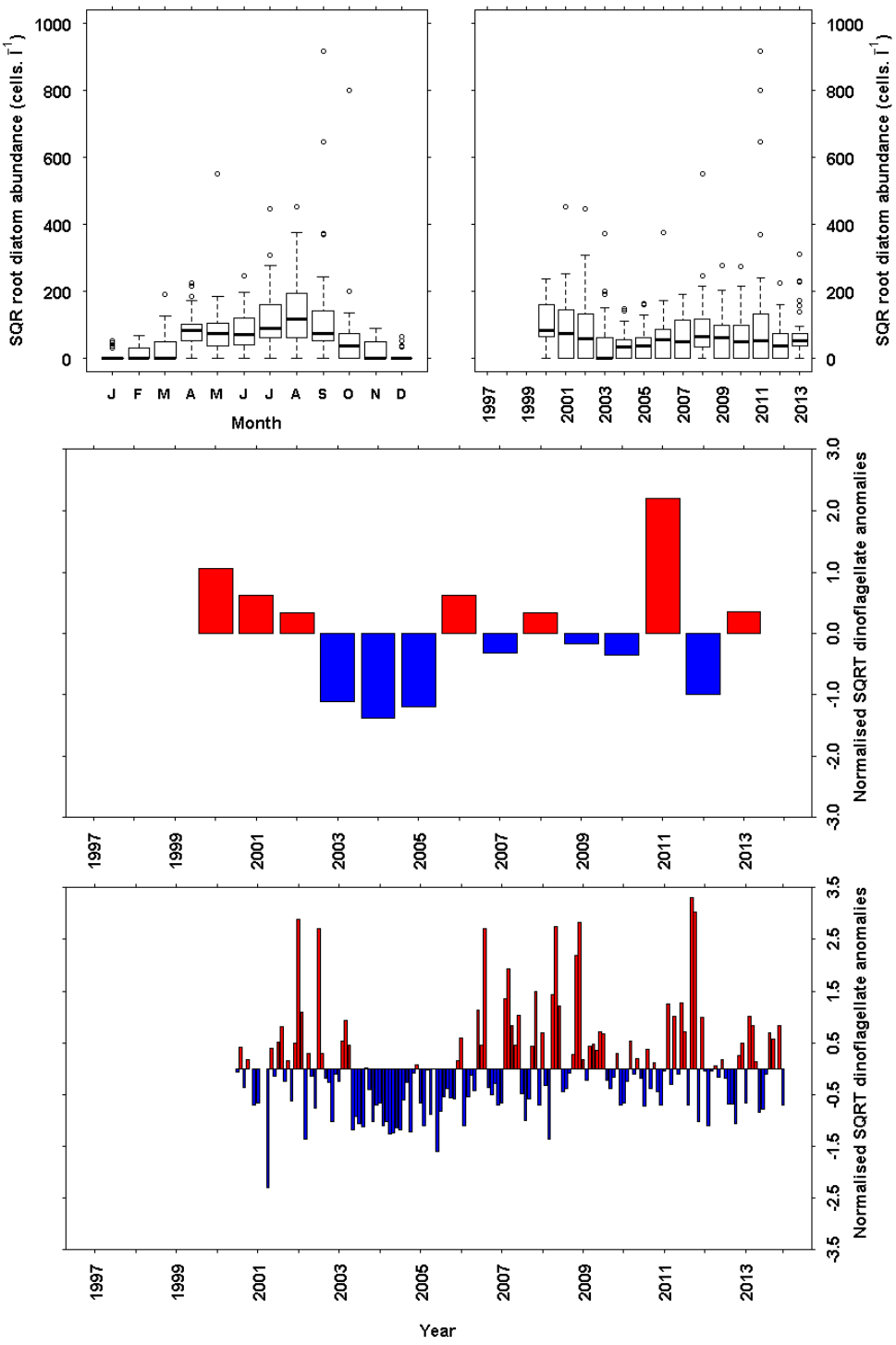

Figure 9.10 Dinoflagellate abundance (cells L^{-1}) from the long term monitoring site at Scapa. SQRT transformed data has been plotted. a) Monthly boxplot of dinoflagellate abundance. b) Annual boxplot of dinoflagellate abundance. c) Annual mean anomaly time series d) Monthly mean anomaly time series. Sampling began in 2001. The full data set was used as the base period for the anomaly calculations.

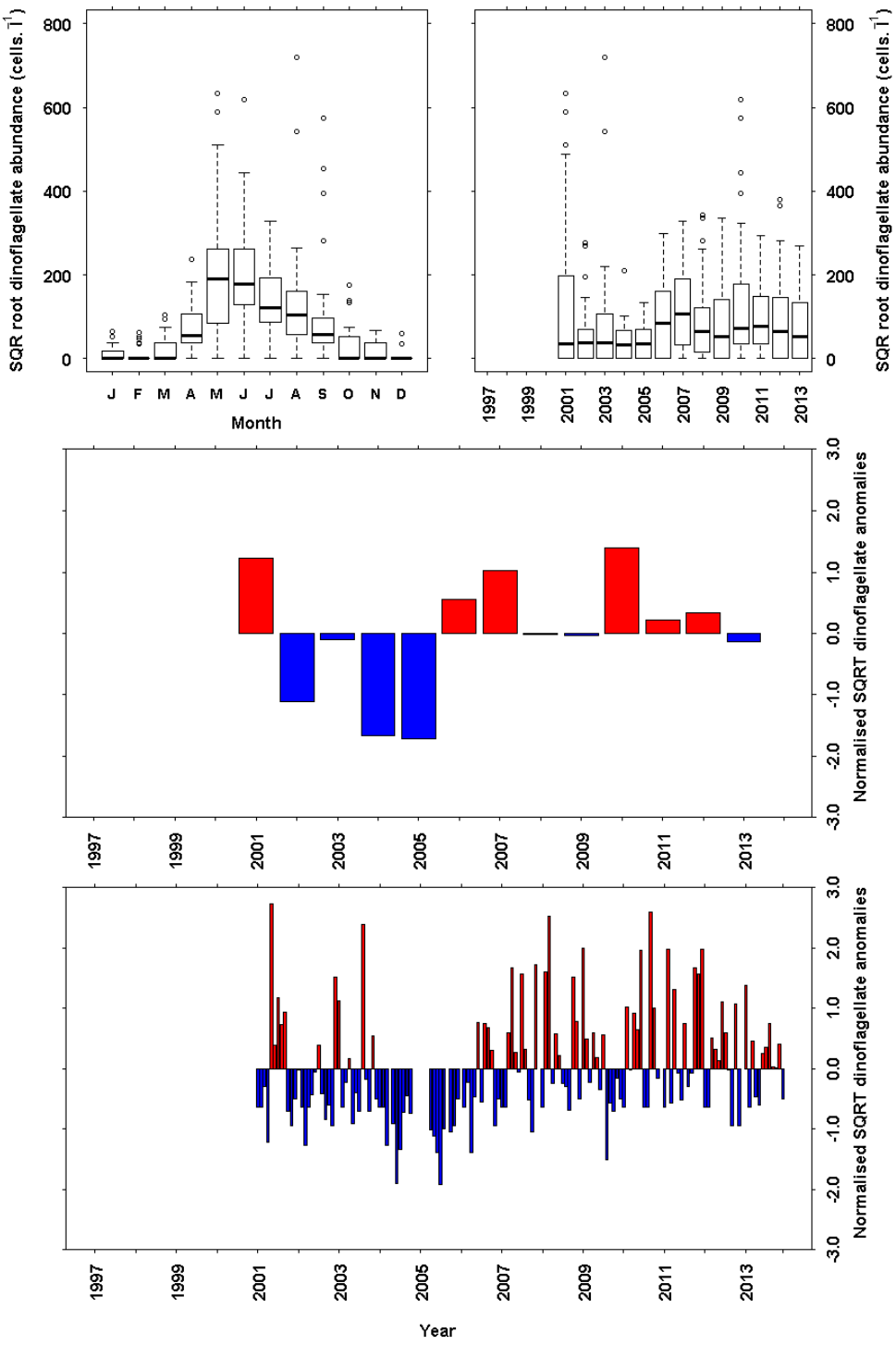

Figure 9.11 Dinoflagellate abundance (cells L^{-1}) from the long term monitoring site at Scalloway. SQRT transformed data has been plotted. a) Monthly boxplot of dinoflagellate abundance. b) Annual boxplot of dinoflagellate abundance. c) Annual mean anomaly time series d) Monthly mean anomaly time series. Sampling began in 2001. The full data set was used as the base period for the anomaly calculations.

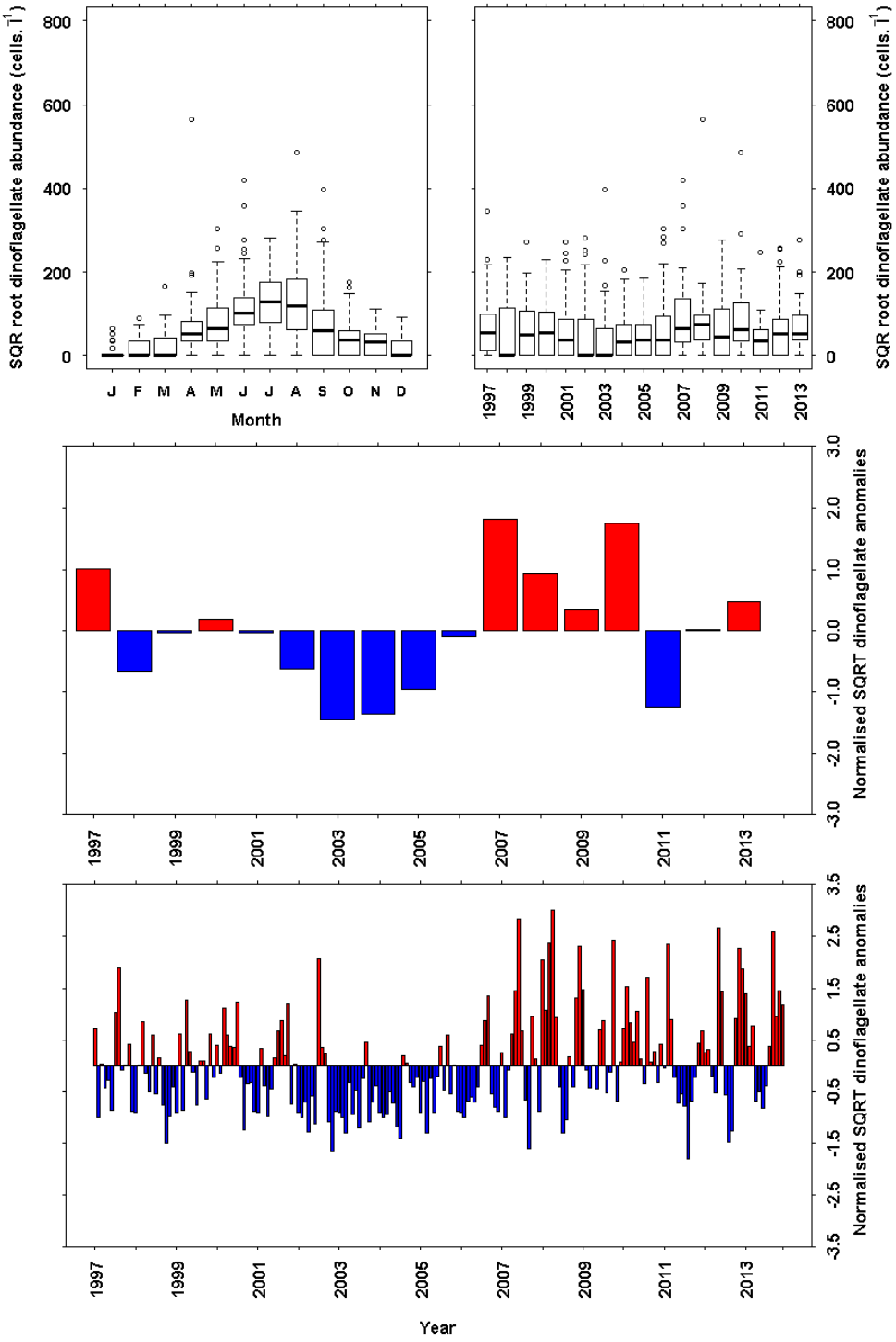

Figure 9.12 Dinoflagellate abundance (cells L^{-1}) from the long term monitoring site at Stonehaven. SQRT transformed data has been plotted. a) Monthly boxplot of dinoflagellate abundance. b) Annual boxplot of dinoflagellate abundance. c) Annual mean anomaly time series d) Monthly mean anomaly time series. Sampling began in 1997. The full data set was used as the base period for the anomaly calculations.

9.7 Results – *Alexandrium*

Species within the dinoflagellate genus *Alexandrium* are confirmed producers of the toxins responsible for paralytic shellfish poisoning (PSP) in Scottish waters. Shellfish accumulate the PSP toxins in their flesh through filter feeding the *Alexandrium* cells where they can pose a serious risk to human health if consumed. Monitoring for PSP toxins began in 1968 in the region from the Firth of Forth to the Humber (Ayres and Cullum 1968). Routine monitoring was extended around the Scottish coast and into Northern Ireland in the early 1990s in response to an extensive bloom of *Gonyaulax tamarense* var *excavata* (now considered part of the *Alexandrium fundyense/tamarense/catenella* complex). During the 1990s the east coast of Scotland along with the Orkney Islands were considered a hot spot for the *Alexandrium* genus and shellfish in this region were observed to contain high concentrations of PSP toxins.

The taxonomy of the *Alexandrium fundyense/tamarense/catenella* complex is not straightforward and at the time of press is currently under revision (John et al., 2014, Fraga et al., 2015). *Alexandrium* cells cannot be identified to species level using routine light microscopy with a lugol's iodine fixative. Cells are identified to genus level only. Members of the *A. fundyense/tamarense/catenella* complex are morphologically similar. Using the taxonomic nomenclature of Lily et al., (2007), early studies during PSP events in Scottish waters revealed the presence of the toxin producing *A. tamarense* Group I strain while the non-toxin producing *A. tamarense* Group III was observed along the south coast of England (Medlin et al., 1998).

More recent investigations into the diversity of Scottish *Alexandrium* revealed the presence of *A. ostenfeldii*, *A. minutum*, *A. tamutum*, *A. tamarense* Group I and *A. tamarense* Group III (Collins et al., 2009a, Brown et al., 2011). In addition *A. tamarense* Group I and Group III cells were observed in the same location in the Shetland islands (Touzet et al., 2010).

PSP toxicity in Scottish shellfish observed a period of less frequent PSP toxicity at the beginning of this century (Bresnan et al., 2008). The relationship between this decrease in toxicity and the diversity of *Alexandrium* populations in Scottish waters is currently under investigation.

A molecular quantitative polymerase chain reaction(qPCR) method was developed to examine the diversity of the *Alexandrium* population at the different monitoring sites (Collins et al., 2009b). This reveals the toxin producing *A. tamarense* Group I to be the dominant signal observed at Loch Ewe, Scapa and Stonehaven while the non-toxin producing *A. tamarense* Group III is the dominant signal at Scalloway (see Figure 9.19).

Alexandrium: Millport

Alexandrium cells were present in low numbers (< 500 cells L^{-1}) during the spring and summer over most of the monitoring period. Only three samples contained more than 1,000 *Alexandrium* cells L^{-1} with the highest cell density of 5,760 cells L^{-1}

observed in 2011. A slight increase in cell abundance can be observed during the latter part of this monitoring period.

Alexandrium: Loch Maddy

Alexandrium cells densities were also low (< 500 cells L^{-1}) in Loch Maddy during the course of the monitoring programme, occurring in the summer months. The highest cell density recorded was 2,600 cells L^{-1}. Infrequent sampling at this site makes any trends difficult to interpret.

Alexandrium: Loch Ewe

Alexandrium cells were present in low numbers (mostly < 500 cells L^{-1}) at the Loch Ewe monitoring site. Highest cell densities were observed in April and May. Only two samples contained *Alexandrium* cell densities greater than 1,000 cells L^{-1}. Both of these samples were collected in 2013 with a maximum of 1,640 cells L^{-1} being observed. An increase can be seen in cell densities during the duration of the monitoring programme.

Alexandrium: Scapa

Maximum *Alexandrium* concentrations are observed in April/May at this site with *Alexandrium* cell densities at the start of the monitoring programme exceeding 3,000 cells L^{-1}. A high degree of interannual variation can be observed with the temporal period over which *Alexandrium* is observed in the water column increasing in later years.

Alexandrium: Scalloway

Alexandrium populations can reach high cell densities at the Scalloway monitoring site with a maximum cell density of 24,000 cells L^{-1} observed in 2007. This is the highest *Alexandrium* cell density recorded as part of this monitoring programme. In contrast to other sites, the maximum *Alexandrium* cell densities are observed later in the summer in June and July.

Alexandrium: Stonehaven

Highest *Alexandrium* cell densities were observed in April and May at Stonehaven. The maximum *Alexandrium* cell density observed was 5,950 cells L^{-1} in 2012. Since 2005 the temporal spread of this genus throughout the summer months has increased.

9.8 Plots – *Alexandrium*

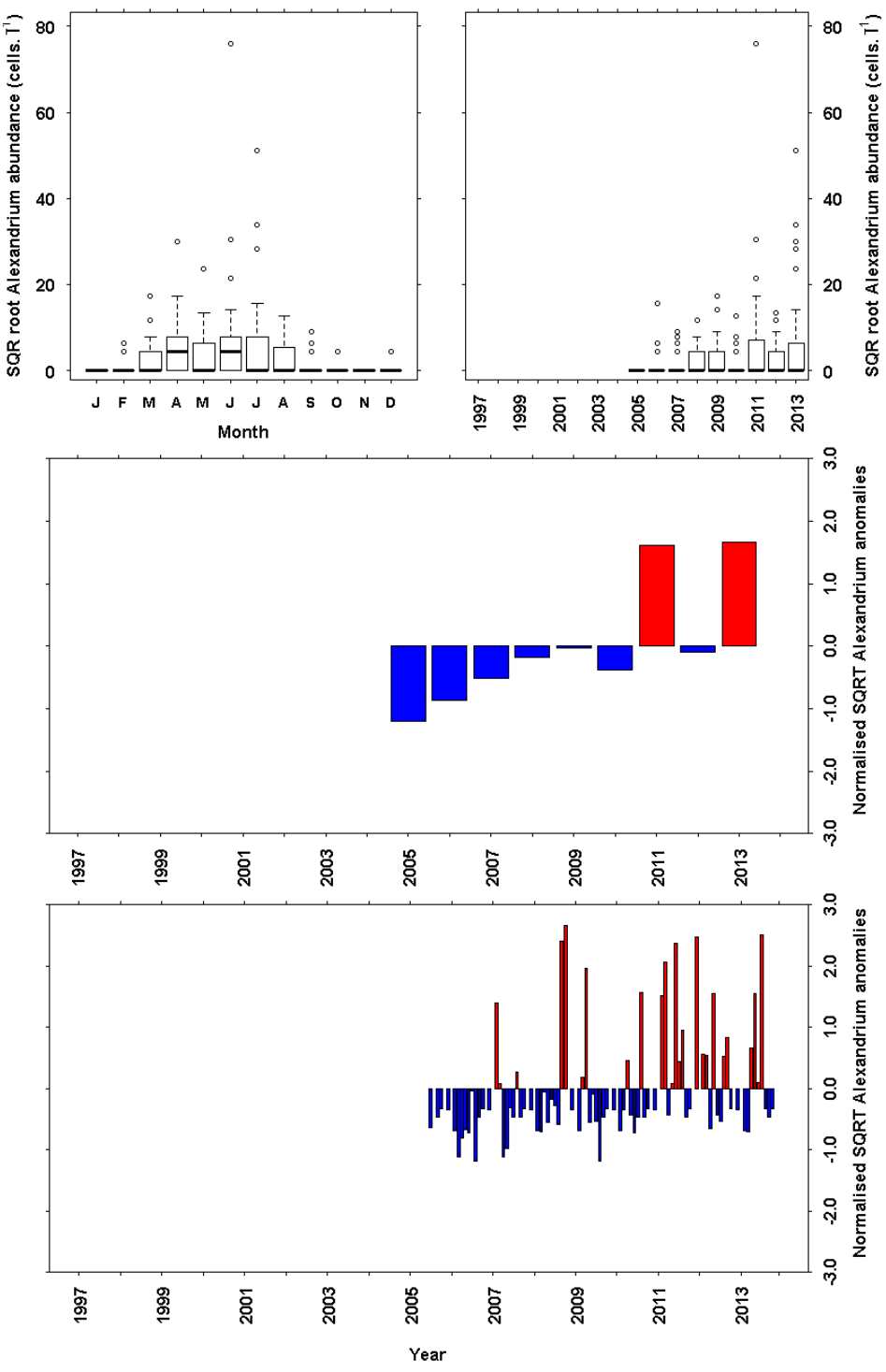

Figure 9.13 *Alexandrium* abundance (cells L^{-1}) from the long term monitoring site at Millport. SQRT transformed data has been plotted. a) Monthly boxplot of *Alexandrium* abundance. b) Annual boxplot of *Alexandrium* abundance. c) Annual mean anomaly time series d) Monthly mean anomaly time series. Sampling began in 2005. The full data set was used as the base period for the anomaly calculations.

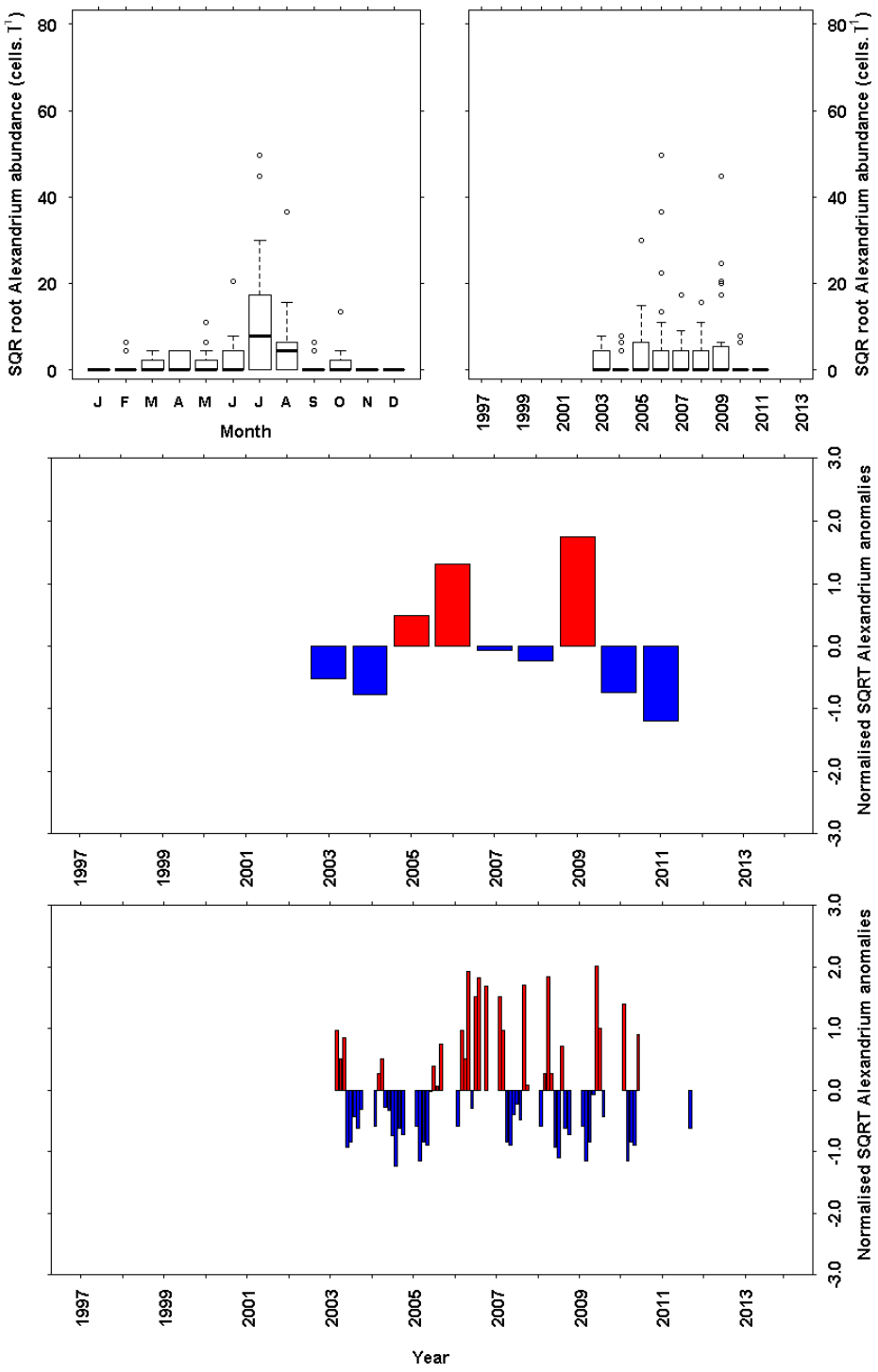

Figure 9.14 *Alexandrium* abundance (cells L^{-1}) from the long term monitoring site at Loch Maddy. SQRT transformed data has been plotted. a) Monthly boxplot of *Alexandrium* abundance. b) Annual boxplot of *Alexandrium* abundance. c) Annual mean anomaly time series d) Monthly mean anomaly time series. Sampling began in 2003. The full data set was used as the base period for the anomaly calculations.

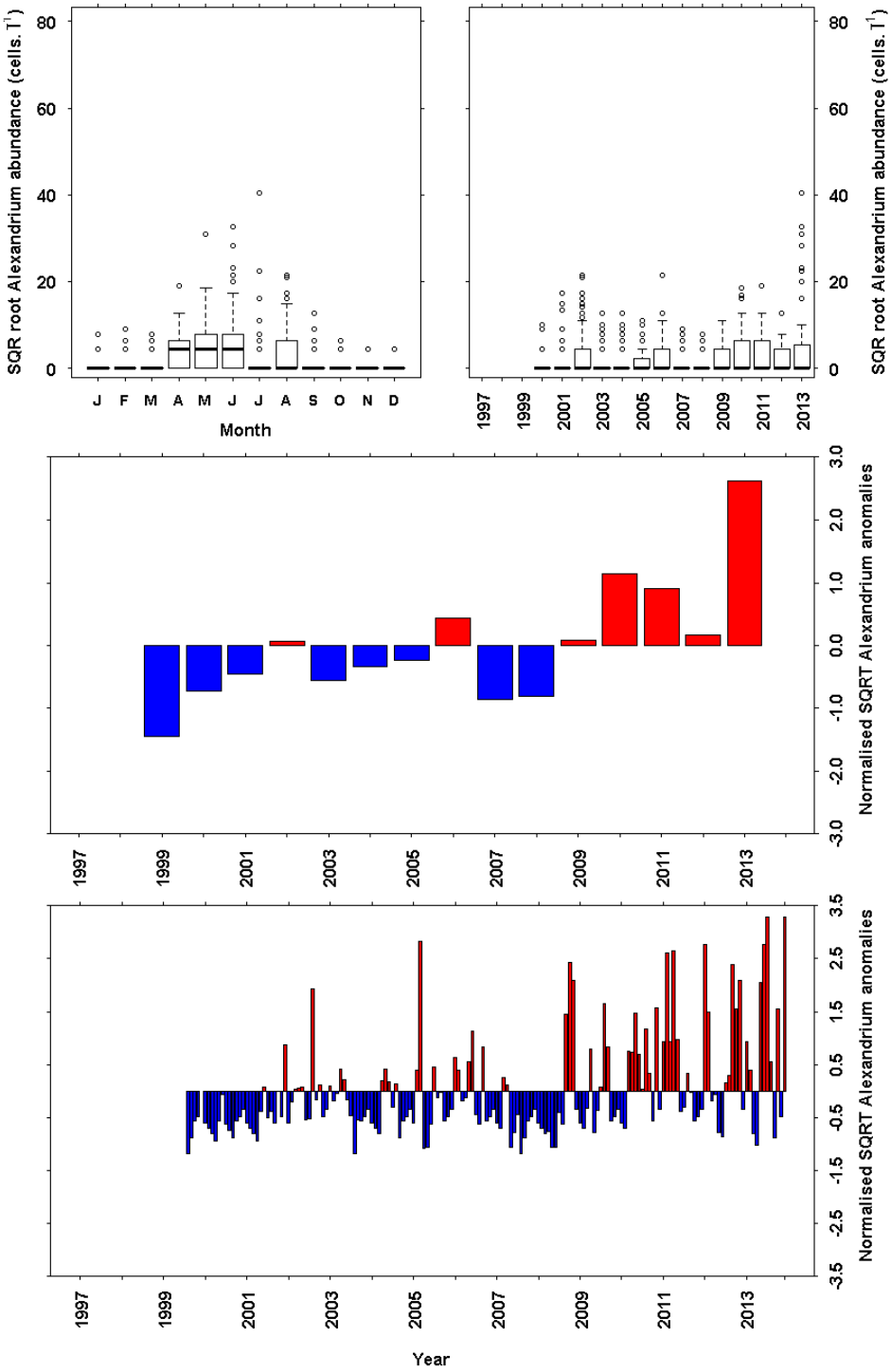

Figure 9.15 *Alexandrium* abundance (cells L^{-1}) from the long term monitoring site at Loch Ewe. SQRT transformed data has been plotted. a) Monthly boxplot of *Alexandrium* abundance. b) Annual boxplot of *Alexandrium* abundance. c) Annual mean anomaly time series d) Monthly mean anomaly time series. Sampling for harmful species began in 1998. The full data set was used as the base period for the anomaly calculations.

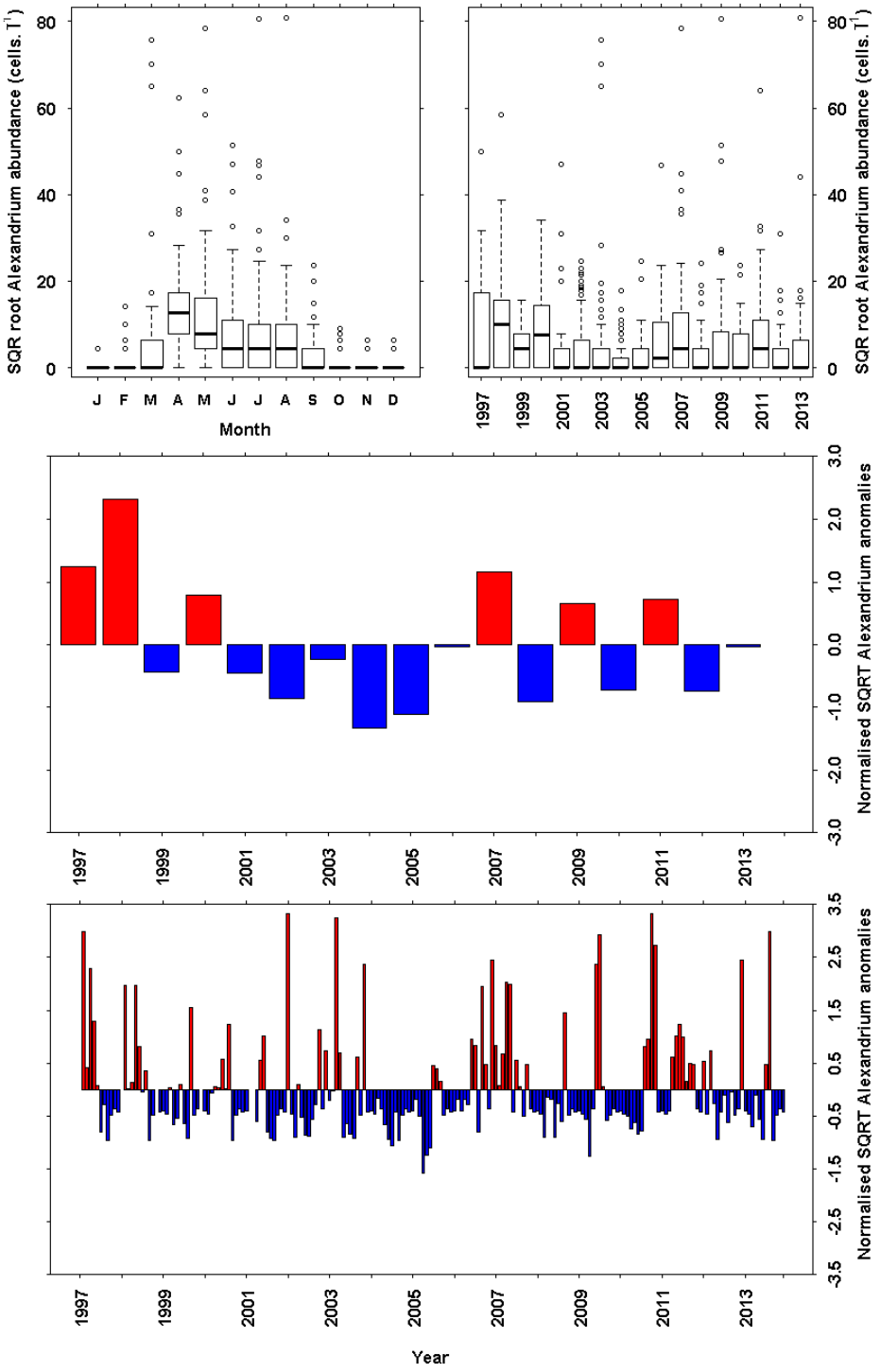

Figure 9.16 *Alexandrium* abundance (cells L^{-1}) from the long term monitoring site at Scapa. SQRT transformed data has been plotted. a) Monthly boxplot of *Alexandrium* abundance. b) Annual boxplot of *Alexandrium* abundance. c) Annual mean anomaly time series d) Monthly mean anomaly time series. Sampling for harmful species began in 1997. The full data set was used as the base period for the anomaly calculations.

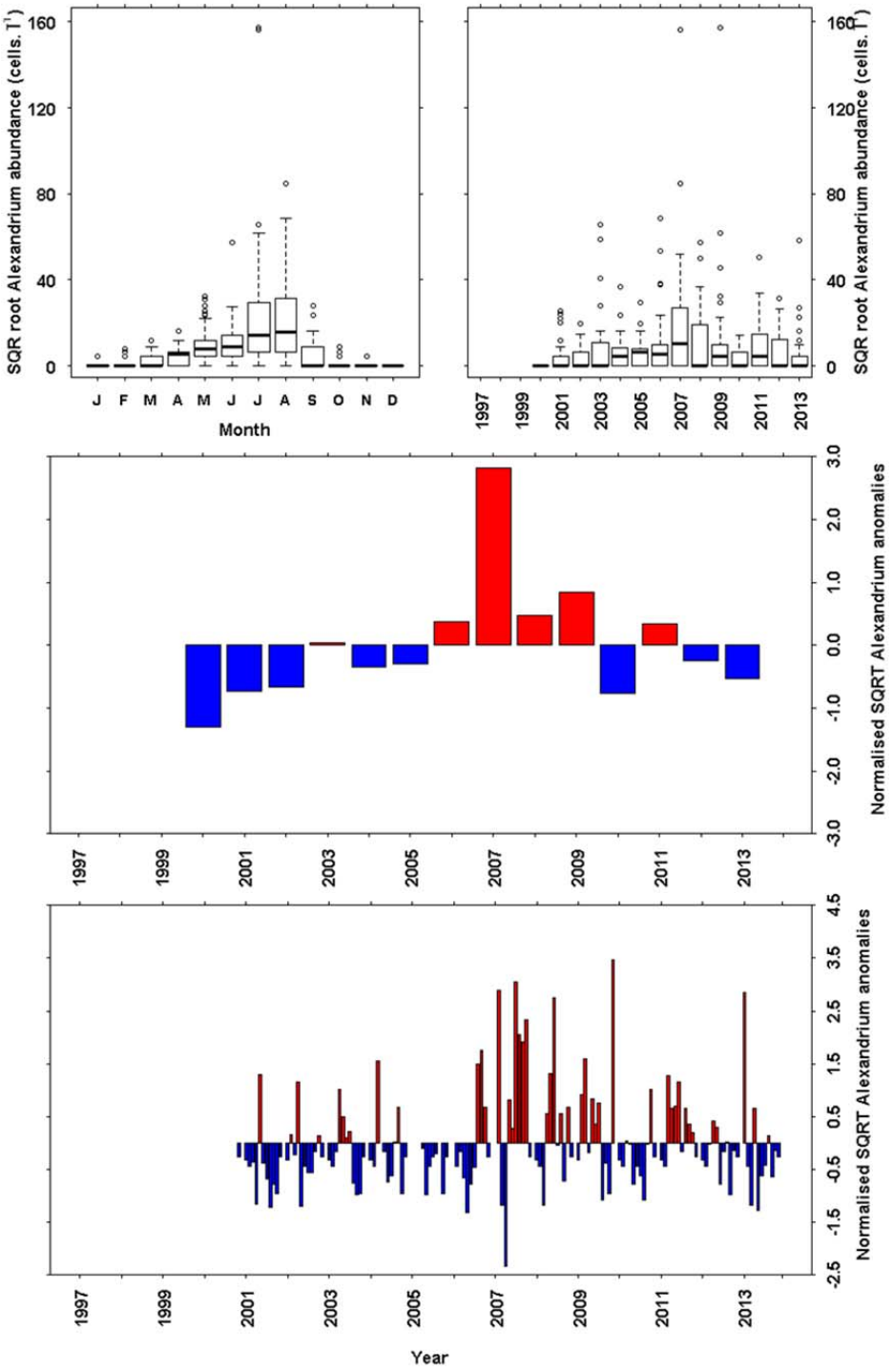

Figure 9.17 *Alexandrium* abundance (cells L^{-1}) from the long term monitoring site at Scalloway. SQRT transformed data has been plotted. a) Monthly boxplot of *Alexandrium* abundance. b) Annual boxplot of *Alexandrium* abundance. c) Annual mean anomaly time series d) Monthly mean anomaly time series. Sampling for harmful species began in 2000. The full data set was used as the base period for the anomaly calculations.

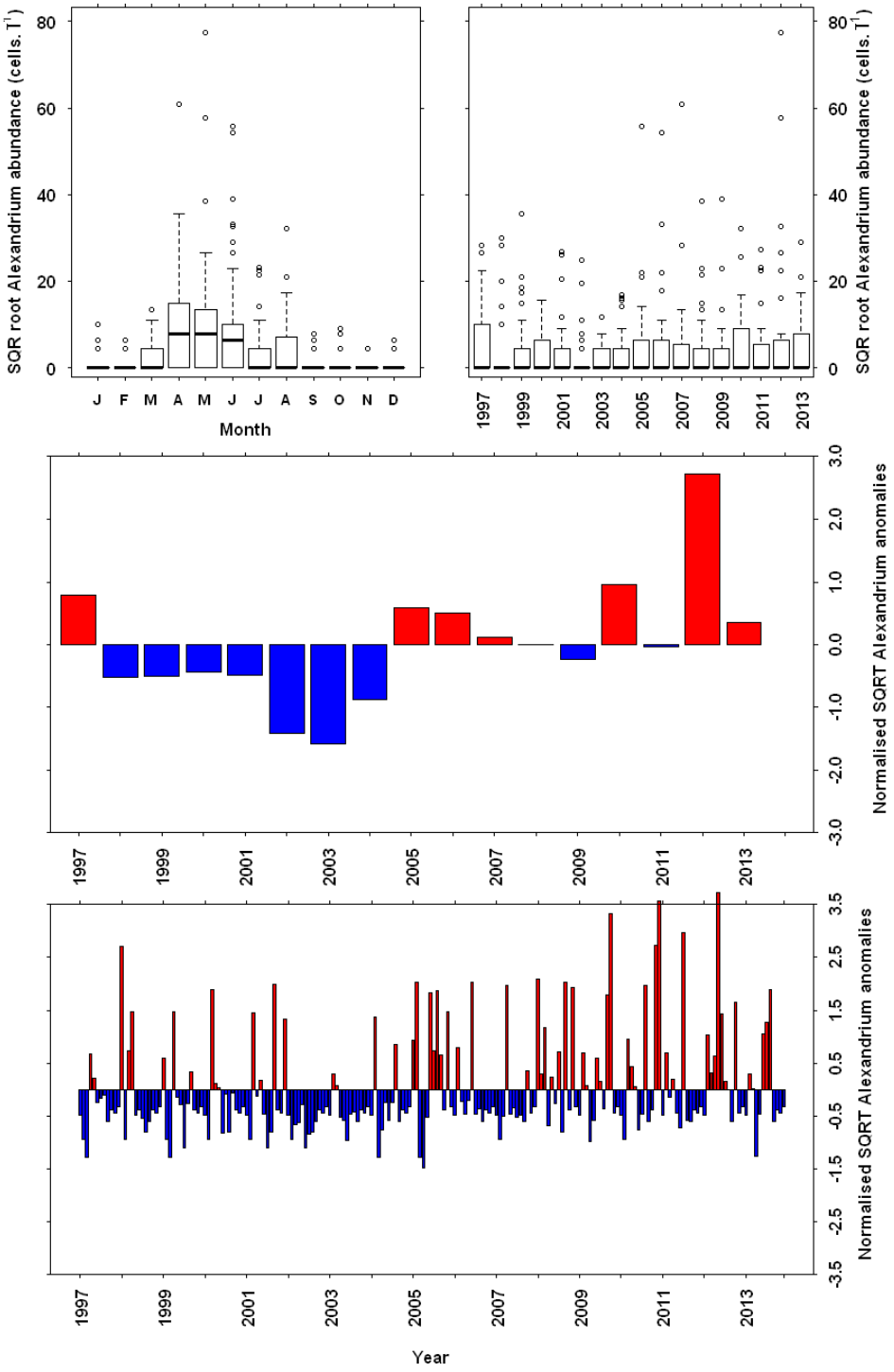

Figure 9.18 *Alexandrium* abundance (cells L^{-1}) from the long term monitoring site at Stonehaven. SQRT transformed data has been plotted. a) Monthly boxplot of *Alexandrium* abundance. b) Annual boxplot of *Alexandrium* abundance. c) Annual mean anomaly time series d) Monthly mean anomaly time series. Sampling for harmful species began in 1997. The full data set was used as the base period for the anomaly calculations.

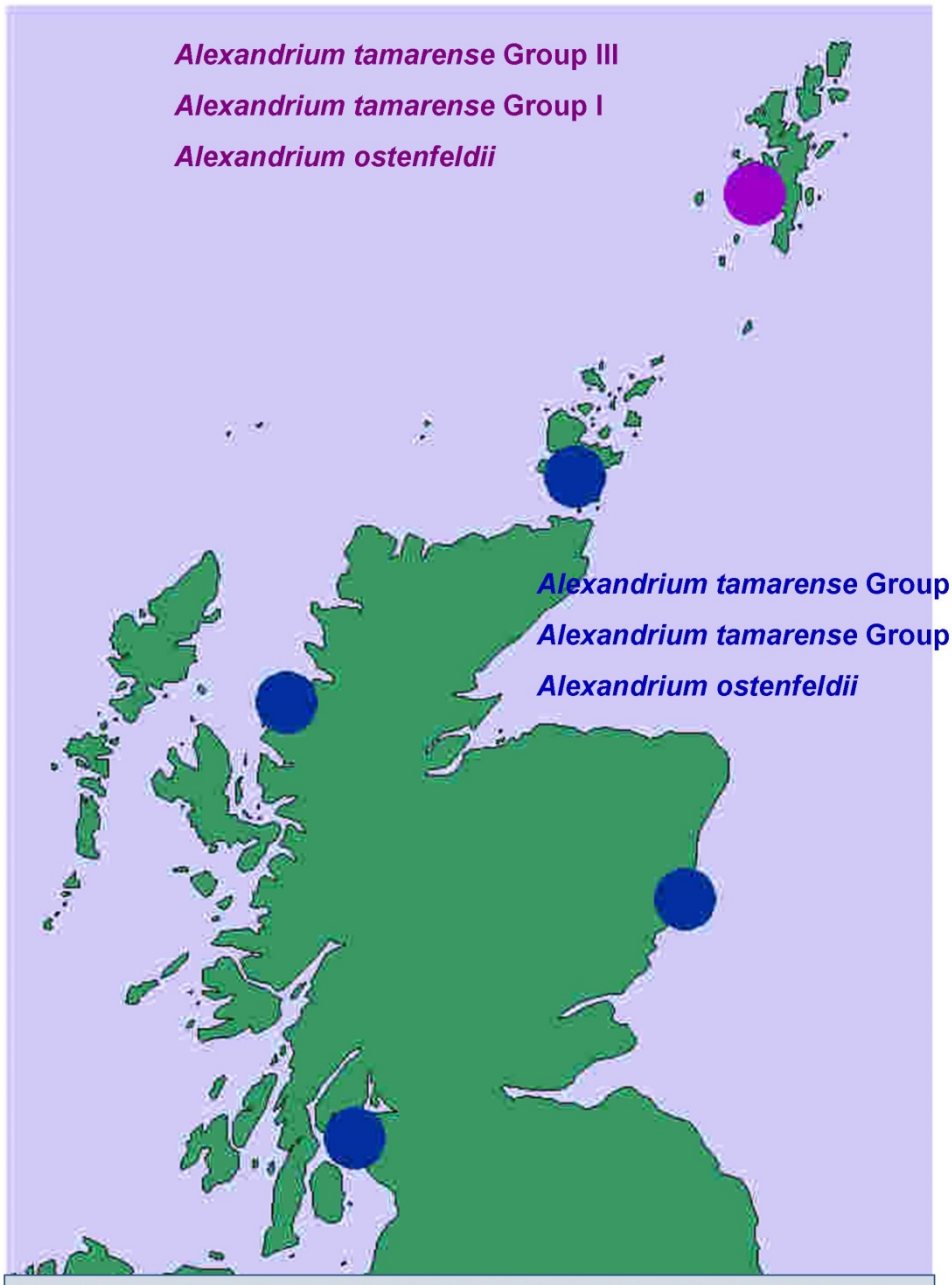

A QPCR method was developed to identify the *Alexandrium* cells to species level (Collins et al., 2009b). Samples from the coastal ecosystem monitoring programme were analysed using this method. These results showed a regional difference in the diversity of *Alexandrium* present with *Alexandrium tamarense* Group III the dominant strain observed using this technique in Shetland while *Alexandrium tamarense* Group I was the dominant strain observed in Millport, Loch Ewe, Scapa and Stonehaven. *A. minutum* and *A. ostenfeldii* were also observed.

Figure 9.19 Map showing the diversity of *Alexandrium* communities at sites in the monitoring programme identified using a qPCR method.

9.9 Results - *Dinophysis*

Members of the dinoflagellate genus *Dinophysis* produce the lipophilic shellfish toxins responsible for Diarhetic Shellfish Poisoning (DSP). A description of these toxins are presented in Chapter 11, Algal toxins. Phytoplankton records from the early 1900s (Herdman and Riddell 1911, 1912, 1913) have recorded the presence of the *Dinophysis* genus in samples collected from the west coast of Scotland which suggest it is an established part of the phytoplankton community in this region.

DSP toxins have been detected in Scottish shellfish since monitoring began in 1992 and *Dinophysis* has been identified as a common member of the summer phytoplankton community since routine monitoring began in fulfilment of the EU Shellfish Hygiene Directive in 1996 (Stern et al., 2014). A moderate correlation between the presence of *Dinophysis* in the water column and DSP toxins in shellfish flesh has been observed (Bresnan et al., 2005).

Dinophysis acuminata and *Dinophysis acuta* are the dominant *Dinophysis* species recorded in Scottish waters. Morphological ambiguity in species identification has been confirmed by molecular techniques (Hart et al., 2007, Stern et al., 2014) with the dominant species identified as *D. acuminata*.

Multidecadal studies have revealed a shift in the spatial distribution of *Dinophysis* within the North Sea (Edwards et al., 2006). Data from the continuous plankton recorder (CPR) reveals that hotspots of *Dinophysis* along the east coast of England recorded in the 1970s appear to have shifted to the western part of the North Sea in the 1990s. *Dinophysis* is typically found in stratified waters (Raine et al., 2010) and can form high density thin layers which can be transported in coastal currents (Farrell et al., 2012). In some areas along the west coast (i.e. Loch Fyne) closures of shellfish harvesting areas resulting from high concentrations of DSP toxins can be prolonged with closures of over nine weeks recorded (Bresnan et al., 2013). A sudden shift in wind direction has been implicated in a DSP intoxication event in 2013 caused by mussels from the Shetland Islands (Whyte et al., 2014).

Dinophysis: Millport

Dinophysis cells are observed at the Millport monitoring site during the summer months with highest densities recorded between June and August. *D. acuminata* was the dominant species observed during the monitoring period. An increase in the numbers of *Dinophysis* was observed over the duration of the time series with maximum cell densities reaching 2,520 cells L^{-1}.

Dinophysis: Loch Maddy

Dinophysis cells are observed at the Loch Maddy monitoring site during the summer months. *D. acuminata* was the dominant species observed in the water column. A decrease in the numbers of *Dinophysis* was observed over the duration of the time series but this may be an artefact of the infrequent sampling during the latter part of the time series.

Dinophysis: Loch Ewe

Dinophysis has been routinely observed in Loch Ewe during the summer. High cell densities during the summer months were observed between 2000-2003 (maximum of 5,000 cells L^{-1}) and numbers decreased until 2010. *D. acuminata* is the dominant species at this site.

Dinophysis: Scapa

Dinophysis has been routinely observed at Scapa Bay since monitoring began in 1997. A decrease in the abundance of *Dinophysis* has been observed since monitoring began but this may reflect a change in the location of the sampling point in 2003.

Dinophysis: Scalloway

Dinophysis cells are observed during the summer months in Scalloway. Highest cell abundances have been observed during 2006 and 2013. The 2013 event (23,000 cells L^{-1}) has been associated with wind driven advection (Whyte et al., 2014). The dominant species at this site is *D. acuminata*.

Dinophysis: Stonehaven

Dinophysis cells are observed during the summer months at Stonehaven. High cell densities (3,000 cells L^{-1}) were observed at the start of the time series. Numbers decreased until 2005 and then began to increase with high concentrations of *D. acuminata* once more recorded (6,000 cells L^{-1}).

9.10 Plots – *Dinophysis*

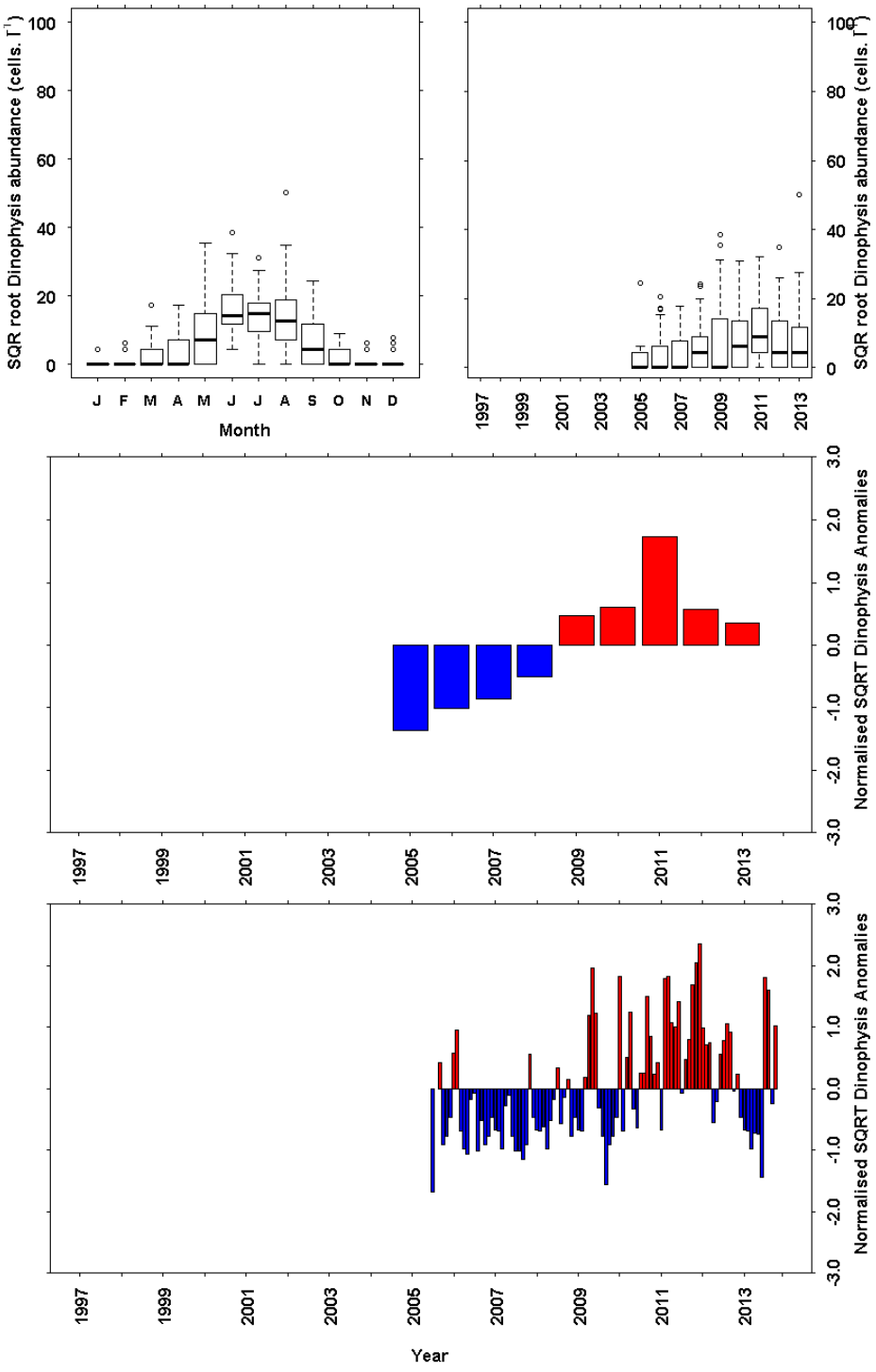

Figure 9.20 *Dinophysis* abundance (cells L^{-1}) from the long term monitoring site at Millport. SQRT transformed data has been plotted. a) Monthly boxplot of *Dinophysis* abundance. b) Annual boxplot of *Dinophysis* abundance. c) Annual mean anomaly time series d) Monthly mean anomaly time series. Sampling for harmful species began in 2005. The full data set was used as the base period for the anomaly calculations.

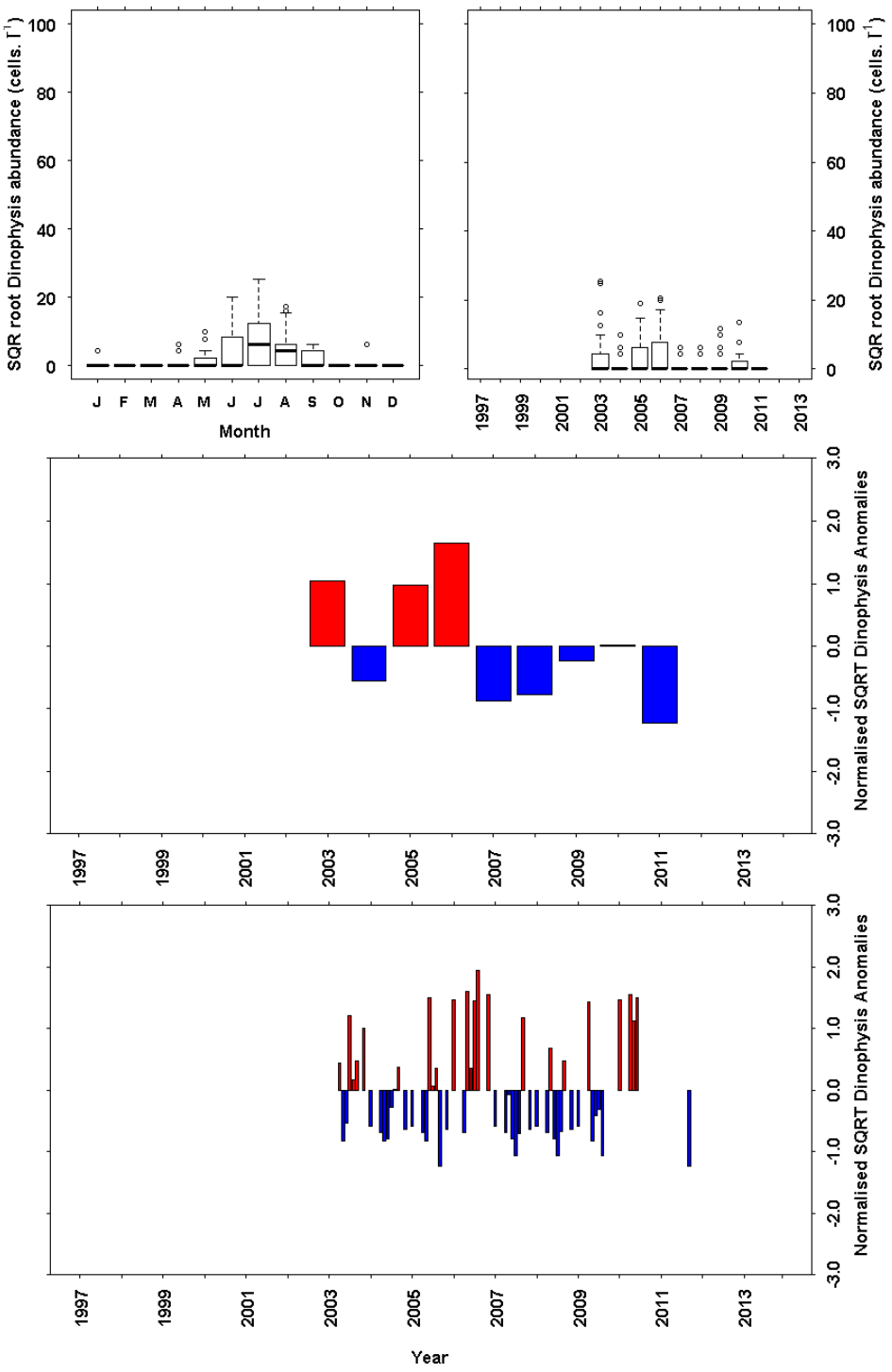

Figure 9.21 *Dinophysis* abundance (cells L^{-1}) from the long term monitoring site at Loch Maddy. SQRT transformed data has been plotted. a) Monthly boxplot of *Dinophysis* abundance. b) Annual boxplot of *Dinophysis* abundance. c) Annual mean anomaly time series d) Monthly mean anomaly time series. Sampling for harmful species began in 2005. The full data set was used as the base period for the anomaly calculations.

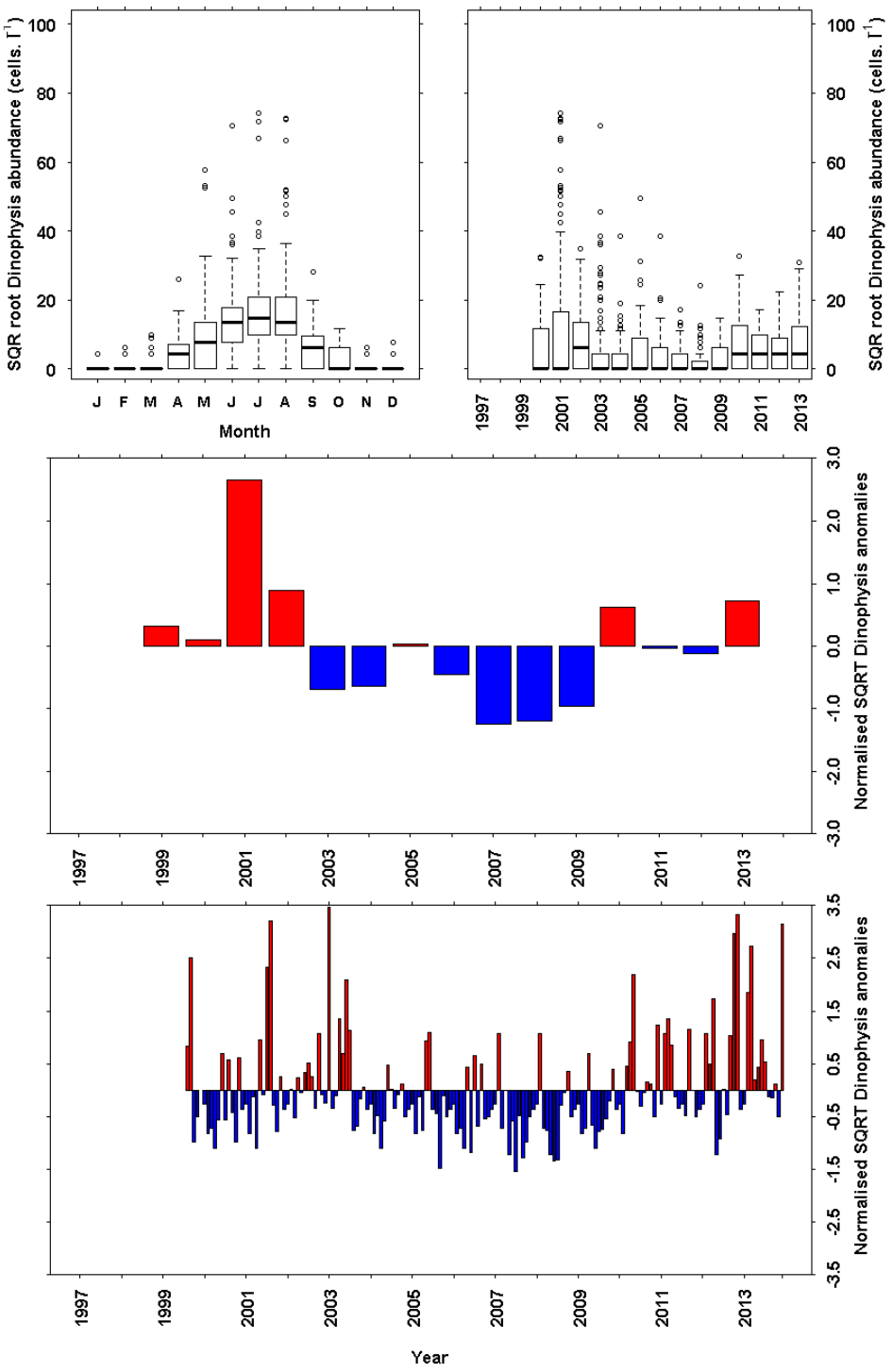

Figure 9.22 *Dinophysis* abundance (cells L^{-1}) from the long term monitoring site at Loch Ewe. SQRT transformed data has been plotted. a) Monthly boxplot of *Dinophysis* abundance. b) Annual boxplot of *Dinophysis* abundance. c) Annual mean anomaly time series d) Monthly mean anomaly time series. Sampling for harmful species began in 2005. The full data set was used as the base period for the anomaly calculations.

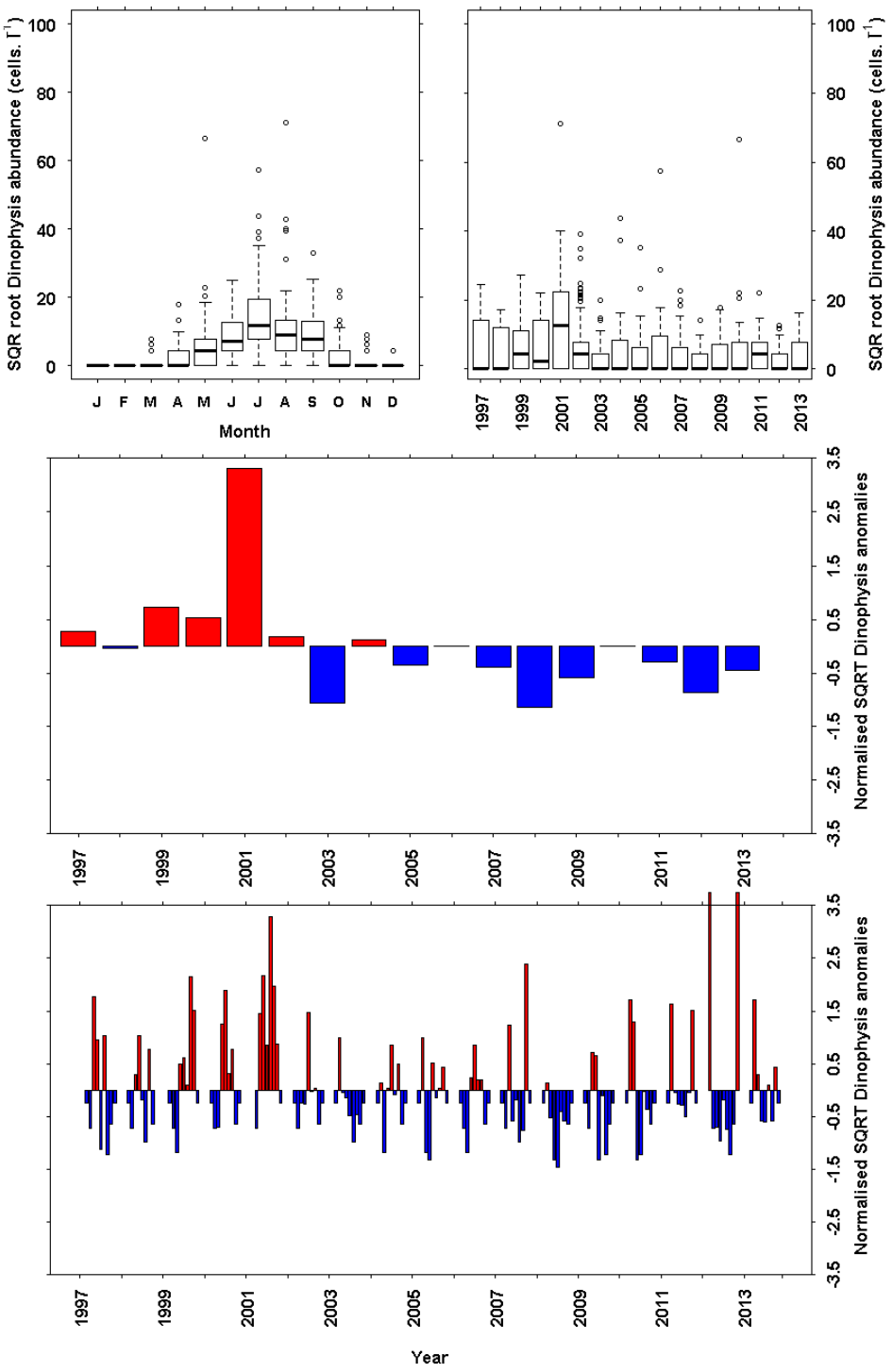

Figure 9.23 *Dinophysis* abundance (cells L^{-1}) from the long term monitoring site at Scapa. SQRT transformed data has been plotted. a) Monthly boxplot of *Dinophysis* abundance. b) Annual boxplot of *Dinophysis* abundance. c) Annual mean anomaly time series d) Monthly mean anomaly time series. Sampling for harmful species began in 1997. The full data set was used as the base period for the anomaly calculations.

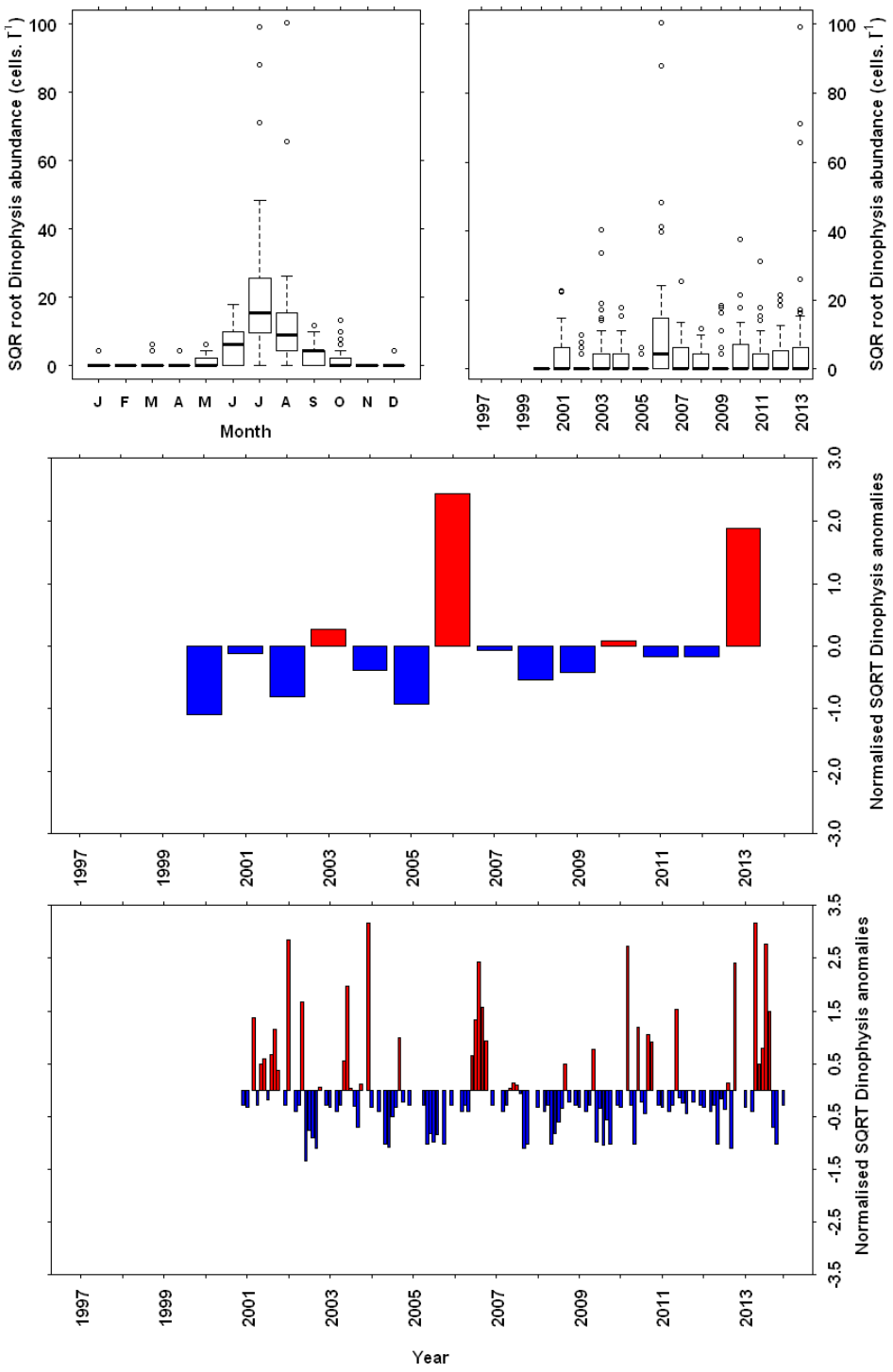

Figure 9.24 *Dinophysis* abundance (cells L^{-1}) from the long term monitoring site at Scalloway. SQRT transformed data has been plotted. a) Monthly boxplot of *Dinophysis* abundance. b) Annual boxplot of *Dinophysis* abundance. c) Annual mean anomaly time series d) Monthly mean anomaly time series. Sampling for harmful species began in 2005. The full data set was used as the base period for the anomaly calculations.

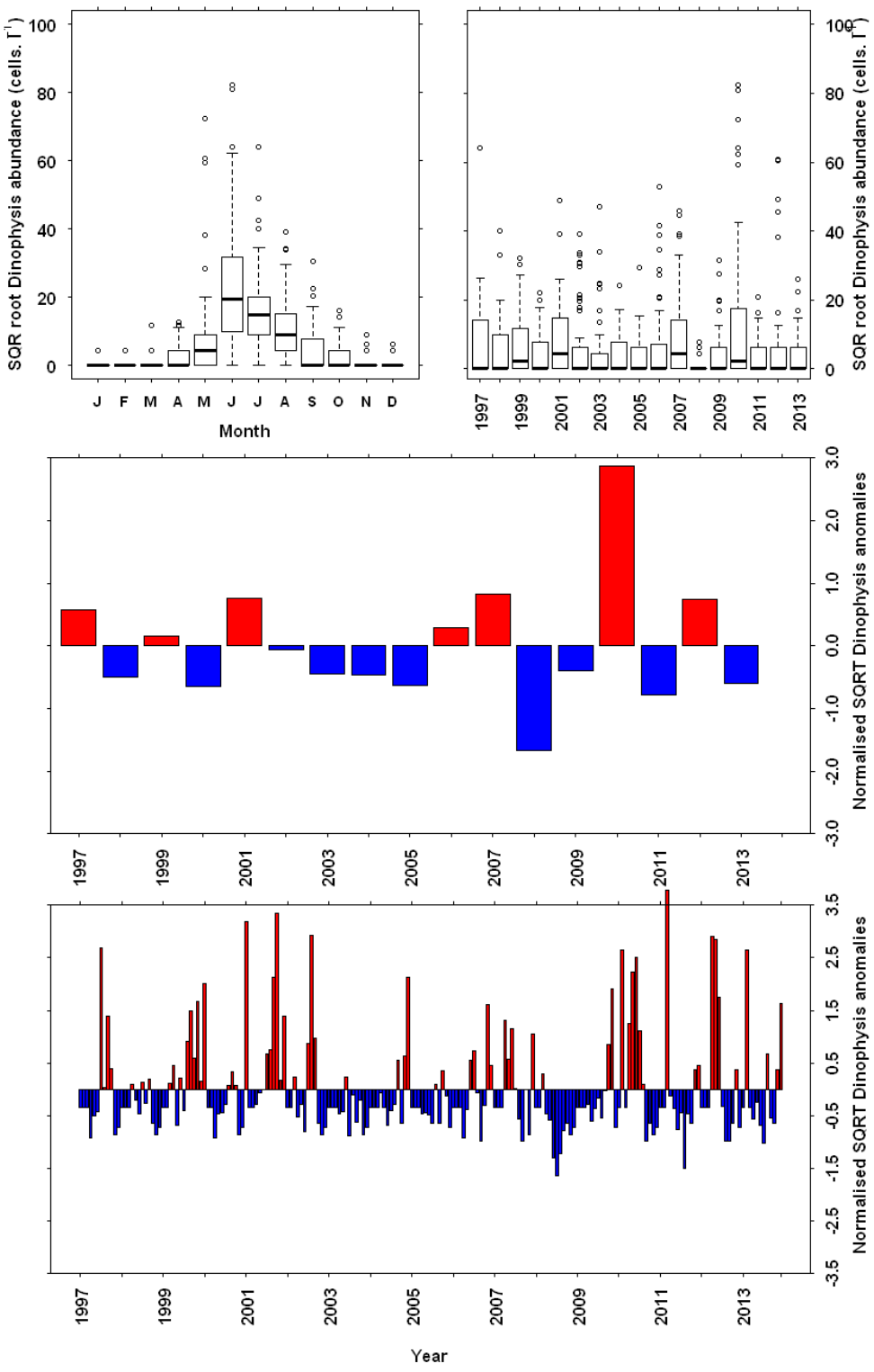

Figure 9.25 *Dinophysis* abundance (cells L^{-1}) from the long term monitoring site at Stonehaven. SQRT transformed data has been plotted. a) Monthly boxplot of *Dinophysis* abundance. b) Annual boxplot of *Dinophysis* abundance. c) Annual mean anomaly time series d) Monthly mean anomaly time series. Sampling for harmful species began in 1997. The full data set was used as the base period for the anomaly calculations.

9.11 Results - *Pseudo-nitzschia*

Pseudo-nitzschia is a diatom that is routinely detected in Scottish coastal waters throughout the year. It is in practically every phytoplankton sample collected by MSS. Herdman and Riddell (1911, 1912, 1913) recorded the presence of *Nitzschia seriata* and *Nitzschia delicatissima* (now called *Pseudo-nitzschia*) in samples collected from the west coast of Scotland in the early 1900s which suggests it is an established part of the phytoplankton community in this region.

Pseudo-nitzschia produces the neurotoxin domoic acid (DA) which is the toxin responsible for Amnesic Shellfish Poisoning (ASP). Closures of shellfish harvesting areas as a result of high concentrations of DA in the gonad tissue of King Scallops, *Pecten maximus*, were enforced in Scottish waters from 1998 (Gallacher et al., 2001) until the EU shellfish hygiene directive for end product testing changed in 2005. More recently DA in harbour seals has been flagged as a concern in relation to their decreasing numbers in Scottish waters (Hall and Frame 2010, Jensen et al., 2015).

Pseudo-nitzschia cells cannot be identified to species level using routine light microscopy. They can be separated in two different size categories </> 5 µm diameter and termed *Pseudo-nitzschia* '*delicatissima* type' and *Pseudo-nitzschia 'seriata* type' cells respectively. Electron microscopy or molecular techniques are required to identify *Pseudo-nitzschia* cells to species level. To date 14 different species have been recorded in Scottish waters; *P. americana*, *P. australis*, *P. caciantha*, *P. cuspidata*, *P. delicatissima*, *P. decepiens*, *P. fraudulenta*, *P. heimii*, *P. multiseries*, *P. plurisecta*, *P. pungens*, *P. pseudodelicatissima*, *P. subpacifica*, *P. seriata* (Fehling et al., 2005, Bresnan et al., 2005, Brown and Bresnan 2008, Bresnan et al., 2015b) of which *P. australis* and *P. seriata* have been confirmed as producers of domoic acid (DA), the toxin responsible for amnesic shellfish poisoning ASP) (Fehling et al., 2005).

Pseudo-nitzschia populations can be diverse and can comprise of up to six species at any one time in Scottish waters (Bresnan et al., 2005). Diversity can vary spatially with different species observed on and off the shelf break (Fehling et al., 2012) and within the North Sea (Bresnan et al., 2015b). A recent study of CPR data has shown an increase in the abundance of *Pseudo-nitzschia* in the North East Atlantic area in response to changing wind direction and increased intensity (Hinder et al., 2012).

Pseudo-nitzschia: Millport

Pseudo-nitzschia cells are present throughout the year at the Millport monitoring site In contrast to other sites (Loch Ewe, Scapa, Stonehaven) *Pseudo-nitzschia* does not increase during the spring bloom. Instead the abundance increases during the late summer and early autumn. A high degree of interannual variation can be found at this site and during most years maximum cell densities observed (~ 200,000 cells L^{-1}) are less than other sites participating in this monitoring programme.

Pseudo-nitzschia: Loch Maddy

Pseudo-nitzschia cell densities are observed throughout the year at this site with highest cell densities observed in late summer (~300,000 cells L-1). As in the Millport monitoring site, *Pseudo-nitzschia* abundance remains low during spring time. A decrease in the abundance of *Pseudo-nitzschia* can be observed over the duration of the monitoring programme at this site. The sporadic sampling in the latter part of this monitoring programme may have contributed to this.

Pseudo-nitzschia: Loch Ewe

Pseudo-nitzschia cells are found throughout the year at this site. *P. delicatissima* type cells are dominant during the spring bloom while *P. seriata* type cells are dominant in the late spring and early autumn. Seven different species of *Pseudo-nitzschia* have been identified at this site using TEM (Brown and Bresnan 2008, Bresnan et al., 2015b). *P. americana*, *P. australis*, *P. delicatissima*, *P. fraudulenta*, *P. pungens* and *P.* cf. *plurisecta*. Higher cell densities of *Pseudo-nitzschia* were observed throughout the year from 2006-2011 with maximum cell densities exceeding 1,000,000 cells L^{-1}.

Pseudo-nitzschia: Scapa

Pseudo-nitzschia cells increase in abundance during the spring bloom at the Scapa monitoring site. Higher cell densities were observed in the early part of the year and in the summer months. A total of six species have been recorded using electron microscopy; *P. americana*, *P. australis*, *P. fraudulenta*, *P. pungens* and *P.* cf. *pseudodelicatissima*. The highest cell densities of *Pseudo-nitzschia* (1,000,000 cells L^{-1}) were observed at this site in 2006 in the aftermath of an extensive *Karenia mikimotoi* bloom. This species was identified using TEM as *P. plurisecta*.

Pseudo-nitzschia: Scalloway

In contrast to Loch Ewe and Scapa *Pseudo-nitzschia* does not constitute a major part of the spring bloom community at the Scalloway monitoring site. High cell densities (> 1,000,000 cells L^{-1}) observed during the summer months have been identified as *P. subpacificia*. To date, Scalloway harbour is the only site in Scotland where blooms of this *Pseudo-nitzschia* species have been observed. An increase in *Pseudo-nitzschia* abundance can be observed between 2008 and 2012.

Pseudo-nitzschia: Stonehaven

Pseudo-nitzschia comprises a large part of the spring bloom population at this site since monitoring began. This was particularly so in 2007. To date seven species of *Pseudo-nitzschia* have been observed at this site; *P. australis*, *P* cf. *delicatissima*, *P. pungens*, *P*. cf. *pseudodelicatissima*, *P. plurisecta*, *P. subpacifica* and *P*. *seriata* (Bresnan et al., 2015b) with lower cell abundances observed in late summer/early autumn compared to other sites. Higher abundances of *Pseudo-nitzschia* (>500,000 cells L^{-1}) throughout the summer months can be observed from 2005.

9.12 Plots - *Pseudo-nitzschia*

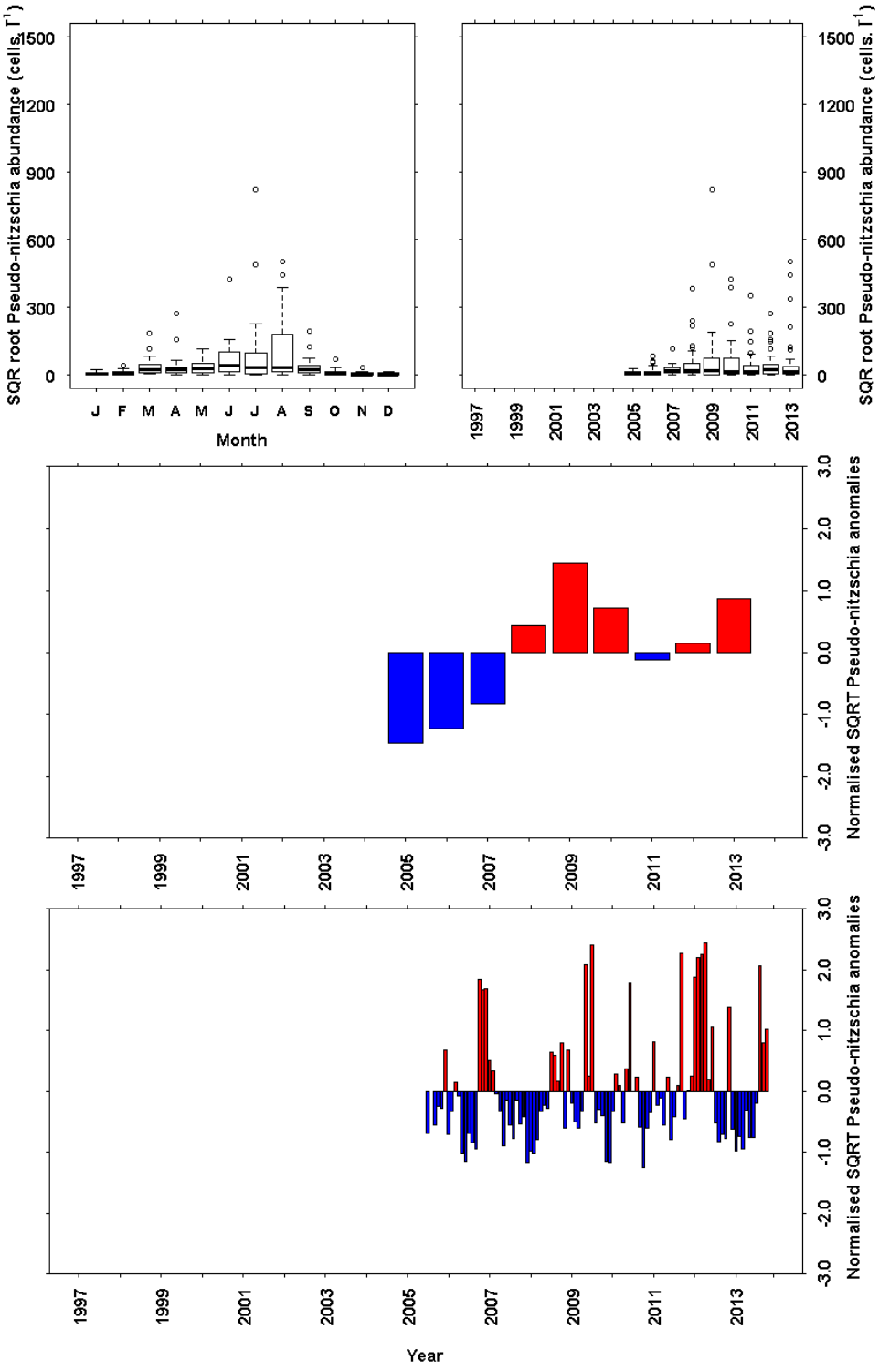

Figure 9.26 *Pseudo-nitzschia* abundance (cells L^{-1}) from the long term monitoring site at Millport. SQRT transformed data has been plotted. a) Monthly boxplot of *Pseudo-nitzschia* abundance. b) Annual boxplot of *Pseudo-nitzschia* abundance. c) Annual mean anomaly time series d) Monthly mean anomaly time series. Sampling for harmful species began in 2005. The full data set was used as the base period for the anomaly calculations.

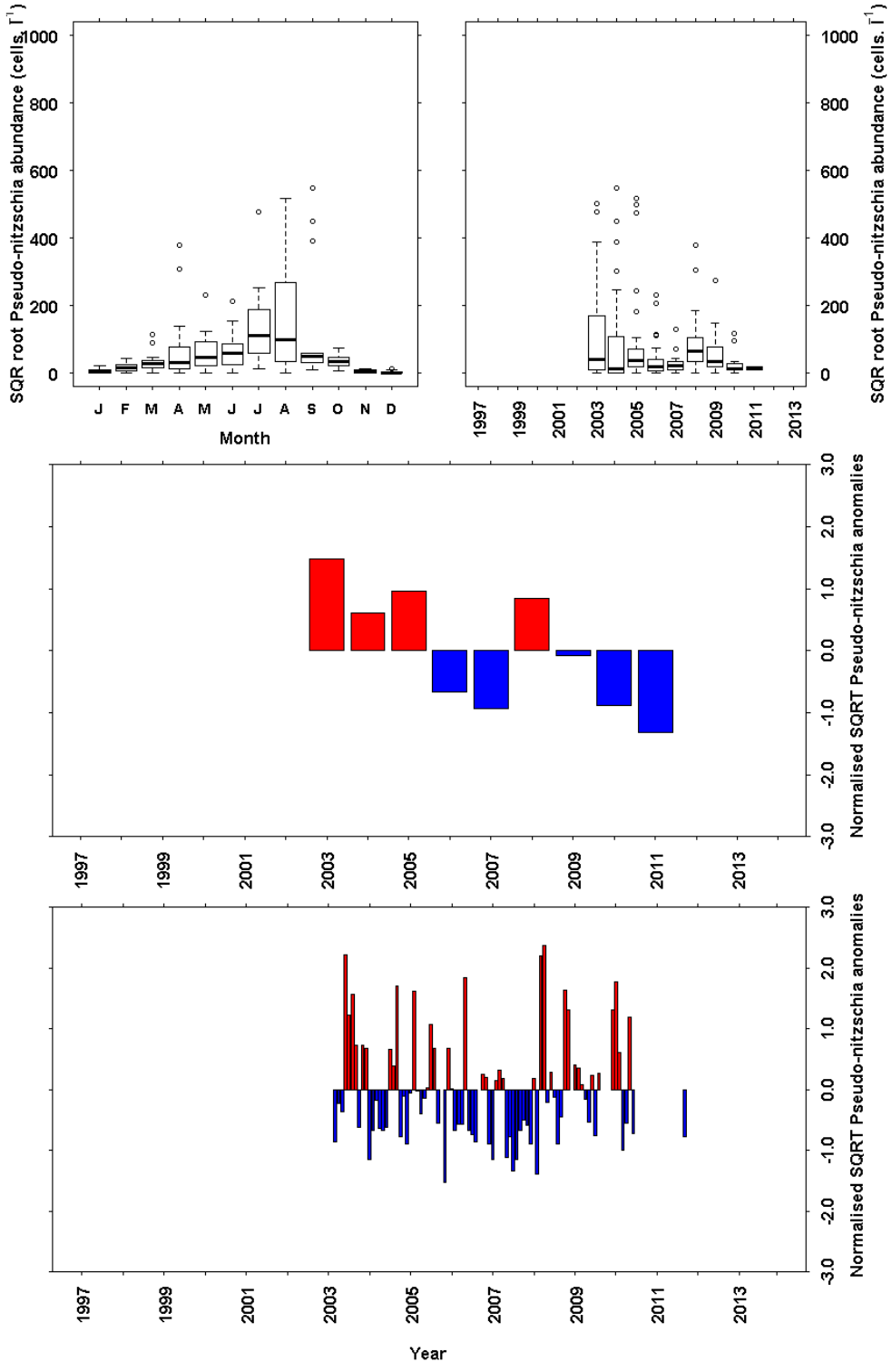

Figure 9.27 *Pseudo-nitzschia* abundance (cells L^{-1}) from the long term monitoring site at Loch Maddy. SQRT transformed data has been plotted. a) Monthly boxplot of *Pseudo-nitzschia* abundance. b) Annual boxplot of *Pseudo-nitzschia* abundance. c) Annual mean anomaly time series d) Monthly mean anomaly time series. Sampling for harmful species began in 2003. The full data set was used as the base period for the anomaly calculations.

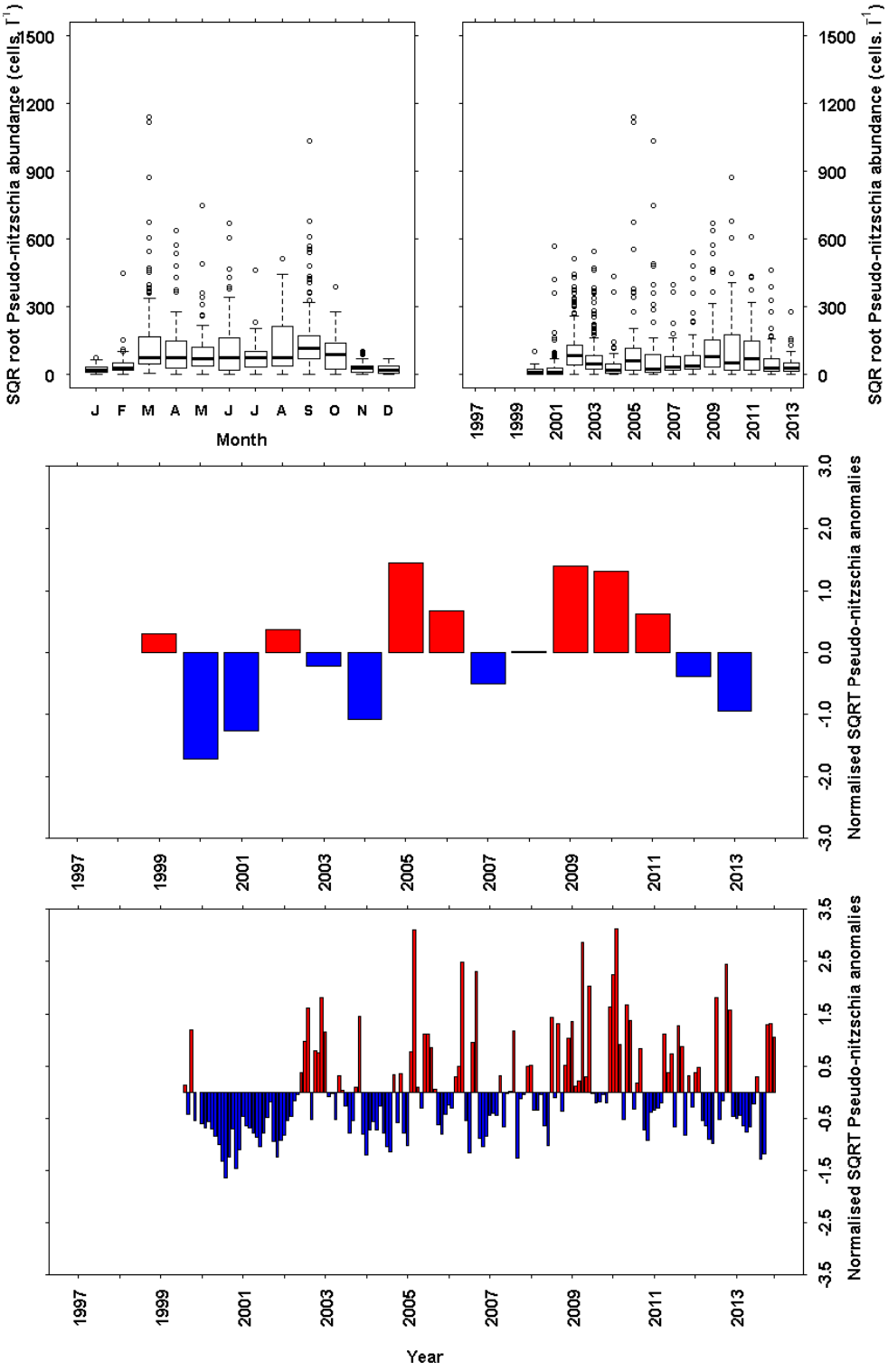

Figure 9.28 *Pseudo-nitzschia* abundance (cells L^{-1}) from the long term monitoring site at Loch Ewe. SQRT transformed data has been plotted. a) Monthly boxplot of *Pseudo-nitzschia* abundance. b) Annual boxplot of *Pseudo-nitzschia* abundance. c) Annual mean anomaly time series d) Monthly mean anomaly time series. Sampling for harmful species began in 2000. The full data set was used as the base period for the anomaly calculations.

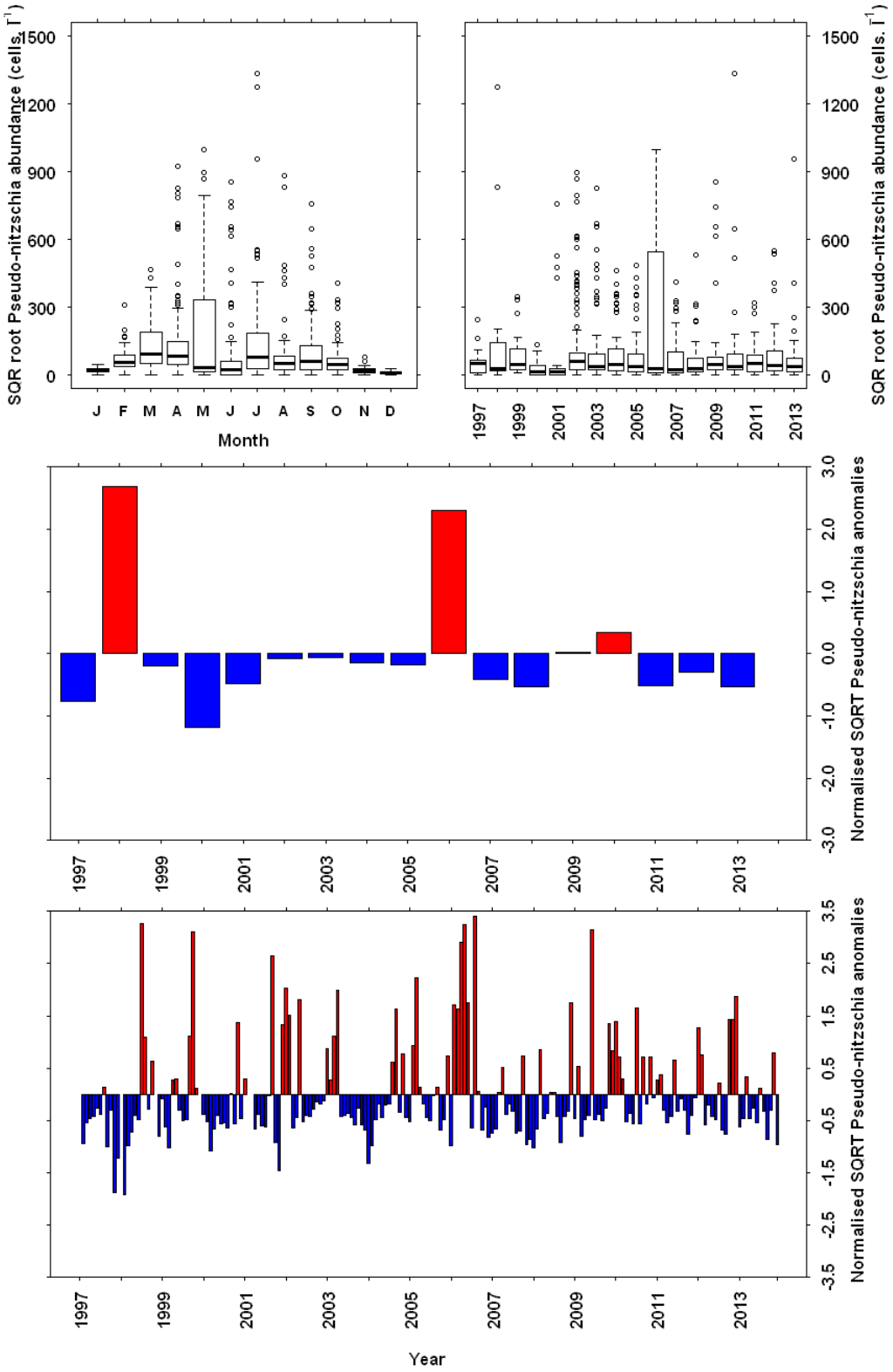

Figure 9.29 *Pseudo-nitzschia* abundance (cells L^{-1}) from the long term monitoring site at Scapa. SQRT transformed data has been plotted. a) Monthly boxplot of *Pseudo-nitzschia* abundance. b) Annual boxplot of *Pseudo-nitzschia* abundance. c) Annual mean anomaly time series d) Monthly mean anomaly time series. Sampling for harmful species began in 1997. The full data set was used as the base period for the anomaly calculations.

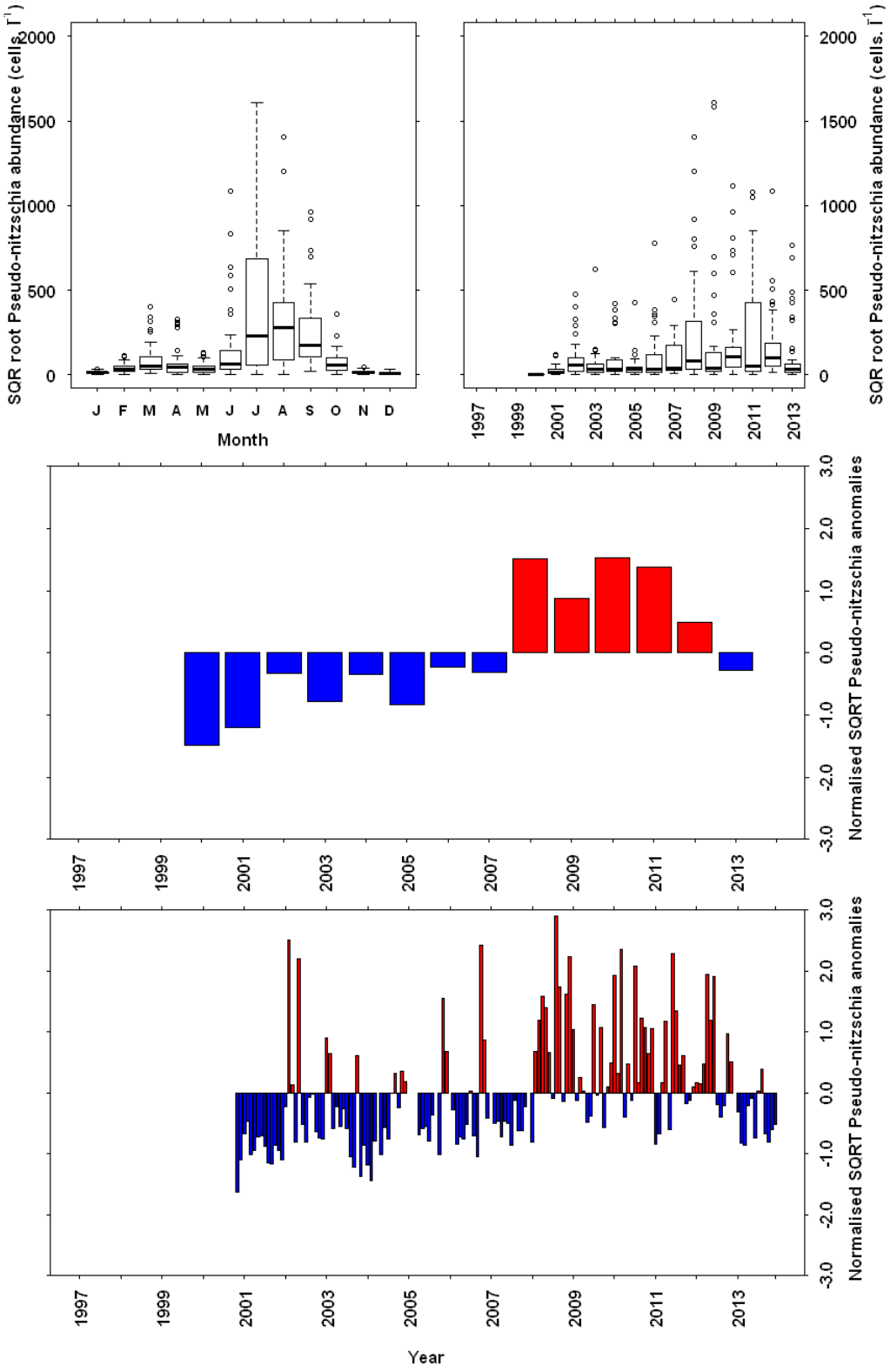

Figure 9.30 *Pseudo-nitzschia* abundance (cells L^{-1}) from the long term monitoring site at Scalloway. SQRT transformed data has been plotted. a) Monthly boxplot of *Pseudo-nitzschia* abundance. b) Annual boxplot of *Pseudo-nitzschia* abundance. c) Annual mean anomaly time series d) Monthly mean anomaly time series. Sampling for harmful species began in 2000. The full data set was used as the base period for the anomaly calculations.

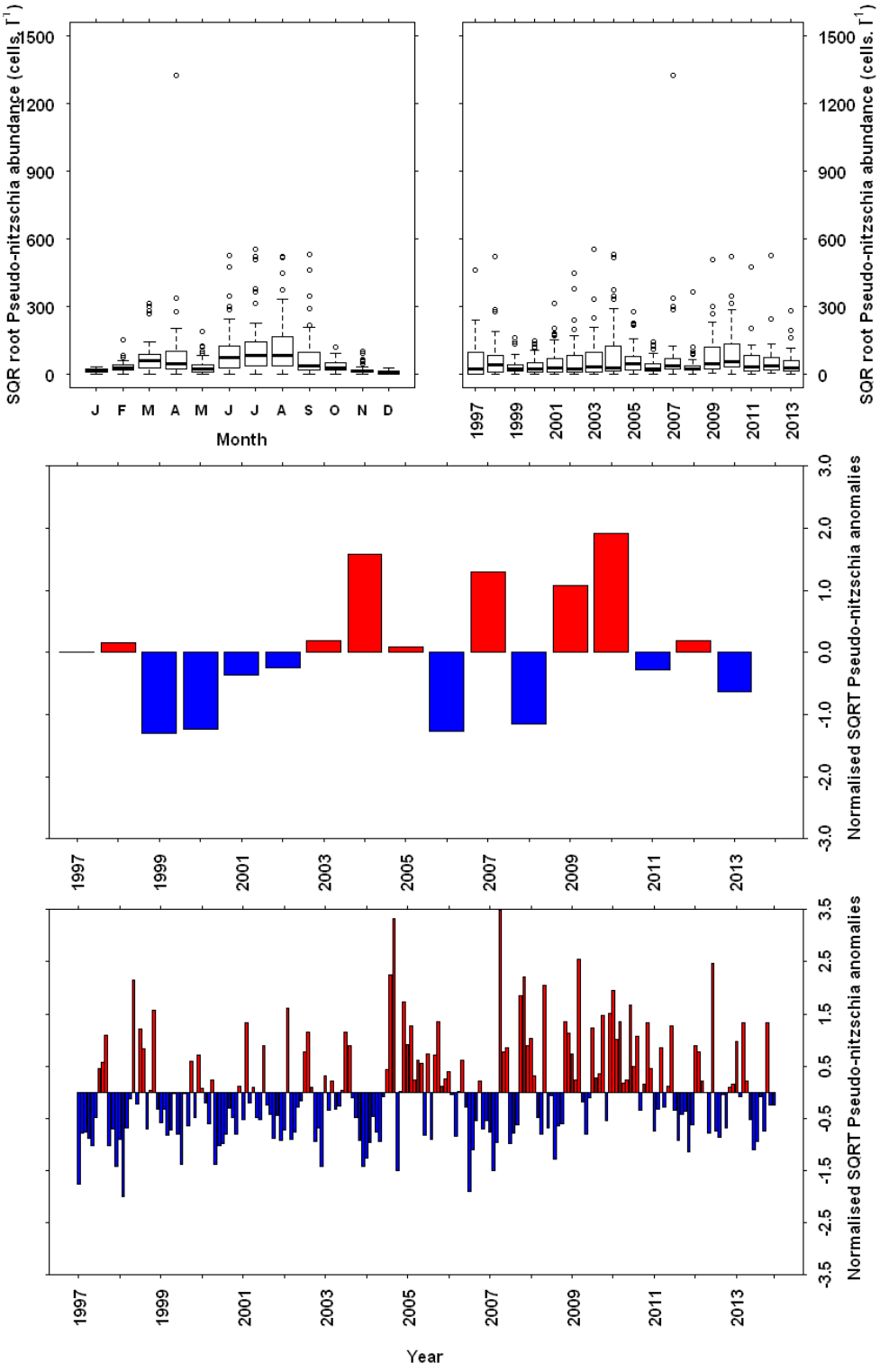

Figure 9.31 *Pseudo-nitzschia* abundance (cells L^{-1}) from the long term monitoring site at Stonehaven. SQRT transformed data has been plotted. a) Monthly boxplot of *Pseudo-nitzschia* abundance. b) Annual boxplot of *Pseudo-nitzschia* abundance. c) Annual mean anomaly time series d) Monthly mean anomaly time series. Sampling for harmful species began in 1997. The full data set was used as the base period for the anomaly calculations.

9.13 Summary – Phytoplankton

- The phytoplankton community in Scottish coastal waters shows a high degree of seasonal and interannual variability.
- Low diatom cell densities were observed from 2000-2004 at most sites. At the Stonehaven site this is coincident with a period of low chlorophyll and positive silicate (DSi) anomalies.
- *Alexandrium* cell densities show an increase in abundance at two west coast sites.
- *Dinophysis* shows considerable regional variability in abundance increasing at Millport, decreasing at Scapa and variable at other sites.
- *Pseudo-nitzschia* cells were present in almost every sample analysed in the programme. It was less abundant in Millport and followed a different seasonal pattern in Scalloway where it was not a component of the spring diatom bloom.

9.14 References - Phytoplankton

Alvarez-Fernandez, S., Lindeboom, H., Meesters, E. (2012) Temporal changes in plankton of the North Sea: community shifts and environmental drivers. Marine Ecology Progress Series, 462, 21-38.

Ayres, P.A. and Cullum, M. (1978) Paralytic shellfish poisoning: An account of investigations into mussel toxicity 1968-77. Fisheries Research Technical Report, MAFF Directorate of Fisheries Research, Lowestoft, 40.

Beaugrand G., Harlay X., Edwards M. (2014) Detecting plankton shifts in the North Sea: a new abrupt ecosystem shift between 1996 and 2003. Marine Ecology Progress Series, 502, 85-104.

Bresnan, E., Cook, K., Hughes, S., Hay, S., Smith, K., Walsham, P. L. Webster. (2015a) Seasonality of the plankton community at an east and west coast monitoring site in Scottish waters. Journal of Sea Research, 105:16-29.

Bresnan, E., Davidson, K., Edwards, M., Fernand, L., Gowen, R., Hall, A., Kennington, K., McKinney, A., Milligan, S., Raine, R., Silke, J. (2013). Harmful Algal Bloom Report Card. MCCIP Science Review 2013, 236-243, doi:10.14465/2013.arc24.236-243.

Bresnan, E., Fryer, R., Hart, M., Percy, P. (2005) Correlation between algal presence in water and toxin presence in shellfish. Fisheries Research Services Contract Report 04/05.

Bresnan, E., Hay, S., Hughes, S.L., Fraser, S., Rasmussen, J., Webster, L., Slesser, G., Dunn, J., Heath, M.R. (2009) Seasonal and interannual variation in the phytoplankton community in the north east of Scotland. Journal of Sea Research, 61, 17-25.

Bresnan, E., Kraberg, A., Fraser, S., Amorim, A.–L., Janisch, S., Wiltshire, K.H. (2015b) A comparison of *Pseudo-nitzschia* diversity and seasonality at two long-term monitoring sites in the North Sea with new records of *P. multiseries* and *P. americana* at Helgoland Roads. Helgoland Marine Research, 69, 193 – 204.

Bresnan, E., Turrell, E. A., Fraser S. (2008) Monitoring PSP and *Alexandrium* hotspots in Scottish waters. In: Proceedings of the 12th International Conference on Harmful Algae. (Moestrup, Ø., Doucette, G., Enevoldson, H., Godhe, A., Hallegraeff, G., Luckas, B., Lundholm, N., Lewis, J., Rengefors, K., Sellner, K., Steidinger, K., Tester, P., Zingone, A., eds), Intergovernmental Oceanographic Commission of UNESCO, Copenhagen, 51-54.

Brown, L. and Bresnan, E. (2008) Seasonal occurrence of *Pseudo-nitzschia* species in the west coast and Shetland Isles, Scotland. In: Proceedings of the 12th International Conference on Harmful Algae. (Moestrup, Ø., Doucette, G., Enevoldson, H., Godhe, A., Hallegraeff, G., Luckas, B., Lundholm, N., Lewis, J., Rengefors, K., Sellner, K., Steidinger, K., Tester, P., Zingone, A., eds), Intergovernmental Oceanographic Commission of UNESCO, Copenhagen, 165 - 167.

Brown, L., Bresnan, E., Graham, J., Lacaze, J.P., Turrell, E., Collins, C. (2011) Distribution, diversity and toxin composition of the genus *Alexandrium* (Dinophyceae) in Scottish waters. European Journal of Phycology, 45(4), 375-393.

Chavez, F.P., Messie, M., Pennington, J.T. (2011) Marine Primary Production in Relation to Climate Variability and Change. Annual Review of Marine Science, 3, 227-260.

Collins, C., Graham, J., Brown, L., Bresnan, E., Lacaze, J-P., Turrell, E. A. (2009a) Identification and toxicity of *Alexandrium tamarense* (Dinophyceae) in Scottish waters. Journal of Phycology, 45, 692-703.

Collins, C., Graham, J., Brown, L., Bresnan, E., Lacaze, J-P., Turrell, E. A. (2009b) Evaluation of Quantitative Real-Time TaqMan PCRs for detection and quantification of *Alexandrium* species in

Scottish waters. 7th International Conference on Molluscan Shellfish Safety, Nantes, France. http://symposcience.lyon.cemagref.fr/exl-doc/colloque/ART-00002534.pdf.

Cushing, D.H. (1989) A difference in structure between ecosystems in strongly stratified waters and in those that are only weakly stratified. Journal of Plankton Research, 11, 1 – 13.

Davidson, K. and Bresnan, E. (2009) Shellfish toxicity in UK waters: a threat to human health? Environmental Health, 8 (Suppl 1), S12.

Davidson, K., Miller, P., Wilding, T.A., Shutler, J., Bresnan, E., Kennington, K., Swan, S. (2009) A large and prolonged bloom of *Karenia mikimotoi* in Scottish waters in 2006. Harmful Algae, 8(2), 349-361.

DEFRA (2010). EU Marine Strategy Framework Directive. http://jncc.defra.gov.uk/page-5193.

Devlin, M., Best, M., Coates, D., Bresnan, E., O'Boyle, S., Park, R., Silke, J., Cusack, C., Skeats, J. (2007) Establishing boundary classes for the classification of UK marine waters using phytoplankton communities. Marine Pollution Bulletin, 55, 1 - 6.

Devlin, M.J., Best, M., Bresnan, E., Baptie, M. (2013) Water Framework Directive: The development and status of phytoplankton tools for ecological assessment of coastal and transitional waters. United Kingdom. Update Report to UK Technical Advisory Group for the Environment Agency (May 2013).

Edwards, M., Beaugrand, G., Reid, P.C., Rowden, A.A., Jones, M.B. (2002) Ocean climate anomalies and the ecology of the North Sea. Marine Ecology-Progress Series, 239, 1-10.

Edwards, M., Beaugrand, G., Helaouët, P., Alheit, J., Coombs, S. (2013) Marine ecosystem response to the Atlantic Multidecadal Oscillation. PLoS ONE, 8(2), e57212.

Edwards, M., Johns, D.G., Leterme, S.C., Svendsen, E., Richardson, A.J. (2006) Regional climate change and harmful algal blooms in the northeast Atlantic. Limnology and Oceanography, 51(2), 820-829.

Farrell, H., Gentien, P., Fernand, L., Lunven, M., Reguera, B., Gonzalez-Gil, S., Raine, R. (2012) Scales characterising a high density thin layer of *Dinophysis acuta* Ehrenberg and its transport within a coastal jet. Harmful Algae, 15, 36-46.

Fehling J., Green D.H., Davidson K., Bolch C.J., Bates S.S. (2004) Domoic acid production by *Pseudo-nitzschia seriata* (Bacillariophyceae) in Scottish waters. Journal of Phycology, 40 (4), 622-630.

Fehling, J., Davidson, K., Bates, S.S. (2005) Growth dynamics of non-toxic *Pseudo-nitzschia delicatissima* and toxic *P. seriata* (Bacillariophyceae) under simulated spring and summer photoperiods. Harmful Algae, 4(4), 763-769.

Fehling, J., Davidson, K., Bolch, C.J., Tett, P. (2006) Seasonality of *Pseudo-nitzschia* spp. (Bacillariophyceae) in western Scottish waters. Marine Ecology Progress Series, 323, 91-105.

Fehling, J., Davidson, K., Bolch, C.J.S., Brand, T.D., Narayanaswamy, B.E. (2012) The relationship between phytoplankton distribution and water column characteristics in north west European shelf sea waters. Plos One, 7(3), e34098.

Fraga, S., Sampedro, N., Larsen, J., Moestrup, Ø, Calado, AJ. (2015) Arguments against the proposal 2302 by John & al. to reject the name *Gonyaulax catenella* (*Alexandrium catenella*) Taxon, 64 (3), 634-635.

Gamble, J.C., Davies, J.M., and Steele, J.H. (1977) Loch Ewe Bag Experiment, 1974. Bulletin of Marine Science, 27(1), 146-175.

Gallacher, S., Howard, G., Hess, P., MacDonald, E., Kelly, M.C., Bates, L.A., Brown, N., MacKenzie, M., Gillibrand, P., Turrell, W.L. (2001) The occurrence of amnesic shellfish poisons in shellfish from Scottish waters. In: Harmful Algal Blooms 2000, UNESCO, Paris, p 30-33.

Gomez, F. (2012) A quantitative review of the lifestyle, habitat and trophic diversity of dinoflagellates (Dinoflagellata, Alveolata). Systematics and Biodiversity, 10, 267 – 275.

Gowen, R.J., Tett, P., Jones, K.J. (1983) The hydrography and phytoplankton ecology of Loch Ardbhair: A small sea loch on the west coast of Scotland. Journal of Experimental Marine Biology and Ecology, 71, 1 – 16.

Gowen, R.J., Tett, P., Bresnan, E., Davidson, K., McKinney, A., Harrison, P.J., Milligan, S., Mills, D.K., Silke, J., Crooks, A.M. (2012) Anthropogenic nutrient enrichment and blooms of harmful phytoplankton. Oceanography and Marine Biology: An Annual Review, 50, 65–126.

Hall, A.J. and Frame, E. (2010) Evidence of domoic acid exposure in harbour seals from Scotland: A potential factor in the decline in abundance? Harmful Algae, 9(5), 489-493.

Hart, M.C., Green, D.H., Bresnan, E., Bolch, C.J. (2007) Large subunit ribosomal RNA gene variation and sequence heterogeneity of *Dinophysis* species from Scottish coastal waters. Harmful Algae, 6, 271 – 287.

Herdman, W.A. and Riddell, W. (1911) The plankton of the west coast of Scotland in relation to that of the Irish Sea. Transactions of the Biological Society of Liverpool, XXV, 132 – 185.

Herdman, W. A. and Riddell, W. (1912) The plankton of the west coast of Scotland in relation to that of the Irish Sea – part II. Transactions of the Biological Society of Liverpool, XXVI, 225 – 245.

Herdman, W. A. and Riddell, W. (1913) The plankton of the west coast of Scotland in relation to that of the Irish Sea – part II. Transactions of the Biological Society of Liverpool, XXVI, 344 – 371.

Hinder, S.L., Hays, G.C., Edwards, M., Roberts, E.C., Walne, A.W., Gravenor, M.B. (2012) Changes in marine dinoflagellate and diatom abundance under climate change. Nature Climate Change, 2(4), 271-275.

Jensen, S.-K., Lacaze, J.-P., Hermann, G., Kershaw, J., Brownlow, A., Turner, A., Hall, A. (2015) Detection and effects of harmful algal toxins in Scottish harbour seals and potential links to population decline. Toxicon, 97, 1 – 14.

John, U., Littaker, R.W., Montressor, M., Murray, S., Brosnahan, M.L., Anderson, D. (2014) Formal Revision of the *Alexandrium tamarense* Species Complex (Dinophyceae) Taxonomy: The Introduction of Five Species with Emphasis on Molecular-based (rDNA) Classification. Protist, 165, 779 – 804.

Joint, I.R., Pomroy, A.J., Robinson, G.A., Morris, R.J., McCArtney, M.I. (1987) Morphological changes in *Skeletonema costatum* (Bacillariophyceae) during a spring bloom in a marine ecosystem enclosure. British Phycological Journal, 22, 119 – 124.

Jones, K.J., Gowen, R.J., Tett, P. (1984) Water column structure and summer phytoplankton distribution in the Sound of Jura, Scotland. Journal of Experimental Marine Biology and Ecology, 78, 269 – 289.

Kelly, M. and Fraser, S. (1999) Toxic algal monitoring in Scotland 1988. Fisheries Research Services Internal Report, 8/99, 32pp. http://www.gov.scot/uploads/documents/coll0899.pdf.

Lilly, E.L., Halanych, K.M., Anderson, D.M. (2007) Species boundaries and global biogeography of the *Alexandrium tamarense* complex (Dinophyceae). Journal of Phycology, 43,1329-1338.

Medlin, L.K., Lange, M., Wellbrock, U., Donner, G., Elbrachter, M., Hummert, C., Luckas, B. (1998) Sequence comparisons link toxic European isolates of *Alexandrium tamarense* from the Orkney Islands to toxic North American stocks. European Journal of Protistology, 34, 329-335.

Morris, R.J. (1984) Studies of a spring phytoplankton bloom in an enclosed experimental ecosystem II. Changes in the component fatty acids and sterols. Journal of Experimental Marine Biology and Ecology, 75, 59 – 70.

Raine, R., McDermott, G., Silke, J., Lyons, K., Nolan, G., Cusack, C. (2010) A simple short range model for the prediction of harmful algal events in the bays of southwestern Ireland. Journal of Marine Systems, 83(3-4), 150-157.

Savidge, G. and Lennon, H.J. (1987) Hydrography and phytoplankton distributions in north-west Scottish waters. Continental Shelf Research, 7, 45 -66.

Scherer, C., Gowen, R.J., Tett, P., Atkinson, A., Baptie, M., Best, M., Bresnan, E., Cook, K., Forster, R., Keeble, S., McQuatters-Gollop, A. (2015) Development of a UK integrated plankton monitoring programme. Report to DEFRA. http://randd.defra.gov.uk/Document.aspx?Document=13580_ME5312LifeformFinalReport.pdf.

Siemering B, Bresnan E, Painter SC, Daniels CJ, Inall M, Davidson K (2016) Phytoplankton Distribution in Relation to Environmental Drivers on the North West European Shelf Sea. PLoS ONE 11(10): e0164482. doi:10.1371/journal.pone.0164482.

Stern R., Amorim A., Bresnan E. (2014) Diversity and plastid types in *Dinophysis acuminata* complex (Dinophyceae) in Scottish waters. Harmful Algae, 39, 223 – 231.

Tett P. (2013) Net Microplankton Production in Loch Creran and its Approaches in September 2013. Scottish Association for Marine Science Report, 39pp.

Tett, P. and Wallis, A. (1978) The general annual cycle of chlorophyll standing crop in Loch Creran. Journal of Ecology, 66, 227 – 239.

Throndsen, J. (1978) Preservation and storage. In: Sournia A. (Ed), Phytoplankton Manual. UNESCO. Paris, 69-74.

Touzet, N., Davidson, K., Pete, R., Flanagan, K., McCoy, G.R., Amzil, Z., Maher, M., Chapelle, A., Raine, R. (2010) Co-Occurrence of the West European (Gr.III) and North American (Gr.I) Ribotypes of *Alexandrium tamarense* (Dinophyceae) in Shetland, Scotland. Protist, 161(3), 370- 384.

Utermöhl, H. (1958) Zur Vervollkommnung der quantitativen Phytoplanktonmethodik. Mitteilungen Internationale Vereinigung für Theoretische und Angewandte Limnologie, 9, 1 – 38.

Whyte, C. (2012) An Investigation into changes in the phytoplankton community in Loch Creran, a Scottish sealoch. Ph.D. thesis, Napier University, 360pp.

Whyte, C., Swann, S., Davidson, K. (2014) Changing wind patterns linked to unusually high *Dinophysis* blooms around the Shetland Islands, Scotland. Harmful Algae, 39, 365 – 373.

Wiltshire, K.H., Malzahn, A.M., Wirtz, K., Greve, W., Janisch, S., Mangelsdorf, P., Manly, B.F.J., Boersma, M. (2008) Resilience of North Sea phytoplankton spring bloom dynamics: An analysis of long-term data at Helgoland Roads. Limnology and Oceanography, 53(4), 1294-1302.

10. Chlorophyll 'a'

10.1 Introduction

Phytoplankton contain a range of pigments in their cells. These pigments have a variety of functions. All photosynthetic phytoplankton have the pigment chlorophyll 'a' in a structure in their cells called the chloroplast. This pigment captures light energy (electrons) which they use to fuel the photosynthetic reaction which converts CO_2 and H_2O to carbohydrates and O_2. Some pigments (assessory chlorophylls, *b*, c_1, c_2 etc.) help capture photons during low light conditions while others (such as carotenoids) have a photoprotective role during periods of high light intensity (Hall and Rao 2011). Selected pigments can be used to identify different phytoplankton groups. Peridinin can be used to estimate dinoflagellate biomass while gyroxanthin is a pigment that is unique to the dinoflagellate genus *Karenia* (Brand et al., 2012). Standard monitoring methods such as fluorometry and spectrophotometry measure chlorophyll 'a'. For a more detailed breakdown of the pigment profile of the phytoplankton community high performance liquid chromatography (HPLC) methodology is used.

Chlorophyll 'a' is an important measurement used to assess the state of the ecosystem as it can provide a bulk estimate of the biomass that is available in the lower parts of the food web (Cloern and Jassby 2010). As phytoplankton come in a variety of shapes and sizes chlorophyll 'a' concentration in the water column is used as an estimate of phytoplankton biomass although the chlorophyll 'a' content per cell can vary depending on the environmental conditions (Kruskopf and Flynn 2006). It has become a standard biological/oceanographic measurement and is used to assess the performance of ecosystem models. Satellites, fixed point sensors as well as mobile operated equipment such as gliders can measure fluorescence in the water column which can be calibrated against standard chlorophyll 'a' measurements to give highly resolved temporal and spatial data.

In some instances (Gowen et al., 2012) anthropogenic nutrient enrichment can result in increased phytoplankton cell densities with an associated increase in chlorophyll 'a' concentration that can be sustained over a period of time. As a result, water quality objectives such as the OSPAR eutrophication assessment, Water Framework Directive and Marine Strategy Framework Directive have threshold concentrations of chlorophyll 'a' above which 'surveillance' of the state of the ecosystem is instigated.

Chlorophyll 'a' is has been measured at the Stonehaven monitoring site since 1997 and the Loch Ewe monitoring site since 2002. These data from are being used to assess the status of the phytoplankton community to fulfil the requirements of the WFD and MSFD.

10.2 Methods

Sample Collection and Storage

Samples for pigment analysis are collected from the Stonehaven monitoring sites using a 10 m integrated tube sampler. At Loch Ewe water samples for pigment analysis were collected using a water bottles only at 5m depth from April 2003 – Dec

2007 and 30 m from April 2003 – Dec 2004. From Jan 2008 – Jun 2011 both 5m water bottle and 10 m integrated tube samples were collected and from June 2011 10 m integrated tube samples only were collected. Depending on the time of year a 500 mL to 2 L aliquot is filtered through a GF/F filter, frozen and stored at -80^{o}C until analysis. Chlorophyll 'a' has been analysed using the fluorometric method of Arar and Collins (1992) which included an acidification step to 'correct' for the presence of phaeopigments. Following a review of analysis procedure (Smith et al., 2007) little difference was found between corrected and uncorrected chlorophyll 'a' (r^2 = 0.999). As a result uncorrected data has been reported since 2007.

Data has been analysed using a Turner AU fluorometer and data is stored in a LIMS database system. This protocol received UKAS accreditation in 2007 and follows the associated data quality procedures.

10.3 Results

Chlorophyll 'a': Loch Ewe

Chlorophyll 'a' concentrations in Loch Ewe follow a typical seasonal pattern observed in temperate latitudes. Concentrations are low during the winter months but increase with day length during spring. Chlorophyll 'a' concentrations reach a maximum in April. This is associated with an increase in the growth of diatoms, a natural event known as the spring bloom. Chlorophyll 'a' concentrations are lower during the summer months; the period when diatom density is less and dinoflagellates dominate. Concentrations peak again during late summer/early autumn when diatoms increase in abundance. Interannual variation can be observed in the chlorophyll 'a' concentrations at Loch Ewe.

Chlorophyll 'a': Stonehaven

The seasonality of chlorophyll 'a' at the Stonehaven monitoring site differs from that observed in Loch Ewe. The increase in chlorophyll 'a' associated with the spring bloom occurs up to one month later at Stonehaven and the late summer/early autumn increase in chlorophyll 'a' is infrequently observed. One exception to this is the period from 2000-2004 when the maximum chlorophyll 'a' concentrations were at times observed during autumn. Considerable interannual variation in the timing and intensity of the spring bloom has been observed at Stonehaven.

10.4 Summary- Chlorophyll 'a'

- Chlorophyll 'a' concentrations follow a different seasonal pattern in Loch Ewe and Stonehaven with chlorophyll 'a' increasing in the water about one month earlier in Loch Ewe than in Stonehaven.
- Higher concentrations of chlorophyll 'a' are observed in the autumn in Loch Ewe than in Stonehaven. This is associated with higher diatom cell densities.
- A period of low chlorophyll concentrations were observed during the spring at Stonehaven between 2000-2004. This coincides with a period of low diatom cell densities.

- During some years in this period highest annual chlorophyll ‘a’ concentrations at Stonehaven were observed during the late summer/early autumn.

10.5 References – Chlorophyll 'a'

Arar, E.J. and Collins, G.B. (1992) Method 445.0: In vitro determination of chlorophyll *a* and phaeophytin a in marine and freshwater phytoplankton by fluorescence. USEPA, Ohio EPA. 14pp.

Hall, D. and Rao, K. (2011) Photosynthesis, 6th Edition, Cambridge University Press.

Brand, L., Campbell, L., Bresnan, E. (2012) Karenia: The biology and ecology of a toxic genus. Harmful Algae, 14, 156 – 178.

Cloern, J.E. and Jassby, A.D. (2010) Patterns and Scales of Phytoplankton Variability in Estuarine-Coastal Ecosystems. Estuaries and Coasts, 33, 230 - 241.

Kruskopf, M. and Flynn, K. (2006) Chlorophyll content and fluorescence responses cannot be used to gauge reliably phytoplankton biomass, nutrient status or growth rate. New Phytologist, 169, 525–536.

Gowen, R.J., Tett, P., Bresnan, E., Davidson, K., McKinney, A., Harrison, PJ., Milligan, S., Mills, D.K., Silke, J., Crooks, A.M. (2012) Anthropogenic nutrient enrichment and blooms of harmful phytoplankton. Oceanography and Marine Biology: An Annual Review, 50, 65 -126.

Smith, K., Webster, L., Bresnan, E., Hay, S.J., Fraser, S., Moffat C. (2007) A review of analytical methodology used to determine phytoplankton pigments in the marine environment and the development of an analytical method to determine uncorrected chlorophyll 'a' and phaeophytin in marine phytoplankton. Fisheries Research Services Internal Report No 03/07, 25pp. http://134.19.161.249/Uploads/Documents/IR0307.pdf.

10.6 Plots – Chlorophyll ‘a’

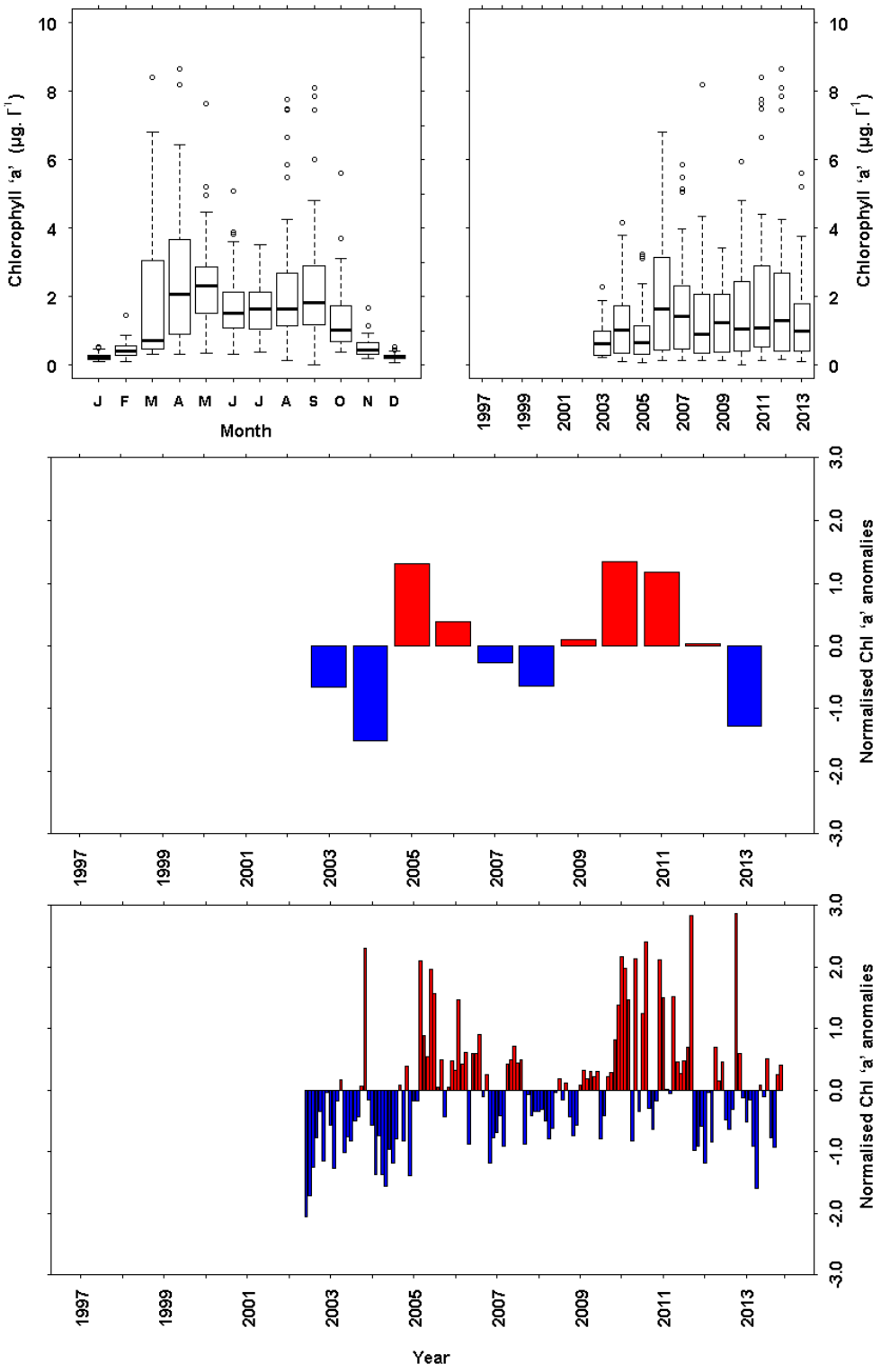

Figure 10.1. Chlorophyll ‘a’ concentration (µg L^{-1}) from the long term monitoring site at Loch Ewe. a) Monthly boxplot of chlorophyll ‘a’ concentration. b) Annual boxplot of chlorophyll ‘a’ concentration. c) Annual mean anomaly time series d) Monthly mean anomaly time series. Sampling for chlorophyll ‘a’ began in 2002. The full data set was used as the base period for the anomaly calculations.

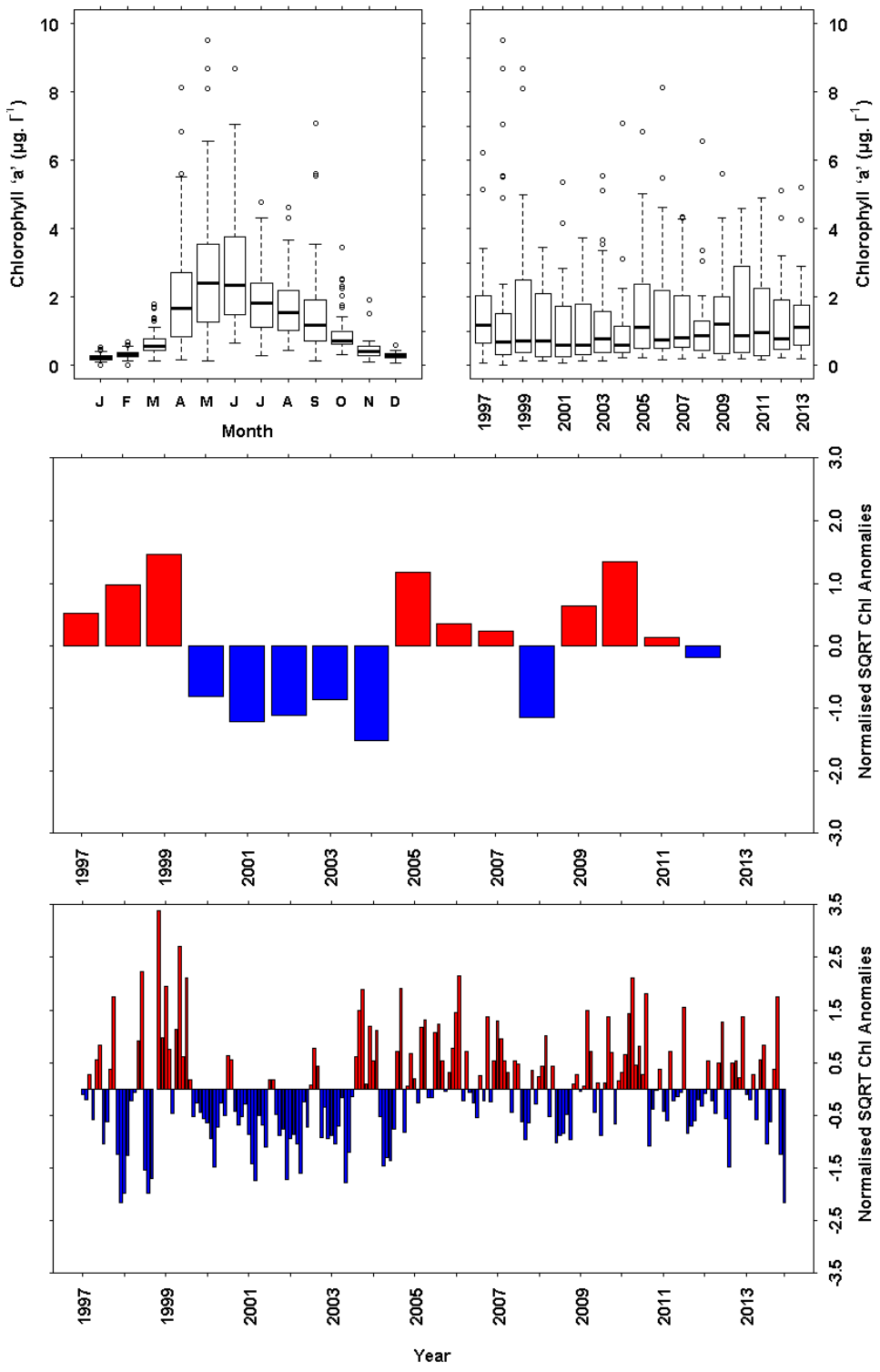

Figure 10.2 Chlorophyll 'a' concentration (µg L^{-1}) from the long term monitoring site at Stonehaven. a) Monthly boxplot of chlorophyll 'a' concentration. b) Annual boxplot of chlorophyll 'a' concentration. c) Annual mean anomaly time series d) Monthly mean anomaly time series. Sampling for chlorophyll 'a' began in 1997. The full data set was used as the base period for the anomaly calculations.

11. Algal Toxins

11.1 Introduction

Among the thousands of phytoplankton species currently described, a few dozen have the ability to produce toxic secondary metabolites (Hallegraeff, 1993); organic compounds non-essential for the basic metabolism and growth of the producing species (Tubaro and Hungerford, 2007) also known as algal toxins. When favourable environmental conditions are met, the abundance of toxin-producing phytoplankton can increase leading to the formation of what is termed a harmful algal bloom (HAB). Bivalve filter-feeding shellfish such as mussels, oysters, scallops and clams grazing on these phytoplankton species can accumulate algal toxins in their flesh especially in their digestive glands. Although the true effect of accumulated algal toxins on shellfish remains largely unknown, consumption of contaminated seafood by humans can result in poisoning, ranging from mild gastrointestinal discomfort and neurological issues to life-threatening heart and respiratory failures. Algal toxins can also accumulate in other marine species such as fish (anchovies, sardines), crustaceans (crabs, lobsters), birds, marine mammals (whales, sea lions) (Scholin et al., 2000). In Scottish waters, algal toxins have been recorded in the faeces and urine of harbour seals (Hall and Frame, 2010, Jensen et al., 2015). Thus, algal toxins can not only present a food safety hazard for seafood consumers but can also adversely impact marine wildlife.

In Scottish coastal waters, the most prevalent toxins can be grouped into four categories, identified by the human syndrome they may cause. These are:

- Paralytic shellfish poisoning (PSP) caused by saxitoxin (STX) and its analogues.
- Diarrhetic shellfish poisoning (DSP) caused by okadaic acid (OA) and its dinophysistoxins analogues (DTX-1, DTX-2 and DTX-3).
- Amnesic shellfish poisoning (ASP) caused by domoic acid (DA) and its analogues.
- Azaspiracid shellfish poisoning (AZP) caused by toxins from the azaspiracid (AZA) group.

Toxins belonging to the pectenotoxin (PTX) and yessotoxin (YTX) groups can also be regularly found in shellfish from UK waters, however, their oral toxicity to humans has yet to be fully confirmed. Together with the DSP and AZP toxin groups, they possess similar chemical properties which led them to be grouped under the “lipophilic marine biotoxins” terminology. The structures of these lipophilic toxins are presented in Figure 11.1.

The worldwide development of fin and shellfish aquaculture in coastal waters has led to a greater awareness of HABs and marine biotoxins (Hallegraeff, 2010). In the west and north of Scotland, salmon and shellfish aquaculture represent an increasingly important industry, helping to sustain economic growth in those rural and coastal communities. There is, therefore, a pressing requirement to monitor the plankton community to provide advice on the impacts of climate change, ocean acidification and eutrophication on the marine ecosystem and the development of

aquaculture, but also to meet the requirements of EU water quality directives (Bresnan et al., 2015).

Light microscopy is the current and most widely used technique to identify and enumerate phytoplankton in official control biotoxin monitoring (live bivalve molluscs) programmes. However, this technique does not provide information about the toxin content of a phytoplankton cell.

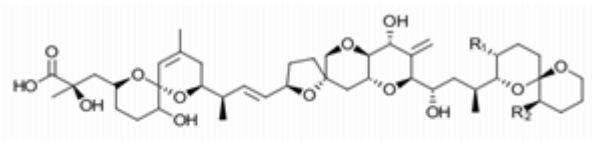

Toxin	R1	R2
Okadaic acid	CH_3	H
Dinophysistoxin-1	CH_3	CH_3
Dinophysistoxin-2	H	CH_3

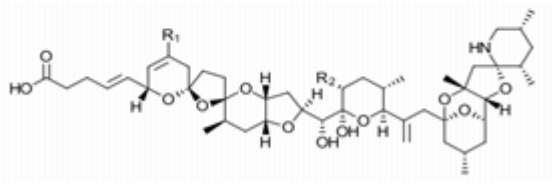

Toxin	R1	R2
Azaspiracid-1	H	CH_3
Azaspiracid-2	CH_3	CH_3
Azaspiracid-3	H	H

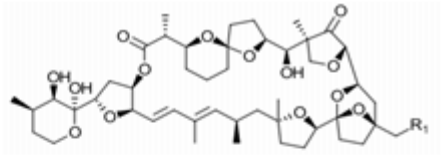

Toxin	R1
Pectenotoxin-1	OH
Pectenotoxin-2	H

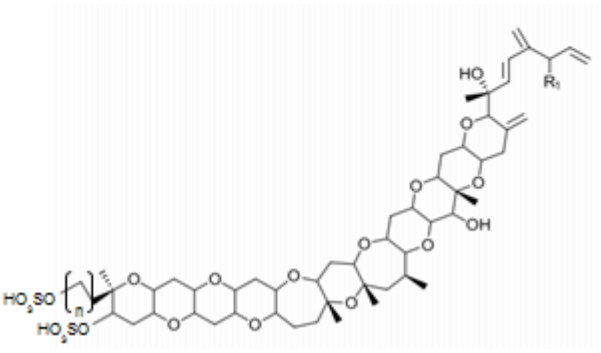

Toxin	R1	n
Yessotoxin	H	1
Homo Yessotoxin	H	2
45 OH Yessotoxin	OH	3
45 OH Homo Yessotoxin	OH	4

Figure 11.1 Structures of main marine lipophilic biotoxins

Extracellular algal toxins can be detected in the water column during blooms of toxin producing phytoplankton (Mackenzie et al., 1998). Monitoring the presence of extracellular algal toxins alongside light microscopy phytoplankton enumeration provides vital information on the presence (or absence) of toxin-producing algal species in the water column.

In 2005, Loch Ewe became the first site where dissolved algal toxins were monitored alongside potentially toxic phytoplankton species. Two more sites, Scapa and

Scalloway, were added in 2011. These three sites were chosen because of the history of algal toxin events in these areas.

The monitoring of lipophilic algal toxins carried out at MSS is based on a passive sampling technique called SPATT (Solid Phase Adsorption Toxin Tracking) developed originally in New Zealand (Mackenzie et al., 2004) which uses the capability of a synthetic resin to passively adsorb and retain the dissolved lipophilic toxins present in the water column. Laboratory and field studies of the SPATT technique have been carried out at various coastal locations around the world such as Ireland (Fux et al., 2009), Norway (Rundberget et al., 2009), Spain (Mallat et al., 2007), Australia (Takahashi et al., 2007) and Canada (Garnett et al., 2006). These studies have shown that a wide range of algal toxins, mainly lipophilic, could be detected by SPATT and demonstrated this technique had the potential to provide reliable, sensitive, time-integrated sampling to monitor the occurrence of toxic algal bloom events (MacKenzie, 2010).

11.2 Methods

Sample Collection and Storage

The SPATT sampler in use at MSS (Figure 11.2) consists of a 100 µm nylon mesh bag (Carbis Filtration, Stockton-On-Tees, UK) of relatively small dimensions (15 x 5 cm) filled with ca. 12 g of synthetic resin (Sepabeads® SP-700, Mitsubishi Chemical Corporation) which demonstrated during method development (Turrell et al., 2007) good adsorption capabilities towards diarrhetic shellfish poisoning (DSP) toxins and other lipophilic toxins such as yessotoxins (YTXs), pectenotoxins (PTXs) and azaspiracids (AZAs).

Figure 11.2 SPATT bag used by MSS for lipophilic toxins monitoring.

The SPATT bags were tagged for identification and closed half way with a non-releasable cable tie. A Holdon® Midi clip (Holdon® Systems, Båstad, Sweden) was used to seal the top of each bag, serving at the same time as anchor point. The SPATT bags prepared at MSS, along with a sample sheet, were placed into individually sealed Ziploc bags to prevent the resin drying, and sent to the sampling personnel in a polystyrene box with ice packs, generally on the same day or the day

after their preparation. After arrival at the sampling site, the bags containing the SPATT bags were immediately stored in a fridge until deployment.

On sampling day, the SPATT bag which had been in the water attached to the mooring line was removed and swapped with a new one. The retrieved SPATT bag was put straight away in an empty Ziploc bag to prevent the resin drying before storage back on land in a freezer. The SPATT bags were sent back to the MSS laboratory in a polystyrene box with ice packs and completed sample sheets. Upon reception, the passive samplers were stored in a freezer until processing and lipophilic toxins analysis.

The SPATT bags were attached to a mooring line at the different sampling sites, generally a few meters below the surface. At Loch Ewe, the SPATTs were attached 7 meters below the surface, while at Scapa and Scalloway they were 4 and 1.5 meters below the surface respectively. The passive samplers were aimed at being deployed on a weekly basis. However, this was dependent on the weather and on the availability of the sampling personnel. The weekly deployment was rigorously adhered to at the Loch Ewe monitoring site where, between April 2005 and December 2013, only five SPATT bags corresponding to five weeks of toxin monitoring could not be analysed due to losses or damage (lost resin). More recently, passive samplers were also deployed at Scapa and Scalloway monitoring sites from May and June 2011 respectively. The weekly deployment was mostly adhered to at these two sites although on a few occasions the SPATT bags were left in the water up to two consecutive weeks. There are gaps in the time series at Scalloway where no SPATT bags were deployed. As a result these data are not presented here. A summary describing the period of the year for which SPATT bags have been deployed and analysed is detailed in Table 11.1.

Table 11.1 Summary of SPATT monitoring

Site name	SPATT deployment period	Number of analysed SPATT
Loch Ewe	04/04/2005 – 30/12/2013	452
Scapa	16/05/2011 – 09/12/2013	131
Scalloway	10/06/2011 - 09/09/2011	12
	04/05/2012 - 17/08/2012	10
	07/06/2013 - 31/12/2013	31

SPATT Extraction Processing

Extraction of the lipophilic toxins from the resin-filled SPATT bags was performed using a procedure previously described (Turrell et al., 2007) with some small modifications. Frozen SPATT bags (ten to twelve bags per batch) were left to defrost on a bench at room temperature for one hour. The Midi clips were then removed from each SPATT bag and the cable ties cut using pliers. The bags were cut open using a pair of scissors and the resin was transferred into 250 mL glass Duran® bottles using a funnel. The resin beads were rinsed from the bags and the

funnels into Duran® bottles with deionised water. The final volume of deionised water was made up to 200 mL and the bottles containing the resin were shaken by hand for one minute.

For each sample, the resin slurry was poured into a couple of 25 mL polypropylene reservoirs (Grace, Carnforth, UK) fitted with 20 µm polyethylene frits (Grace, Carnforth, UK) and installed on a solid phase extraction 12-port manifold (Hichrom, Theale, UK). A reservoir containing blank SP700 resin (4.7 ± 0.1 g) was also installed on the manifold and was used as method blank. The resin bed height of the method blank was used as a reference during the aliquoting of the samples.

A small volume of deionised water was used to ensure all the resin was transferred from the Duran® bottles to the reservoirs. In the end, the resin from each SPATT sample ended up aliquoted into two reservoirs, one containing ca. 4.7 g of resin and used for the extraction of lipophilic toxins and a second containing ca. 7 g of resin and used as a back-up if necessary. Both resin fractions were further rinsed with deionised water (100 ± 5 mL) in order to remove salts still potentially present at this stage of the procedure.

Thereafter, a low vacuum was applied to the manifold to gently remove interstitial water from the washed resin. The second reservoir was capped at both ends using Alltech™ inlet and outlet caps (Fischer Scientific, Loughborough, UK) and stored in a freezer.

Extraction of the lipophilic toxins was carried out using methanol. The solvent (10 mL) was added using a pipette to the reservoir which was then capped. The contents were vortex-mixed for one minute before the reservoir was installed back on the manifold where the resin was left to soak for 30 minutes. A glass Duran® bottle (100 mL) was installed in the manifold and the eluent was collected (1 to 2 drops per sec.).

The resin was further extracted with methanol (90 mL) so that a total extraction volume of 100 mL was used to extract the lipophilic toxins. The Duran® bottle was capped and the extract was mixed by inversion several times. An aliquot (10 mL) was then transferred into a borosilicate glass tube (15 mL), evaporated to dryness using a Turbovap® LV (Biotage, Hengoed, UK) and re-suspended in 80% methanol (500 µL).

The concentrated sample was filtered by centrifugation (10,000 rpm for three minutes) using an Ultrafree-MC GV 0.22 µm PVDF centrifugal concentrator (Millipore, Watford, UK) and the cleaned extract was transferred into an amber vial with a 350 µL fused insert prior to LC-MS analysis.

SPATT extracts analysis by LC-MS

The resin extracts were analysed for lipophilic toxins by liquid chromatography-mass spectrometry (LC-MS) according to a method developed at MSS (Stobo et al., 2005). The toxins analysed were: okadaic acid (OA), dinophysistoxins 1 and 2 (DTX-1 and DTX-2), pectenotoxins 1 and 2 (PTX-1 & PTX-2), yessotoxin (YTX), homoyessotoxin, 45-hydroxy-yessotoxin (45-OH-YTX), 45-hydroxy-homoyessotoxin

(45-OH-homoYTX) and azaspiracids 1-3 (AZA-1, AZA-2 & AZA-3). These are the lipophilic toxins included in Decision 2002/225/EC which have to be monitored in bivalve molluscs as part of an official control program undertaken by a country's competent authority.

The toxins were separated in an Agilent 1100 series LC system (Agilent Technologies, West Lothian, UK) consisting of a G1323B control module, G1354A quaternary pump, G1379A degasser, G1313A autosampler, and a G1316A column oven. An Applied Biosystems API 150EX (Warrington, UK) mass spectrometer with a TurboIonspray® atmospheric pressure ionization interface was used for the detection of the toxins. A switching valve (Valco, Schenkon, Switzerland) was included as part of the system set-up, to divert the post-column flow of mobile phase to waste for the initial two minutes of the LC-MS toxin analysis and also after 16 minutes. The mass spectrometer was operated in both ionization modes (positive and negative) and selected ion monitoring (SIM) acquisition mode. The ions, ionspray voltages, declustering, and focusing potentials are detailed in Stobo et al., (2005).

Chromatographic separation of the lipophilic toxins was achieved with a Hypersil BDS C8 column (50 x 2.1 mm, 3 µm) attached with a guard column (10 x 2.1 mm, 3 µm) of the same stationary phase (Thermo Fisher Scientific, Hemel Hampstead, UK). Elution of the toxins from the column was performed using a binary gradient, with phase A consisting of water and phase B of 95% acetonitrile (both containing 5 mM ammonium acetate, pH 6.8). The gradient ran from 20% to 100% B for the first 12.5 minutes of the analysis, held for five minutes and returned to 20% B over one minute before re-equilibration for 5.5 minutes. The flow rate, injection volume, and column temperature were set at 0.25 mL/min, 5 µL, and 25ºC respectively.

Analysis of the SPATT extracts followed a two-step process. During the first analysis, the extracts were screened for the presence of lipophilic toxins. This involved analysis of the extracts alongside some standards (low and high concentration) and a laboratory reference material (LRM – spiked resin extract) to identify the toxins present. Standard addition was then carried out in a second step on extracts which contained quantifiable amount of toxins. These extracts were analysed with an LRM and a full calibration set of standards in what was the final quantitative analysis.

SPATT Extracts Archiving

Vials containing the analysed SPATT sample extracts were re-capped after LC-MS analysis and were stored in a freezer up to two years. Additionally, aliquots (ca. 20 mL) of non-diluted SPATT extracts collected during the toxin extraction process were stored in glass sample vials (Wheaton, Millville, NJ, USA) and kept at -20ºC for five years in the eventuality of further required analyses.

Data Quality, Handling and Archiving

All solvents and reagents were of LC grade and were used without further purification.

Certified solutions of OA, YTX, PTX-2 and AZA-1 in methanol, were obtained from the Certified Reference Materials Program from the National Research Council Canada (Halifax, Nova Scotia, Canada). These certified solutions were used to prepare calibration standard solutions. DTX-1 was purchased from Wako Chemicals (Osaka, Japan) while 45-OH-YTX standard (Norwegian School of Veterinary Science, Norway), PTX-1 standard (Tohoku University, Sendai, Japan), semi-purified extracts of DTX-2, AZA-2 and AZA-3 (Marine Institute, Ireland), and homoYTX and 45-OH-homoYTX (Centro Ricerche Marine, Italy) were received as generous gifts and used to prepare the laboratory reference material.

Stock standard solutions (400 ng/mL for OA, PTX-2, and AZA-1; 1000 ng/mL for YTX) were prepared gravimetrically in methanol and were stored at -20ºC until use. For calibration of the LC-MS and the quantification of lipophilic toxins, a working standard solution (100 ng/mL for OA, PTX-2, and AZA-1; 250 ng/mL for YTX) was prepared in 80% methanol from dilution of the stock standard solution. The working standard solution was then diluted (gravimetrically) to obtain six calibration standards ranging from 2.5 to 40 ng/mL for OA, PTX-2, and AZA-1 and from 6 to 96 ng/mL for YTX. All standards were stored at –20°C until required.

All calibration curves were linear for all the toxins (OA, YTX, PTX-2 and AXA-1) with a correlation coefficient $r^2 > 0.99$. Standard additions were carried out on samples found in the initial screen analyses to contain toxins as a way of dealing with any signal suppression or enhancement. Equimolar relative response factors where toxins have similar structures within a toxin group, i.e., OA and DTXs, YTXs, PTXs, and AZAs were used to quantify those toxins without a certified standard.

A methanol blank was injected at least four times at the beginning of a sequence to allow the LC column to equilibrate. This was followed by the injection of a system suitability before the first standard to ensure the toxins eluted at the correct retention time and to check the signal responses of the toxins were satisfactory.

LC-MS data were processed using the Analyst® software (v1.1 initially then upgraded to v1.3, Applied Biosystems, Warrington, UK) and peak integrations were checked and corrected manually when necessary. Final toxins concentrations in the resin were calculated taking into account any dilution and enhancement/suppression correction factor. The results were finally entered in LIMS once they had been QC checked by the technical manager.

11.3 Results

Loch Ewe

The seasonal distribution of the main lipophilic toxins (OA, DTX-1, DTX-2, PTX-2, AZA-1 and YTX) recovered from the SPATT bags at Loch Ewe follows different trends as illustrated by the monthly boxplots shown in Figures 11.3a to 11.8a.

For OA, DTX-1, PTX-2 and YTX, the seasonal distribution is characterised by a gradual increase in toxin concentration from a minimum in April (March for DTX-1) to a maximum toxin concentration around August-September. The highest recorded concentration of OA, DTX-1, PTX-2 and YTX in SPATT since algal toxin monitoring

began in 2005 was 566 ng g^{-1} of resin (09/09/2013), 96 ng g^{-1} of resin (25/07/2013), 535 ng g^{-1} of resin (01/08/2005) and 71 ng g^{-1} of resin (29/07/2013) respectively.

The seasonal trend for AZA-1 and DTX-2 is very different from the seasonal pattern described for the previous toxins. The seasonal distribution for AZA-1 is characterised by higher toxin concentrations during the winter months (November-February) while the lowest concentration can be observed during the summer months (minimum in July). The highest recorded concentration of AZA-1 in SPATT was 72 ng g^{-1} of resin (04/02/2013).

The monthly DTX-2 boxplot shows an ambiguous seasonal distribution pattern, with the highest median DTX-2 concentrations recorded between January and May. The highest recorded concentration of DTX-2 in SPATT was 72 ng g^{-1} of resin (24/10/2011).

The concentration of OA, DTX-1 and PTX-2 is most variable during the period May-October when toxin-producing *Dinophysis* cells are more abundant, while YTX concentration is most variable during a shorter summer period (June-September). This is very different for AZA-1 with the most variable concentration during the period October-February and the least variable concentration during the summer (June-July). Finally, the concentration of DTX-2 appears to be slightly more variable in October than the rest of the year.

Yearly boxplots for OA and PTX-2 (Figures 11.3b and 11.4b) are very similar and show a substantial decrease in the concentration of these toxins in the water column between 2005 and 2007. It is important though to bear in mind that SPATT monitoring only started in April 2005, thus positively skewing the data for 2005. There seems to be a trend characterised by an overall increase in concentration for OA and PTX-2 between 2007 and 2013. This temporal trend appears to be confirmed by the anomaly plots (annual) of OA and PTX-2 concentrations (Figures 11.3c and 11.4c) which show gradually decreasing negative anomalies from 2007 to 2013. The anomaly was positive for OA in 2013 and slightly negative for PTX-2 for the same year. This is driven by an increase for these two toxins in the number of positive monthly anomalies (Figures 11.3d and 11.4d) since 2012 and a decrease in the severity of the negative anomalies since 2007 for OA and 2009 for PTX-2.

The annual DTX-1 boxplot (Figure 11.5b) does not appear to exhibit any temporal trend. The annual anomaly plot for DTX-1 concentration (Figure 11.5c) shows for the last three monitoring years (2011-2013) slightly positive anomalies. This follows negative DTX-1 concentration anomalies during the period 2006-2010. The monthly concentration anomaly plot for DTX-1 (Figure 11.5d) highlights the absence of DTX-1 in the water during the first three months of the year. This has been regularly occurring since 2006, the first complete year of SPATT algal toxin monitoring at Loch Ewe.

The yearly YTX boxplot (Figure 11.8b) does not exhibit any key temporal trend. The 2007-2008 two year period stands out, however, due to the absence of YTX detected in the SPATT bags deployed during that time. The lack of temporal trend for YTX is also shown in both monthly and annually concentration anomalies plots

(Figures 11.8c and 11.8d) where negative and positive anomalies alternate since 2009.

The yearly AZA-1 boxplot (Figure 11.7b) seems to exhibit a temporal trend between 2009 and 2013, characterised by gradual yearly higher AZA-1 concentration in SPATT culminating in 2013. This is confirmed by the annual AZA-1 concentration anomalies plot (Figure 11.7c) which shows gradually decreasing negative toxin concentration anomalies between 2009 and 2013. The AZA-1 annual concentration anomaly became largely positive in 2013 driven by a series of consecutive monthly positive AZA-1 concentration anomalies spreading from January through September (Figure 11.7d).

Finally, the yearly DTX-2 boxplot (Figure 11.6b) shows, following a 5-year period (2006-2010) where DTX-2 was present at low levels, a sudden increase in the occurrence of DTX-2 in 2011 characterised by the highest DTX-2 concentrations recorded in SPATT during the 2005-2013 monitoring period. This was followed by gradual lower DTX-2 concentration recovered from SPATT in 2012 and 2013. The later observation is confirmed by the DTX-2 concentration anomalies plot (annual and monthly, Figure 11.6c) which shows decreasing anomalies, from positive (2011 and 2012) to negative (2013). The DTX-2 annual concentration anomaly became largely negative in 2013 driven by monthly negative DTX-2 concentration anomalies throughout the whole year (Figure 11.6d).

Scapa

SPATT monitoring at Scapa started in May 2011 and was carried out uninterrupted throughout 2012 and 2013. This 30 month monitoring period is relatively short, making the observation of trends for the various toxins difficult. The main lipophilic toxins (OA, DTX-1, DTX-2, PTX-2, AZA-1 and YTX) found in SPATT bags deployed at Loch Ewe were also detected in SPATT bags deployed at Scapa. The seasonal distribution of these toxins follows different trends as illustrated by the monthly boxplots shown in Figures 11.9a to 11.14a. For OA, DTX-1 and PTX-2, the seasonal distribution is characterised by a gradual increase in toxin concentration from a minimum in April to a maximum in September. The highest recorded concentration of OA, DTX-1 and PTX-2 in SPATT since algal toxin monitoring began at Scapa was 412 ng g^{-1} of resin (21/08/2013), 49 ng g^{-1} of resin (21/08/2013) and 154 ng g^{-1} of resin (21/08/2013) respectively.

The monthly YTX boxplot illustrates the infrequent presence of this toxin at Scapa between the periods March to September. The highest recorded concentration of YTX in SPATT was 135 ng g^{-1} of resin (05/08/2013). YTX has not been detected in the SPATT samplers deployed during the period October to February.

The seasonal trend for AZA-1 and DTX-2 is very different from the seasonality pattern described for the previous toxins. The seasonal distribution for AZA-1 is characterised by higher toxin concentrations during the winter months (November-February) while the lowest concentration can be observed during the summer months (minimum in July). The highest recorded concentration of AZA-1 in SPATT was 129 ng g^{-1} of resin (19/09/2011).

The monthly DTX-2 boxplot shows an ambiguous seasonal distribution pattern, with the highest median DTX-2 concentration recorded during the period September-October. The highest recorded concentration of DTX-2 in SPATT was 51 ng g^{-1} of resin (12/09/2011). Overall, DTX-2 accumulates in SPATT bags at Scapa between June and February. Furthermore, DTX-2 has not been detected in SPATT bags deployed during the month of April (2012 and 2013).

The concentration of OA, DTX-1 and PTX-2 is most variable in July when toxin-producing *Dinophysis* cells are more abundant, while YTX concentration is most variable in May and August. This is very different for AZA-1 for which the most variable concentration spans from November-February and April-May. It is during the summer months (June-September) that the AZA-1 concentration is the least variable. Finally, the concentration of DTX-2 appears to be more variable in late autumn (October and November).

Yearly boxplots for OA, PTX-2, DTX-1 and to a certain extent YTX (Figures 11.9b, 11.10b, 11.11b and 11.14b) are very similar and show that the overall concentration of these toxins in the water column at Scapa was higher in 2013 than in 2012. Owing to the start mid-May 2011 of the SPATT monitoring, the 2011 box plot is positively skewed, making the assessment of the partial data collected that year difficult to interpret. The annual anomaly plots for these four toxins (Figures 11.9c, 11.10c, 11.11c and 11.14c) show large negative anomalies for 2012 followed by positive anomalies for 2013. This is driven by a large majority of negative monthly anomalies for OA, PTX-2, DTX-1 and YTX (Figures 11.9d, 11.10d, 11.11d and 11.14d) in 2012 and a large majority of positive monthly anomalies for the same toxins in 2013.

The yearly AZA-1 boxplot (Figure 11.13b) shows an increase in the overall concentration of this toxin in the water column at Scapa between 2012 and 2013. This is confirmed by the annual AZA-1 concentration anomalies plot (Figure 11.13c) which shows a large negative toxin concentration anomaly in 2012 followed by a marginally negative AZA-1 concentration anomaly in 2013. This evolution between 2012 and 2013 was driven by a series of monthly positive AZA-1 concentration anomalies spreading from January through August 2013 (Figure 11.13d).

Finally, the yearly DTX-2 boxplot (Figure 11.12b) shows a decrease in the overall concentration of this toxin in the water column at Scapa between 2012 and 2013. This is confirmed by the annual DTX-2 concentration anomalies plot (Figure 11.12c) which shows a negative toxin concentration anomaly in 2012 followed by a larger negative DTX-2 concentration anomaly in 2013. This evolution between 2012 and 2013 was driven by a series of consecutive monthly negative DTX-2 concentration anomalies spreading throughout 2013 (Figure 11.12d).

11.4 Discussion

OA, PTX-2, DTX-1 and DTX-2 are algal toxins known to be produced by some species of planktonic marine dinoflagellates belonging to the genus *Dinophysis* (Reguera et al., 2014). *Dinophysis* cells are present in the water column at both Loch Ewe and Scapa monitoring sites mainly between April and October as shown in Figure 9.22a and 9.23a. SPATT results, especially at Loch Ewe, correlate well with

this observation with increased detection of OA, PTX-2 and DTX-1 in the water column from a low in April to a maximum towards the end of the summer season (August-September). The SPATT results at Scapa show an overall seasonal trend for OA, PTX-2 and DTX-1 similar to Loch Ewe (April low and September high), though with more variability between consecutive months, probably the result of a much shorter monitoring period (2.5 years at Scapa compared to 8.5 years at Loch Ewe). Further examination of this data highlighted the presence of a slight time lag between the emergence of *Dinophysis* cells in April, and an increase in the detection of OA, PTX-2 and DTX-1 concentrations in SPATT deployed in May at both sites.

Another interesting observation is the yearlong persistence of OA and PTX-2 in the water column at Loch Ewe and Scapa even during the winter months in the absence of *Dinophysis* cells. OA was detected at Loch Ewe in all 452 deployed SPATT bags while PTX-2 was detected in ca. 96% of the passive samplers. At Scapa, OA and PTX-2 were detected in 97% and 93% respectively of the deployed SPATT bags.

DTX-1 and 2 are regularly detected in SPATT bags deployed at Loch Ewe and Scapa, albeit in much lower abundance than OA and PTX-2. As previously mentioned, DTX-1 follows a similar seasonal distribution to OA and PTX-2. However, detection of DTX-1 in SPATT starts generally in May at Loch Ewe, a month earlier than at Scapa. Accumulation of DTX-1 in SPATT peaks in August at Loch Ewe, also a month earlier than at Scapa. The presence of DTX-2 in SPATT reaches a maximum slightly later in autumn, around September-October. Increased levels of DTX-2 can also be detected in winter around January-February at Loch Ewe and Scapa when *Dinophysis* sp. cells are absent from the water column. This is also valid for OA and PTX-2.

YTX and its analogues (ca. 100) are known to be produced by the phytoplanktonic dinoflagellates *Protoceratium reticulatum* (Satake et al., 1997), *Lingulodinium polyedrum* (Tubaro et al., 1998) and *Gonyaulax spinifera* (Rhodes et al., 2006). At Loch Ewe, YTX especially but also 45-OH-YTX more occasionally are the main yessotoxin analogues detected in SPATT primarily during the summer months (June-September). Their detection coincides with the presence of low numbers of *P. reticulatum* cells in the water column (*L. polyedrum* being very rarely detected), thus confirming this dinoflagellate species as the most likely source of YTXs at Loch Ewe. During the period 2007-2008, YTXs were not detected in SPATT. However since 2009, a small increase in the concentration of dissolved YTX in SPATT could be associated with an increase in the number of *P. reticulatum* cells in the water column.

At Scapa, YTX has been the only yessotoxin analogue detected in SPATT between March and September, with a peak in August. The detection of YTX also coincides with the presence of low numbers of *P. reticulatum* cells in the water column (*L. polyedrum* not detected), thus confirming this dinoflagellate species as the most likely source of YTX at Scapa. Higher levels of YTX were detected in SPATT bags deployed at Scapa in 2013 compared to 2012.

Since the isolation and identification of *Azadinium spinosum*, the first AZA-producing organism discovered in the North Sea in 2007 (Krock et al., 2009, Tillmann et al., 2009), a number of new species of the genus *Azadinium* also originating from the

North Sea have been discovered: *A. obesum* (Tillmann et al., 2010), *A. poporum* (Tillmann et al., 2011*)* and *A. polongum* (Tillmann et al., 2012). While initially *A. spinosum* was found to be the only species to produce azaspiracids, namely AZA-1 and AZA-2 (Tillmann et al., 2009), more recently other species of dinoflagellates have also been shown to produce AZAs (Krock et al., 2012, 2014).

Light microscopy assessment of the presence of *Azadinium* sp*.* in the water is very difficult due to the small size (11-18 µm in length) of this organism. Moreover, molecular techniques such as real time PCR are under development and optimisation before it can be confidently integrated into a monitoring programme setup. Analysis of the SPATT passive samplers deployed at Loch Ewe revealed the presence of AZA-1 mainly, but also occasional traces of AZA-2 and possible traces of AZA-3, indicating the occurrence of one or several azaspiracid-producing phytoplankton species. At Scapa, AZA-1 was also the main azaspiracid analogue detected in SPATT bags, but also occasional traces of AZA-2. The seasonal distribution of AZA-1 is similar at Loch Ewe and Scapa and is very distinct from the other lipophilic toxins. Indeed, the presence in the SPATT bags of AZA-1 occurs mainly between September and March, in other words during autumn and winter. July is the month where AZA-1 concentration is at its lowest in the SPATT samplers deployed at Loch Ewe and Scapa. The overall concentration of AZA-1 in the water column shows an increasing trend since 2009.

SPATT monitoring at Scalloway started mid-2011 and although deployment of the passive samplers occurred generally on a weekly basis, there were large periods with no SPATT deployment. Out of the 53 SPATT bags deployed at Scalloway, OA, DTX-1, PTX-2, AZA-1 and YTX were the only toxins detected. Unlike at Loch Ewe and Scapa, DTX-2 and AZA-2 were not detected at Scalloway in any of the SPATT bags deployed. An interesting event happened in 2013 where a large toxin-producing *Dinophysis* sp. bloom (maximum 23,800 cells/L) took place at Scalloway in July 2013. This led a few weeks later to a significant increase in the amount of OA (maximum 344 ng g^{-1} of resin) and PTX-2 (164 ng g^{-1} of resin) detected in the SPATT bags. However, no co-occurring dinophysistoxins were detected in SPATT during this bloom event suggesting the *Dinophysis* species responsible for this event was different from the *Dinophysi*s species regularly blooming at Loch Ewe and Scapa.

11.5 Summary – Biotoxins

- SPATT is a straight forward passive sampling technique allowing the detection of extra cellular marine toxins produced by various species of phytoplankton.
- OA is the only monitored lipophilic toxin which has been found to be persistent at Loch Ewe all year long since SPATT monitoring started in April 2005.
- Other lipophilic toxins such as PTX-2, DTX-1, DTX-2, YTX and AZA-1 are also regularly detected at Loch Ewe and Scapa.
- At Loch Ewe and Scapa, OA, PTX-2 and DTX-1 follow a seasonal distribution characterised by an increased detection in SPATT from May until August/September followed by a decrease abundance throughout the autumn/winter months.

- AZA-1 follows a totally opposite seasonal pattern with a maximum abundance recorded at Loch Ewe and Scapa in the winter between November and February.
- In the absence of monitoring for *Azadinium* cells, SPATT can be a useful tool by accumulating azaspiracid toxins, thus providing direct information on the presence of toxin-producing *Azadinium* spp. in the water column of a monitored site.
- SPATT monitoring at Loch Ewe seems to suggest a gradual increase in the presence of dissolved lipophilic toxins since the period 2007-2009, culminating in 2013.

11.6 References – Algal toxins

Bresnan, E., Cook, K.B., Hughes, S.L., Hay, S.J., Smith, K., Walsham, P., Webster, L. 2015. Seasonality of the plankton community at an east and west coast monitoring site in Scottish waters. Journal of Sea Research, 105, 16-29.

Fux, E., Bire, R., Hess, P. 2009. Comparative accumulation and composition of lipophilic marine biotoxins in passive samples and in mussels (*M. edulis*) on the West coast of Ireland. Harmful Algae, 8, 523-537.

Garnett, C.M., Rafuse, C.M., Lewis, N.I., Kirchoff, S., Cullen, J., Quilliam, M.A. 2006. Monitoring of lipophilic shellfish toxins using SPATT (solid-phase adsorption toxin tracking) in Nova Scotia, Canada. In: abstract O.19-02 of the 12th International Conference on Harmful Algae, Copenhagen, Denmark, 4–8 September 2006, p. 72.

Hall, A.J. and Frame, E. 2010. Evidence of domoic acid exposure in harbour seals from Scotland: A potential factor in the decline of abundance? Harmful Algae, 9, 489-493.

Hallegraeff, G.M. 1993. A review of harmful algal blooms and their apparent global increase. Phycologia, 32, 79-99.

Hallegraeff, G.M. 2010. Ocean climate change, phytoplankton community responses, and harmful algal blooms: a formidable predictive challenge. Journal of Phycology, 46, 220-235.

Jensen, S-K., Lacaze, J-P., Hermann, G., Kershaw, J., Brownlow, A., Turner, A., Hall, A. 2015. Detection and effects of harmful algal toxins in Scottish harbour seals and potential links to population decline. Toxicon, 97, 1-14.

Krock, B., Tillmann, U., John, U., Cembella, A.D. 2009. Characterization of azaspiracids in plankton size-fractions and isolation of an azaspiracid-producing dinoflagellate from the North Sea. Harmful Algae, 8, 254–263.

Krock, B., Tillmann, U., Voß, D., Koch, B.P., Salas, R., Witt, M., Potvin, E., Jeong, H. J. 2012. New azaspiracids in Amphidomataceae (Dinophyceae). Toxicon, 60, 830-839.

Krock, B., Tillmann, U., Witt, M., Gu, H. 2014. Azaspiracid variability of *Azadinium poporum* (Dinophyceae) from the China Sea. Harmful Algae, 36, 22-28.

Mackenzie, L., Truman, P., Satake, M., Yasumoto, T., Adamson, J., Mountfort, D., White, D. 1998. Dinoflagellate blooms and associated DSP-toxicity in shellfish in New Zealand. In: Reguera, B., Blanco, J., Fernandez, M.L., Wyatt, T. eds. Harmful Algae. Santiago de Compostela, Xunta de Galicia and Intergovernmental Oceanographic Commission of UNESCO, 74-77.

Mackenzie, L., Beuzenberg, V., Holland, P., McNabb, P., Selwood, A. 2004. Solid phase adsorption toxin tracking (SPATT): a new monitoring tool that simulates the biotoxin contamination of filter feeding bivalves. Toxicon, 44, 901-918.

Mackenzie, L. 2010. In situ passive solid-phase adsorption of micro-algal biotoxins as a monitoring tool. Current Opinion in Biotechnology, 21, 326-331.

Mallat, E., Krock, B., Ferández-Tejedor, M., Caillaud, A., Cañete, E., Elandaloussi, J., Franco, J., Cembella, A., Diogène, J. 2007. First approach towards the implementation of passive sampling adsorption devices for the identification of lipophilic toxins in the coastal embayments of the Ebro Delta. In: Proceedings of the 6th International Conference on Molluscan Shellfish Safety Blenheim, New Zealand, 18–23 March 2007, P. Busby (Ed), pp 336-342.

Reguera, B., Riobo, P., Rodríguez, F., Diaz, P.A., Pizarro, G., Paz, B., Franco, J.M. and Blanco, J. 2014. *Dinophysis* Toxins: Causative Organisms, Distribution and Fate in shellfish. Marine Drugs, 12, 394-461.

Rhodes, L., McNabb, P., de Salas, M., Briggs, L., Beuzenberg, V., Gladstone, M. 2006. Yessotoxin production by *Gonyaulax spinifera*. Harmful Algae, 5, 148-155.

Rundberget, T., Gustad, E., Samdal, I.A., Sandvik, M., Miles, C.O. 2009. A convenient and cost-effective method for monitoring marine algal toxins with passive samplers. Toxicon, 53, 543-550.

Satake, M., Mackenzie, L., Yasumoto, T. 1997. Identification of *Protoceratium reticulatum* as the biogenetic origin of yessotoxin. Natural Toxins, 5, 164-167.

Scholin, C.A., Gulland, F., Doucette, G.J., Benson, S., Busman, M., Chavez, F.P., Cordaro, J., DeLong, R., De Vogelaere, A., Harvey, J., Haulena, M., Lefebvre, K., Lipscomb, T., Loscutoff, S., Lowenstine, L.J., Marin III, R., Miller, P.E., McLellan, W.A., Moeller, P.D.R., Powell, C.L., Rowles, T., Silvagni, P., Silver, M., Spraker, T., Trainer, V., Van Dolah, F.M. 2000. Mortality of sea lions along the central California coast linked to a toxic diatom bloom. Nature, 430, 80-84.

Stobo, L., Scott, A., Lacaze, J-P., Gallacher, S., Smith, E., Quilliam, M. 2005. Liquid chromatography with mass spectrometry-detection of lipophilic shellfish toxins. Journal of the Association of Official Analytical Chemist International, 88, 1371-1382.

Takahashi, E., Yu, Q., Eaglesham, G., Connell, D.W., McBroom, J., Costanzo, S., Shaw, G.R. 2007. Occurrence and seasonal variations of algal toxins in water, phytoplankton and shellfish from North Stradbroke Island, Queensland, Australia. Marine Environmental Research, 64, 429-442.

Tillmann, U., Elbrächter, M., Krock, B., John, U., Cembella, A.D. 2009. *Azadinium spinosum* gen. et sp. nov. (Dinophyceae) identified as a primary producer of azaspiracid toxins. European Journal of Phycology, 44, 63–79.

Tillmann, U., Elbrächter, M., John, U., Krock, B., Cembella, A.D. 2010. *Azadinium obesum* (Dinophyceae), a new nontoxic species in the genus that can produce azaspiracid toxins. Phycologia, 49, 169–182.

Tillmann, U., Elbrächter, M., John, U., Krock, B. 2011. A new non-toxic species in the dinoflagellate genus *Azadinium*: *A. poporum* sp. nov. European Journal of Phycology, 46, 74–87.

Tillmann, U., Soehner, S., Nézan, E., Krock, B. 2012. First record of the genus *Azadinium* (Dinophyceae) from the Shetland Islands, including the description of *Azadinium polongum* sp. nov. Harmful Algae, 20, 142–155.

Tubaro, A., Sidari, L., Della Loggia, R., Yasumoto, T. 1998. Occurrence of yessotoxin-like toxins in phytoplankton and mussels from northern Adriatic Sea. In: Reguera, B., Blanco, J., Fernandez, M.L., Wyatt, T. eds. Harmful Algae. Santiago de Compostela, Xunta de Galicia and Intergovernmental Oceanographic Commission of UNESCO 1998, 470-472.

Tubaro, A. and Hungerford, J. 2007. Toxicology of marine toxins. In: Gupta, R.C. ed. Veterinary toxicology: basic and clinical principles. New York, Academic Press, 725-752.

Turrell, E., Stobo, L., Lacaze, J-P., Bresnan, E., Gowland, D. 2007. Development of an 'early warning system' for harmful algal blooms using solid-phase adsorption toxin tracking (SPATT). In: Oceans'07 IEEE Aberdeen Conference Proceedings, 'MarineChallenges Coastline to Deep Sea' Paper No. 070131-028.

11.7 Plots – Algal toxins

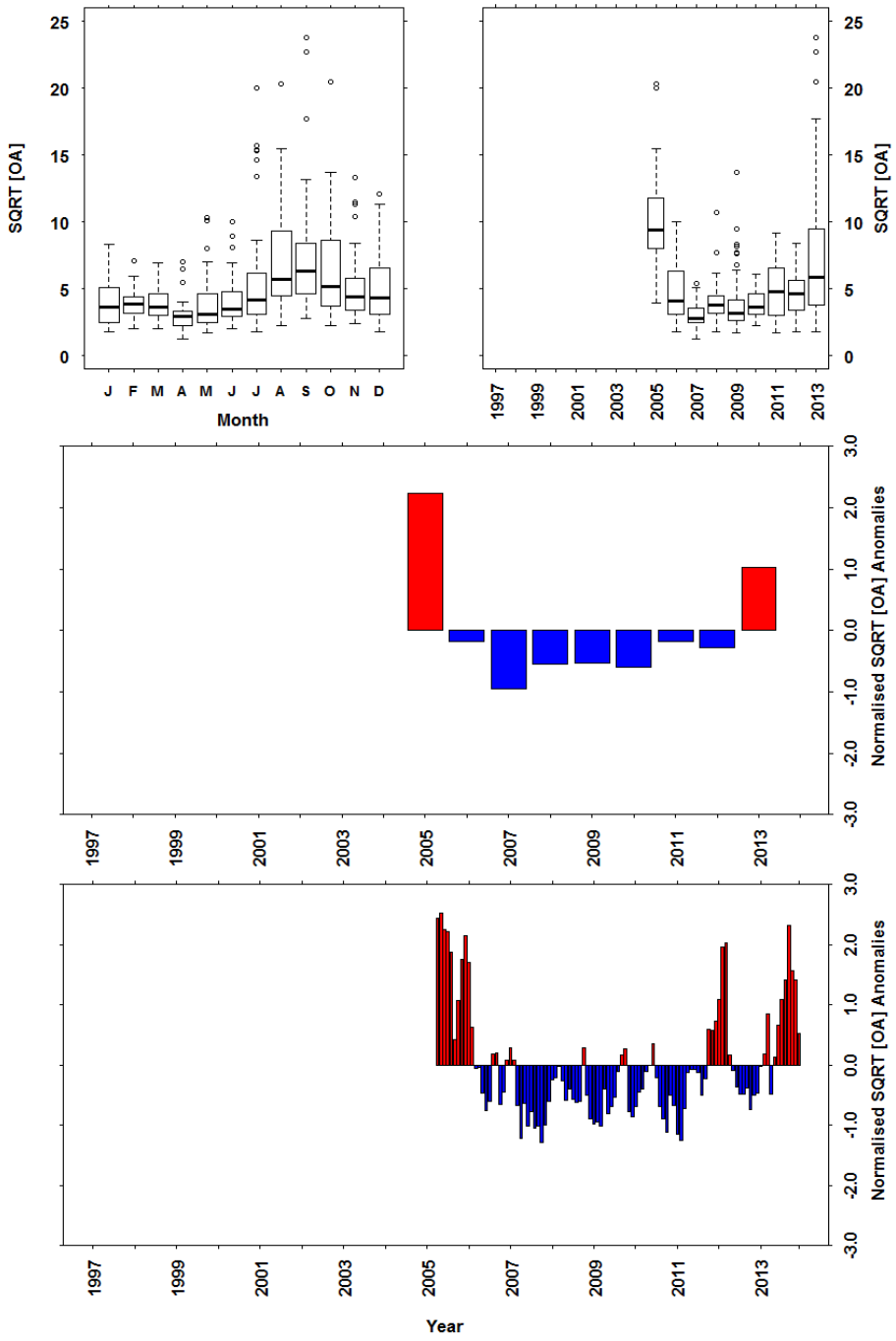

Figure 11.3 Square root transformed OA concentration in SPATT passive samplers deployed at Loch Ewe since April 2005. Monthly a) and annual b) boxplots of OA transformed concentration data. Annual c) and monthly d) mean anomaly time series plots of OA transformed concentration data. Note: Vertical axis units in figures a) and b) are ng toxin g^{-1} of resin. The full data set was used as the base period for the anomaly calculations.

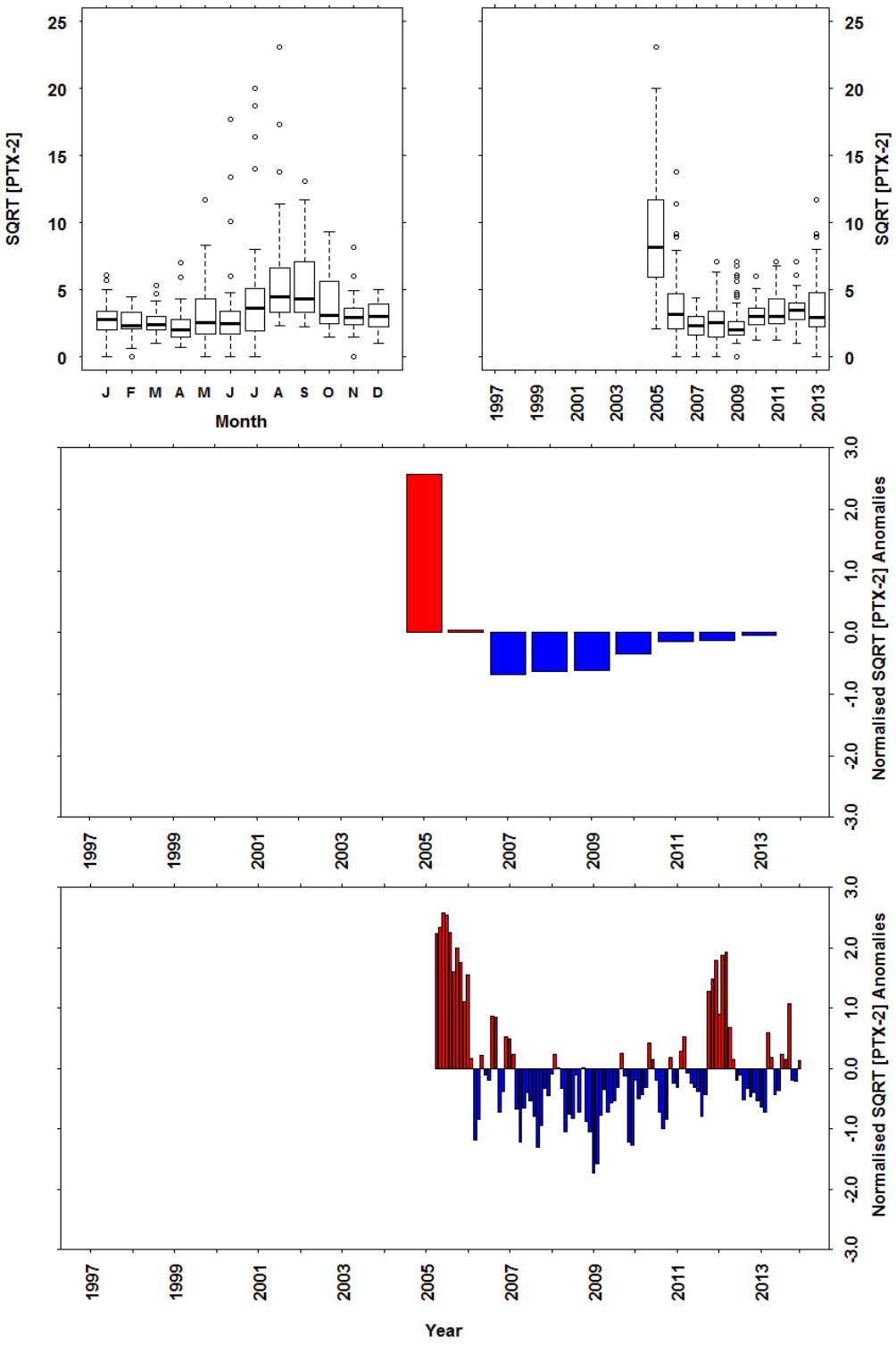

Figure 11.4. Square root transformed PTX-2 concentration in SPATT passive samplers deployed at Loch Ewe since April 2005. Monthly a) and annual b) boxplots of PTX-2 transformed concentration data. Annual c) and monthly d) mean anomaly time series plots of PTX-2 transformed concentration data. Note: Vertical axis units in figures a) and b) are ng toxin g^{-1} of resin. The full data set was used as the base period for the anomaly calculations.

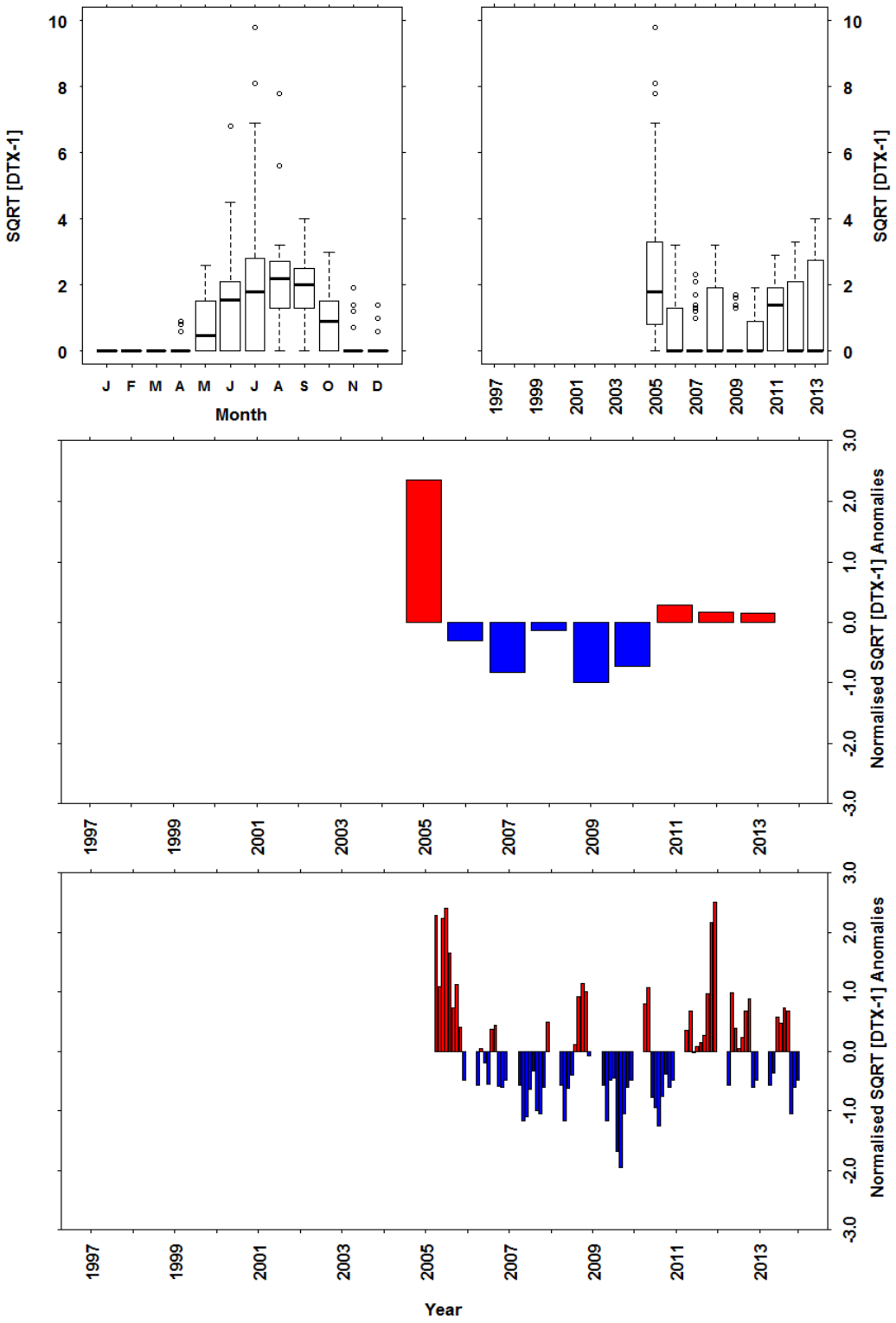

Figure 11.5 Square root transformed DTX-1 concentration in SPATT passive samplers deployed at Loch Ewe since April 2005. Monthly a) and annual b) boxplots of DTX-1 transformed concentration data. Annual c) and monthly d) mean anomaly time series plots of DTX-1 transformed concentration data. Note: Vertical axis units in figures a) and b) are ng toxin g^{-1} of resin. The full data set was used as the base period for the anomaly calculations.

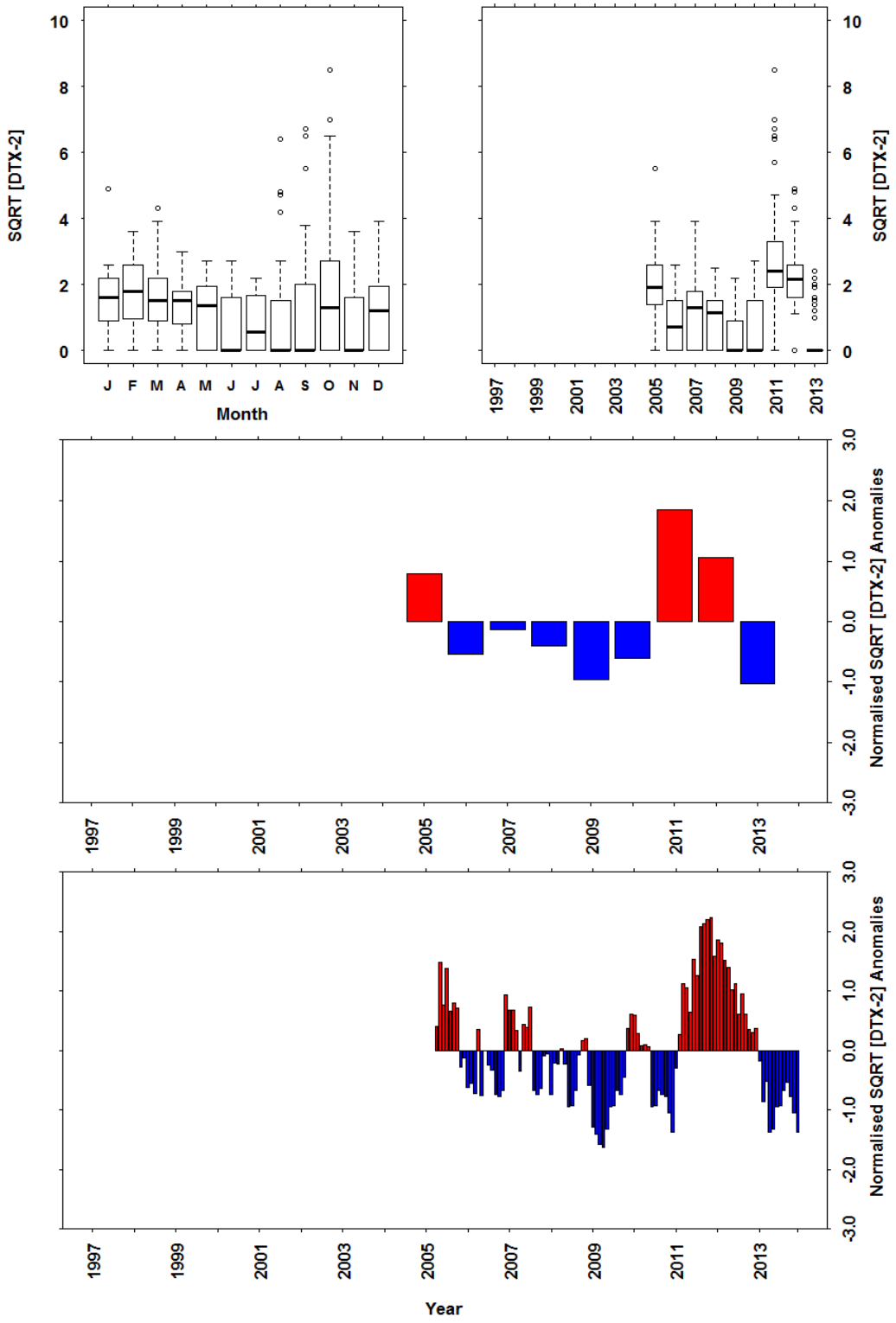

Figure 11.6 Square root transformed DTX-2 concentration in SPATT passive samplers deployed at Loch Ewe since April 2005. Monthly a) and annual b) boxplots of DTX-2 transformed concentration data. Annual c) and monthly d) mean anomaly time series plots of DTX-2 transformed concentration data. Note: Vertical axis units in figures a) and b) are ng toxin g^{-1} of resin. The full data set was used as the base period for the anomaly calculations.

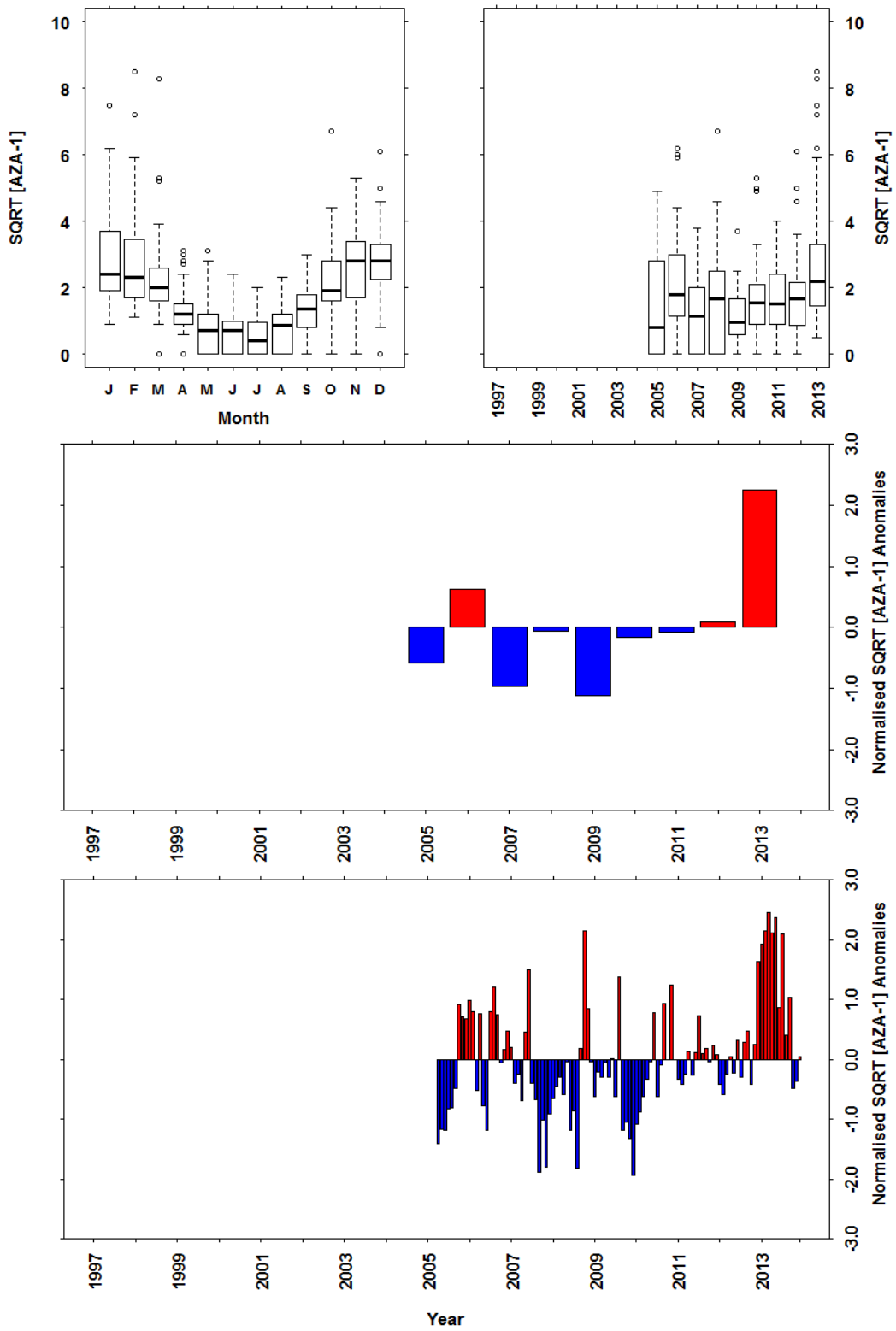

Figure 11.7 Square root transformed AZA-1 concentration in SPATT passive samplers deployed at Loch Ewe since April 2005. Monthly a) and annual b) boxplots of AZA-1 transformed concentration data. Annual c) and monthly d) mean anomaly time series plots of AZA-1 transformed concentration data. Note: Vertical axis units in figures a) and b) are ng toxin g^{-1} of resin. The full data set was used as the base period for the anomaly calculations.

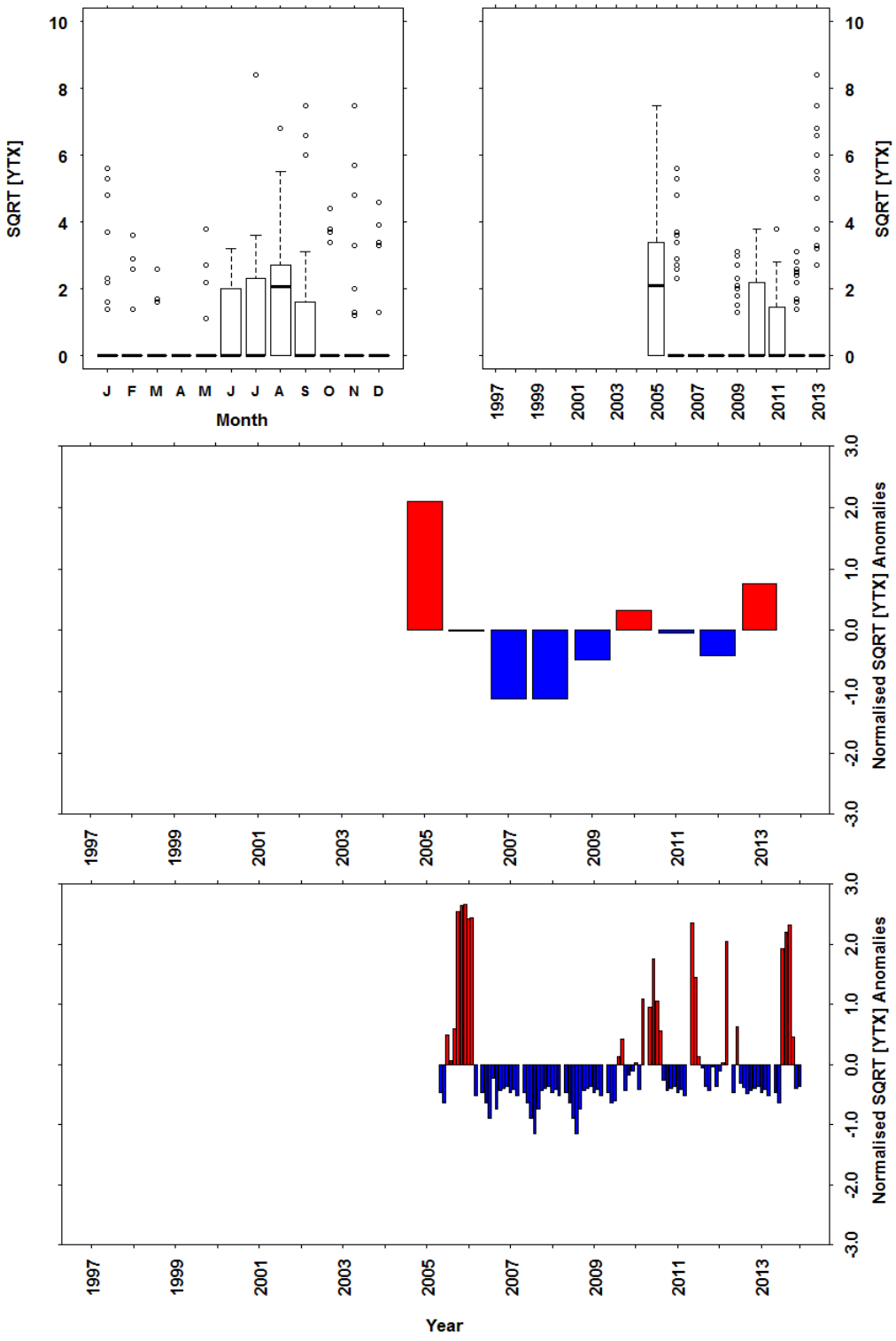

Figure 11.8 Square root transformed YTX concentration in SPATT passive samplers deployed at Loch Ewe since April 2005. Monthly a) and annual b) boxplots of YTX transformed concentration data. Annual c) and monthly d) mean anomaly time series plots of YTX transformed concentration data. Note: Vertical axis units in figures a) and b) are ng toxin g^{-1} of resin. The full data set was used as the base period for the anomaly calculations.

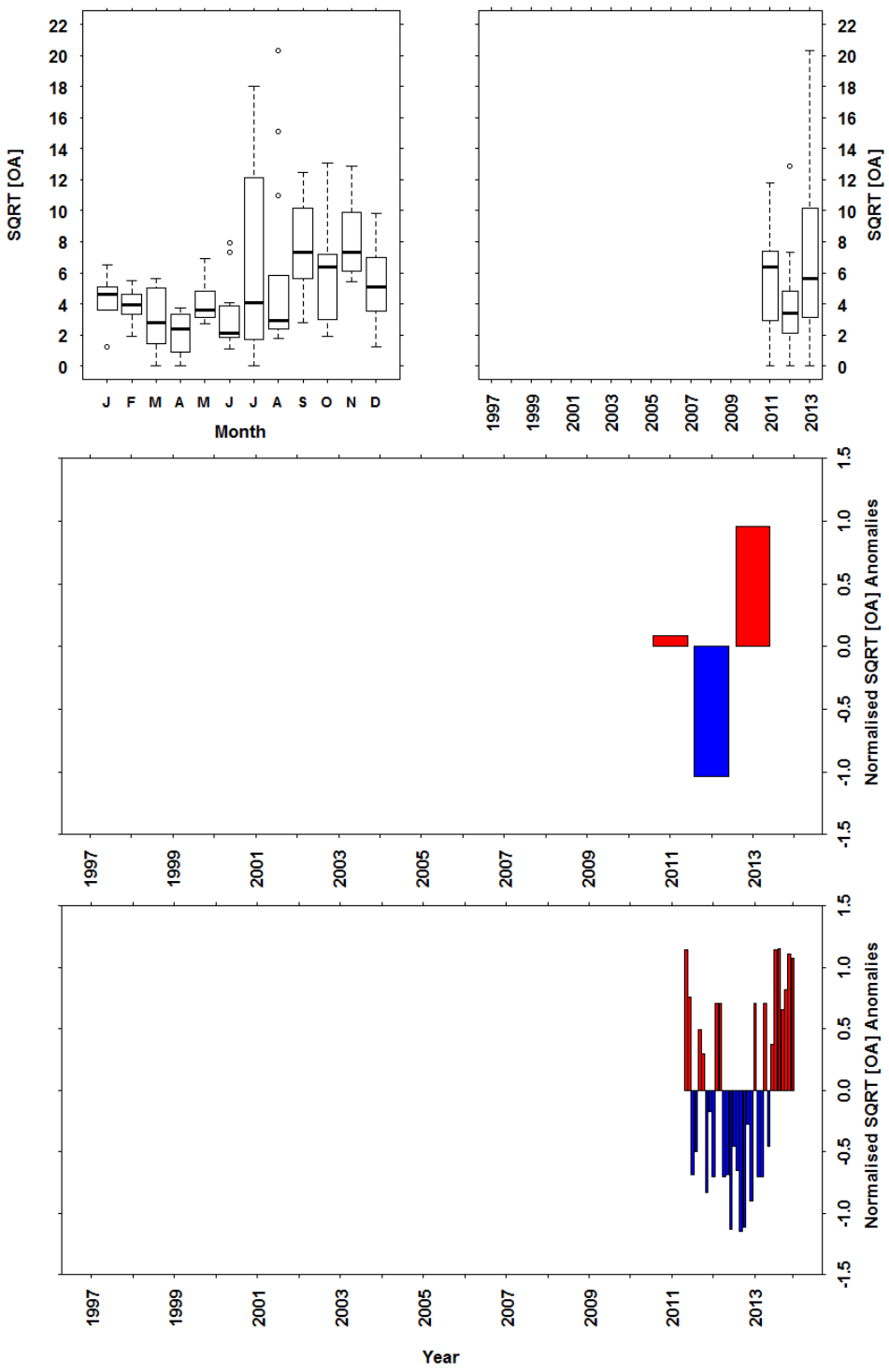

Figure 11.9 Square root transformed OA concentration in SPATT passive samplers deployed at Scapa since May 2011. Monthly a) and annual b) boxplots of OA transformed concentration data. Annual c) and monthly d) mean anomaly time series plots of OA transformed concentration data. Note: Vertical axis units in figures a) and b) are ng toxin g^{-1} of resin. The full data set was used as the base period for the anomaly calculations.

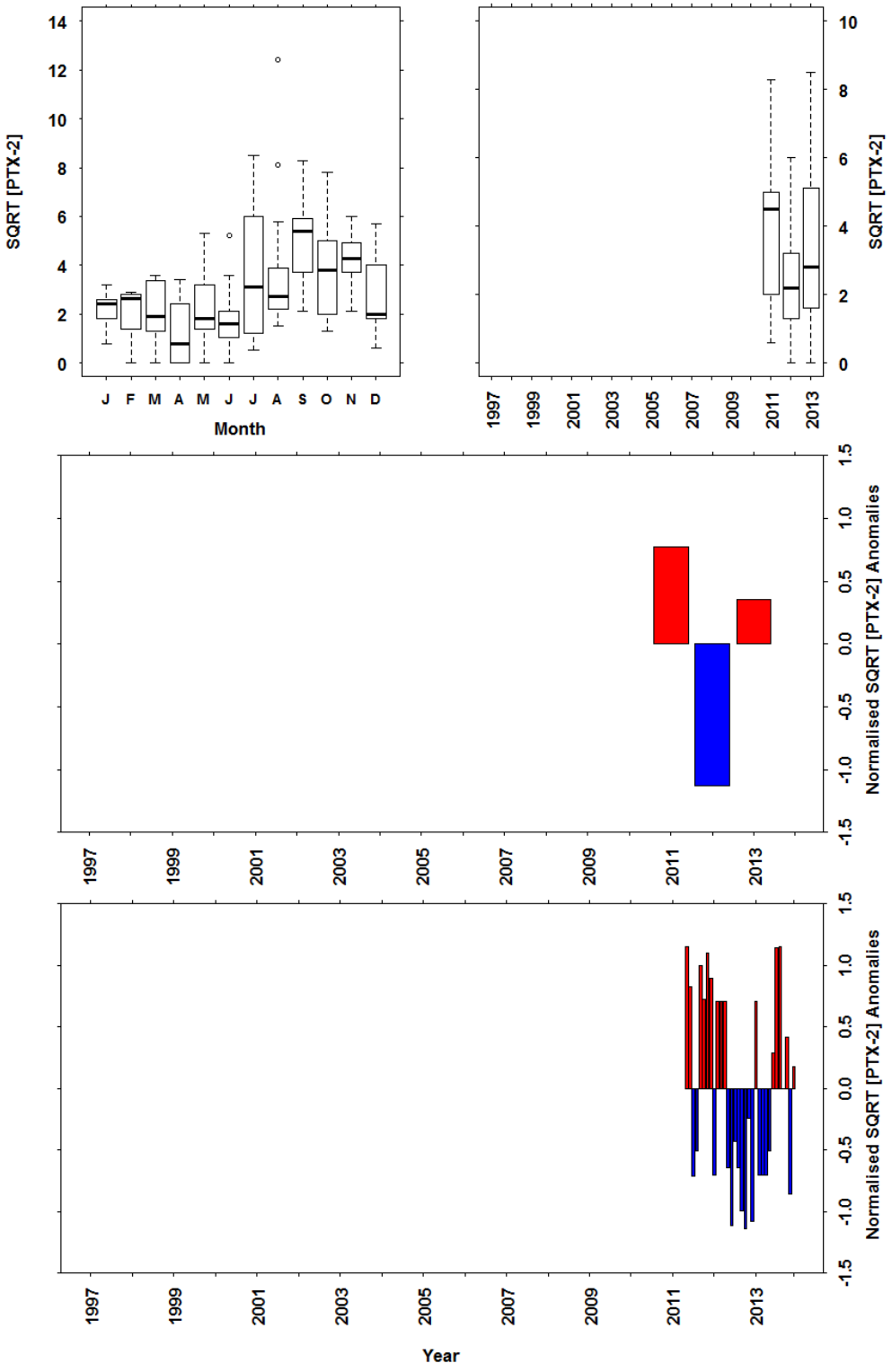

Figure 11.10 Square root transformed PTX-2 concentration in SPATT passive samplers deployed at Scapa since May 2011. Monthly a) and annual b) boxplots of PTX-2 transformed concentration data. Annual c) and monthly d) mean anomaly time series plots of PTX-2 transformed concentration data. Note: Vertical axis units in figures a) and b) are ng toxin g^{-1} of resin. The full data set was used as the base period for the anomaly calculations.

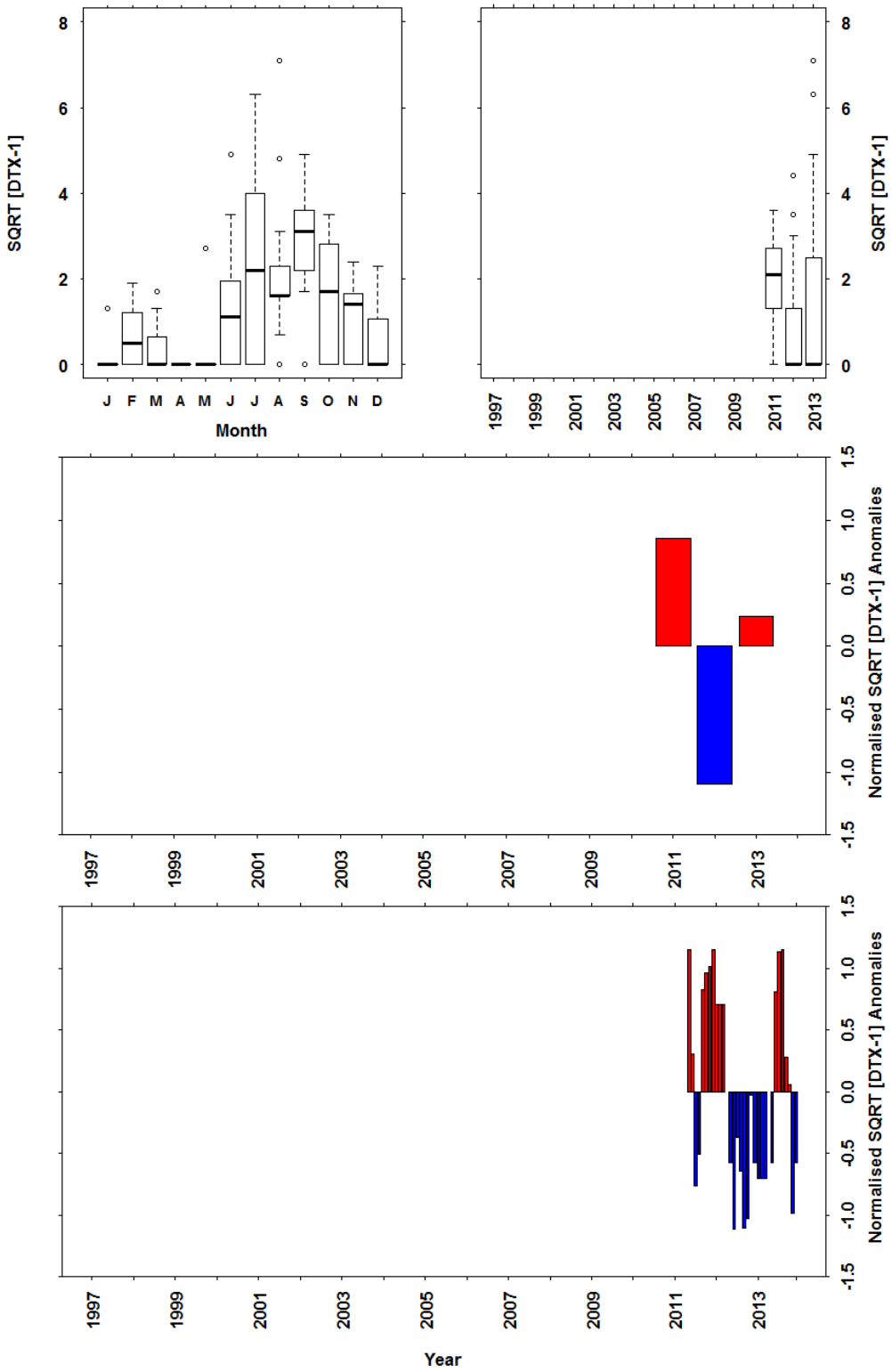

Figure 11.11 Square root transformed DTX-1 concentration in SPATT passive samplers deployed at Scapa since May 2011. Monthly a) and annual b) boxplots of DTX-1 transformed concentration data. Annual c) and monthly d) mean anomaly time series plots of DTX-1 transformed concentration data. Note: Vertical axis units in figures a) and b) are ng toxin g^{-1} of resin. The full data set was used as the base period for the anomaly calculations.

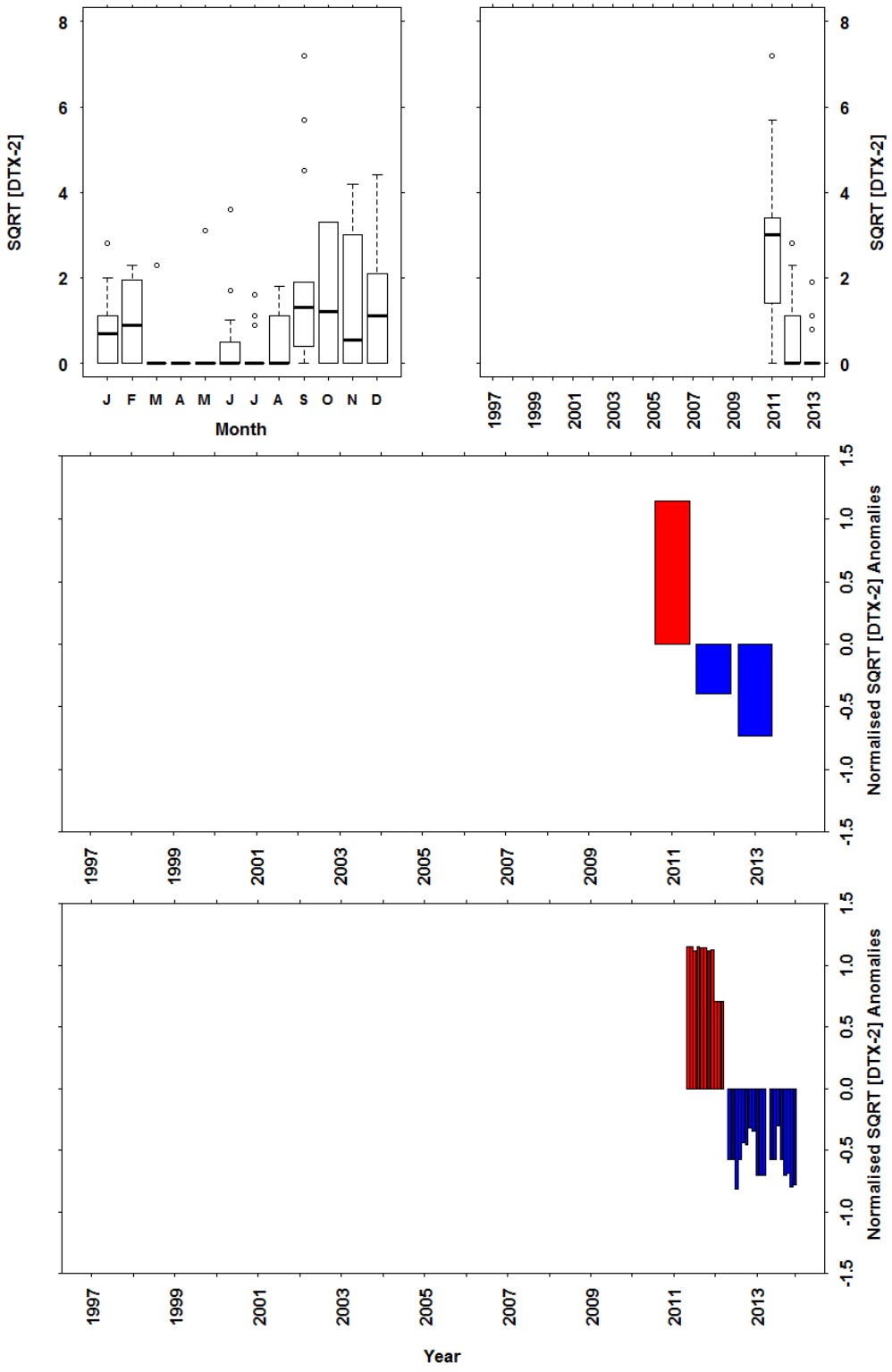

Figure 11.12 Square root transformed DTX-2 concentration in SPATT passive samplers deployed at Scapa since May 2011. Monthly a) and annual b) boxplots of DTX-2 transformed concentration data. Annual c) and monthly d) mean anomaly time series plots of DTX-2 transformed concentration data. Note: Vertical axis units in figures a) and b) are ng toxin g^{-1} of resin. The full data set was used as the base period for the anomaly calculations.

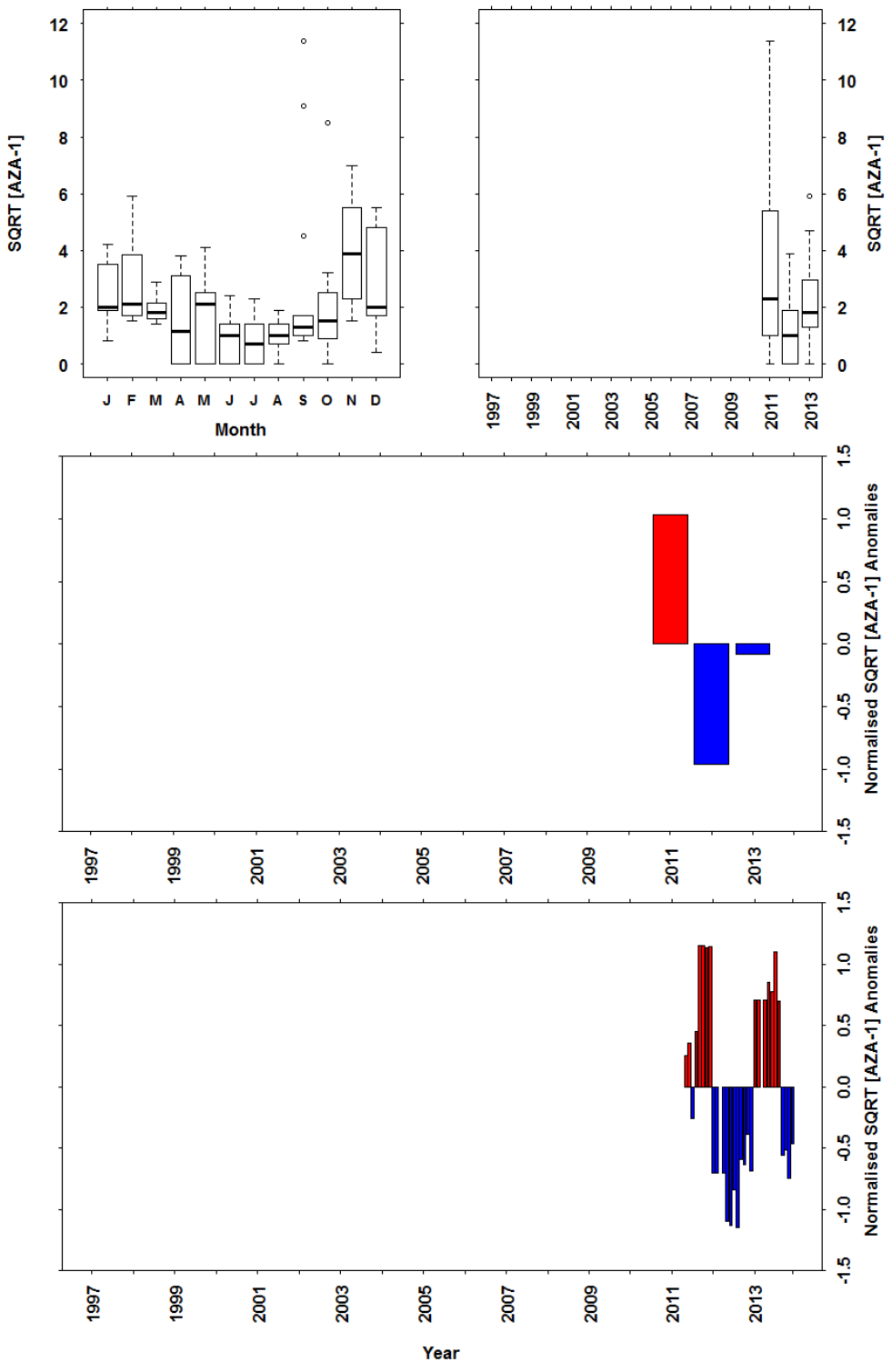

Figure 11.13 Square root transformed AZA-1 concentration in SPATT passive samplers deployed at Scapa since May 2011. Monthly a) and annual b) boxplots of transformed AZA-1 data. Annual c) and monthly d) mean anomaly time series plots of transformed AZA-1 data. Note: Vertical axis units in figures a) and b) are ng toxin g^{-1} of resin. The full data set was used as the base period

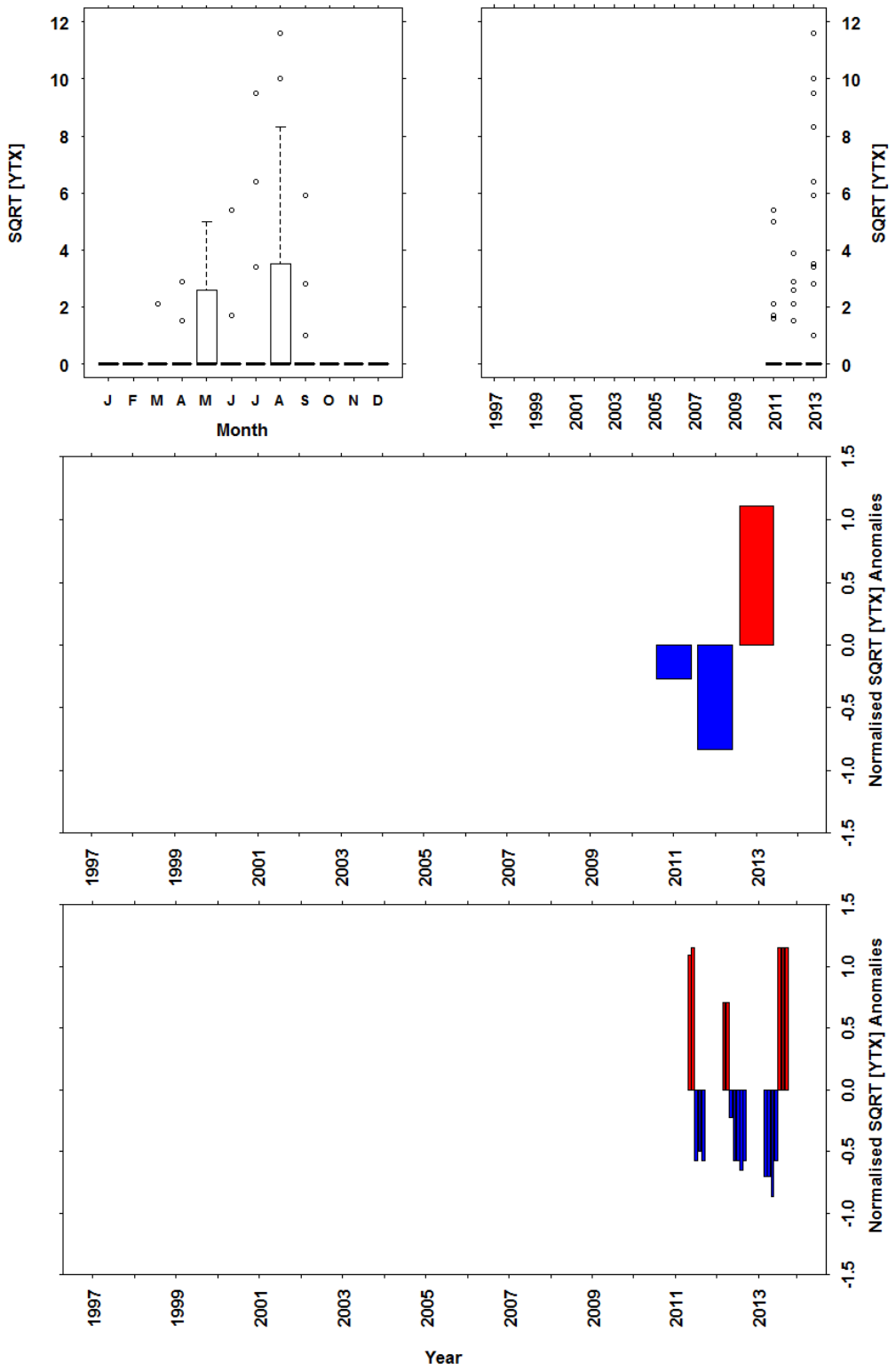

Figure 11.14 Square root transformed YTX concentration in SPATT passive samplers deployed at Scapa since May 2011. Monthly a) and annual b) boxplots of YTX transformed concentration data. Annual c) and monthly d) mean anomaly time series plots of YTX transformed concentration data. Note: Vertical axis units in figures a) and b) are ng toxin g^{-1} of resin. The full data set was used as the base period for the anomaly calculations.

12. Zooplankton

12.1 Introduction

Zooplankton are animals that live in the sea that are not strong enough to swim against tides and currents and so drift along with the water that they are living in. There are tens of thousands of species of zooplankton which range in size from a few hundredths of a millimetre up to giant jellyfish that can reach a couple of meters in diameter. Zooplankton are divided into several categories based on their size (e.g. microzooplankton, mesozooplankton, macrozooplankton, megazooplankton). Usually when people talk about zooplankton, they are referring to mesozooplankton which is in the size range 0.2mm to 2.0cm. Marine Scotland Science has sampled mesozooplankton at Stonehaven on the east coast of Scotland since 1997 and Loch Ewe on the west coast of Scotland since 2002. Until the MSS zooplankton monitoring began in Loch Ewe there had been no sustained measurements of the zooplankton community in the west of Scotland and the zooplankton in Scottish sea lochs has not been described for decades (e.g. Marshall 1949, Gamble et al., 1977, Heath 1995). Even further offshore, CPR coverage in the west coast of Scotland is poor (Scherer et al., 2015).

Mesozooplankton form an important link in food webs by transferring energy made by phytoplankton to higher trophic levels such as fish that eat the zooplankton. The availability of these zooplankton at the right place and time to provide food to fish larvae is thought to be an important factor in determining the size of fish stocks. Zooplankton faecal pellets that sink out of the water column can also provide an important source of food to the benthos. Within the mesozooplankton there are two further important categories: the holoplankton, which are animals that spend their whole life as part of the plankton, and the meroplankton, which are animals that only spend some of their lifecycle as part of the plankton, e.g. crab and starfish larvae. As most animals in the zooplankton, especially the holoplankton, have short lifecycles (less than one year) that are largely controlled by temperature, long-term monitoring of zooplankton provides an ideal indicator of the impacts of climate change in the marine ecosystem.

Full Community Analysis

There are about 230 taxonomic categories that are counted in zooplankton samples as part of the full community analysis. These categories range from the developmental stage level for the most common and easily identifiable species (e.g. copepods that make up about 60% of the taxonomic categories counted) to the Class level for hard to identify species (e.g. gastropod and polychaete larvae) and even to the Phylum level for rarely observed species (e.g. cephalochordates).

The full species list describing the zooplankton community analysis from which the summary figures and data presented in this report are derived is given in Appendix G, in Part 3 of this report.

This report and the accompanying data set uses a sub-set of zooplankton species categories in order to summarise the full data. These are described below.

Total Copepod Biomass

Total copepod biomass can be used as a proxy for total mesozooplankton biomass. Copepods are often the most important component of the mesozooplankton throughout the North Atlantic (O'Brien et al., 2013), and the availability of counts and biomass measurements for individual stages produce the most accurate signal of seasonal variability. Copepods are also one of the life-forms proposed as an indicator for the pelagic habitat under the MSFD by the UK and OSPAR (Defra 2014, Scherer et al., 2015). Recent studies have predicted that zooplankton biomass in the North Sea will decrease in response to a warming climate (Chust et al., 2014a). The calanoid copepods *Acartia clausi*, *Calanus* spp., *Centropages* spp., *Paracalanus parvus*, *Pseudocalanus* spp., *Temora longicornis* and the cyclopoids copepod *Oithona* spp. make up 97.2% and 98.7% of the total copepod abundance at Loch Ewe and Stonehaven respectively (Cook et al., 2010). Other life-forms proposed for MSFD monitoring are large (adult size > 2mm) and small (adult size < 2mm) copepods. *Calanus* spp. made up 96.3% and 97.2% of the large copepod abundance at Loch Ewe and Stonehaven respectively up to the end of 2013. *Acartia clausi*, *Centropages* spp., *Paracalanus parvus*, *Pseudocalanus* spp., *Temora longicornis* and *Oithona* spp. made up 97.9% and 98.7% of the small copepod abundance at Loch Ewe and Stonehaven respectively over the same time periods.

Calanus

In Scottish waters, the important copepod genus *Calanus* is represented by two congeneric species: the artic-boreal *C. finmarchicus* which is at the southern limit of its distribution in the NE Atlantic (peak abundances occur between 6 to 11°C (Helaouët and Beaugrand 2007)) and *C. helgolandicus* which is towards the northern limit of its distribution (peak abundances from 11 to 16°C (Helaouët and Beaugrand 2007)). Historically, *C. finmarchicus* has been the dominant *Calanus* species in most of the North Atlantic and is probably the most intensively studied species of copepod because of their importance as food to the larvae of commercially important spring spawning fish species (Cushing 1990). Recent studies based on CPR data have shown that the abundance of *C. finmarchicus* is declining in the northern North Sea as their geographic distribution is shifting north (Chust et al., 2014b, Hinder et al., 2014) and the percent ratio of *C. finmarchicus* and the more southerly *C. helgolandicus* has been proposed as a useful indicator of North Sea warming (Edwards et al., 2013). *C. finmarchicus* is not resident in shallow coastal and North Sea waters all year round as they overwinter in deep water (>500m) as stage C4-5 (Heath et al., 2004). Results are presented for copepodite stages 5 and 6 as it is only in these stages that it is possible to distinguish *C. finmarchicus* and *C. helgolandicus*.

Centropages

The genus *Centropages* is also represented by two congeneric species in UK waters: the cold-temperate neritic *C. hamatus* which is resident in the North Sea and the more oceanic *C. typicus* which is considered an indicator of temperate Atlantic water (See reviews by Fransz et al., 1991, Halsband-Lenk et al., 2002). *C. hamatus* is known to overwinter using resting eggs (Engel and Hirche 2004) but there is no evidence that *C. typicus* does the same (See review by Ianora et al., 2007).

Halsband-Lenk et al., (2002) determined the optimal reproductive thermal temperature to be 12.5°C for *C. hamatus* and 20°C for *C. typicus* from the North Sea whilst a review by Bonnet et al (2007) concluded that temperatures above 10°C for *C. hamatus* and 15°C for *C. typicus* are optimal for reproduction.

Acartia clausi

Acartia clausi is by far the dominant species in this genus in Scottish waters, but other representatives seen at Stonehaven and Loch Ewe include *A. longiremis*, *A. bifilosa* and *A. discaudata*. Although species of *Acartia* are known to produce resting eggs (reviewed by Marcus 1996) there is no evidence that *A. clausi* do so in the North Sea (Engel and Hirche 2004). Halsband and Hirche (2001) suggest that *A. clausi* overwinters as adult females in the North Sea. *A. clausi* is tolerant of a wide range in temperature and salinity (Gaudy et al., 2000) but has shown evidence of temperature related shifts in seasonal timing (i.e. appearing earlier in warmer years) in the western English Channel (Atkinson et al., 2015).

Paracalanus parvus

Paracalanus parvus is a species complex found almost globally in coastal regions, but recent molecular studies have provided evidence that *P. parvus* s.s is in fact restricted to the NE Atlantic (Cornils and Held 2014). In UK waters there are a number of copepod species belonging to the families Clausocalanidae (e.g. *Clausocalanus* spp., *Ctenocalanus vanus* and *Pseudocalanus* spp.) and *Paracalanidae* (e.g. *Paracalanus parvus*) that are very difficult to distinguish in the juvenile stages. In many datasets they are often combined into a small calanoid copepod category, which in Scottish waters would be dominated by *Pseudocalanus* spp. and, as a result, there is very little information about *P. parvus* dynamics in the NE Atlantic.

Pseudocalanus spp.

Pseudocalanus spp. is another well studied genus of copepod as it is one of the most common copepods in the N. Atlantic and North Sea (see review by Corkett and McLaren 1978) and thought to be an important copepod for larval fish survival (Beaugrand et al., 2003). *Pseudocalanus* is a genus of copepod that carries its eggs in egg sacs until they hatch instead of releasing them directly into the water column. There are a number of different species of *Pseudocalanus* that are very hard to distinguish morphologically (Frost 1989). Historically, it had been thought that only *P. elongatus* was present in the North Atlantic and North Sea but recent molecular studies have revealed the presence of *P. moultoni* (Aarbakke et al., 2011, Laakmann et al., 2013) and it is possible that *P. acuspes* could also be found in Scottish waters (Aarbakke et al., 2014). *P. elongatus* has shown evidence of temperature related shifts in seasonal timing (i.e. appearing earlier in warmer years) in the western English Channel (Atkinson et al., 2015) but Klein Breteler et al (1995) found that mortality of North Sea *P. elongatus* was higher at 20°C compared to 15°C.

Temora longicornis

Temora longicornis is also a well-studied and abundant copepod species with a widespread North Atlantic distribution, and is the only representative of this genus known to be found in Scottish waters. Other members of the family Temoridae are present but tend to have a more estuarine distribution. *T. longicornis* has been found to be fairly tolerant to changes in temperature up to 22°C with no clear optimum (Halsband-Lenk et al., 2002). *T. longicornis* is known to be able to produce resting eggs (Lindley 1990) but has also been observed to reproduce all year round in the southern North Sea (Halsband and Hirche 2001, Halsband-Lenk et al., 2004) and eastern Irish Sea (Castellani and Altunbas 2006) and nauplii have been observed during winter in Loch Striven (Marshall 1949) and Northumberland coastal waters (Evans 1977).

Oithonidae

The Oithonidae, and especially those of the genus *Oithona*, are considered one of the most widespread, important and yet understudied group of copepods in the world (Gallienne and Robins 2001, Dahms et al., 2015), although they form an important component of the North Sea food web (Nielsen and Sabatini 1996). The Oithonidae carry their eggs in egg sacs until they hatch instead of releasing them directly into the water column. They are tolerant of a wide range of temperatures (e.g. egg hatching rates have been measured between -1 to 20°C (Nielsen et al., 2002)) and have a very low metabolic rate compared to other similarly sized copepods (Castellani et al., 2005). This is thought to give them an advantage in low food conditions for example during winter. There are a number of different species of Oithonidae that are very similar morphologically so they are not distinguished during the routine analysis at Stonehaven and Loch Ewe. The most common species found is *Oithona similis* but others are regular members of the North Atlantic zooplankton community (e.g. *Oithona nana*, *Oithona plumifera*).

Benthic, Decapod, Bivalve and Barnacle Larvae Biomass

Most marine organisms have larval stages that spend time in the plankton (meroplankton). The meroplankton are one of the life-forms proposed as an indicator for the pelagic habitat under the MSFD by the UK and OSPAR (Defra 2014, Scherer et al., 2015). The benthic larvae that are seen in the plankton at Stonehaven and Loch Ewe include the larvae of most of the animals that can be seen living on the sea floor in Scottish waters, e.g. barnacles, worms, crabs, starfish and shellfish. The decapod larvae found at Stonehaven and Loch Ewe, which include commercially important species of crabs and lobster, have been relatively well studied and their planktonic and settlement seasonal cycles and interannual variation described (Pan and Hay 2010, Pan et al., 2011a, Pan et al., 2011b). These studies concluded that there was high interannual variability in the abundance of decapod larvae relating to chlorophyll availability and water temperature. However, it is time-consuming to identify decapod larvae to species so this is not done routinely. Bivalve larvae and barnacle larvae are also extremely difficult to identify to species under a binocular microscope so this is not done as part of the routine sample analysis at Stonehaven and Loch Ewe. The bivalve larvae found here will include commercially important species such as mussels and scallops. Most bivalve

larvae generally appear in the plankton during either optimum food or temperature conditions for a particular species (Philippart et al., 2014). It is thought that the release of barnacle larvae is highly coupled with phytoplankton bloom conditions (Starr et al., 1991).

Cnidaria Biomass

Many Cnidaria are only abundant seasonally as they live as sexually reproducing medusa for only a few weeks or months. The rest of the life cycle is a long lived colonial polyp stage which lives and grows attached to a seabed or substrate. The animals that we commonly think of as jellyfish are the Scyphozoa. It is thought that jellyfish blooms are increasing in size and number due to climate change and ecosystem degradation (Attrill et al., 2007, Purcell et al., 2007, Richardson et al., 2009, Lynam et al., 2011) but, in fact, recent publications have concluded that there is not enough data available to understand jellyfish ecology, especially about where and when they occur (Lynam et al., 2010, Condon et al., 2012, Gibbons and Richardson 2013, Hosia et al., 2014, Pikesley et al., 2014), and that factors affecting the benthic stage may be more important (Lucas et al., 2012, Makabe et al., 2014, Marques et al., 2015, Van Walraven et al., 2015). The Cnidaria found in mesozooplankton samples are dominated by a number of other species not commonly thought of as jellyfish, including the small hydrozoan medusae *Obelia* spp., *Clytia hemisphaerica*, *Lizzia blondina*, *Euphysa* spp., *Rathkea octopunctata*, *Bougainvillia* spp., *Sarsia* spp., *Hydractinia* spp., *Phialella quadrata*, the anthozoan *Cerianthus* spp. and the siphonophores which form floating colonies. Gelatinous zooplankton are one of the life-forms proposed as an indicator for the pelagic habitat under the MSFD by the UK and OSPAR (Defra 2014, Scherer et al., 2015).

Calcifying Plankton Biomass

There is increasing interest in the possible effects of ocean acidification on marine animals that rely on calcification as part of their physiology. Increased acidity dissolves, and can make it harder to form, structures such as shells and calcareous skeletons (Fabry et al., 2008). However, recent studies have concluded that the effects of temperature are more important on the abundance of calcifying plankton than ocean acidification (Beaugrand et al., 2013). Animals in this category are planktonic snails (gastropod larvae and the holoplanktonic pteropods *Limacina retroversa* and *Clione limacina* which has no shell has an adult), bivalve larvae and starfish larvae (which form calcareous skeletons).

12.2 Methods

Sample Collection and Storage

Zooplankton samples were collected using 40 cm diameter bongo nets fitted with 200 µm mesh. The nets were hauled vertically from near bottom (45 m at Stonehaven and 35 m at Loch Ewe) to surface at a speed of 2-3 $m.s^{-2}$. The samples were immediately preserved in 4% borax buffered formaldehyde for later analysis in the laboratory.

Sample Processing, Analysis and Archiving

Zooplankton samples were analysed in the laboratory using a Zeiss Stemi-11 stereomicroscope. Larger zooplankton categories (such as *Calanus* spp., chaetognaths, jellyfish, euphausiids etc.) were identified and enumerated from the whole sample. The remaining zooplankton categories were identified and enumerated from a series of subsamples (of variable volume depending on concentration of animals but a minimum 2.5% of the whole sample) so that at least 100 animals were recorded. All copepods were identified to the lowest taxonomic level possible, whilst others animals were grouped into categories. Zooplankton counts were converted to abundance using filtered volume estimated from vertical distance towed, net mouth area and a 70% filtration efficiency (MSS unpublished data). Zooplankton abundance was converted to biomass using historical dry weight data measured from the North Sea and North Atlantic (Hay et al., 1988, Hay et al., 1991, Marine Scotland Science, unpublished data). If there was no dry weight data for a particular species or stage, the dry weight of another similar animal was used (e.g. values for *Eucalanus elongatus* were used for *Subeucalanus crassus*). The samples are archived for future use.

Data Quality, Handling and archiving

Zooplankton quality assurance follows the MSS joint code of practice and analysts participate in NMBAQC external identification ring trials as they arise. All calculations and data entry into the zooplankton database are double checked by a second analyst. The calculated abundances of each zooplankton category are checked against a nine week running mean and any value that is greater than ±3 standard deviations from the mean is checked and, if necessary, the sample is reanalysed.

Sample information, zooplankton count and abundance data from the species analyses, and zooplankton biomass measurements are held in dedicated Microsoft Access databases for Stonehaven and Loch Ewe. Only authorised staff members are able to edit information on the databases.

12.3 Results - Total Copepod Biomass

Zooplankton sampling at Loch Ewe began in April 2002, therefore, the figures that show annual values (b, c) begin at 2003 whereas those that show monthly values also (a, d) incorporate the 2002 data.

The seasonality in total copepod biomass observed at Loch Ewe (Figure 12.1a) is typical for zooplankton grazers in the NE Atlantic. Biomass began to increase in March and high values were generally observed between April/May and September/October. Copepod biomass was usually slightly higher between July and September than the rest of the growing season, although variability within May and June was very high and peak biomass levels occurred in these months in some years. There was no trend in the normalised annual anomalies (Figure 12.1c), which oscillated between positive and negative anomalies since 2008.

At Stonehaven, total copepod biomass began to increase in April, a month later than was seen at Loch Ewe, and increased at a slower rate than at Loch Ewe until peak biomass values were observed around August (Figure 12.2a). The differences between Stonehaven and Loch Ewe were probably due to the lower winter and spring water temperatures seen at Stonehaven (Figures 5.16a and 5.8a). Copepod biomass at Stonehaven declines in June, but this month was also highly variable. There was a positive trend in the normalised annual anomalies in copepod biomass between 1999 and 2008 (Figure 12.2d). Since 2008 the annual anomalies were all low positive or negative, but without the sharp oscillations seen at Loch Ewe.

12.4 Plots – Total Copepod Biomass

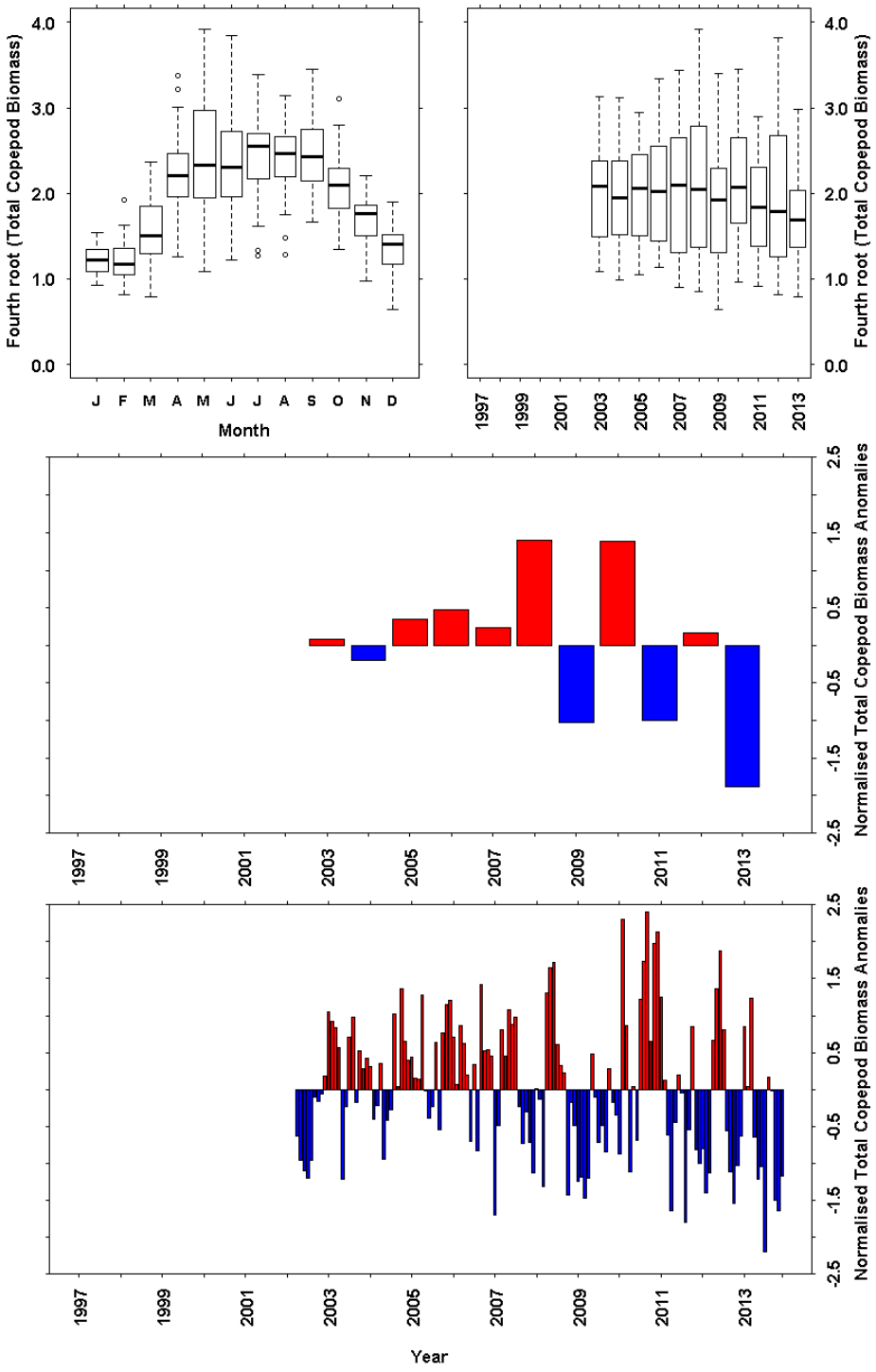

Figure 12.1 Total Copepod Biomass (mg dry weight m^{-3}) data from the long term monitoring site at Loch Ewe. a) Monthly boxplot of total copepod biomass data. b) Annual boxplot of total copepod biomass data. c) Annual mean anomaly time series d) Monthly mean anomaly time series. Sampling began in April 2002. Figures b and d only include data from January 2003. The full data set was used as the base period for the anomaly calculations.

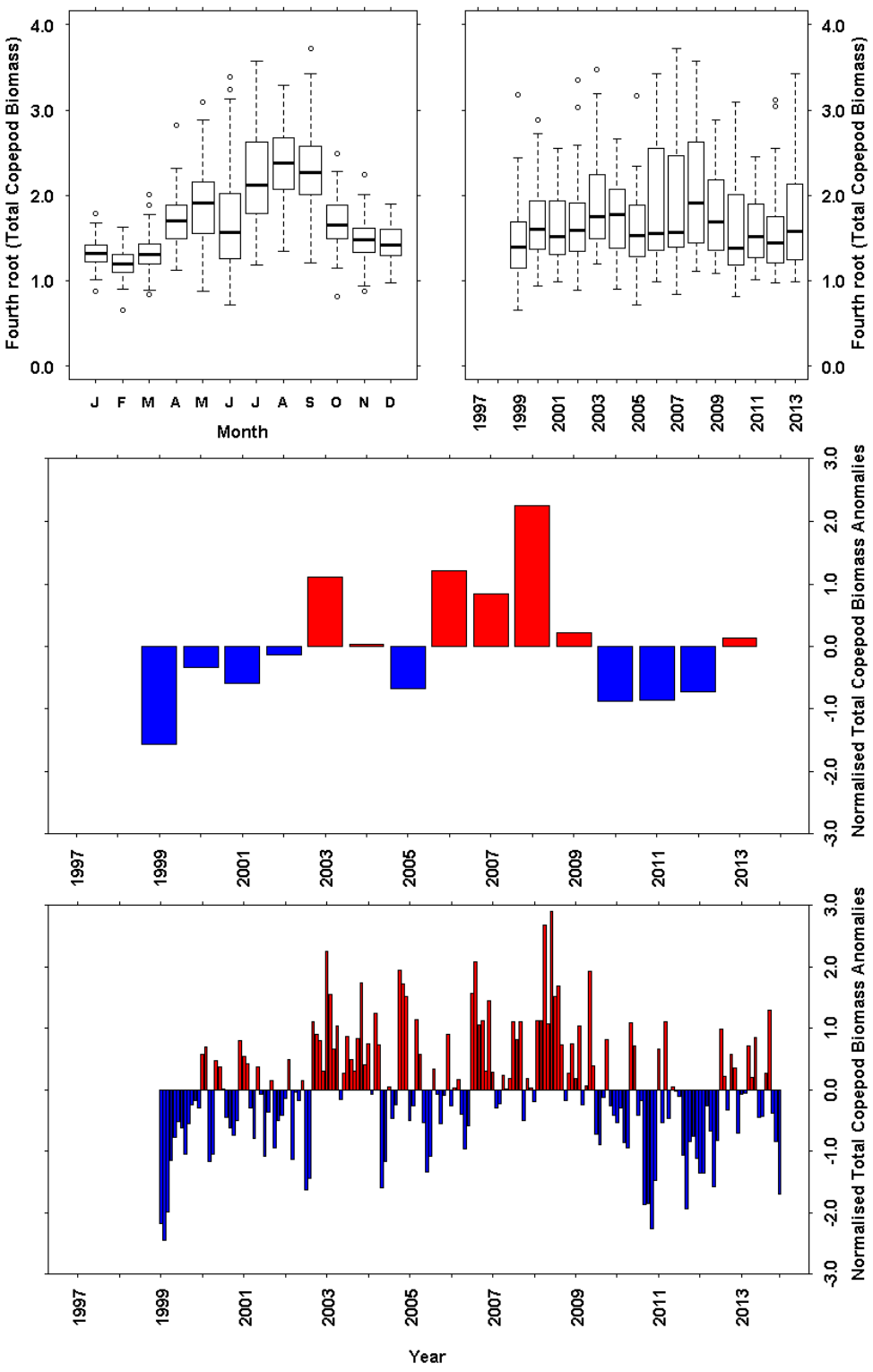

Figure 12.2 Total Copepod Biomass (mg dry weight m^{-3}) data from the long term monitoring site at Stonehaven. a) Monthly boxplot of total copepod biomass data. b) Annual boxplot of total copepod biomass data. c) Annual mean anomaly time series d) Monthly mean anomaly time series. The full data set was used as the base period for the anomaly calculations.

12.5 Results - *Calanus finmarchicus* Stages C5-6 Biomass

At Loch Ewe there was very little *C. finmarchicus* present in the water column between September and February (Figure 12.3a), although biomass during autumn was more variable than during winter. The levels of *C. finmarchicus* biomass recorded at Loch Ewe were not high. They began to increase in March and remained elevated until August. The month of peak *C. finmarchicus* biomass was usually May, but this was also the most variable month. Biomass declined slightly between May and July before increasing again in August. A higher median value of *C. finmarchicus* biomass was observed between 2006 to 2011 compared to the rest of the time series (Figure 12.3b).

A positive trend in normalised annual anomalies was observed until 2008 (Figure 12.3c). Between 2006-2009 almost all monthly anomalies were positive between July 2006 and June 2009 resulting in a higher annual anomaly. The only exceptions were January and February 2007 and September 2008.

At Stonehaven, the seasonal cycle in *C. finmarchicus* biomass was similar to that seen at Loch Ewe. Biomass began to increase in March and peaked in May (Figure 12.4a), but then the biomass decreased slowly and remained at intermediate levels until December. There was a brief dip in biomass in June before a small late summer peak in July. Extremely low *C. finmarchicus* biomass was observed during 2010 (Figure 12.4b).

12.6 Plots - *Calanus finmarchicus* Stages C5-6 Biomass

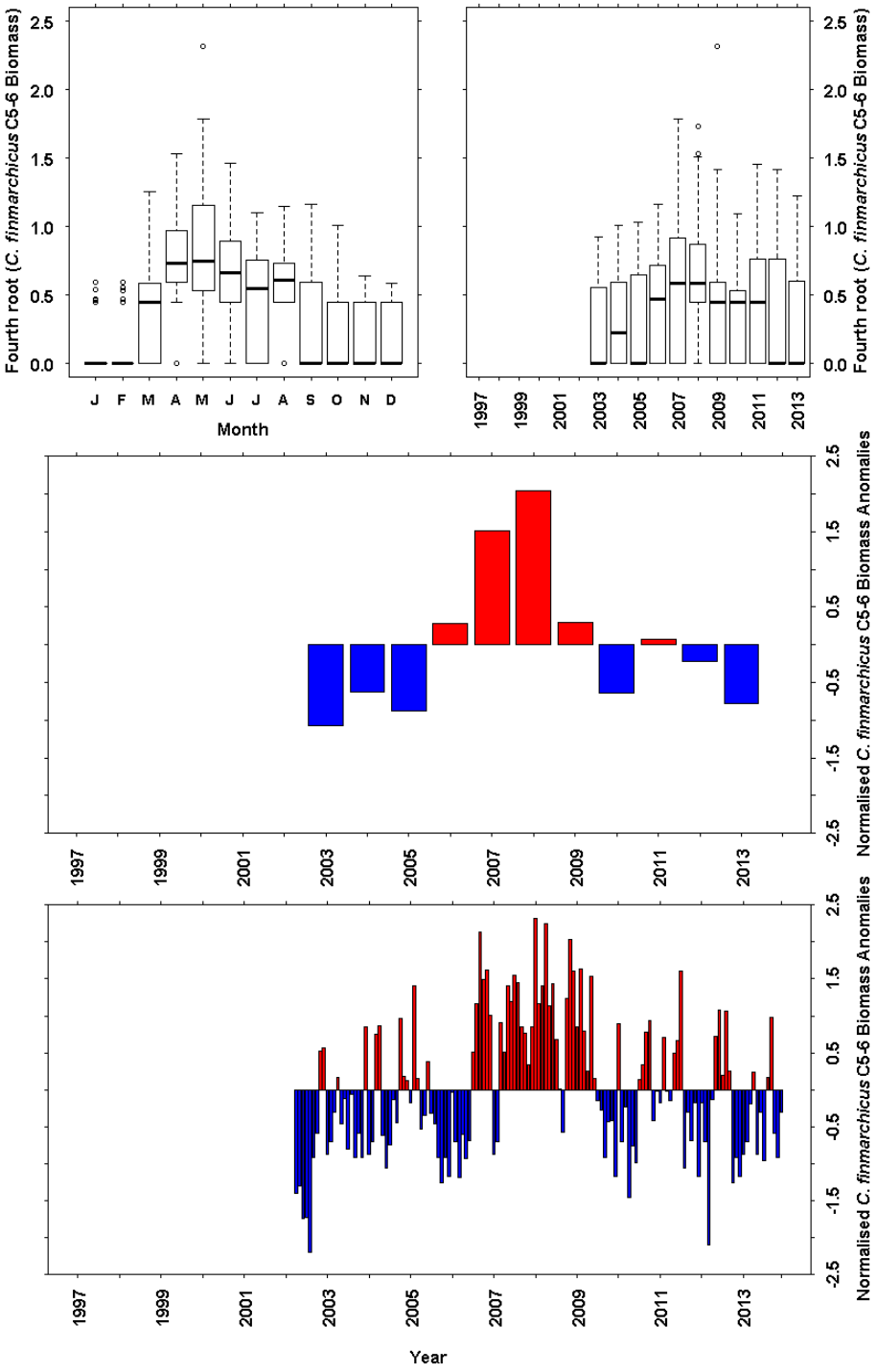

Figure 12.3 *Calanus finmarchicus* Stages C5-6 Biomass (mg dry weight m^{-3}) data from the long term monitoring site at Loch Ewe. a) Monthly boxplot of *C. finmarchicus* stages C5-6 biomass data. b) Annual boxplot of *C. finmarchicus* stages C5-6 biomass data. c) Annual mean anomaly time series d) Monthly mean anomaly time series. Sampling began in April 2002. Figures b and d only include data from January 2003. The full data set was used as the base period for the anomaly calculations.

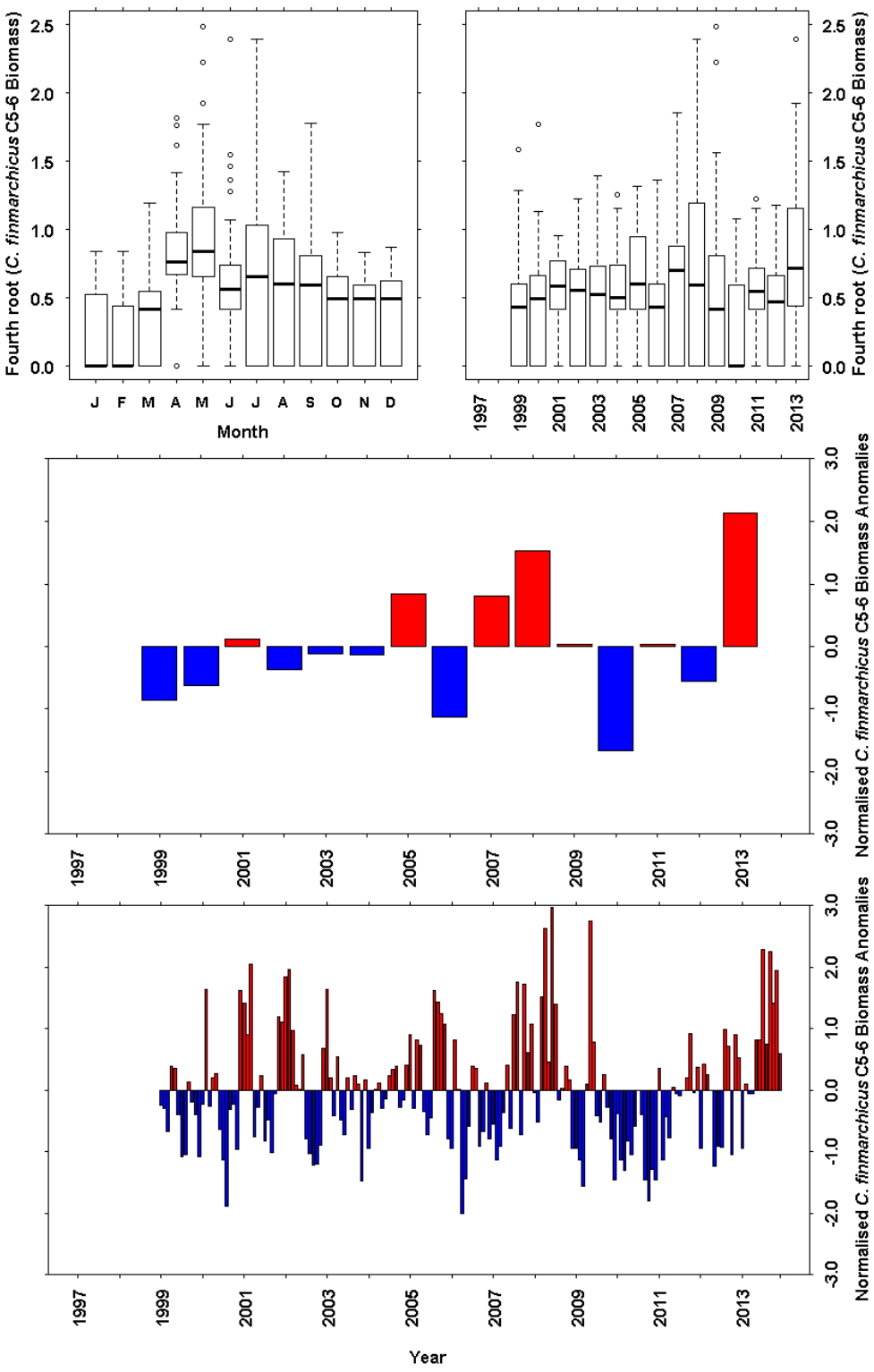

Figure 12.4 *Calanus finmarchicus* Stages C5-6 Biomass (mg dry weight m^{-3}) data from the long term monitoring site at Stonehaven. a) Monthly boxplot of *C. finmarchicus* stages C5-6 biomass data. b) Annual boxplot of *C. finmarchicus* stages C5-6 biomass data. c) Annual mean anomaly time series d) Monthly mean anomaly time series. The full data set was used as the base period for the anomaly calculations.

12.7 Results - *Calanus helgolandicus* Stages C5-6 Biomass

At Loch Ewe *C. helgolandicus* was present at low levels all year round with two distinct, almost equally sized, peaks of biomass occurring in April-May and August-October (Figure 12.5a). 2013 was a year of extremely low *C. helgolandicus* biomass compared to the rest of the time series (Figure 12.5b). Normalised annual anomalies were all positive between 2003-2008 (Figure 12.5c). The year 2013 was the only year where all normalised monthly anomalies were negative (Figure 12.5d).

At Stonehaven, the seasonal cycle in *C. helgolandicus* biomass was very different to that seen at Loch Ewe (Figure 12.6a). *C. helgolandicus* was present at low levels during winter. There was a small spring increase in April-May but then biomass was low and highly variable in June-July before increasing to the main biomass peak in August-September. This autumn peak in biomass was nearly double that observed in Loch Ewe. Relatively low average *C. helgolandicus* biomass was observed at Stonehaven between 2009-2011 (Figure 12.6b) with very low variability. These years were also a period of negative annual anomalies (Figure 12.6c) due to most of the individual months having negative anomalies (Figure 12.6d).

12.8 Plots - *Calanus helgolandicus* Stages C5-6 Biomass

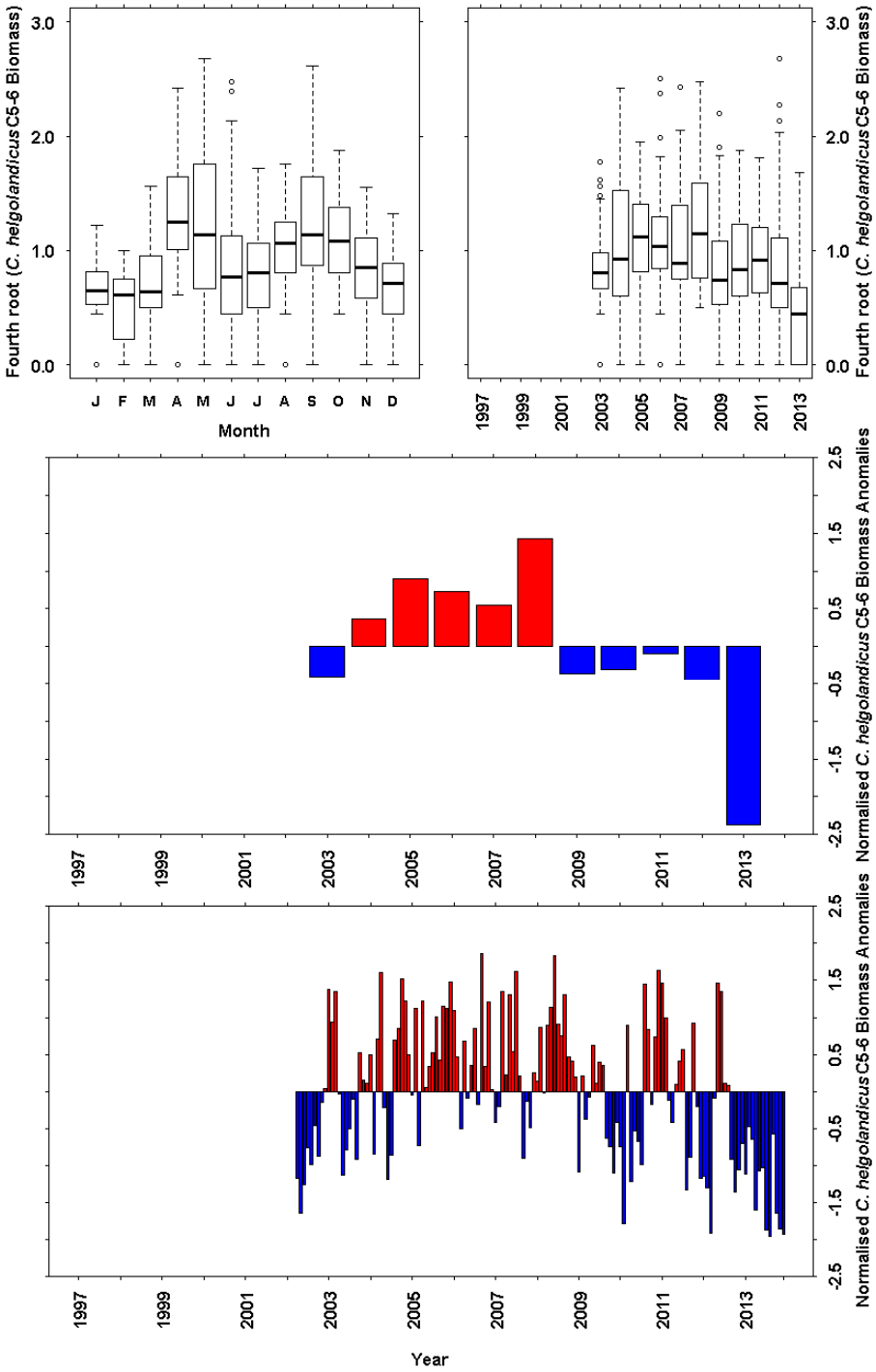

Figure 12.5 *Calanus helgolandicus* Stages C5-6 Biomass (mg dry weight m^{-3}) data from the long term monitoring site at Loch Ewe. a) Monthly boxplot of *C. helgolandicus* stages C5-6 biomass data. b) Annual boxplot of *C. helgolandicus* stages C5-6 biomass data. c) Annual mean anomaly time series d) Monthly mean anomaly time series. Sampling began in April 2002. Figures b and d only include data from January 2003. The full data set was used as the base period for the anomaly calculations.

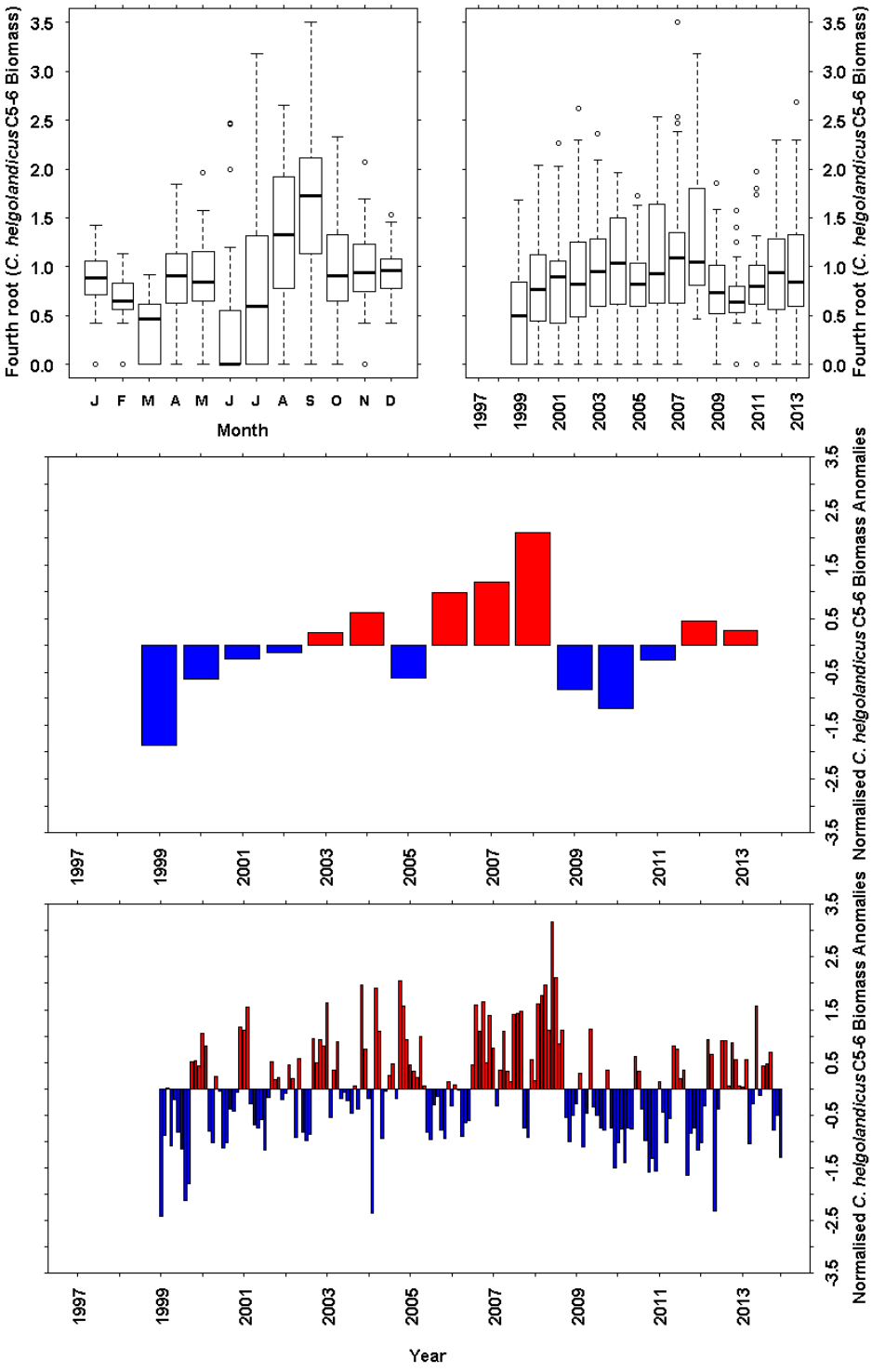

Figure 12.6 *Calanus helgolandicus* Stages C5-6 Biomass (mg dry weight m^{-3}) data from the long term monitoring site at Stonehaven. a) Monthly boxplot of *C. helgolandicus* stages C5-6 biomass data. b) Annual boxplot of *C. helgolandicus* stages C5-6 biomass data. c) Annual mean anomaly time series d) Monthly mean anomaly time series. The full data set was used as the base period for the anomaly calculations.

12.9 Results - *Centropages hamatus* Stages C1-6 Biomass

At Loch Ewe *C. hamatus* was virtually absent during November and January, and was never recorded in December or February (Figure 12.7a). Biomass began to increase in March, peaked in June-July and then decreased until October, although August-October showed relatively high variability compared to the spring and summer months. The annual biomass of *C. hamatus* at Loch Ewe was fairly low and variable, and in the majority of years the median was zero (Figure 12.7b). The years 2003, 2007, 2012 and 2013 were exceptions to this, whilst 2009 was a year of exceptionally low biomass. There was a period of negative annual anomalies between 2004-2010 (Figure 12.7c).

At Stonehaven, the seasonal cycle in *C. hamatus* biomass was very similar to that seen at Loch Ewe. *C. hamatus* was virtually absent during the winter months of December-February (Figure 12.8a). Biomass began to increase in March, peaked slightly later than Loch Ewe in July-August and then decreased until November. June and July were highly variable months. *C. hamatus* was more abundant annually at Stonehaven than at Loch Ewe. The year 2006 had a very low median biomass, but some extremely high values (Figure 12.8b). There was a period of low negative annual anomalies between 2004-2012 (Figure 12.8c).

12.10 Plots - *Centropages hamatus* Stages C1-6 Biomass

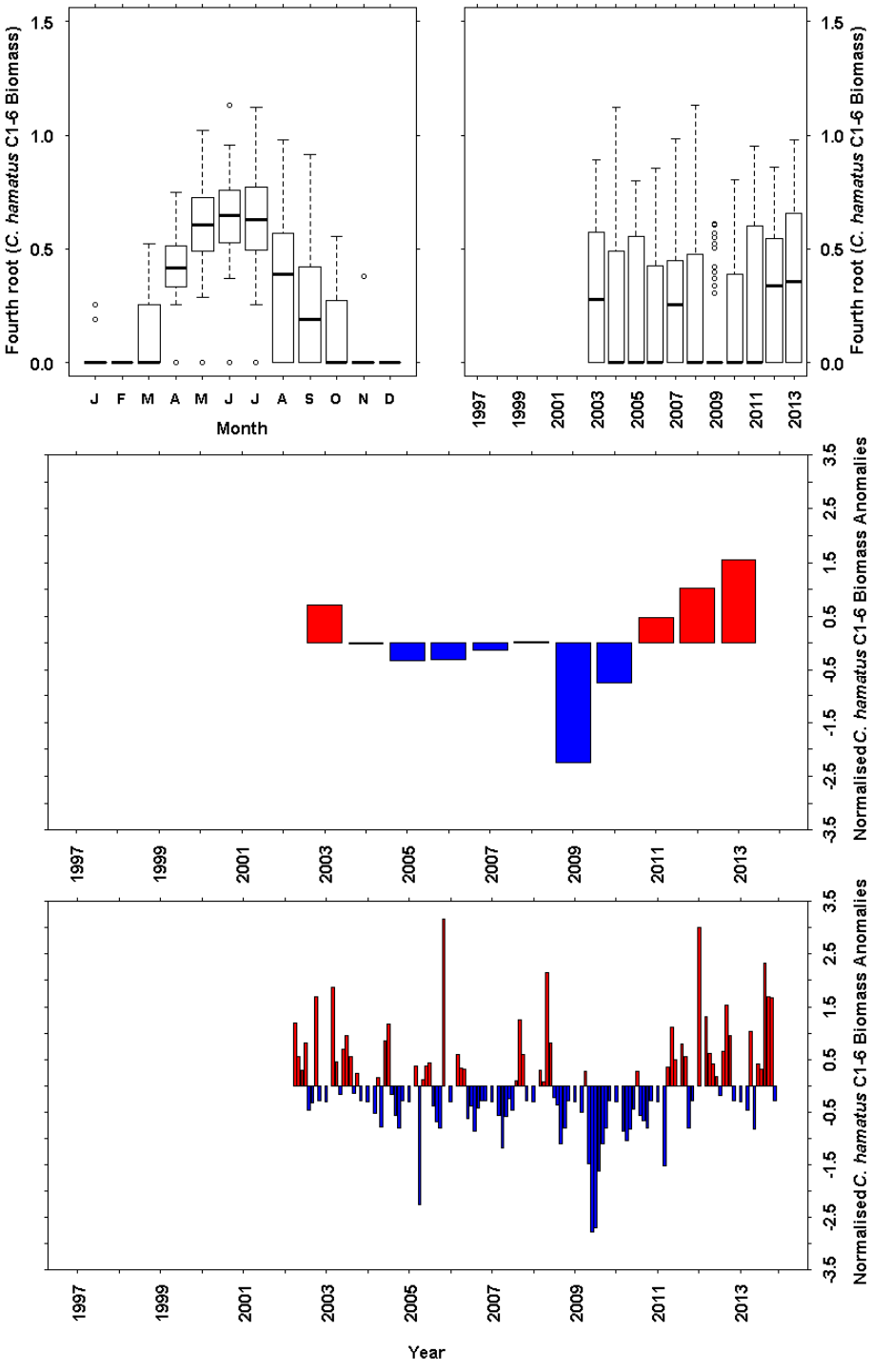

Figure 12.7 *Centropages hamatus* Stages C1-6 Biomass (mg dry weight m^{-3}) data from the long term monitoring site at Loch Ewe. a) Monthly boxplot of *C. hamatus* stages C1-6 biomass data. b) Annual boxplot of *C. hamatus* stages C1-6 biomass data. c) Annual mean anomaly time series d) Monthly mean anomaly time series. Sampling began in April 2002. Figures b and d only include data from January 2003. The full data set was used as the base period for the anomaly calculations.

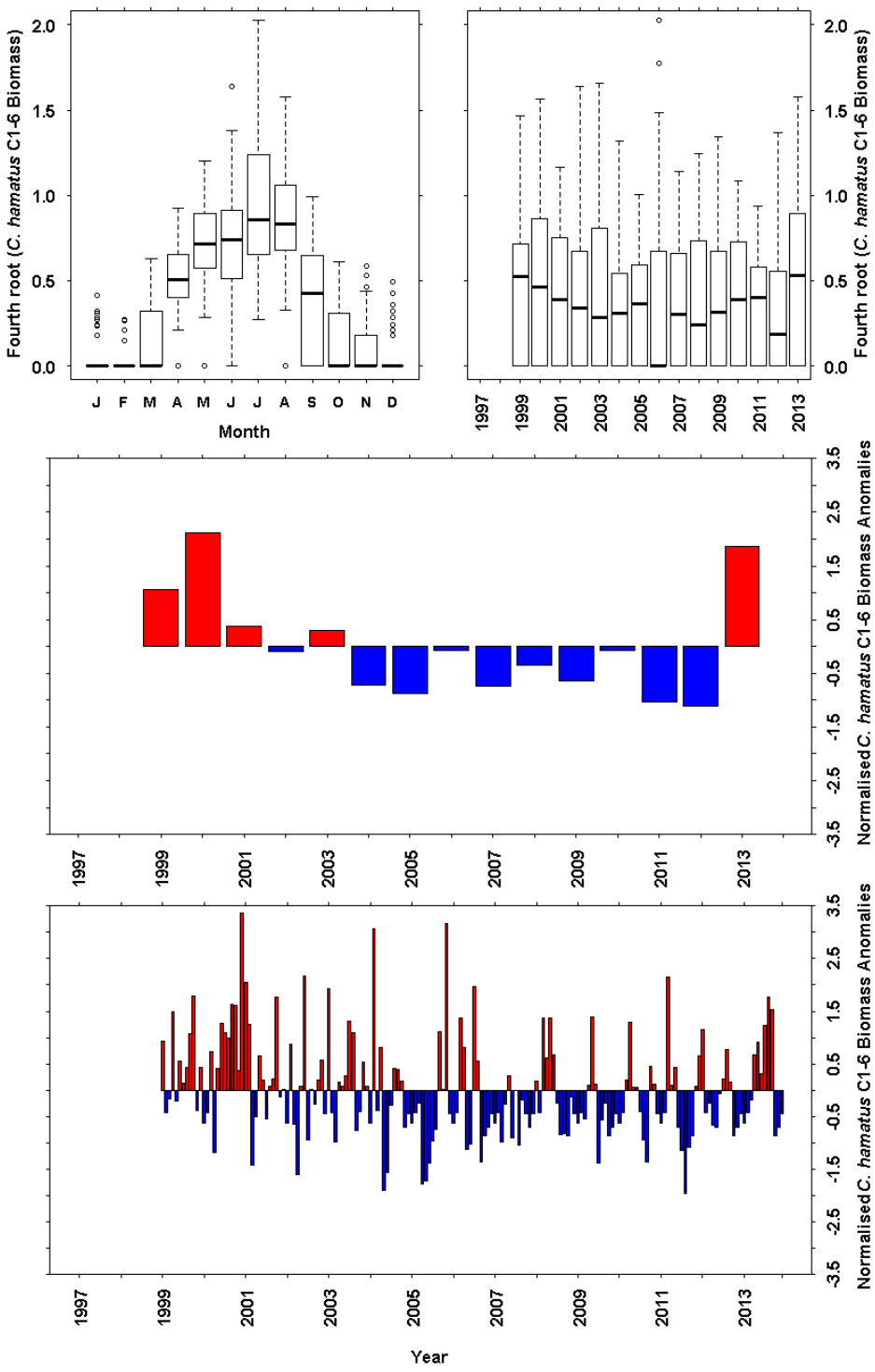

Figure 12.8 *Centropages hamatus* Stages C1-6 Biomass (mg dry weight m^{-3}) data from the long term monitoring site at Stonehaven. a) Monthly boxplot of *C. hamatus* stages C1-6 biomass data. b) Annual boxplot of *C. hamatus* stages C1-6 biomass data. c) Annual mean anomaly time series d) Monthly mean anomaly time series. The full data set was used as the base period for the anomaly calculations.

12.11 Results - *Centropages typicus* Stages C1-6 Biomass

At Loch Ewe *C. typicus* was virtually absent during February-March (Figure 12.9a). Biomass began to increase in April, peaked in September and then decreased until January, although variability was high in most months. The annual biomass of *C. typicus* at Loch Ewe (Figure 12.9b) was higher than that of *C. hamatus* (Figure 12.7b) but 2004 and 2012-2013 were years of low median annual biomass. There was a period of positive annual anomalies between 2005-2010 (Figure 12.9c) which coincided with the period of negative anomalies in *C. hamatus* biomass (Figure 12.7c).

At Stonehaven, the seasonal cycle in *C. typicus* biomass began later in the year than at Loch Ewe. *C. typicus* was virtually absent during the spring/summer months of March-June (Figure 12.10a). Biomass began to increase in July, peaked in the same month as Loch Ewe in September and then decreased until February. *C. hamatus* was more abundant annually at Stonehaven (Figure 12.10b) than *C. typicus* (Figure 12.8b). The period 1999-2000, 2002 and 2013 were years of low median biomass although 2013 also saw the highest outlying values. The highest median biomass was recorded in 2008(Figure 12.10b). There was a period of mostly positive annual anomalies since 2003 (Figure 12.10c) which coincided with the period of negative anomalies in *C. hamatus* (Figure 12.8c).

12.12 Plots - *Centropages typicus* Stages C1-6 Biomass

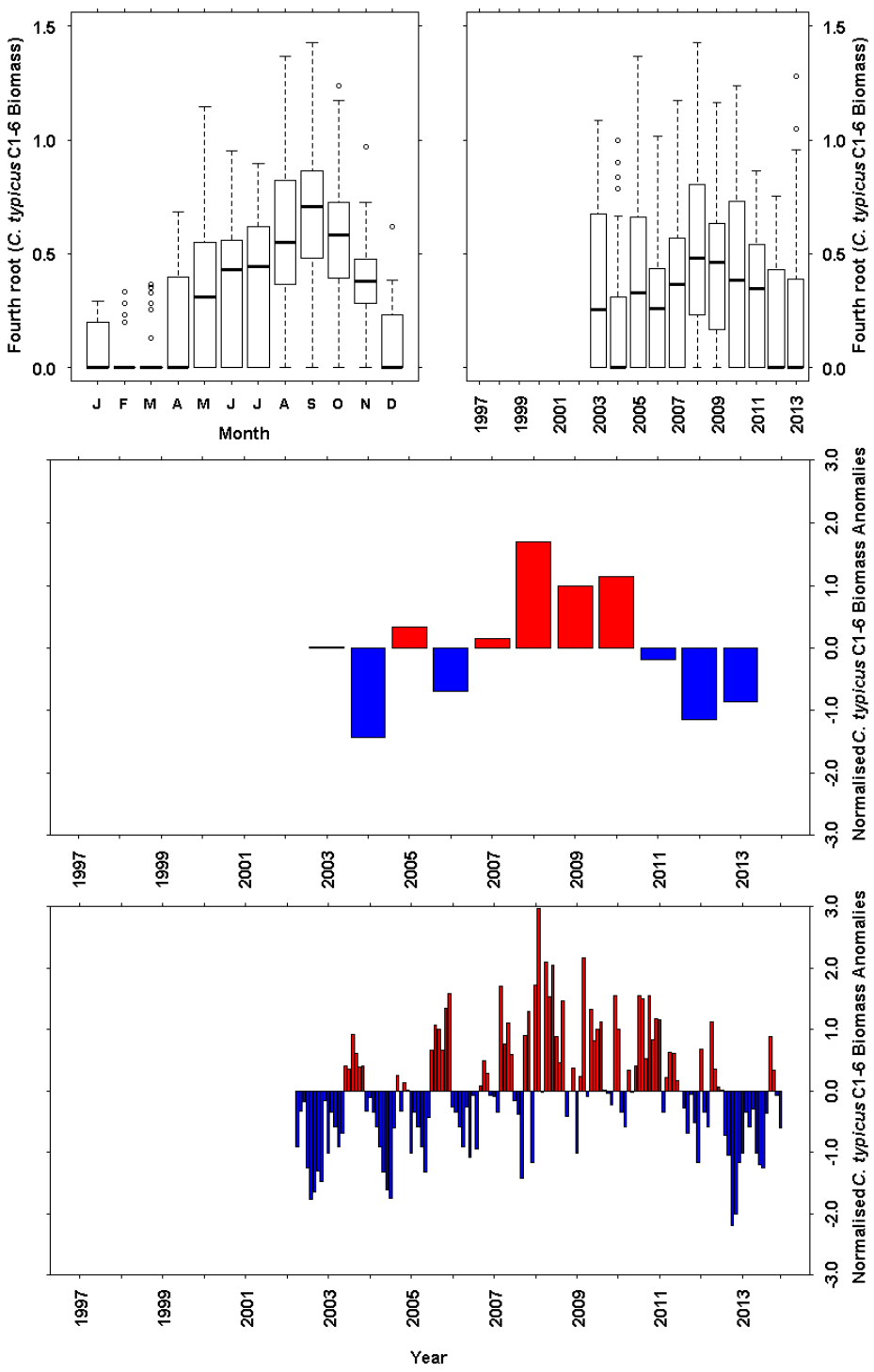

Figure 12.9 *Centropages typicus* Stages C1-6 Biomass (mg dry weight m^{-3}) data from the long term monitoring site at Loch Ewe. a) Monthly boxplot of *C. typicus* stages C1-6 biomass data. b) Annual boxplot of *C. typicus* stages C1-6 biomass data. c) Annual mean anomaly time series d) Monthly mean anomaly time series. Sampling began in April 2002. Figures b and d only include data from January 2003. The full data set was used as the base period for the anomaly calculations.

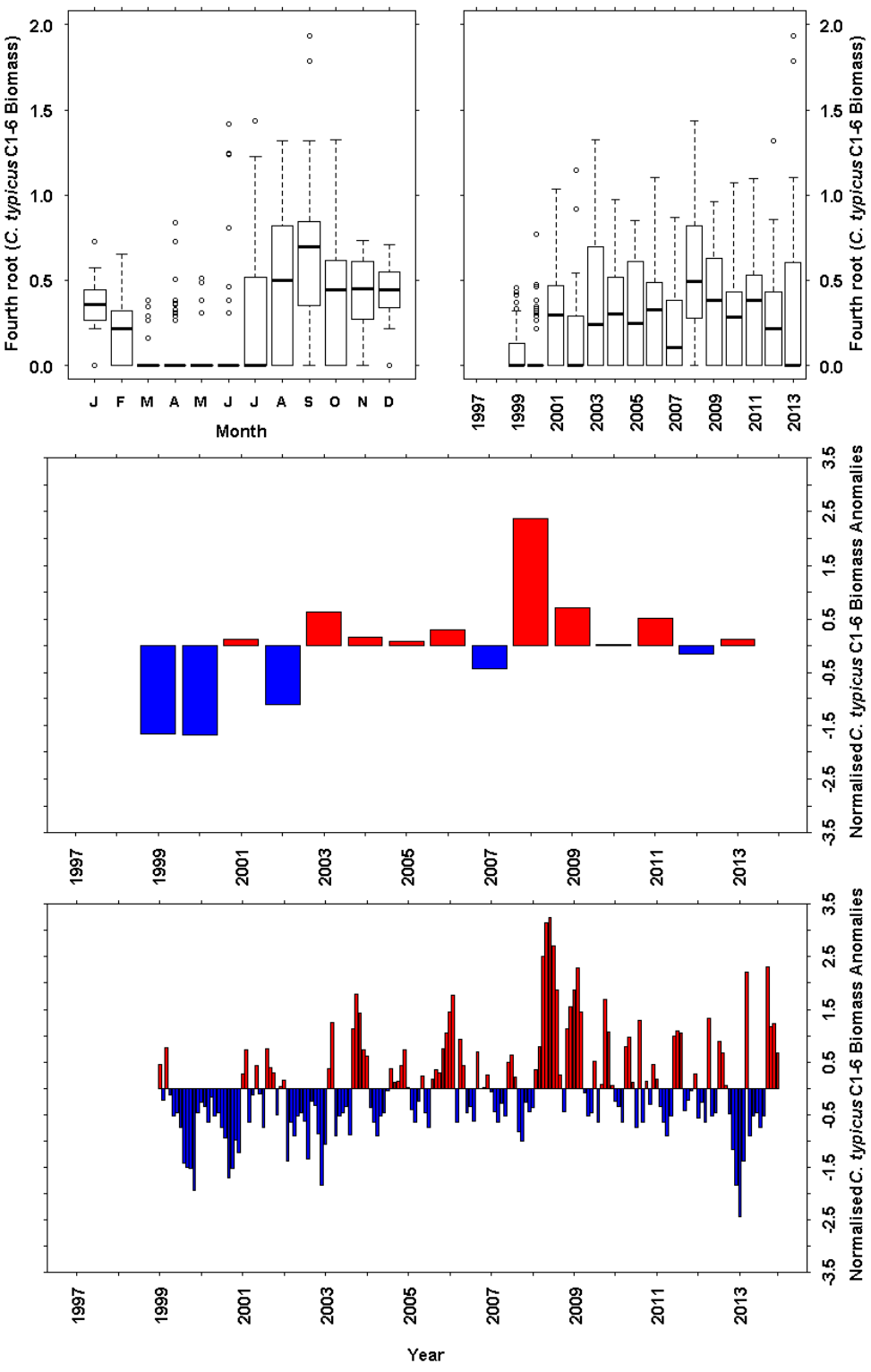

Figure 12.10 *Centropages typicus* Stages C1-6 Biomass (mg dry weight m^{-3}) data from the long term monitoring site at Stonehaven. a) Monthly boxplot of *C. typicus* stages C1-6 biomass data. b) Annual boxplot of *C. typicus* stages C1-6 biomass data. c) Annual mean anomaly time series d) Monthly mean anomaly time series. The full data set was used as the base period for the anomaly calculations.

12.13 Results - *Acartia clausi* Stages C1-6 Biomass

At Loch Ewe, *A. clausi* was present all year round (Figure 12.11a). Biomass started to increase from low winter levels in April and peaked in July. The median annual biomass and variability in annual biomass of *A. clausi* at Loch Ewe was fairly consistent, although 2008 was a year of higher median biomass and 2012-2013 were years of low median biomass (Figure 12.11b, 12.11d). The period 2006-2010 was a period of mostly positive annual anomalies (Figure 12.11c).

At Stonehaven, the seasonal cycle in *A. clausi* was almost identical to that seen at Loch Ewe but at slightly lower biomass levels. *A. clausi* was present at low levels throughout the winter (Figure 12.12a), began to increase in April and peaked in July. The annual biomass of *A. clausi* at Stonehaven was highly variable (Figure 12.12b). The years 2003 and 2010 were particularly variable whereas 2005 and 2011-2012 had low variability. A period of mostly positive annual anomalies (Figure 12.12c) was observed between 2006-2010 as at Loch Ewe, but seen in the context of the longer time series it appears to be part of broader fluctuations (Figure 12.12d).

12.14 Plots - *Acartia clausi* Stages C1-6 Biomass

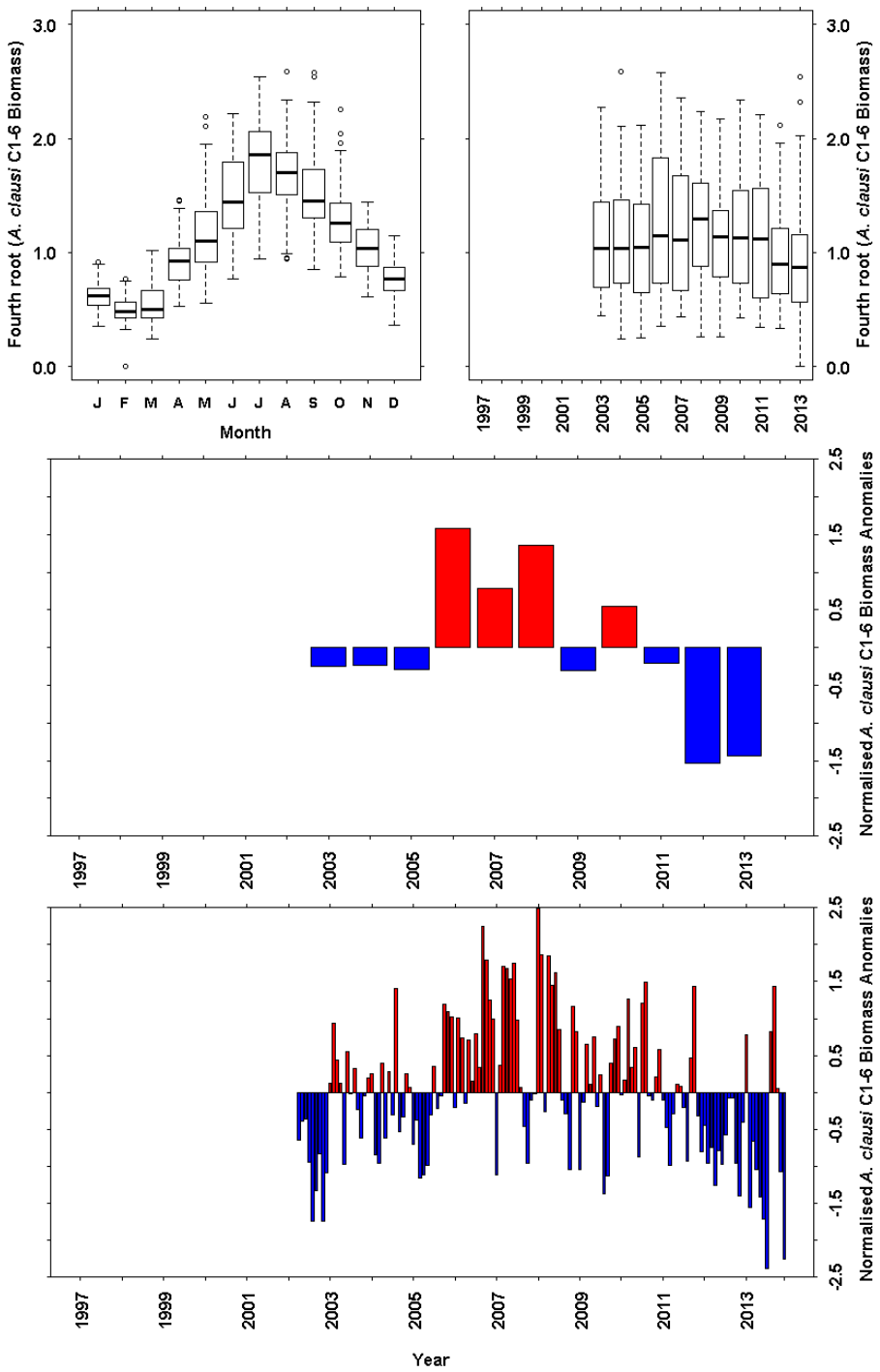

Figure 12.11 *Acartia clausi* Stages C1-6 Biomass (mg dry weight m^{-3}) data from the long term monitoring site at Loch Ewe. a) Monthly boxplot of *A. clausi* stages C1-6 biomass data. b) Annual boxplot of *A. clausi* stages C1-6 biomass data. c) Annual mean anomaly time series d) Monthly mean anomaly time series. Sampling began in April 2002. Figures b and d only include data from January 2003. The full data set was used as the base period for the anomaly calculations.

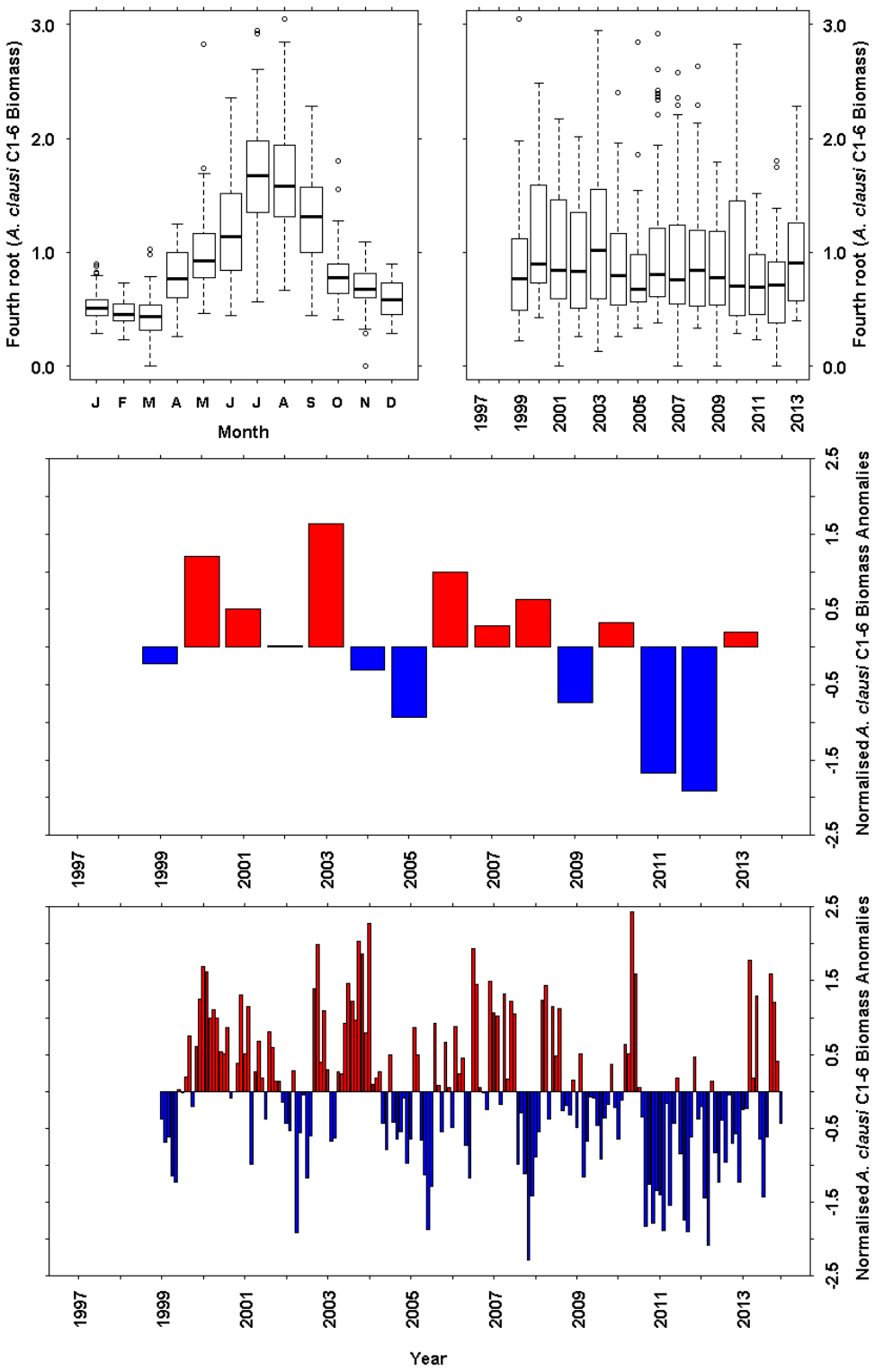

Figure 12.12 *Acartia clausi* Stages C1-6 Biomass (mg dry weight m^{-3}) data from the long term monitoring site at Stonehaven. a) Monthly boxplot of *A. clausi* stages C1-6 biomass data. b) Annual boxplot of *A. clausi* stages C1-6 biomass data. c) Annual mean anomaly time series d) Monthly mean anomaly time series.

12.15 Results - *Paracalanus parvus* Stages C1-6 Biomass

At Loch Ewe, low biomass of *P. parvus* was recorded during the winter months. Biomass began to increase between March and April (Figure 12.13a), peaking in September. Highmedian annual biomass were observed during 2003 and 2008 with high annual variability recorded during 2008 (Figure 12.13b). In contrast, 2013 was a year of very low median annual biomass.

At Stonehaven, *P. parvus* biomass was lower than at Loch Ewe but was it was recorded at this site all year round. Winter (November-January) median biomass levels were about the same as late spring (April-May) levels but there were dips in biomass in early spring (February-March) and summer (June-July) (Figure 12.14a). The peak biomass levels were reached in autumn (September-October). The annual median biomass of *P. parvus* at Stonehaven was variable (Figure 12.14b) but 2003 and 2008 were years of high median annual biomass and high positive annual anomalies (Figure 12.14c) as also seen at Loch Ewe. Low median annual biomass and a negative annual anomaly were also observed in 2013. The annual anomalies in *P. parvus* biomass increased between 1999-2003 and 2004-2008. The negative trend in annual anomalies from 2008-2013 seen at Loch Ewe was not as evident at Stonehaven.

12.16 Plots - *Paracalanus parvus* Stages C1-6 Biomass

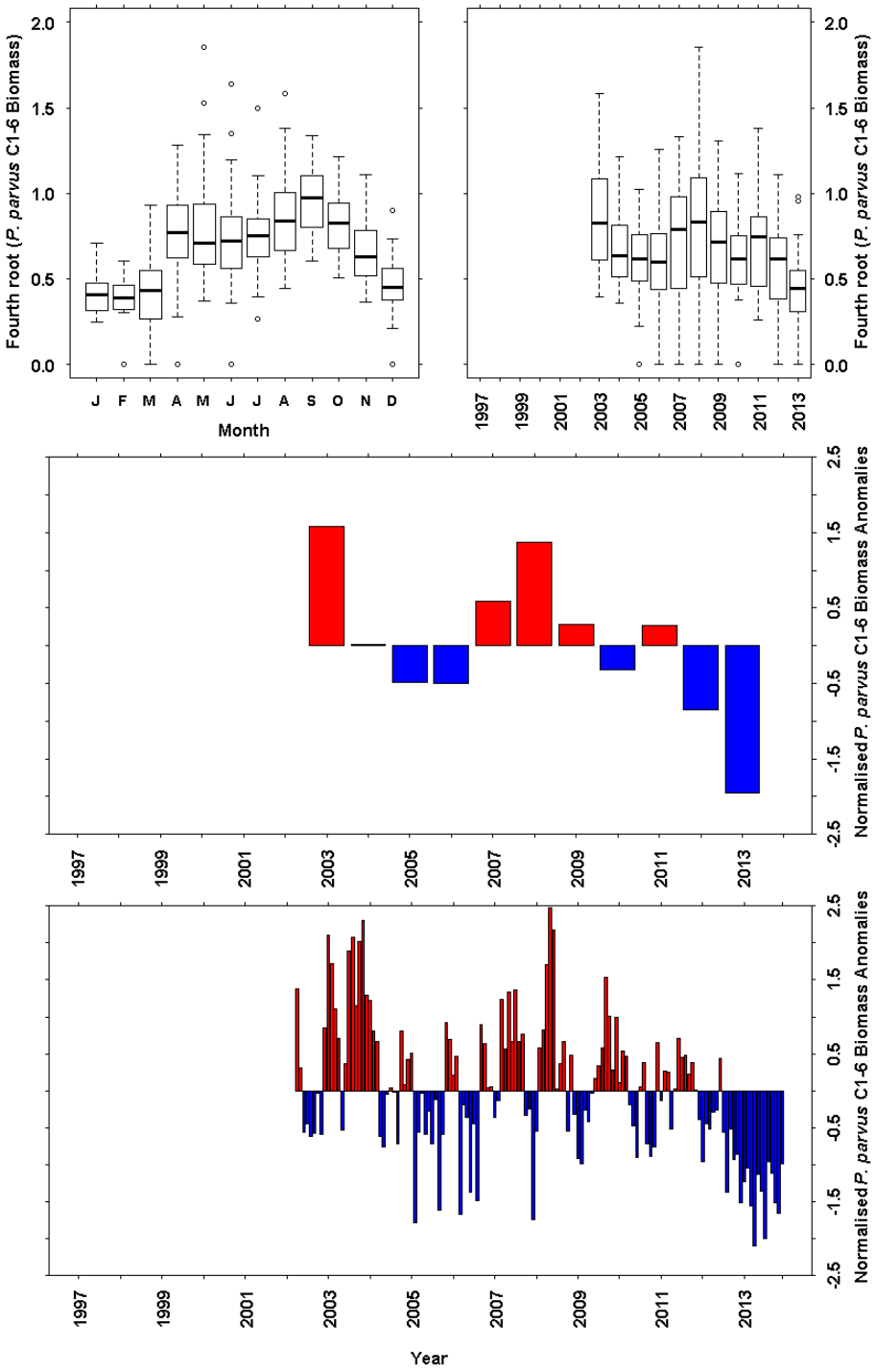

Figure 12.13 *Paracalanus parvus* Stages C1-6 Biomass (mg dry weight m^{-3}) data from the long term monitoring site at Loch Ewe. a) Monthly boxplot of *P. parvus* stages C1-6 biomass data. b) Annual boxplot of *P. parvus* stages C1-6 biomass data. c) Annual mean anomaly time series d) Monthly mean anomaly time series. Sampling began in April 2002. Figures b and d only include data from January 2003. The full data set was used as the base period for the anomaly calculations.

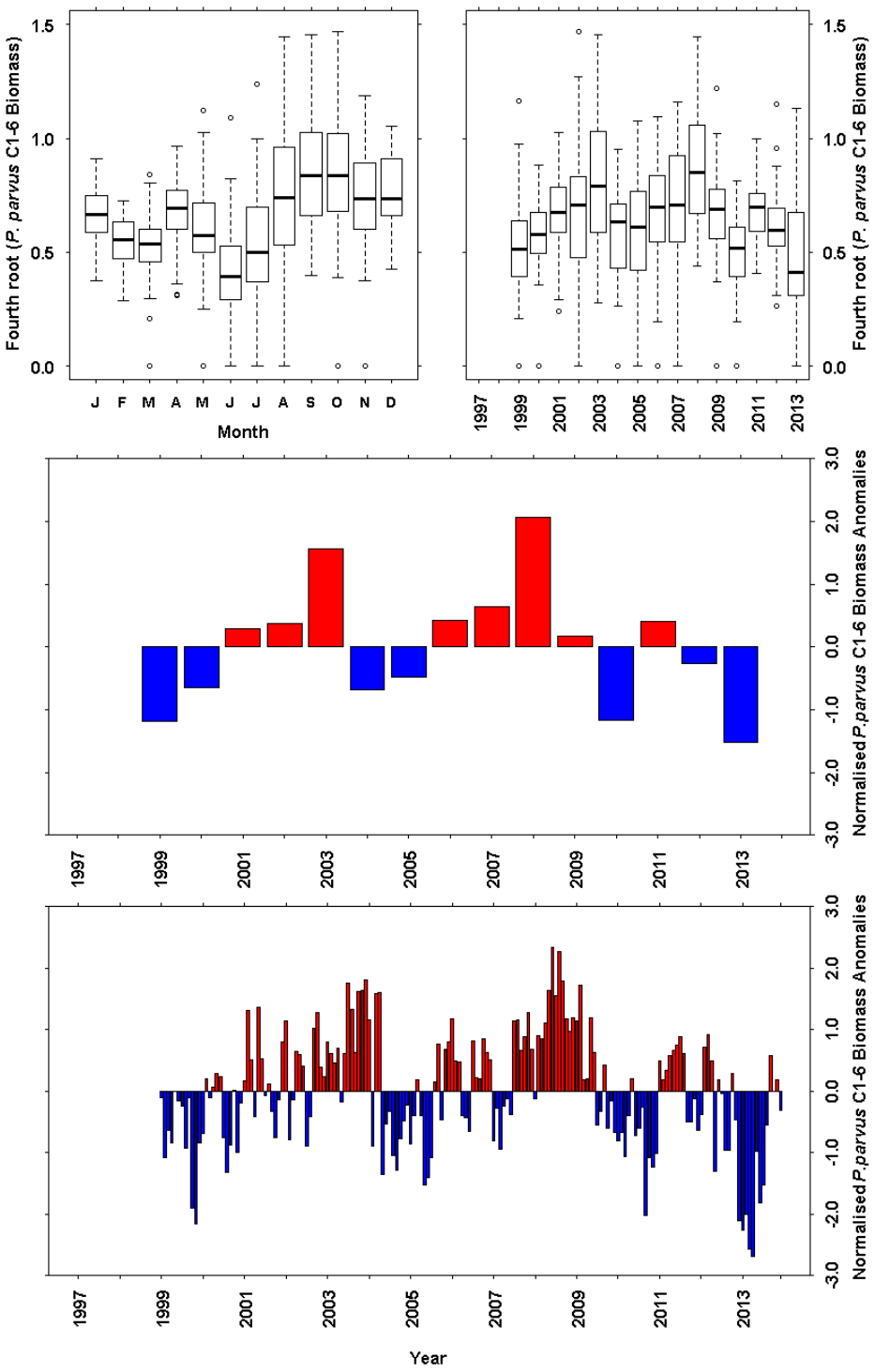

Figure 12.14 *Paracalanus parvus* Stages C1-6 Biomass (mg dry weight m^{-3}) data from the long term monitoring site at Stonehaven. a) Monthly boxplot of *P. parvus* stages C1-6 biomass data. b) Annual boxplot of *P. parvus* stages C1-6 biomass data. c) Annual mean anomaly time series d) Monthly mean anomaly time series. The full data set was used as the base period for the anomaly calculations.

12.17 Results - *Pseudocalanus* spp. Stages C1-6 Biomass

At Loch Ewe, *Pseudocalanus* spp. was present at low levels throughout the winter. Biomass began to increase in March and peaking in April (Figure 12.15a). Biomass declined in June before increasing again in July and remaining high until October. The summer months where the median biomass dips show high variability suggesting that this does not occur in all years. The highest positive annual biomass anomaly (Figure 12.15c) was observed in 2012 but not the highest median annual biomass (Figure 12.15b), although variability was relatively high.

At Stonehaven, the seasonal pattern in *Pseudocalanus* spp. biomass was similar to that seen at Loch Ewe but with a slight lag and median biomass levels were lower than those seen at Loch Ewe. Biomass started to slowly increase from winter levels around March and reached the spring peak in April-May (Figure 12.16a). The June-July dip in biomass reached very low levels at Stonehaven that were comparable to winter biomass levels although with fairly high variability. The autumn peak was reached in Autumn-September. There was no obvious pattern in annual median biomass of *Pseudocalanus* spp. at Stonehaven (Figure 12.16b) or in the annual anomalies (Figure 12.16c and d).

12.18 Plots - *Pseudocalanus* spp. Stages C1-6 Biomass

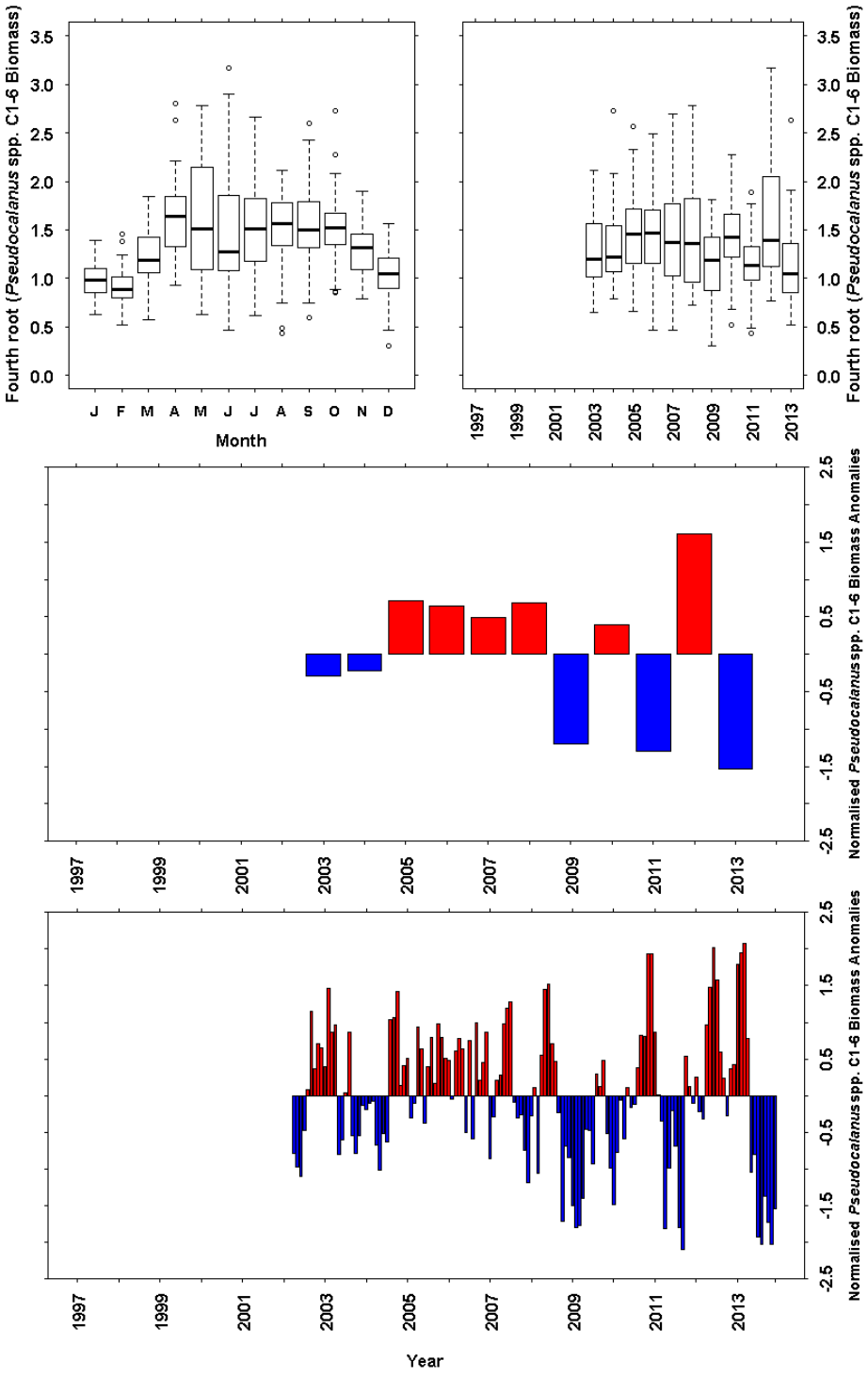

Figure 12.15 *Pseudocalanus* spp. Stages C1-6 Biomass (mg dry weight m^{-3}) data from the long term monitoring site at Loch Ewe. a) Monthly boxplot of *Pseudocalanus* spp. stages C1-6 biomass data. b) Annual boxplot of *Pseudocalanus* spp. stages C1-6 biomass data. c) Annual mean anomaly time series d) Monthly mean anomaly time series. Sampling began in April 2002. Figures b and d only include data from January 2003. The full data set was used as the base period for the anomaly calculations.

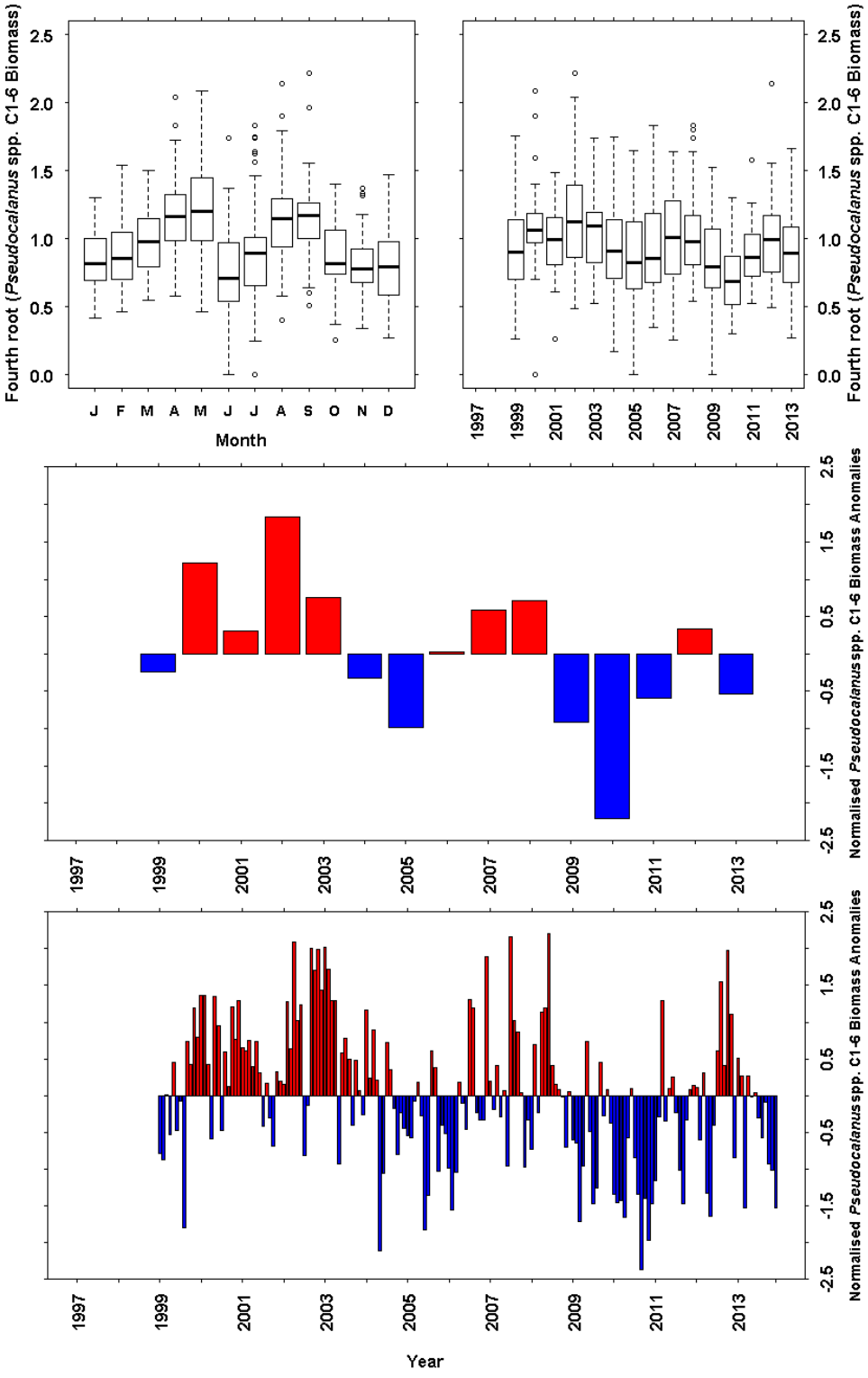

Figure 12.16 *Pseudocalanus* spp. Stages C1-6 Biomass (mg dry weight m^{-3}) data from the long term monitoring site at Stonehaven. a) Monthly boxplot of *Pseudocalanus* spp. stages C1-6 biomass data. b) Annual boxplot of *Pseudocalanus* spp. stages C1-6 biomass data. c) Annual mean anomaly time series d) Monthly mean anomaly time series. The full data set was used as the base period for the anomaly calculations.

12.19 Results - *Temora longicornis* stages C1-6 biomass

Very low biomass of *T. longicornis* was observed during the winter months at Loch Ewe, especially January-February (Figure 12.17a). Biomass increased quite rapidly between February and May and then continued to increase at a slower rate until the annual peak was reached around August. Biomass then declined steadily to winter levels. The variability in May and June biomass levels were high compared to other months indicating that the spring/early summer bloom may be more important in some years. In the period 2006-2008 these months were the only ones that showed positive monthly biomass anomalies (Figure 12.17d). High median annual biomass was observed during 2003 (Figure 12.17b and c)..

Biomass of *T. longicornis* was higher during winter at Stonehaven compared to Loch Ewe (Figure 12.18a). The annual low occurred in February and biomass increased from March to a spring/early summer peak in May. There was a slight decline in biomass in June before an increase to the annual peak in August. Variability was high in May as it was in Loch Ewe..

12.20 Plots - *Temora longicornis* stages C1-6 biomass

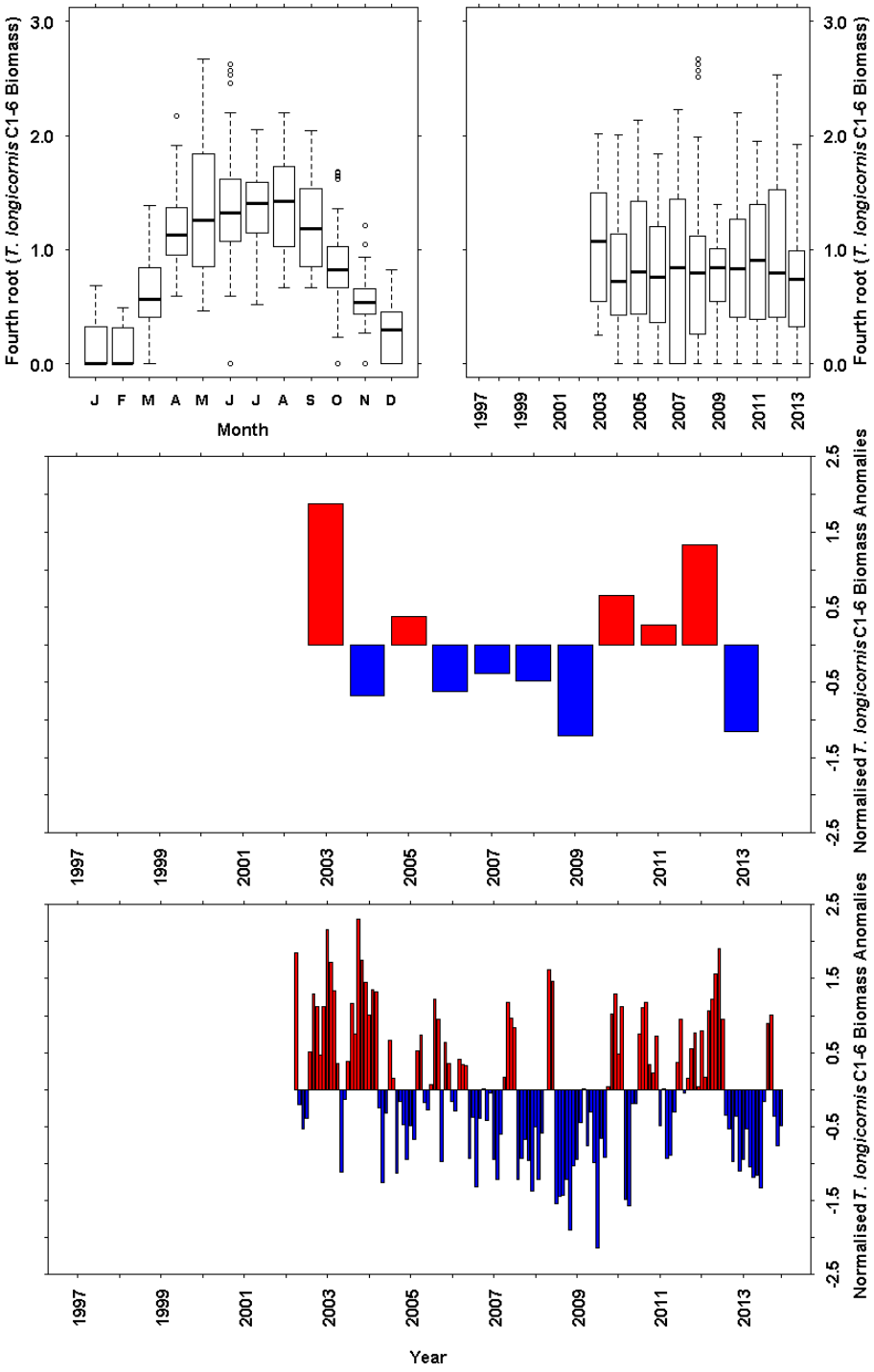

Figure 12.17 *Temora longicornis* Stages C1-6 Biomass (mg dry weight m^{-3}) data from the long term monitoring site at Loch Ewe. a) Monthly boxplot of *T. longicornis* stages C1-6 biomass data. b) Annual boxplot *of T. longicornis* stages C1-6 biomass data. c) Annual mean anomaly time series d) Monthly mean anomaly time series. Sampling began in April 2002. Figures b and d only include data from January 2003. The full data set was used as the base period for the anomaly calculations.

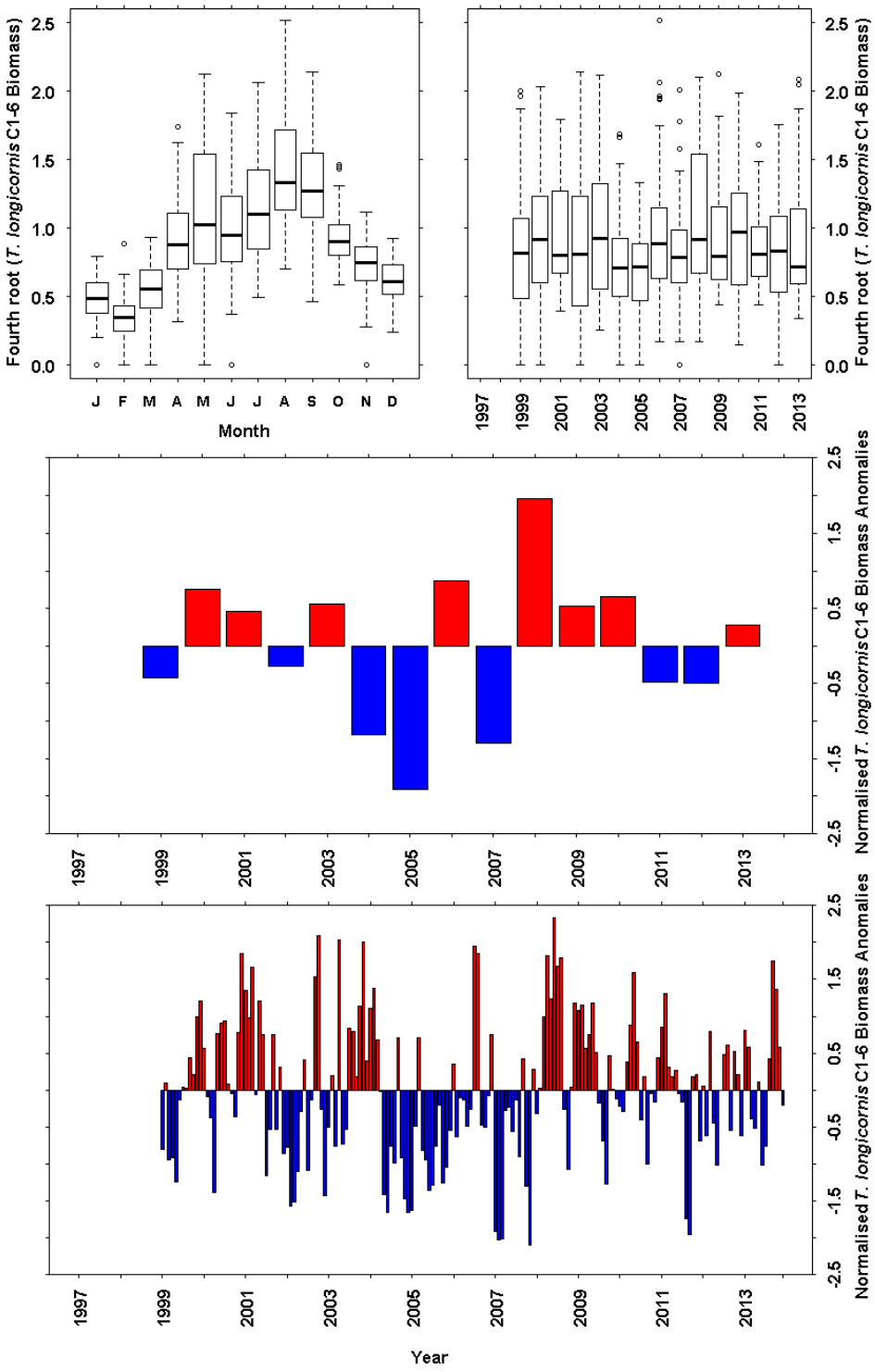

Figure 12.18 *Temora longicornis* Stages C1-6 Biomass (mg dry weight m^{-3}) data from the long term monitoring site at Stonehaven. a) Monthly boxplot of *T. longicornis* stages C1-6 biomass data. b) Annual boxplot of *T. longicornis* stages C1-6 biomass data. c) Annual mean anomaly time series d) Monthly mean anomaly time series. The full data set was used as the base period for the anomaly calculations.

12.21 Results - Oithonidae stages C1-6 biomass

At Loch Ewe there was relatively high biomass of Oithonidae during the winter months. The biomass began to increase steadily in March, reached a maximum in August and then declined until the lowest biomass in January (Figure 12.19a). High Oithonidae biomass was observed in 2010 (Figure 12.19b) with almost all months (except June) having positive monthly anomalies (Figure 12.19c & d).

At Stonehaven there was a lower biomass of Oithonidae compared to Loch Ewe, and the seasonal cycle had a less defined pattern (Figure 12.20a). Winter biomass levels were similar to those observed at Loch Ewe, but the biomass stayed at these levels well into the summer. Biomass increased slightly between July-September, although variability in these months was extremely high. There were three groups of years with respect to median biomass levels: 1999-2001 with low biomass, 2002-2008 with high biomass and 2009-2013 with low biomass (Figure 12.20b). It should be noted that the way the Oithonidae were analysed at Stonehaven changed in 2002. Before this the copepods were just counted, but since 2002 each copepod was staged. Although this shouldn't affect the numbers, there may have been an unconscious increase in effort looking for Oithonidae by analysts which could have artificially increased biomass estimates.

12.22 Plots - Oithonidae stages C1-6 biomass

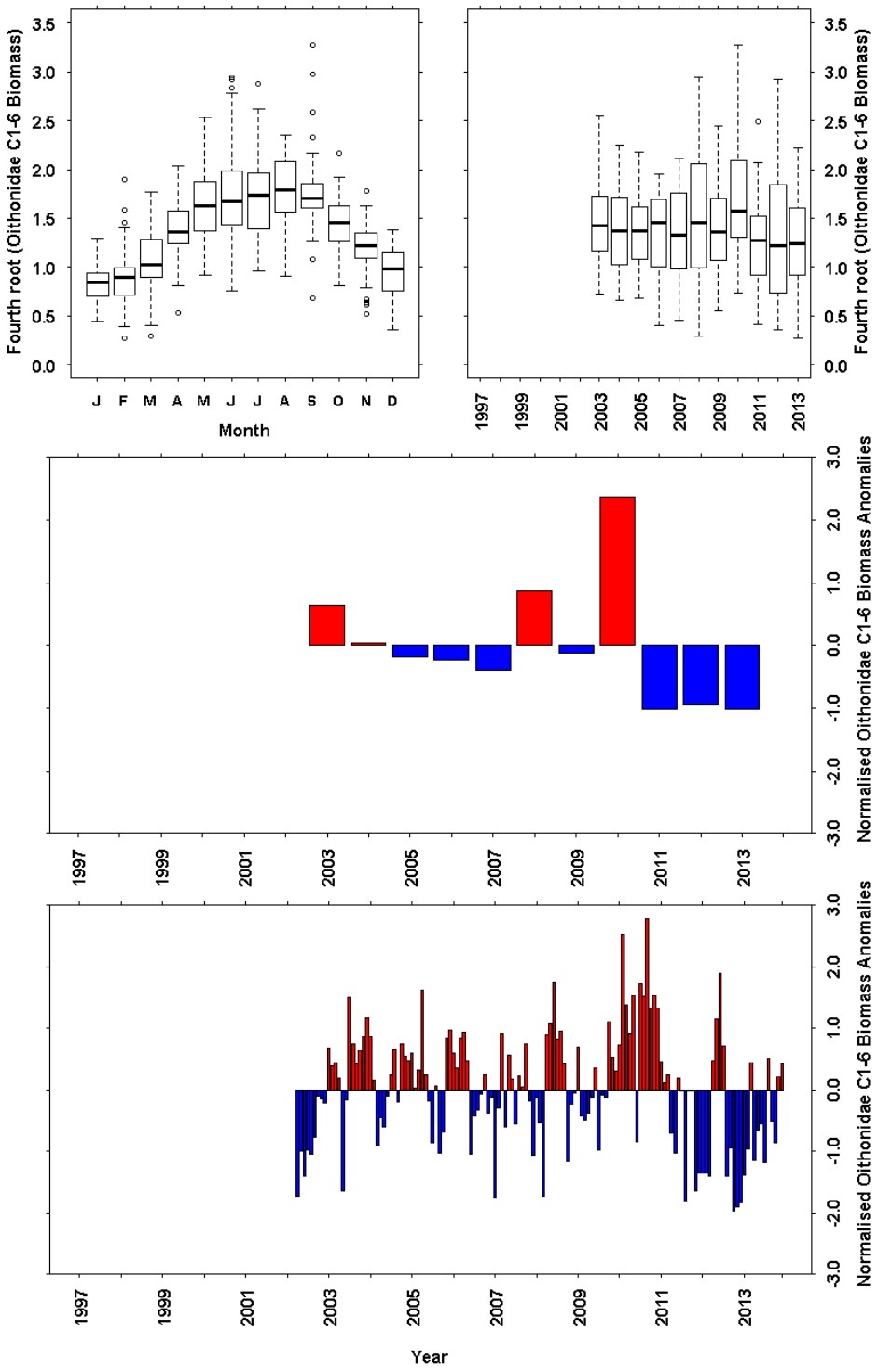

Figure 12.19 Oithonidae Stages C1-6 Biomass (mg dry weight m^{-3}) data from the long term monitoring site at Loch Ewe. a) Monthly boxplot of Oithonidae stages C1-6 biomass data. b) Annual boxplot of Oithonidae stages C1-6 biomass data. c) Annual mean anomaly time series d) Monthly mean anomaly time series. Sampling began in April 2002. Figures b and d only include data from January 2003. The full data set was used as the base period for the anomaly calculations.

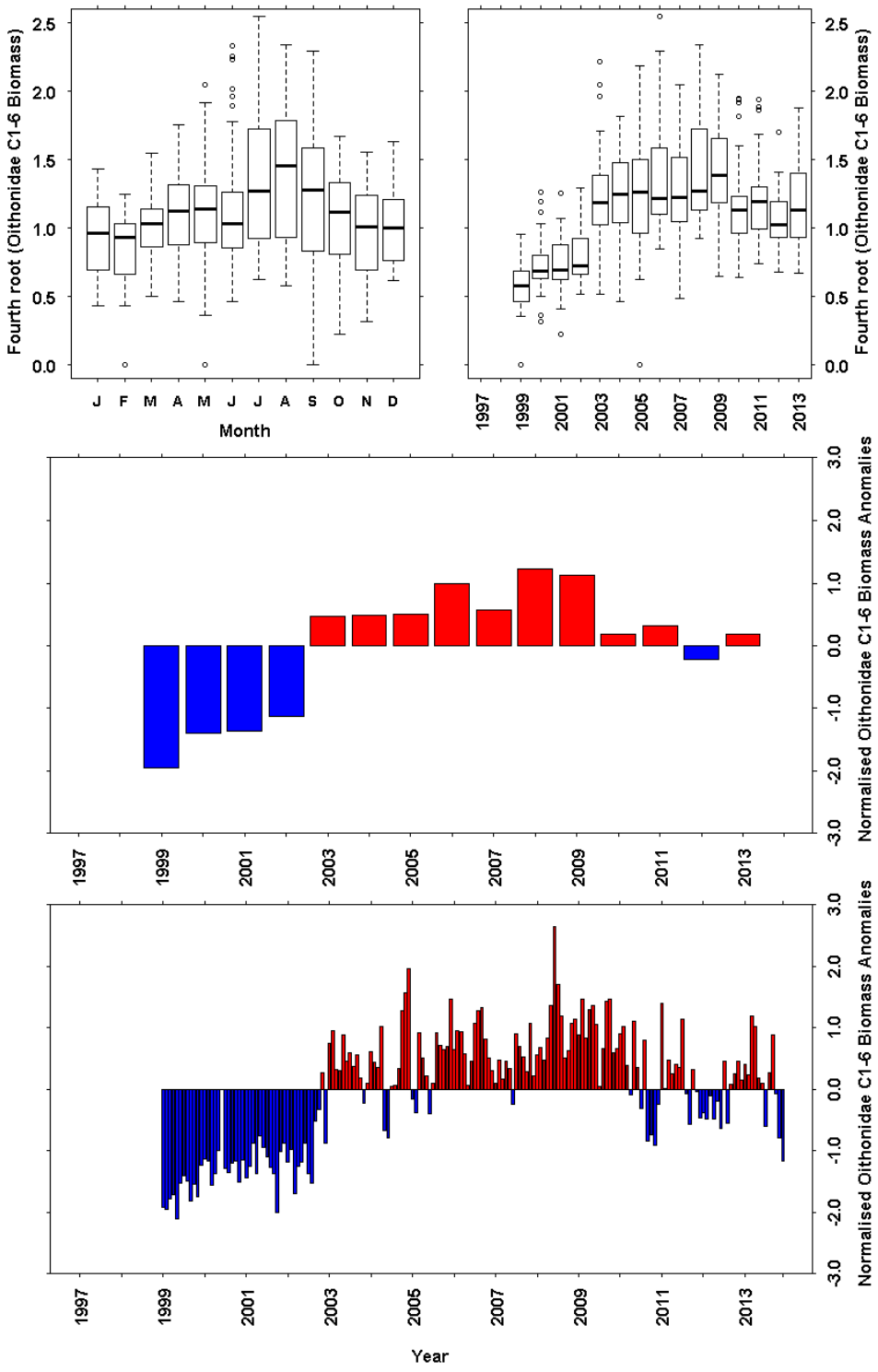

Figure 12.20 Oithonidae Stages C1-6 Biomass (mg dry weight m^{-3}) data from the long term monitoring site at Stonehaven. a) Monthly boxplot of Oithonidae stages C1-6 biomass data. b) Annual boxplot of Oithonidae stages C1-6 biomass data. c) Annual mean anomaly time series d) Monthly mean anomaly time series. The full data set was used as the base period for the anomaly calculations.

12.23 Results - Benthic Larvae Biomass

A low biomass of benthic larvae was observed in the water column during winter at Loch Ewe (Figure 12.21a), and biomass began to increase in February. A spring peak in biomass was recorded in April and a similarly sized summer/autumn peak in July-September. The variability in March was relatively high compared to the other months. There were no obvious patterns in annual biomass (Figure 12.21b) but annual anomalies were positive between 2003-2008 and then became mostly negative (except 2010, Figure 12.21c and d) giving the appearance of a negative trend.

The seasonal cycle of benthic larvae biomass at Stonehaven was similar to that at Loch Ewe. There were low biomass levels throughout the winter months, but biomass began to increase in March and reached a peak in April/May (Figure 12.22a). A second peak in July/August was slightly higher than the spring peak. There was no obvious pattern in annual benthic larvae biomass (Figure 12.22b). Since 2003, the annual benthic larvae biomass anomalies have mostly been positive, except in 2005, 2010 and 2011 (Figure 12.22c). Years with negative annual anomalies generally had lower autumn monthly anomalies than years with positive annual anomalies (Figure 12.22d).

12.24 Plots - Benthic Larvae Biomass

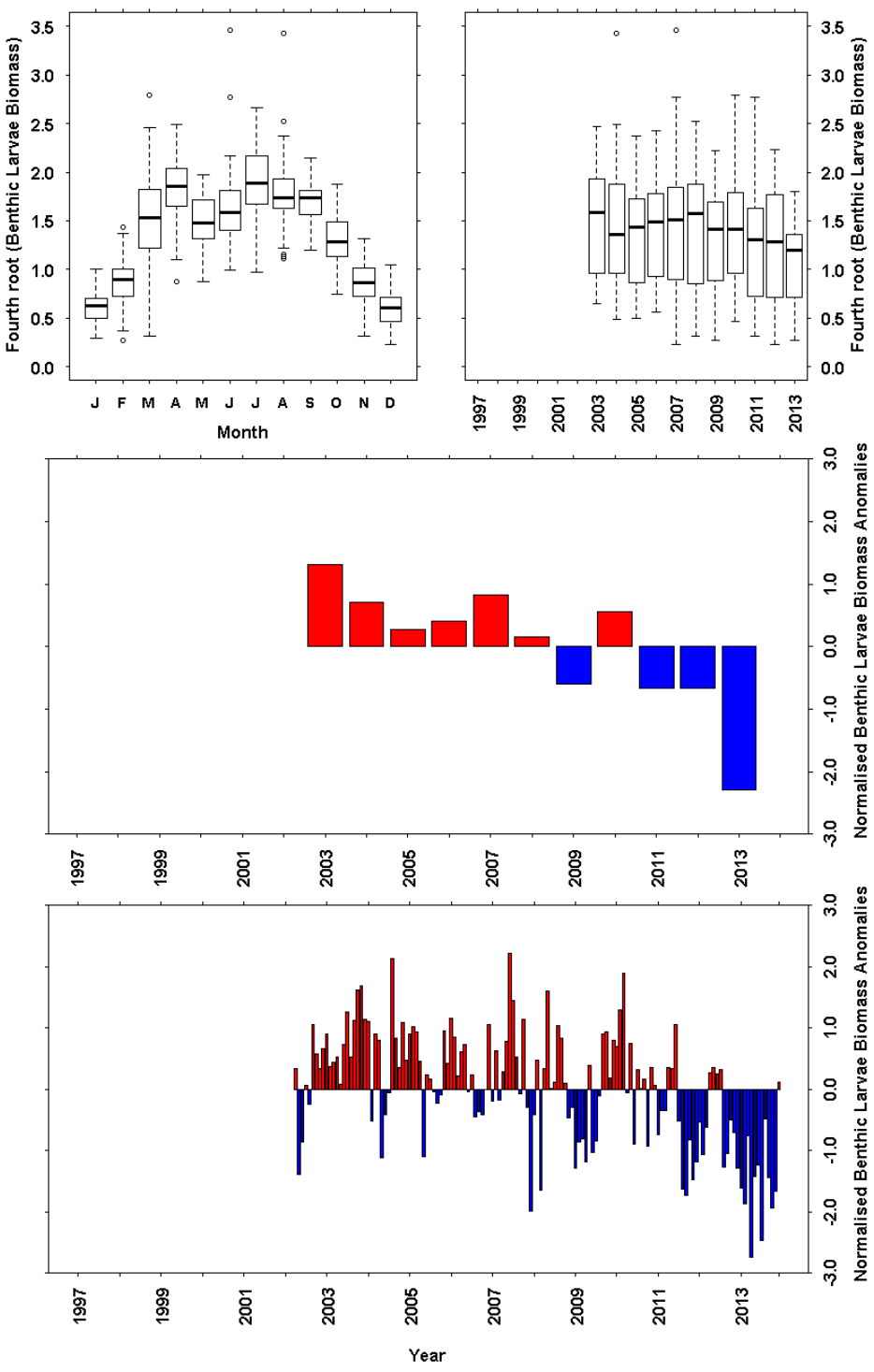

Figure 12.21 Benthic Larvae Biomass (mg dry weight m^{-3}) data from the long term monitoring site at Loch Ewe. a) Monthly boxplot of benthic larvae biomass data. b) Annual boxplot of benthic larvae biomass data. c) Annual mean anomaly time series d) Monthly mean anomaly time series. Sampling began in April 2002. Figures b and d only include data from January 2003. The full data set was used as the base period for the anomaly calculations.

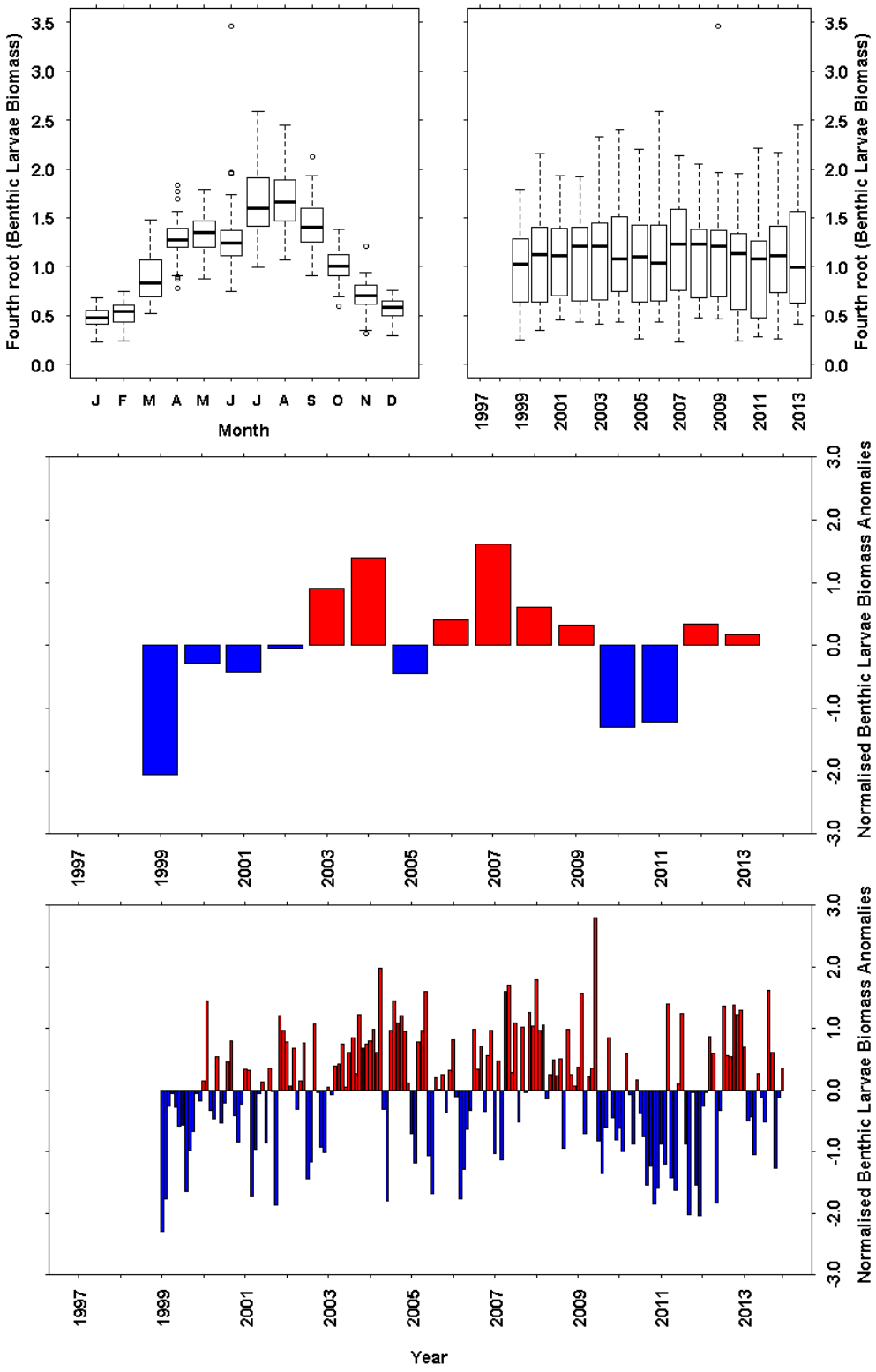

Figure 12.22 Benthic Larvae Biomass (mg dry weight m^{-3}) data from the long term monitoring site at Stonehaven. a) Monthly boxplot of benthic larvae biomass data. b) Annual boxplot of benthic larvae biomass data. c) Annual mean anomaly time series d) Monthly mean anomaly time series. The full data set was used as the base period for the anomaly calculations.

12.25 Results - Decapod Larvae Biomass

At Loch Ewe there was very low decapod larvae biomass observed during December-January which began to increase in February peaking in April (Figure 12.23a). A second larger peak was observed in July before biomass began to decrease to winter levels. The annual median biomass of decapod larvae could be divided into two groups: higher biomass between 2003-2008 and lower biomass between 2009-2013 (Figure 12.23b). This was also apparent in the decapod larvae biomass anomalies (Figure 12.23c and d) where 2003-2008 had positive annual anomalies whilst 2009-2013 had negative annual anomalies (except 2010). The pattern in annual anomalies was almost identical to that seen for benthic larvae biomass (Figure 12.21c) indicating that decapod larvae are an important component of the benthic larvae community at Loch Ewe in terms of biomass.

At Stonehaven the seasonal cycle in decapod larvae biomass was very similar to that seen at Loch Ewe but with a slight lag. Biomass began to increase in March, reached a spring peak in April/May/June and a larger peak in August (Figure 12.24a). Annual decapod larvae biomass anomalies (Figure 12.24c) increased between 1999-2007. This was associated with an increase in the number of months within a year with positive monthly anomalies (Figure 12.24d). Since 2009, however, most years have had negative annual anomalies except 2012.

12.26 Plots - Decapod Larvae Biomass

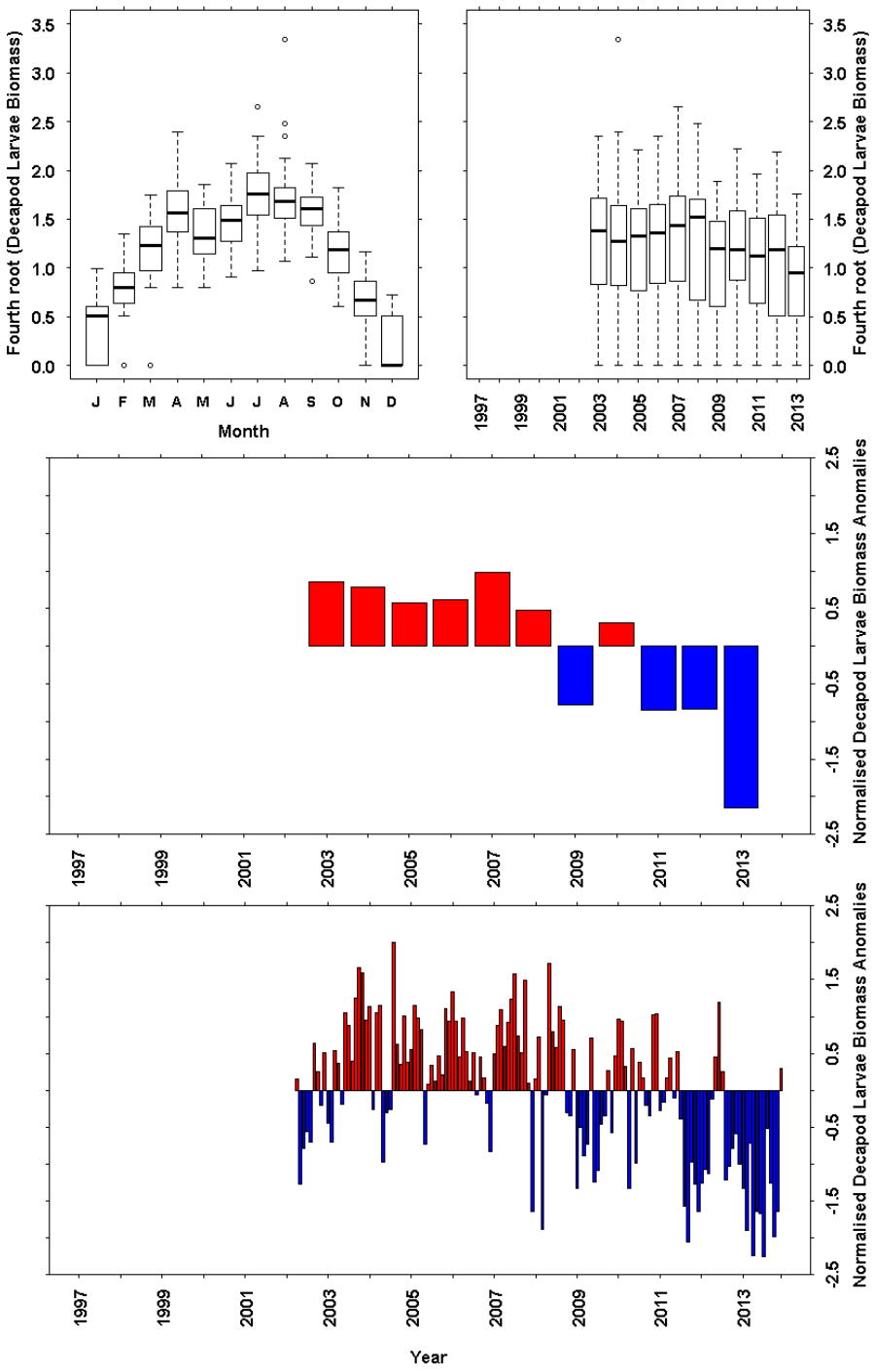

Figure 12.23 Decapod Larvae Biomass (mg dry weight m^{-3}) data from the long term monitoring site at Loch Ewe. a) Monthly boxplot of decapod larvae biomass data. b) Annual boxplot of decapod larvae biomass data. c) Annual mean anomaly time series d) Monthly mean anomaly time series. Sampling began in April 2002. Figures b and d only include data from January 2003. The full data set was used as the base period for the anomaly calculations.

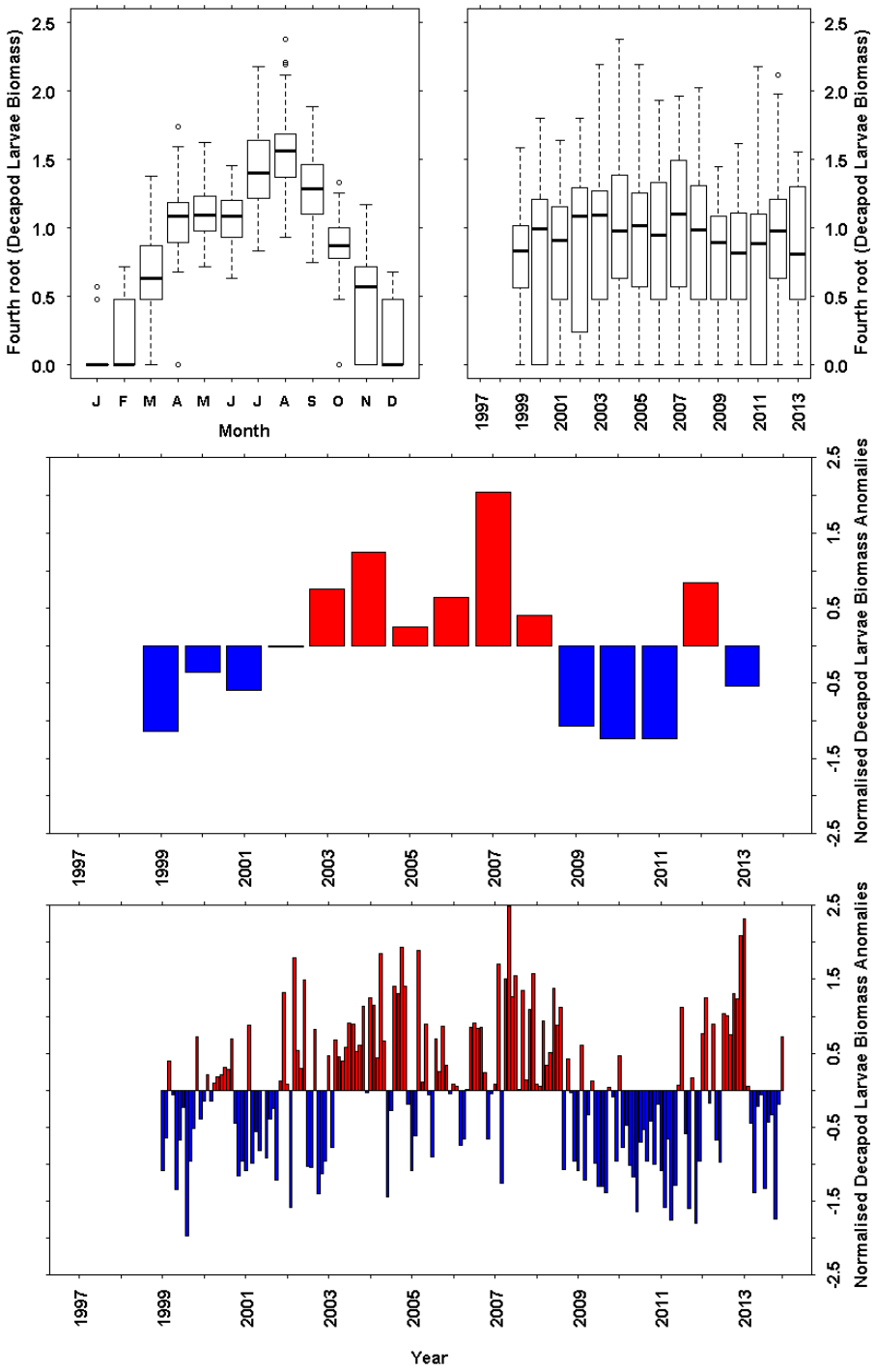

Figure 12.24 Decapod Larvae Biomass (mg dry weight m^{-3}) data from the long term monitoring site at Stonehaven. a) Monthly boxplot of decapod larvae biomass data. b) Annual boxplot of decapod larvae biomass data. c) Annual mean anomaly time series d) Monthly mean anomaly time series. The full data set was used as the base period for the anomaly calculations.

12.27 Results - Bivalve Larvae Biomass

At Loch Ewe there were low levels of bivalve larvae biomass present throughout the winter (Figure 12.25a). There was a slight increase in biomass in early spring (March) but the main biomass peak occurred in late August/September. There was a decline in median annual bivalve larvae biomass between 2003-2008 (Figure 12.25b). This pattern was also seen in annual bivalve larvae biomass anomalies (Figure 12.25c) and the monthly bivalve larvae biomass anomalies (Figure 12.25d).

At Stonehaven the seasonal pattern in bivalve larvae biomass was different to that recorded at Loch Ewe. Biomass started to increase in April, reached a summer peak in May and levels remained high throughout the summer and autumn until they began to decline in October (Figure 12.26a). There was low median annual bivalve larvae biomass between 2004-2007 (Figure 12.26b), which was also a period of relatively high negative annual bivalve larvae biomass anomalies (Figure 12.26c).

12.28 Plots - Bivalve Larvae Biomass

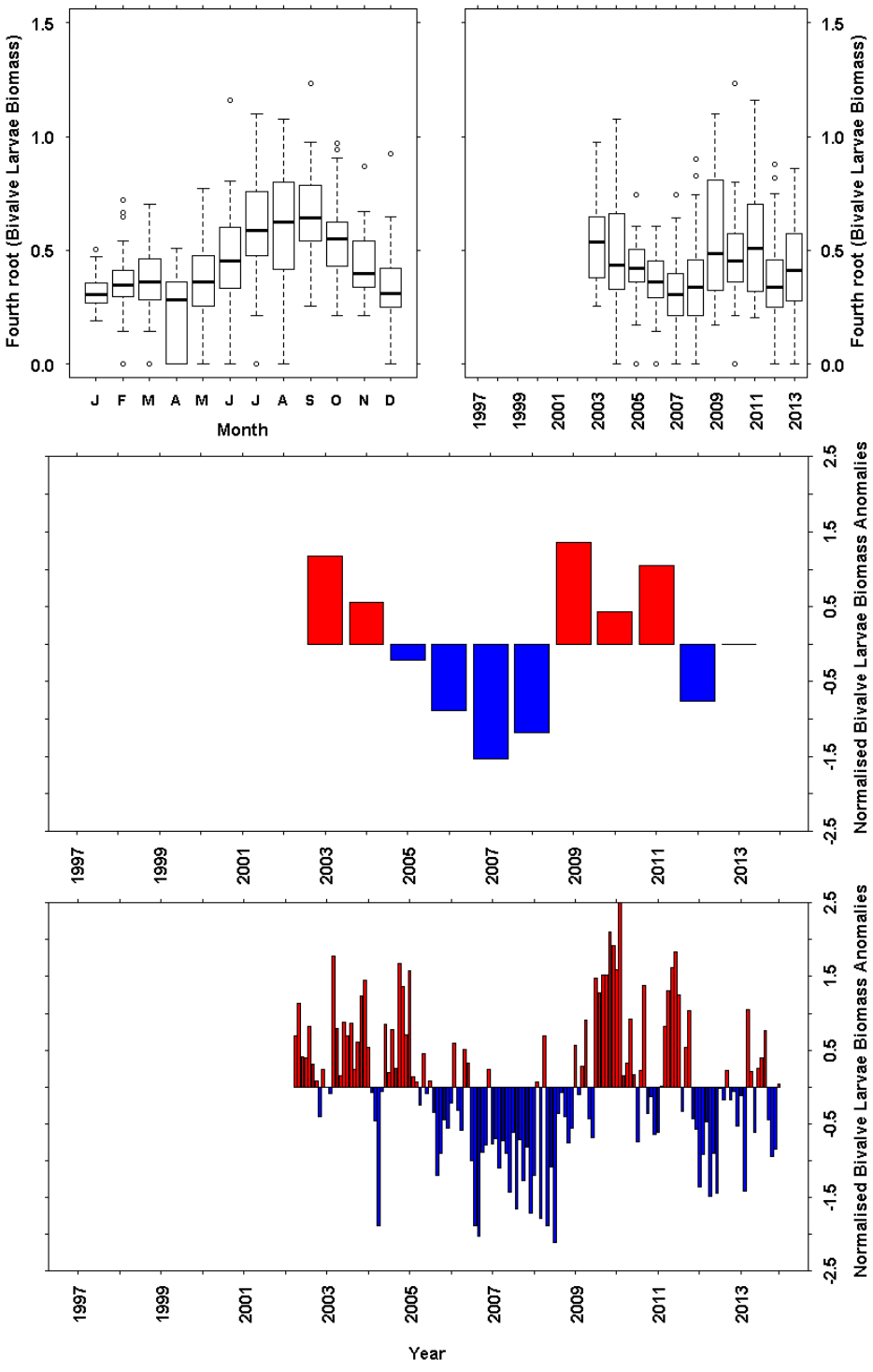

Figure 12.25 Bivalve Larvae Biomass (mg dry weight m^{-3}) data from the long term monitoring site at Loch Ewe. a) Monthly boxplot of bivalve larvae biomass data. b) Annual boxplot of bivalve larvae biomass data. c) Annual mean anomaly time series d) Monthly mean anomaly time series. Sampling began in April 2002. Figures b and d only include data from January 2003. The full data set was used as the base period for the anomaly calculations.

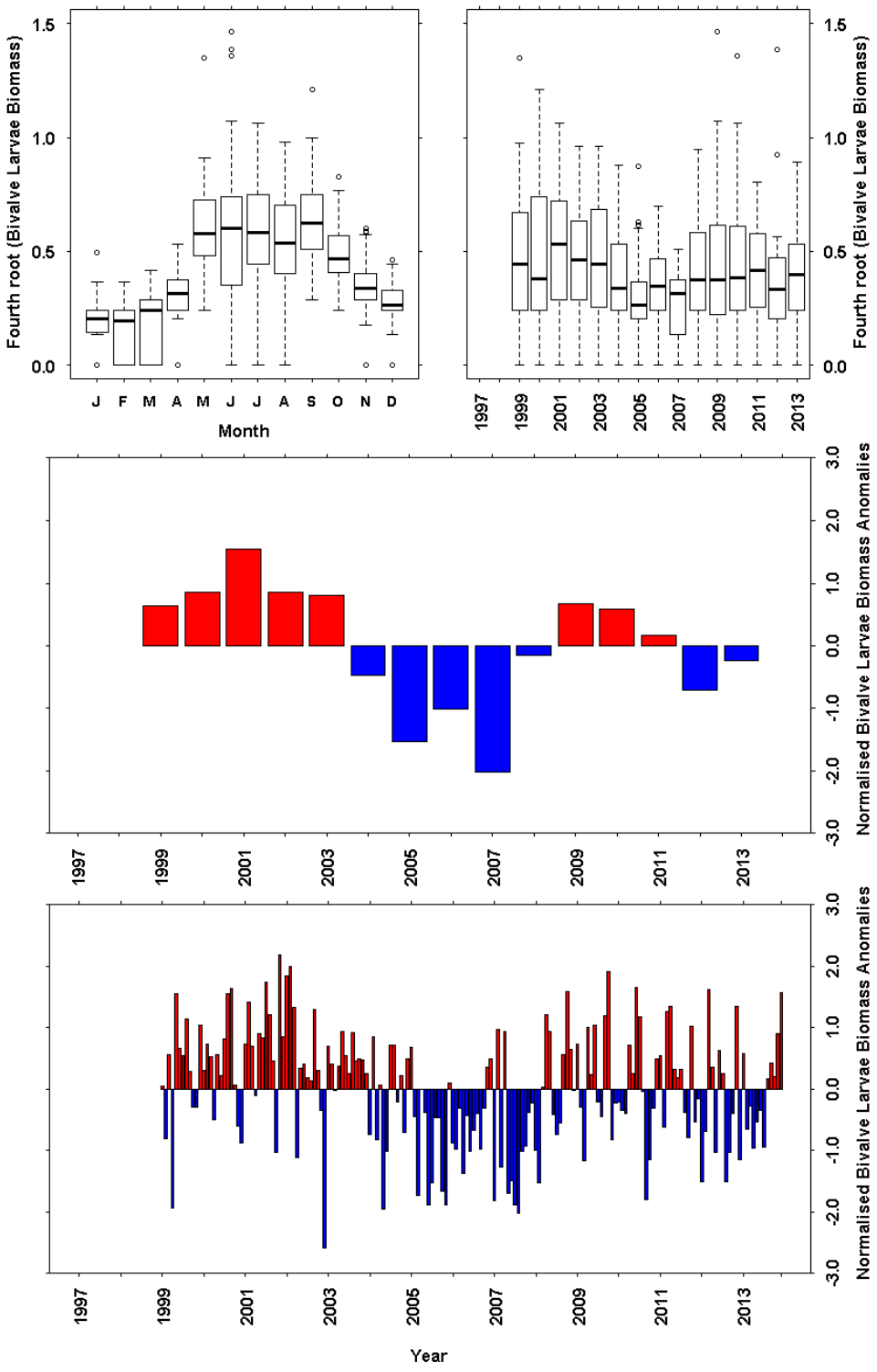

Figure 12.26 Bivalve Larvae Biomass (mg dry weight m^{-3}) data from the long term monitoring site at Stonehaven. a) Monthly boxplot of bivalve larvae biomass data. b) Annual boxplot of bivalve larvae biomass data. c) Annual mean anomaly time series d) Monthly mean anomaly time series. The full data set was used as the base period for the anomaly calculations.

12.29 Results - Barnacle Larvae Biomass

A very low biomass of barnacle larvae was recorded at Loch Ewe in the winter months. Biomass increased rapidly between February and April which formed the annual peak (Figure 12.27a). Biomass then decreased to intermediate levels during the summer months. Median annual barnacle larvae biomass declined between 2003-2008 (Figure 12.27b), as did median annual bivalve larvae biomass at Loch Ewe (Figure 12.25b). Annual barnacle larvae biomass anomalies (Figure 12.27c) and monthly barnacle larvae biomass anomalies (Figure 12.27d) also decreased between 2003-2008. The highest median annual biomass and the highest positive annual anomaly were observed in 2010.

The seasonal pattern in barnacle larvae biomass at Stonehaven was similar to that seen at Loch Ewe although delayed by about a month. Biomass began to increase in March and peaked in May (Figure 12.28a). There was a decline in median annual barnacle larvae biomass between 2000-2005 (Figure 12.28b), similar to that seen for bivalve larvae biomass at Stonehaven (Figure 12.26b). There was also a decrease in annual barnacle larvae biomass anomalies between 2000 and 2006 (Figure 12.28c).

12.30 Plots - Barnacle Larvae Biomass

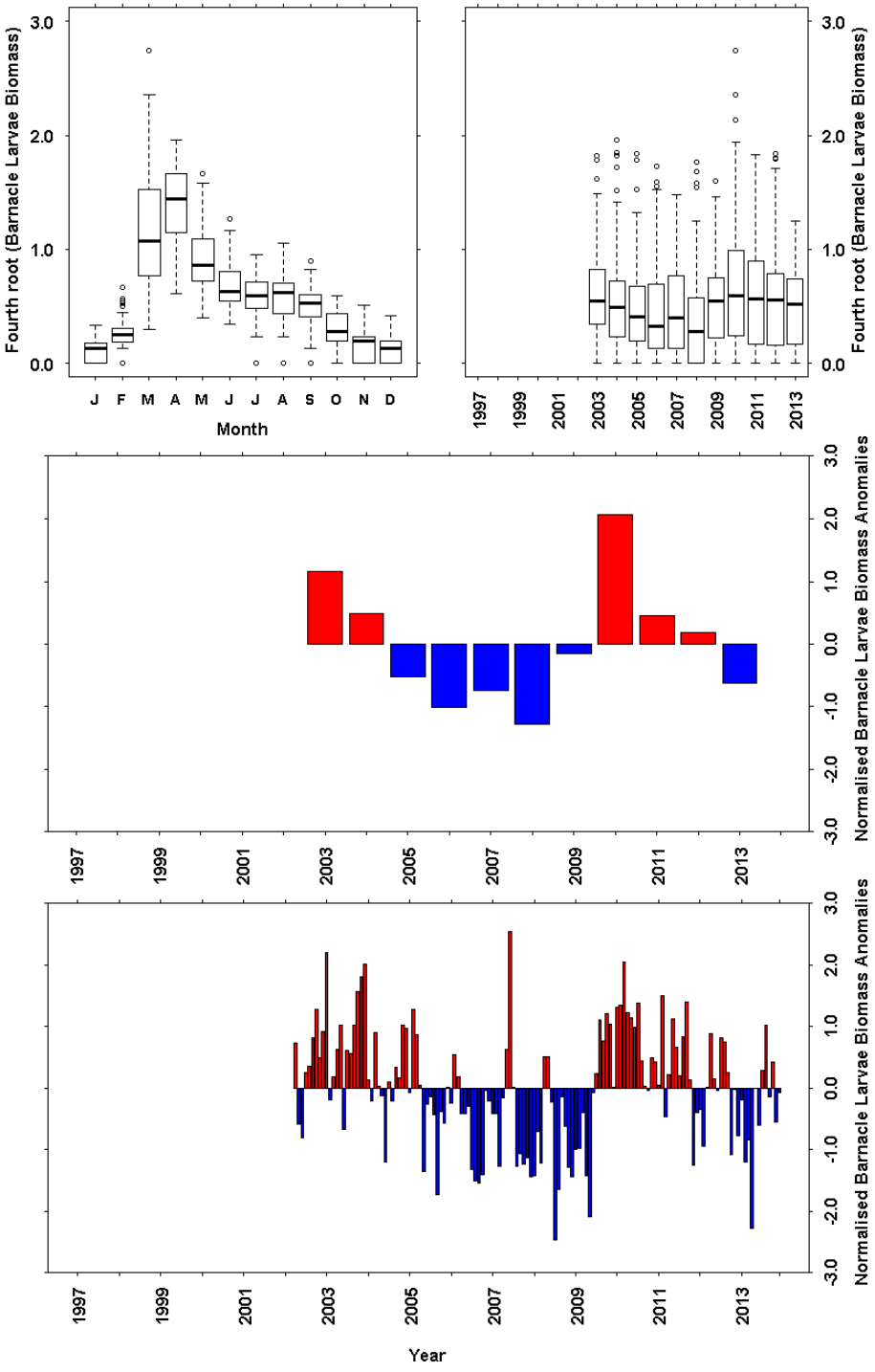

Figure 12.27 Barnacle Larvae Biomass (mg dry weight m^{-3}) data from the long term monitoring site at Loch Ewe. a) Monthly boxplot of barnacle larvae biomass data. b) Annual boxplot of barnacle larvae biomass data. c) Annual mean anomaly time series d) Monthly mean anomaly time series. Sampling began in April 2002. Figures b and d only include data from January 2003. The full data set was used as the base period for the anomaly calculations.

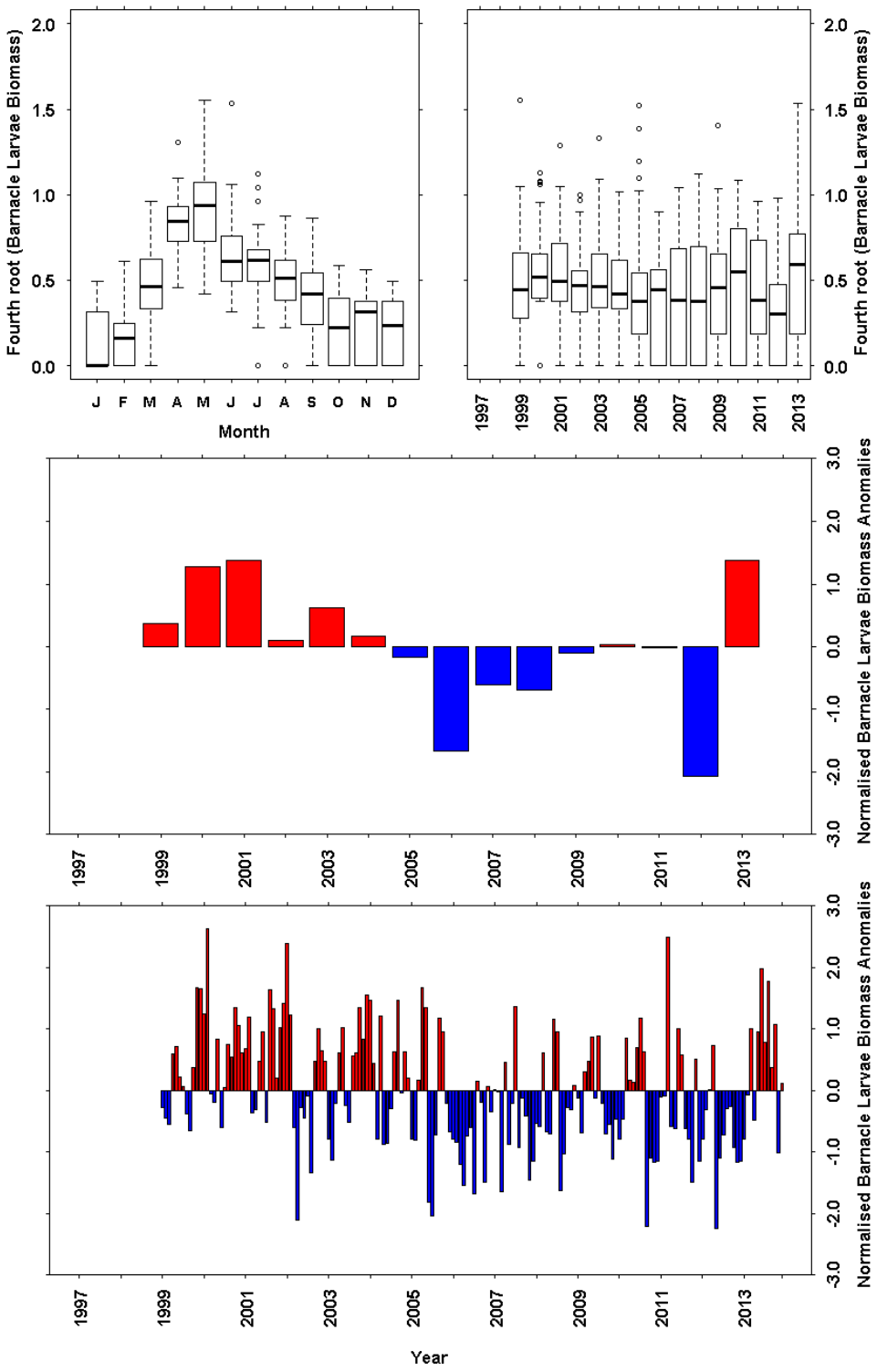

Figure 12.28 Barnacle Larvae Biomass (mg dry weight m-3) data from the long term monitoring site at Stonehaven. a) Monthly boxplot of barnacle larvae biomass data. b) Annual boxplot of barnacle larvae biomass data. c) Annual mean anomaly time series d) Monthly mean anomaly time series. The full data set was used as the base period for the anomaly calculations.

12.31 Results - Cnidaria Biomass

At Loch Ewe, Cnidaria biomass was at its annual low in January and started to increase in February (Figure 12.29a). There was a spring peak in April and a larger autumn peak in September with fairly high biomass throughout the summer. There were no obvious patterns in median annual Cnidaria biomass (Figure 12.29b) or annual Cnidaria biomass anomalies (Figure 12.29c). High positive annual biomass anomalies were observed in 2003 and 2012, whilst 2013 was a year of high negative annual biomass anomaly.

At Stonehaven there was much lower Cnidaria biomass compared to Loch Ewe (Figure 12.30a) and the seasonal cycle was delayed by about a month. There was a spring peak in April/May, a similarly sized autumn peak in September and the winter minimum occurred in February. The median annual Cnidaria biomass (Figure 12.30b) and annual Cnidaria biomass anomalies (Figure 12.30c) fluctuated between periods of higher and lower median biomass and positive and negative anomalies. A high positive annual anomaly was recorded in 2012 as seen at Loch Ewe.

12.32 Plots - Cnidaria Biomass

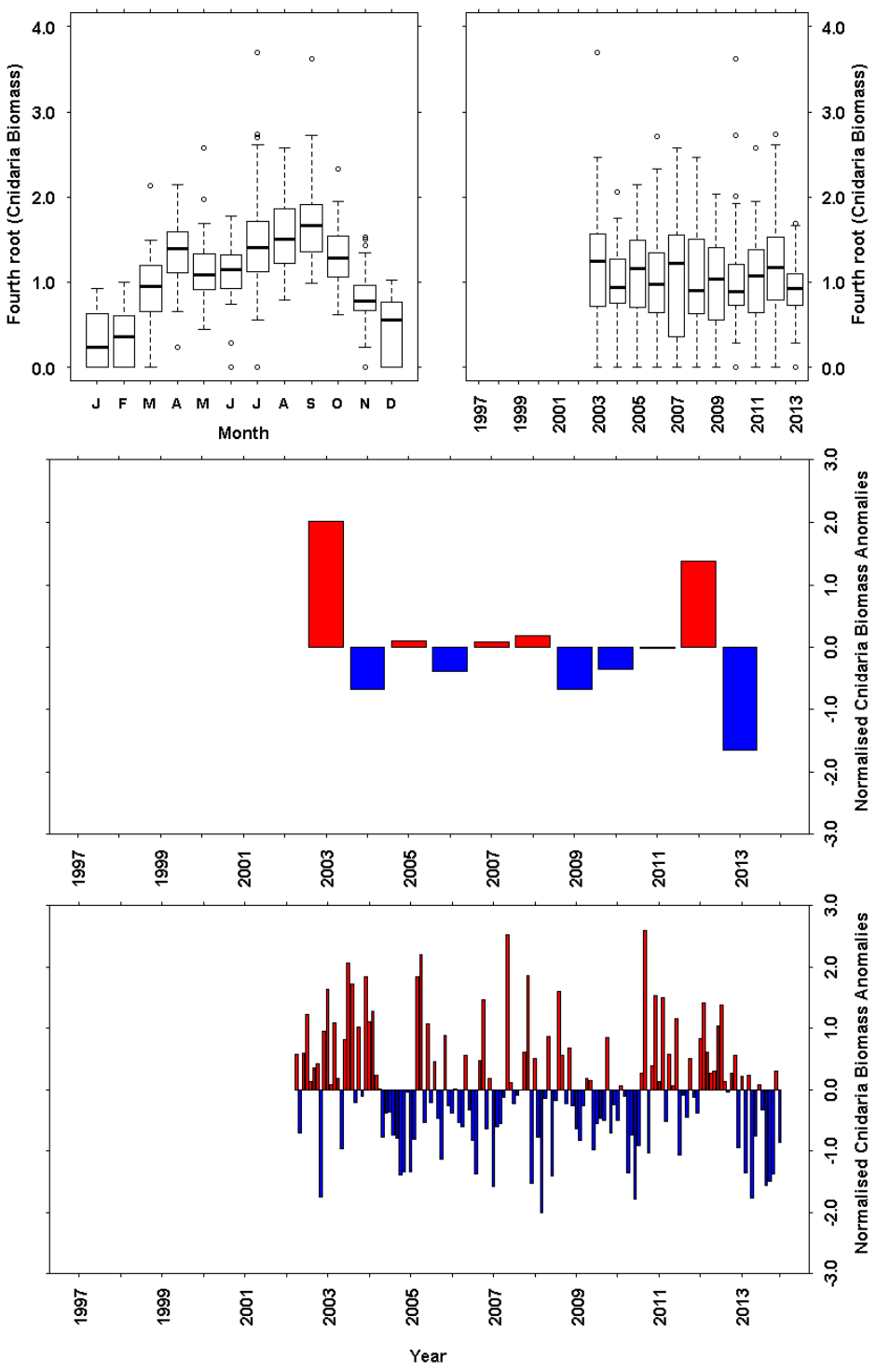

Figure 12.29 Cnidaria Biomass (mg dry weight m^{-3}) data from the long term monitoring site at Loch Ewe. a) Monthly boxplot of Cnidaria biomass data. b) Annual boxplot of Cnidaria biomass data. c) Annual mean anomaly time series d) Monthly mean anomaly time series. Sampling began in April 2002. Figures b and d only include data from January 2003. The full data set was used as the base period for the anomaly calculations.

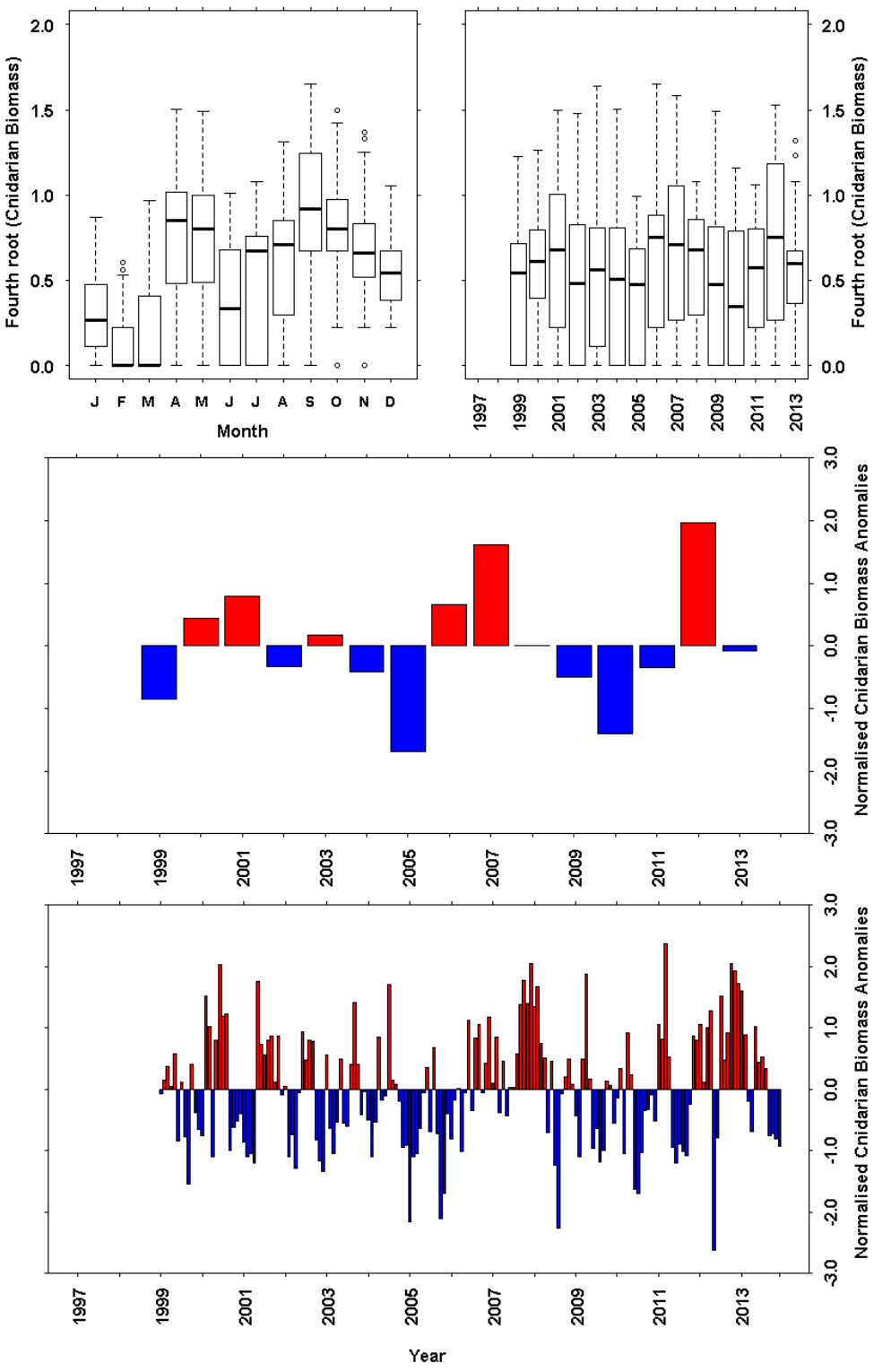

Figure 12.30 Cnidaria Biomass (mg dry weight m^{-3}) data from the long term monitoring site at Stonehaven. a) Monthly boxplot of Cnidaria biomass data. b) Annual boxplot of Cnidaria biomass data. c) Annual mean anomaly time series d) Monthly mean anomaly time series. The full data set was used as the base period for the anomaly calculations.

12.33 Results - Calcifying Plankton Biomass

At Loch Ewe, calcifying plankton biomass was present at low levels throughout the winter and started to increase in February (Figure 12.31a). There was a spring peak in March/April and a larger summer peak in July with fairly high biomass throughout the autumn. Median annual calcifying plankton biomass decreased between 2003-2008 (Figure 12.31b), a pattern also seen in median annual bivalve larvae (Figure 12.25b) and barnacle larvae biomass at Loch Ewe (Figure 12.27b). Annual calcifying plankton biomass anomalies (Figure 12.31c) also decreased between 2003-2008.

The seasonal pattern in calcifying plankton biomass at Stonehaven was similar to that seen at Loch Ewe but delayed by about a month. Biomass began to increase in March and there was a summer peak in May with a larger autumn peak in September (Figure 12.32a). There was no obvious pattern in median annual calcifying plankton biomass (Figure 12.32b). The annual calcifying plankton biomass anomalies have oscillated between periods of positive and negative annual anomalies (Figure 12.32c).

12.34 Plots - Calcifying Plankton Biomass

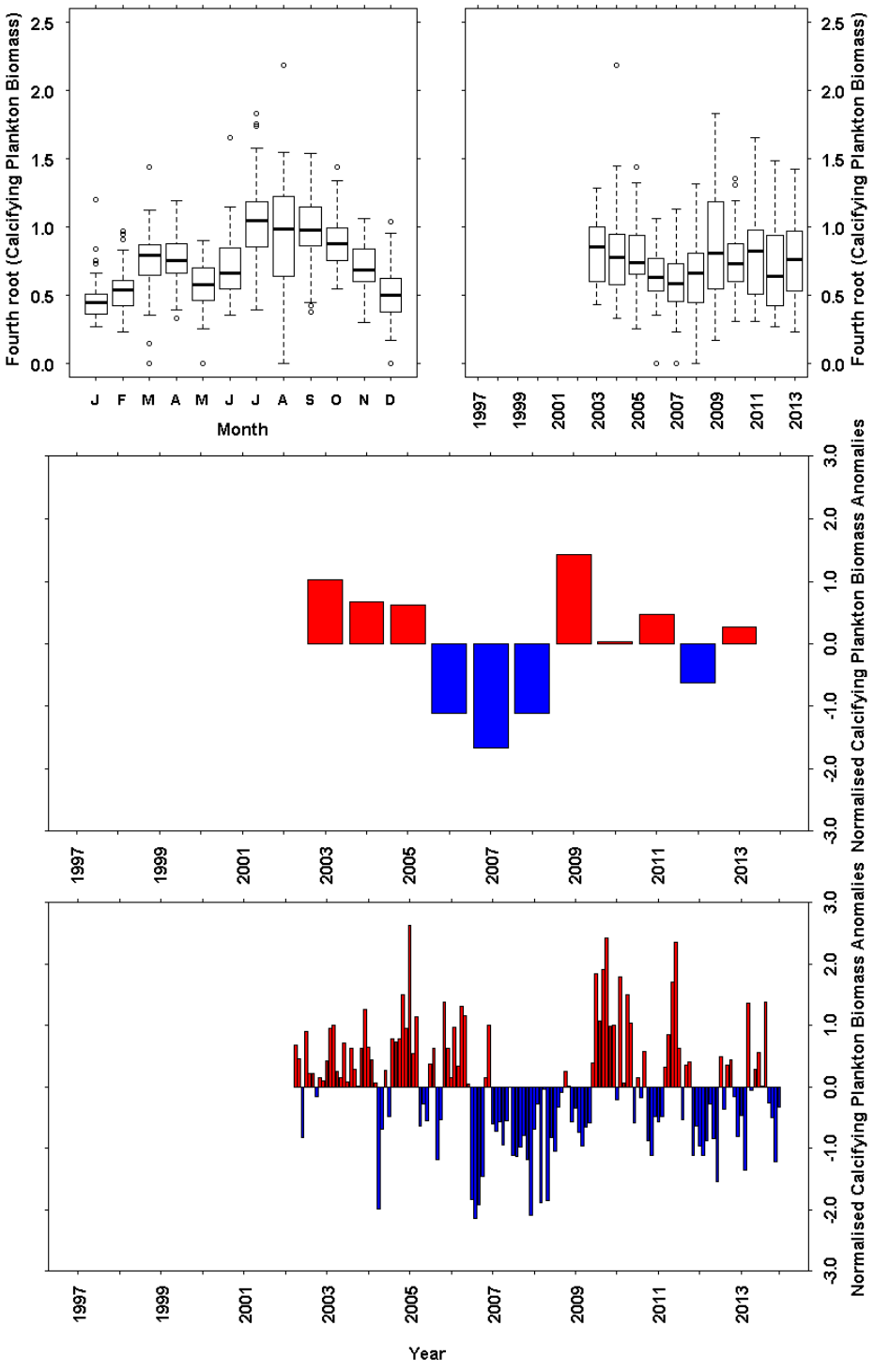

Figure 12.31 Calcifying Plankton Biomass (mg dry weight m^{-3}) data from the long term monitoring site at Loch Ewe. a) Monthly boxplot of calcifying plankton biomass data. b) Annual boxplot of calcifying plankton biomass data. c) Annual mean anomaly time series d) Monthly mean anomaly time series. Sampling began in April 2002. Figures b and d only include data from January 2003. The full data set was used as the base period for the anomaly calculations.

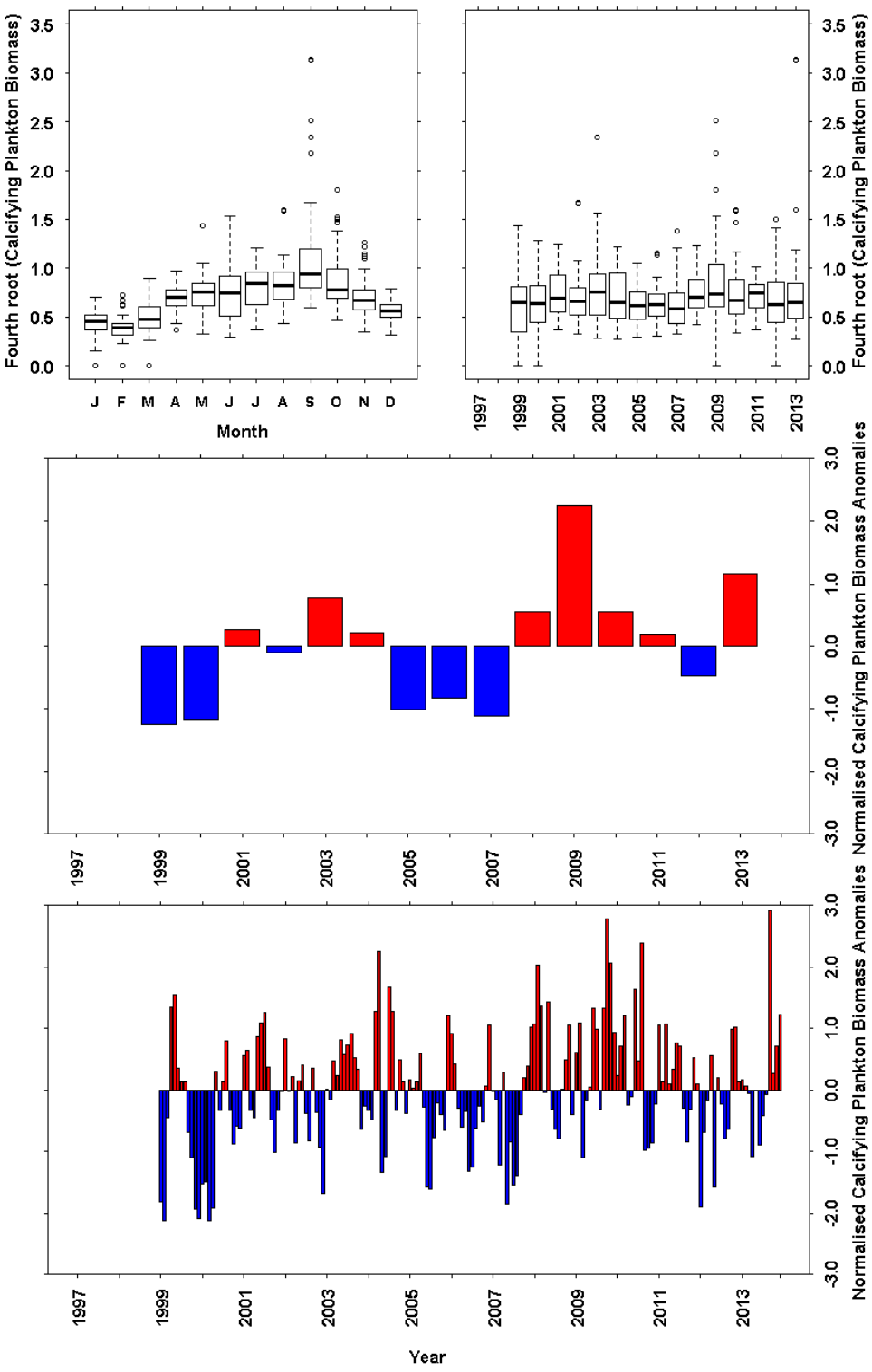

Figure 12.32 Calcifying Plankton Biomass (mg dry weight m^{-3}) data from the long term monitoring site at Stonehaven. a) Monthly boxplot of calcifying plankton biomass data. b) Annual boxplot of calcifying plankton biomass data. c) Annual mean anomaly time series d) Monthly mean anomaly time series. The full data set was used as the base period for the anomaly calculations.

12.35 Summary – Zooplankton

- A high degree of interannual variability can be observed in the Scottish coastal zooplankton community.
- The spring increase in biomass occurs about a month earlier at Loch Ewe compared to Stonehaven for many taxa.
- The autumn biomass peak in *Calanus helgolandicus* at Stonehaven is almost double that seen at Loch Ewe.
- Periods of positive annual anomalies in *Centropages typicus* coincide with periods of negative annual anomalies in *Centropages hamatus* at Loch Ewe and Stonehaven.
- An increase in biomass of total copepods and *Calanus* spp. at Loch Ewe and Stonehaven, and decapod larvae at Stonehaven was observed until 2008.
- The biomass of decapod larvae shows a decrease Loch Ewe.
- A decrease in biomass of bivalve larvae and barnacle larvae at Stonehaven was observed until 2008.
- A decrease in biomass of bivalve larvae, barnacle larvae and calcifying plankton was observed at Loch Ewe until 2008.
- There is no trend in cnidarian biomass observed at either site.

12.36 References - Zooplankton

Aarbakke, O.N.S, Bucklin, A., Halsband, C., Norrbin, F. 2011. Discovery of *Pseudocalanus moultoni* (Frost, 1989) in Northeast Atlantic waters based on mitochondrial COI sequence variation. Journal of Plankton Research, 33, 1487-1495.

Aarbakke, O.N.S., Bucklin, A., Halsband, C., Norrbin, F. 2014. Comparative phylogeography and demographic history of five sibling species of *Pseudocalanus* (Copepoda: Calanoida) in the North Atlantic Ocean. Journal of Experimental Marine Biology and Ecology, 461, 479-488.

Atkinson, A., Harmer, R.A., Widdicombe, C.E., McEvoy, A.J., Smyth, T.J., Cummings, D.G., Somerfield, P.J., Maud, J.L., McConville, K. 2015. Questioning the role of phenology shifts and trophic mismatching in a planktonic food web. Progress in Oceanography, 137, 498-512.

Attrill, M.J., Wright, J., Edwards, M. 2007. Climate-related increases in jellyfish frequency suggest a more gelatinous future for the North Sea. Limnology and Oceanography, 52,4 80-485.

Beaugrand, G., Brander, K.M., Lindley, A.J., Souissi, S., Reid, P.C. 2003. Plankton effect on cod recruitment in the North Sea. Nature, 426, 661-664.

Beaugrand, G., McQuatters-Gollop, A., Edwards, M., Goberville, E. 2013. Long-term responses of North Atlantic calcifying plankton to climate change. Nature Climate Change, 3, 263-267.

Bonnet, D., Harris, R., Lopez-Urrutia, A., Halsband-Lenk, C., Greve, W., Valdes, L., Hirche, H-J., Engel, M., Alvarez-Ossorio, M.T., Wiltshire, K. 2007. Comparative seasonal dynamics of *Centropages typicus* at seven coastal monitoring stations in the North Sea, English Channel and Bay of Biscay. Progress in Oceanography, 72, 233-248.

Castellani, C. and Altunbas, Y. 2006. Factors controlling the temporal dynamics of egg production in the copepod *Temora longicornis*. Marine Ecology Progress Series, 308, 143-153.

Castellani, C., Robinson, C., Smith, T., Lampitt, R.S. 2005. Temperature affects respiration rate of *Oithona similis*. Marine Ecology Progress Series, 285, 129-135.

Chust, G., Allen, J.I., Bopp, L., Schrum, C., Holt, J., Tsiaras, K., Zavatarelli, M., Chifflet, M., Cannaby, H., Dadou, I., Daewel, U., Wakelin, S.L., Machu, E., Pushpadas, D., Butenschon, M., Artioli, Y., Petihakis, G., Smith, C., Garçon, V., Goubanova, K., Le Vu, B., Fach, B.A., Salihoglu, B., Clementi, E., Irigoien, X. 2014a. Biomass changes and trophic amplification of plankton in a warmer ocean. Global Change Biology, 20, 2124-2139.

Chust, G., Castellani, C., Licandro, P., Ibaibarriaga, L., Sagarminaga, Y., Irigoien, X. 2014b. Are *Calanus* spp. shifting poleward in the North Atlantic? A habitat modelling approach. ICES Journal of Marine Science, 71, 241-253.

Condon, R.H., Graham, W.M., Duarte, C.M., Pitt, K.A., Lucas, C.H., Haddock, S.H.D., Sutherland, K.R., Robinson, K.L., Dawson, M.N., Decker, M.B., Mills, C.E., Purcell, J.E., Malej, A., Mianzan, H., Uye, S-I., Gelcich, S., Madin, L.P. 2012. Questioning the rise of gelatinous zooplankton in the world's oceans. Bioscience, 62, 160-169.

Cook, K.B., Bresnan, E., Turrell, E.A. 2010. The influence of naturally occurring algal biotoxins on the biology of pelagic copepods: a review of the literature and data currently available for Scottish waters. Scottish Marine and Freshwater Science, Vol 1, No 15, 71pp.

Corkett, C.J. and McLaren, I.A. 1978. The biology of *Pseudocalanus*. Advances in Marine Biology, 15, 1-231.

Cornils, A., Held, C. 2014. Evidence of cryptic and pseudocryptic speciation in the *Paracalanus parvus* species complex (Crustacea, Copepoda, Calanoida). Frontiers in Zoology, 11, 19.

Cushing, D.H. 1990. Plankton production and year-class strength in fish populations: an update of the match/mismatch hypothesis. Advances in Marine Biology, 26, 249-293.

Dahms, H-U., Tseng, L-C., Hwang, J-S. 2015. Biogeographic distribution of the cyclopoid copepod genus *Oithona* – from mesoscales to global scales. Journal of Experimental Marine Biology and Ecology, 467, 26-32.

Defra 2014. Marine strategy part two: UK marine monitoring programmes. 86pp. https://www.gov.uk/government/publications/marine-strategy-part-two-uk-marine-monitoring-programmes.

Edwards, M., Bresnan, E., Cook, K., Heath, M., Helaouet, P., Lynam, C., Raine, R., Widdicombe, C. 2013. Impacts of climate change on plankton. MCCIP Science Review, 4, 98-112.

Engel, M. and Hirche, H-J. 2004. Seasonal variability and inter-specific differences in hatching of calanoid copepod resting eggs from sediments of the German Bight (North Sea). Journal of Plankton Research, 26, 1083-1093.

Evans, F. 1977. Seasonal density and production estimates of the commoner planktonic copepods of northumberland coastal waters. Estuarine and Coastal Marine Science, 5, 223-241.

Fabry, V.J., Seibel, B.A., Feely, R.A., Orr, J.C. 2008. Impacts of ocean acidification on marine fauna and ecosystem processes. ICES Journal of Marine Science, 65, 414-432.

Fransz, H.G., Colebrook, J.M., Gamble, J.C., Krause, M. 1991. The zooplankton of the North Sea. Netherlands Journal of Sea Research, 28, 1-52.

Frost, B.W. 1989. A taxonomy of the marine calanoid copepod genus *Pseudocalanus*. Canadian Journal of Zoology, 67, 525-551.

Gallienne, C.P. and Robins, D.B. 2001. Is *Oithona* the most important copepod in the world's oceans? Journal of Plankton Research, 23, 1421-1432.

Gamble, J.C., Davies, J.M., Steele, J.H. 1977. Loch Ewe bag experiment, 1974. Bulletin of Marine Science, 27, 146-175.

Gaudy, R., Cervetto, G., Pagano, M. 2000. Comparison of the metabolism of *Acartia clausi* and *A. tonsa*: influence of temperature and salinity. Journal of Experimental Marine Biology and Ecology, 247, 51-65.

Gibbons, M.J. and Richardson, A.J. 2013. Beyond the jellyfish joyride and global oscillations: advancing jellyfish research. Journal of Plankton Research, 35, 929-938.

Halsband-Lenk, C., Carlotti, F., Greve, W. 2004. Life-history strategies of calanoid congeners under two different climate regimes: a comparison. ICES Journal of Marine Science, 61, 709-720.

Halsband-Lenk, C., Hirche, H-J., Carlotti, F. 2002. Temperature impact on reproduction and development of congener copepod populations. Journal of Experimental Marine Biology and Ecology, 271, 121-153.

Halsband, C., Hirche, H.J. 2001. Reproductive cycles of dominant calanoid copepods in the North Sea. Marine Ecology Progress Series, 209, 219-229.

Hay, S.J., Evans, G.T., Gamble, J.C. 1988. Birth, growth and death rates for enclosed populations of calanoid copepods. Journal of Plankton Research, 10, 431-454.

Hay, S.J., Kiørboe, T., Matthews, A. 1991. Zooplankton biomass and production in the North Sea during the Autumn Circulation Experiment, October 1987–March 1988. Continental Shelf Research, 11, 1453-1476.

Heath, M.R. 1995. Size spectrum dynamics and the planktonic ecosystem of Loch Linnhe. ICES Journal of Marine Science, 52, 627-642.

Heath, M.R., Boyle, P.R., Gislason, A., Gurney, W.S.C., Hay, S.J., Head, E.J.H., Holmes, S., Ingvarsdóttir, A., Jónasdóttir, S.H., Lindeque, P., Pollard, R.T., Rasmussen, J., Richards, K., Richardson, K., Smerdon, G., Speirs, D. 2004. Comparative ecology of over-wintering *Calanus finmarchicus* in the northern North Atlantic, and implications for life-cycle patterns. ICES Journal of Marine Science, 61, 698-708.

Helaouët, P., Beaugrand, G. 2007. Macroecology of *Calanus finmarchicus* and *C. helgolandicus* in the North Atlantic Ocean and adjacent seas. Marine Ecology Progress Series, 345, 147-165.

Hinder, S.L., Gravenor, M.B., Edwards, M., Ostle, C., Bodger, O.G., Lee, P.L.M., Walne, A.W., Hays, G.C. 2014. Multi-decadal range changes vs. thermal adaptation for north east Atlantic oceanic copepods in the face of climate change. Global Change Biology, 20, 140-146.

Hosia, A., Falkenhaug, T., Naustvoll, L.J. 2014. Trends in abundance and phenology of *Aurelia aurita* and *Cyanea* spp. at a Skagerrak location, 1992-2011. Marine Ecology Progress Series, 498, 103-115.

Ianora, A., Miralto, A., Halsband-Lenk, C. 2007. Reproduction, hatching success, and early naupliar survival in *Centropages typicus*. Progress in Oceanography, 72, 195-213.

Klein Breteler, W.C.M., Gonzalez, S.R., Schogt, N. 1995. Development of *Pseudocalanus elongatus* (Copepoda, Calanoida) cultures at different temperature and food conditions. Marine Ecology Progress Series, 119, 99-110.

Laakmann, S., Gerdts, G., Erler, R., Knebelsberger, T., Martínez Arbizu, P., Raupach, M.J. 2013. Comparison of molecular species identification for North Sea calanoid copepods (Crustacea) using proteome fingerprints and DNA sequences. Molecular Ecology Resources, 13, 862-876.

Lindley, J.A. 1990. Distribution of overwintering calanoid copepod eggs in sea-bed sediments around southern Britain. Marine Biology, 104, 209-217.

Lucas, C.H., Graham, W.M., Widmer, C. 2012. Jellyfish life histories: role of polyps in forming and maintaining scyphomedusa populations. Advances in Marine Biology, 63, 133-196.

Lynam, C.P., Attrill, M.J., Skogen, M.D. 2010. Climatic and oceanic influences on the abundance of gelatinous zooplankton in the North Sea. Journal of the Marine Biological Association of the United Kingdom, 90, 1153-1159.

Lynam, C.P., Lilley, M.K.S., Bastian, T., Doyle, T.K., Beggs, S.E., Hays, G.C. 2011. Have jellyfish in the Irish Sea benefited from climate change and overfishing? Global Change Biology, 17, 767-782.

Makabe, R., Furukawa, R., Takao, M., Uye, S. 2014. Marine artificial structures as amplifiers of *Aurelia aurita* s.l. blooms: a case study of a newly installed floating pier. Journal of Oceanography, 70, 447-455.

Marcus, N.H. 1996. Ecological and evolutionary significance of resting eggs in marine copepods: past, present, and future studies. Hydrobiologia, 320, 141-152.

Marques, R., Cantou, M., Soriano, S., Molinero, J-C., Bonnet, D. 2015. Mapping distribution and habitats of *Aurelia* sp. polyps in Thau lagoon, north-western Mediterranean Sea (France). Marine Biology, 162, 1441-1449.

Marshall, S.M. 1949. On the biology of the small copepods in Loch Striven. Journal of the Marine Biological Association of the United Kingdom, 28, 45-122.

Nielsen, T.G., Møller, E.F., Satapoomin, S., Ringuette, M., Hopcroft, R.R. 2002. Egg hatching rate of the cyclopoid copepod *Oithona similis* in arctic and temperate waters. Marine Ecology Progress Series, 236, 301-306.

Nielsen, T.G. and Sabatini, M. 1996. Role of cyclopoid copepods *Oithona* spp. in North Sea plankton communities. Marine Ecology Progress Series, 139, 79-93.

O'Brien, T.D., Wiebe, P.H., Falkenhaug, T. 2013. ICES Zooplankton Status Report 2010/2011. ICES Cooperative Research Report, No. 318, 208pp.

Pan, M. and Hay, S. 2010. Decapod crustacean larvae of Scottish coasts. A photographic identification guide (excluding infraorder Brachyura). Scottish Marine and Freshwater Science, Vol 1, No 11, 106pp.

Pan, M., Pierce, G., Cunningham, C., Hay, S. 2011a. Spatiotemporal coupling/decoupling of planktonic larvae and benthic settlement in decapods in the Scottish east coast. Marine Biology, 158, 31-46.

Pan, M., Pierce, G.J., Cunningham, C.O., Hay, S.J. 2011b. Seasonal and interannual variation of decapod larval abundance from two coastal locations in Scotland, UK. Journal of the Marine Biological Association of the United Kingdom, 91, 1443-1451.

Philippart, C.J.M., van Bleijswijk, J.D.L., Kromkamp, J.C., Zuur, A.F., Herman, P.M.J. 2014. Reproductive phenology of coastal marine bivalves in a seasonal environment. Journal of Plankton Research, 36, 1512-1527.

Pikesley, S.K., Godley, B.J., Ranger, S., Richardson, P.B., Witt, M.J. 2014. Cnidaria in UK coastal waters: description of spatio-temporal patterns and inter-annual variability. Journal of the Marine Biological Association of the United Kingdom, 94, 1401-1408.

Purcell, J.E., Uye, S., Lo, W. 2007. Anthropogenic causes of jellyfish blooms and their direct consequences for humans: a review. Marine Ecology Progress Series, 350, 153-174.

Richardson ,A.J., Bakun, A., Hays, G.C., Gibbons, M.J. 2009. The jellyfish joyride: causes, consequences and management responses to a more gelatinous future. Trends in Ecology and Evolution, 24, 312-322.

Scherer, C., Gowen, R.J., Tett, P., Atkinson, A., Baptie, M., Best, M., Bresnan, E., Cook, K., Forster, R., Keeble, S., McQuatters-Gollop, A. 2015. Development of a UK integrated plankton monitoring programme. A final report of the Lifeform and State Space project prepared for Defra. 76pp. http://randd.defra.gov.uk/Document.aspx?Document=13580_ME5312LifeformFinalReport.pdf.

Starr, M., Himmelman, J.H., Therriault, J-C. 1991. Coupling of nauplii release in barnacles with phytoplankton blooms: a parallel strategy to that of spawning in urchins and mussels. Journal of Plankton Research, 13, 561-571.

Van Walraven, L., Langenberg, V.T., Dapper, R., Witte, J.I., Zuur, A.F., van der Veer, H.W. 2015. Long-term patterns in 50 years of scyphomedusae catches in the western Dutch Wadden Sea in relation to climate change and eutrophication. Journal of Plankton Research, 37, 151-167.

13. Acknowledgments

The authors wish to acknowledge the contribution of the many people (volunteers, analysts, administrators) involved in the successful delivery of this body of work. Without their contribution this programme would not be feasible. Amongst many involved in the programme since 1997, we would particularly note the efforts of:

Sample Collection

Millport
Fiona Hannah
Staff of the University Marine Biological Station Millport
Staff of the Field Studies Council

Loch Maddy
The late Dr. John McLeod
Staff of Camann na Mara
Staff of Loch Duart Salmon

Loch Ewe
Jane and Willie Grant (Isle Ewe Shellfish),
Phil McLaughlin

Scapa:
Jenni Kakonnen
Eileen Summers
Alex Simpson
Staff of Orkney Islands Council Marine Services

Scalloway:

Staff of the North Atlantic Fisheries College
Mark Hamilton
Beth Mouat
Luke Bullogh

Mallaig
Ewen Nicholson

Cromarty
Tim Barton (Aberdeen University)

Fair Isle
Dave Wheeler

Stonehaven and Laboratory-Based Work

Boats/skippers

Jim Brown, Raymond Gargill, Ian Gibb, Paul McDonald, Ian Watson

Stonehaven Sampling
Ana–Luisa Amorim, John Beaton, Tanja Betts, Eileen Bresnan, Maria Campbell, John Clarke, Kathryn Cook, Russell Davidson, Pablo Diaz, John Dunn, Dafne Eerkes-Medrano, Matt Geldart, Marie Kelly, Matt Kinghorn, Shona Kinnear, Steve Hay, Mike Heath, Jennifer Hindson, Michelle Inglis, Marine Kelly, Dave Lee, Dougal Lichtman, Emma Lines, Elspeth MacDonald, Tracy McCollin, Laura Morley, Mike Penston, Campbell Pert, Berit Rabe, Jens Rasmussen, Tom Riley, Tim Roberts, Susan Robinson, Stuart Wallace, Katy Urquhart
Staff of Marine Scotland

Sample Analysis

Oceanography (temperature and salinity)
Richard Adams, John Beaton, Bee Berx, John Dunn, Alejandro Gallego, Matt Geldart, Sarah Hughes, Dave Lee, Dougal Lichtman, Jennifer Hindson, Rodney Payne, George Slessor, Bill Turrell

Chemistry (nutrients, chlorophyll ‘a’, carbonate chemistry)
Fiona Brown, John Fraser, Sheila Fraser, Kelly McIntosh, Abbie Morrice, Malcolm Rose, Carrie Shaw, Kerry Smith, Alsion Taylor, Pam Walsham, Lynda Webster, Andy Wilson

Phytoplankton Ecology (phytoplankton, secchi)
Ana-Luisa Amorim, Eileen Bresnan, Lyndsay Brown, Russell Davidson, Pablo Diaz, Sheila Fraser, Marie Kelly, Elspeth MacDonald, Tracy McCollin, Nikki Smith

Molecular Biology (qPCR)
Ana-Luisa Amorim, Catherine Collins, Jennifer Graham

Biotoxins (SPATT)
Nigel Brown, Guillame Hermann, Jean-Pierre Lacaze, Laura Morley, Alaistair Scott, Lesley Stobo, Elizabeth Turrell

Zooplankton Ecology (zooplankton)
Kathryn Cook, John Dunn, John Fraser, Steve Hay, Margarita Machairopoulou, Mike Penston, Jens Rasmussen, Susan Robinson

Data/Quality Management

Gavin Grewar, Helen McGregor, Jens Rasmussen, Pam Walsham

Project Management
Eileen Bresnan, Mike Heath, Colin Moffat, Bill Turrell

This programme is funded under the service level agreement with the Scottish Government ST03p (2016).